Exploring the medicinal potential of secondary metabolites derived from selected medicinal plants of Ethiopia flora: an integrated study of antidiabetic, anticancer, antibacterial and antioxidant activities, phytochemical analysis, ADMET profiling, and molecular docking insights

By

Getachew Tegegn Kibret

A Dissertation Submitted to the Department of Applied Chemistry

School of Applied Natural Science

Presented in Partial Fulfillment of the Requirement for the Degree of Doctor of Philosophy in Applied Chemistry (Natural Product Chemistry)

Office of Graduate Studies

Adama Science and Technology University

June, 2024

Adama, Ethiopia

Exploring the medicinal potential of secondary metabolites derived from selected medicinal plants of Ethiopia flora: an integrated study of antidiabetic, anticancer, antibacterial and antioxidant activities, phytochemical analysis, ADMET profiling, and molecular docking insights

By

Getachew Tegegn Kibret

Supervisors

Main Supervisor: Milkyas Endale (Professor)

Co-supervisor: Yadessa Melaku (Professor)

A Dissertation Submitted to the Department of Applied Chemistry
School of Applied Natural Science

Presented in Partial Fulfillment of the Requirement for the Degree of Doctor of Philosophy in Applied Chemistry (Natural Product Chemistry)

Office of Graduate Studies
Adama Science and Technology University

Declaration and Recommendation

Declaration

I hereby declare that this Dissertation entitled "**Exploring the medicinal potential of secondary metabolites derived from selected medicinal plants of Ethiopia flora: an integrated study of antidiabetic, anticancer, antibacterial and antioxidant activities, phytochemical analysis, ADMET profiling, and molecular docking insights"** is my original work and has not been submitted to any other university for the award of any academic degree. The references used in this dissertation are duly acknowledged by appropriate citations.

Getachew Tegegn	_____	12/6/2024
Name of student	Signature	Date

Recommendation of Supervisors

We, the supervisors of this dissertation, hereby certify that we have read and revised the dissertation entitled "**Exploring the medicinal potential of secondary metabolites derived from selected medicinal plants of Ethiopia flora: an integrated study of antidiabetic, anticancer, antibacterial and antioxidant activities, phytochemical analysis, ADMET profiling, and molecular docking insights**" prepared under our guidance by **Getachew Tegegn** submitted in partial fulfillment of the requirements for the degree of Doctor of Philosophy in Applied Chemistry (**Natural Products Chemistry**). Therefore, we hereby recommend the submission of the dissertation to the department for further review and evaluation.

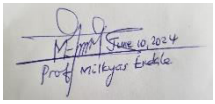

Milkyas Endale (Prof)	_____	12/6/2024
Major Supervisor	Signature	Date
Yadessa Melaku (Prof)	_____	12/6/2024
Co-supervisor	Signature	Date

Approvals

Approval of Supervisors

We hereby certify that the recommendations and suggestions given by the examiners committee are appropriately incorporated into the final version of the dissertation entitled **"Exploring the medicinal potential of secondary metabolites derived from selected medicinal plants of Ethiopia flora: an integrated study of antidiabetic, anticancer, antibacterial and antioxidant activities, phytochemical analysis, ADMET profiling, and molecular docking insights"** by Getachew Tegegn.

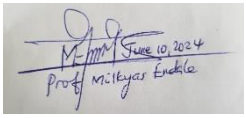

Milkyas Endale (Prof)	_____	12/6/2024
Major Supervisor	Signature	Date
Yadessa Melaku (Prof)	_____	12/6/2024
Co-supervisor	Signature	Date

Approval of Board of Examiners

We, then undersigned, members of the board examiners committee of the dissertation open defense by Getachew Tegegn have read and evaluated the dissertation entitled **"Exploring the medicinal potential of secondary metabolites derived from selected medicinal plants of Ethiopia flora: an integrated study of antidiabetic, anticancer, antibacterial and antioxidant activities, phytochemical analysis, ADMET profiling, and molecular docking insights "** and examined the candidate during open defense. This is, therefore, to certify that the dissertation is accepted for partial fulfillment of the requirement of the Degree of Doctor of Philosophy in Applied Chemistry (**Natural Products Chemistry**)

_____	_____	12/6/2024
Chairperson	Signature	Date
Aman Dekebo (Professor)	_____	12/6/2024
Internal Examiner 1	Signature	Date
Negera Abdissa (PhD)	_____	12/6/2024
External Examiner 1	Signature	Date
Zelalem Yibralegn (PhD)	_____	12/6/2024
External Examiner 2	Signature	Date

Final approval and acceptance of the dissertation is contingent upon the submission of its final copy to the Office of Postgraduate Studies (OPGS) through the candidate's Department Graduate Council (DGC) and School Graduate Committee (SGC).

_____	_____	_____
Department Head	Signature	Date
_____	_____	_____
School Dean	Signature	Date
_____	_____	_____
Office of Postgraduate Studies, Dean	Signature	Date

ACKNOWLEDGEMENTS

First and foremost, I humbly express my deepest feelings to the Almighty God for giving me strength throughout my life and keeping me safe. I am very indebted to express my sincerest gratitude to my advisors, Professor Milkyas Endale and Professor Yadessa Melaku for their kind supervision, invaluable technical support, suggestions, guidance, and encouragement at every stage throughout the whole period of my Ph.D. study. I owe you a big thanks! I have grasped a lot from you, my advisor Professor Milkyas Endale, for your continuous follow-up and unreserved support during the whole period of this work starting from proposal development. I appreciate your commitment to research. Thank you for sharing your indispensable experiences and skillfully helping me to improve my knowledge. Your inspiration raised my eagerness to be a good advisor in the future.

I would like to thank Professor Aman Dekebo profoundly for all of his support during the challenges I've faced since getting my MSc. I also appreciate his thoughtful comments on the dissertation, seminars, proposal development, progress reports, and you collaborated with the Pasteur Institute in St. Petersburg, Russia and Walailak University in Nakhon Si Thammarat, Thailand to evaluate antiviral and anti-acanthamoeba activity, respectively. I am grateful to Dr. Defaru Negera, Head of the Department of Applied Chemistry, Dr. Aschalew Tadesse, former Head of the Applied Chemistry Department, and Dr. Tsegaye Deyou, Academic Vice President of Salale University, for their administrative and material support. I also want to express my gratitude to all academic staff of the Applied Chemistry Department, especially to Dr. Endale Mulugeta, Dr. Worku Dinku, and Dr. Lemma Teshome for their friendly care, encouragement, moral support, and material support to accomplish my study. I sincerely thank Prof. Rajalakshmanan Eswaramoorthy, Ankita Garg, and Muhdin Aliye for their technical support during the computational study of the isolated compounds. I deeply acknowledge: Prof. Rajalakshmanan Eswaramoorthy for carrying out *in vitro* antidiabetic, and anticancer, Mr. Abiy Abebe, Mr. Sileshi Degu, and Mr. Ebisa Firisa conducted the antimicrobial activity, Mr. Kebede Shenkute for GC-MS Analysis, Dr. Taye Demissie, and Japeth Ombito, from the Department of Chemistry, University of Botswana, Professor Mo Hunsen from the Department of Chemistry, Kenyon College, Gambier, USA, Dr. Mesfin Getachew, and

Mr. Yohannes Meaza, from the Department of Chemistry, Addis Abeba University for running the NMR samples, and Mr. Melaku Wondaferash, and Mr. Shambel Alemu, taxonomists at National Herbarium, Addis Ababa University, who helped me during plant identification. I am also grateful to Mr. Yohannes Meaza and Miheretu Samuel from Addis Abeba University's Department of Chemistry, for the material support.

I extend my deepest appreciation to my hero and love, my wife, Wegen Getu, and her sister Mimi, simple thanks are not enough for your continuous support and countless sacrifices to help me get to this point; my children, Beknan Getachew, and Melona Getachew, for the love you showed; my mom, W/ro Wude Alemu, father-in-law, mother-in-law, my beloved sisters, and my brothers for their moral guidance, prayers, and timely help in various ways during this study.

I am also grateful to all my friends, with special thanks to my friends Dagem Tesfaye, Mesay Tamirat, Wondwosen Beyene, Seifu Kedir, Anteneh Getinet, Mikael Endalu and Melese Hailemikael for their invaluable contributions. I also appreciate Dr. Tekalign Begna, Dr. Digafie Zeleke, Dr. Teshome Degifie, Dr. Mamaru Bitew, Dr. Tsegu Kiros, Mr. Bundi Roba, Mr. Enyew Tilahun, Mr. Shewarega Habtamu and Emebet Getaneh for their constructive comments and suggestions that helped me improve this dissertation and my co-workers in ASTU (Tolosa Duguma, Hadush Gebrehiwot, Bihon Abera, and Kibrom Mezgeb). Thank you all for the support, comfort, and good times I have shared with you. Finally, the Applied Chemistry Department, Adama Science, and Technology University is thanked for allowing me to pursue PhD studies and Salale University for study leave.

TABLE OF CONTENTS

ACKNOWLEDGEMENTS ..... **VII**
LIST OF TABLES ..... **XIV**
LIST OF FIGURES ..... **XVI**
LIST OF SCHEMES ..... **XVIII**
LIST OF APPENDICES ..... **XIX**
LIST OF ACRONYMS AND ABBREVIATIONS ..... **XXIV**
ABSTRACT ..... **XXIII**
CHAPTER ONE **1**
1. INTRODUCTION **1**
1.1. Background 1
1.2. Statement of the problem 5
1.3. Justification of the study 6
1.4. Objectives 7
1.4.1. General objective 7
1.4.2. Specific objectives 7
1.5. Significance of the study 8
CHAPTER TWO **10**
2. LITERATURE REVIEW **10**
2.1. Review of studied medicinal plants 10
2.2. Botanical description, and geographical distribution of the studied medicinal plants 10
2.2.1. *Crinum abyssinicum* 10
2.2.2. *Calotropis procera* 11
2.2.3. *Caylusea abyssinica* 12
2.2.4. *Justicia schimperiana* 12
2.2.5. *Verbascum sinaiticum* 13
2.2.6. *Lagenaria abyssinica* 14
2.3. Ethnobotanical uses 14
2.3.1. *Crinum abyssinicum* 14
2.3.2. *Calotropis procera* 15
2.3.3. *Caylusea abyssinica* 16
2.3.4. *Justicia schimperiana* 16
2.3.5. *Verbascum sinaiticum* 16
2.3.6. *Lagenaria abyssinica* 17
2.4. Phytochemistry and biological activities informations 19
2.4.1. *Crinum abyssinicum* 19

2.4.2. *Calotropis procera* 25
2.4.3. *Caylusea abyssinica* 30
2.4.4. *Justicia schimperiana* 31
2.4.5. *Verbascum sinaiticum* 35
2.4.6. *Lagenaria abyssinica* 38
2.5 Current Status and Challenges in the Management of Microbial, Diabetic, and Cancer Diseases 40
CHAPTER THREE 42
3. MATERIALS AND METHODS 42
3.1. General 42
3.2. Plant materials collection, identification, and preparation 42
3.3. Extraction and isolation 43
3.3.1. General extraction method 43
3.3.2. Extraction and isolation of secondary metabolites from the roots of *C. abyssinicum* 45
3.3.3. Extraction and isolation of secondary metabolites from the roots of *C. procera* 46
3.3.4. Extraction and isolation of secondary metabolites from the roots of *C. abyssinica* 47
3.3.5. Extraction and isolation of secondary metabolites from the roots of *J. schimperiana* 48
3.3.6. Extraction and isolation of secondary metabolites from the roots of *V. sinaiticum* 49
3.3.7. Extraction and isolation of secondary metabolites from the roots of *L. abyssinica* 50
3.3.8. Extraction of essential oils from different parts of studied medicinal plants 50
3.3.8.1. GC-MS analysis of the essential oils 51
3.4. Biological activities 53
3.4.1. Antimicrobial study 53
3.4.1.1. Broth microdilution MTT assay 53
3.4.1.2. Disc diffusion method 54
3.4.2. Radical scavenging activity of the extracts and isolated compounds 55
3.4.3. *In vitro* antidiabetic activity 56
3.4.4. *In vitro* cytotoxicity assay 57
3.4.4.1. Cell viability assay 57
3.4.4.2. Cell lines and culture 57
3.4.5. *In vitro* anti-acanthamoeba activity of extracts 58
3.4.5.1. Cultivation of *A. triangularis* 58
3.4.5.2. Screening 58
3.4.6. *In vitro* antiviral activities assays 59
3.5. Computational studies 59
3.5.1. *In silico* molecular docking methodology 60

3.5.1.1. Preparation of ligands 60
3.5.1.2. Preparation of macromolecules 60
3.5.1.3. AutoDock vina analysis 60
3.5.2. *In silico* pharmacokinetics (drug-likeness) properties of the isolated compounds 61
3.5.3. *In silico* prediction of toxicity of isolated compounds 62
3.6. Statistical data analysis 62
CHAPTER FOUR 63
4. RESULTS AND DISCUSSION 63
4.1. Secondary metabolites isolated from the studied medicinal plants 63
4.1.1. Secondary metabolites isolated from the roots of *C. abyssinicum* 63
4.1.2. Secondary metabolites isolated from the root of *Calotropis procera* 73
4.1.3. Secondary metabolites isolated from the root of *Caylusea abyssinica* 86
4.1.4. Secondary metabolites isolated from the root of *Justicia schimperiana* 91
4.1.5. Secondary metabolites isolated from the root of *Verbascum sinaiticum* 101
4.1.6. Secondary metabolites isolated from the root of *Lagenaria abyssinica* 116
4.2. Chemical composition of essential oils extracted from different parts of studied medicinal plants 120
4.2.1. Percentage yield of essential oils 120
4.2.2. Chemical composition of essential oils from bulbs of *C. abyssinicum* and aerial parts of *C. abyssinica* 121
4.2.3. Chemical composition of essential oils from leaves, flowers, and seeds of *C. procera* 122
4.2.4. Chemical composition of essential oils from leaves, and roots of *J. schimperiana* 123
4.2.5. Chemical composition of essential oils from leaves, and roots of *V. siniaticum* 124
4.2.6. Chemical composition of essential oils from seeds, and roots of *L. abyssinica* 125
4.3. Biological activity analysis 126
4.3.1. Antibacterial activity of the extracts and isolated compounds 126
4.3.1.2. Antibacterial activity of the extracts and isolated compounds (97, 234, 96, 87, 231, 232) from roots of *C. procera* 129
4.3.1.3. Antibacterial activity of the extracts and isolated compounds (239-241, 79) from roots of *C. abyssinica* 131
4.3.1.4. Antimicrobial activity of the extracts and isolated compounds (78, 242-246) from roots of *J. schimperiana* 133
4.3.1.5. Antimicrobial activity of the extracts and isolated compounds (247-253, 230) from roots of *V. siniaticum* 135
4.3.2. Antimicrobial evaluation of essential oil extract 136
4.3.3. Antioxidant activity of the extracts and isolated compounds 139

4.3.3.1. Antioxidant activity of the extracts and isolated compounds (224-229) from roots of *C. abyssinicum* 140
4.3.3.2. Antioxidant activity of the extracts and isolated compounds (97, 234, 87, 231, 232) from roots of *C. procera* 141
4.3.3.3. Antioxidant activity of the extracts and isolated compounds (239-241, 79) from roots of *C. abyssinica* 143
4.3.3.4. Antioxidant activity of the extracts and isolated compounds (78, and 242-246) from roots of *J. schimperiana* 144
4.3.3.5. Antioxidant activity of the extracts and isolated compounds (247-253) from roots of *V. sinaiticum* 146
4.3.4. Inhibition of α-amylase by extracts of studied medicinal plants 147
4.3.5. Cytotoxicity analysis 149
4.3.6. Anti-acanthamoeba activity studies of extracts 151
4.3.7. *In vitro* antiviral activities analysis 152
4.9. Computational studies of isolated compounds 153
4.9.1. Molecular docking studies of isolated compounds 153
4.9.2. *In silico* pharmacokinetics (ADME) properties of isolated compounds 163
4.9.3. *In silico* toxicity prediction of isolated compounds 165
CHAPTER FIVE 170
5. CONCLUSION AND RECOMMENDATIONS 170
5.1. Conclusions 170
5.2. Recommendation 173
REFERENCES 175
APPENDICES 204
List of published articles from this work 297

LIST OF TABLES

Table 1: Botanical and ethno-botanical description of studied plants. 18
Table 2: Compounds organized by compound class from different *Crinum* species. 20
Table 3: Compounds isolated from *C. procera* organized by compound class. 26
Table 4: List of compounds isolated from *C. abyssinica* organized by compound class. 31
Table 5: A List of compounds organized by compound class from different *Justica* species. 32
Table 6. A List of compounds organized by compound class from *V. sinaiticum*. 36
Table 7: ^{1}H NMR (400 MHz, $CDCl_3$) and ^{13}C NMR (101 MHz, $CDCl_3$) data of compound **224** and literature ^{13}C-NMR data of stigmast-4-ene-3-one. 64
Table 8: ^{1}H NMR (400 MHz, $CDCl_3$) and ^{13}C NMR (101 MHz, $CDCl_3$) data of compound **225** and literature ^{1}H NMR and ^{13}C-NMR data of 1,3-dilinoleoyl-2-oleine. .. 66
Table 9: ^{1}H NMR (400 MHz, $CDCl_3$) and ^{13}C NMR (101 MHz, $CDCl_3$) data of compound **226** and literature ^{1}H NMR and ^{13}C-NMR data of 6-hydroxy-3,5,7,4′-tetramethoxyflavone. 68
Table 10: ^{1}H NMR (400 MHz, $CDCl_3$) and ^{13}C NMR (101 MHz, $CDCl_3$) data of compound **227** and literature of ^{13}C-NMR data of penicilloitins B. 69
Table 11: ^{1}H NMR (400 MHz, $CDCl_3$) and ^{13}C NMR (101 MHz, $CDCl_3$) data of compound **228** and literature of ^{13}C-NMR data of sitosterol-3-O-*β*-D-glucopyranoside. 71
Table 12: ^{1}H-NMR (400 MHz, $CDCl_3$) and ^{13}C-NMR (101 MHz, $CDCl_3$) spectral data of compound **82** and the reported data for *β*-sitosteryl linoleate. 74
Table 13: ^{1}H-NMR (400 MHz, $CDCl_3$) and ^{13}C-NMR (101 MHz, $CDCl_3$) spectral data of compound **231** and the reported ^{13}C-NMR data for (4*Z*)-dodec-4-en-1-ol. 76
Table 14: ^{1}H NMR (400 MHz, $CDCl_3$) and ^{13}C NMR (101 MHz, $CDCl_3$) data of compound **232** and literature ^{13}C-NMR data of spinasterol. 78
Table 16: The ^{1}H- NMR (400 MHz, $CDCl_3$) and ^{13}C-NMR (101 MHz, $CDCl_3$) spectral data of compound **234** and the data reported in the literature for 11-oxo-α-amyrin ethylated. 85
Table 17: ^{1}H NMR (400 MHz, $CDCl_3$) and ^{13}C NMR (101 MHz, $CDCl_3$) data of compound **239** and literature ^{1}H NMR and ^{13}C-NMR data of bis(2-ethylheptyl) phthalate. 88
Table 18: ^{1}H NMR (400 MHz, $CDCl_3$) and ^{13}C NMR (101 MHz, $CDCl_3$) data of compound **79** and literature ^{13}C-NMR data of stigmasterol. 90
Table 19: ^{1}H-NMR (400 MHz, $CDCl_3$) and ^{13}C-NMR (101 MHz, $CDCl_3$) spectral data of compound **78** and the reported data for *β*-sitosterol. 92
Table 20: ^{1}H NMR (400 MHz, $CDCl_3$) and ^{13}C NMR (101 MHz, $CDCl_3$) data of compound **242** and literature data of 5-methoxy durmillone. 95
Table 21: ^{1}H-NMR (400 MHz, DMSO-d_6) and ^{13}C-NMR (101 MHz, DMSO-d_6) spectral data of compound **243** and the reported data for *trans-resveratr*ol. 96
Table 22: ^{1}H-NMR (400 MHz, DMSO-d_6) and ^{13}C-NMR (101 MHz, DMSO-d_6) spectral data of compound **244** and the reported data for tricuspidatol A. 98
Table 23: Comparison of the ^{1}H-NMR (400 MHz, DMSO-d_6) and ^{13}C-NMR (101 MHz, DMSO-d_6, δ in ppm) spectral data of compounds **245,** and **246** with the reported data. 101
Table 24: Comparison of the ^{1}H-NMR (400 MHz, $CDCl_3$) and ^{13}C-NMR (101 MHz, $CDCl_3$) spectral data of compound **247** and 3′-(4′′-methoxy phenyl)-3′-oxo-propionyl hexadecanoate. 102

Table 25: Comparison of the ^{13}C-NMR (101 MHz, DMSO-d_6) spectral data of compound **248** and harpagoside. 104
Table 26: Comparison of the ^{1}H-NMR spectral data (400 MHz, δ_H in ppm, *J* in Hz) of compounds **249**, **250**, **251**, and **252** with the reported data. 111
Table 27: Comparison of the ^{13}C-NMR spectral data (101 MHz, δ_C in ppm) of compounds **249**, **250**, **251**, **252,** and with reported data. 113
Table 28: Comparison of the ^{13}C-NMR (101 MHz, DMSO-d_6) spectral data of compound **253** and harpagide 6-*O*-β-glucoside. 115
Table 29: ^{1}H NMR (400 MHz, $CDCl_3$) and ^{13}C NMR (101 MHz, $CDCl_3$) data of compound **254** and literature reported ^{13}C-NMR data of 22, 23-dihydrospinasterol acetate. 117
Table 30: ^{1}H NMR (400 MHz, $CDCl_3$) and ^{13}C NMR (101 MHz, $CDCl_3$) data of compound **255** and literature of ^{13}C-NMR data of stigmasterol-3-O-*β*-D-glucoside. 119
Table 31: The mean inhibition zone diameter (IZD) in mm of the root extracts, and isolated compounds (**223-229**) of *C. abyssinicum*. 127
Table 32: The mean inhibition zone diameter (IZD) in mm of the root extracts and isolated compounds (**97, 234, 96, 87, 231, 232**) of *Calotropis procera*. 130
Table 33: The mean inhibition zone diameter (IZD) in mm of the root extracts and isolated compounds (**239-241, 79**) of *C. abyssinica*. 132
Table 34: Antimicrobial activity (MIC) of extracts, and isolated compounds (**78, 242-246**) from roots of *J. schimperiana*. 134
Table 35: Antimicrobial activity of extracts and isolated compounds (**247-253, 230**) from roots of *V. sinaiticum*. 136
Table 36: Antimicrobial Activity of EO extracts of plants against selected microorganisms (MIC in mg/mL). 139
Table 37: Percent radical scavenging activity of the plant extract and isolated compounds (**224-229**). 140
Table 38: Percent radical scavenging activities of the plant root extract and isolated compounds (**97, 234, 87, 231, 232**). 142
Table 39: Percent radical scavenging activities of the plant extract and isolated compounds (**239-241, 79**). 143
Table 40: Percent radical scavenging activities of the root extract and isolated compounds (**78**, and **242-246**) of *J. schimperiana*. 145
Table 41: Percent radical scavenging activities of the root extract and isolated compounds (**247-253**) of *V. siniaticum*. 146
Table 42: % Inhibition of alpha-amylase assay. 148
Table 43: Cytotoxic activities of plant extracts against MCF-7 breast cancer cell line. 150
Table 44: Screening of anti-*Acanthamoeba* activity of extracts against *A. triaugularis* WU19001 and *A. castellanii* ATCC50739 trophozoites. 152
Table 45: Assessment of cytotoxicity and Anti influenza virus A activity of extracts by MTT assay in MDCK cell line. 152
Table 46: Parameters of *in silico* bioavailability prediction and physicochemical properties of isolated compounds. 167
Table 47: Pharmacokinetic (ADME) property prediction of isolated compounds. 168
Table 48: *In silico* toxicity prediction of isolated compounds using PreADMET and PROTOX-II protocols. 169

LIST OF FIGURES

Figure 1: Some natural products isolated from higher plants as clinical agents. 2
Melaku Tegegn, November, 2021).....11
Figure 4: Aerial part (a) and roots (b) of *C. abyssinica* (Illubabor, Oromia, Picture by Melaku Tegegn, November, 2021).....12
Figure 5: Aerial part (a) and root (b) of *J. schimperiana* (Illubabor, Oromia, Picture by Melaku Tegegn, November, 2021).....13
Figure 6: Leaves (a) and roots (b) of *V. sinaiticum* (Arsi, Oromia, Picture by Yalew Amare, November, 2022).....14
Figure 7: Aerial part (a) and root (b) of *L. abyssinica* (Illubabor, Oromia, Picture by Melaku Tegegn, November, 2021).....14
Figure 9: Structure of compounds reported from *C. procera*.....30
Figure 10: Structure of compounds isolated from *C. abyssinica* 31
Figure 11: Structures of compounds reported from the genus *Justicia*.....35
Figure 12: Structures of compounds reported from *V. sinaiticum* 38
Figure 13: Structures of compounds reported from *Lagenaria* species. 39
Figure 14: Map showing the plants collection area in Oromia Regional State. 43
Figure 15: The percentage yield of EOs extract. 121
Figure 16: Most abundant compounds identified from *C. abyssinicum* (bulbs), and *C. abyssinica* (aerial parts) essential oils. 122
Figure 17: Most abundant compounds identified from *C. procera* (leaves, flowers, and seeds) essential oils.....123
Figure 18: Most abundant compounds identified from *J. schimperiana* (leaves, and roots) essential oils.....124
Figure 19: Most abundant compounds identified from *V. siniaticum* (leaves, and roots) essential oils.....125
Figure 20: Most abundant compounds identified from *L. abyssinica* (seeds, and roots) essential oils.....126
Figure 21: The inhibition zone of the extract and isolated compounds of *C. abyssinicum* in mm (mean ± SD) at 500 μg/mL.....129
Figure 22: The inhibition zone of the extract and isolated compounds of *C. procera* in mm (mean ± SD) at 500 μg/mL.....131
Figure 23: The inhibition zone of the extract and isolated compounds of *C. abyssinica* in mm (mean ± SD) at 500 μg/mL.....133
Figure 24: The structure of DPPH radical and its product (DPPH-H). 140
Figure 25: Percentage of DPPH radical scavenging activities of the extract and isolated compounds of *C. abyssinicum*. 141
Figure 28: Percentage of DPPH radical scavenging activities of the extracts, and isolated compounds of *J. schimperiana*. 145
Figure 29: The antioxidant activities of the extract and isolated compounds of *V. siniaticum*. 147
Figure 30: Percentage of α-amylase inhibitory effects of extracts and acarbose (standard drug). 149
Figure 34: The 2D and 3D binding interactions of isolated compounds and standard vosaroxin, and revlimid against human topoisomerase IIα (PDB ID: 4fm9). 161
Figure 35: The 2D and 3D binding interactions of isolated compounds and standard drug amoxicillin against *S. aureus* Gyrase (PDB ID: 2XCT).....161

Figure 37: BOILED-Egg model for predicting gastrointestinal absorption and brain access. 165

LIST OF SCHEMES

Scheme 1: General procedures for extractions of the plant samples. 44
Scheme 2: General procedures of extractions of essential oils.....52

LIST OF APPENDICES

Appendix 1A: ^{1}H NMR (400 MHz, CDCl3) spectrum of (*E*)-octadec-7-enoic acid (**223**). 202

Appendix 1B: ^{13}C NMR (101 MHz, CDCl3) spectrum of (*E*)-octadec-7-enoic acid (**223**) 202

Appendix 1C: DEPT-135 NMR (101 MHz, CDCl3) spectrum of (*E*)-octadec-7-enoic acid (**223**) 203

Appendix 2A: ^{1}H NMR (400 MHz, CDCl3) spectrum of stigmast-4-en-3-one (**224**). 203

Appendix 2B: ^{13}C NMR (101 MHz, CDCl3) spectrum of stigmast-4-en-3-one (**224**) 204

Appendix 2C: DEPT-135 NMR (101 MHz, CDCl3) spectrum of stigmast-4-en-3-one (**224**) 204

Appendix 3A: ^{1}H NMR (400 MHz, CDCl3) spectrum of 1,3-dilinoleoyl-2-oleine (**225**) 205

Appendix 3B: ^{13}C NMR (101 MHz, CDCl3) spectrum of 1,3-dilinoleoyl-2-oleine (**225**) 205

Appendix 3C: DEPT-135 NMR (101 MHz, CDCl3) spectrum of 1,3-dilinoleoyl-2-oleine (**225**) 206

Appendix 4A: ^{1}H NMR (400 MHz, CDCl3) spectrum of 6-hydroxy-3,5,7,4′-tetramethoxyflavone (226). 206

Appendix 4B: ^{13}C NMR (101 MHz, CDCl3) spectrum of 6-hydroxy-3,5,7,4′-tetramethoxyflavone (**226**). 207

Appendix 4C: DEPT-135 NMR (101 MHz, CDCl3) spectrum of 6-hydroxy-3,5,7,4′-tetramethoxyflavone (**226**). 207

Appendix 4D: ^{1}H-^{1}H COSY spectrum of 6-hydroxy-3,5,7,4′-tetramethoxyflavone (**226**). 208

Appendix 4E: HSQC correlation of 6-hydroxy-3,5,7,4′-tetramethoxyflavone (**226**). 208

Appendix 4F: HMBC correlation of 6-hydroxy-3,5,7,4′-tetramethoxyflavone (**226**). 209

Appendix 5A: ^{1}H NMR (400 MHz, CDCl3) spectrum of penicilloitins B (**227**). 209

Appendix 5B: ^{13}C NMR (101 MHz, CDCl3) spectrum of penicilloitins B (**227**). 210

Appendix 5C: DEPT-135 NMR (101 MHz, CDCl3) spectrum of penicilloitins B (**227**). 210

Appendix 6A: ^{1}H NMR (400 MHz, CDCl3) spectrum of *para*-methoxy benzoyl-sitosterol-3-O-*β*-D-glucopyranoside (**228**). 211

Appendix 6B: ^{13}C NMR (101 MHz, CDCl3) spectrum of *para*-methoxy benzoyl-sitosterol-3-O-*β*-D-glucopyranoside (**228**). 211

Appendix 6C: DEPT-135 NMR (101 MHz, CDCl3) spectrum of *para*-methoxy benzoyl-sitosterol-3-O-*β*-D-glucopyranoside (**228**). 212

Appendix 7A: ^{1}H NMR (400 MHz, CDCl3) spectrum of ethyl (E)-octadec-9-enoate (**229**). 212

Appendix 7B: ^{13}C NMR (101 MHz, CDCl3) spectrum of ethyl (E)-octadec-9-enoate (**229**). 213

Appendix 7C: DEPT-135 NMR (101 MHz, CDCl3) spectrum of ethyl (E)-octadec-9-enoate (**229**). 213

Appendix 8A: ^{1}H NMR (400 MHz, MeOD) spectrum of sucrose (**230**). 214
Appendix 8B: ^{13}C NMR (101 MHz, MeOD) spectrum of sucrose (**230**). 214
Appendix 8C: DEPT-135 NMR (101 MHz, MeOD) spectrum of sucrose (**230**). 215
Appendix 9B: ^{13}C NMR (101 MHz, CDCl3) spectrum of calotroproceryl acetate A (**96**). 216
Appendix 9C: DEPT-135 NMR (101 MHz, CDCl3) spectrum of calotroproceryl acetate A (96). 216
Appendix 10A: ^{1}H NMR (400 MHz, CDCl3) spectrum of *β*-sitosteryl linoleate (**82**). 217
Appendix 10B: ^{13}C NMR (101 MHz, CDCl3) spectrum of *β*-sitosteryl linoleate (**82**). 217
Appendix 10C: DEPT-135 NMR (101 MHz, CDCl3) spectrum of *β*-sitosteryl linoleate (**82**). 218
Appendix 11A: ^{1}H NMR (400 MHz, CDCl3) spectrum of α-amyrin (**87**). 218
Appendix 11B: ^{13}C NMR (101 MHz, CDCl3) spectrum of α-amyrin (**87**). 219
Appendix 11C: DEPT-135 NMR (101 MHz, CDCl3) spectrum of α-amyrin (**87**). 219
Appendix 12A: ^{1}H NMR (400 MHz, CDCl3) spectrum of compound (**231**). 220
Appendix 12B: ^{13}C NMR (101 MHz, CDCl3) spectrum of compound (**231**). 220
Appendix 12C: DEPT-135 NMR (101 MHz, CDCl3) spectrum of compound (**231**). 221
Appendix 13A: ^{1}H NMR (400 MHz, CDCl3) spectrum of spinasterol acetate (**232**). 221
Appendix 13B: ^{13}C NMR (101 MHz, CDCl3) spectrum of spinasterol acetate (**232**). 222
Appendix 13C: DEPT-135 NMR (101 MHz, CDCl3) spectrum of spinasterol acetate (**232**). 222
Appendix 14A: ^{1}H NMR (400 MHz, MeOD) spectrum of calotropursenol B (**233**). 223
Appendix 14B: ^{13}C NMR (101 MHz, MeOD) spectrum of calotropursenol B (**233**). 223
Appendix 14C: DEPT-135 NMR (101 MHz, MeOD) spectrum of calotropursenol B (**233**). 224
Appendix 15A: ^{1}H NMR (400 MHz, CDCl3) spectrum of calotroproceroⅼ A (**97**). 224
Appendix 15B: ^{13}C NMR (101 MHz, CDCl3) spectrum of calotroproceroⅼ A (**97**). 225
Appendix 15C: DEPT-135 NMR (101 MHz, CDCl3) spectrum of calotroproceroⅼ A (**97**). 225
Appendix 15D: ^{1}H-^{1}H COSY spectrum of calotroproceroⅼ A (**97**). 226
Appendix 15E: HSQC correlation of calotroproceroⅼ A (**97**). 226
Appendix 15F: HMBC correlation of calotroproceroⅼ A (**97**). 227
Appendix 16A: ^{1}H NMR (400 MHz, CDCl3) spectrum of 11-oxo-α-amyrin ethylated (**234**). 227
Appendix 16B: ^{13}C NMR (101 MHz, CDCl3) spectrum of 11-oxo-α-amyrin ethylated (**234**). 228
Appendix 16C: DEPT-135 NMR (101 MHz, CDCl3) spectrum of 11-oxo-α-amyrin ethylated (**234**). 228
Appendix 16D: ^{1}H-^{1}H COSY spectrum of 11-oxo-α-amyrin ethylated (**234**). 229
Appendix 16E: HSQC correlation of 11-oxo-α-amyrin ethylated (**234**). 229
Appendix 16F: HMBC correlation of 11-oxo-α-amyrin ethylated (**234**). 230
Appendix 17A: ^{1}H NMR (400 MHz, CDCl3) spectrum of calotroprocerol B (**98**). 230

Appendix 17B: ^{13}C NMR (101 MHz, CDCl3) spectrum of calotroprocerol B (**98**). 231
Appendix 17C: DEPT-135 NMR (101 MHz, CDCl3) spectrum of calotroprocerol B (**98**). 231
Appendix 18A: ^{1}H NMR (400 MHz, CDCl3) spectrum of lauric acid (**238**). 232
Appendix 18B: ^{13}C NMR (101 MHz, CDCl3) spectrum of lauric acid (238). 232
Appendix 18C: DEPT-135 NMR (101 MHz, CDCl3) spectrum of lauric acid (**238**). 233
Appendix 18D: ^{1}H-^{1}H COSY spectrum of lauric acid (238). 233
Appendix 18E: HSQC correlation of lauric acid (**238**). 234
Appendix 18F: HMBC correlation of lauric acid (**238**). 234
Appendix 19A: ^{1}H NMR (400 MHz, CDCl3) spectrum of bis(2-ethylheptyl) phthalate (**239**). 235
Appendix 19B: ^{13}C NMR (101 MHz, CDCl3) spectrum of bis(2-ethylheptyl) phthalate (**239**). 235
Appendix 19C: DEPT-135 NMR (101 MHz, CDCl3) spectrum of bis(2-ethylheptyl) phthalate (**239**). 236
Appendix 19D: ^{1}H-^{1}H COSY spectrum of bis(2-ethylheptyl) phthalate (**239**). 236
Appendix 19E: HSQC correlation of bis(2-ethylheptyl) phthalate (**239**). 237
Appendix 19F: HMBC correlation of bis(2-ethylheptyl) phthalate (**239**). 237
Appendix 20A: ^{1}H NMR (400 MHz, CDCl3) spectrum of oleic acid (**240**). 238
Appendix 20B: ^{13}C NMR (101 MHz, CDCl3) spectrum of oleic acid (**240**). 238
Appendix 20C: DEPT-135 NMR (101 MHz, CDCl3) spectrum of compound oleic acid (**240**). 239
Appendix 21A: ^{1}H NMR (400 MHz, CDCl3) spectrum of myristic acid (**241**). 239
Appendix 21B: ^{13}C NMR (101 MHz, CDCl3) spectrum of myristic acid (**241**). 240
Appendix 21C: DEPT-135 NMR (101 MHz, CDCl3) spectrum of myristic acid (**241**). 240
Appendix 21D: ^{1}H-^{1}H COSY spectrum of myristic acid (**241**). 241
Appendix 21E: HSQC correlation of myristic acid (**241**). 241
Appendix 21F: HMBC correlation of myristic acid (**241**). 242
Appendix 22A: ^{1}H NMR (400 MHz, CDCl3) spectrum of stigmasterol (**79**). 242
Appendix 22B: ^{13}C NMR (101 MHz, CDCl3) spectrum of stigmasterol (**79**). 243
Appendix 22C: DEPT-135 NMR (101 MHz, CDCl3) spectrum of stigmasterol (**79**). 243
Appendix 23A: ^{1}H NMR (400 MHz, CDCl3) spectrum of β-sitosterol (**78**). 243
Appendix 23B: ^{13}C NMR (101 MHz, CDCl3) spectrum of β-sitosterol (**78**). 244
Appendix 23C: DEPT-135 NMR (101 MHz, CDCl3) spectrum of β-sitosterol (**78**). 245
Appendix 24A: ^{1}H NMR (400 MHz, CDCl3) spectrum of 5-methoxy durmillone (**242**). 245
Appendix 24B: ^{13}C NMR (101 MHz, CDCl3) spectrum of 5-methoxy durmillone (**242**). 246
Appendix 24C: DEPT-135 NMR (101 MHz, CDCl3) spectrum of 5-methoxy durmillone (**242**). 246
Appendix 24D: ^{1}H-^{1}H COSY spectrum of 5-methoxy durmillone (**242**). 247
Appendix 24E: HSQC correlation of 5-methoxy durmillone (**242**). 247

Appendix 24F: HMBC correlation of 5-methoxy durmillone (**242**). 248
Appendix 25A: ^{1}H NMR (400 MHz, DMSO) spectrum of *trans-resveratr*ol (**243**). 248
Appendix 25B: ^{13}C NMR (101 MHz, DMSO) spectrum of *trans-resveratr*ol (**243**). 249
Appendix 25C: DEPT-135 NMR (101 MHz, DMSO) spectrum of *trans-resveratr*ol (**243**). 249
Appendix 26A: ^{1}H NMR (400 MHz, DMSO) spectrum of tricuspidatol A (**244**). 250
Appendix 26B: ^{13}C NMR (101 MHz, DMSO) spectrum of tricuspidatol A (**244**). 250
Appendix 26C: DEPT-135 NMR (101 MHz, DMSO) spectrum of tricuspidatol A (**244**). 251
Appendix 27A: ^{1}H NMR (400 MHz, Acetone-d_6) spectrum of kaempferol-3-O-α rhamnopyranoside (**245**). 251
Appendix 27B: ^{13}C NMR (101 MHz, Acetone-d6) spectrum of kaempferol-3-O-α rhamnopyranoside (**245**). 252
Appendix 27C: DEPT-135 NMR (101 MHz, Acetone-d6) spectrum of kaempferol-3-O-α rhamnopyranoside (**245**). 252
Appendix 28A: ^{1}H NMR (400 MHz, DMSO) spectrum of kaempferol-3-O-rutinoside (**246**). 253
Appendix 28B: ^{13}C NMR (101 MHz, DMSO) spectrum of kaempferol-3-O-rutinoside (**246**). 253
Appendix 28C: DEPT-135 NMR (101 MHz, DMSO) spectrum of kaempferol-3-O-rutinoside (**246**). 254
Appendix 29A: ^{1}H NMR (400 MHz, CDCl3) spectrum of 3′-(4′′-methoxy phenyl)-3′-oxo-propionyl hexadecanoate (**247**). 254
Appendix 29B: ^{13}C NMR (101 MHz, CDCl3) spectrum of 3′-(4′′-methoxy phenyl)-3′-oxo-propionyl hexadecanoate (**247**). 255
Appendix 29C: DEPT-135 NMR (101 MHz, CDCl3) spectrum of 3′-(4′′-methoxy phenyl)-3′-oxo-propionyl hexadecanoate (**247**). 255
Appendix 30A: IR spectrum of compound **248** 255
Appendix 30B: ^{1}H NMR (400 MHz, DMSO) spectrum of harpagoside (**248**). 256
Appendix 30C: ^{13}C NMR (101 MHz, DMSO) spectrum of harpagoside (**248**). 257
Appendix 30D: DEPT-135 NMR (101 MHz, DMSO) spectrum of harpagoside (**248**). 257
Appendix 31A: IR spectrum of compound **249.** 258
Appendix 31B: ^{1}H NMR (400 MHz, Acetone-d6)spectrum of pulverulentoside I (**249**). 258
Appendix 31C: ^{13}C NMR (101 MHz, Acetone-d6)spectrum of pulverulentoside I (**249**). 259
Appendix 31D: DEPT-135 NMR (101 MHz, Acetone-d6) spectrum of pulverulentoside I (**249**). 259
Appendix 32A: ^{1}H NMR (400 MHz, MeOD)spectrum of scrophuloside B4 (**250**). 260
Appendix 32B: ^{13}C NMR (101 MHz, MeOD)spectrum of scrophuloside B4 (**250**). 260
Appendix 32C: DEPT-135 NMR (101 MHz, MeOD) spectrum of scrophuloside B4 (**250**). 261
Appendix 33A: ^{1}H NMR (400 MHz, MeOD)spectrum of scropolioside A (**251**). 261

Appendix 33B: ^{13}C NMR (101 MHz, MeOD) spectrum of scropolioside A (**251**). 262
Appendix 33C: DEPT-135 NMR (101 MHz, MeOD) spectrum of scropolioside A (**251**). 262
Appendix 34A: ^{1}H NMR (400 MHz, MeOD) spectrum of scropolioside-D2 (**252**). 263
Appendix 34B: ^{13}C NMR (101 MHz, MeOD) spectrum of scropolioside-D2 (**252**). 263
Appendix 34C: DEPT-135 NMR (101 MHz, MeOD) spectrum of scropolioside-D2 (**252**). 264
Appendix 35A: IR spectrum of compound **253.** 264
Appendix 35B: ^{1}H NMR (400 MHz, DMSO) spectrum of harpagide 6-*O*-β-glucoside (**253**). 265
Appendix 35C: ^{13}C NMR (101 MHz, DMSO) spectrum of harpagide 6-*O*-β-glucoside (**253**). 265
Appendix 35D: DEPT-135 NMR (101 MHz, DMSO) spectrum of harpagide 6-*O*-β-glucoside (**253**). 266
Appendix 36A: IR spectrum of compound **230.** 266
Appendix 36B: ^{1}H NMR (400 MHz, DMSO) spectrum of sucrose (**230**). 267
Appendix 36C: ^{13}C NMR (101 MHz, DMSO) spectrum of sucrose (**230**). 267
Appendix 36D: DEPT-135 NMR (101 MHz, DMSO) spectrum of sucrose (**230**). 268
Appendix 37A: ^{1}H NMR (400 MHz, CDCl3) spectrum of 22, 23-dihydrospinasterol acetate (**254**). 268
Appendix 37B: ^{13}C NMR (101 MHz, CDCl3) spectrum of 22, 23-dihydrospinasterol acetate (**254**). 269
Appendix 37C: DEPT-135 NMR (101 MHz, CDCl3) spectrum of 22, 23-dihydrospinasterol acetate (**254**). 269
Appendix 38A: ^{1}H NMR (400 MHz, CDCl3) spectrum of stigmasterol-3-O-*β*-D-glucoside (**255**). 270
Appendix 38B: ^{13}C NMR (101 MHz, CDCl3) spectrum of stigmasterol-3-O-*β*-D-glucoside (**255**). 270
Appendix 38C: DEPT-135 NMR (101 MHz, CDCl3) spectrum of stigmasterol-3-O-*β*-D-glucoside (**255**). 271
Appendix 39A: Chemical composition of the essential oils from bulbs of *C. abyssinicum* (BCA), and aerial parts of *C. abyssinica* (ACA). 271
Appendix 39B: Chemical components (%) of the essential oils from leaves, flowers, and seeds of *C. procera.* 273
Appendix 39C: Chemical compositions of essential oils from *J. schimperiana* roots, and leaves essential oils. 276
Appendix 39D: Chemical compositions of essential oils from leaves, and roots of *V. siniaticum*. 278
Appendix 39E: Chemical compositions of essential oils from seeds, and roots of *L. abyssinica* 280
Appendix 40A: The GC-MS chromatogram of *C. abyssinicum* bulbs (a), and *C. abyssinica* aerial parts (b) essential oils. 282
Appendix 40B: The GC-MS chromatogram of *C. procera* leaves (a), flowers (b), and seeds (c) essential oils. 283

Appendix 40C: The GC-MS chromatogram of *J. schimperiana* roots (a), and leaves (b) essential oils. 285
Appendix 40D: The GC-MS chromatogram of *V. siniaticum* leaves (a), and roots (b) essential oils. 286
Appendix 40E: The GC-MS chromatogram of *L. abyssinica* seeds (a), and roots (b) essential oils. 287
Appendix 41A: Molecular docking results of isolated compounds against *E. coli* Gyrase B (PDB ID 7P2W). 287
Appendix 41B: Molecular docking results of isolated compounds against human myeloperoxidase (PDB ID 1DNU). 289
Appendix 41C: Molecular docking value of isolated compounds against human topoisomerase IIα (PDB ID: 4fm9). 291
Appendix 41D: Molecular docking results of isolated compounds against *S. aureus* Gyrase (PDB ID 2XCT). 292
Appendix 41E: Molecular docking results of isolated compounds against N-Terminal Domain of PqsA in a Complex with 6-Fluoroanthraniloyl-AMP (PDB ID 5OE3). 293

LIST OF ACRONYMS AND ABBREVIATIONS

1D	1-Dimensional
^{1}H-NMR	Proton Nuclear Magnetic Resonance
^{13}C-NMR	Carbon-13 Nuclear Magnetic Resonance
2D	2-Dimensional
ADME	Adsorption, distribution, metabolism and excretion
ANOVA	Analysis of Variance
ATCC	American type cell culture
bro. s	broad singlet
CAM	Complementary and Alternative Medicine
CC	Column Chromatography
d	doublet
DCM	Dichloromethane
dd	doublet of doublet
DEPT-135	Distortionless Enhancement by Polarization Transfer-135
DM	Diabetes Mellitus
DMSO	Dimethyl sulfoxide
DPPH	2,2-diphenyl-1-picryl hydrazyl
EtOAc	Ethyl acetate
FDA	Food and Drug Administration
GC-MS	Gas chromatograph-Mass spectrometry
HMBC	Heteronuclear Multiple Bond Correlation
HSQC	Heteronuclear Single Quantum Correlation
Hz	Hertz
IC_{50}	50% Inhibition Concentration
IDDM	Insulin-dependent diabetes mellitus
IDF	International Diabetes Federation
IR	Infra-Red
m	multiplet
MeOH	Methanol
NIST	National Institute of Standards and Technology
PTLC	Preparative Thin Layer Chromatography
Rf	Retardation factor
s	singlet
SD	Standard Deviation
SEM	Standard Error of Mean
t	triplet
TCM	Traditional China Medicine
TLC	Thin Layer Chromatography
TM	Traditional Medicine
UV-Vis	Ultra Violet -Visible
WHO	World Health Organization

ABSTRACT

Since ancient time, human beings have utilized medicinal plants for a variety of purposes, such as food, flavors, cosmetics, clothing dying, and, most importantly, medicine to treat a wide range of diseases. In these studies, six medicinal plants; *Crinum abyssinicum*, *Calotropis procera*, *Caylusea abyssinica*, *Justicia schimperiana*, *Verbascum sinaiticum*, and *Lagenaria abyssinica* with a variety of traditional uses were selected. The air-dried powdered sample of the plant's material was extracted successively with dichloromethane/methanol (1:1), and methanol by maceration. Fractionation of the extracts was carried out using silica gel column chromatography. Spectroscopic techniques such as ^{1}H-NMR, ^{13}C-NMR, DEPT-135, COSY, HSQC, and HMBC were used to elucidate the structures of isolated compounds. Essential oils were extracted by hydrodistillation method and their chemical analyses were performed by Gas chromatography coupled to mass spectrometry (GC-MS). The disc diffusion method was used to assess antibacterial activity against four bacterial species. Broth dilution method was also used to test antimicrobial activity against a set of microorganisms (bacterial and 3 fungal strains). The radical scavenging activity of the extracts and isolated compounds were evaluated using DPPH method. Antidiabetic potentials of the plant's crude extracts were evaluated by α-amylase inhibition assay. The cytotoxicity effects of crude extracts were evaluated *in vitro* against MCF-7 human breast cancer cell lines by using MTT assay. The *in vitro* anti-*Acanthamoeba* activity of the extracts has been tested against *Acanthamoeba triaugularis* and *castellanii* using micro dilution method. The MDCK cell line and the MTT method were used to examine the extracts' anti-influenza A virus activities. The molecular docking analysis of the isolated compounds was conducted using AutoDock vina 4.2 open-source program. ADMET was predicted by SwissADME and PreADMET property predictions. Silica gel column chromatographic separation of the extracts of six selected medicinal plants afforded thirty-seven known compounds identified by comprehensive analyses of NMR data and comparison with literature data. The class of compounds obtained were identified as fatty acids, fatty acid esters, steroids, ursane-type triterpenoids, flavonoids, stilbenoids and iridoid phenylethanoid glycosides of which 32 compounds were reported herein for the first time from the studied medicinal plants. The essential oils obtained from the bulb of *C. abyssinicum,* leaves, and roots of *J. schimperiana*, leaves, flowers, and seeds of *C. procera*, roots, and seeds of *L. abyssinica,* leaves, roots of *V. siniaticum,* and aerial parts of *C. abyssinica* were analyzed by GC-MS. The GC-MS analysis of essential oils revealed a total of 62, 52, 54, 59, 46, 45, 35, 41, 61, 32, and 41 chemical constituents, representing 100, 99.73, 98.84, 99.45, 99.34, 100, 100, 99.78, 99.8, 100, and 99.78 % of the total oil contents, respectively. The MeOH and CH_2Cl_2/MeOH (1:1) root extract of *C. abyssinicum* had strong activity against *P. aeruginosa* and *S. aureus* with a maximum zone of inhibition of 16.3 ± 0.3 mm and 16.7 ± 1.2 mm at 250 µg/ml, respectively. Methanolic extract of *J. Schimperiana* and *C. abyssinica* had the maximum zone of inhibition of 17.0 ± 0.3 mm and 15.4 ± 0.3 against *E. coli.*, respectively. Among the plants tested, the methanolic extract of *C. abyssinica* (with the highest zone of inhibition of 18.3 ± 0.4 mm against *S. aureus*) was very promising and showed significant inhibition of all tested bacterial pathogens. For *J. schimperiana* extracts, the smallest MIC value was recorded for the dichloromethane: methanol (1:1) extract against *S. aureus,* and *E. faecalis* which was 4.0 mg/mL. The DCM: MeOH (1:1), and MeOH extracts of *V. sinaiticum* roots showed the highest activity against *S. epidermids* with MIC value of 0.25 mg/mL. For isolated compounds, the

highest mean inhibitory value was recorded by **231** (17.7 ± 0.8) followed by **232 (**17.0 ± 1.2**), 87** (14.3 ± 0.5), **97** (13.9 ± 0.2 mm), and **234** (12.7 ± 0.4 mm), against *E. coli* at 500 µg/mL compared with ciprofloxacin (29.7 ± 0.3) with similar concentration. Compound **79** displayed promising activity against *S. aureus* (14.1 ± 1.0 mm) at 500 *µ*g/mL compared with Gentamycin (19.3 ± 0.5 mm). The *S. aureus* and *S. agalactiae* were highly susceptible to compound **246** with a MIC value of 0.25 mg/mL followed by compounds **242,** and **243** with MIC values of 0.5 mg/mL against *S. agalactiae*. The strongest antibacterial effects were demonstrated with *S. epidermidis*, which exhibited a 0.0625 mg/mL MIC for compound **247**, followed by compounds **248, 249**, and **250** against *S. aureus, S. typhimurium*, and *S. epidermidis* with a MIC value of 0.5 mg/mL for each, respectively, from *V. sinaiticum*. The DCM: MeOH (1:1) extract of *C. abyssinicum* (IC_{50} value 12.8 µg/mL) and *C. abyssinica* (IC_{50} value 12.5 µg/mL), MeOH extract of *C. Procera* (IC_{50} value 15.3 µg/mL), *J. Schimperiana* (IC_{50} value 10.8 µg/mL), and *C. abyssinica* (IC_{50} value 12.6 µg/mL) showed good antioxidant potential compared to ascorbic acid (IC_{50} value 3.1 µg/mL), and for isolated compounds, the results showed that, compounds **226** (70.8 ± 0.2, IC50 = 10.20 µg/mL), and **228** (79.6 ± 0.6, IC_{50} = 0.60 µg/mL) showed promising antioxidant potential. In comparison to ascorbic acid (88.1%) at a concentration of 200 g/mL, compounds **97** and **234** reduced the stable DPPH radical by 63.5% and 75.0%, respectively, indicating potential radical scavengers. Better anti-DPPH action was demonstrated by bis(2-ethylheptyl) phthalate (**239**) at a concentration of 200 g/mL with an IC_{50} value of 10.2 g/mL (70.8 ± 0.2). In comparison to ascorbic acid (89.9%, IC_{50} = 1.3), compounds **245** (73.3%), **246** (77.9%), **249** (72.7%, IC_{50} =3.8), **250** (74.8%, IC_{50} = 4.2), **251**(72.8%, IC_{50} =3.6), **252**(73.2%, IC_{50} =3.38), **253** (71.1%, IC_{50} = 4.2), and **248** (70.7%, IC_{50} =4.7), displayed the highest radical scavenging activity. The *in vitro* antidiabetic activity results showed, the methanol roots extracts of *C. abyssinica*, and DCM/MeOH (1:1) leaves extract of *J. schimperiana* exhibited strong α-amylase enzyme inhibition with IC_{50} values of 7.8, and 7.5 mg/mL, respectively, at a concentration of 10.0 mg/mL compared to the positive control acarbose (IC_{50} = 4.4 mg/mL). Of all the studied plants, the DCM/MeOH (1:1) root extract of *C. procera* had the highest cytotoxic effect on the MCF-7 breast cancer cell line with 4.1% viability. The *In vitro* anti-*Acanthamoeba* activity of the extracts showed the dichloromethane: methanol (1:1) root extracts of *V. sinaiticum* showed a good inhibitory activity (% viability < 10) at 2 mg/mL against Acanthamoeba *castellanii* ATCC50739. The study of the antiviral activities of the DCM: MeOH (1:1) leaves extract of *J. schimperiana* displayed more effective at inhibiting A/H1N1/. The results of the molecular docking analysis for compounds revealed minimal binding energies of -5.0 to–8.9, -5.6 to–10.1, -4.3 to -10.8, -5.1 to -11.0, -5.0 to -10.5, -4.5 to -9.9 kcal/mol against DNA gyrase B (PDB ID:7P2W), *S. aureus* Gyrase (PDB ID: 2XCT), human myeloperoxidase (PDB ID: 1DNU), PqsA (PDB ID 5OE3and human topoisomerase IIα (PDB ID: 4fm9), respectively. Of the tested isolated compounds, **226**, **227**, **231**, **238**, **241, 242,** and **243** obeyed Lipinski's rule of five with zero violations. The *in vitro* antibacterial, antioxidant, antidiabetic activity and molecular modeling analysis suggest the potential use of the isolated compounds and crude extracts as medicine which corroborate the traditional uses of the studied plants.

Keywords: *Crinum abyssinicum*, *Calotropis procera*, *Caylusea abyssinica*, *Justicia schimperiana*, *Verbascum sinaiticum*, and *Lagenaria abyssinica*, flavonoids, steroids, iridoids, ursane-type triterpenoids, Inhibition of α-Amylase, Cytotoxicity, anti-a*canthamoeba*, antiviral, antibacterial, antioxidant, ADMET, molecular docking.

CHAPTER ONE

1. INTRODUCTION

1.1. Background

The natural products found in living organisms are a diverse and complex set of chemicals, necessary for survival and adaptation (Phillipson, 2001; Lai *et al*., 2010). Over the past ten years, numerous studies and publications have underscored the significance of natural product derived drugs and potential leads. These encompass various sources including endophytic and epiphytic microbes (Newman & Cragg, 2020), marine drug candidates (Newman & Cragg, 2015), natural product scaffolds (Newman & Cragg, 2016), ACE inhibitors (Newman, 2016), uncultured microbes as a source of natural products (Newman, 2016), antitumor antibody-drug conjugates (Newman & Cragg, 2017), and extremophilic marine fungi (Giddings & Newman, 2019). Natural products have remained an important part of drug discovery and development.

Since ancient times, natural products have been harnessed to alleviate various ailments. Advancements in natural product chemistry have unveiled a plethora of bioactive compounds, including muscarine (**1**), penicillin (**2**), nicotine (**3**), cocaine (**4**), quinine (**5**), morphine (**6**), paclitaxel (**7**) and many others (Figure 1), which have been integral to traditional medicine practices and continue to serve as invaluable resources in drug discovery (Figure 1). In recent years, natural products have played a pivotal role in the development of drugs targeting a diverse range of diseases, including immunosuppressants, anticoagulants, antibiotics, antioxidants, antidiabetics, anti-mutagens, anti-inflammatories, antimicrobials, and anticancer agents (Chin *et al*., 2006; Suffredini *et al*., 2006). Notably, over half of the drugs approved by the FDA trace their origins back to natural products, highlighting their significance in contemporary drug development (Newman *et al*., 2003; Jamil *et al*., 2007).

Herbal medicines are gaining increasing recognition and acceptance worldwide, driven by dissatisfaction with conventional treatments in developed nations and limited access to pharmaceutical drugs in developing regions due to their high costs (Bekele, 2007). Despite this growing interest, only a fraction of medicinal plants have undergone thorough testing for their phytochemical composition and biological activities (Peteros and Mylene, 2010;

Mahesh and Satish, 2008). Thus, there remains vast untapped potential for further exploration and exploitation of natural products in medicine.

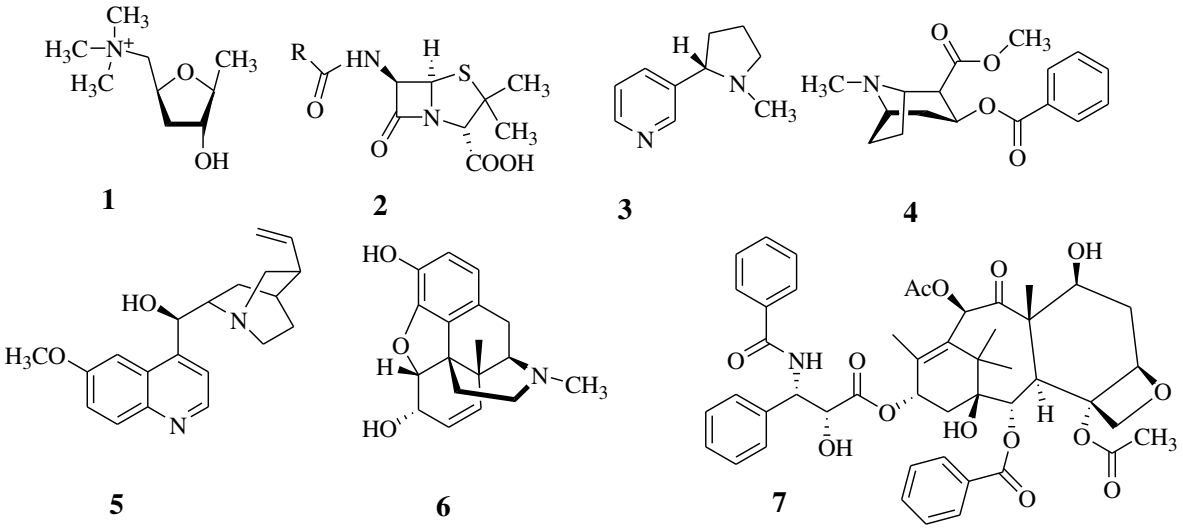

Figure 1: Some natural products isolated from higher plants as clinical agents.

Ethiopia has a rich heritage of traditional medicine, deeply rooted in its ancient history and cultural practices. Drawing upon locally grown plants, animal products, and minerals, this traditional knowledge has been passed down orally through generations, with the exact origins shrouded in the absence of written documentation. The amalgamation of Christian, Islamic, and indigenous beliefs has significantly influenced traditional medicinal practices, as evidenced by the Ge'ez medico-religious texts known as "*Metsafe Fews*" and "*Matsafe Medhanit*" (Asfaw, 2015).

The country's diverse flora comprises approximately 6,500 species of higher plants, with 12% being endemic, reflecting the unique biodiversity of Ethiopia (Tuasha *et al*., 2018). These indigenous plants have demonstrated efficacy in treating a myriad of medical ailments, with an estimated 80% of the population relying on traditional remedies (Yirga, 2010; Birhanu, 2013). Among the commonly utilized plants are *Artemisia* spp., *Boswellia* spp., *Brucea antidysentrica*, *Cinnamomum cassia*, *Commiphora* spp., *Cyperus bulbosus*, *Echinops* spp., *Embelia schimperi*, *Glinus lotoides*, *Hagenia abyssinica*, *Juniperus procera*, *Myrtus communis*, *Ocimum* spp., *Otostegia* spp., *Phytolacca dodecandra*, *Thymus schimperi*, *Moringa stenopetala*, *Stevia rebaudiana*, *Pentas schimperiana*, *Meriandra dianthera*, *Vernonia Amygdalina*, *Justicia Schimperiana*, *Aloe camperi*, *Croton macrostachys*, *Ajuga remota* Benth, *Aloe vera*, *Nigella sativa*, *Otostegia integrifolia*, and

many others. These medicinal plants are often traded alongside spices and food items, reflecting their integral role in local economies and daily life (FAO, 2007; Meresa *et al*., 2017).

In the realm of combating infectious diseases, exploring antimicrobial agents derived from natural products presents a promising avenue. These natural products, sourced from diverse organisms like plants, fungi, marine life, and microorganisms, offer a vast repertoire of bioactive compounds endowed with inherent antimicrobial properties (Newman and Cragg, 2016). Evolving over millennia, these compounds have honed their efficacy against microbial pathogens through intricate biochemical pathways. Numerous studies underscore the invaluable role of natural products in drug discovery, with many clinically significant antimicrobials originating from these sources (Newman and Cragg, 2016; Harvey, Edrada-Ebel, and Quinn, 2015). However, despite their potential, translating antimicrobials derived from natural products into clinical practice encounters various challenges. These include optimizing pharmacokinetic properties, scaling up production, and navigating regulatory hurdles.

Diabetes mellitus is a chronic condition, either acquired or inherited, characterized by insulin deficiency or insensitivity of body organs to produce insulin, or a combination of both (Vadivelan *et al*., 2019). Globally, approximately 537 million adults suffer from diabetes, a number projected to rise to 700 million by 2045. This condition imposes a significant economic burden, with health expenditure totaling USD 966 billion annually and contributing to over 4 million deaths per year (IDF, 2021). Risk factors for diabetes include Multiple lifestyle-related and sociodemographic factors, metabolic and environmental factors, nutritional factors and biological factors such as elevated blood pressure or impaired glucose tolerance. In Ethiopia, studies indicate that 6% of the population has diabetes, with contributing factors including overweight, gestational diabetes, and inadequate nutrition during pregnancy (Bekele *et al*., 2016). Diabetes can be classified into type one diabetes mellitus (T1DM) and type two diabetes mellitus (T2DM), with the latter comprising 90-95% of diabetic cases globally (Anyanwu *et al*., 2019).

Treatment strategies for diabetes may involve medications aimed at reducing postprandial hyperglycemia by inhibiting enzymes responsible for converting complex carbohydrates into absorbable monosaccharides (Nebih *et al*., 2020; Turkan *et al*., 2020). Another approach includes alpha amylase inhibitors, which work by binding polyphenols to the

enzyme through hydrogen bonds, thereby reducing glucose levels (Biçer *et al*., 2020; Altay *et al*., 2019).

Cancer presents a significant challenge in healthcare worldwide, with escalating rates observed in both developing and developed nations (Charoensin, 2014; Arome & Amarachi, 2014; Rahmani-Nezhad *et al*., 2014; Prakash *et al*., 2013). In 2008 alone, there were 7.6 million cancer-related deaths globally, a figure projected to double by 2030 (Arome & Amarachi, 2014). Despite advancements in chemotherapy, the survival rates of cancer patients have seen limited improvement in many countries (Safavi *et al*., 2012). Regrettably, existing cancer treatments are not without limitations, as they are not always 100% effective and can be associated with adverse side effects (Arome & Amarachi, 2014; Rahmani-Nezhad *et al*., 2014; Prakash *et al*., 2013). Hence, there is a pressing need for novel drugs that can combat cancer effectively while circumventing issues such as drug resistance and toxicity associated with current therapies (Rahmani-Nezhad *et al*., 2014). Consequently, considerable attention is being directed towards plants as a natural source to enhance cancer treatment (Adedapo *et al*., 2016; Gordaliza, 2007). Remarkably, approximately 60% of cancer drugs currently in use have been derived from natural products (Adedapo *et al*., 2016).

Natural products and secondary metabolites exhibit various properties that can aid in disease prevention and infection control, including antioxidative, anti-inflammatory, and phytotoxic properties (Abd-ElGawad *et al*., 2020; Assaeed *et al*., 2020; Elshamy *et al*., 2019; Vamanu & Gatea, 2020). Essential oils, integral components of medicinal herbs, also possess a spectrum of bioactivities (Assaeed *et al*., 2020; Abd El-Gawad, 2016; Elshamy *et al*., 2020; Diniz do Nascimento *et al*., 2020). Factors such as altitude, plant age, water availability, and environmental conditions can influence the chemical composition and efficacy of essential oils (Abd-ElGawad *et al*., 2020; Elshamy *et al*., 2019; Amin *et al*., 2019). Given the rampant overuse of antibiotics, there is a growing demand for alternative sources of antimicrobial agents to curb the proliferation of infectious diseases (Esmail, 2016; Cos *et al*., 2006; Spellberg *et al*., 2008).

Natural products have significantly contributed to the discovery of new drugs and innovative disease treatment methods. Among the extensively studied effects of natural substances are their antioxidative properties, crucial for mitigating the damage caused by reactive oxygen species in various illnesses. Computational research methods have

revolutionized the drug discovery process, making it faster and more cost-effective. In recent years, scientists have enhanced the properties of pharmaceuticals by predicting their absorption, distribution, metabolism, excretion, and tolerance within the body (Butina, 2002). This predictive information aids in drug discovery by eliminating compounds that do not meet the "Lipinski rule of 5", thereby streamlining the selection process. Docking studies play a vital role in assessing the binding affinity of lead compounds to receptor targets, facilitating drug design and discovery.

The selection of plants for this study was based on indigenous knowledge and ethnobotanical uses. This study involved the isolation, characterization, and evaluation of biological activity of secondary metabolites derived from six edicinal plants of Ethiopian Flora: *Caylusea abyssinica*, *Justicia schimperiana*, *Calotropis procera*, *Crinum abyssinicum*, *Lagenaria abyssinica*, and *Verbascum sinaiticum*. The study emphasized on *in vitro* antidiabetic, anticancer, anti-Acanthamoeba, antibacterial, and radical scavenging activities of plant extracts and isolated compounds. Furthermore, molecular docking and pharmacokinetic (ADMET) studies, including assessment of drug-likeness based on Lipinski's rule of five, were conducted on isolated compounds to elucidate their binding affinity and interactions, guided by *in vitro* biological results.

1.2. Statement of the problem

The escalating rates of antimicrobial resistance present a significant threat to the efficacy of traditional antibiotics, underscoring the urgent need for alternative antimicrobial agents. Despite the abundance of natural products with antimicrobial properties, there has been limited progress in translating these bioactive compounds into viable clinical treatments, underscoring the importance of systematic screening, isolation, and development processes (Newman and Cragg, 2016). Diabetes mellitus imposes a substantial burden on global health, with conventional treatments often leading to adverse side effects and inadequate control of blood sugar levels in certain patients. While natural products such as medicinal plants and phytochemicals show promise in managing diabetes, the lack of standardized formulations, clinical evidence, and understanding of their mechanisms of action hinders their integration into mainstream diabetes care (Kumar and Narwal, 2013). Despite advancements in cancer treatment modalities like chemotherapy and targeted therapies, many patients continue to face obstacles such as treatment resistance, toxicities, and

disease recurrence. Although natural products have yielded numerous anticancer agents, hurdles like poor bioavailability, limited mechanistic understanding, and inconsistent clinical outcomes impede their effective utilization as cancer treatments. Consequently, further research and development efforts are imperative to address these challenges (Kinghorn et al., 2009).

The persistent threat of viral pandemics, the emergence of drug-resistant strains, and the limited effectiveness of current antiviral therapies underscore the necessity for new antiviral medications. Although natural products have great potential in fighting viral infections, obstacles such as identifying potent and specific compounds, understanding their mechanisms of action, and improving their pharmacokinetic properties create barriers to developing antiviral drugs based on natural products (Chattopadhyay and Khan, 2017). These statements emphasize the urgent challenges and research gaps in utilizing natural products for the treatment of microbial, diabetic, cancer, and antiviral diseases, providing valuable guidance for future research and drug development efforts. More extensive research into the isolation of active compounds, efficacy, mechanism of action, and toxicity of medicinal plants is warranted. Addressing this research gap, investigating the biological properties and chemical constituents of these specific medicinal plants is essential to fill this knowledge void.

1.3. Justification of the study

In Ethiopia, *Crinum abyssinicum*, *Calotropis procera*, *Caylusea abyssinica*, *Justicia schimperiana*, *Verbascum sinaiticum*, and *Lagenaria abyssinica* have long been utilized for treating various issues including diabetes, cancer, and other illnesses (Regassa, 2013; Firaol *et al*., 2013; Yineger *et al*., 2008; Kloos *et al*., 2014; Mekuanent *et al*., 2016; Asnakech *et al*., 2019; Abebe *et al*., 2003; Tesfaye *et al*., 2016). Despite some research conducted on these plants, their bioactive compounds still haven't been fully characterized. Essential oils from the aerial parts of *Caylusea abyssinica*, roots of *Justicia schimperiana,* seeds, and roots of *Lagenaria abyssinica*, flowers of *Calotropis procera*, leaves, and roots of *Verbascum sinaiticum* have not been reported. Therefore, it is imperative to ascertain the chemical constituents, essential oils composition, and biological activities of these plants. Motivated by their extensive traditional uses and the lack of comprehensive prior phytochemical investigation and biological evaluation, this study aimed to bridge this gap

by isolating, characterizing, and assessing the biological activity of extracts and secondary metabolites from these Ethiopian medicinal plants. This endeavor seeks to enhance the scientific understanding of these plants while also exploring their potential as sources of new drug candidates.

1.4. Objectives

1.4.1. General objective

- The overall objective of this study was to extract, isolate, and characterize phytochemicals from selected Ethiopian medicinal plants, and evaluate the in *vitro* antidiabetic, anticancer, antimicrobial, antiviral, anti-*acanthamoeba*, and antioxidant activities of the extracts, and isolated compounds, and computational studies of the isolated compounds.

1.4.2. Specific objectives

- To successively extract the roots of *C. procera, C. abyssinicum, C. abyssinica, J. schimperiana, V. sinaiticum*, and *L. abyssinica* using DCM/MeOH (1:1) and methanol.
- To extract essential oils from the bulb of *C. abyssinicum*; leaves, and roots of *J. schimperiana*; leaves, flowers, and seeds of *C. procera*; roots, and seeds of *L. abyssinica*; leaves, and roots of *V. siniaticum*; and aerial parts of *C. abyssinica* using hydrodistillation.
- To isolate secondary metabolites from the extracts of *C. procera, C. abyssinicum, C. abyssinica, J. schimperiana, V. sinaiticum*, and *L. abyssinica* using silica gel column chromatography.
- To elucidate the structures of the isolated compounds from these six plants using different spectroscopic techniques; ^{1}H NMR, ^{13}CNMR, DEPT-135, COSY, HSQC, HMBC, and comparison with literature reports.
- To identify the chemical composition of essential oils by using GC-MS instrument.
- To evaluate *in vitro* antibacterial activity of the extracts and isolated compounds of *C. procera, C. abyssinicum,* and *C. abyssinica,* against Gram-positive bacteria (*Staphylococcus aureus,* and *Streptococcus pyogenes*) and Gram-negative bacteria (*Pseudomonas aeruginosa*, and *Escherichia coli*) using the disc diffusion method.

- To evaluate the *in vitro* antimicrobial activity of essential oil extracted from all selected plants, and crude extract, isolated compounds of *J. schimperiana,* and *V. sinaiticum* against 6 bacterial strains (*Staphylococcus aureus, Streptococcus agalactiae, Enterococcus faecalis, Escherichia coli, Pseudomonas aeruginosa, Klebsiella pneumoniae*) and 3 fungal strains (*Trichophyton mentagrophytes, Trichophyton rubrum*, *Candida albicans*) by using broth dilution method.
- To evaluate the radical scavenging activity of extracts and isolated compounds using DPPH assay.
- To establish the *in vitro* α-amylase inhibitory assay of the extracts.
- To determine the cytotoxicity of the extracts using MTT assay against MCF-7 breast cancer cell lines.
- To evaluate the *in vitro* anti-*acanthamoeba* activity of the extracts against *Acanthamoeba triaugularis* and *castellanii*.
- To conduct *in silico* molecular docking analysis for compounds that showed promising *in vitro* activity using AutoDock vina version 4.2 software.
- To conduct drug-likeness, ADME predictions and toxicity profile of the isolated compounds using SwissADME, PreADMET, and ProTox-II online servers.

1.5. Significance of the study

The present study in general may have the following significance:

- Provide information on the chemical constituents of the roots of the plants.
- Provide information on essential oils compositions of the plants.
- Provide antibacterial information of the plant extracts and isolated compounds against selected microbial strains to provide scientific support to traditional use of the plant to treat infectious diseases.
- Provide information on antioxidant activities of the plants extract and isolated compounds.
- Provide the *in vitro* α-amylase inhibitory assay information of crude extracts to contribute scientific support to traditional uses of the plants to treat diabetic diseases.
- Provide cytotoxicity information of crude extracts against MCF-7 breast cancer cell lines to provide scientific support to traditional uses of the plants to treat cancer diseases.

- Provide the *in vitro* anti-*Acanthamoeba* activity of the extracts against *Acanthamoeba triaugularis* and *castellanii*.
- Provide information on molecular docking analysis to have better understanding of the molecular mechanisms of interaction between the compounds with promising antibacterial, antioxidant activity and selected protein domains.
- Provide information on drug-likeness, ADME predictions and toxicity profile of the isolated compounds to understand the reason for their interaction and their drug properties.
- Providing scientific evidence to support the claimed ethnomedicinal uses of the selected plant species.
- The information gathered may be used to increase awareness of people on the role of the traditional uses of these plants' species.
- Besides, it could give valuable information to the public and also serves as baseline data for researchers engaged in search of selected medicinal plant species.

CHAPTER TWO

2. LITERATURE REVIEW

2.1. Review of studied medicinal plants

In the present review of the literature, the botanical description, geographic distribution, ethnobotanical uses, phytochemistry, and biological activities for the studied plants: *Crinum abyssinicum, Calotropis procera, Caylusea abyssinica, Justicia schimperiana, Verbascum sinaiticum*, and *Lagenaria abyssinica* were included.

2.2. Botanical description, and geographical distribution of the studied medicinal plants

2.2.1. *Crinum abyssinicum*

The genus *Crinum*, Amaryllidaceae family, encompasses close to 180 species distributed across Africa, America, southern Asia, and Australia (Lawal and Dangoggo, 2014). Among these, four species i.e. *C. abyssinicum*, *C. bambusetum*, *C. macowanii*, and *C. ornatum* are available in Ethiopia (Nordal and Sebsebe, 2010), with *C. abyssinicum* and *C. bambusetum* being endemic to the region (Nordal and Sebsebe, 2010). With a rich diversity of nearly 1,600 species spanning approximately 80 genera, *Crinum* ranks among the most plentiful bulbous flowering plants, characterized by underground stems and straplike leaves (Bastida et al., 2006). Despite this wide array, *Crinum* species are predominantly concentrated in three primary regions: India, South America, and South Africa, along with the Mediterranean basin (Bastida et al., 2006). The visually appealing flowers typically feature three or six petals and produce either dry capsules or fleshy berry fruits. Many *Crinum* species are cultivated as garden ornamentals, while others serve as vital food crops (Bastida *et al*., 2006). In Ethiopia, *C. abyssinicum* (depicted in Figure 2) is known by various names such as shinkurta/bokolo Werabessa/Murquffaa/Chopi in Afan Oromo, Yejib Shinkurt in Amharic, and Galadiweese in Sidamic (Abebe *et al*., 2003).

(a) (b)

Figure 2: Aerial part (a) and bulb (b) of *C. abyssinicum* (Illubabor, Oromia, Picture by Melaku Tegegn, November, 2021).

2.2.2. *Calotropis procera*

Calotropis procera, a perennial evergreen shrub belonging to the Asclepiadaceae family, is characterized by its softwood and toxic properties, making it widely considered a weed. With a distribution spanning Asia, Africa, and America, this species is part of a larger group encompassing 320 genera and approximately 2,000 species (Ramos *et al*., 2006). *C. procera* (depicted in Figure 3) thrives in arid and semi-arid climates, demonstrating remarkable resilience to minimal annual rainfall (as low as 150 mm) and enduring dry seasons of up to 10 months. Typically, the mean annual monthly temperatures in its habitat range from 20 to 30°C, with no tolerance for frost. The species exhibits adaptability to various soil types, including alkaline and saline soils, although it prefers well-draining sandy soils. Its altitudinal range extends from exposed coastal sites to medium elevations, reaching up to 1300 m. In Ethiopia, it is recognized by local names such as Tobiaw in Amharic, Qimbo in Afan Oromo, Ghinde'a in Tigregna, or Galaqto among the Afar people, reflecting its widespread distribution across Asia, Africa, and America (Seifu, *et al*., 2006).

Figure 3: Aerial part of *C. procera* (Adama, Oromia, Picture by Getachew Tegegn, August 2020).

2.2.3. *Caylusea abyssinica*

Caylusea abyssinica (Fresen) (Figure 4) is a member of the Resedaceae family which comprises herbaceous dicotyledonous plants, encompassing approximately 107 recognized species across 8 to 12 genera (Hristenhusz *et al*., 2016). This plant is characterized by an erect herbaceous habit, reaching heights of up to 1.5 m, featuring a slightly woody taproot and a stem devoid of hairs (glabrous). Its habitat predominantly consists of open grasslands, fields, roadsides, and rocky areas situated at altitudes ranging from 1500 to 2750 m above sea level. Widely distributed across the Mediterranean region, as well as Northern and Eastern Africa, *C. abyssinica* is abundant in countries such as Sudan, Ethiopia, Kenya, Uganda, Rwanda, Burundi, Tanzania, and Malawi (Mwai *et al*., 2004; Grubben and Denton, 2004). Locally, it is referred to as "Reenci" or "Illancoo" in Afan Oromo (Kebebew, 2017). This plant serves both culinary and medicinal purposes, contributing to its significance in various communities across the Mediterranean region, and Northern and Eastern Africa (Hoareau and Edgar, 1999; Kebebew, 2017).

(a) (b)

Figure 4: Aerial part (a) and roots (b) of *C. abyssinica* (Illubabor, Oromia, Picture by Melaku Tegegn, November, 2021).

2.2.4. *Justicia schimperiana*

Justicia schimperiana (Figure 5), an erect leafy shrub belonging to the Acanthaceae family, typically reaches heights of 4-5 m, often extensively branched from the base, with individual stems measuring 2-3 m high. Characterized by brittle stems, this plant features simple, opposite leaves that are long oval, approximately 13 x 4 cm in size, with pointed tips and short stalks. Its flowers are inconspicuous and appear in terminal heads on long stalks, protruding prominently above the foliage. Each small flower is enclosed within a green-yellow leafy bract, about 1.5 cm long, with a clear membranous edge. The flowers themselves are white or yellow-white, tubular, up to 3 cm long, and two-lipped, often

exhibiting dark purple throat or lines on the lip. The plant is commonly found in the dry and moist "Weyna Dega" and moist "Dega" agro-climatic zones of Ethiopia. It thrives in moist montane forests, particularly near streams and rivers, as well as in evergreen scrub on hill slopes, forest clearings, coffee plantations, waste ground, and is also frequently planted as hedges around homesteads (Dagne, 2009). In Ethiopia, it is known locally as "Dhumuugaa" in Afan Oromo and "Sensel" or "Smiza" in Amharic.

(a) (b)

Figure 5: Aerial part (a) and root (b) of *J. schimperiana* (Illubabor, Oromia, Picture by Melaku Tegegn, November, 2021).

2.2.5. *Verbascum sinaiticum*

Verbascum sinaiticum is a biennial plant species in the family Scrophulariaceae. It is commonly found in eastern Africa and the Arabian Peninsula. The Scrophulariaceae family is cosmopolitan, consisting of 300 genera and 5400-5500 species (Edwards, 1976; Mahmoud *et al*., 2007). *V. sinaiticum* Benth (Figure 6) is an erect herb up to 2 m tall that flowers perennially. It grows in a wide range of geographic areas in Ethiopia and is commonly known by various local names, including "Ye Ahya joro", and "Yeferes zeng" in Amharic, "Gurra harree", and "Abokena" in Afan Oromo (Yineger *et al*., 2007), "Tirnake", "Handega", "Kunama Luta" in Tigrigna. It can be found in Africa around the Mediterranean region (Chekole, 2017).

(a) (b)

Figure 6: Leaves (a) and roots (b) of *V. sinaiticum* (Arsi, Oromia, Picture by Yalew Amare, November, 2022).

2.2.6. *Lagenaria abyssinica*

Lagenaria is among the genera in the family Cucurbitaceae. Six species belong to the genus *Lagenaria*, all of which may be found in Africa: *Lagenaria abyssinica, Lagenaria breviflora, Lagenaria guineensis, Lagenaria rufa, Lagenaria siceraria,* and *Lagenaria sphaerica*. *Lagenaria abyssinica* (Hook. f) Jeffrey (Figure 7) is a climbing vine and a species of squash plant, covered with spines resembling hair (Arua *et al.,* 2010). It extends from Asia to Africa, and its fruit is used to make bottles and instruments. The genus is well known for its ornamental uses (Morimoto *et al*., 2004). In Ethiopia, it is known as "Buqe Setana" in Afan Oromo or "Yesetan Kil" in Amharic.

(a) (b)

Figure 7: Aerial part (a) and root (b) of *L. abyssinica* (Illubabor, Oromia, Picture by Melaku Tegegn, November, 2021).

2.3. Ethnobotanical uses

2.3.1. *Crinum abyssinicum*

Various species of *Crinum* are traditionally used for the treatment of a diverse range of ailments. They are also reported to exhibit antibacterial, antifungal, antiviral, antiparasitic,

antioxidant, anti-inflammatory, acetylcholinesterase (AChE) inhibition and anticancer activities (Nair and van Staden, 2013). The fresh root *C. abyssinicum* or dried prepared by Concocted, crushed, mixed with water or butter that applied topically or oral. As a traditional medicinal plant, in Ethiopia, *Crinum* species have been reported to be used in various health care systems for the treatment of a variety of diseases such as hypertension and diabetes (Regassa, 2013), animals' internal parasites (Firaol *et al*., 2013), hepatitis B treatment, skin infection (Yineger *et al*., 2008), rheumatoid arthritis and evil spirits (Kloos *et al*., 2014), snake bite (Mekuanent *et al*., 2016), anticancer, asthma, colds, malarial (Asnakech *et al*., 2019), wound, chancroid, hemorrhage, and some forms of tumor (Teklehaymanot T, and Giday M, 2007). Bulbs of *Crinum* species are used to treat several diseases, like antitumor, anti-coughs and colds, immune-stimulating, analgesic, antiviral, anti-malarial, antibacterial, antifungal activities, etc. (Adesanya *et al*., 1992). In Ethiopia, it is reported that, the bulb extract of *C. abyssinicum*, possessed significant antiproliferative activity (Besufekad *et al*., 2020) (Table 1) but, no scientific report could be found in the literature concerning the antidiabetic and antimicrobial effects of the plant. Therefore, it is considered worthy to conduct scientific experiments to prove whether extracts or isolated compounds of the plant have the potential to elicit beneficial pharmacological activities.

2.3.2. *Calotropis procera*

Traditionally, *Calotropis* is used alone or with other medicines (Pathyusha, 2012) to treat common disease such as fever, rheumatism, indigestion, cold, eczema, diarrhea, for the treatment of boils, to remove thorn from body and for the treatment of jaundice. The root was used for the treatment of eczema, leprosy, elephantiasis, asthma, cough, rheumatism, diarrhea and dysentery (Abhishek *et al*., 2010). The plant is poisonous can lead to blindness if its juice is put in to the eyes. The milky exudates from the plant are a corrosive. It is said to have mercury-like effects on the human body and is sometimes referred as vegetable mercury. Moreover, in traditional folk medicine, the plant has been employed as an antifungal and antipyretic agent (Shrivastava *et al*., 2013). In Ethiopia, the latex of *Calotropis procera (*Asclepiadaceae) is among the herbal drugs used in livestock diseases. The peculiar character for this herbal drug is its use for prevention purpose. One healer recommended the drug for preventing blackleg. In a similar ethnobotanical

study, it was reported that the plant is used for the treatment of blackleg by "Zay" people (Giday & Teklehaymanot, 2013) (Table 1).

2.3.3. *Caylusea abyssinica*

The leaves of *Caylusea abyssinica* have been used in the treatment of DM in Ethiopian folk medicine without any scientific proof for safety and efficacy (Abebe *et al*., 2003). The report indicated that, in Tanzania and Ethiopia, its leaves and stems are eaten alone or as vegetables (Martin-Bravo *et al*., 2007). The plant is also known for its medicinal use by people living in areas where it is growing. It is used to treat stomachache, skin diseases diabetes mellitus and amoebiasis (Etana, 2010; Abebe *et al*., 2003; Megersa, 2010). Similarly, its roots are used to treat abdominal pain impotency and Scabies diarrhea and expel intestinal parasites in humans (Tolossa *et al*., 2013; Etana, 2007; Mesfin *et al*., 2009). In Ethiopia, the plant is traditionally used to treat internal diseases, fever, shivering and skin diseases of domestic animals (Tesfaye and Demissew, 2009) (Table 1).

2.3.4. *Justicia schimperiana*

It is locally utilized to treat scabies, fever, asthma, other inflammatory conditions, excessive pellagra, constipation, stomachache, diarrhea, burning, skin lesion, toothache, malaria, gonorrhea, and rabies (Tariku, 2008; Tolera *et al*., 2017; Yirga and Zerabruk, 2012). The leaf macerate of *J. schimperiana* is asserted to have antidiabetic (Tesfaye *et al*., 2016), antimicrobial (Tedila *et al*., 2019; Melaku, 2017), antimalarial (Abdela *et al.*, 2014), antidiarrheal (Mekonnen *et al*., 2018), antioxidant, and hepatoprotective activities (Umer *et al*., 2010) (Table 1).

2.3.5. *Verbascum sinaiticum*

Traditionally, it is used for wound treatment, stomachache (Teklehaymanot *et al*., 2009), viral infection, cancer (Teklehaymanot, 2007), sunstroke fever, abdominal colic, diarrhea, hemorrhage, anthrax (Weldegerima *et al*., 2008), hepatitis (Yineger *et al*., 2007). In Ethiopian, the root of the plant is used for tumors (Abebe, 2016), rheumatic pain, wound healing, ophthalmic diseases, mental illness, amnesia, tapeworm, syphilis, gonorrhea, relapsing fever, elephantiasis, cold and chest diseases (Gondal *et al*., 2020; Lalrinzuali *et al*., 2016; Yeabyo *et al*., 2018). People also chew the root for toothache, crush, and powder it, and cream it with butter on the affected part for wound healing. They also take it orally

or nasally with water for snakebite, leech infection, and lymphadenitis (Teklay *et al*., 2013; Enyew *et al*., 2014; Megersa *et al*., 2019) (Table 1).

2.3.6. *Lagenaria abyssinica*

Traditionally, the fruits, leaves, stems, seeds, flowers, and oil of the genus *Lagenaria* have been used to treat piles, diabetes, ulcers, colitis, insanity, and other skin disorders, as well as for baldness (Kirtikar and Basu ,2005; Rahman, 2003; Duke *et al*., 1985). In Ethiopia, *Lagenaria abyssinica*, preparations made from powdered flower dispersed in water is used in traditional medicine for treating diabetic mellitus and rabies. The botanical and ethno-botanical information of the studied plants discussed above can be summarized in (Table 1).

Table 1: Ethno-botanical description of studied plants.

Scientific name	Family	Local name	Parts used	Method of preparation	Traditional medicinal Uses	Ref
Crinum abyssinicum	Amaryllidaceae	*Shinkurta/bokolo werabessa* or Murquffaa or Chopi (O) Galadiweese (S), Yejib shinkurt (A)	RT	Fresh or dried is Concocted, crushed, mixed with water	Hemorrhage Hepatitis B	Regassa, 2013
Calotropis procera	Asclepiadaceae	Qinbo (O) or Tobiaw (A) or Galaqto (Af) and Ghinde'a (T)	Bl	Not specified	Antitumor, anti-coughs and colds, immune-stimulating, analgesic, antiviral, anti-malarial, antibacterial, antifungal activities,	Adesanya *et al*., 1992
Caylusea absyssinica	Resedaceae	Reenci (O)	Bl	Inhale smoke	Rheumatoid arthritis, evil sprits	Kloos *et al*., 2014
Justicia schimperiana	Acanthaceae	Sensel or Smiza (A) or Dhumuugaa (O)	RT, Bl	Crashed and applied on the affected part	Snake bite	Mekuanent *et al*., 2016
			ST tip (fresh)	The liquid from the shoot tip is squeezed, mixed with water, and drunk	Hypertension, diabetes	Regassa, R., 2013
Verbascum sinaiticum	Scrophulariaceae	*Ye Ahya joro,in Amharic; Gurra harree, Abokena in Afan Oromo*	RT	Chewed Crushed, powdered and creamed on affected part with butter Taken with water	For tooth ache For wound healing For snake bite	(Teklay *et al*., 2013; Enyew *et al*., 2014; Megersa *et al*., 2019).
Lagenaria abyssinica	Cucurbitaceae	Buqe setena (O)	LF	Powder mixed with hyena feces and latex	Anticancer	Teklehaym, 2009

O: Afan Oromo; A: Amharic; T: Tigregna; Af; Afar; S; Sidama; LF; Leaf: RT; Root: FR; Flower; Bl; Bulb; ST; Shoot; Ref: Reference.

2.4. Phytochemistry and biological activities informations

2.4.1. *Crinum abyssinicum*

Crinum species have been subjected to extensive chemical and biological investigations due to their richness in pharmacologically active principles, especially alkaloids whereas the non-alkaloidal constituents received much less attention (Wildman, 1960). A large number of alkaloids and non-alkaloids compounds have been reported from different *Crinum* species (Refaat *et al*., 2012; 2013). Crinine, lycorine and tazettine types are the most common groups among the isolated alkaloids, while montanine-type has not yet been found in *Crinum* species (Ghosal *et al*., 1985). In addition to these common types of Amaryllidaceae alkaloids, *Crinums* yielded other types that are not common in the family like Augustamine (Ali *et al*., 1983; Ramadan *et al*., 1986; Machocho *et al*., 2004), β-carboline (Ramadan *et al*., 1986), Phenanthridine- (Ramadan *et al*., 1986; Razafimbelo *et al*., 1996), *Sceletium*- (Döpke, 1981), Ismine (Razafimbelo *et al*., 1996; Ghosal, 1981; Highet, 1961) and Clivimine (Ghosal, 1981) type alkaloids. The non-alkaloidal constituents isolated so far were represented by a number of flavonoids, chromones, coumarins, terpenoids, steroids, phenolics, simple glycosides, and long chain hydrocarbons (Takagi and Yamaki, 1977). In Ethiopia, methanol extract of *C. abyssinicum* bulbs yielded two compounds, 6-hydroxycrinamine and lycorine (Besufekad *et al*., 2020). The phytochemical analyses revealed the presence of alkaloids, flavonoids, saponins, tannins and phenols in *Crinum abyssinicum* (Besufekad *et al*., 2020). Pharmacologically the species have been used to cure ailments and diseases throughout the world and some of the most noted effects are analgesic, anticholinergic, antitumor antiviral and Alzheimer's (Fennell and Van Staden, 2001; Jäger *et al*., 2004). The list of compounds reported from different *Crinum* species along with their compound class, plant source, plant part and literature references are depicted in Table 2.

Table 2: Compounds organized by compound class from different *Crinum* species.

Compound class	Compound name	Str. No	Plant source	Plant parts	Ref
Alkaloids	Crijaponine A	**8**	*C. asiaticum L.*	Fr,RZ	Yuta *et al*., 2019
	Crijaponine B	**9**	*C. asiaticum L.*	Fr,RZ	Yuta *et al*., 2019
	6-Hydroxycrinamine	**10**	*C. abyscinicum*	B	Besufekad *et al*., 2020
	Lycorine	**11**	*C. abyscinicum*	B	Besufekad *et al*., 2020
	Crinumlatines A	**12**	*C. latifolium*	B	Tian *et al*., 2020
	Crinumlatines B	**13**	*C. latifolium*	B	Tian *et al*., 2020
	Crinumlatines C	**14**	*C. latifolium*	B	Tian *et al*., 2020
	11-*O*-acetylambelline	**15**	*C. latifolium*	B	Ghosal *et al*., 1985
	11-*O*-acetyl-1,2-β-epoxyambelline	**16**	*C. latifolium*	B	Ghosal *et al*., 1985
	1-*O*-Acetyl-bulbisine	**17**	*C. asiaticum var. sinicum*	L	Chen *et al*., 2011
	(-)-2-Epilycorine	**18**	*C. latifolium Linn.*	F. ST	Ghosal *et al*., 1981
	Hippamine	**19**	*C. bulbispermum Milne.*	B	Abou-Ela *et al*., 2004
	Lycorine-1-*O*-β-D-glucoside	**20**	*C. asiaticum L.*	RT	Ghosal *et al*., 1985
	Lycorine-1,2-*O*-β-Ddiglucoside	**21**	*C. asiaticum L.*	Fr	Ghosal, S. *et al*., 1990
	Lycoriside	**22**	*C. asiaticum L.*	L, Fr, RT	Ghosal *et al*., 1985
	(–)-Palmilycorine	**23**	*C. asiaticum L.*	L, Fr, RT	Ghosal *et al*., 1985
	Criasbetaine	**24**	*C. asiaticum L.*	Fr	Ghosal *et al*., 1990
	Criasiaticidine A	**25**	*C. asiaticum var. japonicum*	B	Min *et al*., 2001
	4,5-Dehydro-anhydrolycorine	**26**	*C. latifolium Linn.*	F, ST	Ghosal *et al*., 1989
	9-*O*-Demethyl-pluviine	**27**	*C. stuhlamanii Baker*	B	Machocho *et al*., 1998
	Galanthine	**28**	*C. amabile Donn.*	B	Murav'eva and Popova, 1982
			C. defixum Ker.	B	Boit and Ehmke, 1957
			C. moorei Hook. F.	B	Kintsurashvili, 2006
	Methylpseudolycorine	**29**	*C. moorei Hook F.* *C. powellii Hort.*	B	Döpke, 1962
	(-)-Pseudolycorine	**30**	*C. asiaticum L.*	---	Ghosal, 1981
	Pseudolycorine-1-*O*-β-Dglucoside	**31**	*C. asiaticum*	---	Ghosal, 1981
	8-*O*-Demethyl-vasconine	**32**	*C. kirkii Baker*	B	Bastida *et al*., 1995
	2-Epipancrassidine	**33**	*C. latifolium Linn.*	F, ST	Ghosal *et al*., 1989
	Hippacine	**34**	*C. bulbispermum Milne.*	B	Ramadan *et al*., 2000

	Hippadine (pratorine)	**35**	*C. purpurascens*	---	Nkanwen *et al*., 2009
	8-Hydroxylycorine-7-one	**36**	*C. bulbispermum Milne.*	B	Abou-Ela *et al*., 2004
	Kalbretorine	**37**	*C. asiaticum L.*		Ghosal, 1985
			C. augustum Rox.	---	
	(+)-Kirkine	**38**	*C. kirkii Baker*	B	Machocho *et al*., 2004
			C. stuhlamanii Baker	B	
	Mooreine	**39**	*C. moorei Hook F.*	WP	Elgorashi *et al*., 2001
	Narcissidine	**40**	*C. powellii Hort.*	B	Boit and Döpke, 1959
			C. pratense		
	Oxoassoanine	**41**	*C. latifolium Linn.*	L	Tram *et al*., 2002
	Pratorimine	**42**	*C. 21mericanum L.*	B	Ali, A.A. *Et al*., 1986
			C. asiaticum L	B	Mohamed, 2000
	Pratorinine	**43**	*C. augustum Rox.*	L, B	Refaat *et al*., 2009
			C. kunthianum Roem.	L	Ramirez *et al*., 2001
	Pratosine	**44**	*C. latifolium Linn*	---	Ghosal, S., 1983
	Ungeremine (lycobetaine)	**45**	*C. asiaticum L.*	Fr	Yuta *et al*., 2019
	Zephyranthine	**46**	*C. kirkii Baker*	B	Machocho *et al*., 2004
	Zephyranthine-1, 2-*O*-diacetyl	**47**	*C. kirkii Baker*	B	Machocho *et al*., 2004
	3-*O*-Acetylsanguinine	**48**	*C. kirkii.*	B	Machocho, K., 2004
	(Acetyl-*O* demethylgalanthamine)				
	Epigalanthamine	**49**	*C. asiaticum L.*	B	Kobayashi, 1984
	Epinorgalanthamine	**50**	*C. asiaticum L.*	B	Kim, 2006
	Sanguinine (*O*-demethylgalanthamine)	**51**	*C. kirkii.*	B	Machocho *et al*., 2004
	Isocraugsodine	**52**	*C. asiaticum*	F	Ghosal *et al*., 1988
	Cherylline	**53**	*C. asiaticum L.*	B	Kobayashi *et al*., 1984
Flavonoids	4', 7-dihydroxy-flavan	**54**	*C. latifolium Linn*	L	Nam *et al*., 2004
	4', 7-dihydroxy-3'-methoxy-flavan	**55**	*C. latifolium Linn*	L	Nam *et al*., 2004
	5,6,3'-trihydroxy-7,8,4'-trimethoxy-flavone	**56**	*C. latifolium Linn*	L	Nam *et al*., 2004
	4-hydroxy-7-methoxyflavan	**57**	*C.asiaticumvar. japonicum*	B	Min *et al*., 2001
	7-hydroxyflavanone	**58**	*C.asiaticumvar.sinicum*	B	Min *et al*., 2001
Chromes	Eugenin (5-hydroxy-7-methoxy-2-methylchromone	**59**	*C. moorei Hook F.*	B	Kamel, 1996

	Noreugenin (5,7-dihydroxy-2-methyl-chromone	**60**	*C. moorei Hook F.*	B	Kamel, 1996
	5,7-dihydroxy-6-methoxy-2,8-dimethyl-chromone	**61**	*C. moorei Hook F.*	B	Kamel, 1996
Terpenoids	Cycloart-24-en-3-ol	**62**	*C.asiaticum var. japonicum Bak.*	B	Takagi and Yamaki, 1977
	Cyclolaudenol	**63**	*C.asiaticum var. japonicum Bak.*	B	Takagi and Yamaki, 1977
	31-norcyclolaudenol	**64**	*C.asiaticum var. japonicum Bak.*	B	Takagi and Yamaki, 1977
	Asparthenin	**65**	*C.ensifolium*	B	Khoi *et al*., 2011
	Sitosterol-α D-Glucopyranoside	**66**	*C.purpurascens*	L	Nkanwen *et al*., 2009
Fatty acids and polyketides	S-hydroxyhexacosan-9-one	**67**	*C.auugusrum*	B	ElHafiz *et al*., 1991
	5-hydroxyoctacosan-9-one	**68**	*C.auugusrum*	B	ElHafiz *et al*., 1991
	S-hydroxytriacontan-9-one	**69**	*C.auugusrum*	B	ElHafiz *et al*., 1991
	n-hexadecanoic acid	**70**	*C.asiaticum*	L	Indradevi *et al*., 2012
	9, 12, 15-octadecatrienoic acid	**71**	*C.asiaticum*	L	Indradevi *et al*., 2012
	9,12-octadecadienoic acid	**72**	*C.asiaticum*	L	Indradevi *et al*., 2012
Glycoside	Amabiloside (3-hydroxy-4-*O*-D-glucopyranosylbenzaldehyde)	**73**	*C.amabile*	B	Likhitwitayawuid *et al*., 1993

Ba: Bark, WP: Whole plant, Se: Seed, F: Flower, Fr: Fruit, ST: Stem, L: Leaf, RT: Root, RZ: Rhizome, Str No: structure number; cpd: Ref: Reference.

The structures of compounds reported from the *Crinum* species are given below.

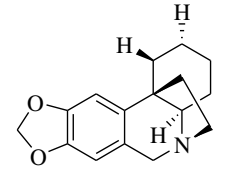

8

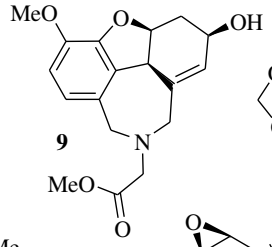

9

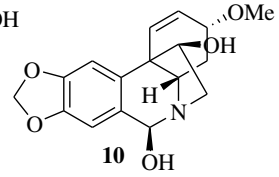

10

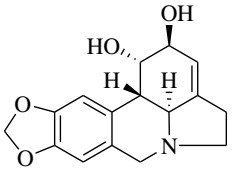

11

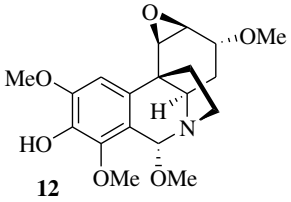

12

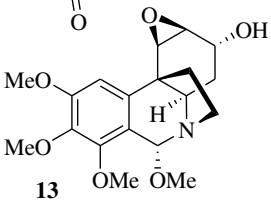

13

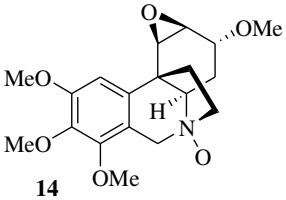

14

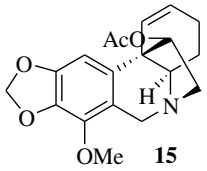

15

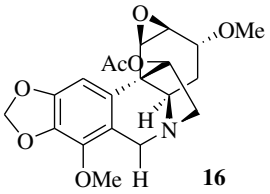

16

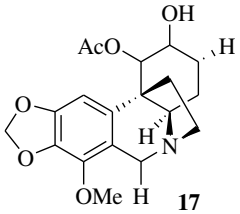

17

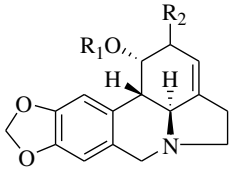

18. R_1 = H, R_2 = αOH
19. R_1 = H, R_2 =βOMe
20. R_1 = H, R_2 =βOH
21. R_1 = Glc., R_2 =β -O-Glc.
22. R_1 = Glc. (6'-palmitoyl), R_2 =βOH
23. R_1 = palmitoyl, R_2 = βOH

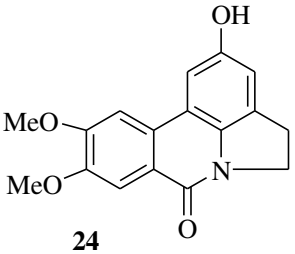

24

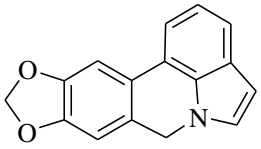

25

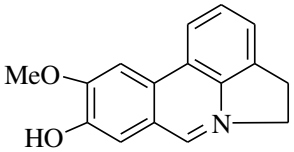

26

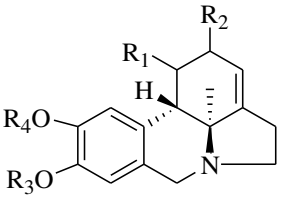

27. R_1 =α OH R_2 = H. R_3 = H, R_4 = H
28. R_1 =α OH R_2 = β OMe. R_3 = Me, R_4 = Me
29. R_1 =α OMe R_2 =β OH. R_3 = Me, R_4 = Me
30. R_1 =α OH R_2 = β OH R_3 = Me, R_4 = Me
31. R_1 = α -O-Glc. R_2 =β OH. R_3 = Me, R_4 = Me

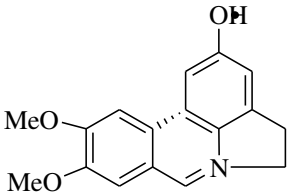

32

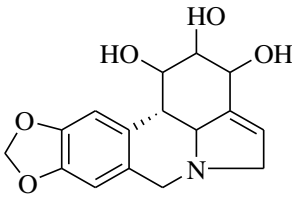

33

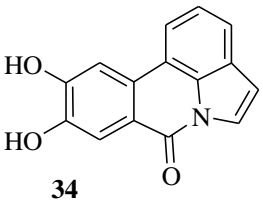

34

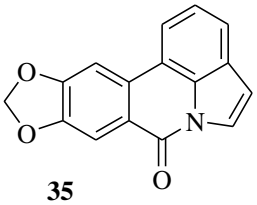

35

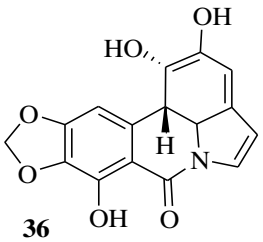

36

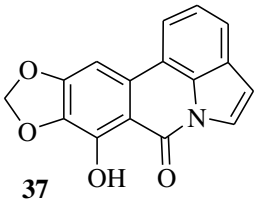

37

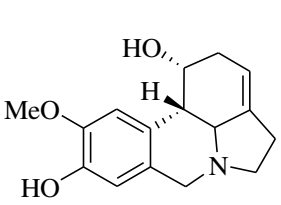

38

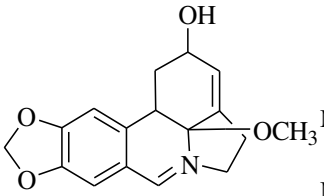

39

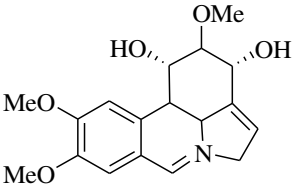

40

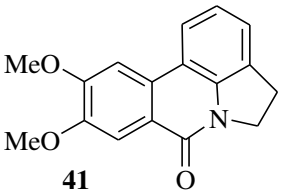

41

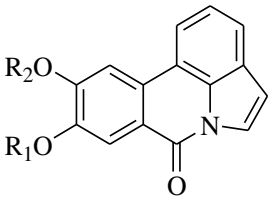

42. R_1 = H, R_2 = Me
43. R_1 = Me, R_2 = H
44. R_1 = Me, R_2 = Me

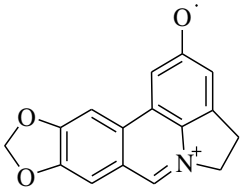

45

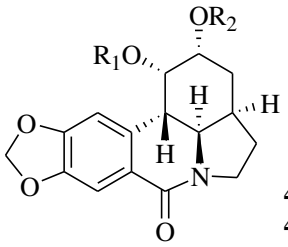

46. R_1 = H, R_2 = H
47. R_1 = Ac, R_2 = Ac

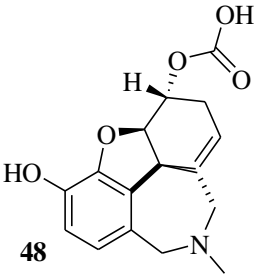

48

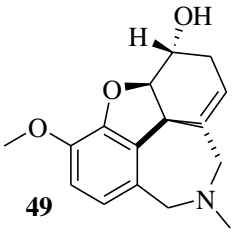

49

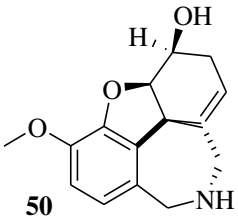

50

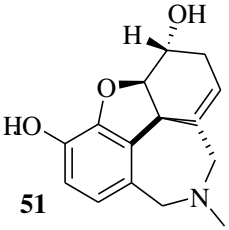

51

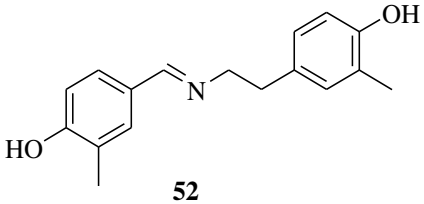

52

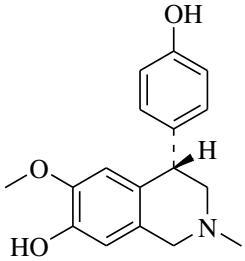

53

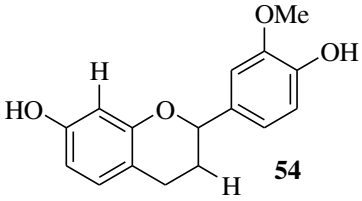

54

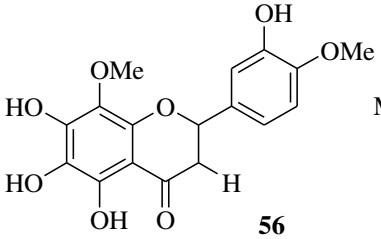

56

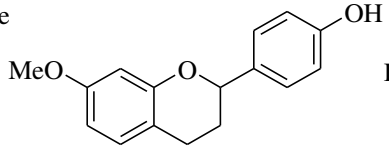

57

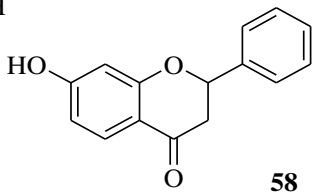

58

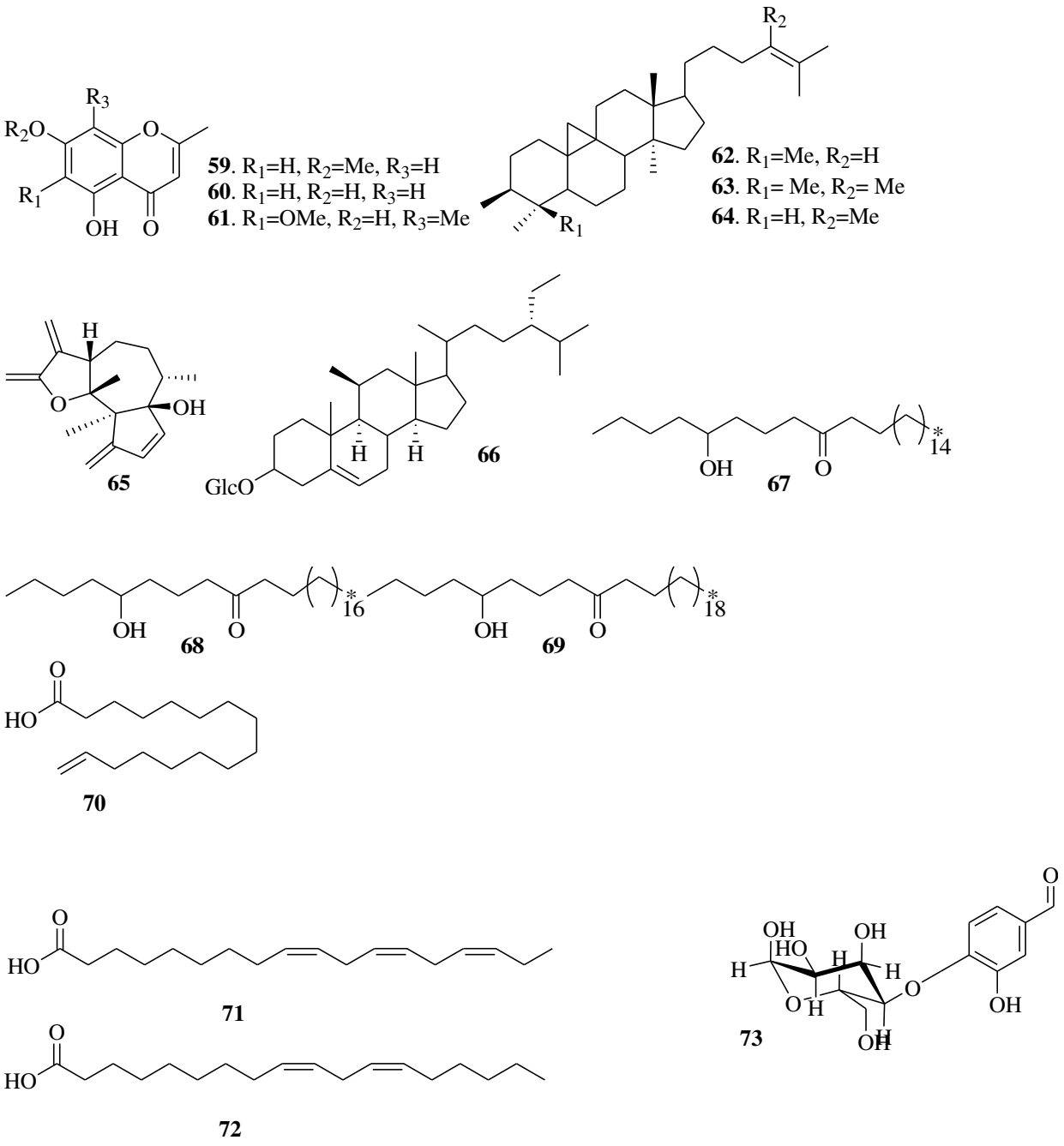

Figure 8: Structure of compounds isolated from different *Crinum* species

2.4.2. *Calotropis procera*

Previous pharmacological reports disclosed that *C. procera* exhibit antimicrobial, anthelmintic, anti-inflammatory, analgesic and antipyretic, anticancer, anti-angiogenic, immunological, antidiabetic, cardiovascular, hypolipidemic, gastroprotective, hepatic

protective, renal protective, antidiarrheal, antifungal, antioxidant, larvicidal activity, anticonvulsant, anti-ulcer effects, enhancement of wound healing, antifertility and smooth muscle relaxant effect (Hassan *et al*., 2006; Al-Snafi, 2015). The root extracts of *C. procera* were investigated for its anti-hyperglycemic effect in Male Wister Albino rats. Glibenclamide 500 µg/kg, petroleum ether, methanol and aqueous extracts of roots of *C. procera* were administered to streptozotocin induced diabetic rats at a dose of 250 mg/kg bw as a single dose per day for 15 days. It appeared that methanol and aqueous extracts were the most effective hypoglycemic extracts (Samy and Chow, 2012). The chloroform extract of *C. procera* seeds exhibited better antimicrobial activity while the extracts obtained from *Calotropis procera* seeds were evaluated for their possible in vitro antibacterial activities using the paper disc method (Bhaskar, 2000). In Ethiopia, pharmacological studies of ethanolic extract of the leaves and latex *C. procera* demonstrated antimicrobial activity against *S. aureus, E. coli, Bacillus cereus, Proteus mirabilis, Proteus vulgaris, Klebsiella pneumoniae, Shigella dysenteriae* and *Pseudomonas aeruginosa* (Asres *et al*.,1992).

The preliminary phytochemical screening of the plant showed the presence of cardenolides, steroids, tannins, glycosides, phenols, terpenoids, sugars, flavonoids, alkaloids and saponins (Šiler *et al*., 2010). Phytochemical studies indicated that extracts of roots of *C. procera* contained alkaloids, flavonoids, glycosides, saponins and terpenes (Šiler *et al*., 2010). The list of compounds reported from *calotropis procera* along with their compound class, plant part and literature references are shown in Table 3.

Table 3: Compounds isolated from *C. procera* organized by compound class.

Compound class	Compound name	Str No	Plant part	Ref
Flavonoids	5-hydroxy-3,7-dimethoxyflavone-4′-*O*-*β*-glucopyranoside	**74**	L	Nenaah, 2013
	Quercetin-3-O-rutinoside	**75**	L	Nenaah, 2013
	kaempferol-3-O-rutinoside	**76**	L	Nenaah, 2013
	Isorhamnetin-3-O-rutinoside	**77**	L	Nenaah, 2013
Steroids	β-Sitosterol	**78**	La	Chundattu *et al*., 2011
	Stigmasterol	**79**	La	Chundattu *et al*., 2011
	Multiflorenol	**80**	La	Chundattu *et al*., 2011
	Procesterol	**81**	F	Saber *et al*., 1969
	β-Sitosteryl linoleate	**82**	RT	Shahania *et al*., 2012
	12β-O-benzoyl-3β,14β,17β-trihydroxypregnane 20-one	**83**	RT	Wang *et al*., 2008
	Gofruside	**84**	RT	Wang *et al*., 2008

	16-α-Hydroxy calotropagenin	**85**	F	Yogesh *et al*., 2011
Terpenoids	β-Amyrin	**86**	RT	Quazi *et al*., 2013
	α-Amyrin	**87**	RT	Quazi *et al*., 2013
	Taraxasterol	**88**	RT, L	Wang *et al*., 2008
	α-amyrin acetate	**89**	RT	Quazi *et al*., 2013
	β-Amyrin acetate	**90**	RT	Quazi *et al*., 2013
	Proceraursenolide	**91**	RT	Mittal and Ali, 2012
	Calotroprocerone-A	**92**	RT	Mittal and Ali, 2012
	Calotropenyl acetate	**93**	RT	Ibrahim *et al*., 2012
	Lupeol	**94**	RT	Ibrahim *et al*., 2012
	3β,27-dihydroxy-urs-18-en-13,28-olide	**95**	La	Chundattu *et al*., 2011
	Calotroproceryl acetate A	**96**	RT	Ibrahim *et al*., 2012
	Calotroprocerol A	**97**	RT	Ibrahim *et al*., 2012
	Calotroprocerol B	**98**	RT	Ibrahim *et al*., 2012
	Urosolic acid	**99**	L	Meena *et al*., 2010
Cardenolide	2β,19-epoxy-3β,14β-dihydroxy-19-methoxy-5α-card-20(22)-enolide	**100**	RT, ST	Kamel *et al*., 2010
	β-anhydroepidigitoxigenin-3β-*O*-glucopyranoside	**101**	RT, ST	Meena *et al*., 2010
	Caroglaucigenin	**102**	RT	Meena *et al*., 2010
	Frugoside	**103**	RT	Meena *et al*., 2010
	Carotoxigenine	**104**	RT	Meena *et al*., 2010
	Calotropagenin	**105**	L	Arun *et al.*, 2012
	Calotropin	**106**	La	Chopra *et al*., 1983; Baquar *et al*., 1984
	Calactin	**107**	La	Arun *et al.*, 2012; Chopra *et al*., 1983
	Calotoxin	**108**	La	Arun *et al.*, 2012; Chopra *et al*., 1983
	Uscharin	**109**	RT	Arun *et al.*, 2012; Chopra *et al*., 1983
	Voruscharin	**110**	La	Arun *et al.*, 2012; Chopra *et al*., 1983
	Uzarigenin	**111**	La	Rastogi *et al*., 1993; Grieve, 1994
	Syriogenin	**112**	La	Baquar *et al*., 1984
	Proceroside	**113**	La	Baquar *et al*., 1984; Rastogi *et al*., 1993
	Proceragenin	**114**	La	Baquar *et al*., 1984; Rastogi *et al*., 1993
Others	O-Pyrocatechuic acid	**115**	F	Khasawneh *et al*., 2011
	Methyl caffeate	**116**	L	Mohamed *et al*., 2011
	Caffeic acid	**117**	L	Mohamed *et al*., 2011

F: Flower, L: Leaf, RT: Root, La: Latex; Str No: structure number; Ref: Reference.

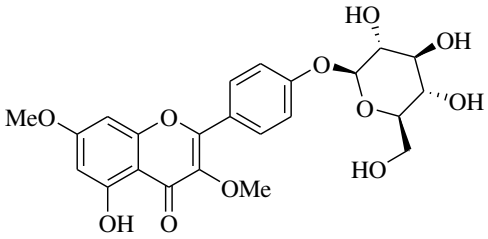

74

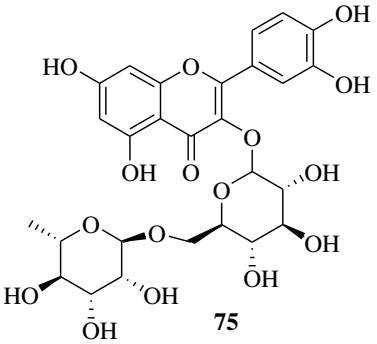

75

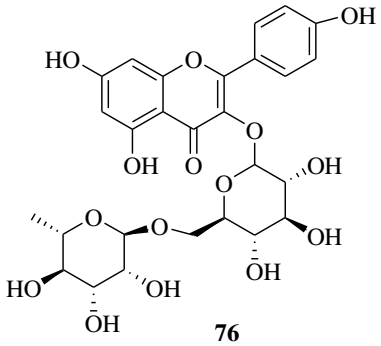

76

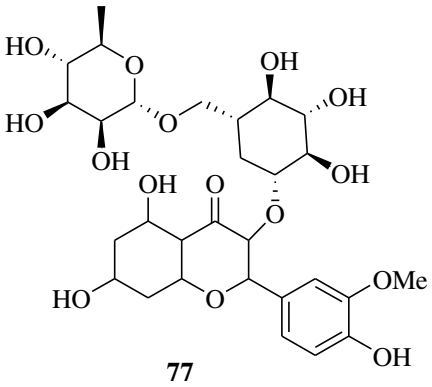

77

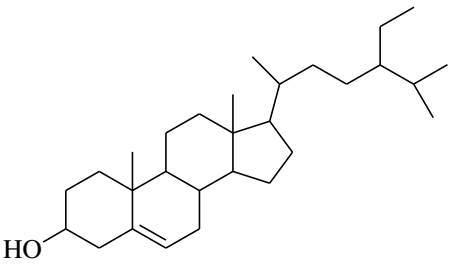

78

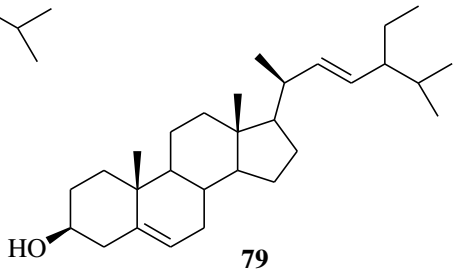

79

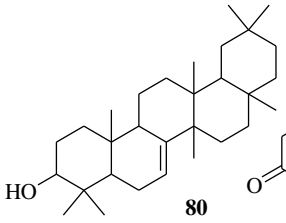

80

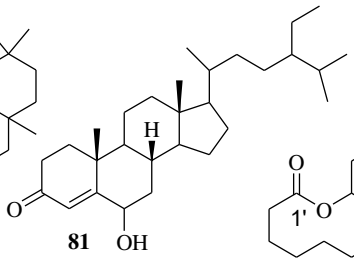

81

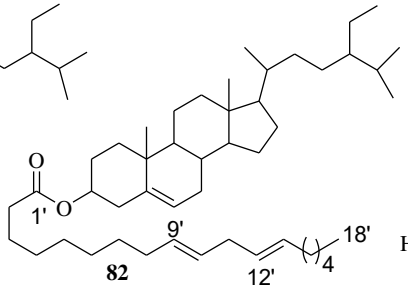

82

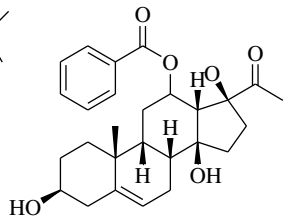

83

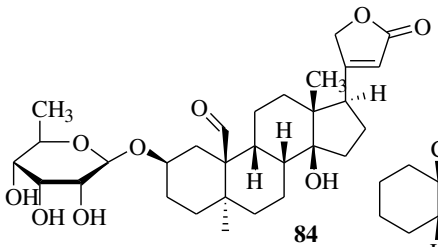

84

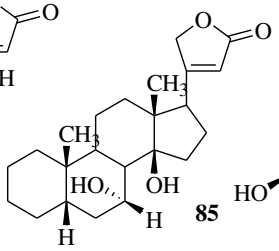

85

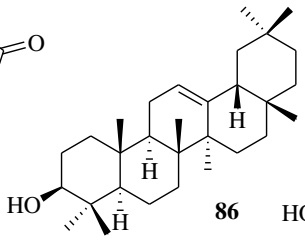

86

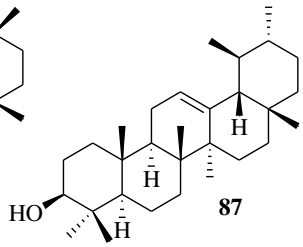

87

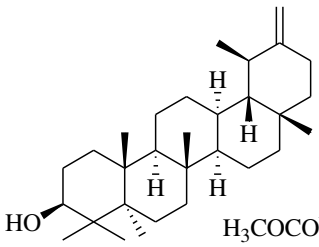

88

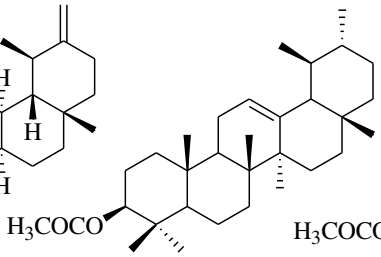

89

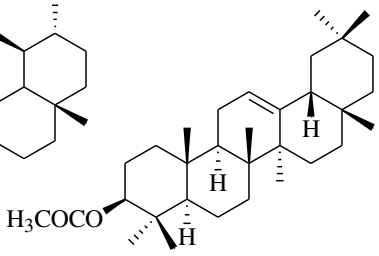

90

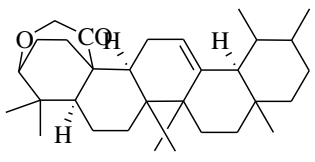

91

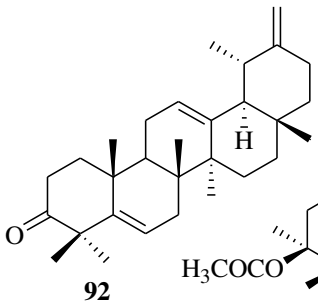

92

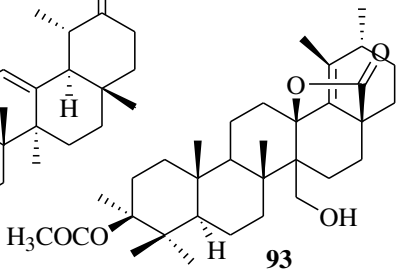

93

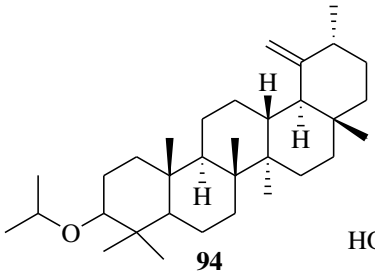

94

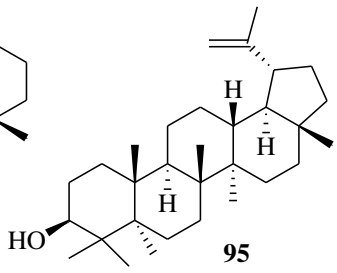

95

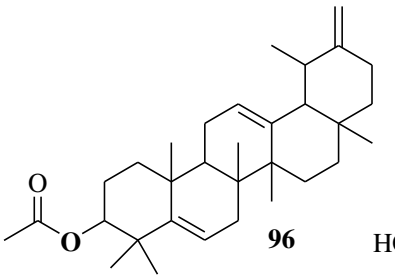

96

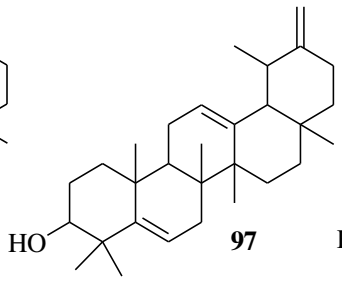

97

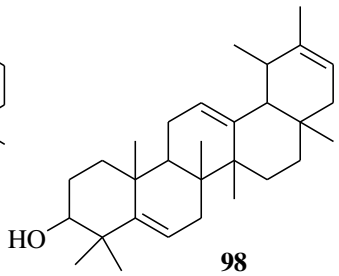

98

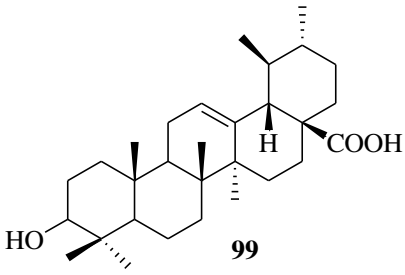

99

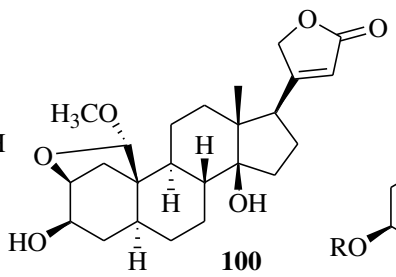

100

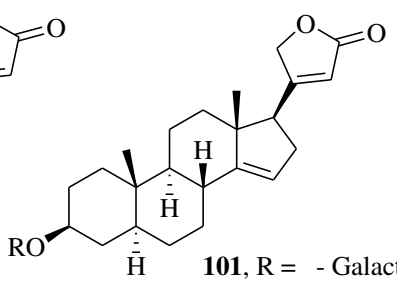

101, R = - Galactopyranose

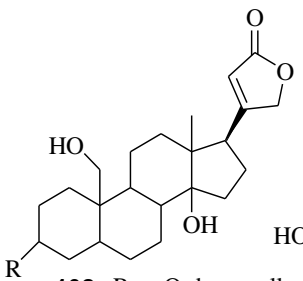

102 R = -O-desoxyallosyl

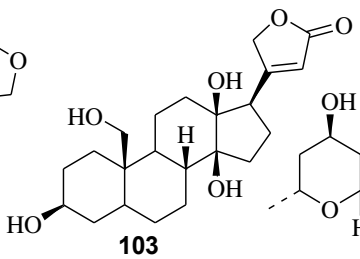

103

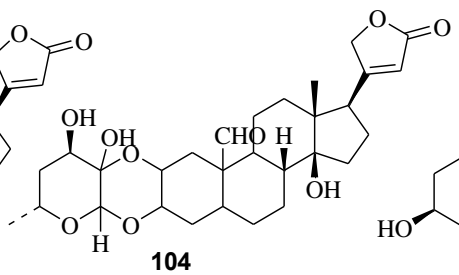

104

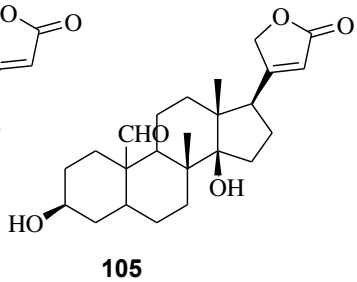

105

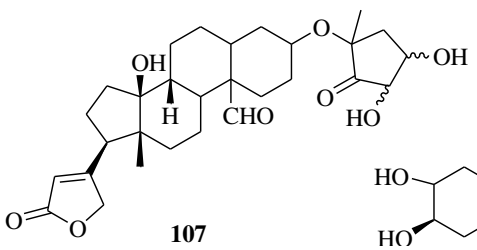

107

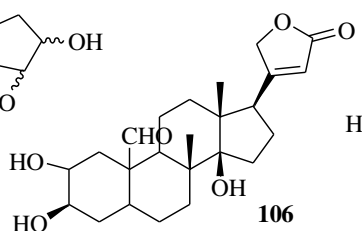

106

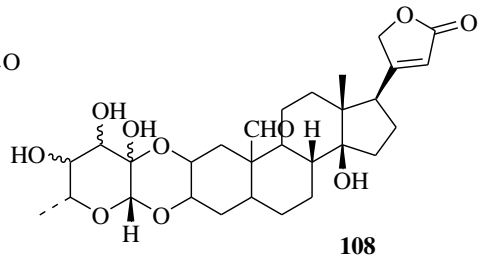

108

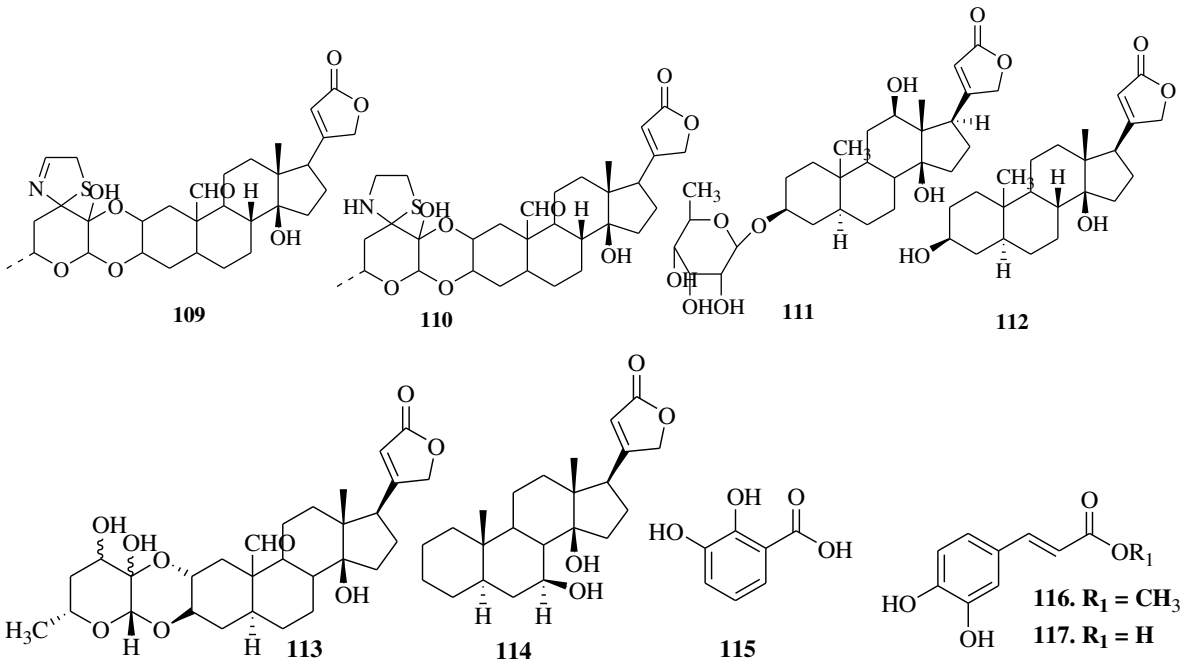

Figure 9: Structure of compounds reported from *C. procera*.

2.4.3. *Caylusea abyssinica*

According to the report, 80 % methanolic leaf extracts of *C. abyssinica* showed antidiabetic and oral glucose tolerance improving actions, particularly at the dose of 200 mg/kg in experimental animals. The report also supported the prevailing traditional claims of the leaves of *C. abyssinica* for management of diabetes mellitus (Tamiru *et al*., 2012). Oral administration of the methanol and aqueous fractions of *C. abyssinica* leaves have beneficial effect in reducing BGLs in normal and streptozotocin induced diabetic rodents (Gebreyohannis *et al*., 2014). Phytochemical screening of *C. abyssinica* revealed the presence of alkaloids, cardiac glycosides, reducing sugars, steroidal compounds, phenolic compounds, tannins, saponins and flavonoids (Edilu *et al*., 2015). The following are some lists of compounds isolated from *C. abyssinica* along with their compound class, compound name, plant part and literature references (Table 4).

Table 4: List of compounds isolated from *C. abyssinica* organized by compound class.

Compound class	Compound name	Str No	Plant part	Ref
	3-(3 carboxyphenyl) alanine	**118**	L	Olsen and Sørensen, 1980
	(3-carboxyphenyl) glycine	**119**	L	Olsen and Sørensen, 1980
	3-(3-carboxy-4 hydroxyphenyl) alanine	**120**	L	Olsen and Sørensen, 1980
Amino acids	(3-carboxy-4 hydroxyphenyl) glycine	**121**	L	Olsen and Sørensen, 1980
	(2S,4S)-4-Hydroxy-4-methylglutamic acid	**122**	L	Olsen and Sørensen, 1980
	(2S,4R)-4-Hydroxy-4-methylglutamic acid	**123**	L	Olsen and Sørensen, 1980
	4-Carboxy-4-hydroxy-2-aminoadipic acid	**124**	L	Olsen and Sørensen, 1980
	2-Aminoadipic acid	**125**	L	Olsen and Sørensen, 1980
	Saccharopine	**126**	L	Olsen and Sørensen, 1980
Steroids	β-Sitosterol	**78**	RT	Edilu *et al*., 2015
	Stigmasterol	**79**	RT	Edilu *et al*., 2015

L: Leaf, RT: Root, Str No: structure number; Ref: Reference.

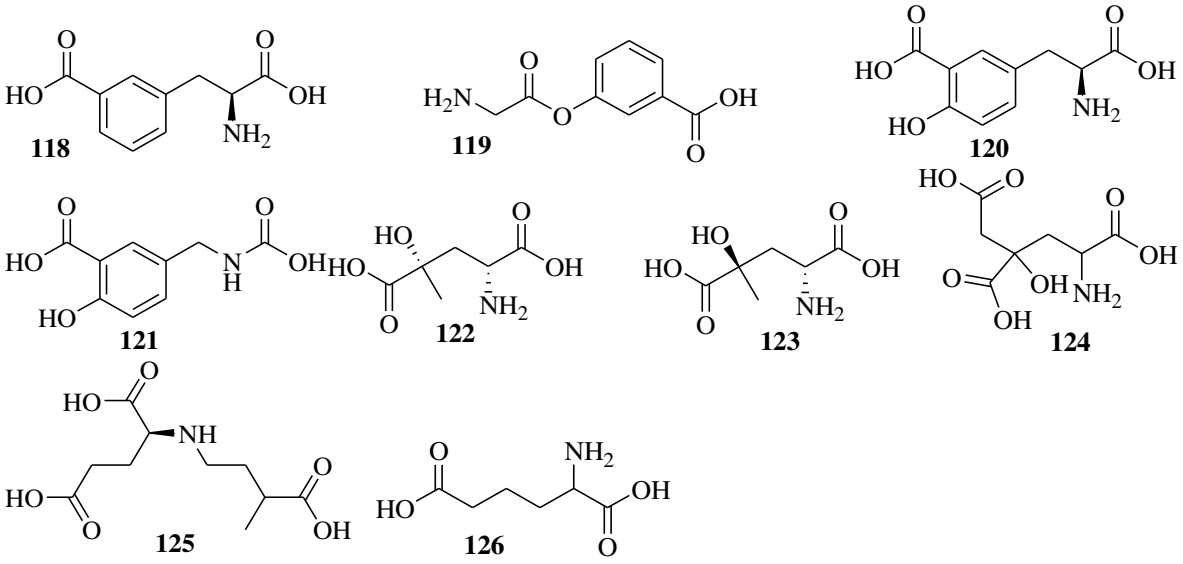

Figure 10: Structure of compounds isolated from *C. abyssinica*

2.4.4. *Justicia schimperiana*

A wide variety of secondary metabolites were reported from the genus *Justicia* such as alkaloids, lignans, flavonoids, and terpenoids (iridoids, diterpenoids, and triterpenoids) (Al-Juaid *et al*., 2004). Some of the compounds identified from this plant species along with their compound class, plant part, and literature references are listed in Table 5. The

primary ingredient in the active extracts of *Justicia* species is lignan and has been assessed for different activities including antiviral, antitumoral, anti-inflammatory, and antiplatelet aggregations activities, which warrant further exploration (Geone and Antônio, 2012).

Table 5: A List of compounds organized by compound class from different *Justica* species.

Compound class	Compound name	Str No	Plant source	Plant part	Ref
Coumarin	Umbelliferone	**127**	*J. pectoralis*	L	Leal *et al*., 2000
Flavonoids	3′,4′-Dihydroxyflavonol	**128**	*Justicia cataractae* Leonard	WP	Woodman and Malakul, 2009
	Apigenin	**129**	*J. gendarussa*	L	Wahi *et al*., 1974
	Kaempferitrin	**130**	*J. spicigera*	L	Cazarolli *et al*., 2006
	Vitexin	**131**	*J. gendarussa*	L	Cazarolli *et al*., 2006
Alkaloids	5*H*,6*H*-Quinindolin-11-one	**132**	*J. betonica*	AP	Subbaraju *et al*., 2004
	10*H*-Quindoline	**133**	*J. betonica*	AP	Subbaraju *et al*., 2004
	Jusbetonin	**134**	*J. betonica*	AP	Rachana *et al*., 2011
	Vasicine	**135**	*J. adhatoda*	RT	Rachana *et al*., 2011
	Vasicinone	**136**	*J. adhatoda*	RT	Rachana *et al*., 2011
	Allantoin	**137**	*J. spicigera*	L	Rachana *et al*., 2011
	6*H*-Quinindoline	**138**	*J. betonica*	AP	Rachana *et al*., 2011
	Vasicinol	**139**	*J. adhatoda*	RT	Rachana *et al*., 2011
Triterpenoidal glycosides	Justicioside A	**140**	*J. betonica*	AP	Konoshima and Atta-Ur-Rahman, 2000
	Justicioside B	**141**	*J. betonica*	AP	Konoshima and Atta-Ur-Rahman, 2000
	Justicioside C	**142**	*J. betonica*	AP	Konoshima and Atta-Ur-Rahman, 2000
	Justicioside D	**143**	*J. betonica*	AP	Konoshima and Atta-Ur-Rahman, 2000
	Justicioside E	**144**	*J. betonica*	AP	Konoshima and Atta-Ur-Rahman, 2000
	Justicioside F	**145**	*J. betonica*	AP	Konoshima and Atta-Ur-Rahman, 2000
	Justicioside G	**146**	*J. betonica*	AP	Konoshima and Atta-Ur-Rahman, 2000
	Justicisaponin	**147**	*J. simplex*	RT	Badami *et al*., 2003
Lignans	Jusmicranthin	**148**	*J. neesii*	WP	Rajasekhar and Subbaraju, 2000
	Jusmicranthin methyl ether	**149**	*J. neesii*	WP	Rajasekhar and Subbaraju, 2000
	Helioxanthin	**150**	*J. flava*	L	Chang *et al*., 2000
	Taiwanin E	**151**	*J. procumbens*	WP	Chang *et al*., 2000
	Taiwanin E methyl ether	**152**	*J. purpurea*	RT	Kavitha *et al*., 2003
	Justicidin E	**153**	*J.*	WP	Fukamiya and Lee,

		procumbens		1986
Neojusticin A	**154**	*J. procumbens*	WP	Fukamiya and Lee, 1986
Justicidin B	**155**	*J. purpurea*	RT	Kavitha *et al*., 2003
Diphyllin	**156**	*J. extensa*	L	Wang and Ripka, 1983
Justicidin A	**157**	*J. extensa*	L	Wang and Ripka, 1983
Cleistanthin B	**158**	*J. purpurea*	WP	Kavitha *et al*., 2003
Neesiinoside A	**159**	*J. neesii*	RT	Subbaraju *et al*., 2001
4′′-*O*-Acetylpatentiflorin B	**160**	*J. patentiflora*	WP	Susplugas *et al*., 2005
Patentiflorin A	**161**	*J. patentiflora*	WP	Susplugas *et al*., 2005
Patentiflorin B	**162**	*J. patentiflora*	WP	Susplugas *et al*., 2005
Tuberculatin	**163**	*J. betonica*	AP	Lu *et al*., 2008
Chinensinaphthol methyl ether	**164**	*J. ciliata*		Day *et al*., 1999
Justalakonin	**165**	*J. purpurea*	WP	Kavitha *et al*., 2003
4′-Dimethyl chinensinaphthol methyl ether	**166**	*J. ciliata*	WP	Day *et al*., 1999
Chinensinaphthol	**167**	*J. betonica*	WP	Day *et al*., 1999
Elenoside	**168**	*J. hyssopifolia*	L	Navarro *et al*., 2001a)
Neojusticin B	**169**	*J. ciliata*	WP	Day *et al*., 1999
Justicidinoside A	**170**	*J. procumbens*	AP	Asano *et al*., 1996
Justicidinoside B	**171**	*J. procumbens*	AP	Asano *et al*., 1996
Justicidinoside C	**172**	*J. procumbens*	AP	Asano *et al*., 1996
Juspurpurin	**173**	*J. purpurea*	WP	Kavitha *et al*., 2003
Carinatone	**174**	*J. patentiflora*	WP	Susplugas *et al*., 2005
Justiflorinol	**175**	*J. patentiflora*	WP	Susplugas *et al*., 2005
(+)-Isolariciresinol	**176**	*J. flava*	-	Küpeli *et al*., 2003
Sesamin	**177**	*J. purpurea*	-	Chung *et al*., 2010
Justiciresinol	**178**	*J. glauca*	-	Subbaraju *et al*., 1991

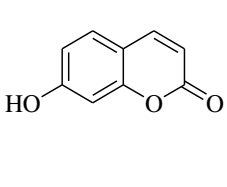

127

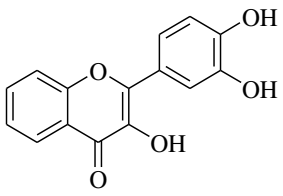

128

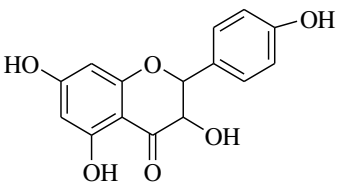

129

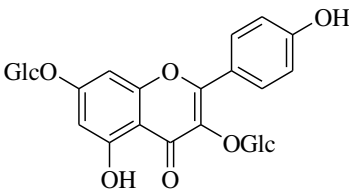

130

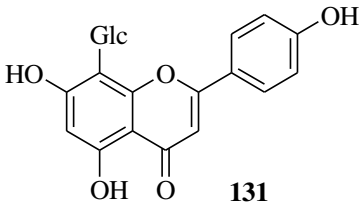

131

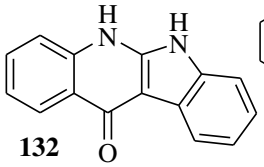

132

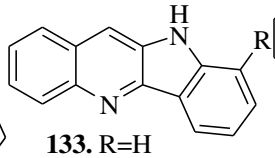

133. R=H
134. R=OGlc

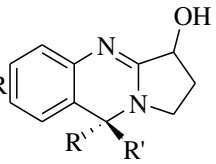

135. R=R'=H
136. R=R'=O

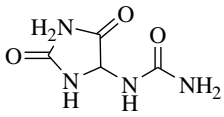

137

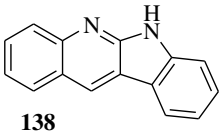

138

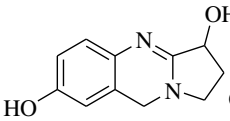

139

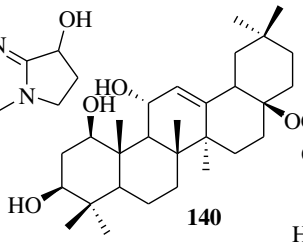

140

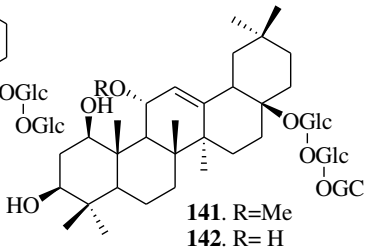

141. R=Me
142. R= H

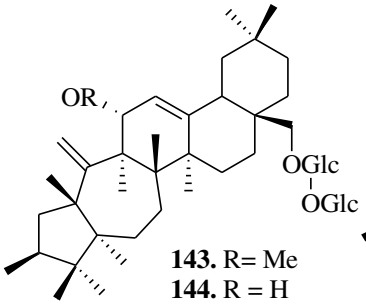

143. R= Me
144. R = H

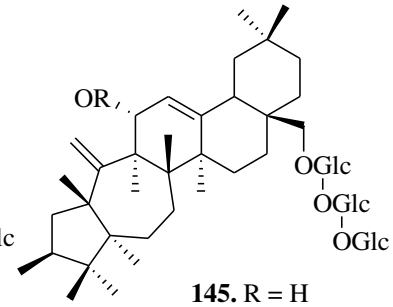

145. R = H
146. R= Me

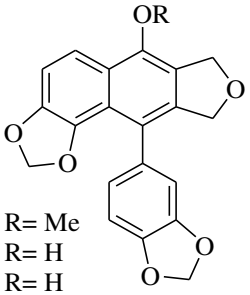

148. R= Me
149. R= H
150. R= H

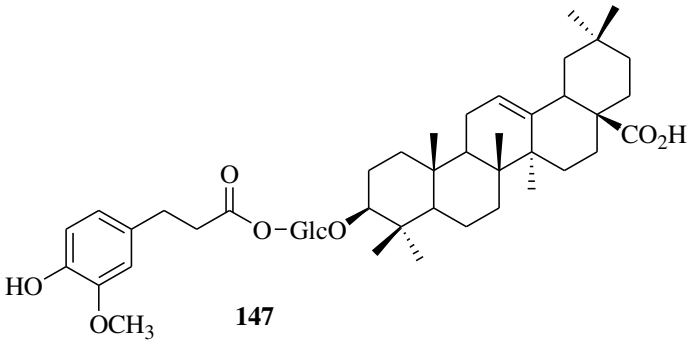

147

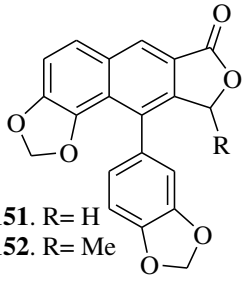

151. R= H
152. R= Me

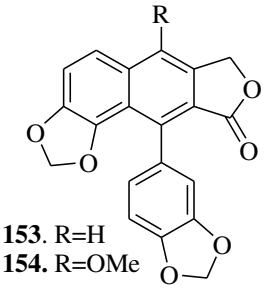

153. R=H
154. R=OMe

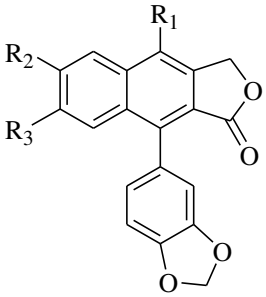

155. R_1=H; R_2=R_3=OMe
156. R_1=OH; R_2=R_3=OMe
157. R_1=R_2=R_3=OMe
158. R_1=OGlc; R_2=R_3=OM
159. R_1=OGlc-OGlc; R_2=R_3=OMe
160. R_1=OGlc-OGlc; R_2=R_3=OMe
161. R_1=OGlc; R_2=R_3=OMe
162. R_1=OGlc; R_2=R_3=OMe
163. R_1=O-D-apiofuranosyl; R_2=R_3=OMe

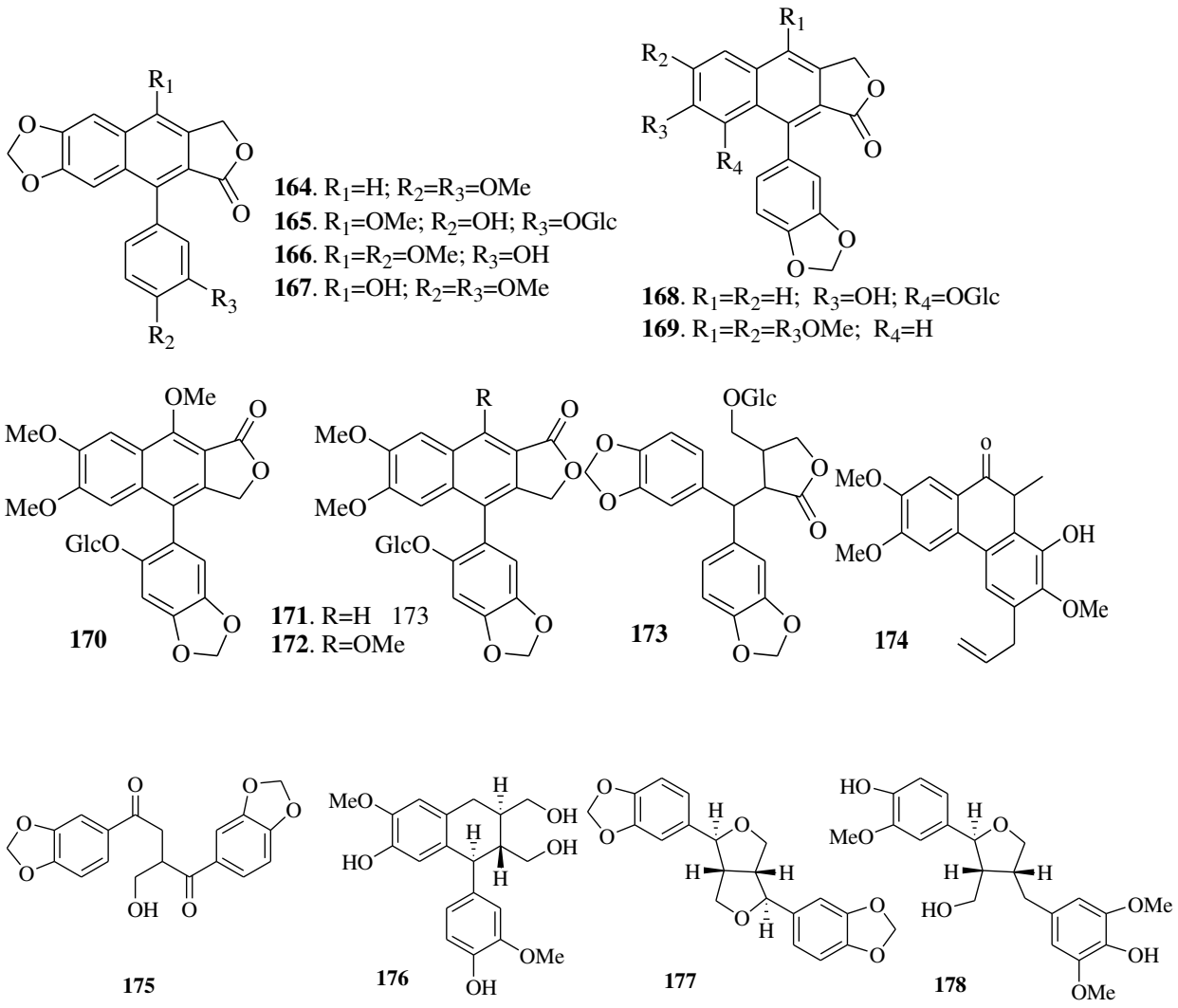

Figure 11: Structures of compounds reported from the genus *Justicia*

2.4.5. *Verbascum sinaiticum*

The pharmacological investigation showed *V. sinaiticum* has hepatoprotective activity (Mahmoud *et al*., 2007), potential antitrypanosomal activity (Mergia *et al*., 2014), antibacterial activity (Yeabyo *et al*., 2018), antioxidant activity, wound healing (Lulsegede *et al*., 2022), and anti-inflammatory activity (Asefa *et al*., 2022). The phytochemical analysis of the leaves of *V. sinaiticum* revealed that the presence of two flavonolignans, hydrocarpin, and the novel *sinaiticum*, as well as two flavones, chrysoeriol, and luteolin and the compounds are exhibited dose-dependent cytotoxicity against leukemia cancer cells (Goll *et al*., 1983). The phytochemical screening of *V. Sinaiticum* species revealed the presence of alkaloids, flavonoids, glycosides, phenolic compounds, saponins, steroids, and

tannins (Yeabyo *et al*., 2018). The list of compounds from *V. Sinaiticum* along with their compound class, compound name, plant part, and literature references are depicted in Table 6.

Table 6: A List of compounds organized by compound class from *V. sinaiticum*.

Compound class	Compound name	Str No	Plant part	Ref
Flavonolignans	Sinaiticin	**179**	L	Afifi *et al*., 1993
	Hydnocarpin	**180**	L	Afifi *et al*., 1993
Flavonoids	Chrysoeriol	**181**	L	Afifi *et al*., 1993
	Luteolin	**182**	L	Mahmoud *et al.*, 2007
	Chrysoeriol-7- *O*-glucoside	**183**	AP	Mahmoud *et al.*, 2007
	Orbol	**184**	AP	Elgindi & Mabry, 2000
	Orbol 7-O-β-D-glucoside	**185**	AP	Elgindi & Mabry, 2000
	5,3',4'-trihydroxy-8-methyl isoflavone 7-O-β-D-glucoside	**186**	AP	Elgindi & Mabry, 2000
	5-hydroxy-3',4' dimethoxyisoflavone7-O-α-Lrhmnoside	**187**	AP	Elgindi & Mabry, 2000
	Rutin	**188**	F	Zengin *et al*., 2021
	Hyperoside	**189**	F	Zengin *et al*., 2021
Phenylethanoid glycosides	Verbascoside	**190**	AP	Gondal *et al*., 2020
	Eukovoside	**191**	AP	Gondal *et al*., 2020
	Martynoside	**192**	AP	Gondal *et al*., 2020
	Jionoside D	**193**	AP	Gondal *et al*., 2020
	Campneoside I	**194**	AP	Gondal *et al*., 2020
	Campneoside II	**195**	AP	Gondal *et al*., 2020
Saponin	Saikosaponin A	**196**	AP	Miyase *et al*., 1997
	Verbascosaponin B	**197**	AP	Miyase *et al*., 1997
Iridoids	Ajugol	**198**	AP	Mahmoud *et al.*, 2007
	Aucubin	**199**	AP	Mahmoud *et al.*, 2007
Others	5-caffeoylquinic acid	**200**	F	Zengin *et al*., 2021
	Vanillic acid	**201**	F	Zengin *et al*., 2021

F: Flower, L: Leaf, AP: Aerial parts, Str No: structure number; Ref: Reference.

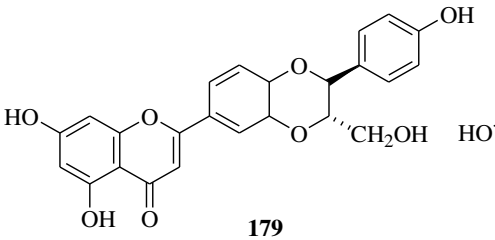

179

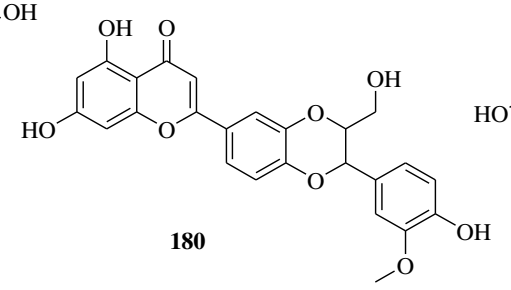

180

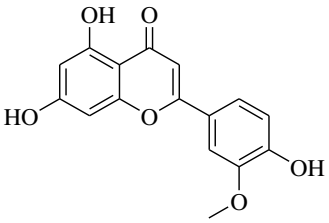

181

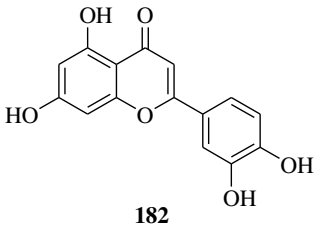

182

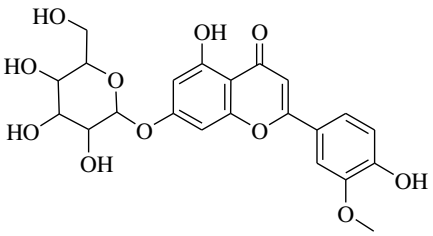

183

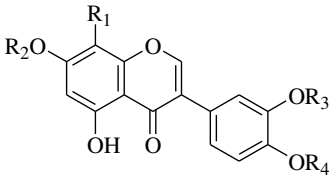

184. $R_1=R_2=R_3=R_4=H$
185. $R_1=R_3=R_4=H$, $R_2=Glc$
186. $R_3=R_4=H$, $R_1=CH_3$, $R_2=Glc$
187. $R_1=H$, $R_2=rha$, $R_3=R_4=CH_3$

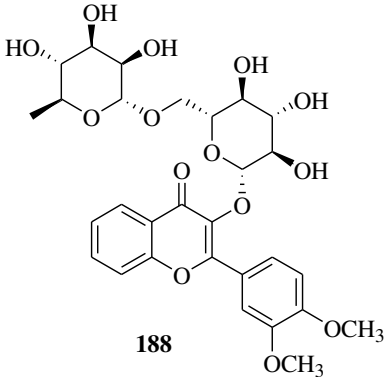

188

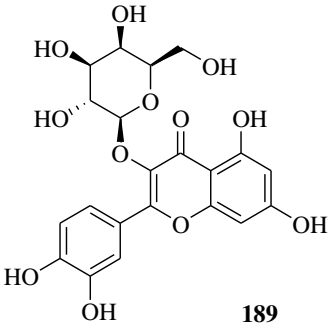

189

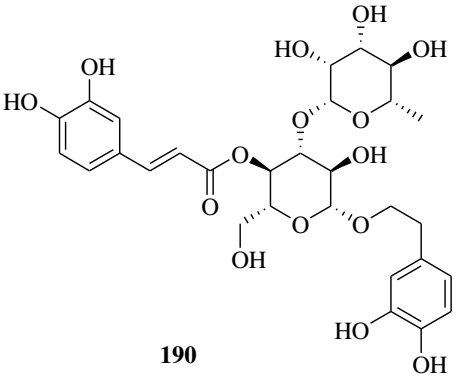

190

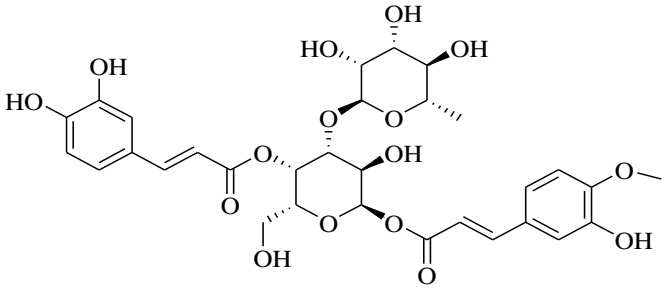

191

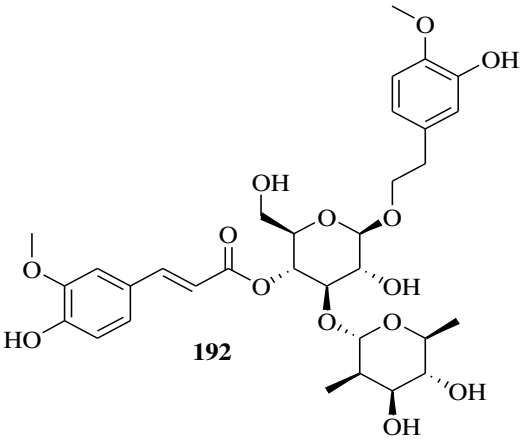

192

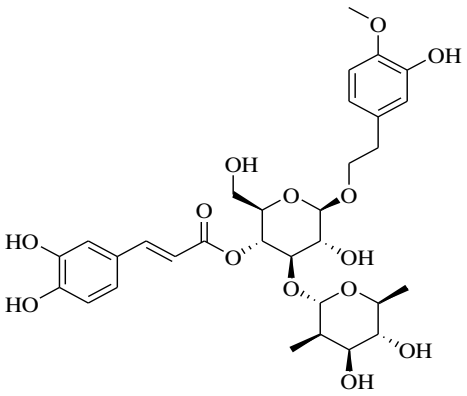

193

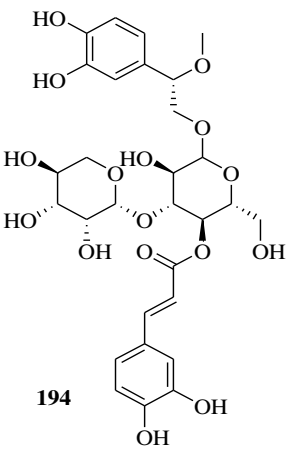

194

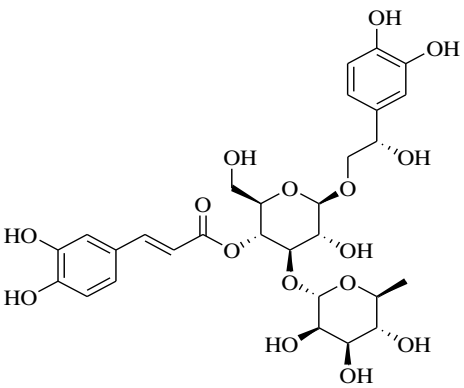

195

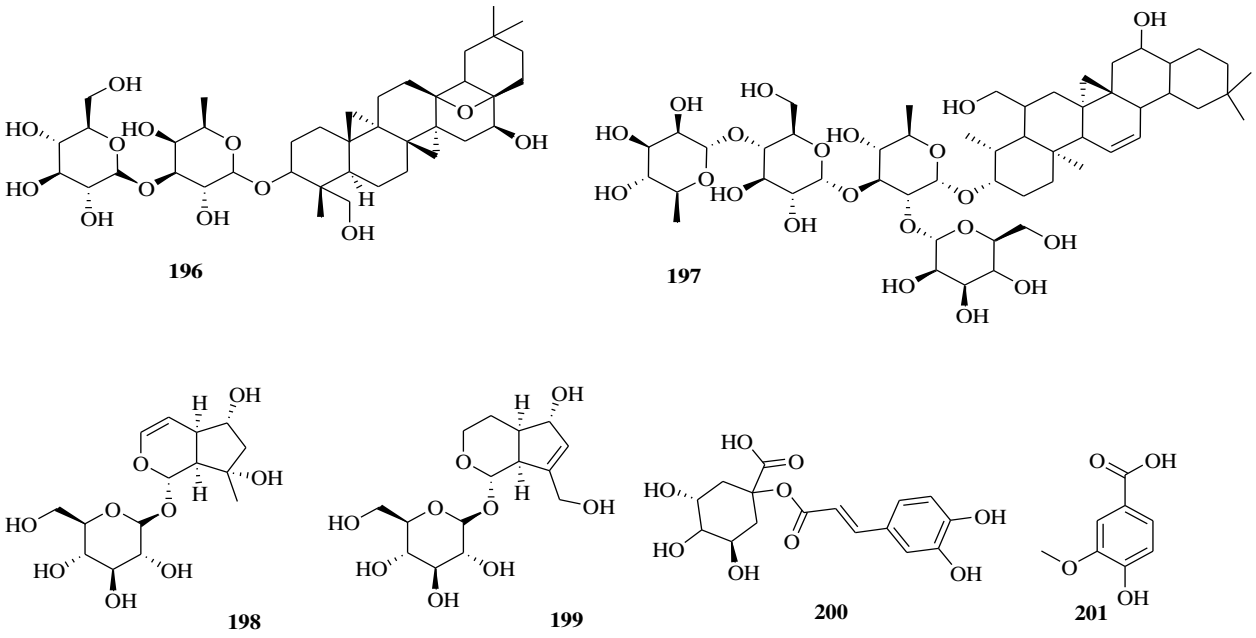

Figure 12: Structures of compounds reported from *V. sinaiticum*

2.4.6. *Lagenaria abyssinica*

Phytochemical screening showed that the genus *Lagenaria* contain compounds such as alkaloids, carbohydrates, phenols, proteins, minerals, tannins, phytosterols, flavonoids and steroidal are the known (Amit Kumar *et al*., 2012). As reported in literature, in pharmacological studies, *Lagenaria* species possess antioxidant activity, laxative, cardioprotective, diuretic, hepatoprotective, antihyperglycemic, hypolipidemic, central nervous system stimulant, anthelmintic, antihypertensive, immunosuppressive analgesic, antidepressant, anticancer, anti-stress, immunomodulatory, antihepatotoxic, analgesic, anti-inflammatory, antimicrobial, adaptogenic and free radical scavenging activity (Pragya *et al*., 2015). Compounds reported from species of *Lagenaria* are flavones with C-glycosides attachment such as isovitexin (**202**), isoorientin (**203**), saponarin (**204**), and saponarin 4'-*O*-glucoside (**205**) (Mirlosawa and Cisowski, 1995), cucurbitacin B (**206**), D (**207**) and E (**208**) (Muhammad and Rahila, 2013), 22-deoxocucurbitacin-D (**209**) , 22-deoxoisocurcubitacin D (**210**) (Rastogi and Melhrotra, 1990), oleanolic acid (**211**), campesterol (**212**), isoquercitrin (**213**) (Gangwal *et al*., 2010), C-friedooleana-7, 9 (11)-dien-29-ol (**214**), 3b-*O*-(*E*)-coumaroyl-D:*C*-friedooleana- 7,9(11)-dien-29-ol (**215**), 3b-*O*-(*E*) coumaroyl-D:*C*-friedooleana-7,9 (11)-dien-29-oic acid (**216**), 3-epikarounidiol (**217**),

3-oxo-D:*C*-friedoolena-7, 9 (11)-dien-29-oic acid (**218**), Methyl 2 β ,3 β -dihydroxy-D:*C*-friedoolean-8-en-29-oate (**219**), bryonolol (**220**), bryononic acid (**221**), and 20-epibryonolic acid **(222**) (Chen *et al*., 2008). Nevertheless, to the best of our knowledge, there are not prior phytochemical reports on *Lagenaria abyssinica,* from Ethiopian flora.

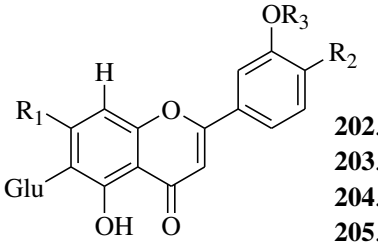

202. R_1=H, R_2=H, R_3=H
203. R_1=H, R_2=OH, R_3=H
204. R_1=Glucose, R_2=H, R_3=H
205. R_1=Glucose, R_2=H, R_3=Glucose

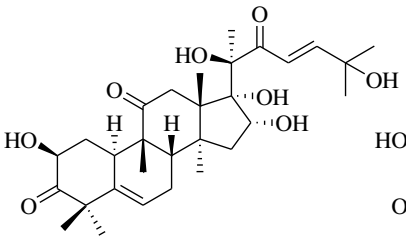

206

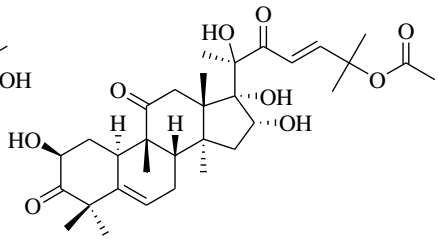

207

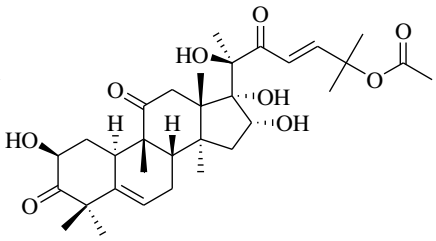

208

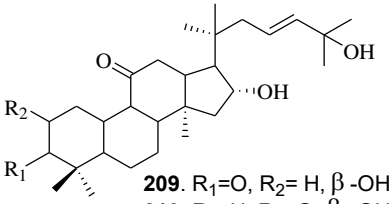

209. R_1=O, R_2= H, β -OH
210. R_1=H, R_2=O, β -OH

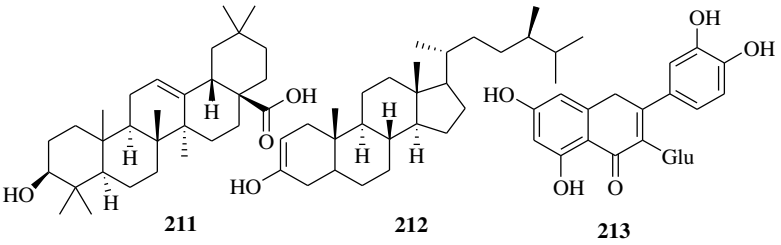

211 **212** **213**

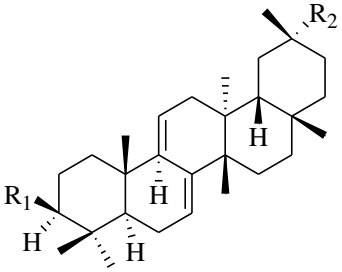

214. R_1=O-(*E*)-feruloyl, R_2=CH_2OH
215. R_1=O-(*E*)-coumaroyl, R_2= CH_2OH
216. R_1= O-(*E*)-coumaroyl, R_2=COOH
217. R_1= OH, R_2=CH_2OH
218. R_1= OH, R_2=COOH

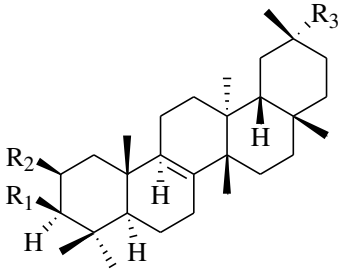

219. R_1= OH, R_2=OH, R_3=$COOCH_3$
220. R_1= OH, R_2= H, R_3= CH_2OH
221. R_1= =O, R_2= H, $R_{3=}$ COOH
222. R_1= OH, R_2=H, R_3=CH_3

Figure 13: Structures of compounds reported from *Lagenaria* species.

Nonetheless, the antidiabetic, anticancer, anti-*Acanthamoeba,* antioxidant, antibacterial activity, and essential oils composition studies on these selected plants have been relatively limited. To the best of our knowledge, in Ethiopia, the antioxidant, antibacterial, antidiabetic, anti-*Acanthamoeba* and anticancer activity of *C. abyssinicum*, *C. abyssinica, Lagenaria abyssinica, V. sinaiticum*, and *J. schimperiana* root extracts have never been reported. Indeed, a study reported by Tamiru *et al*. (2012) on the effects of crude leaf 80 % methanolic extract of *Caylusea abyssinica* was tested on alloxan-induced diabetic mice showed promising activity as well as related phytochemical analysis and in vitro antibacterial activity on the methanolic crude extract of the roots of *C. absyssinica* (Edilu *et al*., 2015). Furthermore, the leaf macerate of *J. schimperiana* is asserted to be antidiabetic (Tesfaye *et al*., 2016), antimicrobial (Tedila *et al*., 2019; Melaku, 2017), and antioxidant activities (Umer *et al*., 2010). As a result, in Ethiopia, this is the first report of an *in-vitro* antidiabetic, anticancer, antioxidant, antibacterial, anti-*Acanthamoeba* activity analysis, and phytochemical studies of the DCM/MeOH (1:1) and methanol root extracts for *Lagenaria abyssinica, V. sinaiticum, C. abyssinicum*, *C. abyssinica, C. procera,* and *J. schimperiana*.

2.5 Current Status and Challenges in the Management of Microbial, Diabetic, and Cancer Diseases

Natural products have historically served as vital sources of antimicrobial agents, with numerous drugs originating from plants, fungi, and marine organisms (Newman and Cragg, 2016). For instance, antibiotics such as penicillin and erythromycin are derived from fungi and bacteria. Present research endeavors are primarily focused on identifying novel natural compounds to combat antibiotic-resistant pathogens. Compounds sourced from plants, such as berberine and curcumin, exhibit antimicrobial properties against a diverse array of pathogens, including bacteria, fungi, and parasites. Moreover, marine-derived peptides and compounds are undergoing investigation for their potential antimicrobial effects.

In the realm of diabetes management, natural products have displayed promising results by modulating blood sugar levels, enhancing insulin function, and safeguarding pancreatic cells (Kumar and Narwal, 2013). Compounds found in plants, such as berberine, curcumin, and resveratrol, have demonstrated efficacy in combating diabetes in both animal and

human studies. Traditional herbal remedies like bitter melon, fenugreek, and ginseng have long been utilized to help manage diabetes. Researchers are also exploring marine-derived compounds like fucoidans and marine polyphenols to evaluate their potential in diabetes management. Furthermore, investigations are underway to ascertain natural products that could mitigate diabetes-related complications such as nerve damage and kidney issues.

The devastating problems associated with microbial, cancer, and diabetic cases and deaths encompass a range of complex challenges that have profound implications for global public health and individual well-being. Antimicrobial resistance (AMR) presents a significant issue in the field of health, as our usual drugs used to combat infections are becoming less effective due to certain microbes developing resistance to them (WHO, 2017; Ventola, 2015). Globally, AMR causes over 700,000 deaths annually, with around 25,000 occurring in the European Union alone. Factors contributing to this issue include the misuse of antibiotics, inadequate infection control measures, and a lack of development of new drugs. Furthermore, AMR can lead to longer hospital stays, increased treatment costs, and limited options for patients. Diabetes poses a substantial global health challenge, with approximately 537 million adults aged between 20 and 79 having diabetes in 2021, projected to increase to 643 million by 2030 (IDF, 2021). Complications from diabetes, such as heart disease, stroke, kidney issues, blindness, and amputations, can be extremely severe, impacting health negatively and placing a burden on finances and healthcare systems (Saeedi *et al*., 2019; IDF, 2021). Cancer remains a significant problem worldwide, causing sickness, death, and financial hardship (WHO, 2020; Jemal *et al*., 2017). Despite progress in treatment, challenges like drug resistance, treatment side effects, and limited access to therapies persist (Vasan *et al*., 2019). Addressing these problems requires developing various strategies to prevent them, detect them early, ensure accessible treatment for all, and continue researching improved methods to assist patients.

CHAPTER THREE

3. MATERIALS AND METHODS

3.1. General

All chemicals, solvents, and reagents were analytical grade. The compound purity was determined by analytical TLC. Analytical TLC was run on a 0.25 mm thick layer of silica gel GF254 (Merck) on aluminum plate. HPTLC plates, Merck 60 F_{254} 20x20 cm, 0.2 mm thickness, were used. Spots were detected by observation under UV light (254 and 365 nm). The vanillin spraying agents were also used to visualize the spot on TLC plates. Column chromatography was performed using silica gel (60-200 mesh) Merck. Samples were applied on column by either adsorbing on silica gel or dissolving in appropriate solvent. Solvent was removed using rotavapor. Melting points were measured using the Gallenkamp MFB-595 equipment. A GC–MS instrument from Agilent Technologies (Santa Clara, CA, USA) equipped with a 7890 N network GC system, 5977 inert mass selective detector was used for analyzing the essential oils. UV-Vis's spectrophotometer was used to record absorbance at 517 nm. NMR spectra were recorded using Bruker Avance 400 spectrometer operating at 400 MHz. Structural assignment was performed based on ^{1}H NMR, ^{13}C NMR, DEPT-135, COSY, HSQC, and HMBC.

3.2. Plant materials collection, identification, and preparation

The leaves and roots of *C. procera* were collected in August 2020 from Adama special administrative zone, around express way (Figure 13). The roots of *C. abyssinicum, L. abyssinica* and aerial parts and roots of *C. abyssinica* and *J. schimperiana* were collected from Illubabor zone, Didesa Woreda, Oromia region 420 km away from Addis Ababa on November, 2021(Figure 14). The leaves, and roots of *V. sinaiticum* were collected from Arsi zone, Inkolo Wabe Woreda, Bokoji Mirt Kebele, Oromia Region 274.1 km away from the capital Addis Ababa on November 21, 2022 (Figure 13). Identification and authentication of the plant's specimen were done by botanist Mr. Melaku Wondaferash, and Mr. Shambel Alemu at the National Herbarium, Addis Ababa University and voucher specimens have been deposited in the Herbarium with voucher code GT 002/2020 for *C. procera*, GT 003/2021 for *C. abyssinicum*, GT 004/2021 for *C. abyssinica*, GT 001/2020 for *J. schimperiana* and GT 005/2021 for *L. abyssinica*, and GT 006/2022 for *V.*

sinaiticum. The plants were chopped into small pieces, air dried under shade at room temperature and pulverized using a Willy electrical mill.

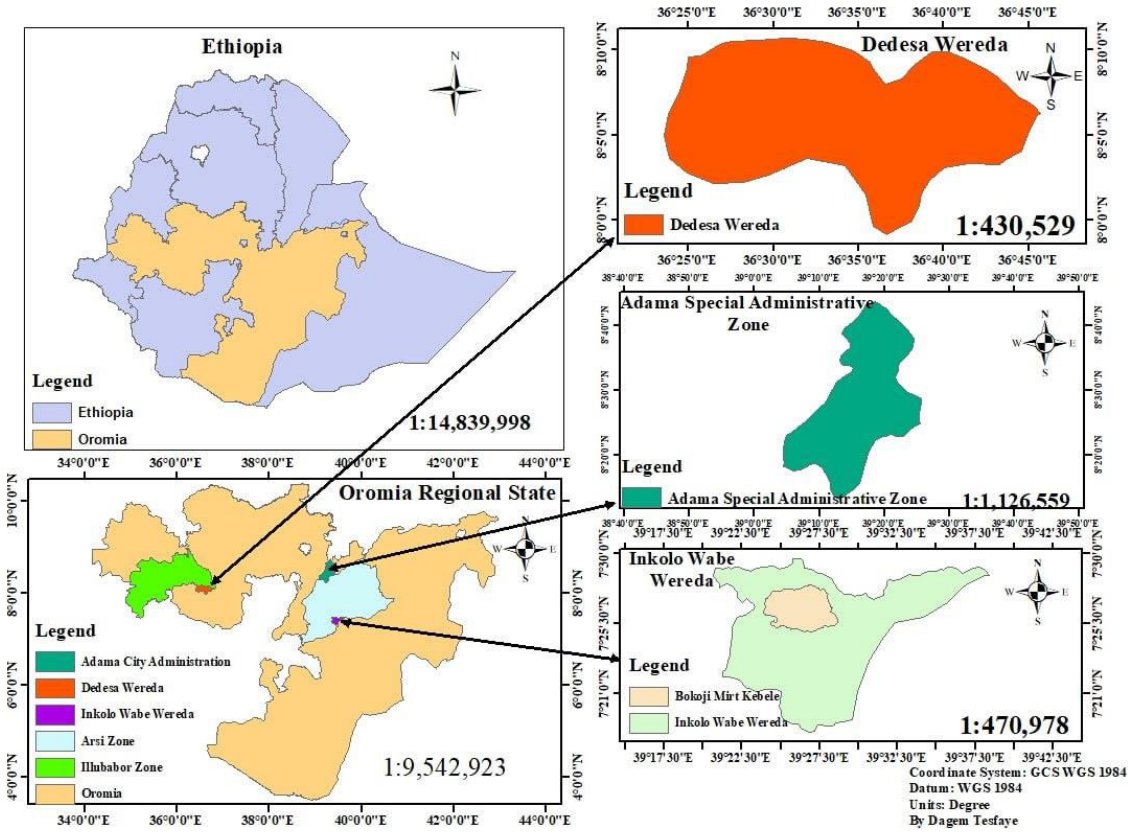

Figure 14: Map showing the plants collection area in Oromia Regional State.

Source: ArcMap V. 10. 5. By Dage Tesfaye.

3.3. Extraction and isolation

3.3.1. General extraction method

The ground plant materials were extracted by maceration with CH_2Cl_2/CH_3OH (1:1) (v/v) 3 L three times for 48 hrs in each case by shaking using a mechanical shaker. The extracts were concentrated using a rotary evaporator to yield crude CH_2Cl_2/CH_3OH (1:1) extract. The marc after CH_2Cl_2/CH_3OH (1:1) extraction was further extracted with CH_3OH 2.5 L two times for 48 hrs in each case and the extract was concentrated using a rotary evaporator to give crude methanol extracts (Scheme 1).

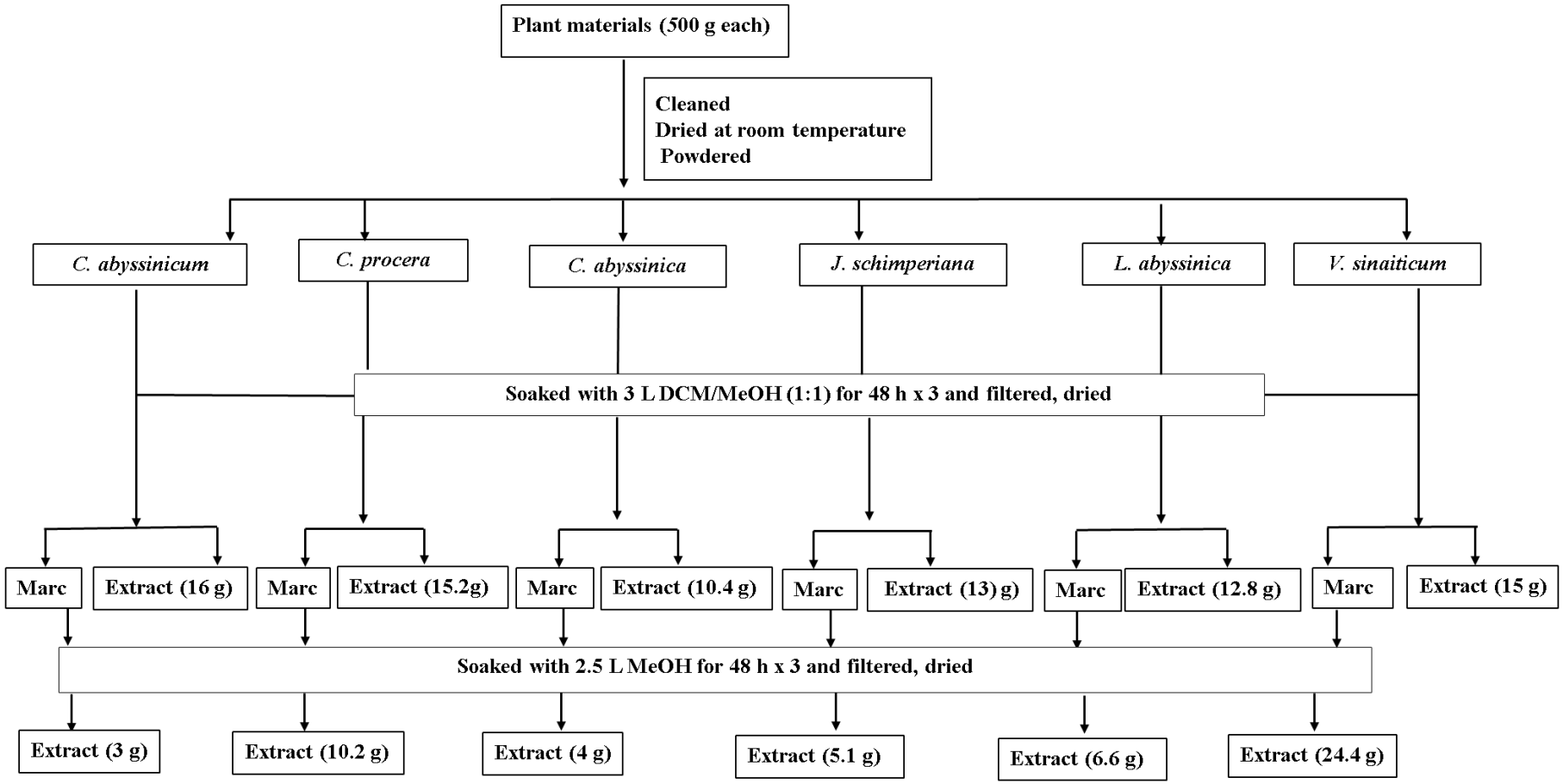

Scheme 1: General procedures for extractions of the plant samples.

3.3.2. Extraction and isolation of secondary metabolites from the roots of *C. abyssinicum*

The powdered roots of *C. abyssinicum* (500 g) were extracted as per the procedure described above (Scheme 1) to yield 16 g (3.2%) and 3 g (0.6%) reddish CH_2Cl_2/CH_3OH (1:1) and methanol crude extracts, respectively (Scheme 1). The crude extract of the roots of *C. abyssinicum* were analyzed using TLC (mobile phase *n*-hexane:EtOAc (7:3). Developed chromatograms were located by observation under short and long ultraviolet light at 254 nm and 360 nm, respectively. 14 g crude dichloromethane/methanol (1:1) extract was adsorbed on silica gel (14 g of silica gel, 60–200 mesh) to make a loading sample. The sample was subjected to silica gel column chromatography (200 g silica gel, 60 – 200 mesh), and the gradient elution method was used to run the column. The column was first eluted with *n*-hexane as the mobile phase, and the polarity of the mobile phase was increased gradually by adding ethyl acetate. After reaching 100% ethyl acetate, the elution was followed by methanol in dichloromethane (Scheme 2). A total of 111 fractions (50 mL each) were collected from the column, and each fraction was concentrated. The concentrated fractions were subjected to thin layer chromatography (TLC) to check homogeneity. Fractions that showed similar R_f values and the same characteristic color on TLC were combined and further purified to get the pure compounds. Combined fractions were dried in glass vials and their yields determined. Pure fractions were then kept at refrigerator for further analysis.

Fractions **10-14** (100 mg) were adsorbed on silica gel and chromatographed over silica gel (20 g). Elution was done using *n*-hexane first followed by hexane:EtOAc (9:1) to afford 21 subfractions (each 50 mL). TLC profile of subfractions **4-6** showed a single spot, which was identified as compound **223** (22 mg). Fractions **15-17** (600 mg) showed the presence of two spots on TLC (*n*-hexane: EtOAc 9:1) which were combined and further purified using column chromatography isocratic (100 % *n*-hexane) to afford 18 subfractions. Subfractions **2** and **6** showed a single spot each on TLC, identified as compounds **224** (12 mg), and **225** (13.5 mg), respectively. Fractions **18-24** (320 mg) were combined and shown to have two spots on TLC (mobile phase *n*-hexane/EtOAc 6.5:3.5) and further purified by column chromatography isocratic (6:4 hexane/EtOAc) to afford ten subfractions (each 50 mL). The TLC profile of the subfraction **6** showed a single spot on TLC, identified as

compound **226** (17 mg. Fractions **27-29** (4.5 % ethyl acetate in *n*-hexane as eluent) were combined and further purified using column chromatography (increasing gradient of ethyl acetate in *n*-hexane as eluent) to give compound **227** (90 mg). Fractions 35-37 (90 % ethyl acetate in n-hexane) were combined and given single spot-on TLC to give compound **228** (80 mg). Fractions 57-59 (0.5 % methanol in dichloromethane) were combined to give compound **229** (40 mg). Fractions 101-103 (4.5 % methanol in dichloromethane) were combined to give compound **230** (80 mg).

3.3.3. Extraction and isolation of secondary metabolites from the roots of *C. procera*

The powdered roots of *C. procera* (500 g) were extracted as per the procedure described above (Scheme 1) to afford 15.2 g (3.04%) and 10.2 g (2.04%) yellowish powder of CH_2Cl_2/CH_3OH (1:1) and methanol extracts, respectively (Scheme 1). The dichloromethane/methanol (1:1) extract of the roots of *C. procera* were analyzed using TLC (mobile phase *n*-hexane: EtOAc (9:1). Crude CH_2Cl_2/CH_3OH (1:1) extract (10 g) was adsorbed on equal mass of silica (10 g of silica, 60–120 mesh) to make a loading sample. The sample was subjected to silica gel column chromatography (200 g silica gel, 60 – 200 mesh) and the gradient elution method was used to run the column. The column was first eluted with n-hexane as the mobile phase, and the polarity of the mobile phase was increased by gradually adding ethyl acetate increments. After reaching 100 % ethyl acetate, the polarity was further increased with a gradient of methanol in dichloromethane. A total of 50 fractions (50 mL each) were collected separately and matched by TLC to check homogeneity. Fractions that showed similar R_f values and the same characteristic color on TLC were combined and crystallized using the methanol.

Fractions **13-14** (2.0g, mobile phase *n*-hexane/EtOAc 4:1) were combined and passed through Sephadex LH-20 (eluent CH_2Cl_2/CH_3OH, 1:1) to give **96** compound (27 mg). Fractions **15-16** (1.82 g) which showed the presence of two spots on TLC (*n*-hexane:EtOAc 4:1) which were combined and further purified using column chromatography (increasing gradient of ethyl acetate in *n*-hexane as eluent) to afford 20 subfractions. Subfractions 12-16 showed a single spot (*n*-hexane: EtOAc, 4:1, 490 mg) to give compound **82**. Fractions 18-19 (320 mg, mobile phase ($CHCl_3$:MeOH, 4.75:0.25) were combined and further purified using column chromatography isocratic to afford compound **87** (160 mL, 60 mg). Fractions 22-30 showed the presence of three spots on

TLC (*n*-hexane:EtOAc 4.75:0.25, 800 mg) and were further purified using column chromatography isocratic (100 % *n*-hexane) to afford 54 subfractions. Subfractions 7-11 showed a single spot (*n*-hexane: EtOAc 4:1) to give compound **231** (70 mg), subfractions 20-31 showed a single spot (*n*- hexane:EtOAc 3.5:1.5) to give compound **232** (120 mL, 60 mg).

Similarly, the methanol extract (10 g) was subjected to column chromatography silica gel with increasing gradient of ethyl acetate in *n*- hexane. A total of 152 fractions were collected. Fractions **6-7** (1.88 g) were adsorbed and chromatographed over silica gel (40 g) using *n*-hexane:EtOAc as eluent to afford twelve subfractions (each 50 mL). Subfractions 1-7 and 8-12 were collected using 100 % *n*-hexane and *n*-hexane:EtOAc (9:1), respectively. Subfractions 8-12 (800 mg) were combined and rechromatographed over silica gel (25 g) column chromatography and 18 subfractions were collected. The first three fractions were eluted using 100 % *n*-hexane and fractions 4-10 and 11-18 were eluted using *n*-hexane:EtOAc (9:1) and (8:2), respectively. The TLC profile of the fractions 1-3 (250 mg) was promising and hence subjected to Sephadex LH20 (eluent $CHCl_3$:MeOH (1:1) to afford ten subfractions (10 mL each). Subfractions 4-6 (70 mg) were similar, combined, and concentrated to give compound **97** (20 mg). Likewise, the other subfractions eluted using *n*-hexane:EtOAc (8:2) (subfraction 15-18, 96 mg) was applied on PTLC developed using hexane:EtOAc (8:2) as a mobile phase to afford two bands. Silica gel was filtered and the filtrate was concentrated and identified as a white solid to afford compounds **233** (9.8 mg). Fractions 19-28 (150 mg, 20 % EtOAc in hexane) were adsorbed and applied on a silica gel (10 g) column. Elution was done first with hexane and then hexane:EtOAc (8:2) of increasing polarities to afford fourteen subfractions. Upon TLC examination, Fr1-2 and Fr5 showed one spot each on TLC which were identified as compound **234** (12.6 mg) and **98** (6 mg)**,** respectively.

3.3.4. Extraction and isolation of secondary metabolites from the roots of *C. abyssinica*

The powdered roots of *C. abyssinica* (500 g) were extracted as per the procedure described above (Scheme 1) to yield 10.4 g (2.08%) and 4 g (0.8%) yellowish solid of CH_2Cl_2/CH_3OH (1:1) and methanol extracts, respectively (Scheme 1). The crude dichloromethane/methanol (1:1) roots extracts of *C. abyssinica* were analyzed using TLC (mobile phase *n*-hexane: EtOAc (7:3). The dichloromethane/methanol (1:1) extract (10 g)

was adsorbed on 10 g silica gel and subjected to silica gel column chromatography (200 g silica gel, 60 – 200 mesh) using *n*-hexane for packing. The column was eluted with increasing gradient of ethyl acetate in *n*-hexane, followed by methanol in dichloromethane to furnish a total of 182 fractions (50 mL each).

Fractions **14-15** (102 mg, mobile phase *n*-hexane/EtOAc 9:1) were combined and further purified by column chromatography (increasing gradient of ethyl acetate in *n*-hexane as eluent) to give **238** compound (24 mg). Fractions **16-19** (300 mg) showed the presence of two spots on TLC (*n*-hexane: EtOAc 8.5:1.5) which were combined and further purified using column chromatography isocratic to afford 25 subfractions. Subfractions **3-6** showed a single spot (*n*-hexane: EtOAc, 8.5:1.5, 20 mg) to give compound **239**. Fractions **22-34** (210 mg) showed the presence of two spots on TLC (*n*-hexane: EtOAc 8:2) were combined and further purified using column chromatography isocratic to afford 28 subfractions. Subfraction 14 showed a single spot (*n*-hexane: EtOAc 8:2) to give compound **240** (22 mg). Fractions **49-53** showed the presence of three spots on TLC (*n*-hexane: EtOAc 6.5:3.5, 120 mg) and were further purified using column chromatography isocratic to afford 22 subfractions. Subfraction **11** showed a single spot (*n*-hexane: EtOAc 6.5:3.5) to give compound **241** (20 mg). Fractions **54–69** (40 % ethyl acetate in *n*-hexane, 350 mg) contained mixtures and showed three major compounds when viewed under UV light at 254 nm, which were combined and afterward subjected to column chromatography, eluted with an increasing gradient of ethyl acetate in *n*-hexane to yield **79** (12 mg).

3.3.5. Extraction and isolation of secondary metabolites from the roots of *J. schimperiana*

The powdered roots of *J. schimperiana* (500 g) were extracted as per the procedure described above (Scheme 1) to afford 13 g (2.6%) and 5.1 g (1.02%) yellowish solid of CH_2Cl_2/CH_3OH (1:1) and methanol extracts, respectively (Scheme 1). The crude CH_2Cl_2/CH_3OH (1:1) extract of the roots of *J. schimperiana* were analyzed using TLC (Mobile phase *n*-hexane:EtOAc (7:3). Crude CH_2Cl_2/CH_3OH (1:1) extract (10 g) was adsorbed on equal mass of silica (10 g of silica, 60–120 mesh) to make a loading sample. The sample was subjected to silica gel column chromatography (100 g silica gel, 60 – 200 mesh) and the gradient elution method was used to run the column. The column was first eluted with n-hexane as the mobile phase, and the polarity of the mobile phase was

increased by gradually adding ethyl acetate increments. After reaching 100 % ethyl acetate, the polarity was further increased with gradient of methanol in ethyl acetate. A total of 69 fractions (50 mL each) were collected separately and matched by TLC to check homogeneity. Fractions that showed similar R_f values and the same characteristic color on TLC were combined and crystallized.

Fractions **3-7** (*n*-hexane:EtOAc 4:1, 210 mg) were combined and further purified using silica gel column chromatography with an increasing gradient of ethyl acetate in *n*-hexane to afford 15 subfractions. Subfraction **8** showed single spot (*n*-hexane: EtOAc, 8.5:1.5, 40 mg) to give compound **78**. Fractions **17–21** (*n*- hexane:EtOAc 6:4, 240 mg) were combined and further purified using column chromatography (increasing gradient of ethyl acetate in *n*-hexane) to give 13 subfractions. Subfractions 9 showed single spot (*n*-hexane: EtOAc 5:5, 16 mg) to give compound **242**. Fractions **38-44** (10 % methanol in dichloromethane, 145 mg) were combined and further purified using silica gel column chromatography (increasing gradient of methanol in dichloromethane) to give compounds **243** (11 mg) and **244** (13 mg). Fractions 47-51 (20 % methanol in dichloromethane, 240 mg) were combined and further purified using silica gel column chromatography (increasing gradient of methanol in dichloromethane) to give 13 subfractions. Subfractions 6-8, and 10-11 showed a single spot each (DCM:MeOH 4:1, 17 mg) to give compounds **245** and **246**, respectively.

3.3.6. Extraction and isolation of secondary metabolites from the roots of *V. sinaiticum*

The ground roots of *V. sinaiticum* (500 g) were extracted by maceration with a *n*-hexane, CH_2Cl_2:CH_3OH (1:1), and with CH_3OH (3 L) three times for 48 hours in each case, with occasional shaking on a machine shaker to afford 4.0 g (0.7%), 15.6 g (2.78%), and 24.4 g (4.4%) black jelly extracts, respectively (Scheme 1). The CH_3OH extract (20 g) of *V. sinaiticum* was loaded over silica gel column chromatography to fractionate using hexane for packing followed by hexane: EtOAc, and EtOAc: CH_3OH mixtures to furnish ninety-six fractions (50 mL each). Fractions 17-19 (5% CH_3OH in CH_2Cl_2, 240 mg) were combined and purified with column chromatography isocratic (100% CH_2Cl_2) to yield compound **247** (21 mg). Fractions **26-36** (10% CH_3OH in CH_2Cl_2, 600 mg) contained mixtures and were adsorbed and chromatographed over silica gel (20 g). Elution was done

using CH_2Cl_2 to afford 38 subfractions (each 10 mL). The TLC profile of subfractions **18-21** showed a single spot, which was identified as compound **248** (18 mg). Subfractions **25-32** (180 mg) showed the presence of three spots on TLC (5% CH_3OH in CH_2Cl_2) which were combined and further purified using column chromatography isocratic (100% CH_2Cl_2) to afford 14 subfractions. Subfractions **7** and **9** showed a single spot each on TLC, identified as compounds **249** (14 mg), and **250** (26 mg), respectively. Fractions **38-52** (20% CH_3OH in CH_2Cl_2, 840 mg) were combined and purified using column chromatography (increasing gradient of CH_3OH in CH_2Cl_2) to afford compound **251** (36 mg), and compound **252** (28 mg). Fractions **46-58** (25% methanol in dichloromethane, 320 mg) were combined and purified using column chromatography (increasing gradient of methanol in dichloromethane) to provide compounds **253** (34 mg), and **230** (110 mg).

3.3.7. Extraction and isolation of secondary metabolites from the roots of *L. abyssinica*

The powdered roots of *L. abyssinica* (500 g) were extracted as per the procedure described above (Scheme 1) to afford 12.8 g (2.56%) and 6.6 g (1.32%) light green of CH_2Cl_2/CH_3OH (1:1) and methanol extracts, respectively (Scheme 1). The CH_2Cl_2/CH_3OH (1:1) extract (10 g) of *L. abyssinica* was adsorbed and subjected to silica gel column chromatography using *n*-hexane for packing. Gradient elution was done using *n*- hexane, *n*-hexane: EtOAc, and EtOAc: MeOH to furnish fifty-one fractions (50 mL each), volume of eluent is missing. Fractions **11-17** (20% ethyl acetate in *n*-hexane, 160 mg) contained mixtures and showed three major compounds when viewed under UV light at 254 nm, which were combined and afterward subjected to column chromatography, eluted with increasing gradient of ethyl acetate in *n*-hexane to yield **254** (8 mg), and **255** (6 mg).

3.3.8. Extraction of essential oils from different parts of studied medicinal plants

Powdered (100 g each) bulbs of *C. abyssinicum*, roots, and leaves of *J. schimperiana,* flowers, leaves, and seeds of *C. procera,* roots, and leaves of *V. sinaiticum,* aerial parts of *C. abyssinica*, roots, and seeds of *L. abyssinica* were separately transferred into a round bottom flask with 1 L distilled water and then subjected to hydrodistillation using a Clevenger apparatus each for 3 h (Scheme 2). The distillate was poured into the separatory funnel with 100 mL of chloroform. The essential oil was consecutively separated from the aqueous layer repeatedly. The organic layer was dried over anhydrous Na_2SO_4 and filtered,

then transferred into small vials and the yield was calculated. The essential oils were stored at 4°C in the refrigerator for further analysis. The yield extract was calculated as follows (Eq. 1).

$$\text{Yield Extract (\%)} = \frac{\text{Extract Obtained (g)}}{\text{Mass of Sample}} \times 100 \quad (1)$$

3.3.8.1. GC-MS analysis of the essential oils

Gas Chromatography-Mass Spectrometry (GC-MS) analyses were carried out using an Agilent Technologies (Santa Clara, CA, USA) equipped with a 7890 N network GC system, 5977 inert mass selective detector, 7683B series autosampler injector (10 µL in size), G1701DA GC/MSD Chem Station and HP5MS column (30 m length × 0.25 mm internal diameter × 0.25 µm film thickness) coated with 5% phenyl 95% methyl poly siloxane for analyzing the samples. 2 µL essential oil solutions was injected through autosampler and analyzed with HP5MS column. Gas chromatography condition: the temperature program was 60ºC for 1 min, rising by 4.0ºC min^{-1} to 240ºC and held for 1 min. A diluted sample in chloroform (2 µL) was injected, and the injector and detector were held at 210ºC. The total run-time was 47 min. The mass spectra transfer line temperature was 280°C. The carrier gas was helium (1 mL/min) with a split ratio equal to 100:1. Mass spectra were recorded by electron ionization (EI) at 70 eV. All spectra were scanned from *m*/*z* 40–450 range. The essential oils chemical components were identified via searches through the mass-hunter libraries W9N11.L, NIST11.L., retention time, peak area, and by their linear retention indices, which were determined by injecting a homologous hydrocarbon series (C7–C31) and compared with previously reported data (Al-Rowaily *et al*., 2020).

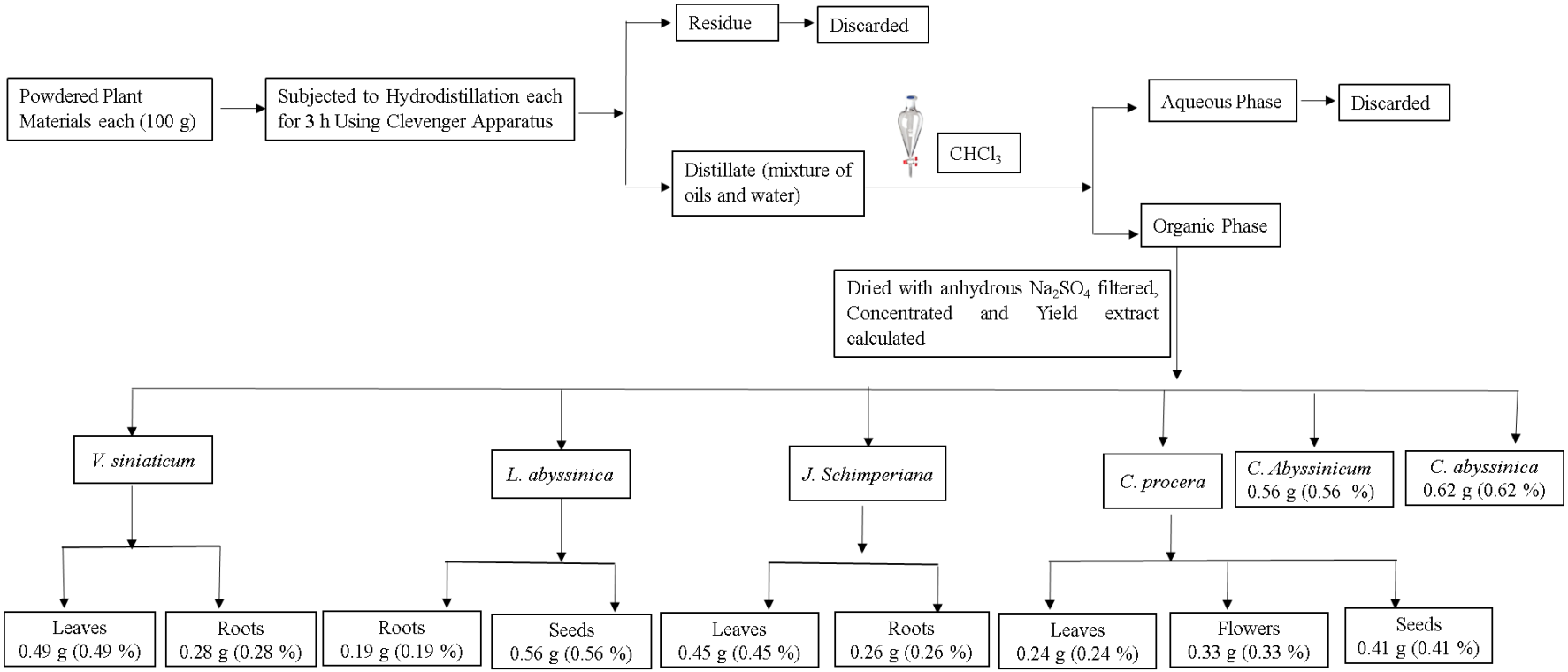

Scheme 2: General procedures of extractions of essential oils.

3.4. Biological activities

3.4.1. Antimicrobial study

3.4.1.1. Broth microdilution MTT assay

The *in vitro* antibacterial activity of the essential oils extracted from the bulbs of *C. abyssinicum*, aerial parts of *C. abyssinica,* leaves, flowers, and seeds of *C. procera*, roots, seeds of *L. abyssinica*, leaves, and roots of *J. Schimperiana*, and *V. sinaiticum,* the DCM: MeOH (1:1), and methanol root extracts of *J. Schimperiana*, and *V. sinaiticum* were evaluated by using the broth dilution method against *Staphylococcus aurous* (ATCC 25923), *Streptococcus agalactiae* (ATCC 12386), *Enterococcus faecalis* (ATCC 29212), *Escherichia coli* (ATCC 25922), *Pseudomonas aeruginosa* (ATCC 27853), *Klebsiella pneumoniae* (ATCC 700603), and fungal cultures used in this study was *Trichophyton mentagrophytes* (ATCC 18748), *Trichophyton rubrum* (ATCC 28188), *Candida albicans* (Clinical isolate) strains were used. The *invitro* antimicrobial activities of all samples were tested in Traditional and Modern Medicine Research Directorate, Ethiopian Public Health Institute, Addis Ababa, Ethiopia.

A microdilution method in 96-well plates, using Mueller-Hinton broth media (for bacteria) and Sabouraud dextrose broth (for fungi), was performed so as to work out minimum inhibitory concentrations. The tested essential oils, crude extract, and isolated compounds were dissolved in 5% Tween 80 in distilled water V/V dilution preparations to prepare a stock solution each sample. A 100 µL of Muller Hinton broth/Sabouraud dextrose broth was added into each well of the 96-well microplates. 100 µL of the essential oils, crude extract, and isolated compounds positive controls (ciprofloxacin (20 µg/mL) for bacteria, ketoconazole (100 µg/mL) and amphotericin B (100 µg/mL) for fungi, negative control (5% tween 80), and sterility control (Mueller-Hinton broth media (for bacteria) and Sabouraud dextrose broth (for fungi) was introduced into the first wells of row A of a 96-well plate and was ready for serial dilution. Thus, row A in columns 1-12 had 200 µL which contain the tested essential oil extracts, crude extract, and isolated compounds, ciprofloxacin, ketoconazole, amphotericin B, and broth alone in a separate micro-plate hole. A multichannel micropipette was used to do systematic twofold serial dilutions through columns 1 to 12 (starting from rows B–H). After proper mixing, 100 µL was removed from the starting concentrations (columns 1-12 in row A) and transferred to the next

row with the 100 µL broth, and the procedure was repeated up to the last row (H) where the last 100 µL was discarded. The refreshed strain was used to prepare the inoculum, following the guidelines set by both the Clinical and Laboratory Standards Institute (CLSI) and Eloff. To standardize, extract 3-5 inoculums from a new, uncontaminated culture of the test organism and mix them with Mueller-Hinton broth or Sabouraud dextrose broth to create a suspension. The absorbance of the prepared suspension was read by UV-visible spectrophotometer (Thermo Scientific Evolution 60s CAT840210100) with a 1 cm light path till obtained an absorbance reading of 0.08 to 0.1 at 625 nm which is proportional to $1x10^8$ CFU/mL bacteria and $1x10^7$ spores/mL fungi. Then, these suspensions were further diluted to $5x10^5$ CFU/mL bacteria and $5x10^4$ spore/mL fungi which were used to evaluate the MIC value of the essential oils. After that, each test and growth control were inoculated with 100 µL of standardized suspensions of tested microorganisms whereas only broth was added into the sterility column. The microdilution trays were incubated at 37ºC for 18-24 h for bacterial strains and at 25ºC for fungal strains for up to 7 days. 18-24 h. Then, 40 µL of MTT, 2,3,5 Triphenyltetrazolium chloride (TTC; Tetrazolium chloride), was added into all 96 well plates as an indicator of microbial growth and incubated at 37ºC for 30 min. After 30 min of incubation, the lowest concentration of each essential oil extract, crude extract, and isolated compounds with a disappearing purple color observed was considered as the MIC value of bacterial/fungal strains in the MTT broth assay (Ohikhena *et al*., 2017). Sterility and growth controls well were also studied for each strain. In order to determine the susceptibility of the bacteria/fungi, positive control experiments were conducted in parallel. A negative control experiment was also conducted using 5% tween 80.

3.4.1.2. Disc diffusion method

The DCM:MeOH (1:1), methanol and the isolated compounds from root extracts of *C. abyssinicum, Calotropis procera, Caylusea abyssinica,* and *Lagenaria abyssinica* were evaluated *in vitro* for antibacterial activity by using the disc diffusion method against two-Gram positive bacteria (*Staphylococcus aureus* (ATCC 25923)*, Streptococcus pyogenes* (ATCC 19615)) and two Gram-negative bacteria (*Pseudomonas aeruginosa* (ATCC 27853), *Escherichia coli* (ATCC 25922)) standard bacterial strains (American Type Culture Collection (ATCC)) were used. The antibacterial activities of all samples were tested in Oromia Public Health Research, Capacity Building and Quality Assurance Laboratory Center, Adama, Ethiopia.

A nutrient agar medium was used for the activation of bacteria. All bacterial test organisms were inoculated into blood agar base enriched with 5% sterile sheep blood. Active cultures for experiments were prepared by transferring a loopful of cells from the stock cultures to test tubes of Mueller-Hinton broth and autoclaved and cooled. 2–3 well isolated colonies of the same morphological type of each bacterial strain were picked up by wire loop from fresh agar plates of bacterial culture and aseptically transferred into pre-labeled test tubes containing the sterile nutrient broth and then incubated for about six hours. The turbidity of the inoculum tube was adjusted visually by either adding colonies or by adding sterile normal saline solution to that of the already prepared 0.5 McFarland standard which is assumed to contain a bacterial concentration of $1x10^8$ CFU/ml.

The sterilized Muller Hinton Agar was poured into sterile Petri plate. The plates were shaken gently to allow evenly mixing of bacterial cells and agar. After the agar solidified, fresh culture of test organisms of bacteria was swabbed uniformly over the surface of agar plates using sterile cotton swab. The plated medium was then allowed to dry at room temperature for 30 min. In each petri dish equidistant bores were made with 6 mm diameter using sterile gel puncher. All the extracts were dissolved in DMSO and adjusted to a concentration of 250 and 125 mg/mL. 20 µg from each dilution, including the positive and negative controls, was loaded onto separate paper discs, followed by putting the discs onto the Petri plates containing the bacterial culture-inoculated MHA, and incubating at 37°C for 18 to 24 h. Ciprofloxacin was used as positive control. After overnight incubation at 37°C, zones of inhibition around the disc were observed. Clear inhibition zones formed around the discs indicated the presence of antibacterial activity. The resulting diameters of zones of inhibition produced by the plant extracts and standard antibiotics were measured using a ruler and reported in millimeter (mm). The mean of zones of inhibition was calculated for each extract and the standard antibiotics. The results are expressed as M ± SEM of triplicate.

3.4.2. Radical scavenging activity of the extracts and isolated compounds

The DPPH radical scavenging activities of the extracts and isolated compounds were evaluated using DPPH assay following procedure (Rivero-Perez *et al*., 2007). Serial dilutions were carried out with the stock solutions 0.5 mg mL^{-1} of the plant extract and its constituents to obtain

concentrations of 200, 100, 50, 25, and 12.5 µg mL^{-1}. The solutions were prepared using methanol as solvent. 4 mL from each four diluted concentrations of the samples were mixed with 1 mL of 2,2-diphenyl-1-picryl hydrazyl (DPPH) solution that was prepared by dissolving 4 mg of DPPH in 100 mL of MeOH. The resulting solution was placed in an oven at 37°C for 30 min and subjected to UV-Vis's spectrophotometer to record absorbance at 517 nm. The percentage DPPH inhibition calculated according to the following formula (Eq. 2) (Proestos *et al*., 2013).

$$(\%)\ \text{inhibition} = \frac{(A_{control} - A_{sample})}{A_{control}} \times 100 \qquad (2)$$

Where $A_{control}$ was the absorbance of the DPPH solution and A_{sample} was the absorbance of a tested sample. Samples were analyzed in triplicate. Ascorbic acid was used as positive control.

3.4.3. *In vitro* antidiabetic activity

The antidiabetic property of the *n*-hexane, DCM: MeOH (1:1), and methanol root extracts of *C. procera*, *C. abyssinica, C. abyssinicum*, *L. abyssinica,* and *J. schimperiana* were evaluated using *In vitro* α-amylase inhibitory assay. The antidiabetic activities of all the extracts were tested at Saveetha Institute of Medical and Technical Sciences (SIMATS), Saveetha University, Chennai. The pancreatic porcine α-amylase assay was adapted with modifications (Parmar & Rupasinghe, 2015). Briefly, the test extracts, enzyme, and soluble starch were dissolved in 20 mM sodium phosphate buffer containing 6 mM NaCl (pH 6.9). The test extracts at different concentrations were dissolved in the buffer solution. To a test tube, 250 µL of pancreatic porcine α-amylase (1 U/mL, dissolved in the buffer (pH 6.9) and 100 µL of test extract at a concentration ranging from 1.25 to 10 mg were added. The mixture was pre-incubated at 37°C for 15 min, before the addition of 250 µL of 0.5% starch. The mixture was then vortexed and incubated again at 37°C for 15 min followed by the reaction termination using 1 mL of dinitro salicylic acid color reagent. The tubes were placed in a boiling water bath for 5 min, cooled to room temperature, and diluted. Two hundred µL of the reaction mixture were taken into a 96-well clear plate, and the absorbance was read at 540 nm using the plate reader. The control α-amylase at 1 U/mL without any inhibitor represented 100% enzyme activity. Appropriate test extract controls containing the reaction mixture except the enzyme were used to correct for the color inter*f*erence. A known α-amylase inhibitor, acarbose was used for comparison studies. The percentage inhibition of the test sample on α-amylase was calculated using (Eq. 3) below:

$$(\%)\ \text{inhibition} = \frac{(\text{Absorbance of control} - \text{Absorbance of sample})}{\text{Absorbance of control}} \times 100 \quad (3)$$

3.4.4. *In vitro* cytotoxicity assay

In the present study, *in vitro* cytotoxicity of DCM/MeOH (1:1), and methanol root extracts of *C. procera*, *C. abyssinica, C. abyssinicum*, and *L. abyssinica*, *n*-hexane, DCM/MeOH (1:1), and methanol leaves extract of *J. schimperiana* against breast cancer cell lines Michigan Cancer Foundation-7 (MCF-7) were evaluated. The breast cancer cell lines MCF-7 were obtained from National Centre for Cell Science (NCCS), Pune, India.

3.4.4.1. Cell viability assay

Cell viability was measured using the MTT assay. The assay detects the reduction of yellow colored MTT by mitochondrial dehydrogenase to purple formazan product, which reflects the normal function of mitochondria and cell viability using MTT assay (Holst & Brünner, 1998).

3.4.4.2. Cell lines and culture

The MCF-7 cells were cultured in a T25 culture flask containing Dulbecco's Modified Eagle Medium (DMEM) containing DMEM supplemented with 10% FBS and 1% antibiotics (100U mL^{-1} penicillin and 100µg mL^{-1} streptomycin). The cells were incubated at 37°C in 5% CO_2 atmosphere. Upon reaching confluence, the cells were detached using Trypsin–EDTA solution and were seeded at a density of 5000 cells per well. At 50% confluence, the culture medium was aspirated and the cells were treated with 20 µg of plant extract in DMSO (20 µL) for 24 h at 37°C in the CO_2 incubator. Later cells were incubated with MTT (4 mg mL^{-1}) for 3 hours. The absorbance was measured at 540 nm with a standard microplate reader. The percentage of viable cells is directly proportional to the level of formazan produced. Therefore, the higher the measured absorbance, the more viable the cells are present. The cell viability was expressed as the percentage of cytotoxicity (% cytotoxicity). The results are presented as the mean of triplicate experiments. The cell viability is calculated using (Equ. 4) below.

$$\%\ \text{Cell viability} = \frac{\text{Absorbance of sample}}{\text{Absorbance of control}} \times 100 \quad (4)$$

3.4.5. *In vitro* anti-acanthamoeba activity of extracts

The DCM: MeOH (1:1), and methanol root extracts of *C. abyssinicum, J. schimperiana* and *V. sinaiticum* were evaluated invitro for anti-*Acanthamoeba* activity against *Acanthamoeba triaugularis* and *castellanii*. The anti-*Acanthamoeba* activities of extracts were tested at Walailak University, Nakhon Si Thammarat-Thailand.

3.4.5.1. Cultivation of *A. triangularis*

A. triangularis WU19001, a strain from the recreational reservoir at Walailak University, Nakhon Si Thammarat-Thailand and *A. castellanii* ATCC50739 (reference pathogen strain) were used in this study. The parasite was grown in protease-peptone yeast glucose (PYG) medium (20 g protease peptone, 2 g yeast extract, 0.98 g $MgSO_4 \cdot 7H_2O$, 0.35 g $Na_2HPO_4 \cdot 7H_2O$, 0.34 g KH_2PO_4, 0.02 g $(NH4)_2Fe(SO_4)_2 \cdot 6H_2O$, 18 g glucose). The trophozoites were observed after 72 h of incubation at room temperature. Trophozoites were centrifuged at 4000 rpm for 5 min and re-suspended in fresh PYG thereafter. For counting, 50 µL of cell suspension was mixed with 50 µL of trypan blue. Viability was investigated under the inverted microscope based on the principle of the dye can cross the membrane of dead cells with blue color, but not in the tact membrane of viable cells with colorless appearances.

3.4.5.2. Screening

The extract (final concentration of 2 mg/mL) were screened for their anti-*Acanthamoeba* activity by the dilution method in a 96-well polystyrene microtiter plate. The stock solutions (100 mg/mL) of extracts were diluted to 4 mg/mL with PYG medium. Then, 100 µL of the extract was transferred to each well. The aliquot of 100 µL (2×10^5 trophozoites/mL) trophozoites were added to give a final concentration (2 mg/mL) and incubated at 25°C for 24 h. The relative percentage of parasite viability was defined as (mean of the treated parasite/mean of the control) × 100.

3.4.6. *In vitro* antiviral activities assays

Cytotoxicity assay

The microtetrazolium test (Mossman, 1983) was used to study the cytotoxicity of the extracts. Briefly, series of three-fold dilutions of each extract in MEM (3.7 – 300 µg/mL) were prepared. MDCK cells were incubated for 48 h at 36°C in 5% CO_2 in the presence of the dissolved specimens. The cells were washed twice with phosphate-buffered saline (PBS), and a solution of 3-(4,5-dimethylthiazolyl-2) 2,5-diphenyltetrazolium bromide (ICN Biochemicals Inc. Aurora, Ohio) (0.5 µg/mL) in PBS was added to the wells. After 1 h incubation, the wells were washed and the formazan residue was dissolved in DMSO (0.1 mL per well). The optical density in the wells was then measured on a Thermo Multiskan FC plate reader at the wavelength of 540 nm and plotted against the concentration of extracts. Each concentration was tested in three parallels. The 50% cytotoxic concentration (CC_{50}) of each extract was calculated from the data obtained.

Cytoprotection assay

The extracts were dissolved in 0.1 mL DMSO to prepare stock solutions, and final serial solutions (300 – 3.7 µg/ml) were prepared by adding MEM with 1 µg/mL trypsin. Extracts were incubated with MDCK cells for 1 h at 36°C. Each concentration of the extracts was tested in triplicate. The cell culture was then infected with influenza virus A/Puerto Rico/8/34 (H1N1) (moi 0.01) for 48 h at 36°C in the presence of 5% CO_2. After this, cell viability was evaluated by MTT assay as described above. Based on the results of photometry, 50% inhibiting concentration (IC_{50}), the concentration that provided protection of 50% cells comparing to the wells without extracts, was calculated for each extract as well as the selectivity index (SI, the ratio of CC_{50} to IC_{50}). For calculations, GraphPad Prism software was used.

3.5. Computational studies

Computational advances played a significant influence on the drug development process. Virtual screening approaches are frequently and widely utilized to minimize the cost and time of drug development. Molecular docking is a technique that is used to discover novel ligands for protein structure and plays a significant role in structure-based drug design (Kitchen *et al*., 2004). The relationship between the compounds and the receptor plays a vital role in the formulation of drugs. Natural products can help cure a wide variety of human ailments, and various medicines

are derived from natural products. Plant-based medicines are the best potential options, given the rise of drug resistance in various diseases, and the negligible side effects of traditional treatments (Khan *et al*.,2019).

3.5.1. *In silico* molecular docking methodology

3.5.1.1. Preparation of ligands

The isolated compounds' 2D structures (mol) were drawn and individually examined using ChemDraw 16.0. ChemBio3D was used to minimize each molecule's energy. Each molecule's 3D coordinates (PDB) were obtained using an optimized structure.

3.5.1.2. Preparation of macromolecules

The crystal structure of receptor molecules *E. coli* DNA gyrase B (PDB ID:7P2W), *S. aureus* Gyrase (PDB ID: 2XCT), Human Myeloperoxidase (PDB ID: 1DNU), N-Terminal Domain of PqsA in a complex with 6-Fluoroanthraniloyl-AMP (PDB ID: 5OE3), and Human Topoisomerase IIα (PDB ID: 4fm9) were downloaded from the protein data bank. The protein preparation was done using the reported standard protocol (Narramore *et al*., 2019), by removing the co-crystallized ligand, selected water molecules, and cofactors, the target protein file was prepared by leaving the associated residue with protein by using Auto Preparation of target protein file Auto Dock 4.2 (MGL tools 1.5.6).

3.5.1.3. AutoDock vina analysis

The graphical user interface program AutoDock 4.2 was used to set the grid box for docking simulations. The grid was set so that it surrounds the region of interest in the macromolecule. The docking algorithm provided with AutoDock Vina was used to search for the best-docked conformation between ligand and protein. During the docking process, a maximum of nine conformers were considered for each ligand. The conformations with the most favorable (least) free binding energy were selected for analyzing the interactions between the target receptor and ligands by Discovery studio visualizer and PyMOL. AutoDock vina with the standard protocol was used to dock the protein *S. aureus* Gyrase (PDB ID 2XCT), Human Topoisomerase IIα (PDB ID: 4fm9), human myeloperoxidase (PDB ID 1DNU), N-Terminal Domain of PqsA in a Complex with 6-Fluoroanthraniloyl-AMP (PDB ID 5OE3), *E. coli* Gyrase B (PDB ID 7P2W) and isolated ligands into the active site of proteins. The molecular docking studies were carried

out using AutoDock Tools (ADT) (Trott & Olson, 2010), which is a free graphic user interface (GUI) for the AutoDock Vina program. The grid box was constructed using 20x20x20, pointing in x, y, and z directions, respectively, with a grid point spacing of 0.375 Å. The center grid box dimensions in XYZ directions are 2.871680, 43.536320, 68.838000 for 2XCT; 150.488431, 142.615272, 136.949942 for 6SJ6; 27.535650, 2.689234, 13.523397 for 1DNU; 29.091339, 22.861116, 30.062947 for 5OE3; -28.158905, 7.244000, 0.816190 for 7P2W, -3.637000, 18.277000, 4.822000 for 6ORI; 28.158905, 7.244000, 0.816190 for 6F86. Nine different conformations were generated for each ligand scored using AutoDock Vina functions and were ranked according to their binding energies. The ligands are represented in a different colour, H-bonds, and the interacting residues are represented in stick model representation.

3.5.2. *In silico* pharmacokinetics (drug-likeness) properties of the isolated compounds

To assess the effectiveness of drugs in the human body, their bioavailability and pharmacokinetic properties, including absorption, distribution, metabolism, and excretion, must be screened and evaluated. In order to determine in-silico pharmacokinetic parameters such as the number of hydrogen donors, hydrogen acceptors, and rotatable bonds, as well as the overall polar surface area of a substance, the structures of isolated compounds are transformed into their canonical simplified molecular-input line-entry systems (SMILEs) (Ibrahim *et al*., 2021). The chosen ligands' SMILES were used as input data and submitted to the SwissADME tool and PreADMET online server. The computer program merged information from various Log P and S prediction programs. This allowed for a comprehensive analysis of the molecules' combined hydrophilicity and lipophilicity. The drug-likeness of the isolated compounds was predicted using Lipinski's Rule of 5 (Lipinski *et al*., 1997; Lipinski, 2000). The establishment of this rule was intended to establish guidelines for the drug-likeness of new molecular entities (NMEs) (Lipinski, 2000). The effectiveness of drug absorption is influenced by various factors, including the drug's water solubility, whether it is a P-glycoprotein substrate, its skin permeability levels (log Kp), Gastro-Intestinal absorption (GSI), and membrane permeability. The distribution of drugs is influenced by the blood-brain barrier (BBB), while excretion is dependent on total clearance and renal OCT2 substrate (Mahanthesh *et al*., 2020: Han *et al*., 2019). CYP models were utilized to assess the volume of distribution and metabolism, including inhibitors for CYP1A2, CYP2C19, CYP2C9, and CYP3A4.

3.5.3. *In silico* prediction of toxicity of isolated compounds

The potential toxicity of individual compounds was assessed using ProTox-II servers to determine various toxicological endpoints such as hepatotoxicity, carcinogenicity, immunotoxicity, and mutagenicity. Additionally, the servers were used to categorize the compounds based on their toxicity class and determine the level of toxicity measured in LD_{50} (mg/Kg) (Banerjee *et al*., 2018; Drwal *et al*., 2014). The compounds organ toxicities and toxicological endpoints of the isolated compounds were predicted using PreADMET and OSIRIS Property (Oduselu *et al*., 2019). The selection of compounds as drug candidates were determined by a parameter called drug score. The higher the drug score value, the higher the compound's chance is considered a drug candidate (Behrouz *et al*., 2018). The results were compared to ciprofloxacin, which is a standard clinical drug.

3.6. Statistical data analysis

Antidiabetic, cytotoxicity, antimicrobial, and antioxidant data obtained by triplicate measurements were reported as mean ± standard error of the mean (SEM). GraphPad Prism version 8.0.2 for Windows was established to perform the analysis. Groups were analyzed for significant differences using a linear model of variance analysis (ANOVA) test for comparisons was performed.

CHAPTER FOUR

4. RESULTS AND DISCUSSION

4.1. Secondary metabolites isolated from the studied medicinal plants

During the course of this study, silica gel column chromatographic separation of the extracts of six selected medicinal plants gave a total of **thirty-seven** compounds categorized as fatty acids, fatty acids esters, steroids, ursane-type triterpenoids, flavonoids, stilbenoids, iridoids glycosides, and others. The structures of the isolated compounds were characterized by UV-Vis, IR, ^{1}H NMR, ^{13}C NMR, DEPT-135, COSY, HSQC, HMBC techniques as well as comparison with literature data.

4.1.1. Secondary metabolites isolated from the roots of *C. abyssinicum*

The dichloromethane/methanol (1:1) extract of the roots of *C. abyssinicum* was subjected to silica gel column chromatography fractionation which afforded eight compounds **223**-**230**. All isolated compounds were reported herein for the first time from *C. abyssinicum*. The detailed characterizations of these compounds are presented below.

Compound **223** was obtained as a yellow oil with an R_f value of 0.40 (*n*-hexane/EtOAc (9:1), as eluent. Its ^{1}H NMR spectrum (400 MHz, $CDCl_3$, Appendix 1A) showed signals at δ 2.3 (t, J = 7.1 Hz, 2H, H-2), δ 5.4 (m, 1H, H-7) and δ 0.9 (t, J = 6.8 Hz, 3H, H-18) attributed to methylene protons attached to a carboxyl group, olefinic proton, and terminal methyl protons, respectively. The ^{13}C NMR (100 MHz, $CDCl_3$, Appendix 1B) spectral data with the aid of DEPT-135 (Appendix 1C) revealed a total of 18 carbon signals of which two olefinic methine signals at δ 130.0, and 127.9, and fourteen methylene signals at δ 34.0, 31.9, 29.7, 29.6, 29.5, 29.4, 29.3, 29.3, 29.2, 29.1, 27.2, 25.6, 24.7 and 22.7 are clearly evident. The most downfield and upfield signals appearing at δ 179.9 and 14.1 attributed to the carboxyl group and terminal methyl, respectively. The above spectral data are in good agreement with data reported for (*E*)-Octadec-7-enoic acid, previously reported from the roots of *C. procera* (Ibrahim *et al*., 2012).

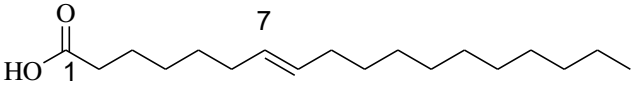

223

Compound **224** was isolated as white crystals, melting point of 79-81 ºC, with an R_f value of 0.5 (10 % EtOAc in *n*-hexane) as eluent on TLC. The ^{1}H-NMR spectrum (400 MHz, $CDCl_3$, Table 7, Appendix 2A) of compound **224** revealed the presence of six methyls at δ 0.75 (3H, *s*), 0.9 (s, 3H), 1.0 (d, J = 6.6 Hz, 3H), 0.84 (d, J = 6.2 Hz, 3H), 0.81 (d, J = 6.8 Hz, 3H), and 0.8 (t, J = 7.7 Hz, 3H). The spectrum also showed the singlet olefinic proton signal at δ 5.8 (*s*, 1H). The presence of a singlet peak in the olefinic proton indicated the absence of proton(s) on the adjacent carbon atom(s) suggesting the presence of adjacent sp^2 quaternary carbon. Other proton signals integrating for 29 hydrogens were observed in the range δ 2.40 to 1.00. The proton decoupled ^{13}C-NMR and DEPT-135 spectra ($CDCl_3$) (Appendix 2B, and 2C) revealed the presence of 29 well resolved carbons, including a conjugated ketone carbonyl group at δ 200.1, one olefinic carbon at δ_C 123.7, one olefinic quaternary carbon δ_C 172.2, two quaternary aliphatic carbon at δ 42.4 and 38.6, eleven methylene groups at δ 35.7, 34.0, 33.0, 32.1, 21.0, 39.6, 24.2, 28.2, 33.9, 26.0, and 23.1, seven aliphatic methine groups at δ 35.6, 53.8, 55.9, 56.0, 36.1, 45.8 and 29.1, six methyl groups at 12.0, 17.4, 18.7, 19.0, 19.9, and 12.0. The ^{13}C NMR spectral data were compared with those previously reported in the literature for stigmast-4-en-3-one (Nurlelasari *et al*., 2017; Udobre *et al*., 2015, Table 7).

Table 7: ^{1}H NMR (400 MHz, $CDCl_3$) and ^{13}C NMR (101 MHz, $CDCl_3$) data of compound **224** and literature ^{13}C-NMR data of stigmast-4-ene-3-one.

Position	Compound **224**		Nurlelasari *et al*., 2017	Udobre *et al*., 2015
	^{1}H-NMR	^{13}C-NMR	^{13}C-NMR	^{13}C-NMR
1		35.7	35.64	35.0
2		34.0	34.00	33.5
3		200.1	199.7	199.0
4	δ 5.8 (*s*, 1H)	123.7	123.7	123.0
5		172.2	171.7	171.0
6		33.0	32.9	32.7
7		32.1	32.1	32.4
8		35.6	35.7	35.0
9		53.8	53.8	53.0
10		38.6	38.6	38.0
11		21.0	21.0	21.8
12		39.6	39.6	39.0
13		42.4	42.4	42.0
14		55.9	55.8	55.0
15		24.2	24.2	24.0
16		28.2	28.2	27.9

17		56.0	56.2	55.1
18	δ 0.75 (3H, *s*)	12.0	11.9	11.2
19	δ 0.9 (3H, *s*)	17.4	17.4	17.7
20		36.1	36.1	35.9
21	1.0 (d, J = 6.6 Hz, 3H)	18.7	18.7	17.5
22		33.9	33.9	32.3
23		26.0	26.1	24.4
24		45.8	45.8	45.0
25		29.1	29.2	28.2
26	0.84 (d, J = 6.2 Hz, 3H)	19.0	19.0	18.3
27	0.81 (d, J = 6.8 Hz, 3H)	19.9	19.8	19.0
28		23.1	23.1	23.1
29	0.8 (t = 7.7 Hz, 3H)	12.0	11.9	11.5

Accordingly, compound **224** was identified as a stigmast-4-en-3-one and was reported for the first time from this species, having been previously reported from the bark of *Chisocheton lasiocarfus*, and stem bark of *Nauclea latifolia*.

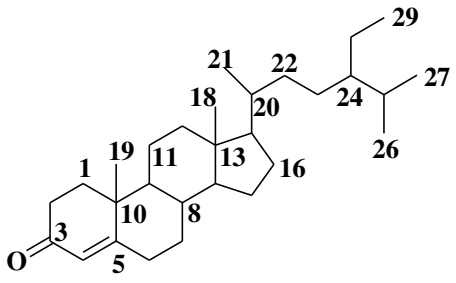

224

Compound **225** was obtained as a yellow oil with R_f value of 0.42 with *n*-hexane:EtOAc (9:1) as a mobile phase. The ^{1}H-NMR spectroscopic data (400 MHz, $CDCl_3$, Table 8, Appendix 3A) varied between δ 0.9 to 5.3. The triplet signal observed at δ 2.3 is attributed to methylene protons attached to a carboxyl group. The multiplet signal at δ 2.0 (m, 2H) are integrated for the allylic methylene protons. The signal showed at δ 2.8 attributed to the methylene protons flanked between the two double bonds. The intense broad singlet signal due to many overlapping methylene protons was observed at δ 1.3 which was supported by the appearance of an intense carbon signal at δ 29.7 in the ^{13}C-NMR spectrum. The spectrum showed signals for olefinic proton at δ 5.3 (*brs*, 1H) and a multiplet at δ 5.1 attributed to oxygenated methine proton. The spectrum also displayed a proton signal at δ_H 4.2 and 4.1 which is evident for the presence of methylene protons. The proton signal showed at δ 0.9 and 0.9 suggesting the presence of two

terminal methyl protons. The ^{13}C-NMR (100 MHz, $CDCl_3$, Table 8, Appendix 3B-C) spectral data with the aid of DEPT-135 revealed the presence of six olefinic signals at δ 130.2, 130.0, 129.8, 129.7, 128.1, and 127.9. The ^{13}C NMR also demonstrated the presence of 14 signals for 24 methylene carbons at δ 34.1, 31.9, 31.5, 29.7, 29.6, 29.5, 29.4, 29.3, 29.2, 29.1, 27.2, 25.6, 24.7, and 22.7 and one oxymethine carbon signal is evident at δ 68.2. The most downfield signals appearing at δ 174.0 and 173.9 are attributed to the ester carbonyl. The most upfield carbon signals at δ 14.1 and 14.0 accounts for the presence of two methyl groups and the downfield signal at δ 64.5 corresponds to an oxygenated methylene carbon. The observed ^{1}H-NMR and ^{13}C-NMR data were found to be consistent with the reported data of 1,3-dilinoleoyl-2-oleine (Hussein *et al*., 2021; Bekele *et al*., 2013).

Table 8: ^{1}H NMR (400 MHz, $CDCl_3$) and ^{13}C NMR (101 MHz, $CDCl_3$) data of compound **225** and literature ^{1}H NMR and ^{13}C-NMR data of 1,3-dilinoleoyl-2-oleine.

Position	Compound **225**		(Hussein *et al*., 2021)		(Bekele *et al*., 2013)	
	^{1}H-NMR	^{13}C-NMR	^{1}H-NMR	^{13}C-NMR	^{1}H-NMR	^{13}C-NMR
1a	4.1	64.5	4.17	65.0	4.20	62.1
1b	4.2		4.17		4.31	
2	5.1	68.2	5.1	68.1	5.25	68.9
3a	4.1	64.5	4.17	65.0	4.12	62.1
3b	4.2		4.17		4.28	
1′, 1″	-	174.0, 173.9	___	174.0, 173.9	-	173.3, 172.8
2′, 2″	2.3	34.1	2.36	34.1	2.33	34.1, 34.2
3′, 3″	1.6	31.9, 31.5	1.64	31.9, 31.5	1.60	31.9, 31.5
4′, 4″	1.3	22.7	1.29	22.7	1.25	22.7
5′, 5″	1.3	22.7	1.29	22.6	1.25	22.7
6′, 6″	1.3	24.7	1.29	24.9	1.25	24.9
7′, 7″	1.3	24.7	1.29	24.9	1.25	24.9
8′, 8″	2.0	27.2	2.05	27.2	2.03	27.2
9′, 9″	5.3	129.7, 130.0	5.37	130.9, 29.7	5.40	129.7, 130.2
10′, 10″	5.3	127.9, 129.8	5.37	128.1,29.7	5.40	127.9, 129.7
11′, 11″	2.8, 2.0	25.6, 27.2	2.05	25.6,29.7	2.80, 2.03	25.6, 27.2
12′, 12″	5.3, 1.3	127.9, 128.1	5.37	130.0, 29.4	5.40, 1.25	127.9, 128.1
13′, 13″	5.3, 1.3	130.2, 130.0	5.37	127.9, 29.4	5.40, 1.25	131.9, 130.2
14′, 14″	2.0, 1.3	27.2	1.29	29.3	2.03, 1.25	27.2
15′, 15″	1.3	29.1–29.7	1.29	29.2	1.25	29.2–29.7
16′, 16″	1.3	29.1–29.7	1.29	29.1	1.25	29.2–29.7
17′, 17″	1.3	29.1–29.7	1.29	29.1	1.25	29.2–29.7
18′, 18″	0.9	14.09, 14.05	0.90	14.2 14.1	0.90	14.2, 14.1

Thus, based on this observation, compound **225** was proposed to be identical to that of 1,3-dilinoleoyl-2-oleine which was reported herein for the first time from *C. abyssinicum*.

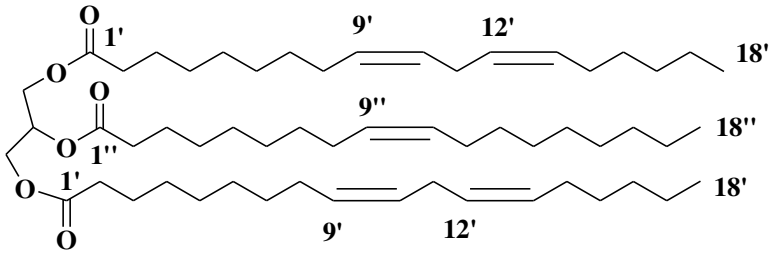

225

Compound **226** was isolated as a yellow solid with melting point 162–164 ºC, R_f value of 0.53 (30 % EtOAc in *n*-hexane as eluent). Its ^{1}H-NMR spectrum (400 MHz, $CDCl_3$, Table 9, Appendix 4A) displayed the aromatic proton signals at δ 7.1 (d, J = 8.6 Hz, 2H), 6.8 (d, J = 8.6 Hz, 2H), and 6.2 (s, 1H). Signals at δ 3.9 (s, 3H), 3.82 (s, 3H), 3.75 (s, 3H), and 3.73 (s, 3H) suggest the presence of four methoxy groups. The ^{13}C-NMR spectrum with the aid of DEPT-135, COSY, HSQC, and HMBC (Table 9, Appendix 4B-F) established the presence of six sp^2 oxygenated quaternary carbons at δ 147.0 (C-2), 159.8 (C-7), 154.6 (C-9), 159.8 (C-4'), δ 137.4 (C-3) and 158.3 (C-5) along with two sp^2 quaternary carbons at δ 108.3 (C-10) and 122.1 (C-1'). The presence of an α, β-unsaturated carbonyl carbon is evident from the appearance of a carbon signal at δ 174.3 (C-4). Four sp^2 methine carbon signals were observed at δ 132.1 (C-6), 96.0 (C-8), 114.0 (C-3', 5'), and 130.1 (C-2', 6'). The ^{1}H-^{1}H COSY spectrum showed a correlation between proton signal at δ 6.8 (H-2') with 7.1 (H-3'), confirming that these protons are symmetrically placed protons on an unsymmetrically *para-substituted* aromatic ring B whereas, whereas ring A of the flavonoid showed singlet protons at δ 6.2, characteristic of H-8. The HSQC showed a correlation such that the methyl proton signals at δ 3.73, 3.75, 3.82, and 3.9 correlate with the carbons at δ 55.3, 61.3, 56.1, and 61.8, respectively. Besides, the HSQC correlations observed were between aromatic protons at δ 7.1, 6.8, and 6.2 with aromatic carbon signals at δ 130.1, 114.0, and 96.0, respectively. The HMBC spectral analysis revealed correlation ~~a~~ between methoxyl group (δ_H 3.9, δ_C 61.8) with oxygenated sp^2 quaternary carbon at δ 158.3 (C-5) suggesting its *peri* position to the carbonyl carbon (C-4). Thus, methoxy at δ 61.8 is located at C-5 of ring A.

Table 9: ^{1}H NMR (400 MHz, $CDCl_3$) and ^{13}C NMR (101 MHz, $CDCl_3$) data of compound **226** and literature ^{1}H NMR and ^{13}C-NMR data of 6-hydroxy-3,5,7,4′-tetramethoxyflavone.

Position	Compound **226**		(Gulcin *et al*., 2004)	
	^{1}H-NMR	^{13}C-NMR	^{1}H-NMR	^{13}C-NMR
2	-	147.0	-	153.2
3	-	137.4	-	139.4
4	-	174.3	-	179.0
5	-	158.3	-	158.4
6	-	132.1	-	132.8
7	-	159.8	-	162.1
8	6.2 (1H)	96.0	6.43 (1H, 1*s*)	90.7
9	-	154.6	-	152.7
10	-	108.3	-	107.0
1′	-	122.1	-	123.2
2′ and 6′	6.8 (d, *J* = 8.6 Hz, 2H)	130.1	6.94 (2H, *d*)	130.5
3′ and 5′	7.1 (d, *J* = 8.6 Hz, 2H)	114.0	7.99 (2H, *d*)	114.4
4′	-	159.4	-	159.4
C-7, OCH_3	3.73 (3H, s)	55.3	3.79 (3H)	55.8
C- 4′, OCH_3	3.75 (3H, s)	56.1	3.83 (3H)	56.7
C-3, OCH_3	3.82 (3H, s)	61.3	3.85 (3H)	60.5
C-5, OCH_3	3.9 (3H, s)	61.8	3.88 (3H)	61.2

The above spectral data is in good agreement with 6-hydroxy-3,5,7,4′-tetramethoxyflavone (Gulcin *et al*., 2004) (Table 9), which has not yet been previously reported from the species.

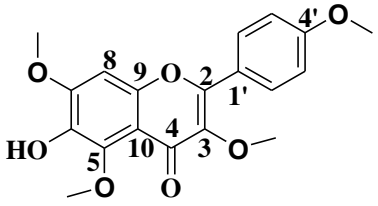

226

Compound **227** was isolated as a yellow oil from the DCM/MeOH (1:1) with an R_f value of 0.6 (*n*-hexane: EtOAc (5.5/4.5), as eluent. Its ^{1}H NMR spectral data (400 MHz, $CDCl_3$, Table 10, Appendix 5A) showed a signal due to terminal methyl proton at δ 0.9 (3H, t, *J*= 6.7 Hz). The spectrum also displayed methylene signals at δ 2.3 (2H, t) and 1.6 (2H, brs) of which the former suggests methylene is connected to a carbonyl group. The proton signal at δ 3.7 (1H, *m,* H-2′) accounted for the presence of oxygenated methine proton connected to oxygen whereas signals at δ 4.1 (dd, *J* = 12.0, 4.5 Hz, 2H, H-1′), 3.9 (m, 1H, H-3′a) and 3.7 (m, 1H, H-3′b) attributed to

oxygenated methylene protons. The ^{13}C NMR spectrum with the aid of the DEPT-135 (Appendix 5B-C) spectrum showed a total of 20 well resolved carbon signals of which four olefinic carbons signals at δ 130.2, 130.0, 128.1, and 127.9, methylene carbon signals at δ 34.2, 31.9, 31.5, 29.7, 29.5, 29.3, 29.1, 27.2, 25.6, 24.9 and 22.7, oxygenated methylene signals at δ 65.1 and 63.3, and sp^3 oxygenated methine at δ 70.3 are clearly observed. Most downfield signals appearing at δ 174.4 are attributed to the ester carbonyl whereas the upfield signal at δ 14.1 suggests a terminal methyl group.

Table 10: ^{1}H NMR (400 MHz, $CDCl_3$) and ^{13}C NMR (101 MHz, $CDCl_3$) data of compound **227** and literature of ^{13}C-NMR data of penicilloitins B.

Position	Compound **227**			Mourshid *et al*., 2016
	^{1}H NMR	^{13}C NMR	Multiplicity	^{13}C NMR
1		174.4	Carbonyl	174.3
2	2.3 (d, *J* = 7.2 Hz, 2H)	34.2	CH_2	34.1
3	1.6 (brs, 2H, H-3,4)	24.9	CH_2	24.8
4		25.6	CH_2	25.7
5	1.3 (d, *J* = 17.1 Hz, H-5,6,7,8)	29.3	CH_2	29.3
6		29.7	CH_2	29.7
7		29.5	CH_2	29.5
8		29.1	CH_2	29.0
9	2.0 (brq, *J* = 13.3, 5.0 Hz, 2H)	27.2	CH_2	27.3
10	5.4 (d, *J* = 11.6 Hz, 1H)	130.2	= CH	133.4
11		127.9	= CH	125.2
12		31.5	CH_2	35.3
13		128.1	= CH	71.5
14		130.0	= CH	36.8
15		31.9	CH_2	31.8
16		22.7	CH_2	22.0
17	0.9 (t, *J* = 5.0 Hz, 3H).	14.1	CH_3	14.0
1’	4.2 (d, *J* = 17.5 Hz, 1H), 4.1 (t, *J* = 6.1 Hz, 1H)	65.1	CH-O	65.3
2’	3.7 (m, 1H)	70.3	CH_2O-	70.2
3’	3.9 (d, *J* = 22.3 Hz, 1H), 3.86 – 3.75 (m, 1H)	63.3	CH_2O-	63.3

The above spectral data is in good agreement with data reported for penicilloitins B, previously reported from marine endophytic *Penicillium* species, where the hydroxyl group at C-13 is dehydrated to double bond in case of compound **227** (Table 10) (Mourshid *et al*., 2016).

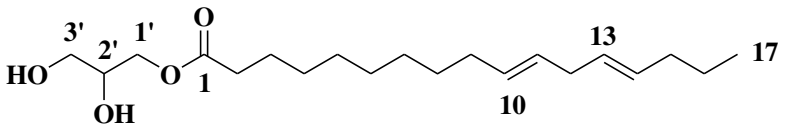

227

Compound **228** was obtained as a white amorphous with R_f value of 0.48 (*n*-hexane/EtOAc, 6:4, as eluent). Its ^{1}H-NMR spectrum (400 MHz, $CDCl_3$, Table 11, Appendix 6A) confirmed the presence of six methyl signals at δ 1.0 (s, 3H), 0.94 (d, J = 6.4 Hz, 3H), 0.87 (d, J = 7.4 Hz, 3H), 0.85 – 0.82 (m, 6H), and 0.70 (s, 3H). Among these the signals at δ 0.7 and 1.0. are due to methyl groups on quaternary carbons. The signal at δ 3.4 (m, 1H, H-3) corresponds to sp^3 oxygenated methine. Other proton signals integrating for 29 hydrogens were observed in the range δ 2.36 to 1.00. The olefinic proton signal at δ 5.38 (1H, *brs*, H-6) along with the six methyl groups are evident for the presence of sterol with one double bond. The ^{1}H NMR spectrum also showed a pair of double doublets appearing at δ 7.90 (d, J = 9.0 Hz, 2H), and 7.05 (d, J = 9.0 Hz, 2H) indicated *para* substituted aromatic ring. A sharp singlet at δ 3.97 (s, 3H) indicated the presence of methoxy group on aromatic ring, which was confirmed by a corresponding signal in its ^{13}C NMR spectrum at δ 55.5. The signals due to an anomeric proton (H-1′) of glucose moiety were observed at δ 4.40 (d, J = 7.7 Hz, 1H, H-1′). The six oxygenated methine proton signals at δ 4.03 (d, J = 6.8 Hz, 1H, H-2′), 3.99 (d, J = 1.0 Hz, 1H, H-5′), 3.91 (d, J = 3.8 Hz, 1H, H-4′), 3.58 (d, J = 9.7 Hz, 1H, H-3′), and the doublet signals at δ 4.12 (d, J = 2.1 Hz,2H, H-6′) are attributed to the glucose moiety. The ^{13}C-NMR spectrum (100 MHz, $CDCl_3$, Table 11) with the help of the DEPT-135 (Appendix 6B-C) spectrum showed 42 well-resolved carbon signals including six quaternary carbon signals at δ 174.6, 161.8, 140.4, 130.3, 42.3, and 36.7. The signals at δ 122.1, and 79.6 were assigned for C-5, and C-3, respectively. Aliphatic methine carbons showed a signal at δ 33.8, 45.8, 56.0, 56.8, 29.2, 50.2, 31.9 and the carbon signal at δ 55.5 was attributed to the aromatic methoxy group. The carbon signals observed at δ 38.9, 34.2, 39.8, 31.9, 21.1, 26.1, 33.8, 24.3, 22.7, 37.3, 29.7, and 25.0 belong to methylene carbons. The methyl group demonstrated signals at δ 11.9, 12.0, 18.8, 19.0, 19.3, and 19.8. The presence of one sugar moiety is evident from the appearance of one anomeric carbon signal at δ 101.2 along with a series of carbon signals at δ 76.1, 73.9, 73.6, 70.2, and 63.3. Additional *para*-methoxy benzoyl moiety was observed at δ 174.6, (C-1′′), 130.3 (C-1′), 127.8 (C-2′′, C-6′′), 114.5 (C-3′, C-5′), and 161.8 (C-4′′). The above spectral data is comparable with literature data of sitosterol-

3-O-*β*-D-glucopyranoside (Yayli *et al*., 2003) with additional *para*-methoxy benzoyl moiety in the case of compound **228**.

Table 11: ^{1}H NMR (400 MHz, $CDCl_3$) and ^{13}C NMR (101 MHz, $CDCl_3$) data of compound **228** and literature of ^{13}C-NMR data of sitosterol-3-O-*β*-D-glucopyranoside.

Position	NMR data of compound **228**		Yayli *et al*., 2003
	^{1}H-NMR	^{13}C-NMR	^{13}C-NMR
1		38.9	38.0
2		34.2	35.9
3	3.4 (m, 1H)	79.8	78.0
4		39.8	39.5
5		140.3	140.5
6	5.38 (1H, *brs*)	122.1	121.5
7		31.9	31.7
8		26.1	28.2
9		45.8	45.6
10		36.7	36.5
11		21.1	19.1
12		33.8	32.7
13		42.3	42.0
14		56.0	55.8
15		24.3	24.1
16		22.7	22.9
17		56.8	56.4
18	1.0 (s, 3H)	18.8	18.6
19	0.70 (s, 3H)	12.0	12.0
20		29.2	29.7
21	0.80 (m, 3H)	11.9	11.7
22		37.3	37.0
23		29.7	29.0
24		50.2	49.0
25		31.9	31.6
26	0.94 (d, *J* = 6.4 Hz, 3H)	19.8	20.8
27	0.80 (m, 3H)	19.3	19.6
28		25.0	26.0
29	0.87 (d, *t* = 6.4 Hz, 3H)	19.0	18.8
1’	4.40 (d, *J* = 7.7 Hz. 1H)	101.2	101,9
2’	4.03 (d, *J* = 6.8 Hz, 1H)	76.1	77.7
3’	3.58 (d, *J* = 9.7 Hz, 1H)	73.9	74.6
4’	3.91 (d, *J* = 3.8 Hz, 1H)	70.2	71.0
5’	3.99 (d, *J* = 1.0 Hz, 1H)	73.6	77.7
6’	4.12 (d, *J* = 2.1 Hz, 2H)	63.3	62.1
Ester carbonyl	-	174.6	-

1″	-	130.3	-
2″, 6″	7.90 (d, *J* = 9.0 Hz, 2H)	127.8	-
3″, 5″	7.05 (d, *J* = 9.0 Hz, 2H)	114.5	-
4″	-	161.8	-

Thus, compound **228** is named *para*-methoxy benzoyl-sitosterol-3-O-*β*-D-glucopyranoside (Table 11) reported herein for the first time from the genus *Crinum.*

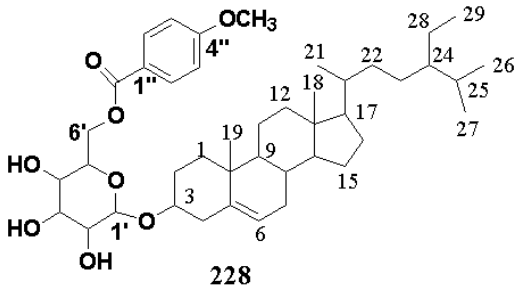

228

Compound **229** was obtained as a reddish crystal with R_f value of 0.56 (DCM: MeOH, 9.5:0.5) as eluent. The ^{1}H NMR spectrum (400 MHz, $CDCl_3$, Appendix 7A) showed the presence of an olefinic proton signal at *δ* 5.3 (brs, 1H, H-6)**.** The compound exhibited the doublet signals at *δ* 4.1 (1H, d, *J* = 8.0 Hz, H-1′a), and 3.8 (1H, d, *J* = 7.8 Hz, H-1′b) were due to oxygenated methylene protons. The signal at *δ* 1.3 (brs*,* 6H) is a characteristic signal for many methylene protons in the compound which was supported by the appearance of an intense carbon signal at *δ* 29.7 in the ^{13}C NMR spectrum. The broad singlet signal observed at *δ* 2.3 is ascribed to methylene protons attached to a carbonyl group. An upfield proton signal at *δ* 0.9 (brs, 6H) is evident for the presence of two terminal methyl protons in the compound. The ^{13}C-NMR (400 MHz, $CHCl_3$) spectrum with the aid of DEPT-135 (Appendix 7B-C) revealed 20 carbon signals of which fourteen methylene carbons at *δ* 34.4, 34.3, 31.9, 31.5, 29.7, 29.5, 29.4, 29.3, 28.6, 27.2, 25.9, 25.0, 24.8 and 22.7. The downfield signals at *δ* 64.4 correspond to an oxygenated methylene carbon and the most upfield carbon signal at *δ* 14.2, and 14.1 account for the presence of two terminal methyl protons. The presence of two olefinic sp^2 signals at *δ* 129.9 and 129.8 suggest the presence of one double bond. The presence of ester carbonyl carbon was evident at *δ* 174.1. On the basis of the above spectral data, the structure of compound **229** was found to be identical to data reported for ethyl (*E*)-octadec-9-enoate (Barange *et al*., 2020) reported herein for the first time from the genus *Crinum.*

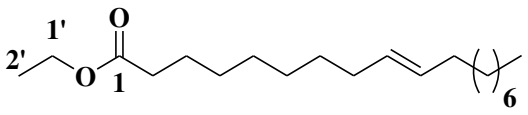

229

Compound **230** was obtained as a white solid. TLC profile showed a spot at R_f 0.48 with (4.5 % methanol in dichloromethane) as a mobile phase. The ^{1}H-NMR (400 MHz, MeOD, Appendix 8A) spectrum of compound **230** displayed signals in the oxygenated region only. The spectrum showed a signal for one anomeric proton at δ 5.13 (d, J = 16.6 Hz, 1H). The remaining proton signals of this compound appeared in the region between 3.00 to 4.00. The proton decoupled ^{13}C-NMR spectrum (101 MHz, MeOD) of compound **230** with the aid of DEPT-135 (Appendix 8B-C) demonstrated the presence of well-resolved carbon resonances of eight methine carbons all of which resonated in the oxygenated region at δ 100.4 (C-1), 93.49 (C-5′), 81.75 (C-3′), 77.16 C-4′), 73.66 (C-3), 73.07 (C-5), 72.37 (C-2), and 71.79 (C-4), one quaternary carbon at δ 103.9 (C-2′) and three oxygenated methylene carbons at δ 61.2 (C-6), 63.2 (C-1´), 64.4 (C-6´). Thus, based on this observation, compound **230** was proposed to be identical to that of sucrose (Hernández-García *et al*., 2019) (**230**) which was reported herein for the first time from *C. abyssinicum*.

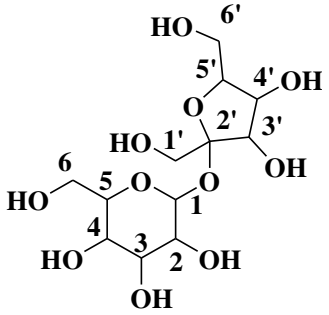

230

4.1.2. Secondary metabolites isolated from the root of *Calotropis procera*

The dichloromethane/methanol (1:1), and methanol extract of the roots of *C. procera* was subjected to silica gel column chromatographic fractionation which afforded five compounds (**96, 82, 87, 231,** and **232)** from dichloromethane/methanol (1:1), and four compounds (**233**, **97, 234,** and **98**) from the methanol root extracts. The structures of the isolated compounds were characterized as discussed here below.

Compound **82** was isolated as a pale-yellow solid with R_f value of 0. 54 (*n*-hexane:EtOAc, 4:1 as eluent). Its ^{1}H NMR spectrum (400 MHz, $CDCl_3$, Table 12, Appendix 10A) showed four olefinic proton signals at δ 5.4 (m, 4H) and seven methyl signals. Methyl signals were observed at δ 1.0 (s, 3H), 0.7 (s, 3H), 0.86 (d, J = 6.8 Hz, 3H), 0.9 (d, J = 6.3 Hz, 3H), 0.85 (d, J = 6.0 Hz, 3H), and 0.82 (t, J = 6.0 Hz, 3H) attributed to H-18, H-19, H-21, H-26, H-27, and H-29, 18′, respectively. The proton signal at δ 4.6 (m, 1H, H-3) corresponds to the oxygenated sp^3 methine proton. A triplet proton signal at δ 2.3 (2H, J = 7.6 Hz) was due to methylene H_2-2′ proton adjacent to the ester group. Other proton signals integrating for hydrogens were detected in the range δ 1.0 to 2.7. The ^{13}C NMR ($CDCl_3$, 101 MHz, Table 12, Appendix 10B-C) spectrum in combination with DEPT-135 displayed 47 well-resolved carbon signals including seven methyl, twenty-three methylene, thirteen methine, and four quaternary carbons of which two sp^2 and two sp^3 quaternary carbons appeared at δ 171.2, 140.7, 36.5, and 42.3 attributed to C- 1′, C-5, C-10, and C-13, respectively, whereas four olefinic methine carbon and one sp^3 oxygenated methine signals were observed at δ 121.7 (C-6), 129.9 (C-9′), 127.9 (C-10′), 128.0 (C-12′), 130.1 (C-13′) and 71.9 (C-3), respectively. The above spectral data are in good agreement with the data reported in the literature for *β*-sitosteryl linoleate (Shahania *et al*., 2012) (Table 12), reported herein for the first time from this plant, having been previously reported from *Geum iranicum*.

Table 12: ^{1}H-NMR (400 MHz, $CDCl_3$) and ^{13}C-NMR (101 MHz, $CDCl_3$) spectral data of compound **82** and the reported data for *β*-sitosteryl linoleate.

Position	Compound **82**		(Shahania *et al*., 2012)	
	^{1}H-NMR	^{13}C-NMR	^{1}H-NMR	^{13}C-NMR
1		37.2		37.0
2		28.2		27.8
3	4.6 (m, 1H)	71.7	4.6 (m, 1H)	73.7
4		42.2		38.4
5		140.7		139.7
6	5.4 (m, 1H)	121.7	5.30 – 5.40 (m, 1H)	122.6
7		31.9		31.8
8		32.4		31.9
9		50.1		50.0
10		36.5		36.5
11		21.1		21.0
12		39.8		39.7
13		42.3		42.3
14		56.7		56.7

15		24.3		24.3
16		31.3		28.3
17		56.0		56.0
18	0.7 (3H, s)	12.0	0.68 (3H, s)	11.8
19	1.0 (3H, s)	19.4	1.03 (3H, s)	19.3
20		36.1		36.2
21	0.9 (3H, d, *J* = 6.3 Hz)	18.7	0.92 (3H, d, *J* = 7 Hz)	18.8
22		33.7		33.9
23		26.1		26.0
24		45.8		45.8
25		29.1		29.1
26	0.86 (3H, d, *J* = 6.0 Hz)	19.8	0.83 (3H, d, *J* = 7 Hz)	19.8
27	0.82 (3H, d, *J* = 6.0 Hz)	19.0	0.81 (3H, d, *J* = 7 Hz)	19.0
28		23.0		23.1
29	0.8 (3H, t, *J* = 7.6 Hz)	11.8	0.84 (3H, m)	11.9
1′		171.2		173.3
2′	2.3 (2H, t, *J* = 7.6 Hz)	34.0	2.29 (2H, t, *J* = 7.5 Hz)	34.4
3′	1.6 (2H, m)	24.7	1.59 – 1.65 (2H, m)	25.1
4′	1.3 (m)	29.2	1.25 – 1.38 (m)	29.2
5′	1.3 (m)	29.3	1.25 – 1.38 (m)	29.3
6′	1.3 (m)	29.6	1.25 – 1.38 (m)	29.6
7′	1.3 (m)	29.7	1.25 – 1.38 (m)	29.7
8′	2.0 (m)	27.2	2.03 – 2.08 (2H, m)	27.2
9′	5.4 (m, 1H)	129.0	5.30 – 5.40 (m, 1H)	130.0
10′	5.4 (m, 1H)	127.9	5.30 – 5.40 (m, 1H)	127.9
11′	2.7 (2H, t, *J* = 6.5 Hz)	25.6	2.76 (2H, t, *J* = 6.5 Hz)	25.6
12′	5.4 (m, 1H)	128.0	5.30 – 5.40 (m, 1H)	128.0
13′	5.4 (m, 1H)	130.1	5.30 – 5.40 (m, 1H)	130.2
14′	2.0 (m)	27.2	2.03 – 2.08 (2H, m)	27.2
15′	1.3 (m)	29.4	1.25 – 1.38 (m)	29.4
16′	1.3 (m)	31.5	1.25 – 1.38 (m)	31.6
17′	1.3 (m)	22.7	1.25 – 1.38 (m)	22.7
18′	0.8 (3H, t, *J* = 7.6 Hz)	14.1	0.88 (3H, t, *J* = 6.5 Hz)	14.1

Thus, from these findings, the structure of compound **82** was assigned as *β*-sitosteryl linoleate.

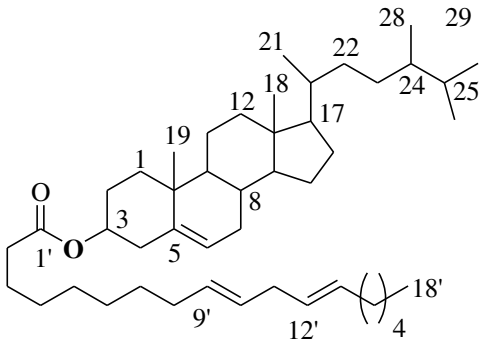

82

Compound **231** was obtained as a yellowish solid with an R_f value of 0.51 (*n*-hexane/Ethyl acetate 4/1) as eluent. Its ^{1}H-NMR spectrum (400 MHz, $CDCl_3$, Table 13, Appendix 12A) showed the presence of an olefinic proton signal at δ 5.4 (m, 1H, H-4) and 5.1 (m, 1H, H-5)**.** Oxygenated methylene protons appeared at δ 4.3-4.1 (m, 1H) and 3.8-3.5 (m, 1H). An upfield proton signal at δ 0.9 (m, 3H) is evident for the presence of methyl group in the compound. The ^{13}C-NMR spectrum with aid of DEPT-135 (Appendix 12B-C) showed a total of well resolved 14 carbon signals including seven methylene signals at δ 33.8, 31.9, 30.4, 29.7, 29.4, 28.9, 23.7, and 22.7, methine carbon at δ 38.7, oxygenated methylene carbons at δ 63.1 and 68.2 and terminal methyl at δ 14.1, and two sp^2 methines at δ 130.9 and 128.8.

Table 13: ^{1}H-NMR (400 MHz, $CDCl_3$) and ^{13}C-NMR (101 MHz, $CDCl_3$) spectral data of compound **231** and the reported ^{13}C-NMR data for (4*Z*)-dodec-4-en-1-ol.

Position	NMR data of compound **231**			(D´yakonov *et al*., 2020)	
	^{1}H-NMR	^{13}C-NMR	Multiplicity	^{13}C-NMR	Multiplicity
1		63.1	CH_2O-	61.9	CH_2O-
2		38.7	CH	35.2	CH_2
3		23.7	CH_2	23.5	CH_2
4	5.38(m,1H)	128.8	= CH	128.8	= CH
5	5.1(m, 1H)	130.0	= CH	130.4	= CH
6		33.8	CH_2	27.1	CH_2
7		31.9	CH_2	31.8	CH_2
8		28.9	CH_2	29.2	CH_2
9		29.4	CH_2	29.2	CH_2
10		29.7	CH_2	29.7	CH_2
11		22.7	CH_2	22.6	CH_2
12	0.9 (m, 3H)	14.1	CH_3	13.9	CH_3
1'		30.4	CH_2	-	-
2'		68.2	CH_2O-	-	-

The above spectral data is comparable with literature reported data for (4*Z*)-dodec-4-en-1-ol (D´yakonov *et al*., 2020) and the only difference is additional hydroxymethyl at C-3 in the case of compound **231** Table 13. This compound has never been reported before from the roots of *C. procera*.

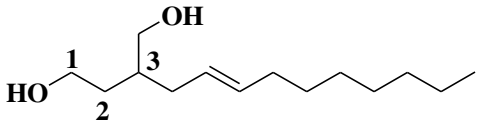

231

Compound **232** was obtained as a white powder with an R_f value of 0.46 (*n-hexane*/EtOAc (3.5:1.5) as eluent. Its ^{1}H-NMR spectrum (400 MHz, $CDCl_3$, Table 14, Appendix 13A) showed three olefinic protons at δ 5.8 (t, J = 7.1 Hz, 1H), 5.4 (m, 1H), 5.2 (dd, J = 15.1, 8.6 Hz, 1H). The signal at δ 4.4 (1H, s, H-3) corresponds to the oxygenated methine proton. The appearance of the singlets at δ 1.4, 0.8, and 0.8 confirm the presence of three methyl groups attached to quaternary carbons. The presence of the peak at δ 2.4 revealed the methyl proton attached to the carbonyl group. The spectrum also revealed the presence of methyl proton signals at δ 1.0 (d, J = 7.4 Hz, 3H), 0.9 (d, J = 7.1 Hz, 3H), 0.9 (d, J = 7.4, 1.9 Hz, 9H) and 0.8 (d, J = 7.1 Hz, 3H). The ^{13}C NMR ($CDCl_3$ 400 MHz, Table 14, Appendix 13B-C) spectrum in combination with DEPT-135 displayed 31 carbon signals corresponding to seven methyl groups at δ 20.2, 19.8, 19.5, 19.0, 14.1, 12.2, and 12.0, nine methylene groups at δ 39.6, 38.6, 37.1, 34.2, 29.7, 28.2, 24.1, 22.7 and 21.0. Eight sp^3 methine carbons were observed at δ 56.0, 55.9, 53.6, 51.2, 45.8, 40.5, 36.1, and 31.9. The peaks observed at δ 38.0 and 42.5 in the ^{13}C NMR spectrum were absent in DEPT-135 spectrum suggesting the presence of two sp^3 quaternary carbon atoms that belong to C-10 and C-13, respectively. The spectrum also showed sp^3 oxygenated methine at δ 73.1 (C-3) and ester carbonyl at δ 168.8 along with olefinic methines at δ 126.2 (C-7), 138.1 (C-23), and 129.4 (C-22).

Table 14: ^{1}H NMR (400 MHz, $CDCl_3$) and ^{13}C NMR (101 MHz, $CDCl_3$) data of compound **232** and literature ^{13}C-NMR data of spinasterol.

Position	Compound **232**			Meneses-Sagrero, *et al*., 2017)	Yang *et al*., 2017
	^{1}H-NMR	^{13}C-NMR	Multiplicity	^{13}C-NMR	^{13}C-NMR
1		37.1	CH_2	37.2	37.2
2		31.9	CH_2	31.5	31.5
3		73.2	CH-O	71.1	71.1
4		38.6	CH_2	38.0	38.0
5		45.8	CH	40.3	40.8
6		29.7	CH_2	29.7	29.7
7	5.8 (t, 1H)	126.2	= CH	117.5	117.5
8		-	-	139.6	139.6
9		53.6	CH	49.5	49.5
10	-	38.0	C	34.2	34.2
11		21.0	CH_2	21.6	21.6
12		39.6	CH_2	39.5	39.5
13	-	42.5	C	43.3	43.3
14		55.9	CH	55.1	55.1
15		23.1	CH_2	23.1	23.0
16		28.2	CH_2	28.5	28.5
17		56.0	CH	55.9	55.9
18		12.2	CH_3	12.0	12.2
19		12.2	CH_3	13.0	13.0
20		40.5	CH	40.8	40.3
21		21.1	CH_3	21.4	19.0
22	5.4 (1H, m)	138.1	CH	138.2	138.2
23	5.2 (1H, m)	129.5	CH	129.5	129.5
24		51.2	CH	51.3	51.3
25		31.9	CH	31.9	31.9
26		21.2	CH_3	21.1	21.4
27		19.5	CH_3	18.99	21.0
28		25.4	CH_2	25.4	25.4
29		12.0	CH_3	12.0	12.1
30	-	168.8	Ester	-	-
31		21.0	CH_3	-	-

The above spectral data of compound **232** is comparable with data reported for the spinasterol skeleton and the only difference is the presence of extra acyl moiety at C-3, in the case of compound **232**. Thus, compound **232** was identified as spinasterol acetate. However, this is the first report of the compound from *C. procera*.

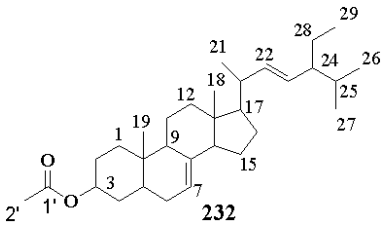

232

Compound **87** as isolated white solid with melting point 164-167 ºC. TLC profile showed a spot at R_f 0.46 with *n*-hexane:EtOAc (3:2) as a mobile phase. The ^{1}H-NMR (400 MHz, $CDCl_3$, Table 15, Appendix 11A) spectra of compound **87** showed the presence of methyl proton signals appeared at δ 1.11 (d, J = 8.8 Hz, 3H), 0.89 (d, J = 6.5 Hz, 3H), 0.8 (brs, 15H), and 0.8 (s, 3H). The presence of seven methyl groups in the ^{1}H-NMR spectrum partly assures the presence of a triterpenoid skeleton in the structure of compound **87**. Other proton signals integrating for 23 protons were observed in the range δ 2.3 to 1.14. The spectrum also showed the olefinic proton signal at δ 5.3 (brs, 1H). Oxygenated sp^3 methine proton was observed at δ 4.5 (m, 1H). The proton decoupled ^{13}C-NMR and DEPT-135 spectra ($CDCl_3$, Appendix 11B-C) of compound **87** revealed the presence of 30 well-resolved carbon signals of which eight methyl, nine methylene, seven methine, and six quaternary carbons. Among them, the signal observed at δ 124.3 belongs to olefinic carbons. The ^{13}C-NMR spectrum also showed methylene signals at δ_C 38.9, 26.9, 18.3, 32.9, 23.4, 28.1, 26.6, 31.3, and 27.9. The spectrum displayed signals due to methyl groups at δ_C 27.9, 15.9, 15.7, 17.5, 23.2, 28.8, 16.9, and 21.3. The carbon signal observed at δ_C 80.6 is detectable for carbon-bearing oxygen. The quaternary carbons were observed at δ_C 139.6, 39.6, 40.0, 36.8, 40.9, and 33.7. The remaining carbon signals for aliphatic methine were displayed at δ_C 55.9, 55.3, 47.6, 39.6, and 39.4. Based on the above spectral data, and comparison with literature report (Table 15), the compound **87** was identified as α-amyrin.

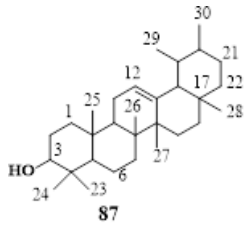

87

Compound **96** was isolated as a colorless powder with melting point 126–129 ºC, R_f value of 0.6 (*n*-hexane: EtOAc, 9:1) as eluent from DCM:MeOH (1:1) extract of the roots of *C. procera*. Its ^{1}H NMR (400 MHz, $CDCl_3$, Table 15, Appendix 9A) spectrum showed two olefinic protons at δ 5.4 (m, 1H) and 5.1 (t, J = 3.5 Hz, 1H) allocated to H-6 and H-12 and pair of doublets of

doublets at δ 4.6 and 4.5 (*J* = 4.6, 2.2 Hz*)* associated with the C-30 exocyclic methylene group. A doublet proton at δ 2.2 was attributed to methine proton H-18 proton. The ^{1}H NMR spectrum also showed signals for eight methyl groups, of these, seven of them were positioned at quaternary carbons corresponding to the singlet signals. The ^{13}C NMR spectrum (Appendix 9B-C) showed carbon signals corresponding to those of the ursane-type triterpenes (Ali *et al*., 1998, 2000). Olefinic carbons appeared at δ 145.2 (C-5), 121.6 (C-6), 124.3 (C-12), and 139.6 (C-13), of which the former is sp^2 quaternary carbon, whereas signals of exocyclic methylene appeared at δ 154.6 (C-20) and 107.2 (C-30). The signal at δ 80.9 is attributed to sp^3 oxygenated methine at C-3.

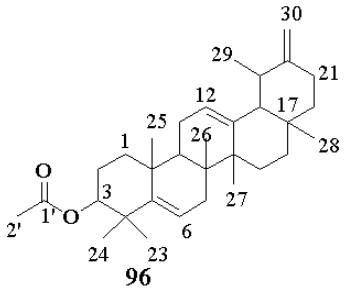

96

Compound **233** was isolated as a colorless powder with an R_f value of 0.48 (*n*-hexane: EtOAc, 8:2) as eluent from the MeOH extract of the roots of *C. procera*. Its ^{1}H NMR (400 MHz, $CDCl_3$, Table 15, Appendix 14A) spectrum showed one olefinic protons at δ 5.3 (t, *J* = 3.7 Hz, 1H) assigned to H-12 and pair of broad singlets at δ 4.65 and 4.7 (brs, 2H)*)* associated with the C-30 exocyclic methylene group. A doublet proton at δ 2.2 (d, *J* = 13.5 Hz, 1H) was attributed to methine proton of H-18 proton. Seven methyl groups also had signals in the ^{1}H NMR spectra, six of which were located at quaternary carbons and corresponded to the singlet signals *δ* 1.1 (s, 3H, H-27), 1.0 (s, 3H, H-25), 0.98 (s, 3H, H-23), 0.90 (s, 3H, H-26), 0.87 (s, 3H, H-24), and 0.80 (s, 3H, H-28). The ^{13}C NMR, and DEPT-135 spectrum (Appendix 14B-C) showed carbon signals corresponding to those of the ursane-type triterpenes (Ali *et al*., 1998, 2000). Olefinic carbon signals were observed at positions 125.5 (C-12) and 138.2 (C-13), the latter is a sp^2 quaternary carbon, while exocyclic methylene carbon signals appeared at 153.1 (C-20) and 103.9 (C-30). The signal at δ 78.3 is attributed to sp^3 oxygenated methine at C-3. The ^{1}H and ^{13}C NMR (Table 15, Appendix 17A-C) data of compound **233** were identical to those of **96** with the exception of the absence of the signals for the acetoxy group and the absence olefinic double bond at δ_C C-

5/C-6 in **233**. The NMR spectral data of compound **233** is in good agreement with data reported for calotropursenol B, previously reported from the same species (Ibrahim *et al*., 2012).

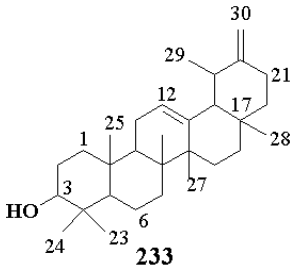

233

Compound **97** was isolated as a colorless powder with a melting point 128-131 ºC, R_f value of 0.5 (*n*-hexane: EtOAc, 1:1) as eluent from the MeOH extract of the roots of *C. procera*. The ^{1}H and ^{13}C NMR (Table 15, Appendix 17A-C) data of compound **97** were identical to those of **96** except the absence of an acetoxy group in **96**. The ^{13}C NMR spectrum (101 MHz, $CDCl_3$, Table 15, Appendix 15B) of compound **97** with the aid of the DEPT-135, COSY, HSQC, and HMBC (Appendix 15C-F) experiments revealed the resonance spectrum of 30 carbons. The ^{13}C NMR spectrum showed signals corresponding to those of the ursane-type triterpenes (Ali *et al*., 2000). The analysis of the ^{13}C NMR spectrum displayed signals corresponding to eight quaternary carbons, including three olefinic carbon signals, and five aliphatic methine carbon signals, two olefinic carbon signals, one exocyclic methylene, three aliphatic methine groups, eight methylene groups and seven methyl groups. The signal at δ 81.0 is attributed to sp^3 oxygenated methine at C-3. This structure was confirmed by analysis of the 2D NMR data, including ^{1}H-^{1}H COSY, HSQC, and HMBC experiments. The NMR spectral data of compound **97** is in good agreement with data reported for calotroprocerol A, previously reported from the same species (Table 15) (Ibrahim *et al*., 2012).

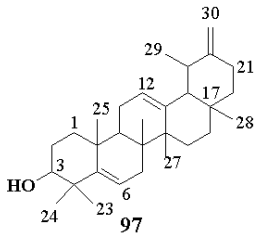

97

Compound **98** was isolated as a white powder with an R_f value of 0.56 (15 % EtOAc in n-hexane) as eluent from the MeOH extract of the roots of *C. procera*. The ^{1}H and ^{13}C NMR (Table 15, Appendix 17A-C) data of compound **98** were identical to those of **97** with the

exception of the absence of the signals for the exocyclic methylene group and the appearance of an additional olefinic double bond at δ_H/δ_C 5.2/118.9 (H-21/C-21) and 139.9 (C-20). The double bond position was established to be at C-20/C-21 based on the literature reported for calotroproceryl acetate B (Ibrahim *et al*., 2012) suggesting the absence of an additional acetoxy group in comparison to **98.**

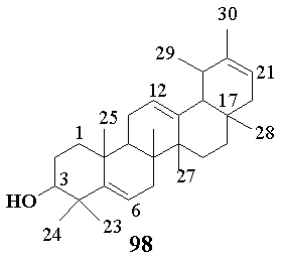

98

Table 15: ^{1}H NMR (400 MHz, $CDCl_3$) and ^{13}C NMR (101 MHz, $CDCl_3$) data of compounds **96, 87, 233, 97,** and **98** with reported data.

Position	96		Ibrahim *et al.*, 2012	87	(Viet *et al.*, 2021)	233	Ibrahim *et al.*, 2012	97	(Ibrahim *et al.*, 2012)	98	(Ibrahim *et al.*, 2012)
	^{1}H-NMR	^{13}C-NMR	^{13}C-NMR	^{13}C-NMR	^{13}C-NMR	^{13}C-NMR	^{13}C-NMR	^{13}C-NMR	^{13}C-NMR	^{13}C-NMR	^{13}C-NMR
1		38.4	38.5	38.9	38.8	38.6	38.8	38.4	38.8	38.8	38.4
2		28.1	28.1	26.9	27.3	27.8	28.8	28.1	28.1	28.1	28.0
3	3.7 (1H, brs)	80.9	81.0	80.6	79.1	78.3	79.0	81.0	79.0	79.1	80.9
4	-	36.8	37.8	39.6	38.8	38.4	38.8	37.0	36.9	38.3	38.2
5		145.2	145.2	55.3	55.2	55.3	55.2	145.2	145.2	145.2	145.2
6	5.4 (t, *J* = 14.5 Hz, 1H)	121.6	121.6	18.3	18.4	18.1	18.4	121.6	121.7	121.7	121.6
7		32.9	33.3	32.9	32.9	32.9	32.9	32.9	32.9	33.8	33.7
8	-	40.0	40.0	40.0	40.0	39.4	40.0	40.0	40.0	40.9	41.5
9		47.6	47.6	47.6	47.7	47.6	47.7	47.6	47.6	48.7	48.7
10		37.7	37.7	36.8	36.9	36.7	36.9	37.7	37.7	37.1	37.7
11		23.6	23.6	23.4	23.3	23.0	23.3	23.4	23.6	23.3	22.5
12	5.14 (t, *J* = 3.5 Hz, 1H)	124.3	124.3	124.3	124.4	125.5	124.4	124.3	124.4	124.4	124.3
13	-	139.6	139.6	139.6	139.6	138.2	139.6	139.6	139.6	139.6	139.6
14	-	40.9	42.1	40.9	41.5	41.8	41.7	42.1	42.1	42.1	42.1
15		26.6	26.9	28.1	28.1	26.5	27.3	26.6	26.9	26.6	26.9
16		23.7	23.7	26.6	26.6	23.9	23.4	23.6	23.7	23.4	23.5
17	-	34.5	34.7	33.7	33.8	32.9	33.8	33.8	34.7	36.7	34.7
18		48.6	48.6	59.1	59.1	53.0	48.7	48.6	48.6	50.4	50.3
19		39.7	41.5	39.6	39.7	39.0	41.5	39.7	41.5	41.5	41.7
20		154.6	154.7	39.4	39.6	153.1	154.7	154.6	154.7	139.9	139.8
21		32.9	32.9	31.3	31.3	31.9	31.3	31.3	32.9	118.9	118.9
22		38.9	39.7	41.5	40.0	38.6	39.6	38.9	39.7	39.2	39.2

23		28.8	29.1	27.9	28.10	30.4	29.7	28.8	29.1	28.8	28.7
24		15.9	15.8	15.9	15.6	15.4	15.6	15.8	15.8	15.4	16.1
25		16.8	16.8	15.7	15.5	15.0	16.3	16.8	16.8	16.3	16.5
26		16.9	16.9	17.5	17.4	16.3	16.9	16.9	16.9	16.9	16.7
27		25.8	26.6	23.2	23.4	27.4	26.6	25.5	26.6	28.0	27.9
28		17.5	17.5	28.8	28.8	16.4	17.5	17.5	17.5	17.5	17.7
29		19.5	18.3	16.9	16.9	20.2	18.4	19.5	18.3	19.5	23.2
30	4.62 (dd, *J* = 4.6, 2.2 Hz, 2H)	107.2	107.1	21.3	21.4	103.9	107.2	107.2	107.2	23.3	23.7
1′	-	171.0	171.1	-	-	-	-	-	-	-	-
2′		21.3	21.3	-	-	-	-	-	-	-	-

Compound **234** was obtained as a white solid with melting point 275-277 ºC, TLC profile showing a spot at R_f 0.48 with *n*-hexane:EtOAc (9:1) as a mobile phase. The ^{1}H-NMR spectrum (400 MHz, $CDCl_3$, Table 16, Appendix 16A) of compound **234** showed resonance signals due to one oxygenated methine at δ 4.45 (dd, *J* = 11.8, 4.8 Hz, 1H), one olefinic proton at δ 5.5 (s, 1H), nine methyl proton signals at δ 0.88 (3H, s), 0.88 (3H, s), 1.1 (3H, s), 1.1 (3H, s), 1.1 (3H, s), 0.76 (3H, s), 0.8 (3H, s), 0.8 (3H, s) and 0.9 (3H, t, *J*= 7.3Hz). The ^{13}C NMR spectrum (101 MHz, $CDCl_3$, Table 16, Appendix 16B-F) of compound **234** revealed resonance signals due to 30 carbons, including a conjugated ketone carbonyl group at δ_C 199.7 (C-12), one olefinic carbon at δ_C 130.4 (C-12), one olefinic quaternary carbon δ_C 165.0 (C-13), five quaternary aliphatic carbon at δ 38.0 (C-4), 39.2 (C-8), 36.8 (C-10), 43.7 (C-14), and 33.9 (C-17), nine methylene groups at δ_C 38.9 (C-1), 28.8 (C-2), 18.7 (C-6), 32.3 (C-7), 27.2 (C-15), 26.4 (C-16), 31.9 (C-21), 40.9 (C-22), 34.5 (C-2′), five aliphatic methine groups at δ_C 55.0 (C-5), 47.7 (C-9), 59.0 (C-18), 36.5 (C-19), and 39.3 (C-20), one O-bearing methine group at δ_C 80.7 (C-3), eight methyl groups at 28.8 (C-23), 16.7 (C-24), 16.6 (C-25), 18.5 (C-26), 23.6 (C-27), 28.1 (C-28), 17.5 (C-29), 21.3 (C-30), and 14.1 (C-2′). The spectrum also showed ester carbonyl at *δ* 171.0 (C-1′).

Table 16: The ^{1}H- NMR (400 MHz, $CDCl_3$) and ^{13}C-NMR (101 MHz, $CDCl_3$) spectral data of compound **234** and the data reported in the literature for 11-oxo-α-amyrin ethylated.

Position	Compound **234**		(Omer *et al*., 2017)	
	^{1}H-NMR	^{13}C-NMR	^{1}H-NMR	^{13}C-NMR
1		38.9		38.9
2		28.8		28.7
3	4.5 (dd, *J* = 11.8, 4.8 Hz, 1H)	80.7	4.50 (1H, dd, J= 10.7, 4.5 Hz, H-3)	80.9
4		38.0	-	38.4
5		55.0		55.3
6		18.7		18.2
7		32.28		32.3
8		39.2		40.2
9		47.7		47.2
10		36.8		36.9
11		199.7		199.6
12	5.5 (s, 1H)	130.4	5.57(1H, s, H-12)	130.4
13		165.0		164.9
14		43.7		42.0
15		27.2		27.1

16		26.4		26.4
17		33.9		33.3
18	2.70 (1H, m)	59.0	2.76 (1H, m)	59.0
19		36.5		36.6
20		39.3		39.2
21		31.9		31.2
22		40.9		41.7
23	0.88 (3H, s)	28.8	0.86 (3H, s)	28.8
24	0.88 (3H, s)	16.7	0.86 (3H, s)	16.3
25	1.1 (3H, s)	16.6	0.95 (3H, s)	15.5
26	1.1 (3H, s)	18.5	0.94 (3H, s)	16.9
27	1.1 (3H, s)	23.6	1.15 (3H, s)	23.7
28	0.76 (3H, s)	28.1	0.79 (3H, s)	28.4
29	0.8 (3H, s)	17.5	0.86 (3H, s)	17.5
30	0.8 (3H, s)	21.3	0.86 (3H, s)	21.3
1′	-	171.0		170.9
2′		34.5	2.02 (2H, q)	34.4
3′	0.9	14.1	0.88 (3H, t, J= 7.3Hz)	14.2

The spectroscopic data of compound **234** agreed well with the literature reported for 11-*oxo*-α-amyrin ethylated which was isolated from *Calotropis gigantea* for the first time (Table 16) (Omer *et al*., 2017). This study represents the first report of compound **234** in *C. procera*.

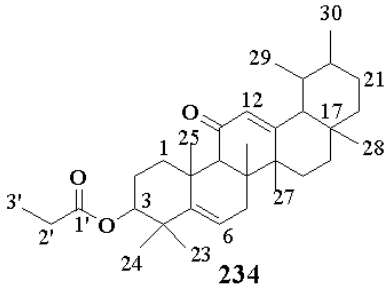

234

4.1.3. Secondary metabolites isolated from the root of *Caylusea abyssinica*

The methanol extract of the roots of *C. abyssinica* was subjected to silica gel column chromatographic fractionation which afforded five compounds (**238, 239, 240, 241,** and **79**). Compounds (**238, 239, 240, and 241)** were reported herein for the first time from *C. abyssinica*. Whereas compound **79** was previously reported from the roots of the same species (Edilu et al., 2015). The detailed characterizations of these compounds are presented below.

Compound **238** (24 mg) was obtained as a white solid with melting point 45-47 ºC. TLC profile showed a spot at R_f 0.58 with *n*-hexane: EtOAc (9:1) as a mobile phase. Its ^{1}H-NMR spectrum (400 MHz, $CDCl_3$, Appendix 18A) showed a triplet signal at δ 2.3 (t, J = 7.3 Hz, 2H) and quintet signal at δ 1.56 (q, J = 6.1 Hz, 2H) are characteristic of methylene protons at α and β positions to a carboxyl group, respectively. The signal due to many overlapping methylene protons was observed at δ 1.2 (brd. s, 16 H) which was supported by the appearance of an intense carbon signal at δ 29.7 in the ^{13}C-NMR spectrum. The presence of a terminal methyl group was evident from the appearance of the proton signal at δ 0.81 (t, J = 6.7 Hz, 3H). The ^{13}C-NMR (101 MHz, $CDCl_3$, Appendix 18B) spectra demonstrated the presence of 12 well-resolved signals. The signal at δ 177.3 is evident for the presence of a carboxyl group. The carbon signal at δ 33.6 is typical of methylene carbon adjacent to the carboxyl group. This was supported by the appearance of a triplet signal at δ 2.3 (2H) in the ^{1}H-NMR spectrum of the compound. The most upfield shifted carbon signal at δ 14.1 in the ^{13}C-NMR spectrum accounts for the presence of a terminal methyl group. The remaining ten methylene carbon signals were observed in the range between δ 31.9 to 22.7. A comparison of the NMR spectral data agreed with those reported in the literature for lauric acid (Yamashita *et al*., 2015). This compound has not been previously reported from this species.

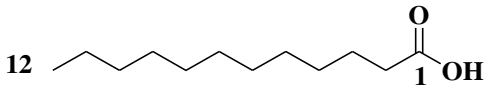

238

Compound **239** was obtained as a yellow amorphous crystal with an R_f value of 0.42 (*n*-hexane/EtOAc (4:1) as eluent. Its ^{1}H NMR (400 MHz, $CDCl_3$, Table 17, Appendix 19A) spectrum showed four symmetric aryl protons at δ 7.6 (dd, J = 5.7, 3.3 Hz, 2H, H-4, 5) and 7.5 (dd, J = 5.7, 3.3 Hz, 2H, H-3,6) with AA'BB' spin system suggesting a symmetrical 1, 2 substituted aromatic system. The methylene protons attached to the ester were observed at δ 4.2 (t, J = 6.1 Hz, 4H, CH_2-1, 1′) integrated into four protons. Besides, ten methylene protons showed a signal at δ 1.6 (p, J = 6.1 Hz, 2H, CH_2-2, 2′), 1.24 (m, 8H CH_2 −3, 3′, 4, 4′), 1.5 (m, 4H, CH_2-8, 8′), 1.35 (m, 4H, CH_2-5, 5′), 1.18 (4H, m, CH_2-6, 6′). The four-terminal methyl protons appeared at δ 0.83 (m, 6H, CH_3-9, 9′) and 0.8 (m, 6H, CH_3-7, 7′). The ^{13}C-NMR spectrum, with the aid of DEPT-135, COSY, HSQC, and HMBC (Appendix 19B-F) spectra, confirmed the presence of well resolved thirteen intense carbon peaks attributed to 26 carbon

numbers indicating that there is a symmetry in compound **239**. The ester carbonyl appeared at δ 167.8 (C-1, 8), three aromatic methines at δ 130.9 (C-3, 6), 128.8 (C-4, 5), and sp^2 quaternary carbon at δ 132.4 (C-2,7), methylene attached to ester oxygen appeared at δ 68.2 (C- 1′,1”). Moreover, the other symmetric carbon peaks were located at δ 38.7 (2′, 2″), 30.4 (3′, 3″), 28.9 (4′, 4″), 29.7, (5′, 5″), 23.0 (6′, 6″) and 23.7 (8′, 8″). The two terminal methyl groups displayed at δ 14.1 (C-7′, 7″) and 11.0 (C-9′,9”). The ^{1}H-^{1}H COSY spectrum showed a correlation between the proton signal at δ 7.5 (H-3) with 7.6 (H-4) and vice versa. The aromatic protons signal at δ 7.5 (H-3) and 7.6 (H-4) showed HSQC correlation with C-3 (δ 128.8) and C-4 (δ 130.9), respectively. The oxygenated protons (H-1′) showed HSQC correlation with C-1′ (δ 68.2) and HMBC correlation with carbons C-2′ (δ 38.7) and C-3′ (δ 30.4). The proton signal observed at δ 0. 8 (H-9″) showed HMBC correlation with the carbon signals at C-2′ (δ 38.7) and C-8″ (δ 23.7). Another HMBC correlation observed was between the proton signal at δ 0,8 (H-7′) and the carbon signals at δ 23.0 (C-6′), (C-5′) 29.7, and (C-4′) 28.9.

Table 17: ^{1}H NMR (400 MHz, $CDCl_3$) and ^{13}C NMR (101 MHz, $CDCl_3$) data of compound **239** and literature ^{1}H NMR and ^{13}C-NMR data of bis(2-ethylheptyl) phthalate.

Position	Compound **239**			(Allahresani *et al*., 2020)	
	^{1}H-NMR	^{13}C-NMR	Multiplicity	^{1}H-NMR	^{13}C-NMR
1	–	167.8 (C-1,8)	C	–	167.7
2	–	132.4 (C-2, 7)	C	–	132.5
3	7.5 (dd, J = 5.7, 3.3 Hz, 2H)	130.9 (C-3, 6)	CH	7.5 (2H, dd (8.8)	130.9
4	7.6 (dd, J = 5.7, 3.3 Hz, 2H)	128.8 (C-4, 5)	CH	7.7 (2H, dd (8.8)	128.8
1′/1"	4.2 (t, J = 6.1 Hz,4H)	68.2	CH_2O-	4.2 (4H, t (6.2)	68.1
2′/2"	1.6 (p, J = 6.1 Hz, 2H)	38.7	CH	1.6 (2H, m)	38.7
3′/3"	1.2 (m, 4H)	30.4	CH_2	1.2 (4H, m)	30.3
4′/4"		28.9	CH_2	1.3 (4H, m)	28.9
5′/5"		29.7	CH_2	1.3 (4H, m)	29.7
6′/6"		23.0	CH_2	1.3(4H, m)	23.0
7′/7"	0.8 (m, 6H)	14.1	CH_3	0.9 (6H, m)	14.1
8″/8"	1.5 (m, 4H)	23.7	CH_2	1.4 (4H, m)	23.7
9″/9"	0.8 (m, 6H)	11.0	CH_3	0.9 (6H, m)	11.0

The above spectral data is in good agreement with literature data (Table 21) reported for bis(2-ethylheptyl) phthalate reported herein for the first time from the species (Allahresani *et al*., 2020).

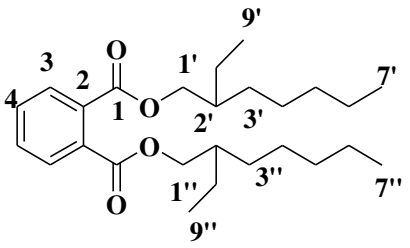

239

Compound **240** was obtained as a white solid with melting point of 13.8-15 ºC, R_f value of 0.41 (*n*-hexane/EtOAc (4:1), as eluent). Its ^{1}H-NMR spectrum (400 MHz, $CDCl_3$, Appendix 20A) showed a signal at δ 5.4 (t, J = 5.3 Hz) attributed to the olefinic proton. The triplet signal at δ 2.4 (t, J = 7.3 Hz, 2H) and quintet signal at δ 2.0 (q, J = 6.3 Hz, 2H) are characteristic of methylene protons at α and β positions to a carboxyl group, respectively. The signal due to many overlapping methylene protons was observed at δ 1.3 (brd. s, 24 H) which was supported by the appearance of an intense carbon signal at δ 29.7 in the ^{13}C-NMR spectrum (101 MHz, $CDCl_3$, Appendix 20B). The presence of a terminal methyl group was evident from the appearance of the proton signal at δ 0.9 (t, J = 6.7 Hz, 3H) with the corresponding carbon signal at δ 14.1. The ^{13}C NMR spectral data with the aid of DEPT-135 (Appendix 20C) displayed well resolved 18 carbon peaks of which the most downfield and upfield signals at δ 177.9 and 14.1 belong to the carboxyl and terminal methyl groups, respectively, whereas two olefinic carbons are evident at δ 130.0 and 129.7. The carbon signal at δ 34.2 is typical of methylene carbon adjacent to the carboxyl group. The remaining carbon signals observed at δ 31.9, 29.7, 29.7, 29.6, 29.5, 29.4, 29.3, 29.2, 29.1, 27.2, 27.2, 24.7, and 22.7 belong to methylene carbons. The above spectral data are in good agreement with the structure of oleic acid, and also complement with literature data (Deivasigamani *et al*., 2016), reported herein for the first time from the species.

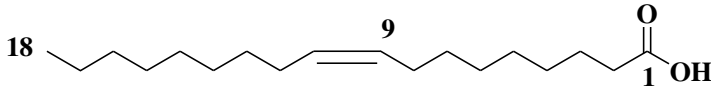

240

Compound **241** (20 mg) was obtained as a white solid with melting point 56-58 ºC, R_f value of 0.39 (*n*-hexane/EtOAc (4:1) as eluent. Its ^{1}H NMR spectrum (400 MHz, $CDCl_3$, Appendix 21A) showed proton signals at δ 2.3 (t, J = 7.5 Hz, 2H, H-2) and 1.6 (p, J = 7.5 Hz, 2H, H-3) attributed to methylene protons at α and β position to a carboxyl group, respectively. The methylene proton signals were observed at δ 1.2 (brs, 20H, H-4-13) and terminal methyl proton at δ 0.8 (t, J = 6.7 Hz, 3H, H-14). The ^{13}C NMR (100 MHz, $CDCl_3$, Appendix 21B) spectral data with the aid of DEPT-135 (Appendix 21C) revealed a total of 14 well resolved carbon signals of which the most downfield and upfield signals observed at δ 178.8 and 14.1 belong to the carboxyl group and terminal methyl, respectively. The carbon signal at δ 33.8 is a typical characteristic peak of methylene carbon adjacent to the carboxyl group. The remaining methylene carbon signals were observed in the range between δ 31.9 to 22.7. Thus, based on the above spectral data, the structure of compound **241** is in good agreement with the structure of myristic acid (Galma *et al*., 2021) reported herein for the first time from the species.

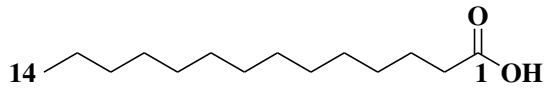

241

Compound **79** was obtained as a white solid with melting point 166-168 ºC, R_f value of 0.46 (*n*-hexane/EtOAc (4:1) solvent system as eluent. Its ^{1}H-NMR spectrum (400 MHz, $CDCl_3$, Table 18, Appendix 22A) showed signals for three olefinic protons at δ 5.3 (d, J = 5.4 Hz, 1H), 5.1 (dd, J = 15.2, 8.5 Hz, 1H), 5.0 (dd, J = 15.2, 8.4 Hz, 1H). The signal at δ 3.5 (1H, m) corresponds to sp^3 oxygenated methine, the characteristic peak for steroids bearing hydroxyl group at the C-3 position. Analysis of the ^{1}H-NMR spectrum demonstrated the presence of six methyl signals at δ 0.9 (s, 3H), 0.8 (m, 3H), 0.7 (s, 3H), 0.74 (t, J = 7.4 Hz, 3H), and 0.6 (d, J = 7.6 Hz, 6H) attributed to H-19, H-21, H-26, H-27, H-18, and H-29, respectively. The ^{13}C-NMR ($CDCl_3$ 400 MHz, Table 18, Appendix 22B) spectral data with the aid of DEPT-135 (Appendix 22C) displayed a total of 29 well resolved carbon signals of which peaks at δ 140.8, 121.7, 129.3, and 138.12 correspond olefinic carbons C-5, C-6, C-22, and C-23, respectively.

Table 18: ^{1}H NMR (400 MHz, $CDCl_3$) and ^{13}C NMR (101 MHz, $CDCl_3$) data of compound **79** and literature ^{13}C-NMR data of stigmasterol.

Position	Compound **79**		(Edilu *et al*., 2015)	
	^{1}H-NMR	^{13}C-NMR	^{1}H-NMR	^{13}C-NMR
1		37.3		37.2
2		31.7		31.6
3	3.46	71.8	3.44	71.8
4		42.2		42.2
5	5.28	140.8	5.26	140.7
6		121.7		121.7
7		31.9		31.9
8		31.9		31.9
9		50.2		50.1
10	-	36.5		36.5
11		21.1		21.0
12		39.7		39.7
13	-	42.3		42.3
14		56.9		56.8
15		24.3		24.3
16		28.9		28.9
17		56.0		55.9
18	0.6	12.2	0.61	12.2
19	0.94	19.4	0.93	19.4
20		40.5		40.5
21	0.77	21.1	0.76	21.1
22	5.08	138.3	5.06	138.3
23	4.95	129.3	4.96	129.2
24		51.3		51.2
25		33.8		33.9
26	0.7	19.0	0.72	19.0
27	0.74	21.2	0.74	21.2
28		25.4		25.4
29	0.6	11.9	0.60	12.0

The above spectral data is in good agreement with stigmasterol and also compliment with literature data, which was previously reported from the roots of the same species (Table 18) (Edilu *et al*., 2015).

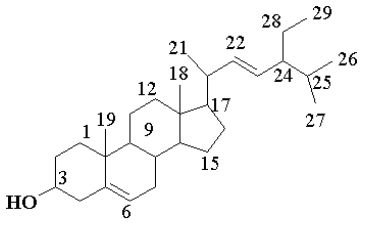

79

4.1.4. Secondary metabolites isolated from the root of *Justicia schimperiana*

The dichloromethane/methanol (1:1) extract of the roots of *J. schimperiana* was subjected to silica gel column chromatographic fractionation which afforded six compounds *β*-sitosterol (**78),** 5-methoxy durmillone (**242**), *trans*-resveratrol (**243**), tricuspidatol A (**244),** kaempferol-3-O-α rhamnopyranoside (**245**), and kaempferol-3-O-rutinoside (**246**). All compounds isolated were reported herein for the first time from the species. The structures of the isolated compounds were characterized by ^{1}H NMR, ^{13}C NMR, and DEPT-135 as discussed here below. All compounds were identified by interpretation of the results of the spectra and comparison with literature data.

Compound **78** was isolated as a white powder with melting point 138-141 ºC, R_f value of 0. 58 (*n*-C_6H_{14}:EtOAc, 4:1 as eluent). Its ^{1}H NMR spectrum (400 MHz, $CDCl_3$, Table 19, Appendix 23A) showed one olefinic proton signal at δ 5.4 (t, J = 3.7 Hz, 1H) along with six methyl signals. Methyl signals were observed at δ 1.0 (s, 3H), 0.7 (s, 3H), 0.86 (d, J = 6.8 Hz, 3H), 0.90 (d, J = 6.2 Hz, 3H), 0.93 (d, J = 6.5 Hz, 3H), and 0.82 (t, J = 7.8 Hz, 3H) attributed to H-29, H-28, H-27, H-26, H-19, and H-24, respectively. The proton signal at δ 3.6 (brs, 1H, H-3) corresponds to the oxygenated sp^3 methine proton. Other proton signals integrating for 29 hydrogens were detected in the range δ 1.0 to 2.3. The ^{13}C NMR ($CDCl_3$, 101 MHz, Table 19, Appendix 23B) spectrum in combination with DEPT-135 (Appendix 23C) displayed 29 well-resolved carbon signals including six methyl, eleven methylene, nine methine, and three quaternary carbons of which one sp^2 and two sp^3 quaternary carbons appeared at δ 140.7, 36.5, and 42.3 attributed to C-5, C-10, and C-13, respectively, whereas one olefinic methine carbon and sp^3 oxygenated methine signals were observed at δ 121.7 (C-6) and 71.9 (C-3).

Table 19: ^{1}H-NMR (400 MHz, $CDCl_3$) and ^{13}C-NMR (101 MHz, $CDCl_3$) spectral data of compound **78** and the reported data for *β*-sitosterol.

Position	Compound **78**		(Chaturvedula, & Prakash, 2012)	
	^{1}H-NMR	^{13}C-NMR	^{1}H-NMR	^{13}C-NMR
1		37.2		37.5
2		31.9		31.9
3	3.6 (brs, 1H)	71.9	3.53 (tdd, 1H, *J* = 4.5, 4.2, 3.8 Hz)	72.0
4		42.0		42.5
5		140.7		140.9
6	5.4 (t, *J* = 3.7 Hz, 1H)	121.7	5.36 (t, 1H, *J* = 6.4 Hz)	121.9
7		31.4		32.1
8		31.9		32.1
9		50.1		50.3
10		36.5		36.7
11		21.1		21.3
12		39.8		39.9
13		42.3		42.6
14		56.8		56.9
15		25.4		26.3
16		28.3		28.5
17		56.1		56.3
18		36.1		36.3
19	0.93 (d, *J* = 6.5 Hz, 3H)	19.0	0.93 (d, 3H, *J* = 6.5 Hz)	19.2
20		33.9		34.2
21		26.1		26.3
22		45.8		46.1
23		23.1		23.3
24	0.82(t, *J* = 7.8 Hz, 3H)	12.2	0.84 (t, 3H, *J* = 7.2 Hz)	12.2
25		29.1		29.4
26	0.90 (d, *J* = 6.2 Hz, 3H)	19.8	0.83 (d, 3H, *J* = 6.4 Hz)	20.1
27	0.86 (d, *J* = 6.8 Hz, 3H)	19.4	0.81 (d, 3H, *J* = 6.4 Hz)	19.6
28	0.7(s, 3H)	18.8	0.68 (s, 3H)	19.0
29	1.0 (s, 3H)	11.9	1.01 (s, 3H)	12.0

The above spectral data are in good agreement with the data reported in the literature for β-sitosterol (Chaturvedula, & Prakash, 2012) (Table 19).

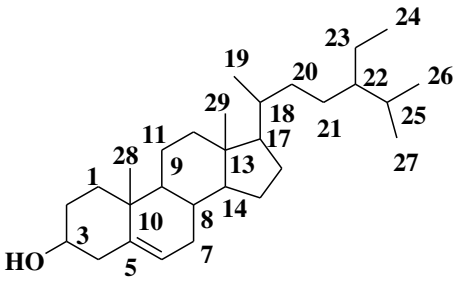

78

Compound **242** was isolated as white crystals solid with melting point 145-147 ºC, R_f value of 0.36 (50 % EtOAc in *n*-hexane) as eluent on TLC. The analysis of the ^{1}H NMR (400 MHz, $CDCl_3$, Table 20, Appendix 24A) spectrum of **242** revealed the presence of four aromatic protons at δ 7.80 (s, 1H), 7.1 (d, J = 1.6 Hz, 1H), 6.9 (d, J = 8.0 Hz, 1H), and 6.8 (d, J = 8.0 Hz, 1H). The aromatic methine proton signals at 7.1 (d, J = 1.6 Hz, H-2′), 6.9 (d, J = 8.0 Hz, H-6′), and 6.8 (d, J = 8.0 Hz, H-5′) confirmed that the presence of disubstituted aromatic ring having ortho coupled ABX pattern. The proton signals at δ 5.67 (d, J = 10.0 Hz, 1H) and δ 6.75 (d, J = 10.0 Hz, 1H) indicated that the two protons are on the adjacent sp^2 carbon atoms coupled to each other. The singlet proton signal at δ_H 6.00 (s, 2H) represented the methylenedioxy proton. The presence of two methoxy groups was suggested by two singlets proton signals at δ 3.94, and 3.88. A high-intensity singlet proton signal appeared at δ_H 1.53 (s, 6H) in the proton spectrum, indicating the presence of the symmetrical methyl group in the compound. The ^{13}C-NMR spectrum, with the aid of DEPT-135, COSY, HSQC, and HMBC (Table 20, Appendix 24B-F, respectively) spectra of compound **242** confirmed the presence of well-resolved 21 carbon peaks corresponding to 22 carbons including 12 quaternary carbons, 6 methine carbons, 2 methoxy carbons, 1 methylenedioxy carbon, and two symmetrical methyl carbons. The presence of six sp^2 oxygenated quaternary carbons signals were showed at δ 151.3 (C-5), 140.1 (C-6), 149.2 (C-7), 153.1 (C-8a), 147.7 (C-3′), and 147.7 (C-3′) along with four sp^2 quaternary carbons at δ 125.4 (C-3), 106.8 (C-4a), 113.2.8 (C-8), and 125.8 (C-1′). Six methine carbon signals were observed at δ 150.5 (C-2), 110.1 (C-2′), 108.4 (C-5′), 122.6 (C-6′), 129.3 (C-10), and 115.1 (C-11). The methylenedioxy and sp^3 oxygenated quaternary carbon appeared at δ_C 101.2 (C-12) and 78.3 (C-9), respectively. The signals due to the two methoxy carbons and the symmetry methyl group showed at δ C 62.3, 61.6, and 28.2, respectively. The presence of an α, β-unsaturated carbonyl carbon is evident from the appearance of a carbon signal at δ 175.3 (C-4). The ^{1}H-^{1}H COSY

spectrum showed a correlation between the proton signal at δ 5.67 with 6.75 and *vice versa*. The HSQC showed a correlation such that the methine proton signals at δ 7.80, 7.1, 6.8, 6.9, 5.67, and 6.75 correlates with the carbons at δ 150.5, 110.1, 108.4, 122.6, 129.2, and 115.1, respectively. Besides, the HSQC correlations observed were between the two methoxy proton signals at δ 3.94, 3.88, and one methylenedioxy proton at 6.0 with carbon signals at δ 62.3, 61.6, and 101.2, respectively. However, the HMBC spectrum showed that the H-2 proton correlates with the quaternary carbons at δ 125.4 (C-3), 175.3 (C-4), and 149.2 (C-7). Further HMBC correlation showed that the methine proton signal at δ 7.1 (H-2′) showed correlations with the carbon signals at δ 147.7 (C-3′), and 122.6 (C-6′), aromatic methine proton signal at δ 6.8 (H-5′) correlates with the carbons at δ 147.7 (C-4′), and 125.8 (C-1′), proton signals at δ 6.9 (H-6′) correlates with the carbons at δ 147.7 (C-4′). Additional HMBC connectivity was detected between the proton signal at δ 5.67 with the quaternary carbon signals at δ 106.8 and 78.3, and the proton signal at δ 6.75 with quaternary carbon signals at δ 151.3, and 78.3. Furthermore, the methoxy proton signal at δ 3.94, and 3.88 correlates with the carbon signal at δ 153.1 (C-8a), and 140.1 (C-6), the methyl proton signal at δ 1.5 correlates with the carbon signals at δ 78.3 (C-9), and 129.2 (C-10), and the methylenedioxy proton signal at δ 6.0 correlates with 147.7 (C-3′), and 147.7 (C-4′).

Table 20: ^{1}H NMR (400 MHz, $CDCl_3$) and ^{13}C NMR (101 MHz, $CDCl_3$) data of compound **242** and literature data of 5-methoxy durmillone.

Position	Compound **242**				**(Eribo *et al*., 2016)**	
	^{1}H-NMR	^{13}C-NMR	HSQC	HMBC	^{1}H-NMR	^{13}C-NMR
2	7.80 (s)	150.5	H-2 → C-2	C-4, C-3, C-7	7.81 (H-2, s)	150.4
3	-	125.4			-	125.4
4	-	175.3			-	175.0
4a	-	106.8			-	106.7
5	-	151.3			-	151.2
6	-	140.1			-	140.1
7	-	149.2			-	149.2
8	-	113.2			-	113.2
8a	-	153.1			-	153.0
1′	-	125.8			-	125.7
2′	7.1 (d, *J* = 1.6 Hz)	110.1	H-2′→ C-2′	C-3′, C-6′	7.1 (d, *J* = 2.4 Hz)	110.1
3′	-	147.7			-	147.6
4′	-	147.7			-	147.6
5′	6.8 (d, *J* = 8.0 Hz)	108.4	H-5′→ C-5′	C-4′, C-1′	6.83 (d, *J* = 7.8 Hz)	108.3
6′	6.9 (d, *J* = 8.0, Hz)	122.6	H-6′ → C-6′	C-4′	6.96 (d, *J* = 2.4, 7.8 Hz)	122.6
9	-	78.3				78.2

10	5.67 (d, *J* = 10.0 Hz)	129.2	H-10 → C-10	C-4a, C-9	5.70 (d, *J* = 8.0 Hz)	129.2
11	6.75 (d, *J* = 10.0 Hz)	115.1	H-11 → C-11	C-9, C-5	6.76 (d, *J* = 8.0 Hz)	115.1
9-CH_3	1.5 (s, 3H)	28.2		C-10, C-9	1.56 (s, 3H)	28.1
5-OCH_3	3.94 (s, 3H)	62.3		C-8a	3.96 (s, 3H)	62.2
6-OCH_3	3.88 (s, 3H)	61.6		C-6	3.92 (s, 3H)	61.5
12	6.00 (s, 2H)	101.2	H-12 → C-12	C-3′, C-4′	6.00 (s, 2H)	101.1

Thus, based on the above spectroscopic evidence the compound **242** was characterized as 5-methoxy durmillone, previously isolated from the roots of *Millettia ferruginea* (Eribo *et al*., 2016; Dagne et.al, 1989). However, this is the first report of the compound from *J. schimperiana*.

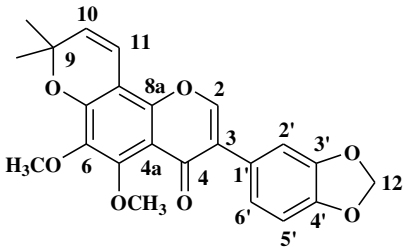

242

Compound **243** was obtained as light brown solid with melting point 154-157 ºC with an R_f value of 0.49 (*n*-C_6H_{14}:EtOAc, 1:4 as eluent, 11 mg). Its ^{1}H NMR (400 MHz, DMSO, Table 21, Appendix 25A) showed a pair of doublets at δ 7.1 (d, *J* = 8.2 Hz, 2H) and δ 6.8 (d, *J* = 8.2 Hz, 2H) attributed to AA'XX' spin system aromatic ring. The aromatic proton at δ 6.2 (d, *J* = 1.9 Hz, 2H, C-2, 6), and 6.1 (s, 1H, C-4) attributed to 1, 3, 5 tri-substituted aromatic ring. The pair of doublet peaks at δ 6.6 (d, *J* = 16.0 Hz, 1H) and 6.2 (d, *J* = 16.0 Hz, 1H) correspond to the *trans* orientation of olefinic protons. The ^{13}C-NMR and DEPT-135 spectra (101 MHz, DMSO, Table 21, Appendix 25B, and 25C, respectively) displayed the presence of 10 signals for 14 carbons of which signals at δ 115.9 (C-3′,5′) and δ 128.2 (C-2',6') belong to AA'XX' spin system aromatic sp^2 methine carbons whereas signals at δ 105.9 (C-2, 6) and δ 99.7 (C-4) belong to the presence of a 1,3,5-trisubstituted aromatic ring. The olefinic carbons appeared at δ 127.5 (C-7), and δ 126.6 (C-8) whereas sp^2 quaternary carbons appeared at δ 154.3 (C-3, 5), 157.8 (C-4′), 146.5 (C-1), and 130.3 (C-1′). Compared to those reported in the literature, the ^{13}C NMR spectral data of compound **243** are in good agreement with those reported for *trans-resveratr*ol (Degfie *et al*., 2022) (Table 21), reported herein for the first time from this plant.

Table 21: ^{1}H-NMR (400 MHz, DMSO-d_6) and ^{13}C-NMR (101 MHz, DMSO-d_6) spectral data of compound **243** and the reported data for *trans-resveratr*ol.

Position	Compound **243**		(Degfie *et al*., 2022)
	^{1}H-NMR	^{13}C-NMR	^{13}C-NMR
1	-	146.5	141.2
2	6.2 (*d*, *J* = 1.9 Hz, 2H)	105.9	105.7
3	-	154.3	159.5
4	6.1 (s, 1H)	99.7	102.4
5	-	154.3	159.5
6	6.2 (*d*, *J* = 1.9 Hz, 2H)	105.9	105.7
7	6.2 (d, *J* = 16.0 Hz, 1H)	127.5	129.3
8	6.6 (d, *J* = 16.0 Hz, 1H)	126.6	126.9
1′	-	130.3	130.3
2′	7.1 (*d*, *J* = 8.2 Hz, 2H)	128.2	128.7
3′	6.8 (*d*, *J* = 8.2 Hz, 2H)	115.9	116.4
4′	-	157.8	158.2
5′	6.8 (*d*, *J* = 8.2 Hz, 2H)	115.9	116.4
6′	7.1 (*d*, *J* = 8.2 Hz, 2H)	128.2	128.7

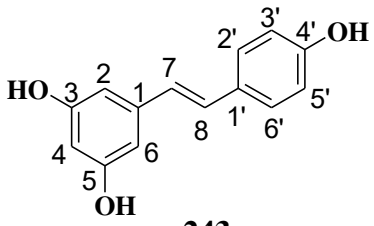

243

Compound **244** was isolated as a light brown solid with melting point 159-l63 ºC with an R_f value of 0.43 in 10 % methanol/ dichloromethane as eluent. Its ^{1}H-NMR (400 MHz, DMSO-d_6, Table 22, Appendix 26A) spectrum showed the presence of four methine proton signals at δ 7.2 (d, *J* = 8.2 Hz, 4H), 6.7 (d, *J* = 8.3 Hz, 4H), 6.6 (brs, 2H), and 5.9 (brs, 4H). The spectrum showed the presence of two symmetrically placed AA'BB' type spin systems at δ 7.2 (d, *J* = 8.2 Hz, 4H, H-2, 6, and 2', 6') and 6.7 (d, *J* = 8.3 Hz, 4H, H-3, 5, and 3', 5') suggested the presence *para-substituted* phenyl moieties (ring A and C) (Degfie *et al*., 2022; Cichewicz *et al*., 2000). The broad singlet proton signal at δ 6.6 (2H, H-12,12'), and high-intensity singlet signal at δ 5.9 (4H, H-10, 14, and 10', 14') attributed to the protons of the two 1,3,5-trisubstituted resorcinol moieties (B and D rings) (Degfie *et al*., 2022; Cichewicz *et al*., 2000). The four remaining aliphatic protons resonances have vicinal coupling patterns at δ 5.2 (brs, 2H, H-7, 7′), 3.9 (d, J= 4.4 Hz, 2H, H-8, 8′) ascribed to the tetrahydrofuran (ring E). The ^{13}C-NMR and DEPT-135

spectra (101 MHz, DMSO, Table 22, Appendix 26B, and 26C) exhibited the presence of 10 signals for 20 carbons of which methine carbons appeared at δ 128.2 (C-2, 6, and 2', 6') and 115.4 (C-3, 5 and 3', 5') with AA'BB' spin system indicating the presence of a 1,4 substituted phenyl ring at C-4 position. The compound displayed sp^2 oxygenated aromatic quaternary carbons at δ 158.9 (C-11, 13 and 11′, 13′), δ 157.9 (C-4, 4′), δ 144.1 (C-9, 9′), and δ 132.5 (C-1, 1′). In addition, the methine carbon showed symmetrically placed aromatic signals at δ 107.8 (C-10, 14, and 10′,14′), and δ 101.1 (C-12, 12′) attributed to two 1,3,5-trisubstituted resorcinol moieties (Degfie *et al*., 2022; Cichewicz *et al*., 2000). The aliphatic carbon signal at δ 84.8 (C-7, 7') and δ 55.9 (C-8, 8') are attributed to a tetrahydrofuran moiety. Thus, based on the above spectroscopic evidence, the spectral data of compound **244** is in good agreement with those reported in the literature for tricuspidatol A (Degfie *et al*., 2022; Cichewicz *et al*., 2000) (Table 22). However, this is the first report of the isolation of the compound from *J. schimperiana*.

Table 22: ^{1}H-NMR (400 MHz, DMSO-d_6) and ^{13}C-NMR (101 MHz, DMSO-d_6) spectral data of compound **244** and the reported data for tricuspidatol A.

Position	Compound **244**		(Degfie *et al*., 2022)	(Cichewicz *et al*., 2000)
	^{1}H-NMR	^{13}C-NMR	^{13}C-NMR	^{13}C-NMR
1, 1′	-	132.5	133.9	131.7
2, 6, 2′, 6′	7.2 (d, J = 8.2 Hz)	128.2	128.8	128.1
3, 5, 3′, 5′	6.7 (d, J = 8.3 Hz)	115.4	116.1	114.2
4, 4′	-	157.9	158.1	155.9
7, 7′	5.2 (brs)	84.8	85.9	84.2
8, 8′	3.9 (d, J = 4.4 Hz)	55.9	59.0	57.6
9, 9′	-	144.1	142.2	142.6
10, 14, 10′, 14′	5.9 (brs)	107.8	109.0	108.0
11, 13, 11′, 13′	-	158.9	158.8	157.7
12, 12′	6.6 (brs)	101.1	101.8	100.5

The NMR spectral analysis described above allowed the identification of compound **244** as tricuspidatol A (**244**).

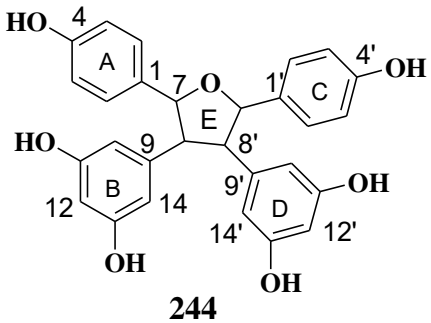

244

Compound **245** was isolated as a yellow solid with an R_f value of 0.48 (10 % MeOH in DCM) as eluent. Its ^{1}H-NMR spectrum (400 MHz, DMSO, Table 23, Appendix 27A) showed two *meta*-coupled doublets at δ 6.3 (J = 2.00 Hz) and δ 6.5 (J = 2.00 Hz) attributed to H-6 and H-8, respectively, of ring A. The two sets of aromatic proton signals at δ 7.8 (d, J = 8.7 Hz, 2H, H-2′/H-6′) and 6.8 (d, J = 8.7 Hz, 2H, H-3′/H-5′) with AA′XX′ spin system attributed to 4′-substituted B-ring of a kaempferol moiety. The presence of a 5-hydroxy substitution on ring A of a flavonoid is evident from the appearance of a downfield signal at δ 12.7 (1H, *s*) corresponding to a chelated hydroxyl group in the compound. The presence of a rhamnose moiety was evident from anomeric proton at δ 4.9 (*d*, J = 1.59 Hz, 1H, H-1′), methyl protons signal at δ 0.9 (*d*, J = 5.46Hz, 3H, H-6″), and signals in between δ 3.2-4.0. The proton decoupled ^{13}C-NMR together with the DEPT-135 spectrum (101 MHz, DMSO, Table 23, Appendix 27B, and 27C, respectively) displayed six oxygenated aromatic quaternary carbons signal at δ 160.1(C-2), 134.8 (C-3), 162.3 (C-5), 164.3 (C-7), 156.7 (C-9), 157.1 (C-4′), and two non-oxygenated aromatic quaternary carbons at δ 121.5 (C-1'), and 104.8 (C-10). The sp^2 quaternary carbon signal at δ 178.4 suggest the presence of α, β-unsaturated carbonyl carbon. The methine carbons at δ 115.4 (C-3', 5') and 130.7 (C-2', 6') showed AA'BB' spin system indicating the presence of a 1,4 substituted phenyl ring at C-4 position. Other methine signals were observed at δ 98.8 (C-6) and 95.3 (C-8). A series of signals in between δ 72.1 to 66.1 combined with the signals at δ 101.8 (C-1") are evident for the presence of one sugar unit. The methyl signal of rhamnose group appeared at 16.9 (C-6"). Based on the above spectroscopic data, compound **245** was therefore identified as kaempferol-3-O-α rhamnopyranoside (Emam *et al*., 2010) (Table 23), reported herein for the first time from this plant. Based on the above spectroscopic data, compound **245** was therefore identified as kaempferol-3-O-α rhamnopyranoside (Emam *et al*., 2010), reported herein for the first time from this plant.

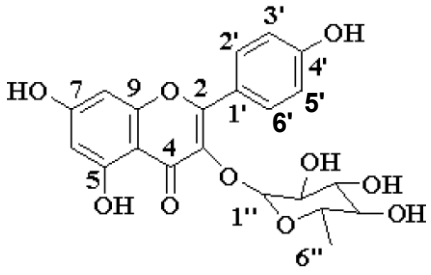

245

Compound **246** was isolated as a yellow solid with an R_f value of 0.38 (10 % MeOH in DCM) as eluent. NMR spectral data of **5** (400 MHz, DMSO, Table 23, Appendix 28A) was comparable to compound **245** with only additional glucose group at C-3. The ^{1}H-NMR spectrum of compound **245** disclosed the presence of four aromatic protons signal region at δ 7.8 (d, J = 8.08 Hz, 2H), 6.9 (d, J = 8.08 Hz, 2H), 6.7 (d, J = 11.3 Hz, 1H), and 6.4 (d, J = 10.7 Hz, 1H). The aromatic proton signals showed at δ 7.8 (d, J = 8.08 Hz, 2H, H-2′, H-6′), and 6.9 (d, J = 8.08 Hz, 2H, H-3′, H-5′) with AA′XX′ spin system attributed to 4′-substituted B-ring. The two doublets' peaks observed at δ 6.7 (d, J = 2.3 Hz, 1H, H-8) and 6.43 (d, J = 2.0 Hz, 1H, H-6) are characteristic of AB spin pattern ring A in a flavonoid skeleton. The presence of downfield signal at δ 12.6 (1H, s) correspond to a chelated OH group suggesting 5-hydroxy substitution on its ring A. The anomeric protons of the glucose, H-1′′, and rhamnose H-1‴ moieties are allocated to the two doublets at δ 5.3 (d, J = 21.1 Hz, 1H) and 5.0 (d, J = 18.0 Hz, 1H), respectively. The oxygenated methylene proton appeared at δ 4.7 (d, J = 12.3 Hz, 2H). The presence of the rhamnopyranose moiety was confirmed by the multiplet signal at δ 0.9 (d, J = 5.5 Hz, 3H) for a secondary methyl group. A series of peaks in the spectrum between δ 4.0 and 3.1 attributed to the presence of sugar moieties. The singlet signal at δ 5.9, and 5.7 belong to hydroxyl groups. The ^{13}C-NMR with the aid of DEPT-135 (101 MHz, DMSO, Table 23, Appendix 28B, and 28C, respectively) displayed nine quaternary, fourteen methine carbons, one oxygenated methylene, and one methyl carbon. The sp^2 oxygenated quaternary carbons signal showed at δ 157.0 (C-2), 134.6 (C-3), 161.7 (C-5), 164.8 (C-7), 156.7 (C-9), 160.4 (C-4′), and sp^2 non-oxygenated quaternary carbons at δ 121.0 (C-1'), and 104.5 (C-10). The olefinic methine carbons signal at δ 115.9 (C-3', 5') and 131.1 (C-2', 6') suggest AA'BB' spin system 1,4 substituted phenyl ring at C-4 position. The carbon signals at δ 95.5, and δ 94.5 belong to sp^2 methines (C-6 and C-8, respectively). The occurrence of an α, β-unsaturated carbonyl carbon was evident from the appearance of a carbon signal at δ 178.1 (C-4). A series of signals in the region between δ 79.6 to 63.1 combined with the signals at

δ 102.2 (C-1''), and 99.2 (C-1‴) are evident for the presence of two sugar units. The methyl signal of rhamnose group appeared at δ 17.9 (C-6‴). The spectral data of the compound is in good agreement with literature data reported for kaempferol-3-O-rutinoside (Dehaghani *et al*., 2017), confirming the compound **246** is kaempferol-3-*O*-rutinoside (Table 23), reported herein for the first time from this plant. Kaempferol-3-O-rutinoside (**246**), which was first reported from *J. schimperiana*.

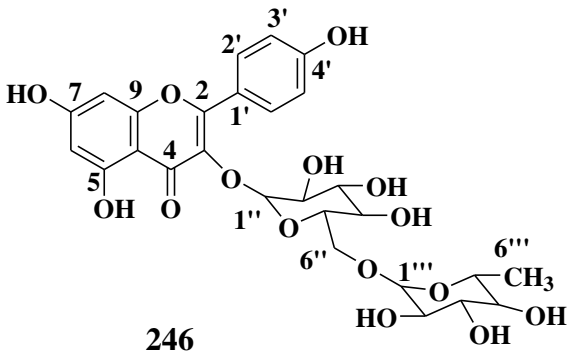

246

Table 23: Comparison of the ^{1}H-NMR (400 MHz, DMSO-d_6) and ^{13}C-NMR (101 MHz, DMSO-d_6, δ in ppm) spectral data of compounds **245,** and **246** with the reported data.

Position	**Compound 245**		**(Emam *et al*., 2010)**		**Compound 246**		**(Dehaghani *et al*., 2017)**	
	^{1}H-NMR	^{13}C-NMR	^{1}H-NMR	^{13}C-NMR	^{1}H-NMR	^{13}C-NMR	^{1}H-NMR	^{13}C-NMR
2	-	160.1	-	161.3	-	157.0	-	158.3
3	-	134.8	-	133.8	-	134.6	-	134.5
4	-	178.4	-	179.1	-	178.1	-	178.8
5	-	162.3	-	162.9	-	161.7	-	161.7
6	6.3 (*J* = 2.00 Hz)	98.8	6.19 (d, *J* = 2.1)	100.7	6.2 (s, 1H)	95.6	6.23 (s, 1H)	99.8
7	-	164.3	-	167.2	-	164.8	-	165.8
8	6.5 (*J* = 2.00 Hz)	95.3	6.35 (d, *J* = 2.1)	96.8	6.4 (d, *J* = 2.0 Hz)	94.5	6.43 (s, 1H)	94.95
9	-	156.7	-	158.7	-	156.7	-	158.3
10	-	104.8	-	105.4	-	104.5	-	104.8
1′	-	121.5	-	122.6	-	121.0	-	122.6
2′, 6′	7.8 (d, *J* = 8.7 Hz)	130.7	7.8 (d, *J* = 8.4)	131.2	7.8 (d, *J* = 8.08 Hz)	131.1	8.08 (d, 1H, *J* = 8.9)	132.4
3′, 5′	6.8 (d, *J* = 8.7 Hz)	115.4	6.8 (d, *J* = 8.1)	115.9	6.9 (d, *J* = 8.08 Hz)	115.9	6.90 (d, 1H, *J* = 8.9)	116.09
4′	-	157.1	-	161.7	-	160.4	-	160.4
Rha					Glucose			
1″	4.9 (*d*, *J* = 1.59 Hz)	101.8	5.7 (d, *J* = 1.8)	101.6	5.3 (d, *J* = 21.1Hz)	102.2	5.15 (d, 1H, *J* = 7.5)	104.61
2″	3.2-4.0 m	70.6	3.3-3.6 m	69.8	3.2-4.0 m	75.7	3.21-3.85	75.77
3″	3.2-4.0 m	71.3	3.3-3.6 m	71.9	3.2-4.0 m	78.5	3.21-3.85	78.14

4″	3.2-4.0 m	72.1	3.3-3.6 m	72.8	3.2-4.0 m	70.5	3.21-3.85	71.44
5″	3.2-4.0 m	66.1	3.3-3.6 m	68.5	3.2-4.0 m	71.1	3.21-3.85	72.1
6″	0.9 (*d*, *J* = 5.46 Hz)	16.9	0.9 (d, *J* = 6)	17.5	4.7 (d, *J* = 12.3 Hz)	63.1	3.21-3.85	68.56
					Rha			
1‴	-	-	-	-	5.0 (d, *J* = 18.0Hz)	99.2	4.54 (bs, 1H)	102.21
2‴	-	-	-	-	3.1-4.0	67.3	3.21-3.85	72.10
3‴	-	-	-	-	3.1-4.0	71.5	3.21-3.85	72.29
4‴	-	-	-	-	3.1-4.0	70.8	3.21-3.85	73.89
5‴	-	-	-	-	3.1-4.0	65.4	3.21-3.85	69.75
6‴	-	-	-	-	0.9 (d, *J* = 5.5 Hz)	17.9	1.14 (d, *J* = 6.0)	17.94

4.1.5. Secondary metabolites isolated from the root of *Verbascum sinaiticum*

The CH_3OH root extract of *V. sinaiticum* was fractionated over silica gel column chromatographic which provided eight compounds (**247**, **248**, **249**, **250**, **251**, **252**, **253**, and **230**). This paper represents the first report of all compounds derived from *V. sinaiticum*. Different NMR spectroscopic techniques were used to characterize the structure of the isolated compounds, as shall be discussed below. All of the isolated compounds were identified by comparing the results of the analysis of the spectra with information obtained from the literature.

Compound **247** was isolated as a yellow solid with melting point 83-85 ºC, R_f 0.41 (5 % MeOH in CH_2Cl_2) as eluent. The proton NMR spectrum (400 MHz, $CDCl_3$, Table 24**,** Appendix 29A) of compound **247** showed a pair of double doublets appearing at δ 7.52 and 6.9 (J = 8.7 Hz) indicating a 1, 4 disubstituted aromatic ring. The methoxy proton signal on aromatic ring was detected as a sharp singlet at δ 3.86 (s, 3H), which was supported by an analogous signal in its carbon spectra at δ 55.4. The triplet and multiplet signals observed at δ_H 2.3, and 2.1 were accounted for methylene protons adjacent to a carbonyl carbon. An aliphatic chain with 12 methylenes was suggested by a broad singlet signal at δ 1.3 integrating for 24 protons. The terminal proton signal showed at 0.9 (J = 6.7 Hz, 3H), indicating that the compound terminal methyl group. The ^{13}C-NMR (400 MHz, $CHCl_3$, Table 24, Appendix 29B and C) spectrum along with the DEPT-135 of compound **247** showed the presence of 26 carbons, including one methyl, fifteen methylenes, two methines, one oxygenated methylene, one methoxy, and four quaternary carbons. The most downfield signal at δ 195.5, and 170.7 were corresponding to ketone, and ester carbonyl, respectively. The other quaternary carbons appeared at δ 164.9, and 135.2. The

other signal appearing at δ 31.9-22.7 was ascribed to the methylenes carbon. The presence of carbon signal at δ 14.1 accounts for a terminal methyl group.

Table 24: Comparison of the ^{1}H-NMR (400 MHz, $CDCl_3$) and ^{13}C-NMR (101 MHz, $CDCl_3$) spectral data of compound **247** and 3′-(4′′-methoxy phenyl)-3′-oxo-propionyl hexadecanoate.

Position	NMR data of compound **247**		(Jao *et al*., 2005)	
	^{1}H-NMR	^{13}C-NMR	^{1}H-NMR	^{13}C-NMR
1	-	170.7	-	173.53
2	2.34 (t, *J* = 7.7 Hz)	33.9	2.25 (2H, t, H-2)	34.26
3-15	2.1 (m, 1H, H-3), 1.3 (brs. 24H, H-4-115)	31.9-22.7	1.60 (2H, m, H-3), 1.25 (24H, s, H-4-15)	32.01-22.78
16	0.9 (t, *J* = 6.7 Hz, 3H)	14.1	0.90 (3H, t, H-16)	14.24
1′	4.50 (m, 2H)	68.9	4.50 (2H, t, H-1′)	69.80
2′		38.3	3.22 (2H, t, H-2′)	37.13
3′	-	195.5	-	195.11
1′′	-	135.2	-	129.96
2′′, 6′′	7.52 (d, *J* = 8.7 Hz, 2′′, 6′′)	130.0	7.92 (2H, d, *J* = 8 Hz, H-2′′, 6′′)	130.42
3′′, 5′′	6.93 (d, *J* = 8.7 Hz, 3′′, 5′′)	114.4	6.92 (2H, d, *J* = 8 Hz, H-3′′, 5′′)	113.81
4′′	-	164.9	-	163.69
OCH_3	3.86 (s, 3H)	55.4	3.85 (3H, s)	55.37

The above spectral data agree with 3-(4-methoxy phenyl)-3-oxo-propionyl hexadecanoate (Jao *et al*., 2005) (Table 24), which has not yet been reported from the roots of *V. sinaiticum*.

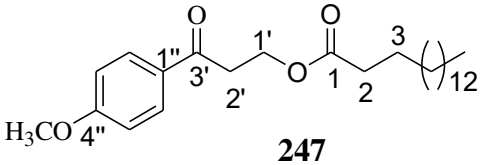

247

Compound **248** was obtained as a white powder, R_f 0.38 (10 % MeOH in CH_2Cl_2) as eluent. The IR spectral (Appendix 30A) analysis displayed peaks at 3431, 2951, 2838, 1647, and 1020 cm^{-1} suggesting the presence of hydroxy, methylene, sp^3 aliphatic C-H, olefinic C=C, and C-O stretching, respectively. The proton NMR spectrum (DMSO-d_6, Table 25**,** Appendix 30B) of compound **248** demonstrated 5 aromatic protons signal at δ 7.7 (dd, *J* = 6.7, 3.1 Hz, 2H), and 7.4 (d, *J* = 6.4 Hz, 2H). The spectrum also disclosed two olefinic proton signals at δ 6.4 (d, *J* = 6.4

Hz, 1H, H-3), 6.0 (d, *J* = 2.4 Hz, 1H, H-4, and the signal at *δ* 7.6 (d, *J* = 16.2 Hz, 1H) and 6.6 (d, *J* = 16.2 Hz, 1H) suggesting the existence of *trans* double bond. A glucose moiety's anomeric proton (H-1″) and acetal carbinol (H-1) signals were shown at *δ* 4.9 (d, *J* = 6.4 Hz) and 4.4 (d, *J* = 7.9 Hz), respectively. The six oxygenated methine proton signals at 3.2 (*d*, J = 8.8 Hz, 1H, H-2″), 3.1 (*d*, J = 8.9 Hz, 1H, H-4″), 3.44 – 3.38 (m, H-3″ and 5″), and the signals at δ 3.72 (*d*, *J* = 12.0 Hz, 2H, H-6″) are ascribed to the glucose moiety. However, the proton NMR spectrum also revealed signals due to methine protons at *δ* 3.0 (*d*, *J* = 8.3 Hz, 1H, H-6), 3.6 (s, 1H, H-9), and methylene protons at δ 2.2 (*d*, *J* = 14.7 Hz, 1H, H-7a), 1.8 (dd, *J* = 14.7, 4.5 Hz, 1H, H-7b). The methyl signals on quaternary carbon were evident from the appearance of a singlet peak at *δ* 1.5 (s, 3H, Me-10). The ^{13}C-NMR spectrum (DMSO-d_6, Table 25**,** Appendix 30C) of compound **248** along with the DEPT-135 (Appendix 30D) confirmed the presence of 23 carbons. The spectrum displayed the most downfield carbon at *δ* 166.4 (C-9′) and the two olefinic carbon signals at *δ* 144.6 (C-**7′**) and 120.0 (C-8′) were apparent for the existence of the α, *β*-unsaturated ester carbonyl group of the cinnamic acid moiety. Five olefinic carbon signals were observed at *δ* 130.9 (C-4′), 129.4 (C-2′, C-6′), and 128.8 (C-3′, C-5′). The methine carbons of the pyran moiety were revealed at *δ* 141.7 (C-3) and 107.9 (C-4). The signal appearing at *δ* 134.6 (C-1′) correlated to the presence of aliphatic quaternary carbon. The spectrum also exhibited two oxygenated aliphatic quaternary carbons signal at *δ* 87.4 (C-8), and 71.9 (C-5). The signals at *δ* 22.7 (C-10) are attributed to the quaternary methyl groups in the compound. The characteristic carbon signal of an acetal carbinol is shown at *δ* 92.9 (C-1). Oxygenated methine carbon signals at *δ* 61.6 (C-6″), 70.6 (C-4″), 73.6 (C-2″), 76.2 (C-5″), and 76.7 (C-3″) together with the anomeric carbon signal at *δ* 97.7 (C-1″) is apparent for the presence of one sugar moiety in the compound. The spectrum also revealed an oxygenated methine carbon signal at *δ* 77.7 (C-6). The spectrum also showed that methine and methylene groups were present at 54.8 (C-9) and 45.0 (C-7) respectively. These spectral data fully agree with those reported for harpagoside (**248**) isolated previously from *Harpagophytum procumbens* (Jin *et al*., 2006). Based on the above-stated spectroscopic data and comparison of the NMR data with literature, compound **248** was identified as harpagoside (Table 25).

Table 25: Comparison of the ^{13}C-NMR (101 MHz, DMSO-d_6) spectral data of compound **248** and harpagoside.

Position	NMR data of compound **248**		(Jin *et al*., 2006)
	^{1}H-NMR	^{13}C-NMR	^{13}C-NMR
Aglycone			
1	4.9 (d, *J* = 6.4 Hz)	92.9	94.8
3	6.4 (d, *J* = 6.4 Hz, 1H)	141.7	142.5
4	6.0 (d, *J* = 2.4 Hz, 1H)	107.9	108.1
5	-	71.9	73.4
6	3.0 (d, *J* = 8.3 Hz, 1H)	77.7	77.0
7	2.2 (d, *J* = 14.7 Hz, 1H, (1.8 (dd, *J* = 14.7, 4.5 Hz, 1H)	45.0	46.1
8	-	87.4	87.6
9	3.6 (*s,* 1H)	54.8	55.3
10	1.5 (s, 3H)	22.7	22.8
Cinnamoyl			
1′	-	134.6	135.0
2′, 6′	7.4 (d, *J* = 6.4 Hz, 2H)	129.4	129.3
3′, 5′	7.7 (dd, *J* = 6.7, 3.1 Hz, 2H)	128.8	128.6
4′	7.7 (dd, *J* = 6.7, 3.1 Hz, 1H)	130.9	130.5
7′	6.6 (d, *J* = 16.0 Hz, 1H)	120.0	144.5
8′	7.6 (d, *J* = 16.0 Hz, 1H)	144.6	120.3
9′	-	166.4	166.9
Glucose			
1″	4.4 (d, *J* = 7.9 Hz)	97.7	99.3
2″	3.2 (d, J = 8.8 Hz, 1H)	73.6	74.9
3″	3.44 – 3.38 (m, 1H)	76.7	78.8
4″	3.1 (d, J = 8.9 Hz, 1H)	70.6	71.7
5″	3.44 – 3.38 (m, 1H)	76.2	78.5
6″	3.72 (d, *J* = 12.0 Hz, 2H)	61.6	62.9

This compound (**248**) has never been reported before from the roots of *V. sinaiticum*.

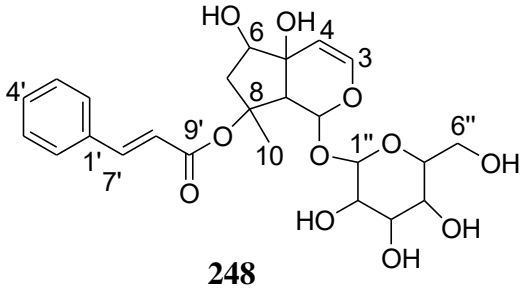

248

Compound **249** was isolated as amorphous powder, R_f 0.35 in 10 % MeOH/CH_2Cl_2 as mobile phase. The IR spectrum (Appendix 31A) exhibited absorption bands at 3329, 2923, 1598, and 1035 cm^{-1} due to O-H, sp^3 aliphatic C-H, C=C and C-O stretching, respectively. The proton NMR (400 MHz, Acetone, Table 26**,** Appendix 31B) showed the presence of a pairs of *ortho*-coupled doublet aromatic protons at δ 7.0 (*J* = 8.4 Hz) and (7.7, *J* = 8.4 Hz), trans olefinic protons at δ_H 6.4 (d, *J* = 16.0 Hz), 7.5 (d, *J* = 16.0 Hz) and one aromatic methoxy group (3.9, *s*) indicating the acyl moiety was trans *p*- methoxy cinnamoyl group. The ^{1}H NMR spectrum also revealed the presence of the following representative signals: δ 1.4 (d, *J* = 6.1 Hz, 3H), 1.96 (s, 3H), 2.5 (m, 1H), 4.5 (s, 2H), as well as the anomeric protons signal at δ 6.5 (d, *J* = 5.9 Hz, 1H), 5.4 (d, J = 4.0 Hz). The signals due to anomeric proton (H-1′), acetal carbinol (H-1) of glucose, and rhamnose (H-1′′) moieties were observed at *δ* 4.9 (d, *J* = 7.7 Hz), and 5.1 (d, *J* = 6.1 Hz), and 5.10 (brs), respectively. A series of peaks in the spectrum between *δ* 4.1 and 3.3 attributed to the existence of sugar moieties. The ^{13}C-NMR (101 MHz, Acetone, Table 27, Appendix 31C) spectrum of compound **249** along with the DEPT-135 (Appendix 31D) confirmed 31 carbons. The spectrum displayed two olefinic carbon signals at δ_C 102.4 and 141.0, indicating the presence of an iridoid moiety. The most downfield carbon signal at *δ* 169.7 (C-9′′′) and the two olefinic carbon atoms at *δ* 145.3 (C-7′′′) and 115.9 (C-8′′′) with the aromatic methoxy carbon 54.9 were evident for the existence of the α, *β*-unsaturated ester carbonyl group of the trans *p*-methoxy cinnamoyl moiety. The presence of aromatic carbons signal was observed at *δ* 130.1 (C-2′′′, 6′′′), and 114.4 (C-3′′′, 5′′′). The sp^2 oxygenated quaternary carbons signal showed at *δ* 129.9 (C-1′′′), 161.9 (C-4′′′). The spectrum also exhibited oxygenated aliphatic quaternary carbons signal at *δ* 65.5 (C-8), quaternary methyl group δ_C 20.0 (C-2′′′′). A series of oxygenated carbon signals in the region between *δ* 77.2 to 60.5 together with the carbon signals at *δ* 98.7 (C-1′), and 96.6 (C-1′′) are apparent for the presence of two sugar units. The methyl signal of the rhamnose group appeared at *δ* 17.2 (C-6′′). Besides, the spectrum revealed an acetyl group at *δ* 165.5 (C-1′′′′) attached to the rhamnose moiety. The spectral results provided above were in good agreement with those for pulverulentoside I (Akdemir *et al*., 2004). Thus, compound **249** was elucidated to be pulverulentoside I (6-*O*-(3′′-*O*-acetyl-4′′′ -*O*-*trans*-*p*-methoxycinnamoyl)-*α* L rhamnopyranosyl catalpol) (Table 26, and 27), this compound has never been reported before from the roots of *V. sinaiticum*.

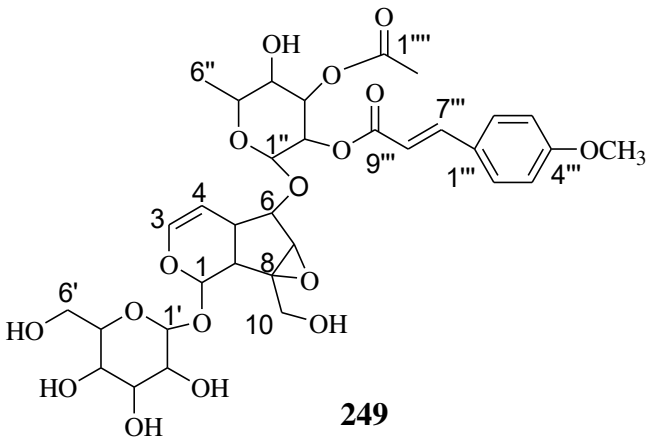

249

Compound **250** was isolated as amorphous powder, R_f 0.31 (20 % MeOH in CH_2Cl_2) mobile phase. The proton spectrum (400 MHz, methanol-d_4, Table 26**,** Appendix 32A) displayed signals of the two anomeric protons at δ 4.75 (d, *J* = 7.9 Hz), 4.60 (d, *J* = 7.8 Hz), and the methyl group at δ 1.32 (d, *J* = 6.2 Hz), demonstrating the existence of two sugar moieties: β-D-glucose, and α-L-rhamnose moiety, respectively (Agrawal, 1992). The proton signals in the region 3.2-3.9 showed the presence of β-D-glucosyl, and α-L-rhamnosyl units. The proton signals at δ 5.05 (m), 6.46 (d, *J* = 5.9 Hz), 5. 10 (m), 2.76 (d, *J* = 6.1 Hz), 4.13 (d, *J* = 13.2 Hz), 3.63 (d, *J* = 8.6 Hz), 2.55 (dd, *J* = 9.7, 7.6 Hz), and 4.03 (d, *J* = 8.2 Hz) of the aglycone. The doublet signals at δ 7.40 (*J* = 16.0 Hz, 1H), and 6.58 (*J* = 16.0 Hz, 1H) of *trans* olefinic protons, along with *ortho*-coupled doublet aromatic protons at δ 7.56 (*J* = 8.8 Hz), 6.94 (*J* = 8.8 Hz), and an aromatic methoxy at δ 3.81 (s, 3H), indicates the acyl moiety was trans *p*- methoxy cinnamoyl group. Besides these signals, the proton spectrum displayed signals for a cinnamoyl moiety, evidenced from protons signal at δ 7.38 (dd, *J* = 6.1, 2.3 Hz), 6.65 (dd, *J* = 8.1, 2.3 Hz), 6.79 (dd, *J* = 8.7, 2.6 Hz), 6.75 (dd, *J* = 8.1, 2.3 Hz), 7.39 (d, *J* = 6.0, 2.1, Hz), and the two olefinic proton signals at 6.6 (d, *J* = 15.9 Hz), 7.7 (d, *J* = 15.9 Hz) which are trans to each other. The ^{13}C-NMR spectrum (101 MHz, methanol-d_4, Table 27**,** Appendix 32B) of compound **250** along with the DEPT-135 (Appendix 32C) confirmed the presence of methine carbon signals at δ 141.0, 102.0, 35.9, 83.0, 41.9, and the epoxy group at 58.0, and 65.2, indicating a cyclopentanopyran ring of an iridoid skeleton. The quaternary carbon signal at *δ* 167.4 and the two olefinic carbon atoms at *δ* 145.9 and 114.0) with the aromatic methoxy carbon 54.6 were evident for the existence of the α, *β*-unsaturated ester carbonyl group of the trans *p*- methoxy cinnamoyl moiety. In addition, the spectrum displayed an unsubstituted cinnamoyl moiety: 134.4, 128.1, 128.8, 130.2, 128.7, 127.9, 115.6,

144.8, and 166.6. A series of oxygenated carbon signals in the region between δ 61.6 to 77.3 together with the carbon signals at δ 98.3 (C-1′), and 96.5 (C-1″) are apparent for the presence of two sugar units. The methyl signal of the rhamnose group appeared at δ 17.2 (C-6″). Besides, the spectrum revealed an acetyl group at δ 171.0 (C-1) attached to the rhamnose moiety. The spectral results provided above were in good agreement with those for scrophuloside B4 previously isolated from *Scrophularia ningpoensis* (Nguyen *et al*., 2005)**,** thus, compound **250** was elucidated to be scrophuloside B4 (6-*O*-(2″-*O*-acetyl-3″-*O*-cinnamoyl-4″-*O*-p-methoxycinnamoyl-α-L-rhamnopyranosyl) catalpol) (Table 26, and 27), which has not yet been reported from the root of *V. sinaiticum*.

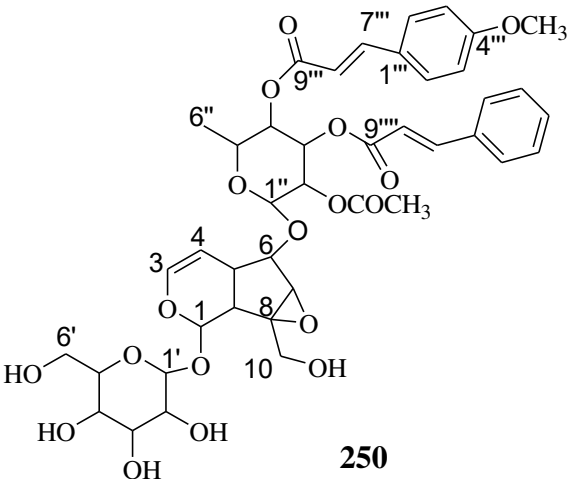

250

Compound **251** was obtained as amorphous powder, R_f 0.33 (10% MeOH in CH_2Cl_2) as eluent. The ^{1}H NMR spectra (400 MHz, methanol-d_4, Table 26**,** Appendix 33A) of compound **251** revealed the identification of an iridoid skeleton proton signals at δ: 5.08 (d, *J* = 6.1 Hz, 1H), 6.36 (d, *J* = 4.1 Hz, 1H), 5.10 (d, *J* = 3.6 Hz, 1H), 2.5 (brs, 1H), 4.04 (d, *J* = 7.0 Hz, 1H), 3.63 (brs, 1H), 2.6 (m, 1H), 4.13 (d, *J* = 13.1 Hz, 2H), and 3.78 (d, *J* = 13.1 Hz, 1H). The anomeric proton showed signals at δ 4.75 (d, *J* = 7.9 Hz, 1H), and 5.1 (d, *J* = 13.0 Hz, 1H). The double doublet proton signals at δ 7.67, and 6.94 (*J* = 15.9 Hz) of *trans* olefinic protons, along with *ortho*-coupled doublet aromatic protons at δ 7.56 (*J* = 8.9 Hz), 6.94 (*J* = 8.8 Hz), and an aromatic methoxy at δ 3.81 (s, 3H), indicates the acyl moiety was trans *p*- methoxy cinnamoyl group. The two singlet acetoxyl proton signals at 2.0 and 1.9 ppm, suggest the presence of two acetyl moieties. The ^{13}C-NMR spectra (400 MHz, methanol-d_4, Table 27**,** Appendix 33A and B) and the DEPT-135 confirmed the presence of 33 carbons. The carbon spectrum revealed the presence of

eight carbon resonances for a *p*- methoxy cinnamoyl moiety at δ 126.8, 129.9, 114.2, 162.1, 145.9, 114.0, 166.6 and the methoxy carbon at δ 54.6. The two anomeric carbon signals at 98.3 and 96.5 along with 8 oxygenated methine carbon signals at 73.4, 76.3, 71.9, 77.3, 70.1, 69.9, 70.5, 68.9, and one oxygenated methylene group at δ 61.6 suggested the presence of two sugar unit. The methyl signal of rhamnose moiety appeared at 16.7. The iridoid skeleton carbon signals were shown at δ 93.4, 141.0, 102.0, 35.6, 83.0, 58.0, 65.2, 41.9, and 60.1. The quaternary carbon signals showed at δ 171.0, and 171.0 indicating the carbonyl carbons of acetyl groups. Compound **251** was identified as scropolioside A [6-*O*-(2",4"-di-*O*-acetyl-3"-*O*-p-methoxy-trans cinnamoyl)-α-L-rhamnopyranosylcatalpol], previously identified from *Scrophularia scopolii* (Calis *et al*., 1998). This compound has never been reported before from the roots of *V. sinaiticum*.

Compound **252** was obtained as amorphous powder, R_f 0.3 (10 % MeOH in CH_2Cl_2) as eluent. The ^{1}H NMR spectrum (400 MHz, methanol-d_4, Table 26**,** Appendix 34A) of compound **252** showed the presence of an iridoid skeleton proton signals at δ: 6.2 (d, *J* = 1.4 Hz, 1H), 6.38 (d, *J* = 6.1 Hz, 1H), 5.05 (dd, *J* = 5.7, 2.4 Hz, 1H), 2.5 (m, 1H), 4.03 (d, *J* = 8.1 Hz, 1H), 3.8 (brs, 1H), 2.9 (d, *J* = 1.8 Hz), 4.13 (d, *J* = 13.1 Hz, 1H), and 3.88 (d, *J* = 13.4 Hz, 1H), anomeric proton signals at δ 4.61 (d, *J* = 7.9 Hz, 1H), and 5.1 (d, *J* = 1.4 Hz, 1H), proton signals due to a cinnamoyl moiety showed at δ 7.6 (m, 2H), 6.94 (dd, *J* = 9.0, 2.7 Hz, 2H), 7.40 – 7.35 (m, 1H), 7.64 (d, *J* = 16.0 Hz, 1H), and 6.5 (d, *J* = 16.1 Hz, 1H). The ^{13}C-NMR and DEPT-135 spectra (400 MHz, methanol-d_4, Table 27**,** Appendix 34B, and 34C, respectively) of compound **252** confirmed the presence of 36 carbons. The carbon spectrum revealed the presence of seven carbon resonances for a cinnamoyl moiety at δ 134.4, 128.7, 127.9, 130.2, 144.8, 118.8, and 167.4. The anomeric carbon signals at *δ* 98.7, and 98.3 along with oxygenated carbon signals at 76.8, 77.3, 71.9, 76.3, 70.1, 70.4, 73.5, 68.9, and 60.1 suggested the presence of two sugar units. The methyl signal of the rhamnose group appeared at *δ* 16.7. The iridoid skeleton carbon signals were shown at δ 93.8, 142.7, 105.4, 35.8, 83.0, 58.0, 65.2, 41.9, and 60.1. The quaternary carbon signals showed at δ 171.1, 171.0, and 170.6 indicating the carbonyl carbons of acetyl groups. Compound **252** was identified as scropolioside-D_2, previously identified from *Scrophularia deserti* (Ahmed *et al*., 2003), based on the data in Table 26, and 27. This compound has never been reported before from the roots of *V. sinaiticum*.

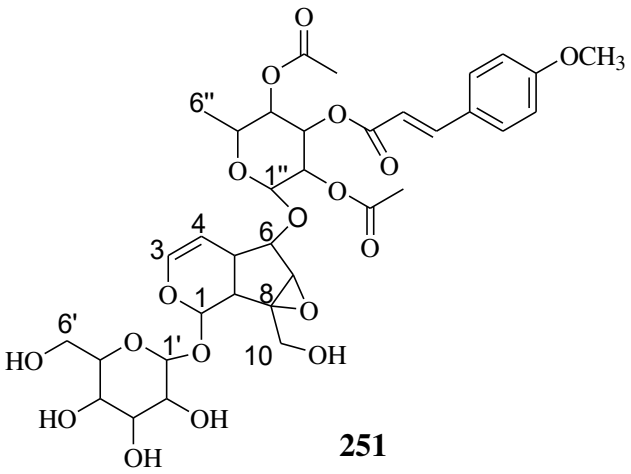

251

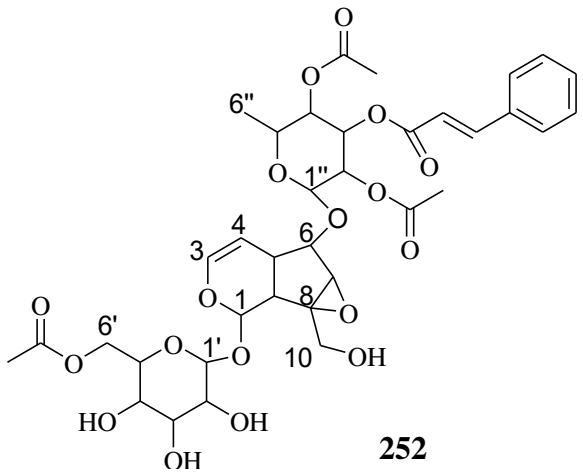

252

Table 26: Comparison of the ^{1}H-NMR spectral data (400 MHz, δ_H in ppm, *J* in Hz) of compounds **249**, **250**, **251**, and **252** with the reported data.

Position	249	(Akdemir *et al*., 2004)	250	(Nguyen *et al*., 2005)	251	(Calis *et al*., 1998)	252
Aglycone							
1	5.1 (d, *J* = 6.1 Hz)	5.01	5.05 (m, 1H)	4.92 d (9.6)	5.08 (d, *J* = 6.1 Hz)	5.09d (9.5)	6.2 (d, *J* = 1.4 Hz, 1H)
3	6.5 (d, *J* = 5.9 Hz)	6.43 (d, *J* = 5.5 Hz)	6.46 (d, *J* = 5.9 Hz)	6.36 d (5.8)	6.36 (d, *J* = 4.1 Hz)	6.39dd (6/1.7)	6.38 (d, *J* = 6.1 Hz, 1H)
4	5.4 (d, *J* = 4.0 Hz)	5.12 (d, *J* = 4.4 Hz)	5. 10 (m, 1H)	5.13 dd (5.8, 4.7)	5.10 (d, *J* = 3.6 Hz)	5.ldd (4.4/6)	5.05 (dd, *J* = 5.7, 2.4 Hz, 1H)
5	2.0 (brs)	2.31 m	2.76 (d, *J* = 6.1 Hz)	2.55 m	2.5 (brs)	2.49m	2.5 (m, 1H)
6	4.1	3.95 (d, *J* = 7.5 Hz)	4.13 (d, *J* = 13.2 Hz)	4.02 dd (8.7, 2.1)	4.04 (d, *J* = 7.0 Hz)	4.06dd (8.9/0.9)	4.03 (d, *J* = 8.1 Hz, 1H)
7	3.7	3.68 (brs)	3.63 (d, *J* = 8.6 Hz)	3.65 d (2.1)	3.63 (brs)	3.67 (br.s)	3.8 (brs, 1H)
8	-	-	-	-	-		-
9	2.5 m	2.43 m	2.55 (dd, *J* = 9.7, 7.6 Hz)	2.66 dd (9.6, 7.8)	2.6 (m)	2.59 dd (9.5/7.6)	2.9 (d, *J* = 1.8 Hz)
10	4.5	3.66, 3.90 d	4.03 (d, *J* = 8.2 Hz)	a. 3.98 dd (11.0, 2.0) b. 4.00 dd (5.5, 11.0)	4.13 (d, *J* = 13.1 Hz), and 3.78 (d, *J* = 13.1 Hz)	3.83 d (13.1), 4.15d(13.1)	4.13 (d, *J* = 13.1 Hz, 1H), 3.88 (d, *J* = 13.4 Hz, 1H)
***β*-D-Glucose**							
1′	4.9 (d, *J* = 7.7 Hz)	4.59 (d, *J* = 7.5 Hz)	4.75 (d, *J* = 7.9 Hz)	4.82 d (7.8)	4.75 (d, *J* = 7.9 Hz)	4.77d (7.8)	4.61 (d, *J* = 7.9 Hz, 1H)
2′	3.3	3.03	3.36 (m)	3.36 dd (7.8, 7.2)	3.4 (m)	3.44–3.23	3.4 (m, 1H)
3′	3.4	3.16	3.38 (m)	3.51 dd (7.2, 7.8)	3.4 (m)	3.44–3.23	3.4 (m, 1H)
4′	3.3	3.01	3.32 (dd)	3.49 dd (7.8, 7.2)	3.2 (m)	3.44–3.23	3.2 (m, 1H)
5′	3.4	3.14	3.21 (m)	3.38 m	3.2 (m)	3.44–3.23	3.2 (m, 1H)
6′	3.4	3.43, 3.73	3.88 (dd, *J* = 12.1, 2.0 Hz)	a. 3.88 dd (11.4, 5.5) b. 3.77 dd (2.0, 11.4)	3.89 (dd, *J* = 11.9, 2.0 Hz)	3.63 dd (11.8/6.2), 3.92dd (11.8/1.6)	4.13 (d, *J* = 13.1 Hz, 1H), 3.88 (d, *J* = 13.4 Hz, 1H)
7′							-
8′							2.1 (s, 3H)
α-L-Rhamnose							
1″	5.10 (brs)	5.00 (brs)	4.60 (d, *J* = 7.8 Hz)	5.03 d (1.2)	5.1 (d, *J* = 13.0 Hz)	5.07d (1.7)	5.1 (d, *J* = 1.4 Hz, 1H)
2″	3.7	5.22	3.63 (m)	5.41 dd (1.2, 3.0)	5.12 (m)	5.3dd (1.7/3.4)	5.09 (m, 1H)
3″	4.1	4.98	5.34 (m)	5.53 dd (3.0, 9.6)	5.33 (dd, *J* = 3.5, 1.8 Hz)	5.37 dd (3.4/10.1)	5.0 (m, 1H)
4″	3.6	3.46	3.52 (m)	5.34 t (9.6)	5.0 (m)	5.l7bt (10)	4.75 (m, 1H)

5″	3.8	3.78	3.59 (m)	4.10 m		4.07 dq (10/6.3)	
6″	1.4 (d, *J* = 6.1 Hz)	1.24 (d, *J* = 5.8 Hz)	1.32 (d, *J* = 6.2 Hz)	1.28 d (6.6)	1.32 (d, *J* = 6.4 Hz)	1.22d (6.3)	1.32 (d, *J* = 6.4 Hz)
7″	-	-	-	-	-	-	-
8″	1.96 (s)	1.94 (s)	1.99 (s)	2.20 (s)	-	-	1.9 (s)
9″	-	-	-	-	2.0 (s)	2.16 (s)	-
10″	-	-	-	-	1.9 (s)	1.93 (s)	1.9 (s)
***p*-methoxy cinnamoyl**							
1‴	-	-	-	-	-	-	-
2‴	7.7 (d, *J* = 8.4 Hz)	7.73 (d, *J* = 8.4 Hz)	7.56 (d, *J* = 8.8 Hz)	7.46 d (9.0)	7.56 (d, *J* = 8.9 Hz)	7.56 d (8.8)	-
3‴	7.0 (d, *J* = 8.4 Hz)	6.97 (d, *J* = 8.4 Hz)	6.94 (d, *J* = 8.8 Hz)	6.89 d (9.0)	6.94 (d, *J* = 8.8 Hz)	6.95 d (8.8)	-
4‴	-	-	-	-	-	-	-
5‴	7.0 (d, *J* = 8.4 Hz)	6.97 (d, *J* = 8.4 Hz)	6.94 (d, *J* = 8.8 Hz)	6.89 d (9.0)	6.94 (d, *J* = 8.8 Hz)	6.95 d (8.8)	-
6‴	7.7 (d, *J* = 8.4 Hz)	7.73 (d, *J* = 8.4 Hz)	7.56 (d, *J* = 8.8 Hz)	7.46 d (9.0)	7.56 (d, *J* = 8.9 Hz)	7.56 d (8.8)	-
7‴	6.4 (d, *J* = 16.0 Hz)	6.56 (d, *J* = 16.0 Hz)	6.58 (d, *J* = 16.0 Hz)	6.25 d (16.2)	7.6 (d, *J* = 15.9 Hz)	7.67d (15.8)	-
8‴	7.5 (d, *J* = 16.0 Hz)	7.65 (d, *J* = 16.0 Hz)	7.40 (d, *J* = 16.0 Hz)	7.64 d (16.2)	6.4 (d, J = 15.9 Hz)	6.63d (15.8)	-
9‴	-	-	-	-	-	-	-
O<u>C</u>H$_3$	3.9 (s)	3.80 (s)	3.81 (s)	3.83 (s)	3.81 (s)	3.82 (s)	
Cinnamoyl							
1⁗	-	-	-	-	-	-	-
2⁗	-	-	7.38 (dd, *J* = 6.1, 2.3 Hz)	7.47 dd (2.5, 8.5)	-	-	7.6 (m)
3⁗	-	-	6.65 (dd, *J* = 8.1, 2.3 Hz)	7.36 dd (8.5, 8.5)	-	-	6.94 (dd, *J* = 9.0, 2.7 Hz)
4⁗	-	-	6.79 (dd, *J* = 8.7, 2.6 Hz)	7.35 dd (8.5, 8.5)	-	-	7.40 – 7.35 (m)
5⁗	-	-	6.75 (dd, *J* = 8.1, 2.3 Hz)	7.36 dd (8.5, 8.5)	-	-	6.94 (dd, *J* = 9.0, 2.7 Hz)
6⁗	-	-	7.39 (d, *J* = 6.0, 2.1, Hz)	7.49 dd (8.5, 2.5)	-	-	7.6 (m)
7⁗	-	-	6.6 (d, *J* = 15.9 Hz)	6.33 d (16.0)	-	-	7.64 (d, *J* = 16.0 Hz)
8⁗	-	-	7.7 (d, *J* = 15.9 Hz)	7.63 d (16.0)	-	-	6.5 (d, *J* = 16.1 Hz)
9⁗	-	-	-	-	-	-	-

Table 27: Comparison of the ^{13}C-NMR spectral data (101 MHz, δ_C in ppm) of compounds **249**, **250**, **251**, **252,** and with reported data.

Position	249	(Akdemir *et al*., 2004)	250	(Nguyen *et al*., 2005)	251	(Calis *et al*., 1998)	252	(Ahmed *et al*., 2003)
Aglycone								
1	93.9	94.0	93.8	94.6	93.8	95.2	93.8	95.7
3	141.0	142.0	141.0	141.3	141.0	142.5	142.7	142.9
4	102.4	103.0	102.0	102.5	102.0	103.2	105.4	103.8
5	35.9	36.3	35.9	35.9	35.6	37.25	35.8	37.6
6	83.1	83.0	83.0	83.6	83.0	84.9	83.0	85.5
7	57.7	58.2	58.0	58.4	58.0	59.5	58.0	59.8
8	65.5	66.3	65.2	65.0	65.2	66.6	65.2	66.8
9	42.3	42.8	41.9	42.6	41.9	43.3	41.9	43.7
10	60.5	59.5	60.1	60.9	60.1	61.4	60.1	61.9
β-D-Glucose								
1′	98.7	98.7	98.3	99.0	98.3	99.78	98.7	100.3
2′	73.9	74.3	73.5	73.2	73.4	74.8	76.8	75.2
3′	76.7	77.3	76.8	76.2	76.3	77.3	77.3	77.8
4′	70.6	71.1	70.4	69.6	71.9	71.8	71.9	71.7
5′	77.2	78.3	77.3	76.7	77.3	78.6	76.3	76.12
6′	62.0	62.2	61.6	61.4	61.6	63.0	61.6	64.6
7′	-	-	-	-	-	-	171.1	173.2
8′	-	-	-	-	-	-	19.6	21.2
α-L-Rhamnose								
1″	96.6	96.7	96.5	96.6	96.5	97.8	98.3	98.1
2″	71.9	72.4	71.0	70.4	70.1	71.3	70.1	71.1
3″	70.6	70.2	70.1	69.1	69.9	70.7	70.4	71.7
4″	70.1	70.1	76.3	71.7	70.5	72.0	73.5	72.7
5″	69.1	69.6	68.9	67.7	68.9	68.3	68.9	68.5
6″	17.2	18.5	17.2	17.5	16.7	17.8	16.7	18.2
Acyl moiety								
7″	165.8	162.7	171.0	170.5	171.0	171.6	171.0	172.4
8″	20.0	21.6	19.6	21.0	171.0	171.6	21.3	21.3
9″	-	-	-	-	22.5	20.9	170.6	172.1
10″	-	-	-	-	19.6	20.9	22.6	21.3
p-methoxy cinnamoyl								
1‴	129.9	127.3	126.8	126.8	126.8	128.1	-	-
2‴	130.1	131.3	129.9	130.2	129.9	131.3	-	-
3‴	114.4	115.3	114.2	114.4	114.2	115.5	-	-
4‴	161.9	162.2	162.0	161.7	162.1	163.4	-	-
5‴	114.4	115.3	114.2	114.4	114.2	115.5	-	-
6‴	130.1	131.3	129.9	130.2	129.9	131.3	-	-
7‴	145.3	146.3	114.0	114.3	145.9	147.4	-	-
8‴	115.9	115.4	145.9	146.1	114.0	115.1	-	-
9‴	169.7	170.8	167.4	166.9	166.6	167.9	-	-
$O\underline{C}H_3$	54.9	56.2	54.6	55.5	54.6	56.0	-	-

Cinnamoyl								
1′′′′	-	-	134.4	134.1	-	-	134.4	135.9
2′′′′	-	-	128.1	128.9	-	-	128.7	129.8
3′′′′	-	-	128.8	129.0	-	-	127.9	130.6
4′′′′	-	-	130.2	130.6	-	-	130.2	132.3
5′′′′	-	-	128.7	128.9	-	-	127.9	
6′′′′	-	-	127.9	128.3	-	-	128.7	
7′′′′	-	-	115.6	117.0	-	-	144.8	147.8
8′′′′	-	-	144.8	146.2	-	-	118.8	118.3
9′′′′	-	-	166.6	166.1	-	-	167.4	167.7

Compound (**253**) was obtained as a colorless amorphous powder with a TLC profile that showed an R_f value of 0.32 (20 % MeOH in CH_2Cl_2) as eluent. The IR spectrum (Appendix 35A) showed an absorption band at 3432, 2945, 2836, 1651, and 1024 cm^{-1} suggesting the presence of hydroxy, methylene, sp^3 aliphatic C-H, olefinic C=C, and C-O stretching, respectively. The proton NMR spectrum (400 MHz, DMSO-d_6, Table 28**,** Appendix 35B) of compound **253** demonstrated the olefinic protons signal at δ 6.3 (d, J = 6.2 Hz, 1H), and 5.6 (d, J = 3.6 Hz, 1H) ascribed to the H-3 and H-4 of pyran ring of aglycone moiety. The carbon signal of the acetal carbinol at δ_H 4.90 (d, J = 3.6 Hz, 1H), and the two anomeric signals of the proton were observed at δ_H 4.83 (d, J = 7.5 Hz, 1H) and 5.01 (d, J = 7.5 Hz, 1H) along with the signals in the region 3.0-4.2 indicated the presence of two β -glucopyranosyl moieties. The proton decoupled ^{13}C-NMR spectrum of compound **253** (101 MHz, DMSO-d_6, Table 28**,** Appendix 35C and D) displayed the two olefinic carbon signals at δ_C 109.0 and 140.4, which is suggestive of the presence of an iridoid moiety. The spectrum also exhibited oxygenated aliphatic quaternary carbons signal at δ 75.7 (C-5), 77.4 (C-8), and quaternary methyl at δ 25.2 (C-10) in the compound. Moreover, the carbon signals at δ 76.6, 47.4, and 58.9 are due to C-6, C-7, and C-9, respectively. The compound showed the presence of a carbinol carbon signal at δ 92.6. A series of oxygenated carbon signals at δ 61.6 (C-6′), 76.8 (C-4′), 74.0 (C-2′), 76.1 (C-3′), 76.8 (C-5′), 73.6 (C-2′′), 76.5 (C-3′′), 70.4 (C-4′′), 77.0 (C-5′′), and 60.9 (C-6′′) together with the anomeric carbon signal at δ 97.3 (C-1′), and 97.9 (C-1′′) was apparent for the presence of two sugars moiety in the compound.

Table 28: Comparison of the ^{13}C-NMR (101 MHz, DMSO-d_6) spectral data of compound **253** and harpagide 6-*O*-β-glucoside.

Position	NMR data of compound **253**		(Manguro *et al*., 2007)
	^{1}H-NMR	^{13}C-NMR	^{13}C-NMR
Aglycone			
1	4.90 (d, *J* = 3.6 Hz, 1H)	92.6	95.7
3	6.3 (d, *J* = 6.2 Hz, 1H)	140.4	146.0
4	5.6 (d, *J* = 3.6 Hz, 1H)	109.0	107.8
5	-	75.7	75.1
6		76.6	76.6
7		47.4	48.3
8	-	77.4	73.4
9		58.8	55.5
10		25.2	21.4
Glucose			
1′	4.83 (d, *J* = 7.5 Hz, 1H)	97.3	100.4
2′		72.8	74.0
3′		73.5	76.1
4′		69.3	69.9
5′		77.1	76.8
6′	4.3 (d, *J* = 7.9 Hz, 2H)	61.6	61.6
1″	5.01 (d, *J* = 7.5 Hz, 1H)	97.9	101.0
2″		72.4	73.6
3″		75.3	76.5
4″		70.7	70.4
5″		77.6	77.0
6″	4.4 (d, *J* = 7.9 Hz, 2H)	61.0	60.9

The spectral data of compound **253** is in agreement with that of literature reported for harpagide 6-*O*-β-glucoside (Manguro *et al*., 2007) (Table 28), which has not yet been reported from the root of *V. sinaiticum*.

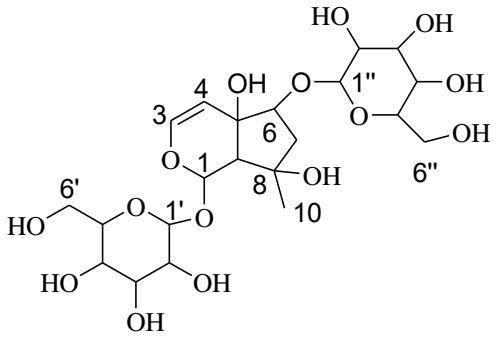

253

Compound **230** was obtained as a white solid with R_f 0.42 with (30 % methanol in dichloromethane) mobile phase. The IR spectrum (Appendix 36A) showed absorption bands at 3317, 2929, and 1047 cm^{-1} due to O-H, aliphatic C-H, and C-O stretching, respectively. The proton NMR spectrum (400 MHz, DMSO-d_6, Appendix 36B) of compound **230** revealed signals in the oxygenated region only. The spectrum displayed a signal for one anomeric proton at δ 5.17 (d, J = 3.6 Hz, 1H). The proton NMR spectrum also showed the oxygenated methylene protons signal at δ_H 4.92 (s, 2H, H-1′), 4.61 (d, J = 6.9 Hz, 2H, H-6), 4.27 (d, J = 7.6 Hz, 2H, H-6′). The remaining oxygenated methine proton signals of this compound looked in the region between 3.00 to 4.00. The proton decoupled ^{13}C-NMR spectrum (101 MHz, DMSO-d_6, Appendix 36C and D) of compound **230** along with the DEPT-135 displayed well-resolved carbon resonances of eight oxygenated methine carbons signal at δ 97.1 (C-1), 92.2 (C-5′), 82.8 (C-3′), 77.4 C-4′), 74.6 (C-3), 73.1 (C-5), 71.9 (C-2), and 70.1 (C-4), one oxygenated quaternary carbon at δ 104.3 (C-2′) and three oxygenated methylene carbons at δ 60.8 (C-6), 61.5 (C-1´), 62.5 (C-6´). Thus, based on this observation, compound **230** was proposed to be identical to that of sucrose (Hernández-García *et al*., 2019), which has not yet been reported from *V. sinaiticum*.

4.1.6. Secondary metabolites isolated from the root of *Lagenaria abyssinica*

The methanol extract of the roots of *L. abyssinica* was subjected to silica gel column chromatographic fractionation which afforded two compounds: 22, 23-dihydrospinasterol acetate (**254**), and stigmasterol-3-O-β-D-glucoside (**255**). Both compounds were reported herein for the first time from this plant. The isolated compounds' structures were characterized using spectroscopic methods, including ^{1}H NMR, ^{13}C NMR, and DEPT-135 spectra as discussed below.

Compound **254** was isolated as a white solid with an R_f value of 0.5 (25 % EtOAc in *n*-hexane) as eluent on TLC. The ^{1}H-NMR spectrum (400 MHz, $CDCl_3$, Table 29, Appendix 37A) of compound **254** revealed the presence of seven methyl's at 1.1 (d, J = 6.8 Hz, 3H), 0.95 (d, J = 6.3 Hz, 3H), 0.85 (s, 3H), 0.8 (s, 3H), 0.82 (d, J = 3.5 Hz, 6H), and 0.6 (d, J = 6.0 Hz, 3H). The signal at δ 3.6 (1H, *m,* H-3) corresponds to a proton attached to an oxygenated carbon. The spectrum also showed a triplet olefinic proton signal at δ 5.2 (t, J = 3.7 Hz, 1H). Other proton signals integrating for 29 hydrogens were observed in the range δ 2.20 to 1.00. The proton decoupled ^{13}C-NMR and DEPT-135 spectra ($CDCl_3$, Table 29, Appendix 37B, and C) revealed the presence of 31 well resolved, including seven methyl's, eleven methylene, nine methine, and four quaternary carbons. The four quaternary carbon signals observed at δ 171.6, 139.6, 43.4, and 34.2 are due to C-8, C-13, and C-10, respectively. The ^{13}C-NMR spectrum (Appendix 38-39) showed a signal in the oxygenated region at δ 71.1 (C-3). The presence of one double bond was evident from the appearance of one olefinic carbon signal attributed to δ 117.4 (C-7). The above spectral data of compound **254** is comparable with data reported for the 22, 23-dihydrospinasterol skeleton, and the only difference is the presence of extra acyl moiety at C-3, in the case of compound **254,** the compound was identified as 22, 23-dihydrospinasterol acetate, with the result given in Table 29.

Table 29: ^{1}H NMR (400 MHz, $CDCl_3$) and ^{13}C NMR (101 MHz, $CDCl_3$) data of compound **254** and literature reported ^{13}C-NMR data of 22, 23-dihydrospinasterol acetate.

Position	Compound **254**		(Ahmed *et al*., 2020)
	^{1}H-NMR	^{13}C-NMR	^{13}C-NMR
1		37.1	37.1
2		31.5	31.4
3		71.1	71.0
4		38.0	37.9
5		40.3	40.2
6		29.7	29.6
7	δ 5.2 (*m*, 1H)	117.4	117.3
8		139.6	139.5
9		49.5	49.4
10		34.2	34.1
11		21.6	21.5
12		39.6	39.5
13		43.4	43.3
14		55.1	55.0
15		23.0	23.0
16		28.0	28.0

17		56.1	56.0
18	δ 0.6 (3H, *s*)	11.9	11.8
19	δ 1.1 (3H, *s*)	13.1	13.0
20		29.2	29.1
21	0.8 (3H, *d*, *J* = 6.4 Hz)	19.8	19.7
22		36.6	36.5
23		29.2	29.1
24		45.8	45.8
25		31.9	31.4
26	0.85 – 0.74 (m, 6H)	19.0	18.8
27		19.0	19.0
28		26.2	26.1
29	0.85 (3H, d, *J* = 6.6 Hz)	12.0	12.0
30	-	171.6	-
31		21.5	-

The above spectral facts in combination with the literature report (Ahmed *et al*., 2020) indicated that compound **254** was identified as 22, 23-dihydrospinasterol acetate, reported herein for the first time from the species.

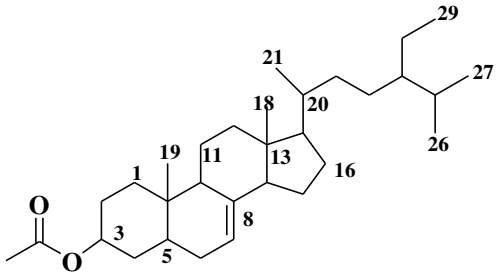

254

Compound **255** was obtained as a yellow crystal with R_f value of 0.43 (*n*-hexane/EtOAc, 6:4, as eluent). Its ^{1}H-NMR spectrum (400 MHz, $CDCl_3$, Table 30, Appendix 38A) demonstrated the presence of six methyl signals at δ 1.0 (s, 3H), 0.93 – 0.83 (m, 9H), 0.8 (d, *J* = 8.4 Hz, 3H), 0.7 (s, 3H). Among these the signals at δ 0.7 and 1.0. are due to methyl groups on quaternary carbons. Other proton signals integrating for 25 hydrogens were detected in the range δ 1.0 to 2.3. The olefinic proton signal at δ 5.3 (1H, *brs*, H-6) and δ 5.1 (1H, dd, *J* = 8.5, 4.1 Hz, H-22), 5.0 (1H, dd, *J* = 8.0, 4.2 Hz, H-23) along with the six methyl groups are evident for the presence of sterol with two double bonds. The proton signal at δ 3.5 (*brs*, 1H, H-3) corresponds to the oxygenated sp^3 methine proton. The presence of anomeric proton at δ 4.32 (d, *J* = 8.0 Hz, 1H, H-

1′), and oxygenated methine protons showed signals in between δ 3.3-4.1. The ^{13}C-NMR spectrum (100 MHz, $CDCl_3$, Table 30) with the help of the DEPT-135 (Appendix 38B-C) spectrum showed 35 well-resolved carbon signals including three quaternary carbon signals at δ 140.4, 42.3, and 36.6, one oxymethine carbon at δ 79.8 (C-3), methine carbons signal at δ 31.5, 31.9, 32.4, 50.1, 51.3, 56.0 and 56.8. The carbon signals observed at δ 39.6, 38.9, 37.3, 34.3, 31.9, 29.1, 25.6, 25.0, and 22.6 belong to methylene carbons. The presences of methyl signals were evident at δ 21.3, 19.8, 19.4, 19.0, 12.2, and 11.8. Two double bonds were evident from the appearance of three olefinic carbon signals attributed at δ 122.0, 129.3, and 138.3. The presence of one sugar moiety is evident from the appearance of one anomeric carbon signal at δ 101.3 along with a series of carbon signals at δ 76.3, 73.7, 73.4, 70.6, and 62.1. The above spectral data is agreed with the literature reported for stigmasterol glycoside (Ridhay*et al.,* 2012; Mailafiya *et al*., 2020).

Table 30: ^{1}H NMR (400 MHz, $CDCl_3$) and ^{13}C NMR (101 MHz, $CDCl_3$) data of compound **255** and literature of ^{13}C-NMR data of stigmasterol-3-O-β-D-glucoside.

Position	Compound **255**		Ridhay *et al*., 2012	Mailafiya *et al*., 2020
	^{1}H-NMR	^{13}C-NMR	^{13}C-NMR	^{13}C-NMR
1		37.3	38.3	38.3
2		34.3	33.3	-
3	3.5 (brs, 1H, H-3)	79.8	76.9	77.4
4		38.9	36.8	39.7
5	-	140.4	140.4	140.9
6	5.3 (1H, brs,)	122.0	121.0	121.7
7		31.9	31.3	31.8
8		31.5	31.4	31.7
9		50.1	49.6	50.1
10		36.7	36.2	35.9
11		22.6	22.6	21.6
12		39.8	41.7	39.9
13		42.3	41.8	45.6
14		56.8	56.2	55.9
15		25.0	24.7	24.3
16		29.1	29.2	29.1
17		56.0	56.1	56.7
18	0.7 (s, 3H,)	11.8	11.8	12.3
19	1.0 (s, 3H)	19.8	18.9	19.6
20		32.4	35.4	33.8
21		21.3	18.8	21.4
22	5.1 (1H, dd, J = 8.5, 4.1 Hz)	138.3	137.8	138.3

23	5.0 (1H, dd, *J* = 8.0, 4.2 Hz)	129.3	128.8	129.3
24		51.3	-	51.1
25		31.9	31.2	31.9
26		19.4	19.3	20.2
27		19.0	18.9	19.4
28		25.6	23.8	25.3
29		12.0	11.6	12.6
1'	4.3 (d, *J* = 8.0 Hz, 1H)	101.3	100.8	101.3
2'	3.64 (d, *J* = 16.2 Hz)	70.6	70.1	73.9
3'	3.4 (1H, brs)	76.3	76.7	77.3
4'	3.9 (d, *J* = 21.5 Hz, 1H)	73.7	73.4	70.6
5'	3.5 (brs, 1H)	73.4	76.6	77.2
6'	4.1 (d, *J* = 21.5 Hz, 2H)	62.1	61.1	61.6

Thus, compound **255** is named stigmasterol-3-O-*β*-D-glucoside (Table 30) reported herein for the first time from this plant.

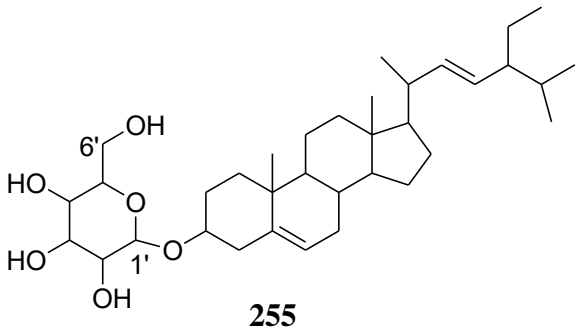

255

4.2. Chemical composition of essential oils extracted from different parts of studied medicinal plants

4.2.1. Percentage yield of essential oils

In this study, essential oils were extracted from various parts of the six selected medicinal plants. The percent yield of essential oils revealed 0.56 g (0.56 %) bulb of *C. abyssinicum* (BCA), 0.45 g (0.45 %) leaves, 0.26 g (0.26 %) roots of *J. schimperiana* (LJS, and RJS), 0.24 g (0.24 %) leaves, 0.33 g (0.33 %) flowers, 0.41 g (0.41 %) seeds of *C. procera* (LCP, FCP, and SCP), 0.19 g (0.19 %) roots, 0.56 g (0.5 %) seeds of *L. abyssinica* (RLA, and SLA), 0.49 g (0.49 %) leaves, 0.28 g (0.28 %) roots of *V. siniaticum* (LVS, and RVS), and 0.62 g (0.62 %) aerial parts of *C. abyssinica* (ACA) (Figure 15). The essential oils were then analyzed by GC-MS using the method described in **Section 3.3.8.1**. The structure of compounds was identified based on their mass spectra value compared with the NIST library databases.

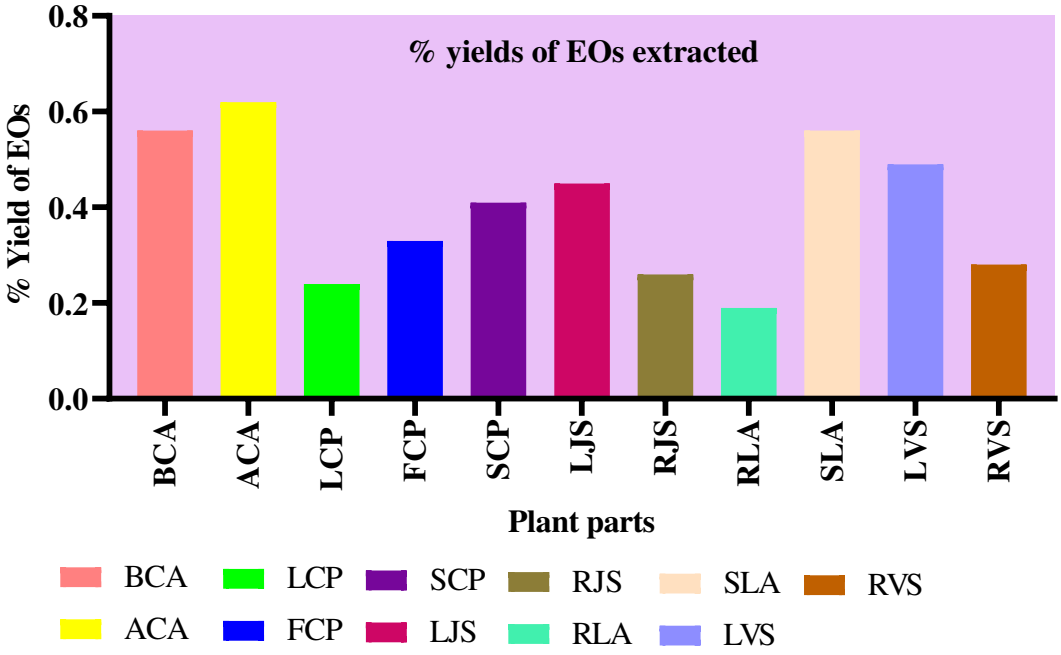

Figure 15: The percentage yield of EOs extract.

4.2.2. Chemical composition of essential oils from bulbs of *C. abyssinicum* and aerial parts of *C. abyssinica*

The dried and powdered (100 g each) bulbs of *C. abyssinicum,* and aerial parts of *C. abyssinica* were extracted by hydrodistillation according to the method described in **Section 3.3.8** and then analyzed by GC-MS (**Section 3.3.8.1**). A total of 62 compounds (Appendix 39A) from the bulbs of *C. abyssinicum,* and area percentage greater than 0.1 were identified and quantified in the oil of *C. abyssinicum* bulbs, representing 100 % of the total oils. Different components were characterized by matching their mass spectra with those of reference compounds recorded in NIST mass spectral library. Palmitic acid (27.15 %), cyclohexadecane (12.7 %), 1,2-benzenedicarboxylic acid, bis(2-methylpropyl) ester (9.07 %), stearic acid (4.52 %), and tricosane (3.91 %) (Figure 16) are the major components derived from bulbs of *C. abyssinicum*. The results are compared to the previous report (Tesfaye *et al*., 2022), on the bulbs of *C. abyssinicum*, which reported that p-menth-2-en-1-ol, cis-(4.02%), p-mentha-2,8-dien-1-ol (4.64%), alloocimene (55.49%) and 1-naphthalenepropanol (7.32%) as the major constituents.

Similarly, the yield of essential oils obtained by hydrodistillation revealed 0.62 % (w/w) from the aerial parts of *C. abyssinica*. In a related study, the GC-MS analysis (Appendix 39A) of essential

oils from the aerial parts of *C. abyssinica,* revealed a total of forty-one chemical compositions representing 99.78 % of the total oil contents. The major compounds identified were benzene, (2-isothiocyanatoethyl)- (33.24 %), benzenepropanenitrile (21.15 %), diisooctylphthalate (11.14 %), cyclohexadecane (9.44 %), and phenol, 2,4-bis(1,1-dimethylethyl)- (4.26 %) (Figure 16). These chemical compositions were reported herein for the first time from *C. abyssinica* and could be considered marker constituents for Ethiopian species. The names of identified compounds with their respective retention times and area percentages are given in Appendix 39A. GC-MS spectra of bulbs, and aerial parts essential oils are presented in Appendix 40A.

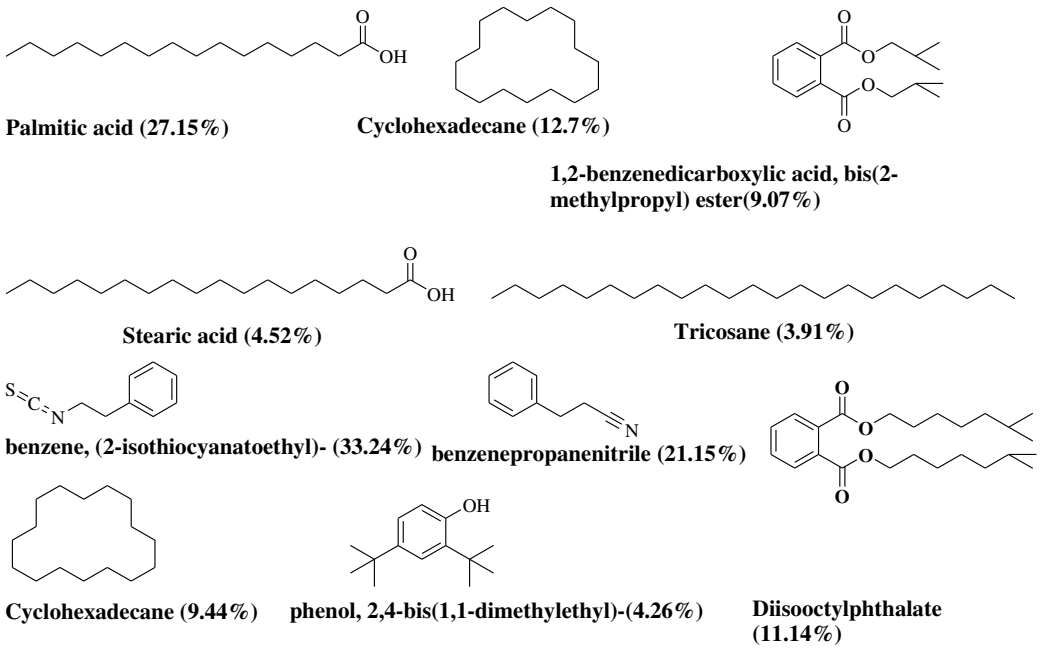

Figure 16: Most abundant compounds identified from *C. abyssinicum* (bulbs), and *C. abyssinica* (aerial parts) essential oils.

4.2.3. Chemical composition of essential oils from leaves, flowers, and seeds of *C. procera*

The names of identified compounds with their respective retention times and area percentages are given in Appendix 39B. Fifty-nine constituents were identified and quantified in the oil of *C. procera* leaves, representing 99.45 % of the total oil. The major components were diisooctylphthalate (27.42 %), phytol (7.54 %), and tridecanal (4.44 %). In the oil of *C. procera* seeds, forty-five constituents (100 %) were identified. phenol, 2,4-bis(1,1-dimethylethyl)- (23.4 %), palmitic acid (20.87 %), cyclohexadecane (14.46 %), and ethyl oleate (5.68 %) were the major compounds. GC-MS analysis of *C. procera* flowers revealed the presence of 46

compounds with a combined area percentage of 99.34 % including *n*-hexadecanoic acid (44.09 %), 1,2-benzenedicarboxylic acid, bis(2-methylpropyl) ester (8.58 %), and tricosane (6.36 %) were the major components (Figure 17). The results are consistent with previous reports (Okiei *et al*., 2009; Al-Rowaily *et al*., 2020), in accordance with the classes of compounds reported from *Calotropis procera*. The previous study showed the major chemical constituents of leaves essential oils of this plant are phytol (25.19 %), 4.6,14-trimethyl-2-pentadecanone (15.31 %), and, 3, 7, 11, 15-tetramethyl-2-hexadecene-1-ol (6.8 %) (Okiei *et al*., 2009). However, the major constituent in the present study was diisooctylphthalate (27.42 %), phytol (7.54 %), and tridecanal (4.44 %) suggesting that compound diisooctylphthalate reported herein for the first time in leaves of *Calotropis procera* whereas tridecanal was found as a minor constituent in the previous study. GC-MS spectra of leaves, flowers, and seeds essential oils are presented in Appendix 40B.

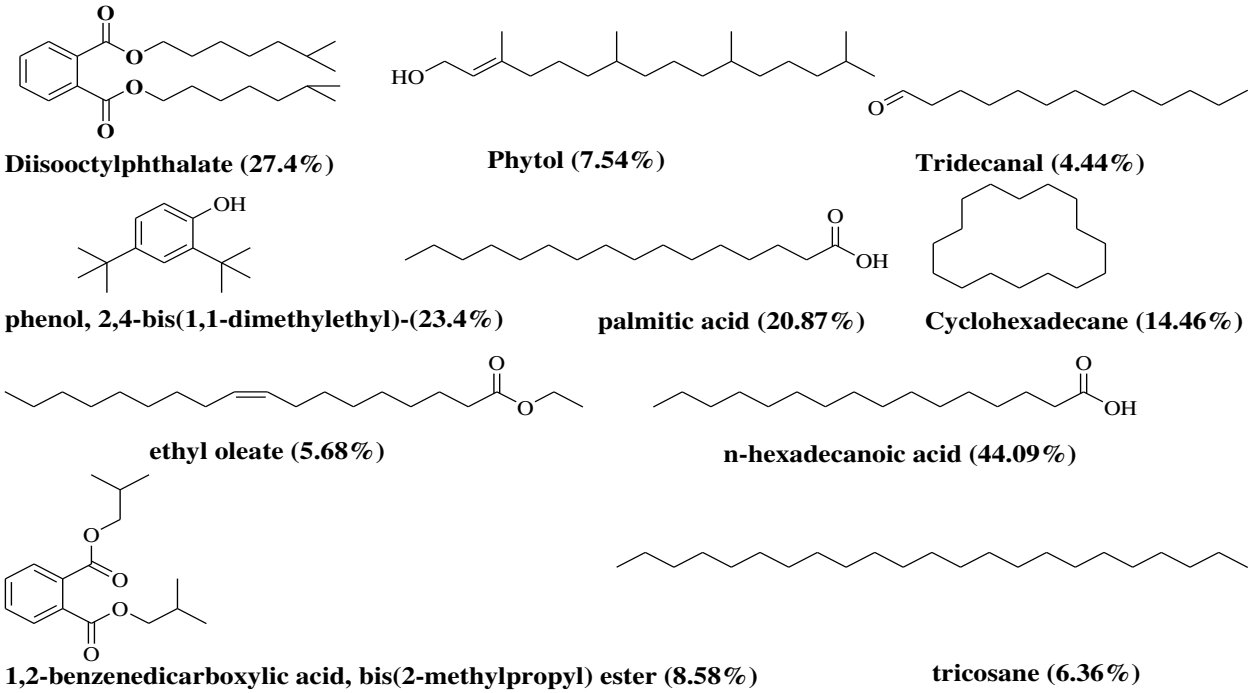

Figure 17: Most abundant compounds identified from *C. procera* (leaves, flowers, and seeds) essential oils.

4.2.4. Chemical composition of essential oils from leaves, and roots of *J. schimperiana*

A total of fifty-four components were identified in the oil of *J. schimperiana* roots, representing 99.73 % of the total oil. The major components were *n*-hexadecanoic acid (32.45 %),

diisooctylphthalate (11.11 %), phenol, 5-methyl-2-(1-methylethyl)- (9.32 %), linoleic acid (6.21 %), and 9,12-octadecadienoic acid (Z, Z)- (5.76 %). Fifty-two constituents were identified and quantified in the oil of *J. schimperiana* leaves, representing 99.84 % of the total oil. n-hexadecanoic acid (30.27 %), 1,2-benzenedicarboxylic acid, bis(2-methylpropyl) ester (12.89 %), diisooctylphthalate (11.29 %), cyclohexadecane (6.32 %), and 2-pentadecanone, 6,10,14-trimethyl- (6.63 %) (Figure 18) were the major components in the leaves of *J. schimperiana* oil. The names of identified compounds with their respective retention times and area percentages are given in Appendix 39C. GC-MS spectra of leaves, and roots essential oils are presented in Appendix 40C.

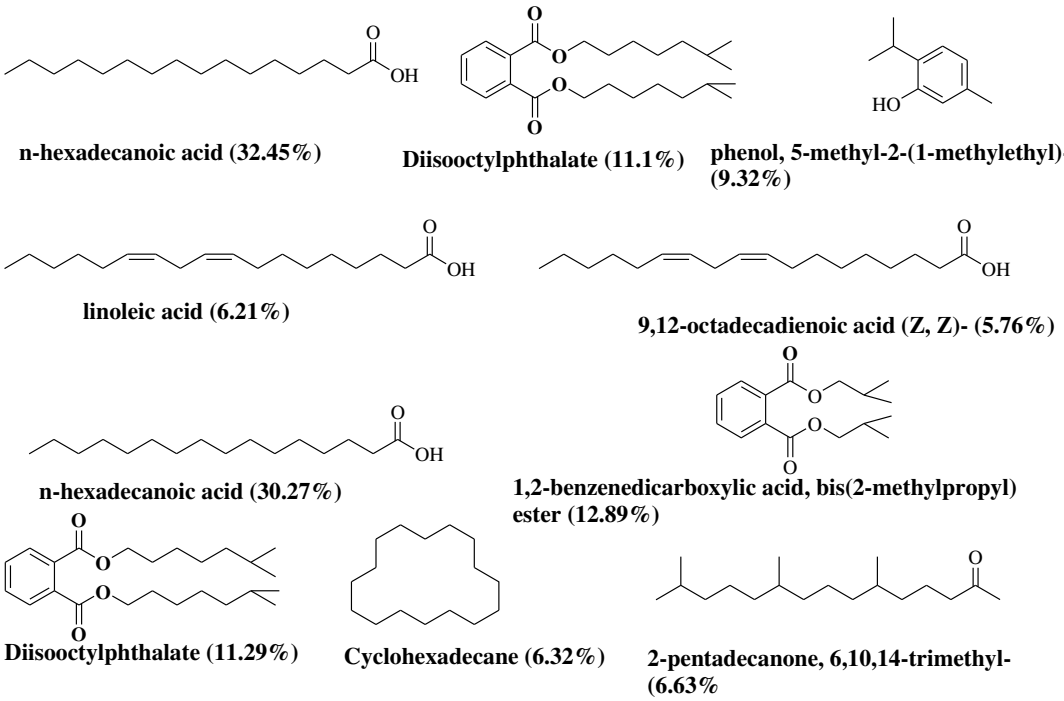

Figure 18: Most abundant compounds identified from *J. schimperiana* (leaves, and roots) essential oils.

4.2.5. Chemical composition of essential oils from leaves, and roots of *V. siniaticum*

GC-MS analysis (Appendix 39D) of essential oils from the leaves of *V. siniaticum,* revealed a total of sixty-one chemical compositions representing 99.8 % of the total oil contents. The major compounds were phenol, 2,4-bis (1,1-dimethyl ethyl)- (30.61 %), of the total composition, followed by cyclohexadecane (15.46 %), benzene, (2-isothiocyanatoethyl)- (7.65 %), palmitic acid (4.42 %). The GC-MS analysis of essential oils from the roots of *V. siniaticum* has led to the identification of thirty-two compounds, accounting for about 100.0 % of the essential oil

compositions. The principal constituents were diisooctylphthalate (36.66 %), cyclohexadecane (34.49 %), and di-isononyl phthalate (8.23 %) (Figure 19). The names of identified compounds with their respective retention times and area percentages are given in Appendix 39D. GC-MS spectra of leaves, and roots essential oils are presented in Appendix 40D.

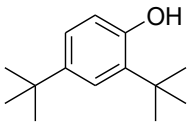

Phenol, 2,4-bis (1,1-dimethyl ethyl)- (30.61%)

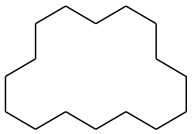

Cyclohexadecane (15.5%)

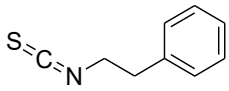

Benzene, (2-isothiocyanatoethyl)- (7.7%)

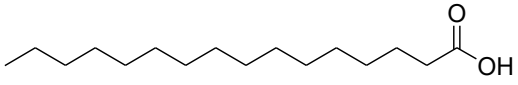

Palmitic acid (4.4%)

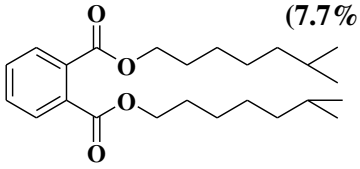

Diisooctylphthalate (36.7%)

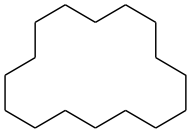

Cyclohexadecane (34.5%)

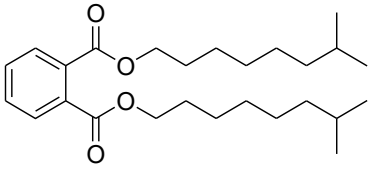

Di-isononyl phthalate (8.2%)

Figure 19: Most abundant compounds identified from *V. siniaticum* (leaves, and roots) essential oils.

4.2.6. Chemical composition of essential oils from seeds, and roots of *L. abyssinica*

The GC-MS analysis (Appendix 39E) of essential oils from the seed of *L. abyssinica* revealed a total of forty-two chemical components, accounting 99.78 % of the total compositions, of which cyclohexadecane (32.22 %), diisooctylphthalate (19.98 %), di-isononyl phthalate (7.98 %), phenol, 2-methoxy- (6.08 %), and 9,12-octadecadienoic acid (Z, Z)- (4.73 %) are the major components identified. Likewise, the GC-MS analysis of essential oil roots of *L. abyssinica* revealed a total of thirty-five chemical components, accounting 100.0 % of the total compositions. The major components identified were diisooctylphthalate (34.3 %), cyclohexadecane (21.66 %), n-hexadecanoic acid (14.49 %), stearyl alcohol (8.61 %), and 1,2-benzenedicarboxylic acid, bis (2-methyl propyl) ester (7.17 %) (Figure 20). This is the first report on the chemical compositions and antimicrobial activities of essential oils obtained from seeds, and roots of *L. abyssinica*. The names of identified compounds with their respective

retention times and area percentages are given in Appendix 39E. GC-MS spectra of seeds, and roots essential oils are presented in Appendix 40E.

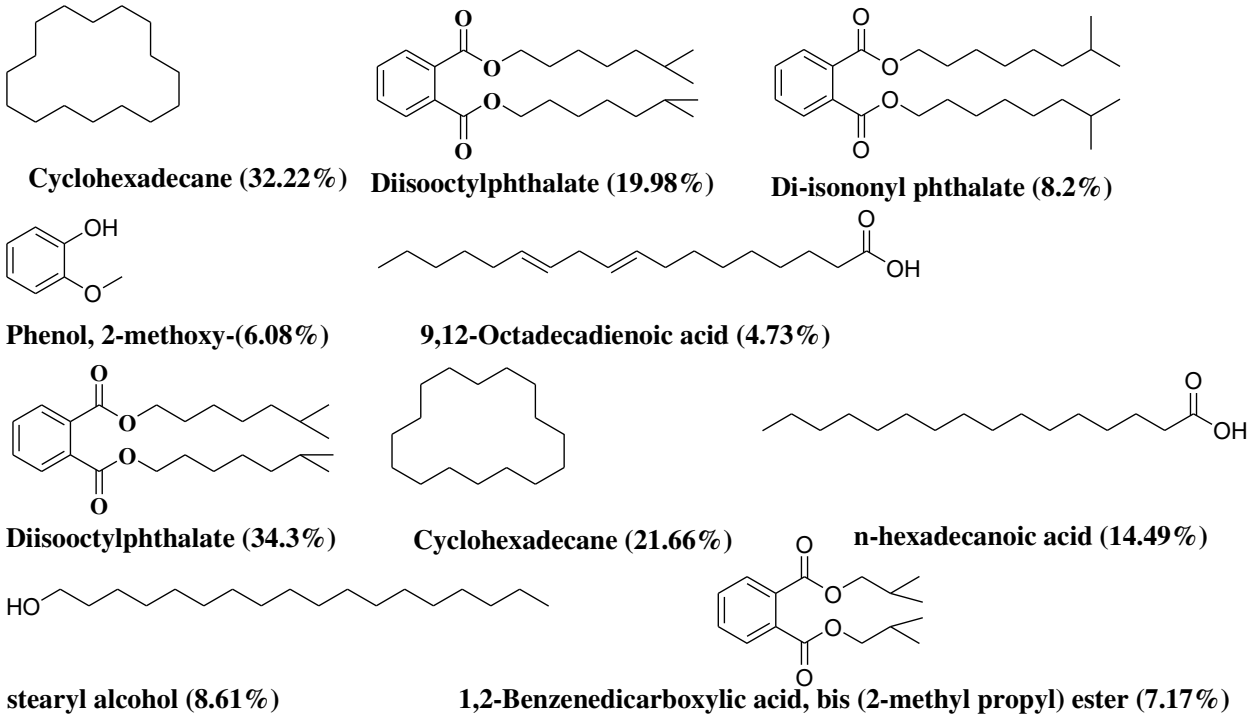

Figure 20: Most abundant compounds identified from *L. abyssinica* (seeds, and roots) essential oils.

4.3. Biological activity analysis

4.3.1. Antibacterial activity of the extracts and isolated compounds

Crude extracts and isolated compounds from the roots of *C. abyssinicum, C. procera*, and *C. abyssinica* were tested for their antibacterial effects against four bacterial strains two-Gram positive bacteria (*Staphylococcus aureus, Streptococcus pyogenes*) and two Gram-negative bacteria (*Pseudomonas aeruginosa*, *Escherichia coli*) using the disc diffusion method. In contrast, extracts and isolated compounds from the roots of *J. schimperiana* and *V. sinaiticum* were tested for their antibacterial effects against six bacterial pathogens *Staphylococcus aurous*, *Streptococcus agalactiae*, *Enterococcus faecalis*, *Escherichia coli*, *Pseudomonas aeruginosa*, *Klebsiella pneumoniae*, and three fungal cultures: *Trichophyton mentagrophytes*, *Trichophyton rubrum*, *Candida albicans* using the previously described microdilution method which was described in detail in Materials and Methods section. As a result, the antibacterial properties

of 30 isolated compounds, as well as the antifungal and antibacterial properties of six selected medicinal plant extracts, were successfully investigated in this study.

4.3.1.1. Antibacterial activity of the extracts and isolated compounds (**223-229**) from roots of *C. abyssinicum*

The DCM/MeOH (1:1) root extracts of *C. abyssinicum* showed antibacterial activity against Gram-negative bacteria *P. aeruginosa* with an inhibition zone of 12.67 ± 1.76 at a concentration of 500 µg/mL and Gram-positive bacteria *S. aureus, S. pyogenes* with 16.67 ± 1.20 and 12.67 ± 1.20 mm diameter zone of inhibition at 500 µg/mL, respectively. The activity showed against *S. aureus* at 500 µg/mL was promising compared to gentamycin used as a standard antibiotic. Whereas the DCM/MeOH (1:1) extract showed no activity at lower concentration (250 µg/mL) against *E. coli*. The zone of inhibition of DCM/MeOH (1:1) and methanol root extracts and isolated compounds of *C. abyssinicum* has been tabulated in (Table 31, Figure 21). The MeOH extracts of the root of *C. abyssinicum* showed activity only against Gram-negative bacteria *P. aeruginosa, E. coli* with a mean inhibition zone of 16.33 ± 0.33 and 10.33 ± 0.33 mm diameter at 500 µg/mL respectively. However, the activity demonstrated against *P. aeruginosa* compared to gentamycin was pronounceable. The DCM/MeOH (1:1) extract of *C. abyssinicum* displayed better activity than the MeOH extract against *S. aureus* and *S. pyogenes*. In contrast, the MeOH extract inhibited better activity against *E. coli* than DCM/MeOH (1:1) extract. Among the tested samples in the present study compounds **224, 225,** and **226** showed growth-inhibitory effects against all the tested bacterial strains in a dose-dependent manner. Compounds **223** and **227** showed moderate activity against *E. coli* with a mean inhibition zone of 13.67 ± 0.67, and 14.67 ± 0.33 mm at 500 µg/mL, respectively, compared to gentamycin (16.7 ± 0.3 mm at 500 µg/mL). Compounds **223, 227,** and **229** were found totally inactive at all concentrations with zero inhibition zone values against *S. pyogenes*. Also, **228** and **229** have zero inhibition zone values against *E. coli*. Compounds **226, 227,** and **228** showed maximum activity against *S. aureus* (11.7 ± 0.1, 13.3 ± 0.7, and 11.7 ± 031mm at 500 µg/mL, respectively) compared to gentamycin (19.5 ± 0.5 mm at 500 µg/mL). The negative control DMSO did not show any inhibition effect against the tested bacterial species.

Table 31: The mean inhibition zone diameter (IZD) in mm of the root extracts, and isolated compounds (**223-229**) of *C. abyssinicum*.

Samples	Conc. µg/mL	Inhibition zone in diameter (mm)			
		P. aeruginosa	*E. coli*	*S. aureus*	*S. pyogenes*
DCME of CRA	500	12.7 ± 1.8	8.9 ± 1.2	16.7 ± 1.2	12.0 ± 1.2
	250	11.3 ± 1.4	NA	15.7 ± 0.3	10.3 ± 0.3
ME of CRA	500	16.3± 0.3	10.3 ± 0.3	8.8 ± 0.8	NA
	250	15.7 ± 0.3	9.7 ± 0.3	NA	NA
223	500	10 ± 1.5	13.7 ± 0.7	NA	NA
	250	9.7 ± 1.2	12 ± 1.5	NA	NA
224	500	9.8 ± 0.4	10.9 ± 0.7	8.0 ± 0.1	7.3 ± 0.4
	250	9.0 ± 0.0	9.4 ± 0.5	7.8 ± 0.1	7.0 ± 0.1
225	500	10.0 ± 0.2	8.7 ± 0.2	10.5 ± 0.1	8.6 ± 0.2
	250	9.7 ± 0.1	8.5 ± 0.0	9.6 ± 0.3	7.8 ± 0.1
226	500	12.6 ± 0.6	11.9 ± 0.2	11.7± 0.1	6.7 ± 0.2
	250	9.9 ± 0.6	10.5 ± 0.3	10.8 ± 0.4	6.2 ± 0.6
227	500	NA	14.7 ± 0.3	13.3 ± 0.7	NA
	250	NA	13 ± 0.6	10.7 ± 0.7	NA
228	500	10.0 ± 0.6	NA	11.7 ± 0.3	8.0 ±0.6
	250	8.3 ± 0.3	NA	10.0 ± 0.6	7.7 ± 0.8
229	500	9.3 ± 0.3	NA	8.6± 1.5	NA
	250	7.7 ± 0.3	NA	7.3 ± 0.3	NA
Gentamycin	500	17.6 ± 0.3	16.7 ± 0.1	19.5 ± 0.5	18.2 ± 0.1
	250	17.2 ± 0.2	16.3 ± 0.3	19.2 ± 0.1	17.8 ± 0.0
DMSO	500	NA	NA	NA	NA
	250	NA	NA	NA	NA

CRA; *Crinum abyssinicum*; DCME; Dichloromethane: methanol (1:1) extract; ME; Methanol extract; NA: No activity; DMSO = Dimethyl sulfoxide; Gentamycin and DMSO were used as the positive and negative controls, respectively.

The morphological differences between Gram-positive and Gram-negative bacteria, with the latter having an outer phospholipidic membrane carrying the structural lipopolysaccharide components, may account for the variation in sensitivity between these microorganisms. As a result, chemicals that act as antimicrobials cannot pass through the cell wall. Conversely, because they only have an outer peptidoglycan layer-which is ineffective as a permeability barrier-Gram-positive bacteria are more vulnerable. Therefore, the cell walls of Gram-negative organisms which are more complex than the Gram-positive ones operate as a diffusional barrier and making them less vulnerable to the antimicrobial drugs than do Gram-positive bacteria (Nostro et al.,

2000; Hodges, 2002). Certain extracts have nevertheless demonstrated some degree of inhibition against Gram-negative pathogens despite these variations in permeability.

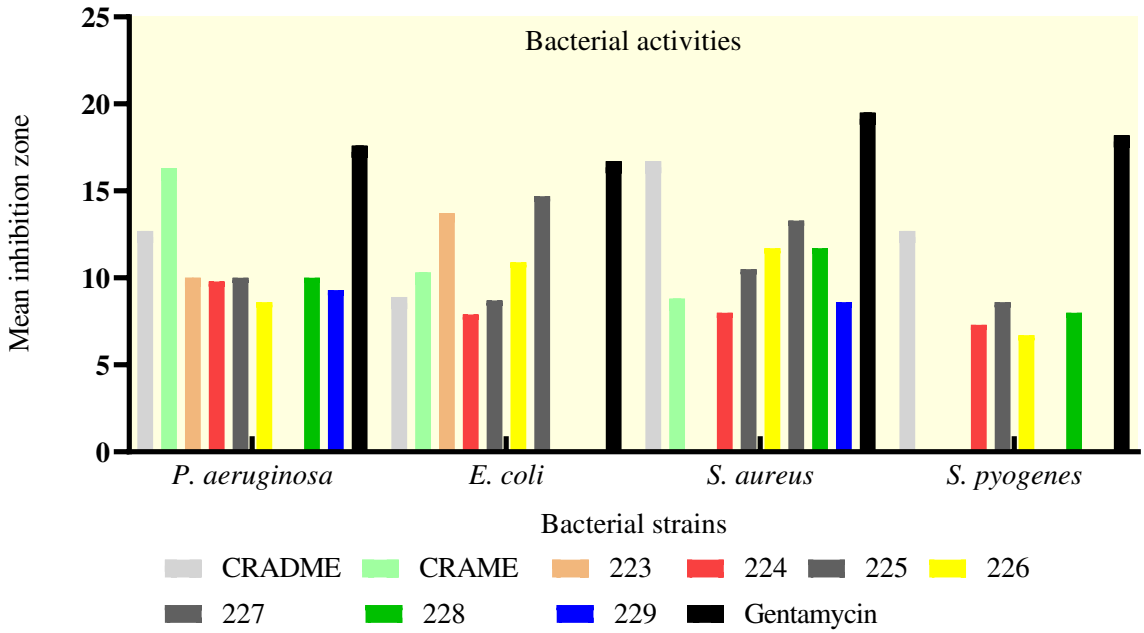

Figure 21: The inhibition zone of the extract and isolated compounds of *C. abyssinicum* in mm (mean ± SD) at 500 μg/mL.

4.3.1.2. Antibacterial activity of the extracts and isolated compounds (**97, 234, 96, 87, 231, 232**) from roots of *C. procera*

In the present investigation, the extract from *C. procera* was tested for antibacterial activity against 4 microbial pathogens. The zone of inhibition of DCM/MeOH (1:1) and methanol root extracts and isolated compounds of *C. procera* has been tabulated in (Table 32, Figure 22). The DCM/MeOH (1:1) root extract of *C. procera* showed medium activity against three of the pathogenic strains such as *P. aeruginosa*, *E. coli*., and *S. pyogenes* with a mean inhibition zone of 11.7 ± 0.3, 11.3 ± 0.7 and 12.6 ± 0.7 mm observed at 500 µg/mL, respectively. Whereas, the MeOH extract of *C. procera* showed no activity against *S. aureus,* and *S. pyogenes* at lower concentration of 250 µg/mL. Besides, the inhibition zone of all the extracts in the present work, the activity increased with increasing concentration in a dose-dependent manner. Among the tested isolated compounds, in the present study calotroprocerol A (**97**) and 11-oxo-α-amyrin ethylated (**234**), **96**, and **87** showed growth inhibitory effects against all the tested bacterial

strains in a dose-dependent manner. The highest mean inhibitory value was recorded by **231** (17.7 ± 0.8) followed by **232 (**17.7 ± 1.2**), 87** (14.3 ± 0.5), **97** (13.9 ± 0.2), and **234** (12.7 ± 0.4 mm), against *E. coli* at 500 µg/mL compared with ciprofloxacin (29.7 ± 0.3) with similar concentration. On the contrary, **97** showed potent activity against *S. pyogenes* (13.2 ± 0.0 mm) at a concentration of 500 µg/mL. **87** and **234** displayed the highest mean inhibition value of 12.5 ± 0.2, and 12.3 ± 0.0 mm against *S. aureus* at 500 *µ*g/mL, respectively, compared with ciprofloxacin (26.7 ± 0.7) at the same concentration. Compounds **231** and **232** were found totally inactive at all concentrations with zero inhibition zone values against *S. aureus*.

Table 32: The mean inhibition zone diameter (IZD) in mm of the root extracts and isolated compounds (**97, 234, 96, 87, 231, 232**) of *Calotropis procera*.

Samples	Conc.	Inhibition zone in diameter (mm)			
	µg/mL	*P. aeruginosa*	*E. coli*	*S. aureus*	*S. pyogenes*
DCME of CP	500	11.7 ± 0.3	11.3 ± 0.7	NA	12.6 ± 0.7
	250	10.3 ± 0.3	10.3 ± 0.3	NA	10.3 ± 0.3
ME of CP	500	8.3 ± 1.1	7.6 ± 0.6	7.9 ± 1.0	7.3 ± 0.9
	250	NA	NA	NA	NA
97	500	11.6 ± 0.6	13.9 ± 0.2	10.6 ± 0.1	13.2 ± 0.1
	250	10.4 ± 0.2	11.5 ± 0.8	9.4 ± 0.3	12.0 ± 0.3
234	500	10.1 ± 0.1	12.7 ± 0.4	12.3 ± 0.1	11.1 ± 0.6
	250	9.3 ± 0.1	12.0 ± 0.5	11.9 ± 0.1	10.5 ± 0.7
96	500	11.9 ± 0.4	13.2 ± 1.4	10.8 ± 0.6	9.9 ± 1.7
	250	11.1 ± 0.6	11.9 ± 1.5	9.2 ± 0.5	7.8 ± 1.8
87	500	9.4 ± 1.0	14.3 ± 0.5	12.5 ± 0.2	7.1 ± 0.3
	250	8.8 ± 1.4	12.8 ± 0.4	11.2 ± 0.2	NA
231	500	12.3 ± 1.5	17.7 ± 0.8	NA	NA
	250	11.7 ± 1.2	16 ± 0.6	NA	NA
232	500	NA	17.0 ± 1.2	NA	11.3 ± 1.2
	250	NA	15.7 ± 0.9	NA	9.3 ± 1.2
Ciprofloxacin	500	29.7 ± 0.3	29.7 ± 0.3	26.7 ± 0.7	29.7 ± 0.4
	250	28.3 ± 0.7	26.7 ± 0.3	26.3 ± 0.3	29.3 ± 0.3
DMSO		NA	NA	NA	NA

CP; *Calotropis procera*; DCME; Dichloromethane: methanol (1:1) extract; ME; Methanol extract; NA: No activity; DMSO = Dimethyl sulfoxide; Ciprofloxacin and DMSO were used as the positive and negative controls, respectively.

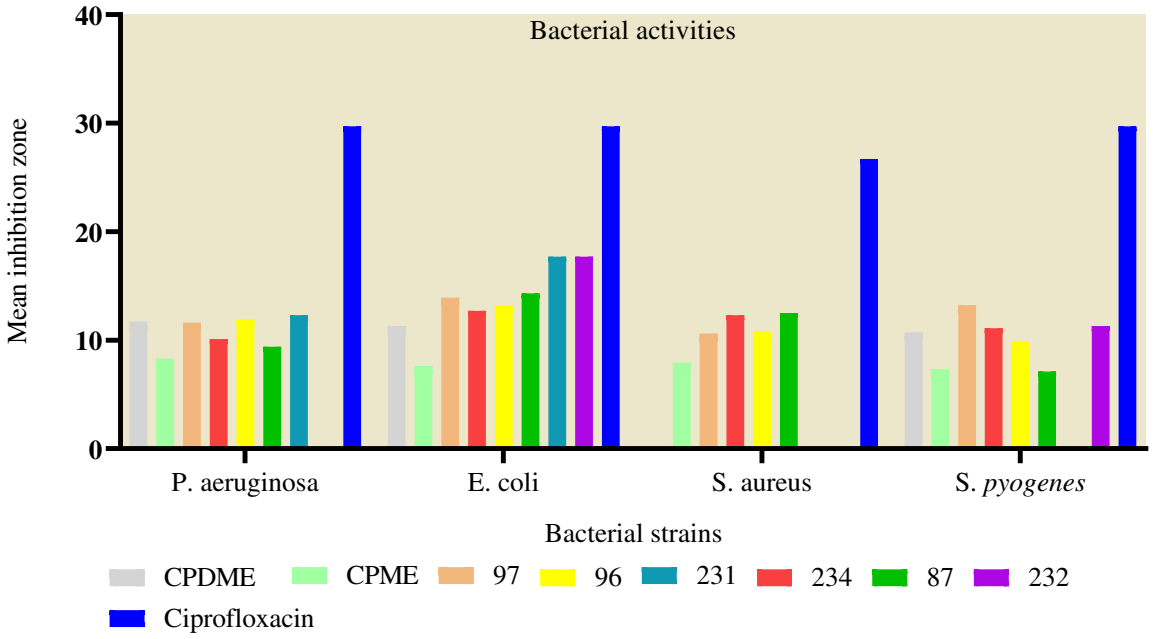

Figure 22: The inhibition zone of the extract and isolated compounds of *C. procera* in mm (mean ± SD) at 500 μg/mL.

4.3.1.3. Antibacterial activity of the extracts and isolated compounds (**239-241, 79**) from roots of *C. abyssinica*

The DCM/MeOH (1:1) and methanolic root extract obtained from *C. abyssinica* (Table 33, Figure 23) revealed appreciable antibacterial activity against four of the pathogenic strains (*P. aeruginosa, E. coli, S. aureus,* and *S. pyogenes*). The methanolic root extract of *C. abyssinica* exhibited an inhibitory effect against four of the pathogenic strains with a mean inhibition zone of 12.3 ± 0.2, 15.4 ± 0.3, 18.3 ± 0.4, and 12.2 ± 0.1 mm observed at 500 µg/ml for *P. aeruginosa, E. coli, S. aureus,* and *S.* pyogenes, respectively. However, the methanolic extract of *C. abyssinica* showed potent inhibitory activity against *S. aureus* (18.3 ± 0.4 mm) and *E. coli.* (15.4 ± 0.3 mm) compared with Gentamycin with IDZ of 19.5 ± 0.5 and 16.7 ± 0.1 mm at 500 μg/mL, respectively. For isolated compounds (Table 37, Figure 23), compounds **241** and **79** displayed better inhibitory activity than compounds **239** and **240** against *E. coli* with a larger zone of inhibition of 13.9 ± 0.2 and 12.3 ± 0.3 mm recorded at a concentration of 500 µg/mL, respectively which was comparable to Gentamycin 16.7 ± 0.1 mm with the same concentration.

Compounds **241** and **79** displayed moderate activity against all tested bacterial strains. Compound **240** was found totally inactive against *P. aeruginosa* at both concentrations with nil inhibition zone values. Compound **79** displayed promising activity against *S. aureus* (14.1 ± 1.0 mm) at 500 µg/mL compared with Gentamycin (19.3 ± 0.5 mm). The concentration of the extract and isolated compounds were significantly associated with a mean zone of inhibition (in mm). An increase in the zone of inhibition was observed with an increase in the concentration of the tested samples. The higher activity of the crude extract may result from the synergistic interactions of various phytochemicals found in the extract; this cannot be the case when evaluating the pure compounds on alone.

Table 33: The mean inhibition zone diameter (IZD) in mm of the root extracts and isolated compounds (**239-241, 79**) of *C. abyssinica*.

Samples	Conc. µg/mL	Inhibition zone in diameter (mm)			
		P. aeruginosa	*E. coli*	*S. aureus*	*S. pyogenes*
DCME of CA	500 µg/mL	8.7 ± 1.2	14.2 ± 0.4	11.7 ± 0.8	9.0 ± 0.4
	250 µg/mL	8.0 ± 1.0	12.8 ± 0.2	11.0 ± 0.6	7.0 ± 0.8
ME of CA	500 µg/mL	12.3 ± 0.2	15.4 ± 0.3	18.3 ± 0.4	12.2 ± 0.1
	250 µg/mL	11.9 ± .6	14.8 ± 0.3	16.7 ± 0.2	10.1 ± 0.4
239	500 µg/mL	7.5 ± 0.2	8.4 ± 0.2	8.3 ± 0.1	NA
	250 µg/mL	7.1 ± 0.5	7.9 ± 0.4	7.5 ± 0.1	NA
240	500 µg/mL	NA	8.9 ± 0.1	9.6 ± 0.1	10.1 ± 0.2
	250 µg/mL	NA	8.4 ± 0.1	9.4 ± 0.0	8.1 ± 0.1
241	500 µg/mL	9.1 ± 0.4	11.8 ± 0.3	8.2 ± 0.6	7.0 ± 0.2
	250 µg/mL	8.7 ± 0.3	10.9 ± 0.2	7.7 ± 0.5	6.7 ± 0.1
79	500 µg/mL	10.8 ± 0.2	12.3 ± 0.3	14.1 ± 0.1	8.8 ± 0.1
	250 µg/mL	9.9 ±0.5	10.6 ± 0.1	12.9 ± 0.6	7.9 ± 0.2
Gentamycin	500 µg/mL	17.6 ± 0.3	16.7 ± 0.1	19.5 ± 0.5	18.2 ± 0.1
	250 µg/mL	17.2 ± 0.2	16.3 ± 0.3	19.2 ± 0.1	17.8 ± 0.0

CA; *Caylusea abyssinica*; DCM; Dichloromethane:methanol (1:1) extract; ME; Methanol extract; Samples were reported as Mean ± SEM; Gentamycin was used as a standard drug.

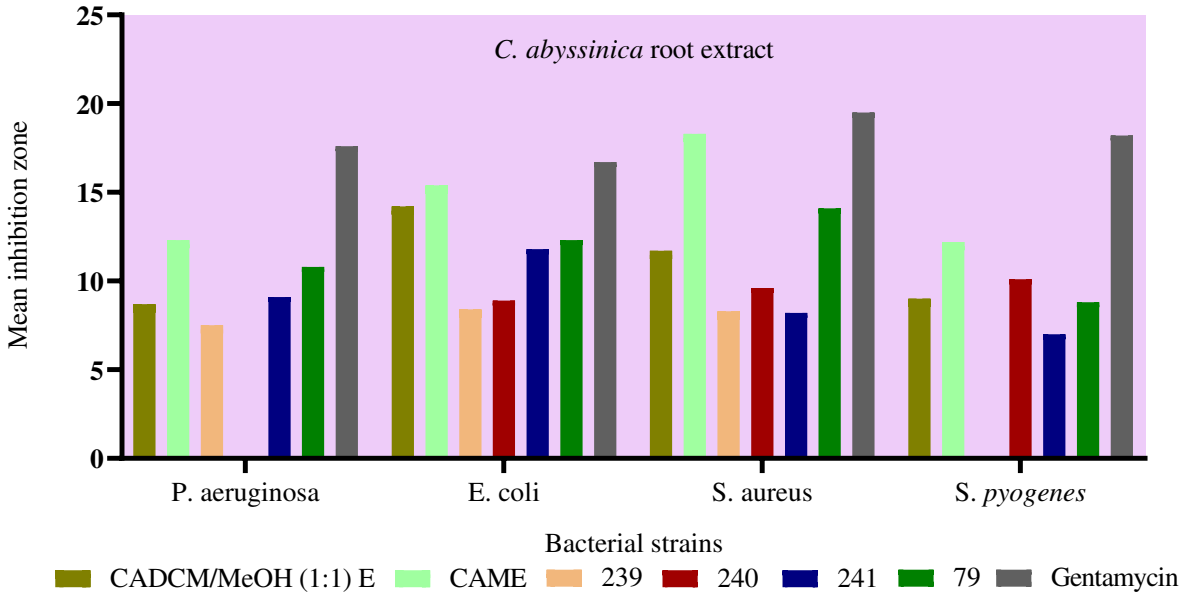

Figure 23: The inhibition zone of the extract and isolated compounds of *C. abyssinica* in mm (mean ± SD) at 500 μg/mL.

4.3.1.4. Antimicrobial activity of the extracts and isolated compounds (**78, 242-246**) from roots of *J. schimperiana*

By using the microdilution method, the antimicrobial activity of the extract and isolated compounds from *J. schimperiana* roots (Table 34) was examined against a total of 9 microorganisms (6 bacteria and 3 fungi) (MIC in mg/mL for extracts, isolated compounds and standard drugs). The result showed, among the tested bacterial strains, Gram-positive bacteria were more susceptible to the crude extract. However, the *n*-hexane extract was less potent than the other extracts against all the tested bacterial pathogens. The smallest MIC value was recorded for the dichloromethane: methanol (1:1) extract against *S. aureus,* and *E. faecalis* which was 4.0 mg/mL. And also, the lowest antimicrobial activities were recorded by *S. aureus, S. agalactiae*, and *E. faecalis* with MIC value of 8 mg/mL for the methanol extract. In comparison to *n*-hexane and methanol extracts, the dichloromethane: methanol (1:1) extracts were found to be more potent against all of the tested bacteria. These could be because of the inherent ability of this bacterial species to produce resistance mechanisms like efflux pump, reduced permeability or biofilm formation which could hinder the antibacterial activity of the bioactive compounds

(Harrient, and Nandita, 2014; Tanya, and Daniel, 2009). Previous studies conducted on 80% methanol leaf extract, aqueous, n-butanol, and ethyl acetate solvent fractions of *Justicia schimperiana* revealed potent antimicrobial activity against tested bacterial pathogens (Melaku, 2017). All the tested fungal species did not respond to lower concentrations they needed higher concentrations of active extracts to be inhibited.

Table 34: Antimicrobial activity (MIC) of extracts, and isolated compounds (**78, 242-246**) from roots of *J. schimperiana*.

Samples	*Gram-positive bacteria*			*Gram-negative bacteria*			*Fungi*		
	S. aurous	*S. agalactiae*	*E. faecalis*	*E. coli*	*P. aeruginosa*	*K. pneumoniae*	*C. albicans*	*T. mentagrophytes*	*T. rubrum*
nHE	16	16	16	>16	>16	>16	>16	>16	>16
DCME	4	8	4	8	8	16	>16	>16	>16
ME	8	8	8	>16	16	>16	>16	>16	>16
78	1	2	2	2	>4	4			
242	2	0.5	1	>2	2	>2			
243	1	0.5	0.5	>1	>1	>1			
244	2	1	1	2	2	2		NT	
245	>2	1	2	>2	2	>2			
246	0.25	0.25	2	0.5	1	2			
Cipro	0.625	0.125	0.125	0.19	0.19	0.19			
Ketoconazole				NT			25	25	50
Amphotericin B							25	100	100
5% Tween 80	G	G	G	G	G	G	G	G	G
Growth control	G	G	G	G	G	G	G	G	G
Sterility control	NG	NG	NG	NG	NG	NG	NG	NG	NG

Keynotes: JS: *J. schimperiana*, nHE: *n*-Hexane extract, DCME: Dichloromethane:methanol (1:1) extract, ME: Methanol extract, NT: Not tested, G: Growth, NG: No growth.

Based on the results of the antibacterial activity, it was found that the isolated compounds (**78**, and **242-246**) have the potential to effectively inhibit the growth of all tested Gram-positive bacteria compared to Gram-negative organisms. The results also showed that *S. aureus* and *S. agalactiae* were highly susceptible to compound **246** with a MIC value of 0.25 mg/mL followed by *S. agalactiae* with a MIC of 0.5 mg/mL to compounds **242**, and **243,** and *E. coli* with a MIC value of 0.5 mg/mL to compound **246**. Additionally, compounds **78**, and **243** were also effective against *S. aureus* (MIC = 1 mg/mL), and compounds **244**, and **246** were effective against all

tested Gram-negative bacteria. The isolated compound **78** showed low bactericidal potential against *P. aeruginosa*, with a MIC greater than 4 mg/mL. The isolated compound **78** showed low bactericidal potential against *P. aeruginosa*, with a minimum inhibitory concentration (MIC) greater than 4 mg/mL. In particular, compounds **243**, and **245** displayed low activity results against all tested Gram-negative bacteria.

4.3.1.5. Antimicrobial activity of the extracts and isolated compounds (**247-253, 230**) from roots of *V. siniaticum*

By using the microdilution method, the antimicrobial activity of the extract and isolated compounds from *V. sinaiticum* roots (Table 35) was examined against a total of nine microorganisms (six bacteria and three fungi) (MIC in mg/mL for extracts, isolated compounds and standard drugs). The findings demonstrated that among the examined bacterial strains, Gram-positive bacteria were more sensitive to the crude extract than Gram-negative bacteria. The CH_2Cl_2:CH_3OH (1:1), and CH_3OH extracts of *V. sinaiticum* roots revealed the highest activity against *S. epidermids* with a MIC value of 0.25 mg/mL, followed by the CH_2Cl_2:CH_3OH (1:1) root extract displayed the activity with a MIC value of 0.5 mg/mL against *S. aureus*. Overall, compared to the other extracts, the *n*-hexane extract was less effective against the tested bacterial pathogens (MIC > 1 mg/mL). The hydroalcoholic leaf extracts of *V. sinaiticum* showed efficacy against *S. aureus* and *P. aeruginosa* with inhibition zones of 25 ± 0.6 mm and 20 ± 0.5 mm, respectively, according to (Tadeg et al., 2005). According to the results of the antibacterial activity, the compounds (**247–253**) can efficiently inhibit the growth of all tested Gram-positive bacteria in comparison to Gram-negative organisms. The highest antibacterial activities were recorded by *S. epidermids* with a MIC value of 0.0625 for compound **247**, and 0.5 mg/mL for compounds **250,** and **253**, followed by *S. aureus*, and *S. typomurium*, with a MIC value of 0.5 mg/mL for compounds **247**, **251**, and, **249** respectively. The isolated compounds **248**, **251**, and **230** showed equipotent activity against *S. epidermids* with a MIC value of 1 mg/mL. In comparison to others, compounds **248**, **249**, and **250** showed the lowest level of antibacterial activity against *K. pneumoniae,* recording the highest MIC value of 2 mg/mL. A MIC value of 2 mg/mL was also recorded for compounds **247** and **250**, against *S. typomurium,* and *E. faecalis*. However, compounds **247**, **250**, and **230** showed good activity against *E. coli* (MIC = 1 mg/mL), and compounds **248**, and **250** showed good activity against *S. aureus* (MIC = 1 mg/mL).

None of the examined fungal species reacted to lower concentrations of the active extracts; they needed higher concentrations to be suppressed. Antibiotics and nanomaterials together exhibit antibacterial efficiency against susceptible and resistant bacterial strains at much lower concentrations, suggesting that combining these nanomaterials with other microbe-fighting compounds can enhance the antibacterial activity of these promising compounds (D'Arrigo *et al.,* 2010).

Table 35: Antimicrobial activity of extracts and isolated compounds (**247-253, 230**) from roots of *V. sinaiticum*.

Samples	*Gram-positive bacteria*			*Gram-negative bacteria*			*Fungi*		
	S. aureus	*S. epidermids*	*E. faecalis*	*E. coli*	*K. pneumoniae*	*S. typomurium*	*C. albicans*	*T. mentagrophytes*	*T. rubrum*
*n*HE	>1	>1	>2	>2	>2	>2	2	>2	>2
DCME	0.5	0.25	1	1	1	2	>2	2	>2
ME	1	0.25	2	2	2	2	2	>2	>2
247	0.5	0.063	2	1	1	2			
248	1	1	1	2	2	>2			
249	>1	>1	>2	>2	2	0.5			
250	1	0.5	2	1	2	2		NT	
251	0.5	1	1	> 1	> 1	> 1			
253	>1	0.5	>2	>1	>2	1			
230	2	1	4	1	4	1			
Cipro	0.25	0.5	0.5	0.13	0.13	0.13			
Ketoconazole				NT			25	25	50
Amphotericin B				NT			25	100	100
5% Tween 80								G	
Growth control				G				G	
Sterility control				NG					

Keynotes: VS: *Verbascum Sinaiticum*, nHE: *n*-hexane extract, DCME: Dichloromethane:methanol (1:1) extract, ME: Methanol extract, NT: Not tested, G: Growth, NG: No growth.

4.3.2. Antimicrobial evaluation of essential oil extract

The results for antimicrobial activity (Table 36) of essential oil extract from the bulbs of *C. abyssinicum* (CRAB), aerial parts of *Caylusea abyssinica* (CAAP), leaves, flowers, and seeds of

Calotropis procera (CPL, CPF, CPS), roots, and seeds of *Lagenaria abyssinica* (LAR, and LAS), leaves, and roots of *Justica schimperiana* (JSL, and JSR), leaves, and roots of *Verbascum sinaiticum* (VSL, and VSR) were tested against selected bacterial strains of *Staphylococcus aureus*, *Streptococcus agalactiae*, *Enterococcus faecalis*, *Escherichia coli*, *Pseudomonas aeruginosa*, *Klebsiella pneumoniae*, and fungal cultures *Trichophyton mentagrophytes*, *Trichophyton rubrum Candida albicans*. Each tested essential oil exhibited various degrees of MIC value, against the tested micro-organisms, ranging from 1 mg/mL to 16 mg/mL. MIC test was included in this study to determine the lowest concentration of EOs that gives the lowest inhibition zone using the broth dilution test. According to the findings, the extracts derived from EO's CRAB, CAAP, LAS, LAR, and CPF showed promising potential in restraining the growth of most Gram-negative bacteria, with varying MIC values. The EO of CRAB, CAAP, and LAS could be identified as effective with MICs ranging from 16 to 2 mg/mL, 16 to 1 mg/mL, and 16 to 4 mg/mL against *S. aureus*, respectively. The Gram-positive bacteria *S. agalactiae* was inhibited by EO of the CRAB, LAR, and LAS at a minimum concentration of 8 mg/mL, 4 mg/mL, and 2 mg/mL respectively. EO of CRAB showed activity against *E. faecalis* with an MIC value of 2 mg/mL; while EO LAS displayed the highest activity with an MIC value of 1 mg/mL. EO of CAAP, and LAS showed equipotent activity against *E. coli* with an MIC value of 2 mg/mL. *S. agalactiae*, *E. coli*, and *P. aeruginosa* exhibited low antimicrobial activity, recording the highest MIC value of 8 mg/mL by CRAB and *E. faecalis*, and *P. aeruginosa* with the highest MIC value of 8 mg/ml by CAAP, in comparison to other bacteria.

Out of the bacteria that were tested, *S. aureus* and *E. faecalis* showed the highest susceptibility with a MIC value of 1.0 mg/mL for CRAB and LAS, respectively. Fungal species such as *C. albicans, T. mentagrophytes,* and *T. rubrum* exhibited greater resistance to CRAB and CAAP, with a minimum inhibitory concentration (MIC) value greater than 16 mg/mL. LAS and LAR extracts showed significantly good fungal inhibitory activity compared to other essential oil extracts, with LAS exhibiting the highest inhibition against *C. albicans* and *T. mentagrophytes* at a MIC value of 4 mg/mL, and LAR showing similar inhibition against *C. albicans, T. mentagrophytes*, and *T. rubrum* at a MIC value of 8 mg/mL as compared to standard antifungal drug, Ketoconazole (25 and 50 µg/mL). The most susceptible bacteria in the treatment of EO of JSL were *E. faecalis* while for JSR *S. aureus*, *S. agalactiae*, and *E. faecalis* with MIC value of 4

mg/mL. Except for the bacteria *E. faecalis,* the lowest antimicrobial activities were recorded by EO of JSL with MIC value of above 4 mg/mL. Similarly, the lowest antimicrobial activities were recorded by *E. coli, P. aeruginosa*, and *K. pneumoniae* with MIC value of above 4 mg/mL for EO of JSR. The EO extracts showed low antifungal activity against *C. albicans, T. mentagrophytes,* and *T. Rubrum*, as their MIC value was higher than 4 mg/mL.

Based on the antimicrobial activity results, it was found that the EO extracts of VSL and VSR have the potential to effectively inhibit the growth of both Gram-positive and Gram-negative bacteria. The EO extracts from VSL were found to be more effective in inhibiting the growth of all tested Gram-negative organisms compared to the EO extracts from VSR. The results also showed that *S. agalactiae* was highly susceptible to both EO extracts of VS (leaves, and roots) with a MIC value of 2 mg/mL, followed by *E. faecalis* with a MIC of 4 mg/mL. Additionally, EO extracts of VSL were also effective against *E. coli* (MIC = 4 mg/mL) and *P. aeruginosa* (MIC = 4 mg/mL). The EO extracts of VSL and VSR showed low bactericidal potential against *K. pneumoniae*, with a minimum inhibitory concentration (MIC) greater than 8 mg/mL. It has been found that EO extracts from VSR may possess fungal inhibition properties against *C. albicans* and *T. mentagrophytes*, with a MIC of 8 mg/mL. The EO extracts of VSL and VSR showed low potential for fungicidal activity against *C. albicans*, *T. mentagrophytes*, and *T. rubrum*, as their MIC value exceeded 8 mg/mL. In particular, the EO extracts of VSR displayed similar results against *T. rubrum*. The activity of EOs on Gram-positive bacteria is said to be slightly more sensitive than that on Gram-negative bacteria. This is explained by the fact that Gram-negative cells' outer membranes are more resistant to the action of EOs and prevent easy diffusion through the lipopolysaccharide membrane (Burt, S., 2004; Fisher & Phillips, 2008). The most vulnerable microbe to EOs is commonly reported to be the Gram-positive *S. aureus* (Burt, S., 2004; Fisher & Phillips, 2008). This study supports previous findings in the literature that antimicrobial activities have a direct relation to increasing the concentration of the EO extract (Bhalodia & Shukla, 2011).

Consequently, these EOs can be used in combination with antimicrobial drugs, which have a synergistic impact against a variety of microorganisms, including those that have become resistant to antibiotics, or they can be used alone when the safety status has been determined (D'Arrigo *et al.,* 2010).

Table 36: Antimicrobial Activity of EO extracts of plants against selected microorganisms (MIC in mg/mL).

EO extracts	*Gram-positive bacteria*			*Gram-negative bacteria*			*Fungi*		
	S. aurous	*S. agalactiae*	*E. faecalis*	*E. coli*	*P. aeruginosa*	*K. pneumoniae*	*C. albicans*	*T. mentagrophytes*	*T. rubrum*
CRAB	2	8	2	8	8	16	>16	>16	>16
CAAP	1	4	4	2	4	> 16	8	>16	>16
LAR	> 8	4	8	4	8	> 8	8	8	8
LAS	4	2	1	2	4	4	4	4	8
CPF	> 4	4	4	> 4	> 4	> 4	> 4	> 4	> 4
CPL	> 4	> 4	> 4	> 4	> 4	> 4	> 4	> 4	> 4
JSL	> 4	> 4	4	> 4	> 4	> 4	> 4	> 4	> 4
JSR	4	4	4	> 4	> 4	> 4	> 4	> 4	> 4
VSL	8	2	4	4	4	> 8	> 8	> 8	> 8
VSR	> 8	2	4	8	8	> 8	8	8	> 8
Cipro	0.625	1.25	1.25	0.19	0.19	0.19	NT	NT	NT
Ketoconazole	NT	NT	NT	NT	NT	NT	25	25	50
Amphotericin B	NT	NT	NT	NT	NT	NT	25	50	100
5% Tween 80	G	G	G	G	G	G	G	G	G
Growth control	G	G	G	G	G	G	G	G	G
Sterility control	NG	NG	NG	NG	NG	NG	NG	NG	NG

Keynotes: EO: Essential oil, CRAB: bulbs of *C. abyssinicum*, CAAP: aerial parts of *Caylusea abyssinica,* CPL, CPF, CPS: leaves, flowers, and seeds of *Calotropis procera*, LAR, LAS: roots, and seeds of *Lagenaria abyssinica*, JSL, JSR: *Justica schimperiana* leaves, and roots, VSL, and VSR: *Verbascum sinaiticum* leaves, and roots, NT: Not tested, G: Growth, NG: No growth.

4.3.3. Antioxidant activity of the extracts and isolated compounds

DPPH is widely used to test the ability of compounds to act as free radical scavengers and to evaluate the antioxidant activity of compounds. It is a stable free radical, because of the delocalized electron. The decreased capability of the DPPH radical is determined by the reduction in its absorbance at 5l7 nm (Hangun-Balkir and McKenney, 2012, Gulcin *et al*., 2010). Furthermore, the color turns from purple to yellow subsequently due to the odd electron of DPPH radical becomes paired with hydrogen from a free radical scavenging antioxidant to form the reduced DPPH-H (Luqman *et al*., 2012) (Figure 24). As a result, the antioxidant activity of **28** isolated compounds and **11** crude extracts of six selected medicinal plants were examined in this work using the DPPH method.

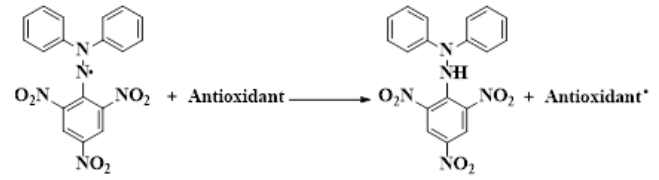

DPPH radical (Purple) DPPH-H (Yellow)

Figure 24: The structure of DPPH radical and its product (DPPH-H).

4.3.3.1. Antioxidant activity of the extracts and isolated compounds (**224-229**) from roots of *C. abyssinicum*

In this study, the DPPH radical scavenging activities of the *C. abyssinicum* extract and isolated compounds were examined by comparison with ascorbic acid which is used as a positive control, and the result is depicted in (Table 37, Figure 25). The results showed that the DCM:MeOH (1:1) and MeOH root extracts of *C. abyssinicum* inhibited the DPPH radical by 70.3 and 64.8 at 100 μg/mL, respectively. The result obtained was moderate compared to ascorbic acid which is used as a positive control with percent inhibition of radical by 90.0 % at the same concentration. The isolated compounds (**224-229**) from the DCM: MeOH (1:1) root extracts of *C. abyssinicum* inhibited the DPPH radical by 50.8, 61.7, 70.8, 57.4, 79.6 and 62.74 at 100 μg/mL, respectively. The IC_{50} values of the isolated compounds were calculated. The lower the IC_{50}, the higher the antioxidant activity of substances. The IC_{50} values of isolated compounds vary from 0.6 µg/mL to 30.0 µg/mL. The isolated compounds displayed lower IC_{50} values for compound **228** (79.64 %, IC_{50} value 0.60 μg/mL) which showed promising antioxidant potential as compared to ascorbic acid (90.0 %, IC_{50} value 0.14 μg/mL) used as a standard antioxidant. The activities shown by isolated compounds showed moderate antioxidant activity.

Table 37: Percent radical scavenging activity of the plant extract and isolated compounds (**224-229**).

Tested samples	Concentration (µg/ml)					
	6.25	12.5	25	50	100	IC_{50}
DCME of CRA	30.1 ± 0.1	36.9 ± 0.2	37.3 ± 0.1	52.9 ± 0.2	70.3 ± 0.7	12.8
ME of CRA	21.1 ± 0.4	23.7 ± 0.1	27.6 ± 0.2	45.6 ± 0.1	64.8 ± 0.9	18.5
224	13.3 ± 2.2	21.7 ± 2.2	24.2 ± 0.8	31.7 ± 2.2	50.8 ± 3.0	30.0
225	16.7 ± 0.8	30.8 ± 3.6	43.3 ± 0.8	53.3 ± 1.7	61.7 ± 0.8	25.5

226	44.2 ± 3.0	49.2 ± 0.0	58.3 ± 2.2	63.3 ± 2.2	70.8 ± 0.2	10.2
227	11.8 ± 0.1	18.5 ± 0.3	25.9 ± 0.4	39.1 ± 0.2	57.4 ± 0.6	8.4
228	28 ± 0.3	46.3 ± 0.5	54.3 ± 0.7	65.9 ± 0.5	79.6 ± 0.6	0.6
229	26.6 ± 0.6	34.2 ± 0.1	45.9 ± 0.1	53.3 ± 0.2	62.7 ± 0.2	3.3
Ascorbic acid	81.7 ± 0.1	85.8 ± 0.1	87.9 ± 0.2	88.1 ± 0.1	90.0 ± 0.3	0.14

CRA; *Crinum abyssinicum,* DCME; Dichloromethane:methanol (1:1) extract; ME; Methanol extract; Samples were reported as Mean± SEM; Ascorbic acid was used as a positive control.

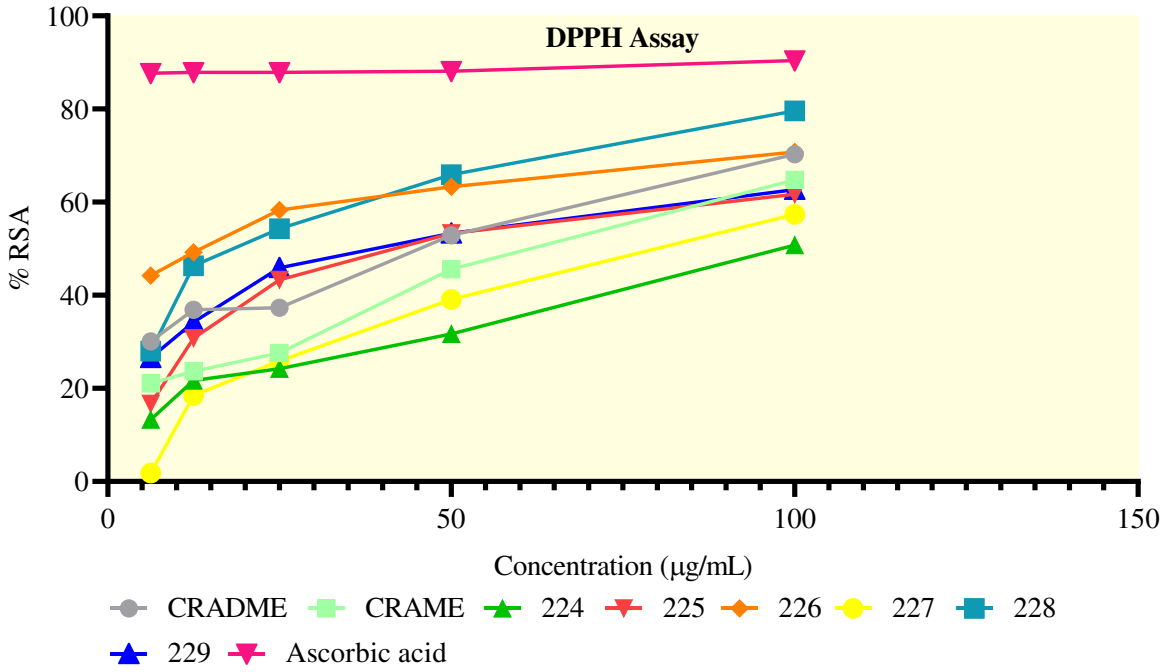

Figure 25: Percentage of DPPH radical scavenging activities of the extract and isolated compounds of *C. abyssinicum*.

4.3.3.2. Antioxidant activity of the extracts and isolated compounds (**97, 234, 87, 231, 232**) from roots of *C. procera*

The DPPH radical scavenging activities of the extracts and isolated compounds of *C. procera* were also examined by comparison with ascorbic acid which is used as a positive control, and the result is depicted in Table 38 and Figure 26. The results showed that the DCM: MeOH (1:1) and methanol root extracts and isolated compounds **97, 234, 87, 231,** and **232** of *C. procera* reduced the stable DPPH radical by 48.4, 70.6, 63.5, 75.0, 62.0, 60.1, and 60.9, respectively, with an IC_{50} value of 20.3, 7.9, 12.6, 8.3, 13.8, 14.6, and 15.3 at 200 μg/mL, respectively. It was observed that the radical scavenging activity increased with an increasing concentration of the

samples in the test. The result revealed that the methanol extract, **97,** and **234** reduced the stable DPPH radical by 70.6 ± 0.8, 63.5 ± 1.0, and 75.0 ± 2.8 at a concentration of 200 µg/mL with an IC_{50} value of 7.9, 12.6, and 8.3, respectively compared with ascorbic acid (IC_{50} value of 0.14) which suggested potential radical scavengers.

Table 38: Percent radical scavenging activities of the plant root extract and isolated compounds (**97, 234, 87, 231, 232**).

Samples	Concentration (µg/mL)					
	12.5	25	50	100	200	IC_{50}
DCME of CP	24.3 ± 0.2	25.8 ± 0.4	27.5 ± 0.1	28.2 ± 0.1	48.4 ± 0.7	20.3
ME of CP	23.5 ± 0.1	26.1 ± 0.3	36.2 ± 0.2	50.5 ± 0.2	70.6 ± 0.8	7.9
97	33.3 ± 2.2	40.8 ± 2.0	46.0 ± 0.8	55.8 ± 2.1	63.5 ± 1.0	12.6
234	48.3 ± 2.2	50.8 ± 2.2	57.5 ± 1.4	65.8 ± 1.7	75.0 ± 2.8	8.3
87	33.3 ± 2.2	40.8 ± 2.0	46.0 ± 0.8	55.8 ± 2.1	62.0 ± 1.8	13.8
231	19.6 ± 0.1	21.07 ± 0.1	31.3 ± 0.1	47.9 ± 0.5	60.1 ± 0.3	14.6
232	27.3 ± 0.3	30.4 ± 0.5	33.1 ± 0.01	55.2 ± 0.0	60.9 ± 0.0	15.3
Ascorbic acid	80.8 ± 0.14	81.7 ± 0.12	85.8 ± 0.12	87.9 ± 0.1	88.1 ± 0.1	0.14

CP; *Calotropis procera*; DCME; Dichloromethane:methanol (1:1) extract; ME; Methanol extract; Samples were reported as Mean ± SEM; Ascorbic acid was used as a positive control.

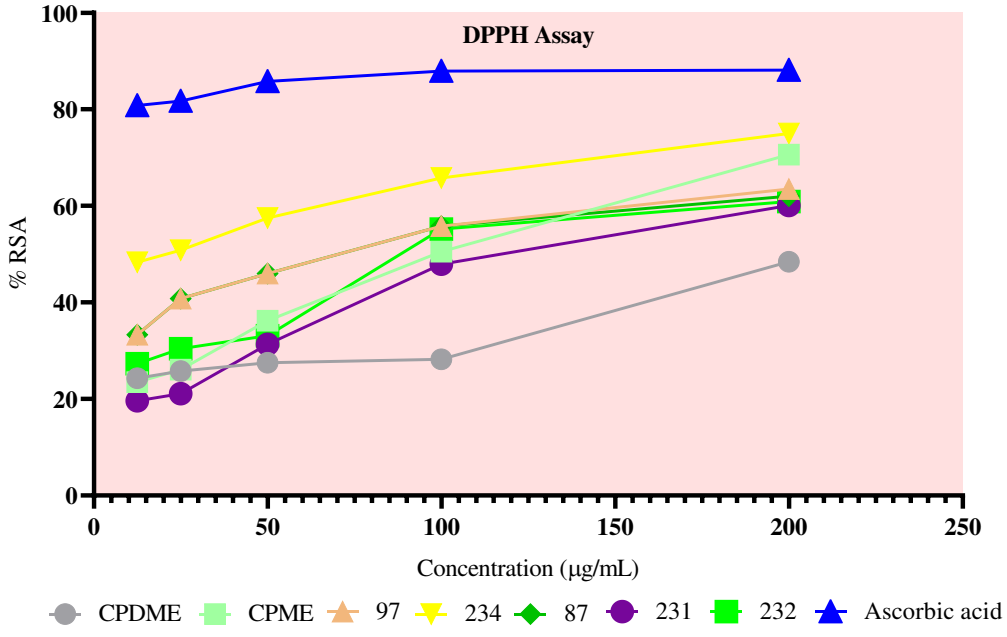

Figure 26: Percentage of DPPH radical scavenging activities of the extract and isolated compounds of *C. procera*.

4.3.3.3. Antioxidant activity of the extracts and isolated compounds (**239-241, 79**) from roots of *C. abyssinica*

The *in vitro* antioxidant potential of the plant extract and isolated compounds were measured by bleaching the purple-colored solution of 1,1-diphenyl-2-picrylhydrazyl radical (DPPH). The DPPH radical scavenging activities of the tested samples were examined by comparison with ascorbic acid which is used as a positive control, and the result is depicted in (Table 39, and Figure 27). The results showed that the DCM: MeOH (1:1), MeOH root extracts, and isolated compounds (**239, 240, 241 and 79**) of *C. abyssinica* inhibited the DPPH radical by 74.3, 71. 3, 70.8, 55.0, 49.2 and 58.0 with an IC_{50} value of 12.5, 12.6, 10.2, 22.8, 23.7 and 34.2 at 200 μg/mL, respectively. The smaller IC_{50} value implies a better DPPH radical scavenging activity and vice versa. The DCM: MeOH (1:1) and MeOH extracts exhibited a better trapping activity (74.3 ± 0.2 and 71. 3 ± 1.7), respectively than compounds isolated on the DPPH radical with respective IC_{50} values of 12.5 and 12.6 μg/mL at a concentration of 200 μg/mL. Compound **239** showed better anti-DPPH activity (70.8 ± 0.2) at a concentration of 200 μg/mL with an IC_{50} value of 10.2 μg/mL. The antioxidant activities of the root extracts and isolated compounds displayed lower IC_{50} values compared to ascorbic acid (IC_{50} value 5.0 µg/mL) the most popular natural antioxidant used as a positive control.

Table 39: Percent radical scavenging activities of the plant extract and isolated compounds (**239-241, 79**).

Samples	Concentration (µg/ml)					
	12.5	25	50	100	200	IC_{50}
DCME of CA	11.2 ± 0.2	37.9 ± 0.1	49.4 ± 0.1	55.9 ± 0.2	74.3 ± 0.2	12.5
ME of CA	25.7 ± 0.9	36.7 ± 0.8	43.7 ± 0.8	52.7 ± 0.4	71. 3 ± 1.7	12.6
239	44.2 ± 3.0	49.2 ± 0.0	58.3 ± 2.2	63.3 ± 2.2	70.8 ± 0.2	10.2
240	23.3 ± 3.0	29.2 ± 2.2	31.7 ± 2.2	43.3 ± 1.7	55.0 ± 1.4	22.8
241	23.3 ± 1.6	25.8 ± 2.0	30.8 ± 1.7	38.3 ± 1.8	49.2 ± 0.2	23.7
79	20.8 ± 3.6	22.4 ± 2.5	29.1± 0.2	43.4 ± 0.6	58.0 ± 0.1	34.2
Ascorbic acid	82.5 ± 1.2	84.2 ± 0.8	86.7 ± 0.8	87.5 ± 1.4	89.2 ± 0.8	5.0

CA; *Caylusea abyssinica*; DCME; Dichloromethane:methanol (1:1) extract; ME; Methanol extract; Samples were reported as Mean ± SEM; Ascorbic acid was used as a positive control; IC_{50} is the 50% inhibitory concentration of the samples.

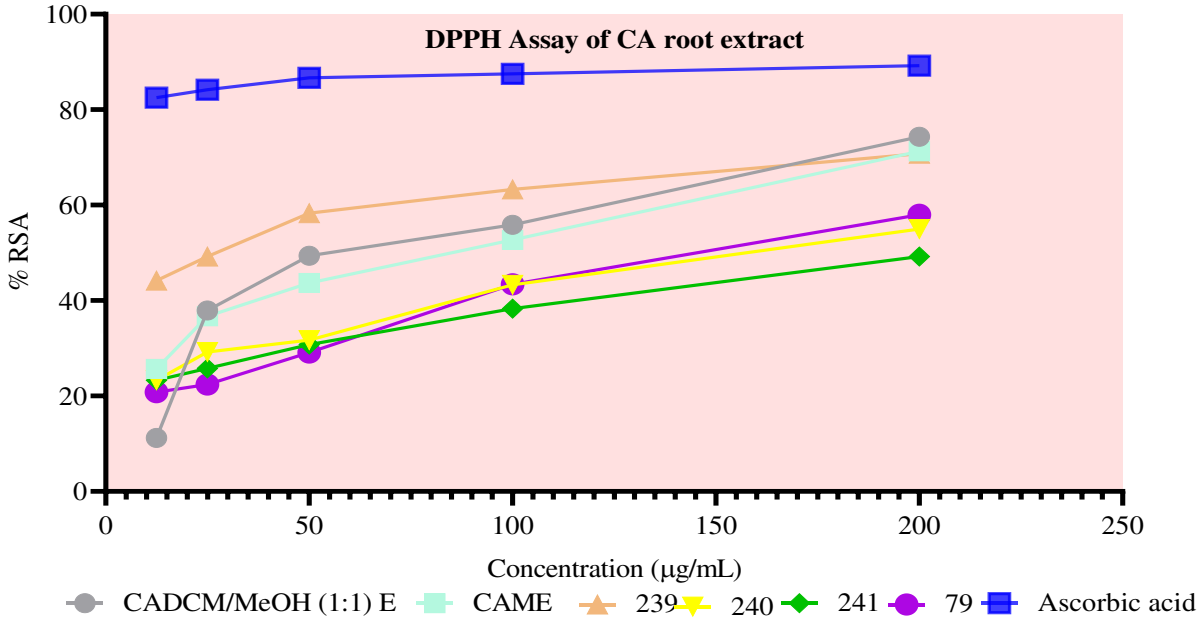

Figure 27: Percentage of DPPH radical scavenging activities of the isolated compounds of C. abyssinica.

4.3.3.4. Antioxidant activity of the extracts and isolated compounds (**78**, and **242-246**) from roots of *J. schimperiana*

In this investigation, radical scavenging activity was carried out on the extracts, and isolated compounds (**78**, and **242-246**) (Table 40). The DPPH radical scavenging activities of the extracts and isolated compounds were examined by comparison with ascorbic acid. The results indicated that the dichloromethane: methanol (1:1), methanol extract, and isolated compounds (**78**, and **242-246**) displayed good free radical scavenging activity with percent inhibition and IC_{50} value at a concentration of 200 µg mL^{-1} depicted in Table 40, and Figure 28. The lower the IC_{50}, the higher the antioxidant activity of substances. In contrast to the DCM: MeOH (1:1), the methanol extract showed the highest antioxidant activities. Furthermore, the methanol extract exhibited the lowest IC_{50} value as compared to the dichloromethane: methanol (1:1) indicating its high scavenging potential. The best radical scavenging activity was displayed by kaempferol-3-O-rutinoside (**246**), and kaempferol-3-O-α rhamnopyranoside (**245**) in comparison with the others with its radical scavenging property comparable with ascorbic acid. This is most likely because of the fact that this compound has the right structural feature (hydroxyl at C-4′) for free radical scavenging activity. Compounds 5-methoxy durmillone (**242**) (IC_{50} value 12.9 µg/mL), *trans*-

*resveratr*ol (**243**) (IC_{50} value 12.1 µg/mL), and tricuspidatol A (**244**) (IC_{50} value 10.2 µg/mL) showed good antioxidant potential compared to ascorbic acid (IC_{50} value 3.1 µg/mL), indicating their strong activities radical as inhibitors.

Table 40: Percent radical scavenging activities of the root extract and isolated compounds (**78**, and **242-246**) of *J. schimperiana*.

Samples	Concentration (µg/ml)					
	12.5	25	50	100	200	IC_{50}
DCM: MeOH (1:1) Extract	32.2 ± 0.1	40.6 ± 0.5	51.3 ± 1.0	57.9 ± 0.7	63.6 ± 0.4	13.3
MeOH extract	44.8 ± 0.6	49.2 ± 0.3	54.9 ± 0.0	65.4 ± 0.1	71.7 ± 0.8	10.8
78	31.7 ± 0.8	37.5 ± 2.5	43.8 ± 0.9	49.2 ± 0.8	53.0 ± 0.3	15.9
242	38.4 ± 1.1	45.1 ± 1.0	54.2 ± 0.7	61.0 ± 0.6	67.5 ± 0.6	12.9
243	45.3 ± 0.4	54.2 ± 0.7	60.1 ± 0.5	65.1 ± 0.4	70.8 ± 1.0	12.1
244	48.6 ± 0.1	56.0 ± 0.3	61.9 ± 0.3	66.7 ± 0.2	71.9 ± 0.9	10.2
245	51.2 ± 1.2	59.7 ± 1.0	63.6 ± 1.1	69.8 ± 1.0	73.3 ± 1.0	7.2
246	54.1 ± 0.9	61.2 ± 1.2	66.1 ± 0.8	71.7 ± 0.8	77.9 ± 0.7	5.9
Ascorbic acid	87.7 ± 0.1	87.9 ± 0.1	87.9 ± 0.1	88.1 ± 0.0	89.8 ± 0.6	3.1

Samples were reported as Mean ± SEM; Ascorbic acid was used as a positive control.

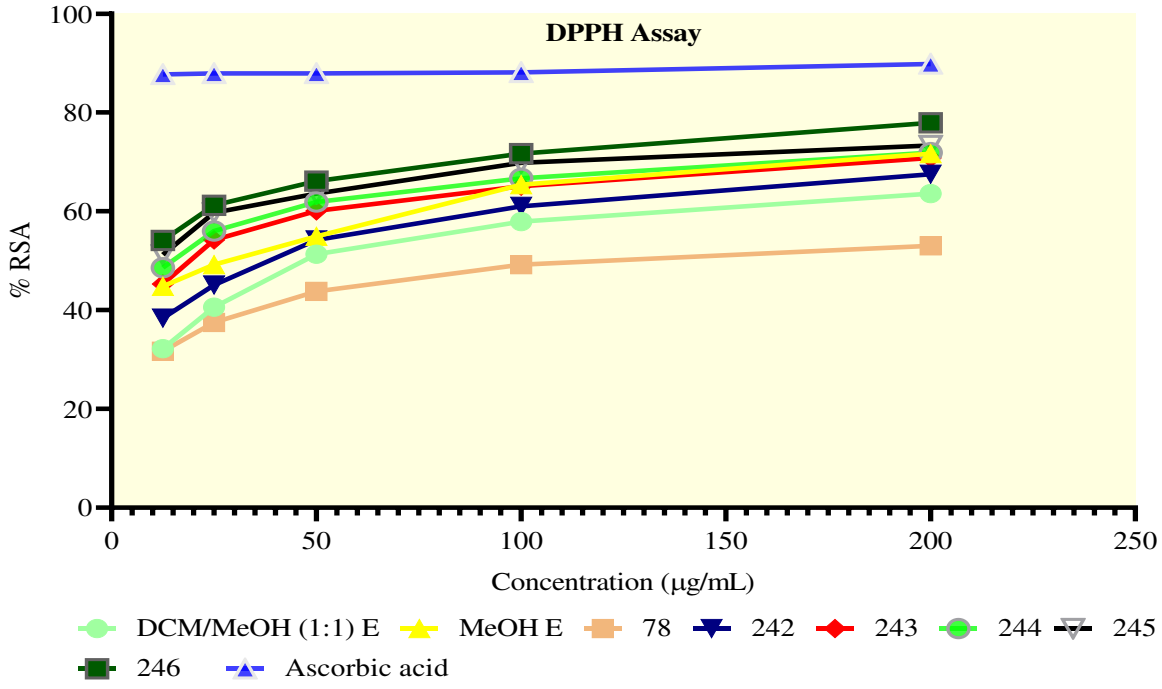

Figure 28: Percentage of DPPH radical scavenging activities of the extracts, and isolated compounds of *J. schimperiana*.

4.3.3.5. Antioxidant activity of the extracts and isolated compounds (**247-253**) from roots of *V. sinaiticum*

In this investigation, radical scavenging activity was carried out on the extracts, and isolated compounds (**247**-**253**) (Table 41, Figure 29). The antioxidant activities of the extracts and isolated compounds were determined by comparison with ascorbic acid. The findings showed the CH_2Cl_2:CH_3OH (1:1), CH_3OH extract, and isolated compounds displayed promising antioxidant activity at a 200 µg/mL concentration. In comparison to the other tested samples, the CH_3OH extract showed the lowest IC_{50} value, suggesting its high scavenging potential. The strongest radical scavenging activity was displayed by the methanol extract (73.8%, IC_{50} =3.4), followed by, compound (**250**) (74.8%, IC_{50} =3.2), compound (**252**) (73.2%, IC_{50} =3.38), compound (**251**) (72.8%, IC_{50} =3.6), compound (**249**) (72.7%, IC_{50} =3.8), compound (**251**) (71.1%, IC_{50} = 4.2), and compound (**248**) (70.7%, IC_{50} =4.7) in comparison with ascorbic acid (89.9%, IC_{50} = 1.3), indicating their strong activity as radical inhibitors. In this report, compound **247** (54.9%) recorded the lowest radical scavenging activity (54.9%) compared to the other compounds.

Table 41: Percent radical scavenging activities of the root extract and isolated compounds (**247-253**) of *V. siniaticum*.

Samples	Concentration (µg/ml)					IC_{50}
	12.5	25	50	100	200	
DCM: MeOH (1:1) Extract	26.6 ± 0.3	38.3 ± 0.5	47.7 ± 0.2	56.1 ± 0.9	67.1 ± 0.8	4.6
MeOH extract	50.2 ± 1.2	57.5 ± 1.0	63.7 ± 0.8	67.1 ± 0.8	73.8 ± 0.6	3.4
247	22.2 ± 0.7	26.1 ± 0.2	35.8 ± 0.2	42.5 ± 0.4	54.9 ± 0.6	11.2
248	54.1 ± 1.0	57.6 ± 0.7	60.3 ± 1.1	65.2 ± 0.8	70.7 ± 0.8	4.7
249	57.2 ± 0.6	59.3 ± 0.4	63.9 ± 0.5	69.3 ± 0.5	72.7 ± 0.3	3.8
250	59.4 ± 1.1	65.1± 0.9	69.7 ± 1.0	71.4 ± 1.4	74.8± 0.8	3.21
251	57.6 ± 0.7	60.7 ± 1.0	63.3 ± 0.9	67.9 ± 0.9	72.8 ± 0.7	3.6
252	56.1 ± 0.9	59.2 ± 0.7	63.8 ± 0.7	68.7 ± 0.6	73.2 ± 0.2	3.38
253	55.8 ± 0.4	58.1 ± 0.6	63.7 ± 0.4	67.4 ± 0.5	71.1 ± 0.7	4.2
Ascorbic acid	84.7 ± 0.1	87.0 ± 0.1	87.9 ± 0.1	88.1 ± 0.2	89.9 ± 0.2	1.3

Samples were reported as Mean ± SEM; Ascorbic acid: a positive control.

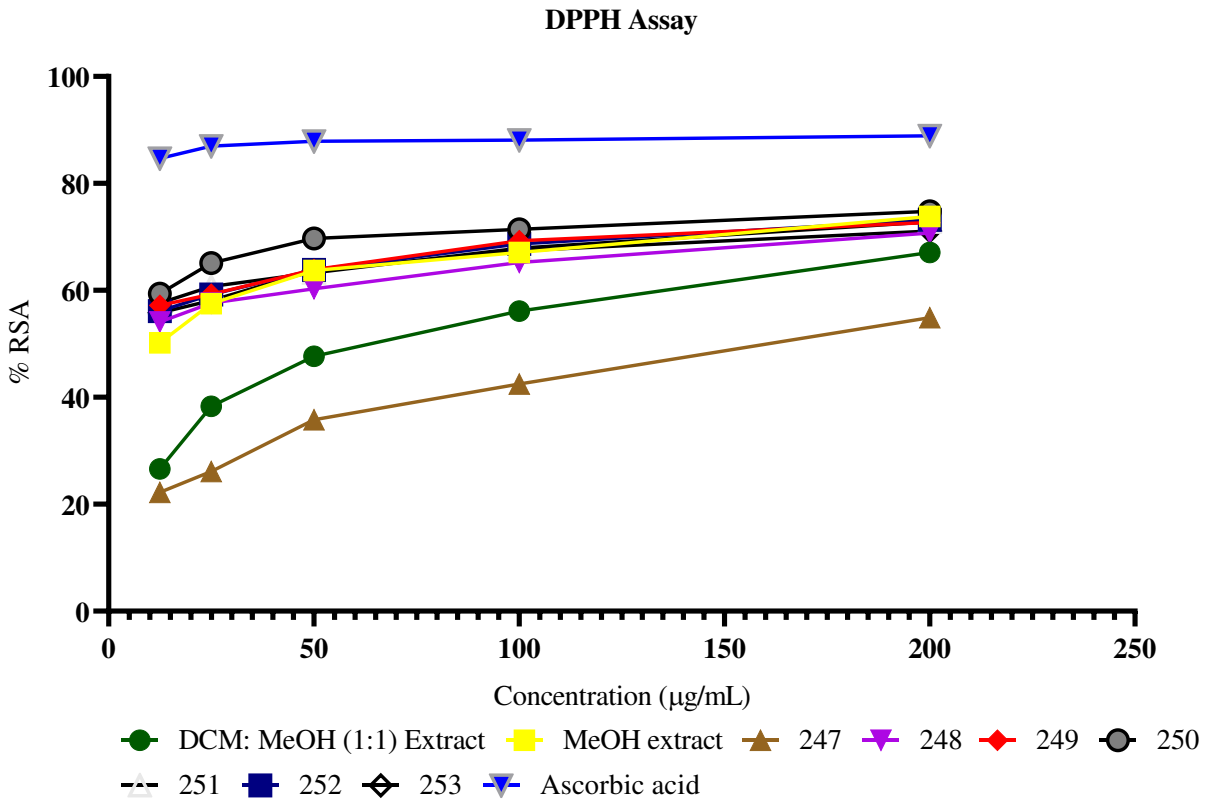

Figure 29: The antioxidant activities of the extract and isolated compounds of *V. siniaticum*.

4.3.4. Inhibition of *α*-amylase by extracts of studied medicinal plants

The present study screened five native antidiabetic medicinal plants for their α-amylase inhibitory potential. It was reported that all of the plant's crude extracts from different solvents exhibited concentration-dependent α-amylase inhibitory action. A total of 13 extracts were screened, and all the extracts showed significant α-amylase inhibitory activity. The IC_{50} values of the extracts were determined (Table 42, Figure 30). The strong inhibitory activity value was recorded by DCM/MeOH (1:1) leaves extract of *J. Schimperiana* (67.1 %) followed by MeOH root extracts of *C. abyssinica* (63.6 %), *C. abyssinicum (*57.7 %*),* and *L. abyssinica* (57.1 %) against the α-amylase enzyme with IC_{50} values of 7.5, 7.8, 8.1, and 8.6 mg/ml, respectively, at a concentration of 10 mg/mL. In addition, the acarbose, the positive control, displayed the highest inhibitory activity (100%) with IC_{50} value 4.4 mg/ml. In all the extracts, the dosage was a factor that affected the inhibition of α-amylase with dichloromethane/methanol (1:1), and methanol root extract of *C. procera*, *L. abyssinica*, and leaves of *J. Schimperiana* having the highest inhibition activity was considered to be mild which is recommended to avoid the side effects

associated with a maximum inhibition of the enzyme. The current study showed that these extracts are potential inhibitors of α-amylase and thus can be used for T2DM (Lebogang *et al*., 2020: Abdel-Hameed *et al*., 2012). The DCM/MeOH (1:1) root extracts *C. abyssinicum, C. abyssinica,* a methanol root extract of *C. abyssinica* showed good α-amylase inhibitory activity of 54.7 % (IC_{50} = 9.1 mg/ml), 55.3 % (IC_{50} = 8.9 mg/ml), 50.0 % (IC_{50} = 9.9 mg/ml), and *n*-hexane leaves extracts of *J. Schimperiana* ((IC_{50} = 9.7 mg/ml) at 10.0 mg/mL, respectively. All the plant extracts have an IC_{50} value that is higher than the positive control acarbose (IC_{50} = 4.4 mg/mL), but this is to be expected. In contrast to acarbose, which is a single compound, plant extracts are composed of several different compounds. Despite being used to control post-prandial hyperglycemia, acarbose has several health side effects (Barakat *et al*., 2020). Thus, of the abovementioned extracts; DCM/MeOH (1:1) and methanol root extract of *C. abyssinicum, C. abyssinica,* methanol root extracts of *C. procera*, and *n*-hexane, and DCM/MeOH (1:1) leaves extract of *J. Schimperiana* exhibited strong that is, ≥ 50 % inhibition against α-amylase enzyme at a concentration of 10 mg/mL. It could thus be speculated that these extracts possess significant α-amylase inhibiting activity.

Table 42: % Inhibition of alpha-amylase assay.

Plant Species	Solvent systems	Inhibitory Concentration (mg/mL)				IC_{50}
		1.25	2.5	5	10	
C. abyssinicum root	DME	4.7 ± 0.2	11.0 ± 0.4	20.5 ± 0.7	54.7 ± 1.3	9.1
	ME	4.4 ± 0.3	10.3 ± 0.4	19.2 ± 1.0	57.7 ± 1.3	8.1
C. procera root	DME	5.9 ± 0.1	13.9 ± 0.3	25.9 ± 0.6	42.7 ± 1.1	12.6
	ME	5.2 ± 0.3	12.1 ± 0.4	22.7 ± 1.2	50.0 ± 1.6	9.9
C. abyssinica root	DME	4.6 ± 1.2	10.8 ± 0.5	20.2 ± 0.6	55.3 ± 2.1	8.9
	ME	3.7 ± 0.1	8.8 ± 0.2	16.5 ± 0.6	63.6 ± 1.2	7.8
J. schimperiana root	DME	6.2 ± 0.1	12.5 ± 0.2	24.8 ± 0.6	49.4 ± 2.1	10.4
	ME	7.8 ± 0.5	15.4 ± 0.7	30.0 ± 1.3	58.4 ± 0.7	8.1
J. schimperiana leaf	nHE	4.9 ± 0.3	11.6 ± 0.5	21.6 ± 1.1	52.3 ± 1.5	9.7
	DME	3.4 ± 0.1	8.0 ± 0.3	14.9 ± 0.6	67.1 ± 1.6	7.5
	ME	5.7 ± 0.4	13.3 ± 0.4	24.9 ± 1.2	44.9 ± 1.4	11.0
L. abyssinica root	DCMME	5.7 ± 0.4	13.3 ± 0.6	25.0 ± 1.6	44.9 ± 2.4	11.4
	ME	4.4 ± 0.2	10.4 ± 0.1	19.4 ± 0.6	57.1 ± 0.8	8.6
Acarbose		14.4 ± 1.2	34.0 ± 1.5	57.0 ± 1.8	100 ± 1.4	4.4

Values are mean ± SEM. Triplicates were done for each sample at different concentrations. DME: Dichloromethane:methanol (1:1) extract; ME: Methanol extract; nHE: *n*-hexane extract: DME: Dichloromethane:methanol (1:1) extract: ME: Methanol extract.

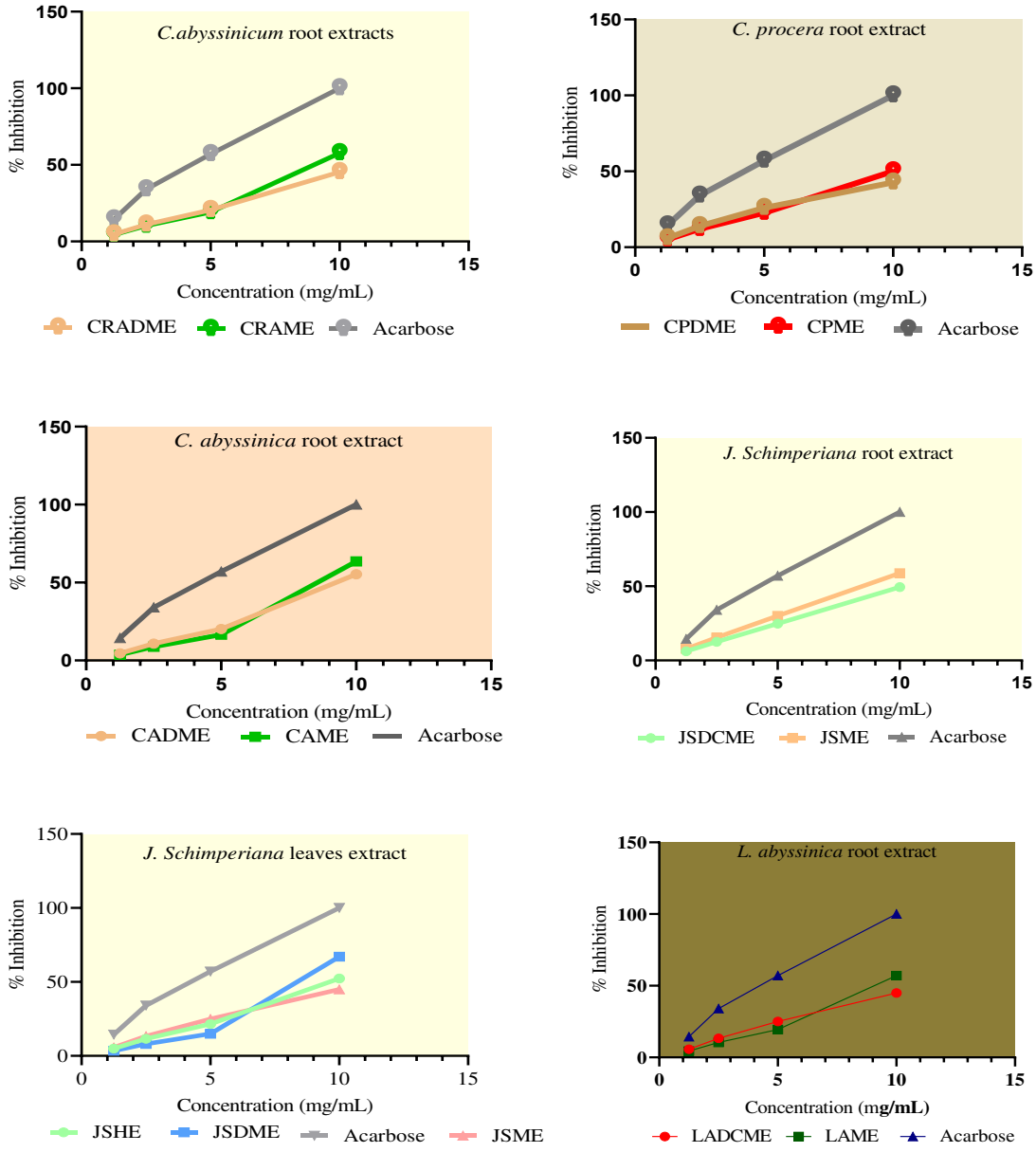

Figure 30: Percentage of α-amylase inhibitory effects of extracts and acarbose (standard drug).

DCM/MeOH (1:1), and methanol root extracts of *C. procera, C. abyssinica, C. abyssinicum, L. abyssinica* and *J. schimperiana*, and *n*-hexane, DCM/MeOH (1:1), and methanol eaves extract of *J. schimperiana*.

4.3.5. Cytotoxicity analysis

MTT assay significantly helps the researchers to determine whether any of the test samples have cell toxicity or proliferative activity (Mosmann, 1983). In the present study, the potential

cytotoxicity of the DCM/MeOH (1:1), and methanol root extracts of *C. procera*, *C. abyssinica, L. abyssinica, C. abyssinicum*, and *n*-hexane, DCM/MeOH (1:1), and methanol leaves extract of *J. schimperiana* were evaluated using MTT assay against MCF-7 breast cancer cell lines at fixed concentrations for an exposure time of 24 h and compared to the control group (Table 43, Figure 31). The MCF-7 cell lines were moderately cytotoxic to the *C. procera* methanol root extract and *J. schimperiana n*-hexane leaves extract, with viability results of 40.3 and 49.0%, respectively. While we found DCM/MeOH (1:1) root extract of *L. abyssinica* (34.4%), methanol leaves extract of *J. schimperiana* (34.8%), DCM/MeOH (1:1) root extract of *C. abyssinicum* (25.2 %), a methanol root extract of *C. abyssinicum* (24.5 %), DCM/MeOH (1:1) root extract of *C. procera* (24.2 %), a methanol root extract of *C. abyssinica* (22.0 %), a methanol root extract of *L. abyssinica* (23.2 %), DCM/MeOH (1:1) leaves extract of *J. schimperiana* (19.0%), and the DCM/MeOH (1:1) root extract of *C. procera* (4.1%) percent viability at the same concentration showed strong cytotoxicity. The American National Cancer Institute (NCI) guidelines set the limit of activity for crude extracts exhibited % cell viability <50% (estimated IC_{50} < 30 µg/mL) after the exposure time of 72 hrs (Abdel-Hameed *et al*., 2012). However, a crude extract with IC_{50} less than 20 µg/mL is considered highly cytotoxic (Mahavorasirikul *et al*., 2010). The tested extracts exhibited cytotoxicity with an estimated IC_{50} < 30 µg/mL, which is acceptable according to the American National Cancer Institute (NCI) criteria of cytotoxic activity for the crude extract. Overall, the experimental result shows that the evaluated extracts exhibited a strong cytotoxicity effect against the MCF-7 cell line.

Table 43: Cytotoxic activities of plant extracts against MCF-7 breast cancer cell line.

Plants extract	% Viability
DCM: MeOH (1:1) root extract of *C. abyssinicum*	25.2 ± 1.2
MeOH root extract of *C. abyssinicum*	24.5 ± 2.1
DCM: MeOH (1:1) root extract of *C. procera*	4.1 ± 1.9
MeOH root extract of *C. procera*	40.3 ± 2.1
DCM: MeOH (1:1) root extract *C. abyssinica*	24.2 ± 1.2
MeOH root extract of *C. abyssinica*	22.0 ± 1.1
n-hexane leave extract of *J. schimperiana*	49.0 ± 3.3
DCM: MeOH (1:1) leave extract of *J. schimperiana*	19.0 ± 1.7
MeOH leaves extract of *J. schimperiana*	34.8 ± 3.2
DCM: MeOH (1:1) root extract of *L. abyssinica*	30.4 ± 1.5
MeOH root extract of *L. abyssinica*	23.2 ± 1.1
Control	100 ± 2.5

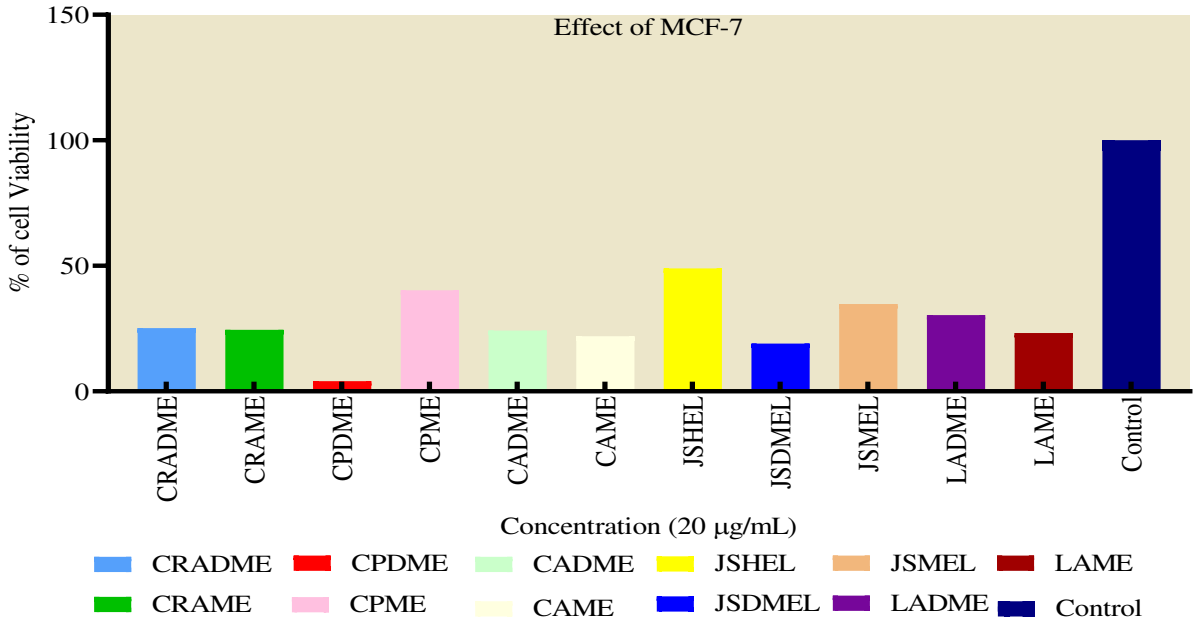

Figure 31: In vitro cytotoxic activity of the extracts and control.

DCM/MeOH (1:1), and methanol root extracts of *C. procera, C. abyssinica, C. abyssinicum, L. abyssinica* and n-hexane, DCM/MeOH (1:1), and methanol leaves extract of *J. schimperiana* on MCF-7 cancer cell lines.

4.3.6. Anti-acanthamoeba activity studies of extracts

The *in-vitro* anti-*acanthamoeba* effects of the CH_2CI_2/CH_3OH (1:1) and methanol extracts of *C. abyssinicum*, *J. schimperiana,* and *V. sinaiticum* have been tested against *Acanthamoeba triaugularis* and *castellanii in-vitro* (Table 44). The result demonstrated that the CH_2CI_2/CH_3OH (1:1) root extract of *V. sinaiticum* showed a promising inhibitory activity (% viability < 10) at 2 mg/mL against *Acanthamoeba castellanii* ATCC50739. Our study, therefore, confirmed for the first time of CH_2CI_2/CH_3OH (1:1) extract from *V. sinaiticum* exhibit anti-*acanthamoeba* activity against *A. castellanii*. However, *C. abyssinicum*, and *J. schimperiana* extracts failed to display anti-acanthamoeba activities against both strains.

Table 44: Screening of anti-*Acanthamoeba* activity of extracts against *A. triaugularis* WU19001 and *A. castellanii* ATCC50739 trophozoites.

Extracts	% viability (Trophozoite)			
	Acanthamoeba triangularis		*Acanthamoeba castellanii*	
	Average	SD	Average	SD
DCMRE of CRA	87.10	0.00	65.12	3.60
MRE of CRA	103.7	5.74	97.37	4.08
DMLE of JS	62.96	5.74	60.53	8.15
MLE of JS	93.55	5.00	60.47	3.60
DCMRE of VS	16.13	5.00	4.65	3.60
MRE of VS	12.90	5.00	41.86	6.24
1% DMSO	96.77	8.66	100.00	3.60
1% MeOH	96.77	8.66	100.00	3.60
1% $CHCl_3$	90.32	5.00	97.67	0.00
Growth control	100.00	0.00	100.00	0.00

SD: standard deviation; CRA; *Crinum abyssinicum*; DCMRE; Dichloromethane: methanol (1:1) root extract; MRE; Methanol root extract, JS; *J. schimperiana*; DCMLE; Dichloromethane: methanol (1:1) leave extract; MLE; Methanol leave extract, VS; *V. sinaiticum*; DCMRE; Dichloromethane: methanol (1:1) root extract.

4.3.7. *In vitro* antiviral activities analysis

In this study, the antiviral potentials of the CH_2CI_2/CH_3OH (1:1) and methanol roots extracts of *C. abyssinicum*, and the leaves extract of *J. schimperiana* (Table 45) were tested against influenza virus A/H1N1 strains. Those demonstrating SI of 10 or higher were deemed to have anti-influenza activity. Findings of this study showed that the CH_2CI_2/CH_3OH (1:1) leaves extract of *J. schimperiana* showed strong activity against influenza A virus.

Table 45: Assessment of cytotoxicity and Anti influenza virus A activity of extracts by MTT assay in MDCK cell line.

Plants extract	CC_{50}, µg/mL	IC_{50}, µg/mL	SI
DCM: MeOH (1:1) leaves extract of *J. schimperiana*	251	13	19
MeOH leaves extract of *J. schimperiana*	>300	>300	1
DCM: MeOH (1:1) root extract of *C. abyssinicum*	1,29	0,8	2
MeOH root extract of *C. abyssinicum*	2,58	2	1

CC_{50}: 50%cytotoxic concentration, IC_{50}: 50%inhibitory concentration; SI: Selectivity index.

4.9. Computational studies of isolated compounds

4.9.1. Molecular docking studies of isolated compounds

During this study, we examined the interactions of twenty-eight (**28**) isolated compounds: **224, 226, 227, 228, 229, 239, 240, 241, 78, 79, 96, 97, 98, 231, 234, 87,** and **243-254.** The selected proteins carried out to study their binding pattern were named: *E. coli* DNA gyrase B (PDB ID:7P2W), *S. aureus* Gyrase (PDB ID: 2XCT), human myeloperoxidase (PDB ID: 1DNU), N-Terminal Domain of PqsA in a complex with 6-Fluoroanthraniloyl-AMP (PDB ID: 5OE3), and human topoisomerase IIα (PDB ID: 4fm9). AutoDock Vina (Trott & Olson, 2010) was used to predict the protein-ligand interactions. The Protein Data Bank (PDB) acquired the protein crystal structures. A more negative value ligand–target complex indicates better binding between the ligand and its target in the AutoDock Vina platform.

Binding mode of analysis of isolated compounds docked against *E. coli* DNA gyrase B (PDB ID:7P2W)

Bacterial DNA gyrase plays a vital role during the investigation of antibacterial agents, as it breaks double-stranded DNA by catalyzing negative supercoiling, which is essential for DNA replication, transcription, and recombination (Lal *et al*., 2013). The analysis of the interaction patterns revealed that the designed candidates were stabilized in the DNA gyrase active site by both hydrogen bonds and hydrophobic interactions. In the present study, the molecular docking analysis of the isolated compounds was carried out to investigate their binding pattern with bacterial gyrase, and the results were compared with the standard antibacterial agent amoxicillin and ascorbic acid**.** The binding energy values of all the ligands against the crystal structure (PDB ID:7P2W) are presented (Appendix 41A and Figure 32).

The molecular docking analysis of the isolated compounds was carried out in the present study to explore their binding pattern with DNA gyrase B and compared with a standard clinical drug (amoxicillin, and ciprofloxacin). The isolated compounds (**224, 226, 227, 228, 229, 239, 240, 241, 78, 79, 96, 97, 98, 231, 234, 87, 243, 244, 245, 246, 247, 248, 249, 253, and 254)** were found to have minimum binding energy ranging from -5.0 to–8.9 kcal/mol (Appendix 41A). Isolated compounds **227** (-6.0 kcal/mol)**, 96** (-6.7 kcal/mol)**, 240** (-6.5 kcal/mol)**, 241** (-6.1 kcal/mol), **243** (-6.3 kcal/mol), **245** (-6.7 kcal/mol), **247** (-6.4 kcal/mol)**,** and **248** (-6.9 kcal/mol) have a moderate binding affinity for target proteins *E. coli* DNA gyrase B when compared with the standard clinical drug amoxicillin (- 7.6 kcal/mol), and ciprofloxacin (-6.7 kcal/mol).

Compounds (**79**) (- 7.5 kcal/mol), **234** (- 7.6 kcal/mol), and **253** (-7.3 kcal/mol) exhibited comparable and compounds **249** (-7.9 kcal/mol)**, 224** (- 8.9 kcal/mol), **226** (- 7.8 kcal/mol), **78** (- 8.7 kcal/mol), **97** (- 8.0 kcal/mol), 9**8** (- 8.6 kcal/mol), **87** (- 8.2 kcal/mol), **246** (-8.1 kcal/mol), and **254** (- 8.6 kcal/mol) have shown better binding affinity to DNA gyrase as compared with amoxicillin (- 7.6 kcal/mol) the standard drug. Compound **234** (–7.6 kcal/mol) shows equivalent binding affinity with amoxicillin. Compounds **224**, **228, 239, 78**, **96, 98, 231,** and **87** interacted with the binding pocket by forming one H-bonds with Gly-77, Arg-76, Arg-76, Asp-73, Asn-46, Thr-165, Asn-46, and His-83, respectively, and compounds **240, 224,** and **243** interacted with the binding pocket by forming three H-bonds, whereas compounds **227, 234, 241, 79,** and **254** interact with the binding pocket by forming two H-bonds. The docking results (high negative binding affinity) agree with the *in vitro* antibacterial results of isolated compounds against *E. coli*. However, compounds **229**, and **97** do not form a hydrogen bond with an amino acid within the binding pocket. The binding affinity of each compound with individual targets with the number of hydrogen bond interactions and residues is summarized in Appendix 41A. The interaction of isolated compounds with DNA gyrase was presented in Figure 32. The Hydrogen bond between isolated compounds and amino acids are shown as green dash lines, hydrophobic interactions are shown as pink lines.

Binding mode of analysis of isolated compounds docked against *S. aureus* Gyrase (PDB ID: 2XCT).

In this study, molecular docking interactions of the isolated compounds (**224, 226, 239, 240, 241, 78, 79, 97, 98, 234, 87, and 254**) against *S. aureus* Gyrase (PDB ID: 2XCT) were studied and compared with amoxicillin used as a standard drug. The isolated compounds were found to have minimum binding energy ranging from -5.6 to–10.1 kcal/mol. Based on the results of molecular docking, compounds **226** (- 9.6 kcal/mol), **98** (- 9.8 kcal/mol), **234** (**-**9.4 kcal/mol), **87** (**-**9.8 kcal/mol), and have shown comparable binding interactions and docking scores with the standard amoxicillin (**-**10.0 kcal/mol). In contrast, compound **97** (**-**10.1 kcal/mol) shows better binding affinity within the binding pockets of *S. aureus* Gyrase. However, compounds **79** (**-**7.9 kcal/mol), **224** (**-**7.5 kcal/mol), **78** (**-**7.0 kcal/mol), and **254** (**-**7.9 kcal/mol) have a moderate binding affinity for target proteins *S. aureus* Gyrase when compared with the standard clinical drug amoxicillin (-10.0 kcal/mol). Hence, these compounds might potentially be promising antibacterial agents, and the *in-silico* results are in good agreement with *in vitro*. Compounds **239**, **240**, and **241** scored

the lowest binding energy of -5.8, 6.0, and 5.6 kcal/mol, respectively, compared to amoxicillin. The binding affinity, H-bond, and residual interaction of isolated compounds (**224, 226, 239, 240, 241, 78, 79, 97, 98, 234, 87,** and **254**) and reference drug amoxicillin were summarized in (Appendix 41D and Figure 35)**.**

Binding mode of analysis of isolated compounds docked against human myeloperoxidase (PDB ID: 1DNU)

Myeloperoxidase (MPO) is a peroxidase enzyme (EC 1.11.1.7) and the most prevalent heme protein for destroying pathogens in neutrophils (Klefanoff, 2005). This enzyme has two functions: peroxidase and halogenation, which can work together or independently (Malle *et al*., 2007). The molecular docking analysis of compounds **239, 240, 241, 79, 97, 234, 87, 245, 246,** and **248-253** were carried out to investigate their binding pattern with Human Myeloperoxidase (PDB ID: 1DNU) and compared with the standard amoxicillin and ascorbic acid. The isolated compounds **239, 240, 241, 79, 97, 234, 87, 245, 246** and **248-253** were found to have minimum binding energy ranging from -4.3 to -10.8 kcal/mol (Appendix 41B). Based on the result of molecular docking analysis, the highest binding energy value has been performed by compounds **79** (-8.2 kcal/mol), **97** (-10.3 kcal/mol), **234** (-10.1 kcal/mol), **87** (-10.8 kcal/mol), **245** (-8.8 kcal/mol), **246** (-10.1 kcal/mol), **248** (-10.3 kcal/mol)**, 249** (-9.2 kcal/mol), **250** (-9.4 kcal/mol), **251** (-9.6 kcal/mol), **252** (-9.5 kcal/mol), and **253** (-9.2 kcal/mol) compared with the standard drugs amoxicillin (-9.2 kcal/mol) and ascorbic acid (-8.1 kcal/mol). Therefore, these compounds might have potential antioxidant agents. The *in-silico* results are in good agreement with the *in vitro* analysis. In the present study, compound **79** showed a binding energy value of - 8.2 kcal/mol similar to ciprofloxacin's binding energy value. The binding affinity, H-bond, and residual interaction of all the isolated compounds are summarized in (Appendix 41B and Figure 33)**.**

Molecular docking binding analysis of isolated compounds docked against human topoisomerase IIα (PDB ID: 4fm9)

Nuclear enzymes called DNA topoisomerases catalyze the addition of topological modifications to the DNA molecule (Nitiss, 2009). Type II topoisomerase known as human topoisomerase II (topo II) has been demonstrated to be a useful target in the treatment of a variety of cancers (Nitiss, 2009). The molecular docking analysis of the isolated compounds (**224, 226, 228, 229, 232, 78, 239, 240, 241, 79, 97, 234, 87, 98,** and **248-254**) was carried out to investigate their

binding pattern with human Topoisomerase IIα (PDB ID: 4fm9) and compared with the vosaroxin and Revlimid. Results obtained from the molecular docking study demonstrated that isolated compounds were found to have minimum binding energy ranging from -4.5 to -9.9 kcal/mol (Appendix 41C). Compared with Vosaroxin (**-**7.2 kcal/mol), and Revlimid (**-**7.4 kcal/mol), isolated compounds **97** (- 9.9 kcal/mol), **234** (- 9.1 kcal/mol), **224** (- 8.5 kcal/mol), **79** (- 8.3 kcal/mol), **87** (- 8.2 kcal/mol), **226** (- 7.4 kcal/mol), **78** (- 7.7 kcal/mol), 9**8** (- 9.1 kcal/mol), **248** (-8.8 kcal/mol), **249** (9.4 kcal/mol), **250** (-9.2 kcal/mol), **251** (-8.6 kcal/mol), **252** (-8.8 kcal/mol), **253** (-8.3 kcal/mol) and **254** (- 7.8 kcal/mol) have shown high binding affinity. Compounds **228** (-6.8 kcal/mol), and **232** (-6.5 kcal/mol) displayed comparable binding affinity values with the standard vosaroxin (- 7.2 kcal/mol), while the modérate binding score for the target protein topoisomerase II α showed by **234** (–6.1 kcal/mol), and **229** (–5.5 kcal/mol). However, compounds **240** (5.1 kcal/mol), and **241** (4.5 kcal/mol) showed the lowest binding score for the target protein topoisomerase IIα. Compound **229** does not form a hydrogen bond with an amino acid within the binding pocket. The binding affinity, H-bond, and residual interaction of compounds and the standard vosaroxin and Revlimid are summarized in (Appendix 41C, Figure 34).

Binding mode of analysis of isolated compounds docked against N-Terminal Domain of PqsA in a complex with 6-Fluoroanthraniloyl-AMP (PDB ID: 5OE3).

The isolated compounds **224, 226, 239, 240, 241, 78, 79, 97, 98, 234, 87, 243, 244, 245, 246, and 254** were docked towards the N-Terminal Domain of PqsA in a Complex with 6-Fluoroanthraniloyl-AMP (PDB ID 5OE3) receptor to determine their binding affinity, and the results were compared to amoxicillin. The minimum binding energies of the isolated compounds **224, 226, 239, 240, 241, 78, 79, 97, 98, 234, 87, 243, 244, 245, 246**, and **254** in the binding pocket of the N-terminal domain of PqsA ranging from -5.1 to -11.0 kcal/mol. Compounds **226** (- 8.5 kcal/mol), 9**8** (- 10.4 kcal/mol), **254** (- 8.2 kcal/mol), **79 (**-8.5 kcal/mol), **97** (-10.2 kcal/mol), **234** (-11.0 kcal/mol), **87** (-9.9 kcal/mol), **244** (-8.6 kcal/mol), **245** (-9.2 kcal/mol), and **246** (-10.4 kcal/mol) have high binding interactions against N-Terminal Domain of PqsA compared with amoxicillin (-8.1 Kcal/mol). Whereas, **224** (- 8.0 kcal/mol), **98** (- 7.9 kcal/mol), and **243** (-7.0 kcal/mol) have shown comparable binding interactions and docking scores with the standard amoxicillin (**-**8.1 kcal/mol). The result showed that the compounds are promising antibacterial agents against *P. aeruginosa*. The *in-silico* results are in good agreement with *in*

vitro results. The binding energy for **239**, **240**, and **241** was found to be -6.4, 5.4, and 5.1 kcal/mol, respectively. The binding affinity, H-bond, and residual interaction of all the isolated compounds are summarized in (Appendix 41E and Figure 36).

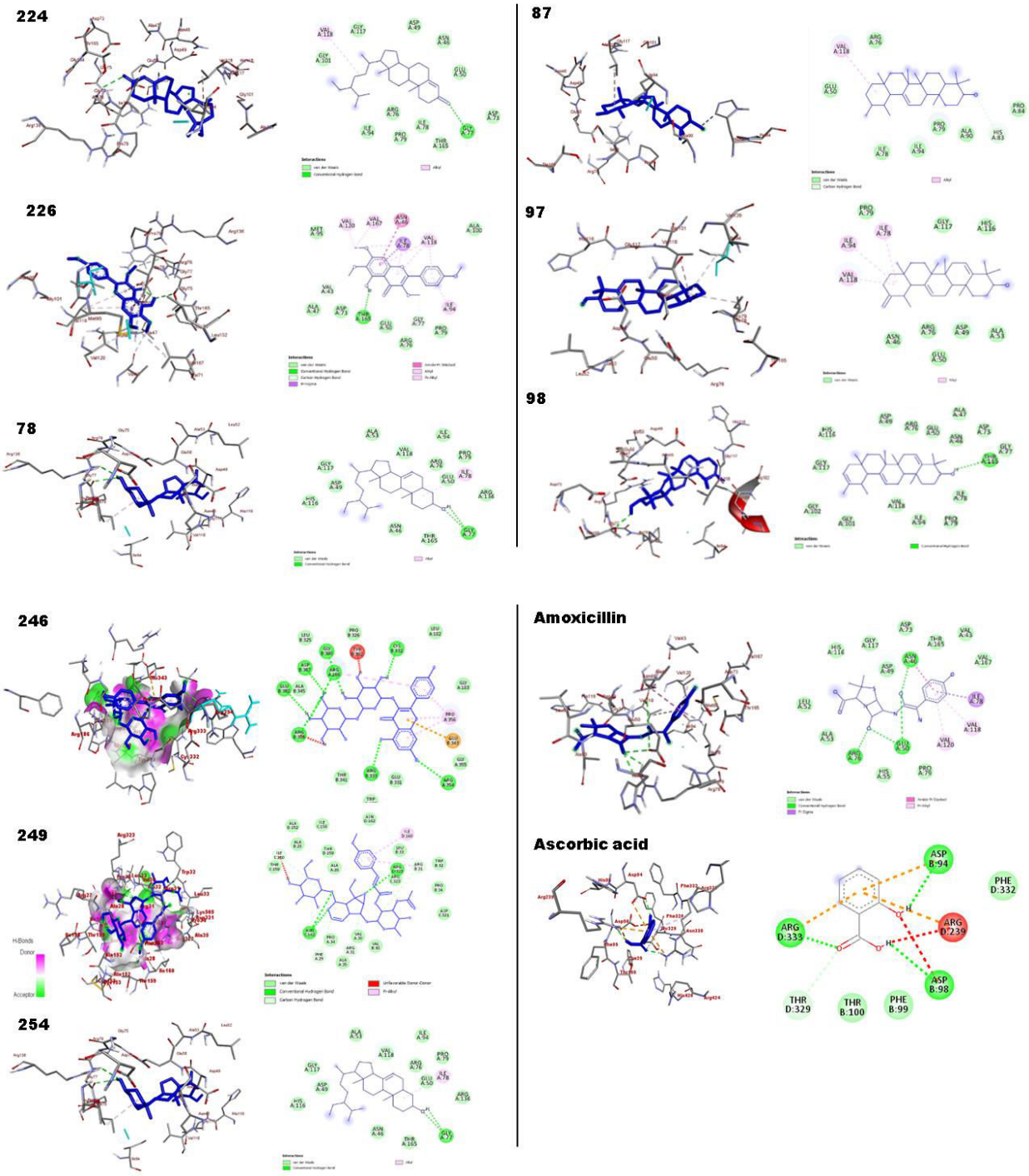

Figure 32: The 2D and 3D binding interactions of isolated compounds and standard drug amoxicillin, and ciprofloxacin against *E. coli* Gyrase B (PDB ID: 7P2W).

79

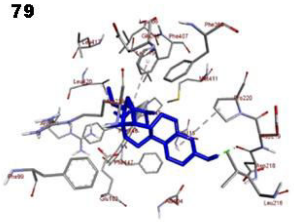

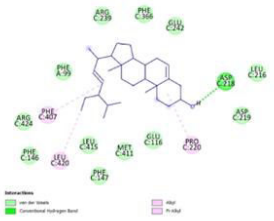

97

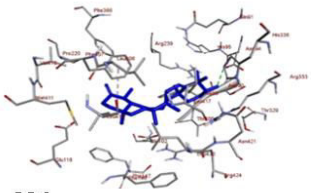

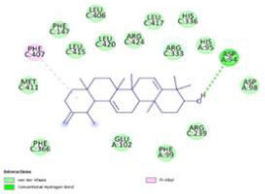

234

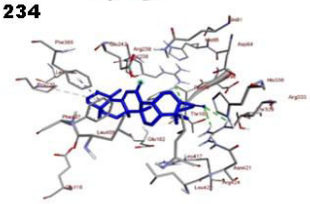

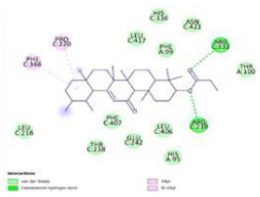

87

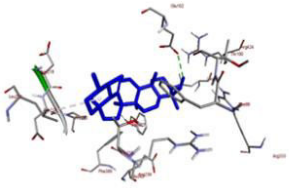

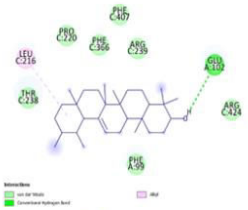

245

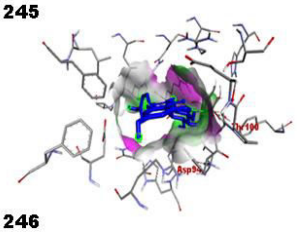

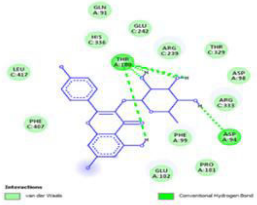

246

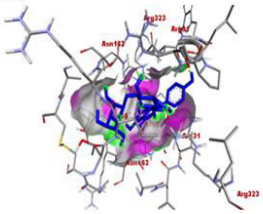

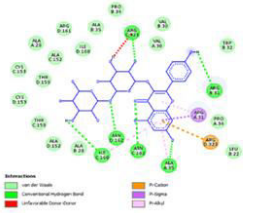

248

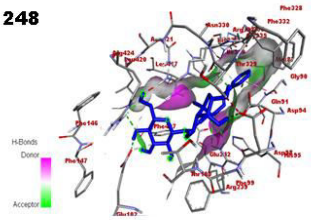

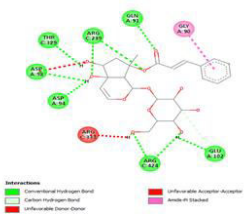

249

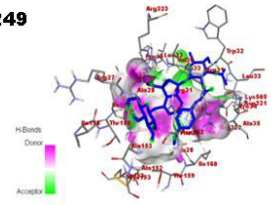

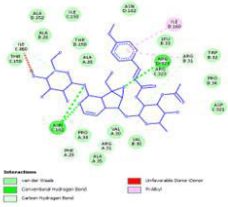

250

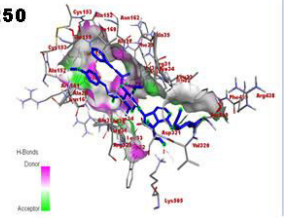

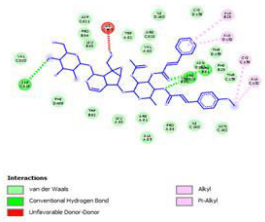

251

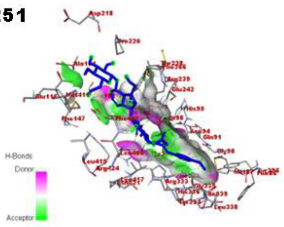

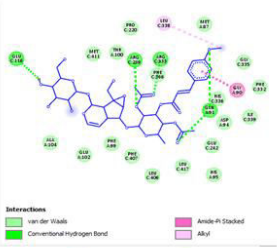

252

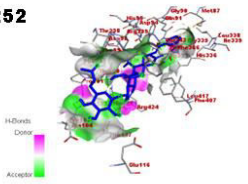

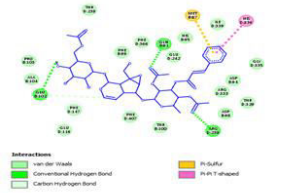

253

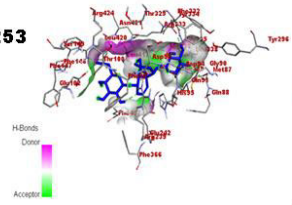

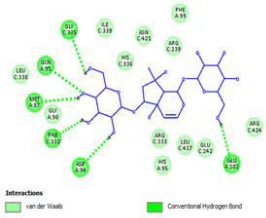

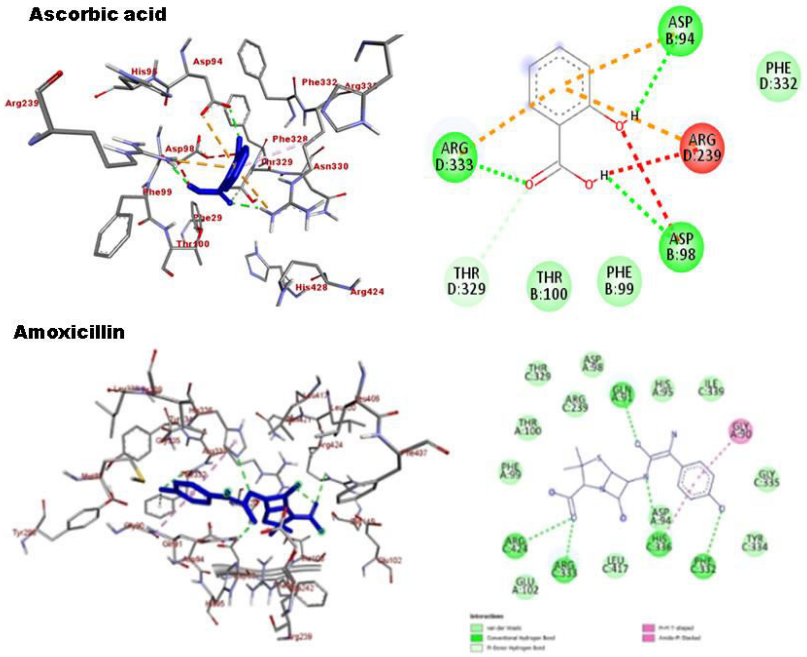

Figure 33: The 2D and 3D binding interactions of isolated compounds (and standard drug amoxicillin and ascorbic acid against human myeloperoxidase (PDB ID: 1DNU).

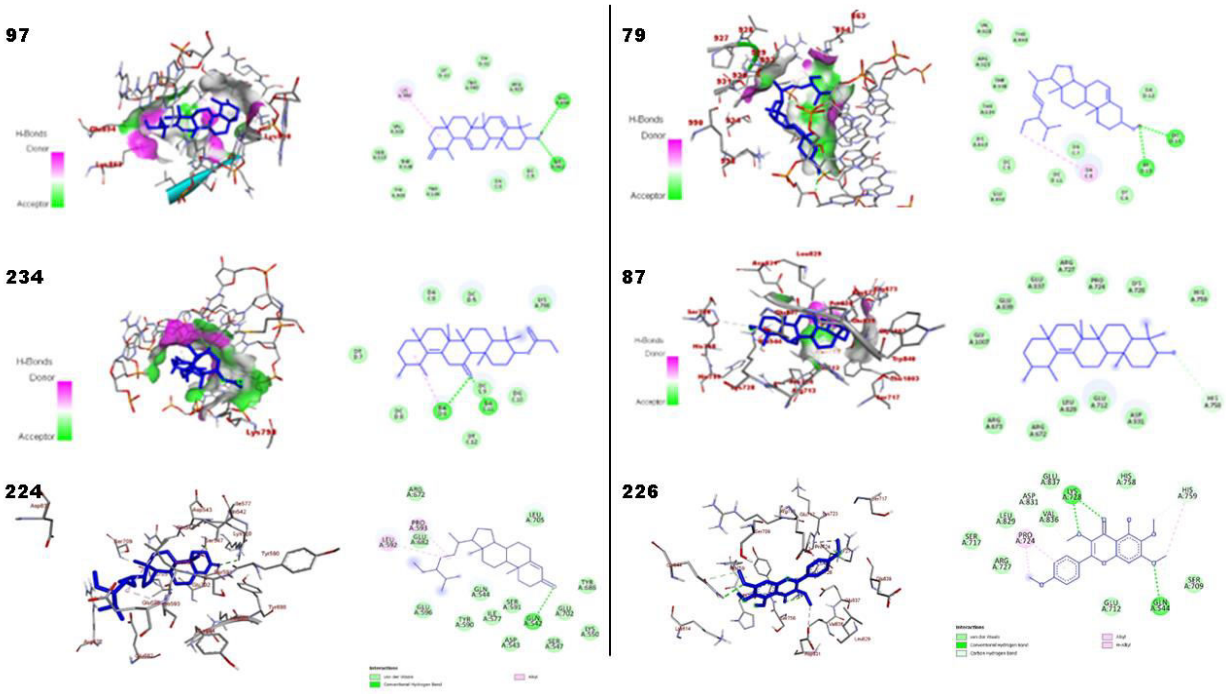

78

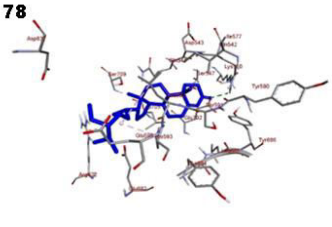

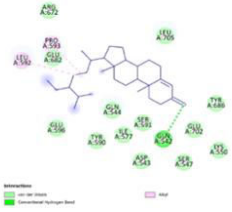

98

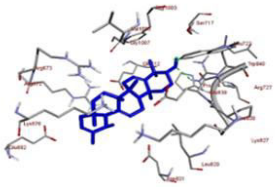

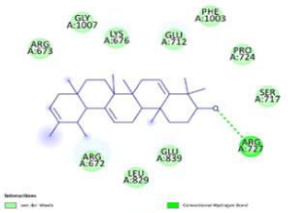

248

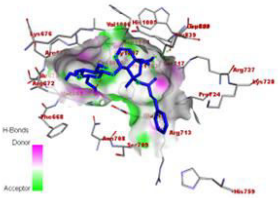

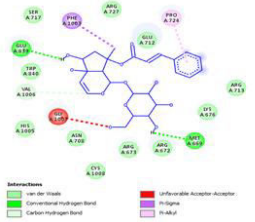

249

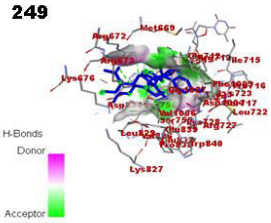

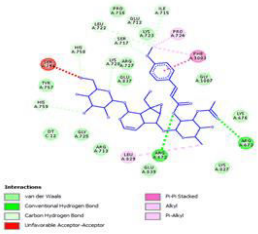

250

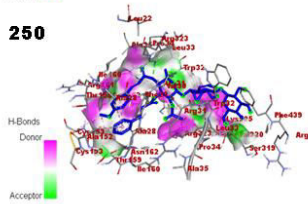

251

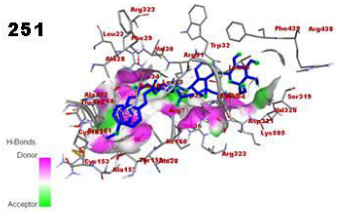

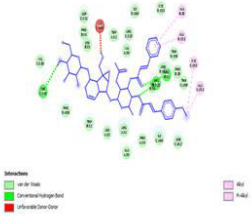

252

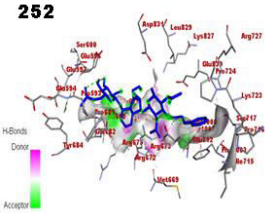

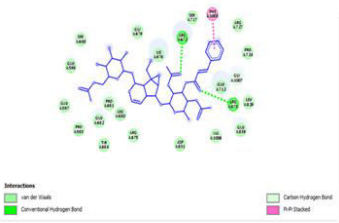

253

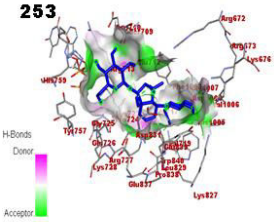

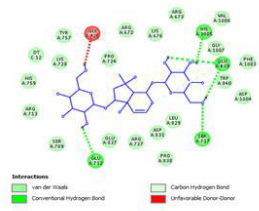

254

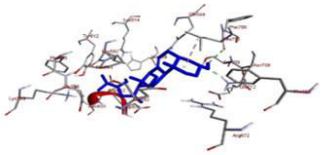

Vosaroxin

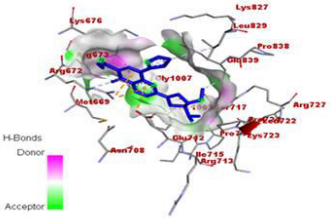

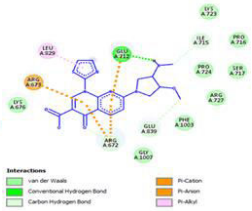

Revlimid

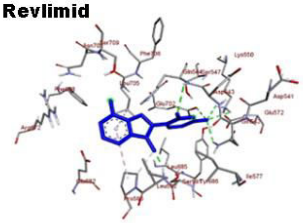

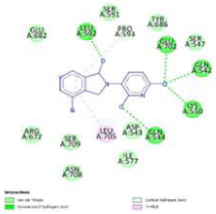

Figure 34: The 2D and 3D binding interactions of isolated compounds and standard vosaroxin, and revlimid against human topoisomerase IIα (PDB ID: 4fm9).

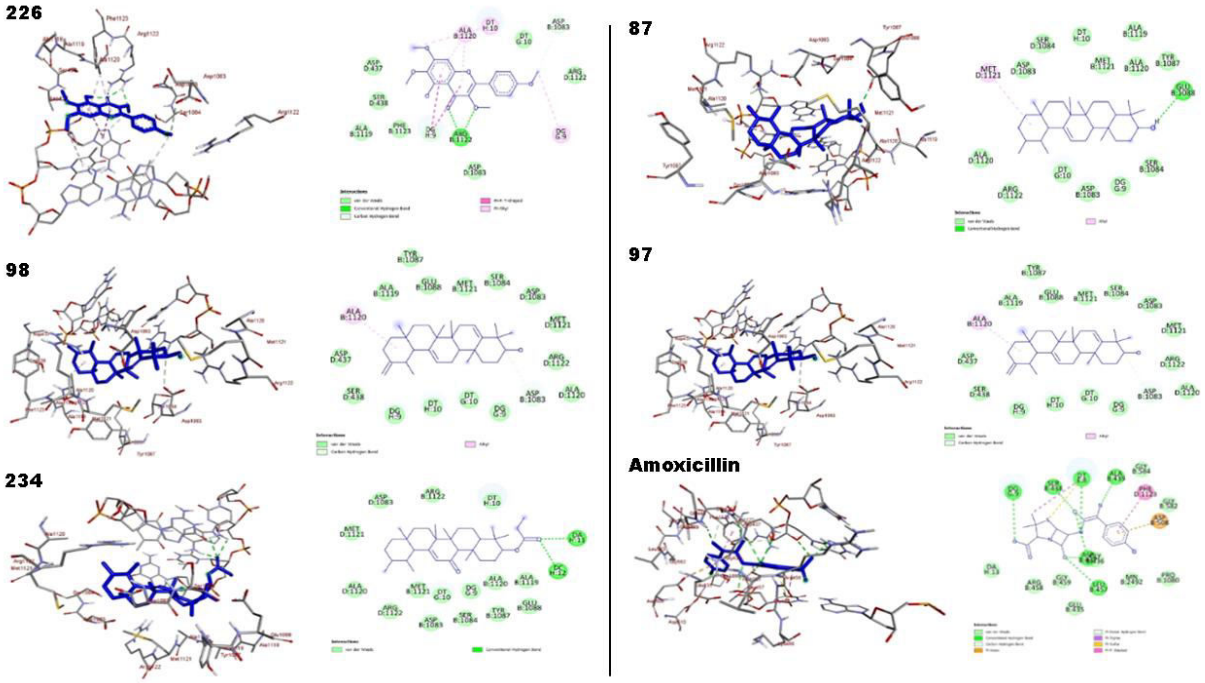

Figure 35: The 2D and 3D binding interactions of isolated compounds and standard drug amoxicillin against *S. aureus* Gyrase (PDB ID: 2XCT).

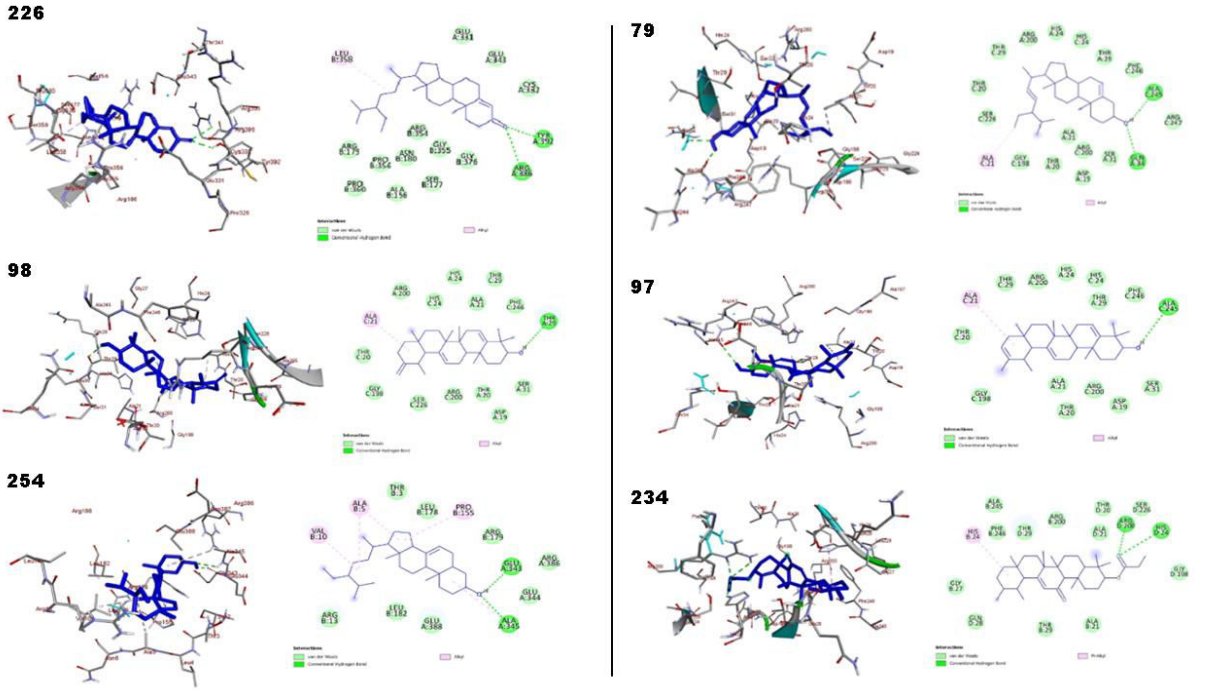

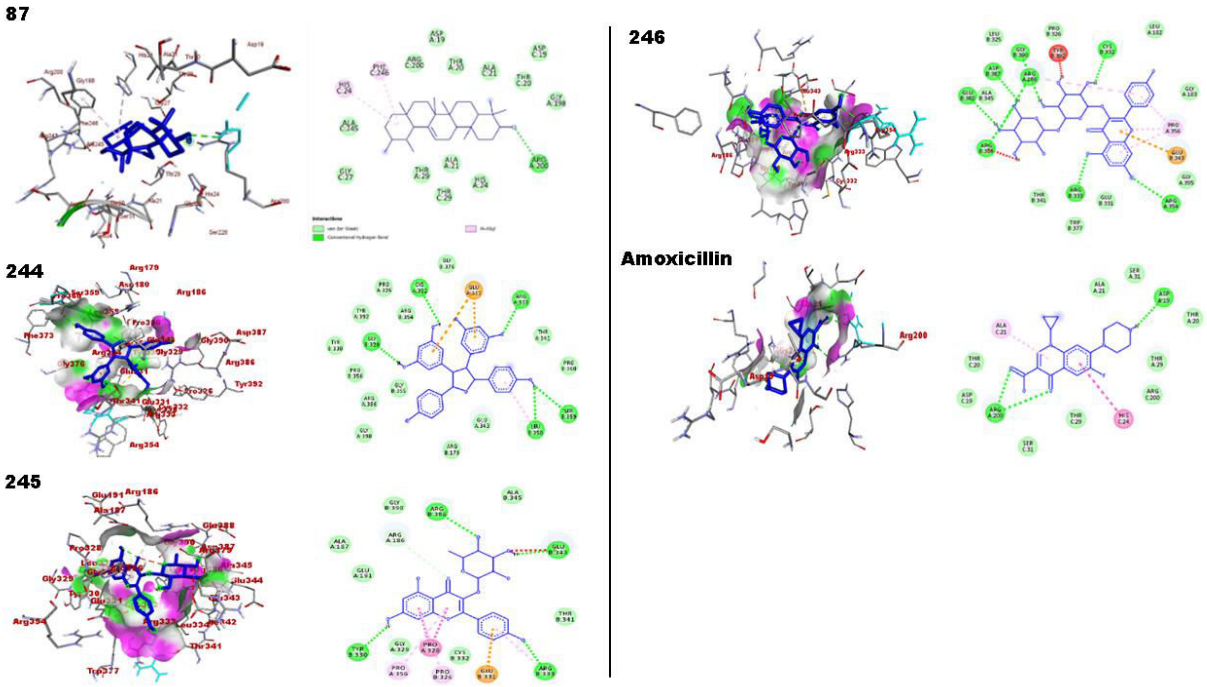

Figure 36: The 2D and 3D binding interactions of isolated compounds standard drug amoxicillin against (PDB ID: 5OE3).

4.9.2. *In silico* pharmacokinetics (ADME) properties of isolated compounds

Physicochemical properties, drug-likeness, boiled-egg model, and pharmacokinetic properties (ADME) of compounds **224**, **226**, **227**, **229**, **96**, **78**, **87**, **231**, **232**, **97**, **234**, **98**, **238**, **239**, **240, 241**, **79, 242, 243, 244, 245, 246, 247, 248, 249, 250, 251, 252,** and **253** were determined using the SwissADME Web tool or PreADMET online server (Daina *et al*., 2017). The percent absorption (% Abs) of the was calculated using the formula % Abs =109 – 0.345 TPSA (Remko, 2009). The toxicity profile of the compounds was predicted using the PreADMET and Protox-II protocols (Banerjee *et al*., 2018). Drug-likeness is a prediction that screens whether a particular organic molecule has properties consistent with being an orally active drug (Lipinski *et al*., 1997).

The drug-likeness of the isolated compounds was characterized according to "Lipinski's rule." In the present study, among the tested compounds, compounds **226**, **227**, **231**, **238**, **241, 242,** and **243** obeyed Lipinski's rule of five with zero violations and is likely to be orally active. Low molecular weight (MW) signifies that the molecules are light and can easily pass through the cell membrane. Low molecular weight (MW< 500) chemicals are favored for oral absorption,

(Lipinski *et al*., 2001) whereas compounds with MW > 500 Da are absorbed via an alternate route, generally the membrane (Refsgaard *et al*., 2005). The present study revealed that all of the molecular weights of the studied (Table 46) compounds except **246, 249, 250, 251, 252,** and **253** were less than 500 Da. The TPSA value of all the studied compounds was noticed in the range of 17.07–249.2 Å2. This indicates that except for compounds **245, 246, 248, 249, 250, 251, 252,** and **253** the results are less than 140 Å2, indicating that intestinal absorption is good and if limits are beyond the score, then the drug does not possess passive cellular permeability (Turner *et al*., 2004). The optimal good bioavailability range of lipophilicity (log P) is between 0 and 3, which refers to the state of a good balance between solubility and permeability. The distribution coefficients (logP) of the isolated compounds (Table 46) were in the range of 0.0 to 5.2. Except for compounds **228**, **238, 243, 244, 245, 246, 247, 249, 250,** and **252** the log(P) of all isolated compounds was found to be greater than three as predicted in (Table 50) which might be due to the small number of hydroxyl groups present in all compounds. Compounds that meet these criteria have been shown to have better pharmacokinetics and bioavailability characteristics. Except for compounds **226, 242, 244, 245, 246, 248, 249, 250, 251, 252,** and **253** the % Abs analysis of the isolated compounds (Table 46) showed that all the isolated compounds have the highest percent absorption than the control. All isolated compounds, except **246**, **248**, **249, 250, 251, 252,** and **253** have a higher bioavailability score of 0.55 and were appropriate for oral administration, indicating drug-like qualities (Martin, 2005). The ability of molecules to penetrate the outer layer of the skin is described by skin permeability (Kp). Except for compounds **246**, **248**, **249, 250, 251, 252,** and **253,** the developed compounds' log Kp values (Table 47) were all determined to be within the permissible range of - 8.0 to - 1.0 (Gaur *et al*., 2015). The SwissADME prediction parameters have shown that the GIA exhibits isolated compounds **226**, **227**, **231**, **238**, **240**, **241, 242**, and **243** that have good oral absorption. The results of the BBB permeability test performed on studied compounds (Table 47) demonstrated that except for compounds **227**, **231, 238, 241,** and **243** the rest lack BBB permeability. The P-gp affects the absorption, distribution, and clearance of a variety of substances. As a result, identifying permeability glycoprotein substrates is critical for identifying prospective medicines and optimizing them. The results show that except for compounds **227, 242, 245, 246, 250, 251, 252, 253,** and clinical drugs, no compounds were substrates of permeability glycoprotein (P-gp). Inhibitory drug metabolism fails when CYP enzymes are inhibited. Knowledge about the

interaction of molecules with cytochromes (CYP) P450 enzymes is essential for the liver's drug metabolism. The study results showed that isolated compounds **227, 229, 231, 240, 241,** and **243** showed inhibitory activity against CYP1A2, compounds **226**, **227**, **232**, **239**, **240**, and **79** showed inhibitory activity against CYP2C9, whereas, compounds **227**, and **242** showed inhibitory activity against CYP2C19, and compounds **227**, **231,** and **252** showed activities against CYP2D6. Compounds **239, 243, 242, 244,** and **247** showed inhibitory activity against CYP3A4.

4.9.3. *In silico* toxicity prediction of isolated compounds

The organ toxicity (hepatotoxicity) and toxicological endpoints (carcinogenicity, immunotoxicity, mutagenicity, and cytotoxicity) of the isolated compounds and their toxicity class and LD_{50} were predicted using Pro Tox II server (Table 48). Toxicological endpoints prediction analysis indicated median lethal dose (LD50) values ranging from 48–70000 mg/Kg. Compounds **229, 96, 234, 239,** and **245** were predicted to be carcinogenic. Compounds **224**, **226**, **96, 78, 87, 232, 97, 234, 98, 79, 242, 245, 246, 248, 249, 250, 251, 252,** and **253** were predicted to be immunotoxic. However, all the tested isolated compounds have shown non-hepatotoxicity and non-mutagenicity. Whereas except for compound **232,** all compounds were predicted to be non-cytotoxic.

The BOILED-Egg model allowed for the correlation between the prediction of gastrointestinal (GI) absorption and blood-brain barrier (BBB) penetration with the alignment between lipophilicity (WlogP) and polarity (TPSA) properties (Daina *et al*., 2017). The BOILED-Egg (Figure 37) prediction model showed that compounds **240,** and **226** were predicted as passively absorbed but not accessing the brain (in the white) and PGP– (red dot), whereas, compounds **227**, and **242** were predicted as brain-penetrant (in the yolk) and actively effluxed (blue dot). Compounds **229, 239, 78, 224, 244**, **245, 247,** and **248** were predicted as not absorbed and not brain penetrant (outside the Egg). Compounds **231, 238, 241**, and **243** were predicted as brain-penetrant (in the yolk) and not subject to active efflux (red dot). Compounds **96, 87, 232, 97, 98, 79**, **246,** and **249-253** were predicted as not absorbed and not BBB permeant because outside of the range of the plot.

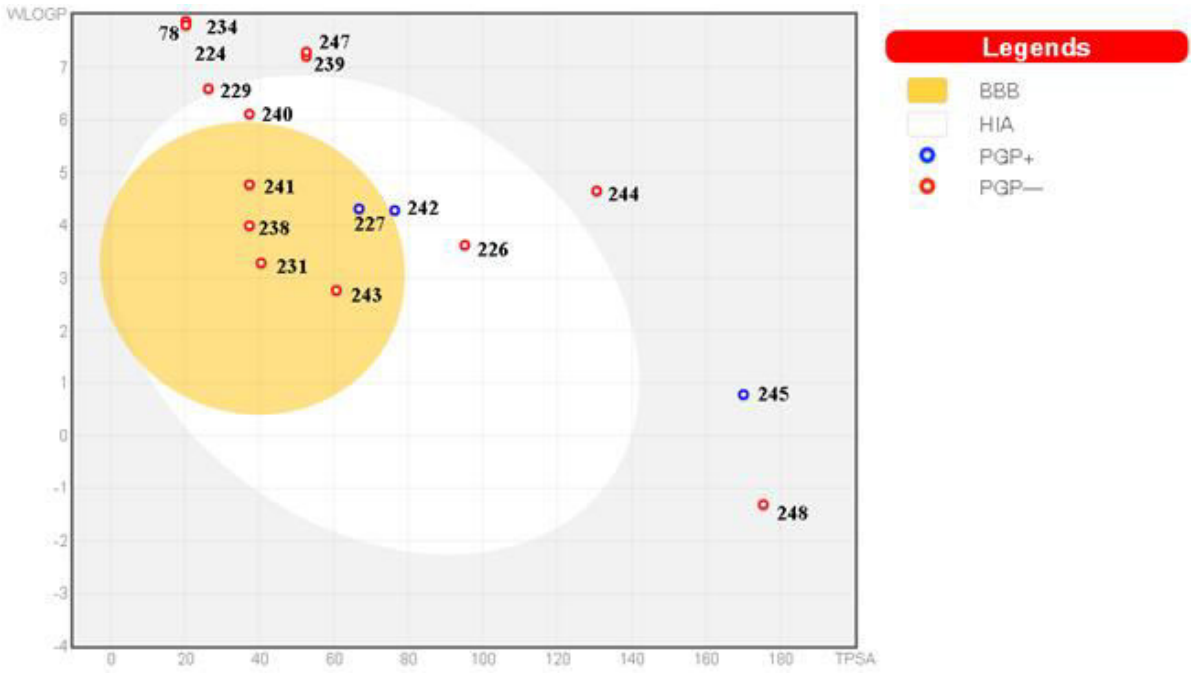

Figure 37: BOILED-Egg model for predicting gastrointestinal absorption and brain access.

The white region was for a high probability of passive absorption by the gastrointestinal tract, and the yellow region (yolk) was for a high probability of brain penetration. Yolk and white areas were not mutually exclusive. In addition, the points were colored in blue if predicted was actively effluxed by P-gp (PGP+) and in red if predicted was as a non-substrate of P-gp (PGP−).

Table 46: Parameters of *in silico* bioavailability prediction and physicochemical properties of isolated compounds.

Compounds	Formula	MW	NRBs	NHBAs	NHBDs	MR	TPSA	%Absn	iLOGP	Lipinski rule of 5	Bioavailability score
224	$C_{29}H_{48}O$	412.7	6	1	0	132.27	17.07	103.1	4.69	1	0.55
226	$C_{19}H_{18}O_7$	358.3	5	7	1	94.54	95.2	76.2	0	0	0.55
227	$C_{20}H_{36}O_4$	340.5	17	4	2	100.91	66.76	86.0	4.76	0	0.55
229	$C_{20}H_{38}O_2$	310.5	17	2	0	99.06	26.3	99.9	5.03	1	0.55
96	$C_{32}H_{48}O_2$	464.7	2	2	0	143.93	26.3	99.9	4.79	1	0.55
78	$C_{29}H_{50}O$	414.7	6	1	1	133.23	20.23	102.0	4.79	1	0.55
87	$C_{30}H_{50}O$	426.7	0	1	1	135.14	20.23	102.0	4.77	1	0.55
231	$C_{14}H_{28}O_2$	228.4	11	2	2	71.26	40.46	95.0	3.36	0	0.55
232	$C_{31}H_{50}O_2$	454.7	7	2	0	142.49	26.3	99.9	5.2	1	0.55
97	$C_{30}H_{46}O$	422.7	0	1	1	134.19	20.23	102.0	4.66	1	0.55
234	$C_{33}H_{52}O_3$	496.8	3	3	0	149.89	43.37	94.0	5	1	0.55
98	$C_{30}H_{46}O$	422.7	0	1	1	134.19	20.23	102.0	4.62	1	0.55
238	$C_{12}H_{24}O_2$	200.3	10	2	1	61.57	37.3	96.1	2.7	0	0.85
239	$C_{26}H_{42}O_4$	418.6	18	4	0	125.91	52.6	90.9	5.23	1	0.55
240	$C_{18}H_{34}O_2$	282.5	15	2	1	89.94	37.3	96.1	4.01	1	0.85
241	$C_{14}H_{28}O_2$	228.4	12	2	1	71.18	37.3	96.1	3.32	0	0.85
79	$C_{29}H_{48}O$	412.7	5	1	1	132.75	20.23	102.0	5.01	1	0.55
242	$C_{23}H_{20}O_7$	408.4	3	7	0	111.09	76.36	82.7	4	0	0.55
243	$C_{14}H_{12}O_3$	228.2	2	3	3	67.88	60.69	88.06	1.71	0	0.55
244	$C_{28}H_{24}O_7$	472.5	4	7	6	130.4	130.6	63.9	2.04	1	0.55
245	$C_{21}H_{20}O_{10}$	432.4	3	10	6	106.97	170.1	50.3	2.4	1	0.55
246	$C_{27}H_{30}O_{15}$	594.5	6	15	9	139.36	249.2	23.03	1.53	3	0.17
247	$C_{26}H_{42}O_4$	418.6	20	4	0	126.13	52.6	90.8	5.33	1	0.55
248	$C_{24}H_{30}O_{11}$	494.5	7	11	6	118.22	175.37	48.5	2.76	2	0.17
249	$C_{33}H_{42}O_{17}$	710.7	13	17	6	163.44	241.89	25.5	4.32	3	0.17
250	$C_{42}H_{48}O_{18}$	840.8	17	18	5	202.79	247.96	23.5	4.43	2	0.17
251	$C_{35}H_{44}O_{18}$	752.7	15	18	5	173.18	247.96	23.5	3.09	2	0.17
252	$C_{36}H_{44}O_{18}$	764.7	16	18	4	176.42	244.8	24.5	3.86	2	0.17
253	$C_{21}H_{34}O_{15}$	526.5	6	15	10	111.25	248.45	23.3	1.51	3	0.17
Cipro.	$C_{17}H_{18}FN_3O_3$	331.3	3	5	2	95.25	74.57	83.3	2.24	0	0.55

NRB = number of rotatable bonds, NHD = number of hydrogen donors, NHA = number of hydrogen acceptors, TPSA = total polar su*rf*ace area, and Cipro = ciprofloxacin.

Table 47: Pharmacokinetic (ADME) property prediction of isolated compounds.

Compounds	log Kp (cm/s)	GI abn	BBB prn	Pgp substrate	CYP1A2 Inh.	CYP2C19 Inh.	CYP2C9 Inh.	CYP2D6 Inh.	CYP3A4 Inh.
224	-2.21	Low	No	No	No	No	No	No	No
226	-5.58	High	No	No	No	No	Yes	No	No
227	-4.65	High	Yes	Yes	Yes	Yes	Yes	Yes	No
229	-2.49	Low	No	No	Yes	No	No	No	No
96	-3.45	Low	No	No	No	No	No	No	No
78	-2.2	Low	No	No	No	No	No	No	No
87	-2.51	Low	No	No	No	No	No	No	No
231	-4.89	High	Yes	No	Yes	No	No	Yes	No
232	-2.78	Low	No	No	No	No	Yes	No	No
97	-3.61	Low	No	No	No	No	No	No	No
234	-2.95	Low	No	No	No	No	No	No	No
98	-3.77	Low	No	No	No	No	No	No	No
238	-4.54	High	Yes	No	No	No	No	No	No
239	-2.8	Low	No	No	No	No	Yes	No	Yes
240	-2.6	High	No	No	Yes	No	Yes	No	No
241	-3.35	High	Yes	No	Yes	No	No	No	No
79	-2.74	Low	No	No	No	No	Yes	No	No
242	-6.05	High	No	Yes	No	Yes	Yes	No	Yes
243	-5.47	High	Yes	No	Yes	No	Yes	No	Yes
244	-6.14	Low	No	No	No	No	No	No	Yes
245	-8.07	Low	No	Yes	No	No	No	No	No
246	-9.91	Low	No	Yes	No	No	No	No	No
247	-2.66	Low	No	No	No	No	No	No	Yes
248	-9.75	Low	No	No	No	No	No	No	No
249	-11.42	Low	No	No	No	No	No	No	No
250	-10.33	Low	No	Yes	No	No	No	No	No
251	-11.27	Low	No	Yes	No	No	No	No	No
252	-11.31	Low	No	Yes	No	No	No	Yes	No
253	-12.96	Low	No	Yes	No	No	No	No	No
Cipro	-9.09	High	No	Yes	No	No	No	No	No

logKp: Skin permeation, GI: Gastro-intestinal; BBB: Blood brain barrier; P-gp: Permeability glycoprotein; CYP: Cytochrome-P, abn: absorption, prn: permission.

Table 48: *In silico* toxicity prediction of isolated compounds using PreADMET and PROTOX-II protocols.

Compounds	Hepatotoxicity	Carcinogenicity	Immunotoxicity	Mutagenicity	Cytotoxicity	LD50 (mg/kg)	Toxicity class
224	Inactive	Inactive	Active	Inactive	Inactive	2300	5
226	Inactive	Inactive	Active	Inactive	Inactive	5000	5
227	Inactive	Inactive	Inactive	Inactive	Inactive	39800	6
229	Inactive	Active	Inactive	Inactive	Inactive	5000	5
96	Inactive	Active	Active	Inactive	Inactive	3000	5
78	Inactive	Inactive	Active	Inactive	Inactive	890	4
87	Inactive	Inactive	Active	Inactive	Inactive	70000	6
231	Inactive	Inactive	Inactive	Inactive	Inactive	4300	5
232	Inactive	Inactive	Active	Inactive	Active	5000	5
97	Inactive	Inactive	Active	Inactive	Inactive	2000	4
234	Inactive	Active	Active	Inactive	Inactive	1000	4
98	Inactive	Inactive	Active	Inactive	Inactive	2000	4
238	Inactive	Inactive	Inactive	Inactive	Inactive	900	4
239	Inactive	Active	Inactive	Inactive	Inactive	1340	4
240	Inactive	Inactive	Inactive	Inactive	Inactive	48	2
241	Inactive	Inactive	Inactive	Inactive	Inactive	900	4
79	Inactive	Inactive	Active	Inactive	Inactive	890	4
242	Inactive	Inactive	Active	Inactive	Inactive	3850	5
243	Inactive	Inactive	Inactive	Inactive	Inactive	1560	4
244	Inactive	Inactive	Inactive	Inactive	Inactive	500	4
245	Inactive	Active	Active	Inactive	Inactive	5000	5
246	Inactive	Inactive	Active	Inactive	Inactive	5000	5
247	Inactive	Inactive	Inactive	Inactive	Inactive	5000	5
248	Inactive	Inactive	Active	Inactive	Inactive	2000	4
249	Inactive	Inactive	Active	Inactive	Inactive	5000	5
250	Inactive	Inactive	Active	Inactive	Inactive	5000	5
251	Inactive	Inactive	Active	Inactive	Inactive	5000	5
252	Inactive	Inactive	Active	Inactive	Inactive	5000	5
253	Inactive	Inactive	Active	Inactive	Inactive	2000	4
Cipro	Inactive	Inactive	Inactive	Active	Inactive	2000	4

CHAPTER FIVE

5. CONCLUSION AND RECOMMENDATIONS

5.1. Conclusions

- During the course of these studies, the *In vitro* antidiabetic, anticancer, anti-Acanthamoeba, antibacterial and antioxidant activities of crude extract and antibacterial and antioxidant activities of isolated compounds along with molecular docking and ADMET properties were examined.
- Silica gel column separation of dichloromethane/methanol (1:1) root extracts of *C. abyssinicum* afforded eight compounds; **223-230**. All compounds were reported herein for the first time from *C. abyssinicum*. Among the tested samples, **224, 225,** and **226** showed growth-inhibitory effects against all the tested bacterial strains in a dose-dependent manner. Compound **228** (79.64 %, IC_{50} value 0.60 μg/mL) displayed lower IC_{50} values which showed promising antioxidant potential as compared to ascorbic acid (90.0 %, IC_{50} value 0.14 μg/mL) used as a standard antioxidant.
- The root extracts of dichloromethane/methanol (1:1) *C. procera* afforded five compounds, **96**, **82**, **87**, **231**, and **232**. In addition, four compounds; **233**, **97**, **234**, and **98** were reported from methanol root extracts of *C. procera*, of which compounds **231**, **232**, **233**, and **234** were isolated herein for the first time from this plant. The highest mean inhibitory value was recorded by **231** (17.7 ± 0.8) followed by **232 (**17.7 ± 1.2**),** **87** (14.3 ± 0.5), **97** (13.9 ± 0.2), and **234** (12.7 ± 0.4 mm), against *E. coli* at 500 µg/mL compared with Ciprofloxacin (29.7 ± 0.3) with similar concentration. **87** and **234** displayed the highest mean inhibition value of 12.5 ± 0.2, and 12.3 ± 0.0 mm against *S. aureus* at 500 μg/mL, respectively, compared with ciprofloxacin (26.7 ± 0.7) at a similar concentration. The antioxidant result revealed that, **97**, and **234** reduced the stable DPPH radical by 63.5 ± 1.0, and 75.0 ± 2.8 at a concentration of 200 µg/mL with an IC_{50} value of 13.8, and 14.6, respectively compared with ascorbic acid (IC_{50} value of 0.14) which suggested potential radical scavengers.
- From the methanol roots extract of *C. abyssinica* **five** compounds were isolated: **238**, **239**, **240**, **241**, and **79**. Except for **79**, all compounds were reported herein for the first time from this plant. Compounds **241**, and **79** displayed better inhibitory activity against *E. coli* with a larger zone of inhibition of 13.9 ± 0.2 and 12.3 ± 0.3 mm,

respectively, recorded at a concentration of 500 µg/mL, besides **79** displayed promising activity against *S. aureus* (14.1 ± 1.0 mm) at 500 μg/mL compared with Gentamycin (19.3 ± 0.5 mm). Compound **239** showed better anti-DPPH activity (70.8 ± 0.2) at a concentration of 200 μg/mL with an IC_{50} value of 10.2 μg/mL.

- The MeOH root extract of the *J. schimperiana* was subjected to silica gel column chromatographic fractionation which afforded six compounds; **78, 242, 243**, **244, 245**, and **246**. All compounds isolated were reported herein for the first time from the species. Compound **246** had a minimum inhibitory concentration (MIC) of 0.25 mg/mL, which was highly susceptible to both *S. aureus* and *S. agalactiae*. Compounds **242,** and **243** with MIC values of 0.5 mg/mL against *S. agalactiae* and compounds **242**, **244**, and **78**, **243** with MIC 1.0 mg/mL against *E. faecalis*, and *S. aureus* respectively. The best radical scavenging activity was displayed by **246** (77.9%), and **45** (73.3%).
- The methanol root extract of *V. sinaiticum* afforded **eight** compounds (**247-253**, and **230**), all compounds were reported herein for the first time from this plant. The highest antibacterial activities were recorded by *S. epidermids* with MIC values of 0.0625 for compound **247**, and 0.5 mg/mL for compounds **250**, and **253**, followed by *S. aureus,* and *S. typomurium* with MIC values of 0.5 mg/mL for compounds **247**, **253**, and **249**, respectively. The highest radical scavenging activity was displayed by the methanol extracts (73.8%), followed by compound (**250**) (74.8%), compound (**252**) (73.2%), compound (**251**) (72.8%), compound (**249**) (72.7%), compound (**253**) (71.1%), and compound (**248**) (70.7%) compared to the standard ascorbic acid (89.9%).
- From the methanol roots extract of *L. abyssinica* **two** compounds **254**, and **255** were isolated, and reported herein for the first time from *L. abyssinica*.
- The GC-MS analysis of bulbs of *C. abyssinicum,* aerial parts of *C. abyssinica*, leaves, seeds, and flowers of *C. procera*, roots, and leaves of *J. schimperiana,* leaves, and roots of *V. siniaticum,* seed, and roots of *L. abyssinica* revealed palmitic acid (27.15 %), benzene, (2-isothiocyanatoethyl)- (33.24 %), diisooctylphthalate (27.42 %), phenol, 2,4-bis(1,1-dimethylethyl)- (23.4 %), *n*-hexadecanoic acid (44.09 %), *n*-hexadecanoic acid (32.45 %), n-hexadecanoic acid (30.27 %), phenol, 2,4-bis (1,1-dimethyl ethyl)- (30.61 %), diisooctylphthalate (36.66 %), cyclohexadecane (32.22 %), and diisooctylphthalate (34.3 %), respectively, as a major compounds.

- For the methanol root extract of *C. abyssinica,* the highest activity was observed against *E. coli* and *S. aureus* with a mean zone of inhibition of 15.4 ± 0.3 and 18.3 ± 0.4 mm at 500 µg/ml, respectively. Among the tested crude extracts, the MeOH and CH_2Cl_2/MeOH (1:1) root extract of *C. abyssinicum* had strong activity against *P. aeruginosa* and *S. aureus* with a maximum zone of inhibition of 16.3 ± 0.3 mm and 16.7 ± 1.2 mm at 500 µg/ml, respectively. The dichloromethane:methanol (1:1) extract against *S. aureus* and *E. faecalis* had the lowest MIC value for *J. schimperiana* extracts, which was 4.0 mg/ml. The antibacterial result of *V. sinaiticum* showed that Gram-positive bacteria were most susceptible to the crude extract among the tested bacterial strains than Gram-negative bacteria.
- Among the plant's crude extract, DCM: MeOH (1:1) extract of *C. abyssinicum*, *C. abyssinica*, and *V. sinaiticum*, MeOH extract of *C. Procera, J. schimperiana*, and *C. abyssinica* had strong (70.3, 74.3, 73.8, 70.6, 71.7, and 71. 3 %) at 200 µg/mL, respectively, radical scavenging activity which turned out to be comparable with ascorbic acid (90.4 %).
- The *in vitro* antidiabetic activity results showed the DCM/MeOH (1:1) and methanol root extract of *C. abyssinicum* and *C. abyssinica,* methanol roots extracts of *C. procera, n*-hexane and DCM/MeOH (1:1) leaves extract of *J. Schimperiana* exhibited strong inhibition of α-amylase enzyme at a concentration of 10 mg/mL.
- Strong cytotoxic effects were observed on the MCF-7 breast cancer cell line with viability percentages of 25.2%, 24.2%, 30.4%, 24.5%, 22.0%, 23.2%, and 34.8% for the DCM/MeOH (1:1) and methanol root extracts of *C. abyssinicum, C. abyssinica, L. abyssinica*, and leave extract of J. *schimperiana*, respectively. With 4.1% viability, the DCM/MeOH (1:1) root extract of *C. procera* had the highest cytotoxic effect of the examined plants on the MCF-7 breast cancer cell line.
- The Dichloromethane: methanol (1:1) root extracts of *V. sinaiticum* showed a good inhibitory activity against Acanthamoeba *castellanii*. The analysis of the antiviral activities of the DCM: MeOH (1:1) leaves extract of *J. schimperiana* revealed strong activity against influenza A virus.
- The analysis of the compounds showed that they had pretty low binding energies, ranging from -5.0 to -8.9, -5.6 to -10.1, -4.3 to -10.8, -5.1 to -11.0, -5.0 to -10.5, and -4.5 to -9.9 kcal/mol against DNA gyrase B (PDB ID: 7P2W), S. aureus Gyrase (PDB

ID: 2XCT), human myeloperoxidase (PDB ID: 1DNU), PqsA (PDB ID: 5OE3), and human topoisomerase IIα (PDB ID: 4fm9), respectively. Of the isolated compounds tested, compounds **226, 227, 231, 238, 241, 242,** and **243** all followed to Lipinski's rule of five with no violations.

- The results obtained from molecular docking, drug-likeness properties, and ADMET analysis are in a good agreement with those obtained from experimental studies of *C. abyssinicum*, *C. abyssinica, C. procera*, *J. schimperiana*, *V. sinaiticum*, and *L. abyssinica* compounds suggesting the potential use of the isolated compounds as medicine which support with the claimed traditional uses of these plants.

5.2. Recommendation

- Phytochemical analysis, and isolation needs to be required on the polar extracts of the plant with the help of reverse phase RP-HPLC to identify, and isolate more polar compounds.
- Biological screening on more bacterial and fungal strains needs to be performed.
- *In vivo* studies against animal models for those active compounds **223**, **227**, **231, 232, 234, 87, 97, 79, 242, 243, 246, 247, 250, and 251** needs be carried out to determine their bioactivity.
- The crude extracts need to be evaluated for their toxicity with normal cell line in different concentrations to determine their toxicity level.
- Isolated compounds **97, 234, 224, 79, 87, 226, 78, 98, 248, 249, 250, 251, 252, 253** and **254** exhibited good binding affinity towards topoisomerase II alpha, cytotoxicity of these compounds, and their structure-activity relationship needs to be studied for providing potential lead drugs.
- Synthetic derivatives of iridoids (**248, 249, 250, 251, 252 and 253**) needs to be synthesized and conduct structure-activity relationship in search for lead drugs.
- For those of active extracts against antidiabetic activity, further isolations of compounds, evaluations of pure compounds against antidiabetic activity, molecular docking against *α*- amylase needs be carried out.
- Further studies need to be investigated the combination of the compounds extracted from these plants with conventional first-line drugs both in vivo and in vitro. Similarly, *in vivo* cytotoxicity study of combination *V. siniaticum*, *C. abyssinicum*, and *l. abyssinica* should be done along with existing first line drugs.

REFERENCES

Abdel Hafiz, M. A., Ramadan, M. A. M., Jung, M. L., Beck, J. P., & Anton, R. (1991). Cytotoxic activity of Amaryllidaceae alkaloids from *Crinum augustum* and *Crinum bulbispermum*. *Planta Med., 57*, 437-439.

Abdela, J. & Shibeshi, W., (2014). *In vivo* antimalarial activity of solvent fractions of the leaf of *Justicia schimperiana* Hochst. Ex Nees (Acanthaceae) against *Plasmodium berghei* in mice. *Ethiop Pharm J,* 30, 95-108. http://dx.doi.org/10.4314/epj.v30i2.3

Abdel-Hameed, E. S., Salih, A., Bazaid, S. A., Shohayeb, M. M., El-Sayed, M. M., & El-Wakil, E. A. (2012). Phytochemical studies and evaluation of antioxidant, anticancer and antimicrobial properties of *Conocarpus erectus* L. growing in Taif, Saudi Arabia. *European J. Med. Plants,* 93-112.

Abebe, D., Debella, A., & Urga, K. (2003). Medicinal plants and other useful plants of Ethiopia: Illustrated Checklist. Addis Ababa: Ethiopian Health and Nutrition Research Institute.

Abebe, W. (2016). An overview of Ethiopian traditional medicinal plants used for cancer treatment. *European J. Med. Plants*, *14*(4),4. doi:10.9734/EJMP/2016/25670.

Abhishek, D., Mohit, C., Ashish, G., & Ameeta, A. (2010). Medicinal utility of *Calotropis procera* (Ait.) R. Br. as used by natives of village Sanwer of Indore District, Madhya Pradesh. *Int. J. Pharm. Life Sci.*, 1(3), 188-190.

Abou-Ela, M. A., El-Lakany, A. M. & Hammoda, H. M. (2004). Alkaloids from the bulbs of *Crinum bulbispermum. Pharmazie*, 59(11), 894–895.

Adedapo, A. A., Oyagbemi, A. A., Fagbohun, O. A., Omobowale, T. O., & Yakubu, M. A. (2016). "Evaluation of the anticancer properties of the methanol leaf extract of *Chromolaena odorata* on HT-29 cell line," *J. Pharmacogn. Phytochem.*, *5*(2), 52–57.

Adesanya, S. A., Olugbade, T. A., Odebiy, O. O., & Aladesanmi, J. A., (1992). Antibacterial Alkaloids in Crinum jagus. *International J. Pharmacognosy*, 4, 303-307.

Afifi, M. S. A., Ahmed, M. M., Pezzuto, J. M., & Douglas Kinghornt, A. (1993). Cytotoxic flavonolignans and flavones from *Verbascum sinaiticum* leaves. *Phytochem., 34*(3), 839–841. doi:10.1016/0031-9422(93)85369-3.

Agrawal, P. K. (1992). NMR spectroscopy in the structural elucidation of oligosaccharides and glycosides. *Phytochem.*, 31, 3307–3330.

Ahmed, B., Al-Rehaily, A. J., Al-Howiriny, T. A., El-Sayed, K. A., & Ahmad, M. S. (2003). Scropolioside-D2 and Harpagoside-B: Two New Iridoid Glycosides from *Scrophularia deserti* and their Antidiabetic and Antinflammatory Activity, *Biol. Pharm. Bull,* 26, 462–467.

Ahmed, M., Qin, P., Ji, M., An, R., Guo, H., & Shafi, J. (2020). Spinasterol, 22,23-Dihydrospinasterol and Fernenol from *Citrullus Colocynthis* L. with Aphicidal Activity against Cabbage Aphid *Brevicoryne Brassicae* L. *Molecules*, *25*, 2184.

Akdemir, Z. Ş., Tatli II, Bedir, E., & Khan, I. A. (2004). Acylated Iridoid Glycosides from *Verbascum lasianthum*. *Turk. J. Chem.*, 28(1), 101 – 109.

Ali, A. A., El-Sayed, H. M., Abdallah, O. M. & Steglich, W. (1986). Oxocrinine and other alkaloids from *Crinum Americanum*. *Phytochem.,* 25(10), 2399–2401.

Ali, A. A., Hambloch, H., & Frahm, A. W. (1983). Relative configuration of the alkaloid Augustamine. *Phytochem.*, 22(1), 283–287.

Ali, M., Gupta, J., Neguerulea, M. V., & Perez-Alonso, M. J. (1998). New ursan-type triterpenic esters from the roots of *Calotropis gigantea. Pharmazie,* 53, 718– 721.

Ali, M., Ravinder, E., & Ramachandram, R. (2000). New ursane-type triterpenic esters from the stem bark of *Thevetia peruviana*. *Pharmazie,* 55, 385–389.

Al-Juaid, S. S., & Abdel-Mojib, M. A. (2004). A novel podophyllotoxin lignan from *Justicia heterocarpa. Chem. Pharm. Bull.,* 52, 507-509.

Allahresani, A., Fatemeh, G., Mohammad, A. N., & Milad, K. (2020). Isolation and characterization of bis(2-ethylheptyl) phthalate from *Cynodon dactylon* (L.) and studies on the catalytic activity of its Cu (II) complex in the green preparation of 1,8-Dioxo-Octahydroxanthenes. *Iran Chem Commun,* 8, 212–227.

Alonso, C., Carrer, V., & Espinosa, S. (2019). Prediction of the skin permeability of topical drugs using in silico and in vitro models. *Eur. J. Pharm. Sci.*, 136.

Al-Rowaily, S. L., Abd-ElGawad, A. M., Assaeed, A. M., Elgamal, A. M., G. El Gendy, A. E., Mohamed, T. A., Dar, B. A., Mohamed, T. K. & Elshamy, A. I. (2020). Essential Oil of *Calotropis procera*: Comparative Chemical Profiles, Antimicrobial Activity, and Allelopathic Potential on Weeds. *Molecules*, *25*, 5203.

Al-Snafi, A. E. (2015). The constituents and pharmacological properties of *calotropis procera* - an overview. *Int. J. Pharm. Rev. Res.*, 5(3), 259-275.

Altay, A., Tohma, H., Durmaz, L., Taslimi, P., Korkmaz, M., Gülçin, I., & Koksal, E. (2019). Preliminary phytochemical analysis and evaluation of *in vitro* antioxidant, antiproliferative, antidiabetic and anticholinergics effects of endemic Gypsophila taxa from Turkey. *J. Food Biochem,* 43 (7), e12908.

Anyanwu, G. O., Iqbal, J., Khan, S. U., Zaib, S., Rauf, K., & Onyeneke, E. (2019). Antidiabetic activities of chloroform fraction of *Anthocleista vogelii* Planch root bark in rats with diet and alloxan-induced obesity-diabetes. *J. Ethno. pharmacol*, 229, 293–302.

Arome, D. & Amarachi, A. (2014). A review on herbal plants with anti-tumour properties. *Int. J. Pharm. Chem. Biol. Sci.*, 2 (2), 43–58.

Arua, C. B., Oyiga, B., & Uguru, M. I., (2010). Variations among some Nigerian *Cucurbita* landraces. *Afr. J. Plant Sci.,* 4 (10), 374 – 386.

Arun, K., Suryavanshi, S., Verma, D., & Dubey, P. (2012). Characterization of Chemical Constituents of *Calotropis procera*. *Chem. Nat. Compd.,* 48(1).

Asano, J., Chiba, K., Tada, M., & Yoshii, T. (1996). Antiviral activity of lignans and their glycosides from *Justicia procumbens. Phytochem.,* 42, 713-717.

Asefa, M., Teshome, N., & Degu, A. (2022). Anti-Inflammatory and Analgesic Activity of Methanolic Root Extract of *Verbascum sinaiticum* Benth. *J. Inflamm. Res.*, 15. 6381–6392.

Asfaw, D. (2015). Proceeding of the Workshop on "Ethiopian Traditional Medicine: Past, Current and Future. *Ethiopian public health institute*.

Asnakech, S., Gure, A., & Feye, T. A., (2019). The Qualitative and Quantitative Phytochemical Investigation of Crinum Species in Ethiopia. *Int. J. Photochem. Photobiol.*, 3(1), 1-9.

Asres, K. (1992). Antimicrobial Screening of *Calotropis Procera*, *Calpurnia aures* and *Melia azedarach* growing in Ethiopia. *Ethiop. Pharm. J.*, 10(1), 43-49.

Badami, S., Aneesh, R., Sankar, S., Sathishkumar, M.N., Suresh, B., & Rajan, S. (2003). Antifertility activity of *Derris brevipes* variety coriacea. *J Ethnopharmacol,* 84, 99-104.

Badmanaban R., Patel C. N., & Patel V. (2010). Determination of polyphenolic content and *in vitro* antioxidant capacity of the leaves of *Lagenaria siceraria* (mol.) standl. *Pharmacogn. J.*, 2(7), 162-169.

Banerjee, P., Eckert, A. O., Schrey, A. K., & Preissner, R. (2018). ProTox-II: a webserver for the prediction of toxicity of chemicals. *Nucleic acids res., 46*(1), 257-263.

Baquar, S. R., & Tasnif, M. (1984). Medicinal plants of southern West Pakistan, Periodical Expert Book Agency, D-42, Vivek Vihar, Delhi., 43.

Barakat, A. Z., Bassuiny, R. I., Abdel-Aty, A. M., & Mohamed, S. A. (2020). Diabetic complications and oxidative stress: The role of phenolic-rich extracts of *saw palmetto* and date palm seeds. *J Food Biochem*, 00:e13416.

Barange, S. H., Raut, S. U., Bhansali, K. J., Balinge, K. R., Patle, D. S., & Bhagat, P. R. (2020). Biodiesel production via esterification of oleic acid catalyzed by Brønsted acid-functionalized porphyrin grafted with benzimidazolium-based ionic liquid as an efficient photocatalyst. *Biomass Convers. Biorefin.* https://doi.org/10.1007/s13399-020-01242-7

Bastida, J., Codina, C., Peeters, P., Rubiralta, M., Orozco, M., Luque, F. J. & Chhabra, S. C. (1995). Alkaloids from *Crinum kirkii*. *Phytochem.,* 40(4), 1291–1293.

Bastida, J., Lavilla, R., & Viladomat, F., (2006). Chemical and biological aspects of Narcissus alkaloids. In: Cordell, G.A. (Ed.), The Alkaloids. 63, Elsevier, Amsterdam, 87–179.

Behrouz, S., Navid, M., Rad, S., Taghavi, B., Mohammad, S., Behrouz, M., & Mirkhani, H. (2018). Design, synthesis, and *in silico* studies of novel eugenyloxy propanol azole derivatives having potent antinociceptive activity and evaluation of their β-adrenoceptor blocking property. *Mol. Divers*., 23, 147–164,

Bekele, A. (2016). Risk factors for chronic non-communicable diseases and prevalence of selected NCDs in Ethiopia special bulletin 18th Annual Review Meeting.

Bekele, B., Adane, L., Tariku, Y., & Hailu, A. (2013). Evaluation of Antileishmanial Activities of Triglycerides Isolated from Roots of *Moringa stenopetala*. *Med. Chem. Res.*, 22(10), 4592-99.

Bekele, E. (2007). Actual Situation of Medicinal Plants in Ethiopia, Prepared for Japan Association for International Collaboration of Agriculture and Forestry, Addis Ababa, Ethiopia, 1-65.

Bernard, A., Clippe, A., Declercq, J. P., Evrard, C., Knoops, B., & Stricht, D.V. (2001). Crystal Structure of Human Peroxiredoxin 5, a Novel Type of Mammalian Peroxiredoxin at 1.5 A Resolution. *J. Mol. Biol*., 311. 751.

Besufekad, A., Tadesse, S., Hymete, A., & Bisrat, D., (2020). Antiproliferative Effects of Alkaloids from the Bulbs of *Crinum abyscinicum* Hochst. ExA. Rich. *J. Evid Based Complementary Altern. Med.,* 8.

Bhalodia, N. R., & Shukla, V. J. (2011). Antibacterial and antifungal activities from leaf extracts of *Cassia fistula* l.: an ethnomedicinal plant. *J. Adv. Pharm. Technol. Res.* 2, 104–109.

Bhaskar, V. H. (2000). Antimicrobial Activity of *Calotropis procera* Seeds. *Asian J. chem.*, 21(7), 5788-5790.

Biçer, A., Kaya, R., Yakali, G., Gültekin, M. S., Turgut, C. G., & Gülçin, I. (2020). Synthesis of novel β-amino carbonyl derivatives and their inhibition effects on some metabolic enzymes. *J. Mol. Struct.,* 1204, 1274–1283.

Birhanu, Z. (2013). Traditional Use of Medicinal Plants By the Ethnic Groups of Gondar Zuria District, North-western Ethiopia. *J. Nat. Remedies,* 13(1), 47-55.

Boit, H. G. & Döpke, W. (1959). Powellamine, ein neues Amaryllidaceen Alkaloid. *Sci. Nat*., 46(15), 475.

Boit, H. G. & Döpke, W. (1960). Krelagine und Crinalbine, zwei neue alkaloide aus *Crinum powellii*. *Sci. Nat.,* 47(21), 498.

Boit, H. G. & Ehmke, H. (1957). XVI. Mitteil. über Amaryllidaceen alkaloide: Alkaloide von *Nerine corusca*, *N. flexusoa*, *Pancratium illyricum*, *Lycoris aurea* und *L. incarnate*. *Chem. Ber.,* 90(3), 369–373.

Boit, H. G., Döpke, W. & Sender, W. (1957). Alkaloide aus *Crinum*, *Zephyranthus*, *Leucojum* und *Clivia*–Arten. *Chem. Ber.,* 99(10), 2203–2207.

Burt, S. (2004). Essential oils: their antibacterial properties and potential applications in foods--a review. *Int. J. Food Microbiol.*, 94(3), 223–253.

Butina, D., Segall, M. D., & Frankcombe, K. (2002). Predicting ADME properties *in silico*: methods and models. *Drug Discov Today,* 7(11), S83-S88.

Calis, I., Gross, G. A., Winkle, T., & Stiche, O. (1998). Isolation and Structure Elucidation of Two Highly Acylated Iridoid Diglycosides from *Scrophularia scopolii*. *Planta med.,* 168-170.

Catharina, E., Fingolo, T. S., Santos, M. D. M., Vianna, F., & Maria, A.C. K (2013). Triterpene Esters: Natural Products from *Dorstenia arifolia* (Moraceae). *Molecules*, 18, 4247-4256. doi:10.3390/molecules18044247.

Cazarolli, L. H., Zanatta, L., Jorge, A. P., Sousa, E. D., Horst, H., Woeh, V. M., Pizzolatti, M. G., Szpoganicz, & Silva, F. R. M. B. (2006). Follow-up studies on glycosylated flavonoids and their complexes with vanadium: their antihyperglycemic potential role in diabetes. *Chem. Biol. Interact.,* 163, 177-191.

Chang, S. T., Wang, D. S. Y., Wu, C. L., Shiah, S. G., Kuo, Y. H., & Chang, C. J. (2000). Cytotoxicity of extractives from *Taiwania cryptomerioides* heartwood. *Phytochem.*, 55, 227-232.

Charoensin, S. (2014). Antioxidant and anticancer activities of *Moringa oleifera* leaves. *J. Med. Plant Res.*, 8 (7), 318–325.

Chattopadhyay, D., & Khan, M. T. H. (2017). Natural Products as Antiviral Agents: Recent Advances and Future Perspectives. *Current Topics in Medicinal Chemistry*, 17(15), 1804–1827. [DOI: 10.2174/1568026617666170111150435]

Chaturvedula, V. S. P, & Prakash, I. (2012). Isolation of Stigmasterol and β-Sitosterol from the dichloromethane extract of *Rubus suavissimus*. *Int. Curr. Pharm. J.*, 1(9), 239-242.

Chekole, G. (2017). Ethnobotanical study of medicinal plants used against human ailments in gubalafto district, Northern Ethiopia. *J Ethnobiol Ethnomed*., *3*, 1–29. doi:10.1186/s13002-017-0182-7.

Chen, C. R., Chen, H. W., & Chang, C. (2008). C-Friedooleanane-type triterpenoids from *Lagenaria siceraria* and their cytotoxic activity. *Chem. Pharm. Bull.,* 56, 335-8.

Chen, C., Lin, F., Tseng, L., Jiang, C., & Lee, S. (2011). Comprehensive study of alkaloids from *Crinum asiaticum* var. *sinicum* assisted by HPLC-DAD-SPE-NMR. *J. Nat. Prod.,* 74(3), 411–419.

Chin, Y., Balunas, M. J., Chai, H. B. & Kinghorn, A. D. (2006). Drug Discovery from Natural Sources. *Arch Aesthetic Plast Surg*, 8, 239-253.

Chopra. T., Abrol, B. K., & Handa, K. L. (1983). Medicinal Plants of the arid zone -t Today and tomorrows, printers and publishers, New Delhi, 25.

Christenhusz, M. J. M. & BYNG, J. W. (2016). The number of known plants species in the world and its annual increase. *Phytotaxa*, 261(3), 201–217.

Chundattu, S. J., Agrawal, V. K., & Ganesh, N. (2011). Phytochemical investigation of *Calotropis procera*. *Arab J Chem*, 48(S1). DOI: 10.1016/j.arabjc.2011.03.011.

Chung, B. H., Lee, J. J., Kim, J. D., Jeoung, D., Lee, H., Choe, J., Ha, K. S., Kwon, Y. G., & Kim, Y. M. (2010). Angiogenic activity of sesamin through the activation of multiple signal pathways. *Biochem Bioph Res Co.,* 391, 254-260.

Cichewicz, R. H., Kouzi, S. A., & Hamann, M. T. (2000). Dimerization of Resveratrol by the Grapevine Pathogen *Botrytis cinerea*. *J. Nat. Prod.*, 63(1), 342-1693.

Cos, P., Vlietinck, A. J., Berghe, D. V., & Maes, L. (2006). Anti-infective potential of natural products: How to develop a stronger *in vitro* 'proof-of-concept. *J. Ethnopharmacol.*, 106, 290–2.

D'Arrigo, M., Ginestra, G., Mandalari, G., Furneri, P. M., & Bisignano, G. (2010). Synergism and postantibiotic effect of tobramycin and *Melaleuca alternifolia* (tea tree) oil against *Staphylococcus aureus* and *Escherichia coli*. *Phytomed.*, 17(5), 317-22.

D´yakonov, V. A., Makarov, A. A., Andreev, E. N., Makarova, E. K. H., Dzhemileva, L. U., Khalilov, L. M., & Dzhemilev, U. M. (2020). Catalytic cycloalumination of 1,2-dienes in the total synthesis of natural grenadamide and lyngbyoic acid. *Russ. Chem. Bull.,* 69 (2), 0386—0389.

Dagne, E. (2009). Natural Database for Africa (NDA). Version 1.0, Addis Ababa, Ethiopia.

Dagne, E., Bekele, A., & Waterman, P. G. (1989). The flavonoids of *Millettia ferruginea* subsp. *ferruginea* and subsp. *darassana* in Ethiopia. *Phytochem.*, 28(7), 1897-1900.

Daina, A., Michielin, O., & Zoete, V. (2017). SwissADME: a free web tool to evaluate pharmacokinetics, drug-likeness and medicinal chemistry friendliness of small molecules. *Sci.Rep.*, 7, 42717.

Day, S., Chiu, N., Won, S., & Lin, C. (1999). Cytotoxic lignans of *Justicia ciliate. J. Nat. Prod.,* 62, 1056-1058.

Degfie, T., Ombito J. O., Demissie T. B., Eswaramoorthy R., Dekebo A., & Endale M (2022). Antibacterial and Antioxidant Activities, in silico Molecular Docking, ADMET and DFT Analysis of Compounds from Roots of *Cyphostemma cyphopetalum*. *Adv Appl Bioinforma Chem.*, 15, 79–97.

Dehaghani, Z. A., Asghari, G., & Dinani, M. S. (2017). Isolation and Identification of Nicotiflorin and Narcissin from the Aerial Parts of *Peucedanum aucheri* Boiss. *J. Agric. Sci. Technol.,* 7, 45-51. doi: 10.17265/2161-6256/2017.01.007.

Deivasigamani, M., Palanirajan, A., Periyasamy, M., Sowmya, S., Enock, O., & Velliyur, K.G. (2016). Isolation, Structural Characterization of Oleic Acid from *Zaleya decandra* Root Extract. *Anal. Chem. Lett.*, 2230-7532. DOI: 10.1080/22297928.2016.1238319

Döpke, W. (1962). Alkaloide aus *Crinum*-Arten. Archiv *der Pharmazie.* 295(12), 868–871.

Döpke, W., Sewerin, E., Trimino, Z. & Juliérrez, C. Z. (1981). Isolation, structure and stereochemistry of a new alkaloid from *Crinum oliganthum. Z Chem*, 21(10), 358.

Dotson, G. S., Chen, C. P., Gadagbui, B., Maier, A., Ahlers, H.W., & Lentz, T.J. (2011). The evolution of skin notations for occupational risk assessment: a new NIOSH strategy. *Regul Toxicol Pharmacol.,* 61(1):53–62.

Drwal, M. N., Banerjee, P., Dunkel, M., Wettig, M. R., & Preissner, R. (2014). ProTox a web server for the in-silico prediction of rodent oral toxicity. *Nucleic Acids Res.*, 42 (W1), W53–W58.

Durcik, M., Skok, Z., Ilas, J., Zidar, N., Zega, A., Szili, P. E., Draskovits, G., Révész, T., Kikelj, D., Nyerges, A., Pál, C., Maši˘c, L. P., & Tomaši˘c, T. (2020). Hybrid inhibitors of DNA gyrase A and B design: Synthesis and evaluation. *Pharmaceutics*, 13(1), 6.

Edilu, A., Adane, L., & Woyessa, D. (2015). In vitro antibacterial activities of compounds isolated from roots of *Caylusea abyssinica*. *Ann. Clin. Microbiol. Antimicrob.,* 14, 15.

Edwards, S. (1976). *Some Wild Flowering Plants of Ethiopia*. Addis Ababa University Press.

Elgindi, M. R., & Mabry, T. J. (2000). Phenylethanoid glycosides from *Verbascum sinaiticum*. *Asian J. Chem., 12*(1), 127-130.

El Sayed, M.T., Sarhan, A. E., Ahmed, E., Khattab, R. R., Elnaggar, M., El-Messery, S. M., Shaldam, M. A., & Hassan, G. S. (2020). Novel pyruvate kinase (PK) inhibitors: new target to overcome bacterial resistance. *ChemistrySelect*, 5(11), 3445-3453.

Elgorashi, E. E., Drewes, S. E. & Van Staden, J. (2001). Alkaloids from *Crinum moorei*. *Phytochem.,* 56(6), 637–640.

Eloff, J. N., Famakin, J. O., & Katerere, D. R. P. (2005). *Combretum woodii* (Combretaceae) leaf extracts have high activity against Gram-negative and Gram-positive bacteria. *Afr. J. Biotechnol.*, 4(10), 1161–1166.

Emam, A. M., Mohamed, A. M., Diab, Y. M., & Megally, Y. N. (2010). Isolation and structure elucidation of antioxidant compounds from leaves of *Laurus nobilis* and *Emex spinosus*. *Drug Discov Ther.*, 4(3), 202-207.

Esmail, A. (2016). Antimicrobial effects of medicinal plants (part 3): plant-based review. *IOSR J. Pharm.,* 10(3), 67-92.

Endale1, M., Eribo, B., Alemayehu, I., Kibret, B., & Mammo, F. (2017). Phytochemical Analysis of Roots of *Aloe gilbertii* and *Millettia ferruginea*. *Int. j. sci. dev.*, 4(1).

Enyew, A., Asfaw, Z., Kelbessa, E., & Nagappan, R. (2014). Ethnobotanical study of traditional medicinal plants in and around Fiche district. *Int J Pharm Clin Res*. *6*, 154-167.

Etana, B. (2010). Ethnobotanical study of traditional medicinal plants of Goma Wereda, Jimma Zone of Oromia Region, Ethiopia (M.Sc Thesis), Ethiopia: Addis Ababa University.

Etana, T. K. (2007). Use and conservation of traditional medicinal plants by indigenous people in Gimbi Woreda, Western Wellega, Ethiopia (M.Sc. Thesis), Ethiopia, Addis Ababa University.

Fennell, C.W & Van Staden, J. (2001). *Crinum* species in traditional and modern medicine. *J. Ethnopharmacol.,* 78(1), 15–26.

Firaol, T., Te*rf*a, W., Kebede, E., Dabessa, G., Roy, R. K., & Sorsa, M., (2013). Ethno-knowledge of plants used in veterinary practices in Dabo Hana District, West Ethiopia. *J. Med. Plant Res.*, 7 (40), 2960- 2971.

Fisher, K., & Phillips, C. (2008). Potential antimicrobial uses of essential oils in food: is *Citrus* the answer. *Trends Food Sci Technol.*, 19(3), 156–164.

Fukamiya, N., & Lee, K. (1986). Antitumor agents, Justicidin-A and diphyllin, two cytotoxic principles from *Justicia procumbens*. *J. Nat. Prod.*, 49, 348-350.

Galma, W., Endale, M., Getaneh, E., Rajalakshmanan, E., Assefa, T., & Melaku, Y. (2021). Antibacterial and antioxidant activities of extracts and isolated compounds from the roots extract of *Cucumis prophetarum* and in silico study on DNA gyrase and human peroxiredoxin 5. *BMC Chemistry,* 15(32).

Gangwal, A. (2010). Scholars Research Library. *Der Pharm. Lett., 2*(1), 307-317.

Gaur, R., Thakur, J. P., Yadav, D. K., Kapkoti, D. S., Verma, R. K., Gupta, N., Khan, F., Saikia, D., & Bhakuni, R. S. (2015). Synthesis, antitubercular activity, and molecular modeling studies of analogues of isoliquiritigenin and liquiritigenin, bioactive components from *Glycyrrhiza glabra*. *Med Chem Res.,* 24(9), 3494 – 3503.

Gebreyohannis, T., Shibeshi, W., & Asres, K. (2014). Effects of Solvent Fractions of *Caylusea abyssinica* (Fresen.) Fisch & Mey on Blood Glucose levels on Normoglycemic, Glucose Loaded and Streptozotocin Induced Diabetic Rodents. *J. Nat. Remedies.,* 14 (1), 2320-3358.

Geone, M., & Antônio, F. (2012). Chemical constituents and biological activities of species of *Justicia* - a review. *Braz. J. Pharmacogn.*, 22(1), 220-238.

Ghosal, S., Rao, P. H., Jaiswal, D. K., Kumar, Y. & Frahm, A. W. (1981). Alkaloids of *Crinum pratense. Phytochem.,* 20(8), 2003–2007.

Ghosal, S., Rao., P. H., & Saini, K. S. (1985). Natural Occurrence of 11-O-Acetylambelline and 11-O-Acetyl-l ,2-β-epoxyambelline in *Crinum latifolium*: Immuno-regulant Alkaloids. *Pharm. Res.,* 2(5), 251-2.

Ghosal, S., Saini, K. S. & Frahm, A. W. (1983). Alkaloids of *Crinum latifolium*. *Phytochem.*, 22(10), 2305–2309.

Ghosal, S., Saini, K. S. & Razdan, S. (1985). *Crinum* alkaloids: their chemistry and biology. *Phytochem.*, 24(10), 2141– 2156.

Ghosal, S., Shanthy, A. & Singh, S. K. (1988). Isocraugsodine, an n arylidenephenethylamine from *Crinum asiaticum* and its ez isomerism. *Phytochem.*, 27, 1849-1852.

Ghosal, S., Shanthy, A., Kumar, A., & Kumar, Y. (1985). Palmilycorine and lycoriside: acyloxy and acylglucosyloxy alkaloids from *crinum asiaticum, Phytochem.,* 24(11), 2703–2706.

Ghosal, S., Singh, S. K. & Unnikrishnan, S. G. (1990). Effects of stress on alkaloid metabolism in *Crinum asiaticum* L. *Phytochem.*, 29(3), 805–811.

Ghosal, S., Unnikrishnan, S. G. & Singh, S. K. (1989). Occurrence of two epimeric alkaloids and metabolism compared with lycorine in *Crinum latifolium. Phytochem.*, 28(9), 2535–2537.

Giday, M., & Teklehaymanot, T. (2013). Ethnobotanical study of plants used in management of livestock health problems by Afar people of Ada'ar District, Afar Regional State, Ethiopia. *J. Ethnobiol. Ethnomed.,* 9(8).

Giddings, L.A., & Newman, D. J. (2019). In Fungi in Extreme Environments: Ecological Role and Biotechnological Significance; Tiquia-Arashiro, S. M.; Grube, M., Eds.; Springer: Cham, Switzerland, 349-3821.

Goll, P. H., Lemma, A., Duncan, J., & Mazengia, B. (1983). Control of schistosomiasis in adwa, ethiopia, using the plant *molluscicide endod* (Phytolacca dodecandra). *Trop. Parasitol, 34*, 177-83.

Gondal, H. Y., Zamir, R., Nisar, M., & Choudhary, M. I. (2020). *Verbascum sinaiticum*, a rich source of antioxidant phenylethanoid glycosides. *Nat Prod J*., *10*, 158–162.

Gordaliza, M. (2007). Natural products as leads to anticancer drugs. *Clin Transl Oncol.*, 9(12), 767–776.

Green, A. K., Haley, S. L., Denise Dearing, M., Barnes, D. M., & Karasov, W. H. (2004). Intestinal capacity of P-glycoprotein is higher in the juniper specialist, Neotoma stephensi, than the sympatric generalist. *Neotoma Albigula*, 139(3), 325–333.

Grieve, M. M. (1994). A Modern Herbal, Tigers Book International London 10, 154.

Grubben, G. J. H. & Denton, O. A. (2004). Plant Resources of Tropical Africa 2: Vegetables, (PROTA). The Netherlands: Buckuys Publishers, 493–501.

Gulcin, I., Huyut, Z., Elmastas, M., & Aboul-Enein, H.Y. (2010). Radical scavenging and antioxidant activity of tannic acid. *Arabian J Chem,* 3, 43–53.

Gulcin, S. C.¸ Betul, S., Sandor, A., Eszter, B. G., & Nurten, A. (2004). Antifungal Diterpenoids and Flavonoids from *Ballota inaequidens*. *Pharm. Biol.*, 42(8), 659–663.

Günsel, A., Bilgiçli, A. T., Barut, B., Taslimi, P., Ozel, A., Gulçin, I., Bıyıklıoglu, Z., & Yarasir, M. N. (2020a). Synthesis of water-soluble tetra-substituted phthalocyanines: investigation of DNA cleavage, cytotoxic effects and metabolic enzyme inhibition. *J. Mol. Struct,* 214,1282. -100.

Gurinder, J. K., & Daljit, S. A. (2009). Antibacterial and phytochemical screening of *Anethum graveolens, Foeniculum vulgare* and *Trachyspermum ammi*. *BMC Complement Altern. Med.,* 9, 30.

Halberstein, R. A. (2005). Medicinal plants: historical and cross-cultural usage patterns. *Ann. Epidemiol.,* 15, 686–699.

Han, Y., Zhang, J., Hu, C.Q., Zhang, X., Ma, B., & Zhang, P. (2019). In silico ADME and toxicity prediction of ceftazidime and its impurities. *Front Pharmacol*. 10.https://doi.org/10.3389/fphar.2019.00434.

Hangun-Balkir, Y., & McKenney, M. (2012). Determination of Antioxidant Activities of Berries and Resveratrol. *Green Chem Lett Rev.,* 5(2), 147–53.

Harrient, U., & Nandita, D. (2014). Mechanism of antibiotic resistance in *Salmonella typhi*. *Int. j. curr. microbiol. appl. sci.*, vol. 3, no 12, 461-476.

Harvey, A. L., Edrada-Ebel, R., & Quinn, R. J. (2015). The re-emergence of natural products for drug discovery in the genomics era. Nature reviews. Drug discovery, 14(2), 111–129.

Hassan, S. W., Bilbis, F. L., Ladan, M. J., Umar, R. A., Dangoggo, S., Saidu, Y., Abubakar, M. K., & Faruk, U. Z. (2006). Evaluation of antifungal acivity and phytochemical analysis of leaves, roots and stem barks extracts of *Calotropis procera* (asclepiadaceae). *Pak. J. Biol. Sci.,* 9 (14), 2624-2629.

Hernández-García, E., García, A., Avalos-Alanís, F. G., Rivas-Galindo, V. M., Delgadillo-Puga, C., & Camacho-Corona, M. D. R. (2019). Nuclear magnetic resonance spectroscopy data of isolated compounds from *Acacia farnesiana* (L) Willd fruits and two esterified derivatives. *Data in Brief*, 22, 255–268.

Highet, R. J. (1961). *Ismine. J. Org. Chem.*, 26(11), 4767–4768.

Hoareau, L.D. & Edgar, J. (1999). Medicinal plants: constituents such as alkaloids, terpenes, flavonoids, A re-emerging health aid. Electron. *J. Biotech., resins, polyphenols, saponnins, steroids and tannins*, 2, 3–4.

Hodges, N., (2002). Pharmaceutical applications of microbiological techniques. In: Aulton, M.E. (Ed.), Pharmaceutics: The Science of Dosage Form Design, 2nd ed. Harcourt Publishers Limited, London, 606.

Holst, H. C. & Brünner, N. (1998). MTT Cell Proliferation assay, Cell Biology: A Laboratory Handbook, San Diego Academic Press 16-18.

Hong, T., Qiao-Jing, L., Jin-Ting, W. & Lu, Z. (2020). Antimicrobial crinane-type alkaloids from the bulbs of *Crinum latifolium*. *J. Asian Nat. Prod. Res.*.

Hussein, K., Eswaramoorthy, R., Melaku, T., & Endale, M. (2021). Antibacterial and Antioxidant Activity of Isoflavans from the Roots of *Rhynchosia ferruginea* and In Silico Study on DNA Gyrase and Human Peroxiredoxin. *Int. J. Sec. Metabolite,* 8(4), 321-336.

Ibrahim, S. R, Mohamed, G.A., Shaala, L.A., Banuls, L.M., Goietsenoven, G.V., & Kiss R. (2012). New ursane-type triterpenes from the root bark of *Calotropis procera*. *Phytochem. Lett.*, 5, 490-5.

Ibrahim, Z. Y., Uzairu, A., Shallangwa, G. A., & Abechi, S. E. (2021). Pharmacokinetic predictions and docking studies of substituted aryl amine-based triazolopyrimidine designed inhibitors of *Plasmodium falciparum* dihydroorotate dehydrogenase (PfDHODH). *Futur. J. Pharm. Sci.*, vol. 7, no. 133, 1826.

Indradevi, S., Ilavenil, S., Kaleeswaran, B., Srigopalram, S., & Ravikumar, S. (2012). Ethanolic extract of Crinum asiaticum attenuates hyperglycemia-mediated oxidative stress and protects hepatocytes in alloxan induced experimental diabetic rats. *J. King Saud Univ. Sci.,* 24, 171-177.

International Diabetes Federation (2021). IDF diabetes atlas. 10th ed.

Jäger, A. K., Adsersen, A., & Fennell, C. W. (2004). Acetylcholinesterase inhibition of *Crinum* sp. *S. Afr. J. Bot.,* 70(2), 323–325.

Jamil, A., Shahid, M., Masud-Ul-Haq Khan, M., & Ashraf, M. (2007). Screening of Some Medicinal Plants for Antifungal Proteins and Peptides, *Pak. J. Bot.*, 39(1), 211–221.

Jao, R. J., Kumar, U. S., Reddy, S.V., Tiwari, A. K., & Rao, J. M. (2005). Antioxidants and a new germacrene sesquiterpene from *Carissa spinarum*. *Nat. Prod. Res.,* 19(8), 763-769. DOI:10.1080/14786410512331330648

Jemal, A., Bray, F., & Center, M. M. (2017). Global cancer statistics. CA: A Cancer Journal for Clinicians, 61(2), 69–90.

Jin, Q., Ji-Jun, C., Zhi-Hong, C., Jia-Hong, Z., Bo-Yang, Y., & Samuel, X. Q. (2006). Iridoid glycosides from *Harpagophytum procumbens* D.C. (devil's claw). *Phytochem.,* 67, 1372–1377.

Kamel, H. S., Nagy, M., Heidi, Z., Johannes. F., & Imhoff, B. S. (2010). Secondary metabolites from *Calotropis procera* (Aiton). *Phytochem. Lett.,* 3, 212–216.

Kamel, M. S. (1996). Non-alkaloidal compounds from bulbs of *Crinum moorei*. *Bull. Pharm. Sci.,* 19, 63–65.

Kanchanapoom, T., Noiarsa, P., Ruchirawat, S., Kasai, R., & Otsuka, H. (2004). Triterpenoidal glycosides from *Justicia betonica. Phytochem.,* 65, 2613-2618.

Kassahun, A., Gashe, F., Mulisa, E., & Rike, W. A. (2016), Nonadherence and factors affecting adherence of diabetic patients to anti-diabetic medication in Assela General Hospital, Oromia Region, Ethiopia. *J. pharm. bioallied sci.,* 8(2), 124.

Kavitha, J., Gopalaiah, K., Rajasekhar, D. G., & Subbaraju, V. (2003). Juspurpurin, an unusual secolignan glycoside from *Justicia purpurea*. *J. Nat. Prod.*. 66, 1113-1115.

Kebebew, M. (2017). Diversity, knowledge and use of medicinal plants in Abay Chomen District, Horo Guduru Wollega Zone, Oromia Region of Ethiopia. *J. Med. Plant Res.*, 11(31), 480–500.

Khan, D., & Zaki, M. J. (2019). The stomatal types in *Sesbania bispinosa* (Jacq.) W. F. Wight seedlings. *Int. J. Biol. Biotech*., 16 (4), 1047-1061.

Khasawneh, M. A., Elwy, H. M., Fawzi, N. M., Hamza, A. A., Chevidenkandy, A. R., & Hassan, A. H. (2011). Antioxidant activity, lipoxygenase inhibitory effect and polyphenolic compounds from *Calotropis procera* (Ait.) R. Br. *Res J Phytochem*, 5, 80-8.

Khoi, N. M., Dat, N. T., Na, M.K., Thuong, P. T., Min, Byung, S., & Bae, Ki, H. (2011). Cytotoxic activity of parthenin, a sesquiterpene isolated from *Crinum ensifolium*. *Nat. Prod. Sci.*, 17, 100-103.

Kim, H., Park, J., Park, H., Badarch, U., Woldemichael, M. & Beutler, A. (2006). Crinamine from *Crinum asiaticum* var.*japonicum* inhibits hypoxia inducible factor-1 activity but not activity of hypoxia inducible factor-2. *Biol. Pharm. Bull.*, 29, 2140-2142.

Kinghorn, A. D., Chin, Y.-W., Swanson, S. M., & Discovery, A. (2009). Discovery of Natural Product Anticancer Agents from Biodiverse Organisms. *Current Opinion in Drug Discovery & Development*, 12(2), 189–196. [PMID: 19333886]

Kintsurashvili, L. G. (2006). Alkaloids from *Crinum moorei* introduced into Georgia. *Chem. Nat. Compd.*, 42(5), 625.

Kirtikar, K. R. & Basu, B.D. (2005). Indian Medicinal Plants, Oriental Enterprises. *International Book distributors*, Dehradun, India, 1116–1117.

Kitchen, D. B., Decornez, H., Furr, J. R., & Bajorath, J. (2004). Docking and scoring in virtual screening for drug discovery: methods and applications. Nat Rev Drug

Discov., 3(11), 935-49. doi: 10.1038/nrd1549.

Klefanoff, S. J. (2005). Myeloperoxidase: friend and foe. *J Leuk Biol*, 77, 598-625.

Kloos, H., Menberu, T., Tadele, A., Chanie, T., Debebe, Y., Abebe, A., Zealiyas, K., Tadele, G., Mohammed, M., & Debella, A., (2014). Traditional medicines sold by vendors in Merkato, Addis Ababa: Aspects of their utilization, trade, and changes between 1973 and 2014. *Ethiop. J. Health Dev.,* 28(2).

Kobayashi, S., Tokumoto, T., Kihara, M., Imakura, Y., Shingu, T. & Taira, Z. (1984). Alkaloidal constituents of *Crinum latifolium L.* and *Crinum bulbispermum* Miln. (Amaryllidaceae). *Chem. Pharm. Bull.,* 32, 3015–3022.

Konoshima, T., & Atta-Ur-Rahman, T. (2000). Anti-tumor-promoting activities (cancer chemopreventive activities) of natural products. *Stud Nat Prod Chem.* 24, 215-267.

Kumar, A., Partap, S., Sharma1, N. K., & Jha, K. K. (2012). Phytochemical, ethnobotanical and pharmacological profile of *Lagenaria siceraria*: - A Review. *J. pharmacogn. phytochem.,* 1(3).

Kumar, S., & Narwal, S. (2013). Antidiabetic Herbal Drugs and Polyherbal Formulations. In Evidence-Based Validation of Herbal Medicine (pp. 389–424). Springer, Berlin, Heidelberg. [DOI: 10.1007/978-3-642-29253-3_14]

Küpeli, E., Erdemoglu, N., Yesilada, E., & Sener, B. (2003). Antiinflammatory and antinociceptive activity of toxoids and lignans from the heartwood of *Taxus baccata* L. *J Ethnopharmacol,* 89, 265-270.

Lai, H. Y., Lim, Y. Y., & Kim, K. H. (2010). *Blenchnum orientale* Linn-a fern with potential as an antioxidant, anticancer and antibacterial agent. *BMC Complement Altern. Med.* 10, 15.

Lal J., Gupta S. K., Thavaselvam, D., & Agarwal, D. D. (2013). Biological activity, design, synthesis, and structure-activity relationship of some novel derivatives of curcumin containing sulfonamides. *Eur. J. Med. Chem. 64,* 579–588.

Lalrinzuali, K., Vabeiryureilai, M., & Jagetia, G. C. (2016). Investigation of the anti-inflammatory and analgesic activities of ethanol extract of stem bark of *sonapatha oroxylum* indicum in vivo. *Int J Inflam*. doi:10.1155/2016/8247014

Lawal, A. & Dangoggo, S. (2014). Phytochemical, Proximate and Toxicity Studies of Aqueous Extract of *Crinum ornatum* (Toad's Onion). *J. Chem. Res.*, 5, 45-50.

Leal, L. K., Ferreira, A. A., Bezerra, G. A., Matos, F. J., & Viana, G. S. (2000). Antinociceptive, anti-inflammatory and bronchodilator activities of Brazilian medicinal plants containing coumarin: a comparative study. *J. Ethnopharmacol.,* 70, 151-159.

Lebogang, M., Wesley, O., & Fanyana, M. (2020). Phytochemical screening, antioxidant activity, and α-amylase inhibition study using different extracts of loquat (*Eriobotrya japonica*) leaves, *Heliyon*, vol. 6, p. e04736.

Lipinski, C. A. (2000). Drug-like properties and the causes of poor solubility and poor permeability. *J Pharmacol Toxicol Methods*, 44 (1), 235–249. doi:10.1016/s1056-8719(00)00107-6.

Lipinski, C. A. (2004). Lead- and drug-like compounds: the rule-of-five revolution. *Drug Discov Today Technol*, 1(4):337–341. https://doi.org/10.101 6/j.ddtec.2004.11.007.

Lipinski, C. A., Franco, L., Dominy, B. W., & Feeney, P. J. (1997). Experimental and computational approaches to estimate solubility and permeability in drug discovery and development settings. *Adv. Drug Deliv. Rev.*, *23*, 3-25.

Lipinski, C. A., Lombardo, F., Dominy, B. W., & Feeney, P. J. (2001). Experimental and computational approaches to estimate solubility and permeability in drug discovery and development settings1. *Adv. Drug Deliv. Rev.,* 46(1-3), 3–26.

Lu, Y. H., Wei, B. L., Ko, H. H., & Lin, C. N. (2008). DNA strand-scission by phloroglucinols and lignans from heartwood of *Garcinia subelliptica* Merr. and *Justicia* plants. *Phytochem.,* 69, 225-233.

Lulsegede, K., Akele, M. Z., & Abiye, A. A. (2022). Wound Healing and Antioxidant Properties of 80% Methanol Leaf Extract of *Verbascum sinaiticum* (Scrophulariaceae): An Ethiopian Medicinal Plant. *J Evid Based Complementary Altern Med.*,10. https://doi.org/10.1155/2022/9836773

Luqman, S., Srivastava, S., Kumar, R., Maurya, A.K., & Chanda, D. (2012). Experimental Assessment of *Moringa oleifera* Leaf and Fruit for Its Antistress, Antioxidant, and Scavenging Potential Using *In vitro* and *In vivo* Assays *J Evid Based Complementary Altern Med.*,1–12.

Machocho, A. K., Bastida, J., Codina, C., Viladomat, F., Brun, R. & Chahabra, S. C. (2004). Augustamine type alkaloids from *Crinum kirkii*. *Phytochem.*, 65(23), 3143–3149.

Machocho, A., Chahabra, S., Viladomat, F., Codina, C. & Bastida, J. (1998). Alkaloids from *Crinum stuhlmanii*, *Planta Med.*, *64*(7), 679–680.

Mahanthesh, M.T., Ranjith, D., Yaligar, R., Jyothi, R., Narappa, G., & Ravi, M.V. (2020). Swiss ADME prediction of phytochemicals present in *Butea monosperma* (Lam.) Tau. *J Pharm Phytochem*., 9(3), 1799-1809.

Mahavorasirikul, W., Viyanant, V., Chaijaroenkul, W., Itharat, A., & Na-Bangchang, K. (2010). Cytotoxic activity of Thai medicinal plants against human cholangiocarcinoma, laryngeal and hepatocarcinoma cells *in vitro*. *BMC Complement Altern Med,* 10, 55.

Mahesh, B. & Satish, S. (2008). Antimicrobial Activity of Some Important Medicinal Plant Against Human and Plant Pathogens. *World J. Agric. Sci.,* 4, 839-843.www.mdpi.com/journal/antioxidants.

Mahmoud, S. M., Abdel-Azim, N. S., Shahat, A. A., Ismail, S. I., & Hammouda, F. M. (2007). Phytochemical and biological studies on *Verbascum sinaiticum* growing in Egypt. *Nat Prod Sci*., *13*,186–189.

Mahmud, T. H. K. (2010). Predictions of the ADMET properties of candidate drug molecules utilizing different QSAR/QSPR modelling approaches. *Curr. Drug Metab.,* 11 (4), 285–295. doi:10.2174/138920010791514306.

Mailafiya, M. M., Pateh, U., Hassan, H. S., Sule, M. I., Yusuf, A. J., & Bila, A. H. (2020). Isolation and Characterization of Stigmasterol Glycoside from the root bark of *Leptadeniahastata. Trends Food Sci Technol.,* 5(2), 394 – 398.

Malle, E., Furtmuller, P. G., Sattler, W., & Obinger, C. (2007). Myeloperoxidase: a target for a new drug development. *Br J Pharmacol*, 152, 838-54.

Manguro, L. O. A., Ogur, J. A., Okora, D. M., Wagai, S. O., & Lemmen, P. (2007). Further flavonol and iridoid glycosides from *Ajuga remota* aerial parts. *J. Asian Nat. Prod. Res.*, 9(7), 617–629.

Martin, Y. C. (2005). "A bioavailability score," *J. Med. Chem.*, 48 (9).

Martin-Bravo, S., Meimberg, H., Luceño, M., Märk, W., Valcárce, V., Bräuchler, C., Vargas, P., & Heub, G. (2007). Molecular systematics and biogeography of Resedaceae based on ITS and trnL-F sequences. *Mol. Phylogenetics Evol.*, 44(1), 105–20.

Mbeng, W. O. (2013). Antifungal evaluation and phytochemical analysis of selected Medicinal plants and other useful plants of Ethiopia. Singapore: Camerapix. in the treatement of fungal diseases associated with HIV infection in the Eastern Cape, South Africa.

Meena, A. K., Yadav, A. K., Niranjan, U. S., Singh, B., Nagariya, A. K., & Sharma, K. (2010). A review on *Calotropis procera* Linn and its ethnobotany, phytochemical, pharmacological profile. *Drug Invent Today,* 2, 185-90.

Megersa, M. (2010). Ethnobotanical study of medicinal plants in Wayu Tuka Wereda, East Wollega Zone of Oromia Region, Ethiopia (M.Sc Thesis). Ethiopia: Addis Ababa University.

Megersa, M., Jima, T. T., & Goro, K. K. (2019). The use of medicinal plants for the treatment of toothache in Ethiopia. *Evid Based Complement Alternat Med*. doi:10.1155/2019/2645174.

Mekonnen, B., Asrie, A. B., & Wubneh, Z. B., (2018). Antidiarrheal Activity of 80% Methanolic Leaf Extract of *Justicia schimperiana*. *Evid Based Complement Alternat Med.,* 10. https://doi.org/10.1155/2018/3037120

Mekuanent, T., Zebene, A., & Solomon, Z., (2016). Ethnobotanical Study of Medicinal Plants in Chilga District, Northwestern Ethiopia. *J. Nat. Remedies.,* 15(2), 88–112.

Melaku, T. (2017). Evaluation of *in-vitro* Antibacterial and Antifungal Activities of Crude extract and Solvent Fractions of the leaves of *Justicia schimperiana* Hochst. Ex Nees (Acanthaceae),'' A thesis submitted to the Department of Pharmacology and Clinical Pharmacy, School of Pharmacy, College of Health Sciences in partial fulfillment of the requirements for the Degree of Master of Science in Pharmacology, Addis Ababa University.

Meneses-Sagrero, S. E., Navarro-Navarro, M., Ruiz-Bustos, E., Del-Toro-Sánchez, C. L., Jiménez-Estrada, M., & Robles-Zepeda, R. E. (2017). Antiproliferative activity of spinasterol isolated of *Stegnospermahalimifolium* (Benth, 1844*). Saudi Pharm J.,* 25, 1137–1143.

Meresa, A., Gemechu, W., Basha, H., & Fekadu, N. (2017). Herbal Medicines for the Management of Diabetic Mellitus in Ethiopia and Eretria including their hytochemical Constituents. *Am. J. Adv. Drug Deliv.*, 040-058.

Mergia, E., Shibeshi, W., Terefe, G., & Teklehaymanot, T. (2014). Phytochemical Screening and *In Vitro* Antitrypanosomal Activity of Aqueous and Methanol Leaf Extract of *Verbascum sinaiticum* (Scrophulariaceae) against *Trypanosoma congolense* Field Isolate. *J Clin Exp Pathol*, 4, 183.

Mesfin, F., Demissew, S., & Teklehaymanot, T. (2009). An ethnobotanical study of medicinal plants in Wonago Woreda, SNNPR, Ethiopia. *J. Ethnobiol. Ethnomed.*, 5, 5–28.

Min, B. S., Gao, J. J., Nakamura, N., Kim, Y. H. & Hattori, M. (2001). Cytotoxic alkaloids and a flavan from the bulbs of *Crinum asiaticum var. japonicum. Chem. Pharm. Bull.*, 49(9), 1217–1219.

Min, B., Fernandez, J. M., Barry, T. N., & McNabb, W. C. (2001). The effect of condensed tannins in *Lotus corniculatus* upon reproductive efficiency and wool production in ewes during autumn. Anim. *Feed Sci. Technol*., 92 (3-4), 185-202.

Mirlosawa, K. B., & Cisowski, W. (1995). Isolation and identification of C-glycosides flavone from *Lagenaria siceraria. L. D Res*, 52, 137-9.

Mittal, A., & Ali, M. (2012). Terpenoid glycosides from the roots of *Calotropis procera* (Ait.) R. Br. *Der Pharm Lett*, 4, 307-13.

Miyase, T., Ishino, M., Akahori, C., Ueno, A., Ohkawa, Y., & Tanizawa, H. (1991). Phenylethanoid glycosides from *Plantago asiatica*. *Phytochem., 30,* 2015–2018.

Mohamed, S. R. (2000). A pharmacognostical study of *Crinum asiaticum* L. cultivated in Egypt. A Thesis for Master Degree submitted to Assiut University, Egypt.

Morimoto, Y., Gikungu, M., & Maundu, P., (2004). Pollinators and biological diversity: the case study of the bottle guard (*Lagenaria siceraria*) in Kenya, 252.

Mosmann, T. (1983). Rapid colorimetric assay for cellular growth and survival: application to proliferation and cytotoxicity assays. *J Immunol Methods,* 65, 55–63.

Mourshid, S. A., Badr, M. J., Risinger, A. L., Susan, Mooberry, L.S., & Youssef, T.A. (2016). Penicilloitins A and B, new antimicrobial fatty acid esters from a marine endophytic Penicillium species. *Z. Naturforsch. C.,* 71(11-12), 387–392. DOI: 10.1515/znc-2015-0242.

Muhammad, A., & Rahila, N. (2013). A review of pharmacognostical, phytochemical and pharmacological properties of *Lagenaria siceraria*, A Miracle Herb. *Int. J. Biomed. Adv. Res*., 4 (5), pp. 269.

Murav'eva, D. A. & Popova, O. I. (1982). Alkaloid composition of the bulbs of *Crinum amabile*, *Khim. Prir. Soedin., 2*, 263– 264.

Nair, J. J., & van Staden, J. (2013). Pharmacological and toxicological insights to the South African Amaryllidaceae, *Food Chem Toxicol,,* 62, 262–275.

Nam, N. H., Kim, Y., You, Y. J., Hong, D. H., Kim, H. M., & Ahn, B. Z. (2004). New constituents from *Crinum latifolium* with inhibitory effects against tubelike formation of human umbilical venous endothelial cells. *Nat. Prod. Res.,* 18(6), 485–491.

Narendiran, S., Janani, D., Keerthana, M., Nivethitha, K. S., Nirmala Devi, S., Padmavathy, S., Supraja, T. S., Sayeedur, R. H., Velvizhi, R., Swathi. N., & Yasaswini. K. G. (2016). Comparative Studies on *in vitro* Phytochemicals Analysis and Larvicidal Efficacy of Medicinal Plant Extracts against *Culex quinquefasciatus*. *Int. J. Life Sci. Res.*, 2(6), 742-748.

Navarro, E., Alonso, S.J., Trujillo, J., Jorge, E., & Pérez, C. (2001a). General behavior, toxicity, and cytotoxic activity of elenoside, a lignan from *Justicia hyssopifolia. J. Nat. Prod.,* 64, 134-135.

Nebih, L., Suleyman, A., Cuneyt, T., Parham, T., Mesut, I., Sukru, B., Gulcin, I., & Mustafa, D. (2020). Synthesis, characterization, inhibition effects, and molecular docking studies as acetylcholinesterase, α-glycosidase, and carbonic anhydrase inhibitors of novel benzene sulfonamides incorporating 1,3,5-triazine structural motifs. *Bioorg. Chem,* 100, 1038–1097.

Nenaah, G. (2013). Antimicrobial activity of *Calotropis procera* Ait. (Asclepiadaceae) and isolation of four flavonoid glycosides as the active constituents. *World J. Microbiol. Biotechnol.,* 29, 1255–1262.

Newman, D. J. (2016). Natural Product-Derived Drugs Based on β-Adrenergic Agents and Nucleosides. *J. Braz. Chem. Soc*., 27, 1320-1333.

Newman, D. J. (2016). Predominately Uncultured Microbes as Sources of Bioactive Agents. *Front. Microbiol*., 7, 1832.

Newman, D. J., & Cragg, G. M. (2015). In Marine Pharmacognosy; from Beach to Bedside; Baker, B., Ed.; CRC Press: Boca Raton, FL, 437-460.

Newman, D. J., & Cragg, G. M. (2016). Natural Products as Sources of New Drugs from 1981 to 2014. *Journal of Natural Products*, 79(3), 629–661. [DOI: 10.1021/acs.jnatprod.5b01055]

Newman, D. J., & Cragg, G. M. (2017). Current Status of Marine-Derived Compounds as Warheads in Anti-Tumor Drug Candidates. *Mar. Drugs*, 15, 99.

Newman, D. J., & Cragg, G. M. (2020). Plant Endophytes and Epiphytes: Burgeoning Sources of Known and "Unknown" Cytotoxic and Antibiotic Agents. *Planta Med*., 86(13-14), 891-905. DOI: 10.1055/a-1095-1111.

Newman, D. J., Cragg, G. M. & Snader, K. M. (2000). The influence of natural products upon drug discovery. *Nat. Prod. Rep.*, 17, 215-234.

Newman, D. J., Cragg, G. M. & Snader, K. M. (2003). Natural products as sources of new drugs over the period. *J. Nat. Prod.*, 66, 1981-2002.

Nguyen, A. T., Fontaine, J., Malonne, H., Claeys, M., Luhmer, M., & Duez, P. (2005). A sugar ester and an iridoid glycoside from *Scrophularia ningpoensis*. *Phytochem.*, 66, 1186–1191.

Nkanwen, E. R. S., Gatsing, D., Ngamga, D., Fodouop, S. P. C. & Tane, P. (2009). Antibacterial agents from the leaves of *Crinum purpurascens* Herb (Amaryllidaceae). *Afr. Health Sci.*, 9, 264–269.

Nordal, I. & Sebsebe, D. (2010). Aloes and Lilies of Ethiopia and Eritrea January, 162-163.

Nostro, A., Germano, M.P., D'Angelo, V., Marino, A., Cannatelli, M.A., (2000). Extraction methods and bioautography for evaluation of medicinal plant antimicrobial activity. Lett. Appl. Microbiol, 30, 379–384.

Nurlelasari, N., Abdullah, F. F., Thufailah, N., Maharani, R., Desi Harneti, D., Hidayat, A. T., & Supratman, U. (2017). Stigmastane-steroid from the bark of *Chisocheton lasiocarfus* (Meliaceae). *J. Akad. Kim.11* (2), 168-173.

Oduselu, G. O., Ajani, O. O., Ajamma, Y. U., Brors, B., & Adebiyi, E. (2019). Homology Modelling and Molecular Docking Studies of Selected Substituted Benzo[d]imidazol-1-yl) methyl) benzimidamide Scaffolds on *Plasmodium falciparum* Adenylosuccinate Lyase Receptor. *Bioinform. Biol. Insights*., 13, 1–10, https://doi.org/10.1177/1177932219865533.

Ohikhena, F. U., Wintola, O. A. & Afolayan, A. J. (2017). Evaluation of the Antibacterial and Antifungal Properties of *Phragmanthera capitata* (Sprengel) Balle (Loranthaceae), a Mistletoe Growing on Rubber Tree, Using the Dilution Techniques. *Sci. World J.*, 9658598.

Okiei, W., Ogunlensi, M., Ofor, E., & Osibote, E. A. S. (2009). Analysis of essential oil constituent in Hydro-Distilates of *Calotropis procera. Res. J. Phytochem.,* 3 (3), 44-53.

Olsen, O., & Sørensen, H. (1980). 4-Carboxy-4-hydroxy-2-aminoadipic acid and other acidic amino acids in *Caylusea abyssinica*. *Phytochem.*, 19, 1717–21.

Omer, I., Abdurrahman, I., & Cai-Xia, Y. (2017). New Triterpenoid from the Roots of *Calotropis gigantea* (L) Dryand (Asclepiadaceae). *Am. J. Org. Chem.,* 7(1), 13-18. DOI: 10.5923/j.ajoc.20170701.03.

Parmar, I., & Rupasinghe, H. (2015). Antioxidant capacity and anti-diabetic activity of wild berry stem infusions. *Euro J Med Plants* 8,11-28. Doi: 10.9734/EJMP/2015/17115.

Pathyusha, R. J. B. (2012). Potential of local anesthetic activity of *Calotropis procera* latex with epinephrine and pH in guinea pig. http//www.pharmatutor.org/ articles/ *Pharmatutor-art*-1043.

Peteros, N. P., & Mylene, M. U. (2010). Antioxidant and Cytotoxic Activities and Phytochemical Screening of Four Philippine Medicinal Plants. *J. Med. Plant Res.,* 4(5), 407-414.

Phillipson, J. D. (2001). Phytochemistry and medicinal plants. *Phytochem.*, 56, 237-243.

Pragya, N., Gidwani, B., Dhongde, H., Gupta, A., & Kaur, C. D. (2015). A review on Pharmacognostical and Pharmacological activities of *Lagenaria siceraria* species. *Int. J. Pertoleum and Pertochemical Eng.,* 1, 55-64.

Prakash, O., Kumar, A., Kumar, P., & Ajeet, A. (2013). Anticancer potential of plants and natural products: a review. *Am. J. Pharmacol. Sci.*, 1 (6), 104–115.

Proestos, C. H., Lytoudi, K., Mavromelanidou, O., Zoumpoulakis, P., & Sinanoglou, V. (2013). "Antioxidant Capacity of Selected Plant Extracts and Their Essential Oils. *Antioxid.,* 2(6), 11–22.

Quazi, S., Mathur, K., & Arora, S. (2013). *Calotropis procera*: An overview of its phytochemistry and pharmacology. *Indian J Drugs,* 1, 63-9.

Rachana, Sujata, B., Mamta, P., Priyanka, K. M., & Sonam, S. (2011). Review and future perspectives of using vasicine, and related compounds. *Indo. Glob. J. Pharm. Res* , 1, 85-98.

Rahman, A. S. H. (2003). Bottle gourd (*Lagenaria siceraria*) a vegetable for good health. *Nat. Prod. Radiance*, 2(5), 249-256.

Rahmani-Nezhad, S., Safavi, M. & Pordeli, M. (2014). Synthesis, in vitro cytotoxicity and apoptosis inducing study of 2-aryl-3- nitro-2H-chromene derivatives as potent anti-breast cancer agents. *Eur. J. Med. Chem.*, 86, 562–569.

Rajasekhar, D., & G.V. Subbaraju (2000). Jusmicranthin, a new arylnaphthalide lignan from *Justicia neesi. Fitoterapia,* 71*,* 598-599.

Ramadan, M. A. (1986). Phytochemical investigation of the minor alkaloids and phenolic compounds of *Crinum bulbispermum* Milne. and *Crinum augustum* Rox. cultivated in Egypt, A Thesis for Ph.D. Degree submitted to Assiut University, Egypt.

Ramadan, M. A., Kamel, M. S., Ohtani, K., Kasai, R., & Yamasaki, K. (2000). Minor phenolics from *Crinum bulbispermum* Miln. Bulbs. *Phytochem.*, 54(8), 891–896.

Ramirez, A., Cabezas, F., Bastida, J., Viladomat, F. & Codina, C. (2001). Alkaloids from the leaves of *Crinum Kunthianum* ROEM. *Revista Latinoamericana De Quimica, Laboratorio Mixim, S.A. de CV*, 9, 26–31.

Ramos, M. V. (2006). Latex constituents from *Calotropis procera* (R. Br.) display toxicity upon egg hatching and larvae of Aedes aegypti (Linn.). *Mem. Inst. Oswaldo Cruz.,* 101(5), 503-510.

Rastogi, R. P. & Mehrotra, B. N. (1993). Compendium of Indian Medicinal Plants, CDRI, Lucknow and PID, New Delhi, India., 2, 174-551.

Rastogi, R. P., & Melhrotra, B. N. (1990). Compendium of Indian Medicinal Plants, New Delhi, India, 1, 237.

Razafimbelo, J., Andriantsiferana, M., Baudouin, G., & Tillequin, F. (1996). Alkaloids from *Crinum firmifolium var. hygrophilum*. *Phytochem.*, 41(1), 323–326.

Refaat, J. (2009). Phytochemical and biological studies of *Crinum augustum* Rox. and *Crinum asiaticum* L. family Amaryllidaceae cultivated in Egypt, A Thesis for Master Degree submitted to Minia University, Egypt.

Refaat, J., Abdel-Lateff, A. A., Kamel, M. S., Ali, A. A., Ramadan, M. A., Okino, T. & Nogata, Y. (2009). Antifouling alkaloids from *Crinum augustum* (Amaryllidaceae). *Pharmacognosy Res.*, 1(2), 43–52.

Refaat, J., Kamel, M. S., Ramadan, M. A., & Ali, A. A., (2012). Crinum; an endless source of bioactive principles: a review, Part II. Crinum Alkaloids: Crinine-Type Alkaloids. *Int. J. Pharm. Sci. Res*., 3(9), 3091-3100.

Refaat, J., Kamel, M. S., Ramadan, M. A., & Ali, A. A., (2013). C*rinum*; an endless source of bioactive principles: a review. Part Iv: non-alkaloidal constituents. *Int. J. Pharm. Sci. Res,,* 4(3), 941-948.

Refsgaard, H. H., Jensen, B. F., Brockhoff, P. B., Padkjaer, S. B., Guldbrandt, M., & Christensen M. S. (2005). In silico prediction of membrane permeability from calculated molecular parameters. *J. Med. Chem.*, 48(3), 805-811.

Regassa, R. (2013). Assessment of indigenous knowledge of medicinal plant practice and mode of service delivery in Hawassa city, southern Ethiopia. *J. Med. Plant Res.*, 7, 517-535.

Remko, M. (2009). Theoretical study of molecular structure, pKa, lipophilicity, solubility, absorption, and polar surface area of some hypoglycemic agents. *J Mol Struc-Theochem,* 897(1-3), 73-82.

Ridhay, A., Noor, A., Soekamto, N. H., Harlim, J., & Altena, I. V. (2012). A Stigmasterol Glycoside from the root wood of *Melochiaumbellata* (Houtt) Stapf var. *degrabrata. Indones. J. Chem.*, 12 (1), 100 – 103.

Rivero-Perez, M. D., Muniz, P., & Sanjase, M. L. (2007). Antioxidant profle of red coines evaluated by total antioxidant capacity, Scavenger activity, and biomarkers of oxidative stress methodologies. *J Agric Food Chem*, 55, 5476–5483.

Saber, H., Maharan, G. H., & Rizkallah, M. M. (1969). Sterols and pentacyclic triterpenes of *Calotropis procera*. *Bull Fac Pharm*, 7, 91-104.

Saeedi, P., Petersohn, I., & Salpea, P. (2019). Global and regional diabetes prevalence estimates for 2019 and projections for 2030 and 2045: Results from the International Diabetes Federation Diabetes Atlas, 9th edition. *Diabetes Research and Clinical Practice*, 157, 107843.

Safavi, M., Esmati, N., Ardestani, S. K. (2012). “Halogenated flavanones as potential apoptosis-inducing agents: synthesis and biological activity evaluation,” *Eur. J. Med. Chem.*, *58*, 573–580.

Samy, R. P. & Chow, V. T. K. (2012). Pilot study with regard to the wound healing activity of protein from *Calotropis Procera* (Ait.). *Evid Based Complement Alternat Med.*

Schimmer, O.& Mauthner, H. (1996). Polymetoxylated xanthones from the herb of *Centaurium erythraea* with strong antimutagenic properties in *Salmonella typhimurium*. *Planta Med.*, 62, 561–564.

Seifu, T., Asres, K., & Gebre-Mariam, T. (2006). Ethnobotanical and Ethnopharmaceutical Studies on Medicinal plants of Chifra District, Afar Region, North Eastern Ethiopia. *Ethiop. Pharm. J.*, 24, 41-58.

Shahania, S., Monsef-Esfahania, H. R., Saeidniab, S., Sanieec, P., Siavoshic, F., Foroumadid, A., Samadie, N., & Goharib, A. R. (2012). Anti-*Helicobacter pylori* Activity of the Methanolic Extract of *Geum iranicum* and its Main Compounds. *Z. Naturforsch*, 67 c, 172 – 180.

Shrivastava, A., Singh, S., & Singh, S. (2013). Phytochemical investigation of different plant parts of *calotropis procera*. *Int. J. Sci. Res. Publ.*, 3(3).

Siler, B., Misić, D., Nestorović, J., Banjanac, T., Glamoclija, J., Soković, M., & Cirić, A. (2010). Antibacterial and Antifungal Screening of *Centaurium pulchellum* crude extracts and main secoiridoid compounds. *Nat. Prod. Commun.*, 5(10), 1525-1530.

Spellberg, B., Guidos, R., Gilbert, D., Bradley, J., Boucher, H. W., Scheld, W. M., Bartlett, J. G., & Edwards, J. (2008). The epidemic of antibiotic-resistant infections: A call to action for the medical community from the Infectious Diseases Society of America. *Clin. Infect. Dis.*, 46, 155-164.

Subbaraju, G. V., Kavitha, J., Rajasekhar, D., & Jimenez, J. I. (2004). Jusbetonin, the first indolo [3,2-b] quinoline alkaloid glycoside, from *Justicia betonica*. *J. Nat. Prod. 67*, 461-462.

Subbaraju, G. V., Kumar, K. K, Raju, B. L., Pillai, K. R., & Reddy, M. C. (1991). Justiciresinol, a new furanoid lignan from *Justicia glauca*. *J. Nat. Prod.*, 6, 1639-1641.

Subbaraju, G. V., Rajasekhar, D., Kavitha, J., & Jimenez, J. I. (2001). Neesiinosides A and B, two new diphyllin glycosides from *Justicia neesii*. *Indian J Chem,* 4, 313-319.

Suffredini, B. I., Paciencia, M. L. B., Nepomuceno, D. C., Younes, R. N., & Varella, A. D. (2006). Antibacterial and cytotoxic activity of Brazilian plant-*Clusiaceau*. *Mem. Inst. Oswaldo Cruz., 101*, 1590-1598.

Susplugas, S., Van Hung, N., Bignon, J., Thoison, O., Kruczynski, A., Sévenet, T., & Guéritte, F. (2005). Cytotoxic arylnaphthalene lignans from a Vietnamese Acanthaceae, *Justicia patentiflora. J. Nat. Prod.,* 68, 734-738.

Tadeg, H., Mohammed, E., Asres, K., & Gebre-Mariam, G., (2005). Antimicrobial activities of some selected traditional Ethiopian medicinal plants used in the treatment of skin disorders. J. Ethnopharmacol. 100, 168–175.

Takagi, S. & Yamaki, M. (1977), On the constituents of the bulbs of *Crinum asiaticum var. japonicum* Bak On the neutral constituents. *Yaku Zasshi,* 97(10), 1155.

Tamiru, W., Engidawork, E., & Asres, K. (2012). Evaluation of the effects of 80% methanolic leaf extract of *Caylusea abyssinica* (fresen.) fisch. & Mey. On glucose handling in normal, glucose loaded and diabetic rodents. *BMC Complement Altern. Med.*, 12, 1–7.

Tanya, S., & Daniel, Y. (2009). *Pseudomonas aeruginosa* – a phenomenon of bacterial resistance. *J. Med. Microbiol.*, 58, 1133-1148.

Tariku, Y. (2008). *In vitro* efficacy study of some selected Medicinal plants against *Leishmania* spp. MSc. thesis in Medicinal Chemistry, Addis Ababa University, Addis Ababa, Ethiopia.

Tedila, H. (2019). In-Vitro Antibacterial Activity of *Ruta Chalepensis* (Tenadam) and *Justicia Schimperiana* (Sensel) Plants against Some Bacterial Human Pathogens. *J. Health, Med. Nurs.*, Vol.63. DOI: 10.7176/JHMN/63-03.

Teklay, A., Abera, B., & Giday, M. (2013). An ethnobotanical study of medicinal plants used in kilte awulaelo district, Tigray region of Ethiopia. *J Ethnobiol Ethnomed*., *9*, 1–23.

Teklehaymanot, T. (2009). Ethnobotanical study of knowledge and medicinal plants use by the people in Dek Island in Ethiopia. *J. Ethnopharmacol.*, 124(1), 69–78.

Teklehaymanot, T., & Giday, M. (2007). Ethnobotanical study of medicinal plants used by people in Zegie Peninsula, Northwestern Ethiopia. *J Ethnobio. Ethnomed.,* 3, 3-12.

Tesfaye, A., & Demissew, S. (2009). Ethnobotanical study of medicinal plants in Kafficho people, southwestern Ethiopia, Proceedings of the 16th International Conference of Ethiopian Studies Trondheim. Trondheim, Norway.

Tesfaye, A., Makonnen, E., & Gedamu, S. (2016). Hypoglycemic and anti-hyperglycemic activity of aqueous extract of *Justicia Schimperiana* leaves in normal and streptozotocin-induced diabetic mice. *Int. J. Pharm. Sci. Res.*, *7*(2).

Tesfaye, D., Endale, M., Getaneh, E., Abdisa, E., Guta, L., & Melaku, Y. (2022). Chemical Composition and Antibacterial Activity of Essential Oils from Various Parts of *Gladiolus Candidus*, *Ranunculus Multifidus*, *Artemisia Abyssinica* and *Crinum Abyscinicum*. *Bull. Chem. Soc. Ethiop*, 36 (4), 865-878.

Tolera, F. F., Shigut, M. M., Hailemariam, T. B., Regassa, t., & Kergano, N. K., (2017). Ethnobotanical study of ethnoveterinary plants in Kelem Wollega Zone, Oromia Region, Ethiopia. *J. Med. Plant Res.,* 11(16), 307-317.

Tolossa, K., Debela, E., Athanasiadou, S., Tolera, A., Ganga, G., & Houdijk, J. G. M. (2013). Ethno-medicinal study of plants used for treatment of human and livestock ailments by traditional healers in South Omo Southern Ethiopia. *J. Ethnobiol. Ethnomed.*, 9, 32.

Tram, N. T., Mitova, M., Bankova, V., Handjieva, N., & Popov, S. S. (2002). GCMS of *Crinum latifolium* L. Alkaloids. *Z NATURFORSCH*, 57c, 239–242.

Trott, O. & Olson, A. J. (2010). AutoDock Vina: improving the speed and accuracy of docking with a new scoring function, efficient optimization, and multithreading. *J. Comput. Chem.*, 31, pp. 455–461.

Tuasha, N., Petros, B., & Asfaw, Z. (2018). Medicinal plants used by traditional healers to treat malignancies and other human ailments in Dalle District, Sidama Zone, Ethiopia. *J. Ethnobiol. Ethnomed.,* 14(1), 1–21.

Turkan, F., Atala, M. N., Aras, A., Gulçin, I., & Bursal, E. (2020). ICP-MS and HPLC analyses, enzyme inhibition and antioxidant potential of *Achillea schischkinii* Sosn. *Bioorg. Chem,* 94, 1033–1043.

Turner, J. V., Maddalena, D. J., & Agatonovic-Kustrin, S. (2004). Bioavailability prediction based on molecular structure for a diverse series of drugs. *Pharm. Res.*, 21(1), 68-82. https://doi.org/10.1023/b:pham.

Udobre, A. S, Etim, E. I., Udobang, J. A. & Udoh, A. E. (2015). Antimicrobial Activity of Stigmast-4-En-3-One And 2,4- Dimethylhexane Isolated From Nauclea Latifolia. *Int. J. Phytopharm.,* 6(2), 65-68.

Umer, S., Asres, K., & Veeresham, C., (2010). Hepatoprotective activities of two Ethiopian medicinal plants. *Pharm. Biol.,* 48(4), 461–468.

Vadivelan, R., Gopala, R., & Kannan, R. (2019). Antidiabetic potential of Asparagus racemosus Willd leaf extracts through inhibition of α-amylase and α-glucosidase. *J. Tradit. Complementary Med.,* 9 (1), 1–4.

Van, Q. E., Simon, G., André, A., Dewelle, J. E., Yazidi, M., & Bruyneel, F. (2005). Identification of a novel cardenolide (2''-oxovoruscharin) from *Calotropis procera* and the hemisynthesis of novel derivatives displaying potent in vitro antitumor activities and high in vivo tolerance: Structure activity relationship analyses. *J Med Chem*, 10, 849-56.

Vasan, N., Baselga, J., & Hyman, D. M. (2019). A view on drug resistance in cancer. Nature, 575(7782), 299–309.

Ventola, C. L. (2015). The antibiotic resistance crisis: part 1: causes and threats. *Pharmacy and Therapeutics*, 40(4), 277–283.

Viet, T. D., Xuan, T. D., & Anh, L. H. (2021). α-Amyrin and β-Amyrin Isolated from *Celastrus hindsii* Leaves and Their Antioxidant, Anti-Xanthine Oxidase, and Anti-Tyrosinase Potentials. *Molecules,* 26, 7248. https://doi.org/10.3390/molecules26237248.

Wahi, S. P. (1974). Chemical study of the leaf of *Justicia gendarussa* Burm. *J. res. innov. manag. sci.*, 9, 65-66.

Wang, C. L. J., & Ripka, W. C. (1983). Total synthesis of justikidin P. A new lignan lactone from *Justicia extensa*. *J Org Chem* 48, 2555-2557.

Wang, Z. N., Wang, M.Y., Mei, W. L., Han, Z., & Dai, H. F. (2008). A new cytotoxic pregnanone from *Calotropis gigantea*. *Molecules*, 13, 3033-9.

Weldegerima, B., Teferra, A., & Muthuswamy, R. (2008). Ethno-Veterinary use of medicinal plants by traditional healers in Dabat District, Northwestern Ethiopia. *Phcog Mag 4*(15).

WHO, E. (2017). Fact sheets on sustainable development goals: health targets: *Antimicrobial Resistance*.

Wildman, W. C. (1960). The Alkaloids: Chemistry and Physiology. Edited by R.H.F. Manske, Academic Press, New York, London, 6.

Woodman, O.L., & Malakul, W. (2009). 3′,4′-Dihydroxyflavonol prevents diabetes-induced endothelial dysfunction in rat aorta. *Life Sci.,* 85, 54-59.

World Health Organization Geneva. (2002-2005). Traditional Medicine Strategy, 1-3.57.

World Health Organization (WHO). (2017). Antimicrobial resistance: Global report on surveillance.

Yamashita, S., Igarashi, M., Hayashi, C., Shitara, T., Nomoto, A., Mizote, T., & Shibasaki, M. (2015). Identification of self-growth-inhibiting compounds lauric acid and 7-(Z)-tetradecenoic acid from Helicobacter pylori. *Microbiol.,* 161(6), 1231-1239. https://doi.org/10.1099/mic.0.000077

Yang, X., Zhou, J., Wang, T., Zhao, L., Ye, G., Shi, F., Li, Y., Tang, H., Dong, Q., Zhou, X., Xu, M., Rong, Q., Chen, H., Yang, X., & Cai, Y. (2017). A Novel Method for Synthesis of α-Spinasterol and its Antibacterial Activities in Combination with Ceftiofur. *Fitoterapia*. Doi: 10.1016/j.fitote.2017.03.011.

Yayli, N, Yildirim, N., Usta, A., Ozkurt, S., & Akgun, V. (2003). Chemical Constituents of *Campanula lactiflora*. *Turk J Chem*, **27**, 749–755.

Yeabyo, S., Teka, M. Z., Gopalakrishnan, V. K., Hagos, Z., & Chaithanya, K. K. (2018). Antibacterial activity of root extracts of *Verbascum sinaiticum* against multidrug-resistant Enterobacteriaceae family Gram-negative and two Gram-positive bacteria. *Drug Invent. Today,*10 (8), 1387-1394.

Yineger, H., Kelbessa, E., Bekele, T., & Molla, E. L., (2008). Plants used in traditional management of human ailments at Bale Mountains National Park, Southeastern Ethiopia. *J. Med. Plant Res.*, 2 (6), 132-153.

Yirga, G. (2010). Assessment of Indigenous Knowledge of Medicinal Plants in Central Zone of Tigray, Northern Ethiopia. *Afr. J. Plant Sci.,* 4(1), 006–011.

Yirga, G., & Zerabruk, S. (2012). Traditional knowledge of medicinal plants in Gindeberet district, Western Ethiopia. *S. Afr. J. Bot.,* 78, 165–169.

Yogesh, M., Abhay, P. S., & Devender, P. (2011). LC-MS/MS Profiling of hydroethanolic extract of *Calotropis procera* leaves. *I Communique*, 3(1).

Yuta, E., Yu, S., Mariko, F., Hiroyuki, K., Masami, I., & Ayumi, O. (2019). Two new alkaloids from *Crinum asiaticum* var. *japonicum. J. Nat. Med., 73*, 648–652. DOI: 10.1007/s11418-019-01304-9.

Zengin, G., Mahomoodally, M. F., Sinan, K. I., Sadeer, N., Maggi, F. Caprioli, G., Angeloni, S., Mollica, A., Stefanucci e, A., & Akan, H. (2021). Evaluation of chemical constituents and biological properties of two endemic *Verbascum* species. *Process Biochem.,* 108 (2021) 110–120.

APPENDICES

Appendix 1A: ^{1}H NMR (400 MHz, $CDCl_3$) spectrum of (*E*)-octadec-7-enoic acid (**223**).

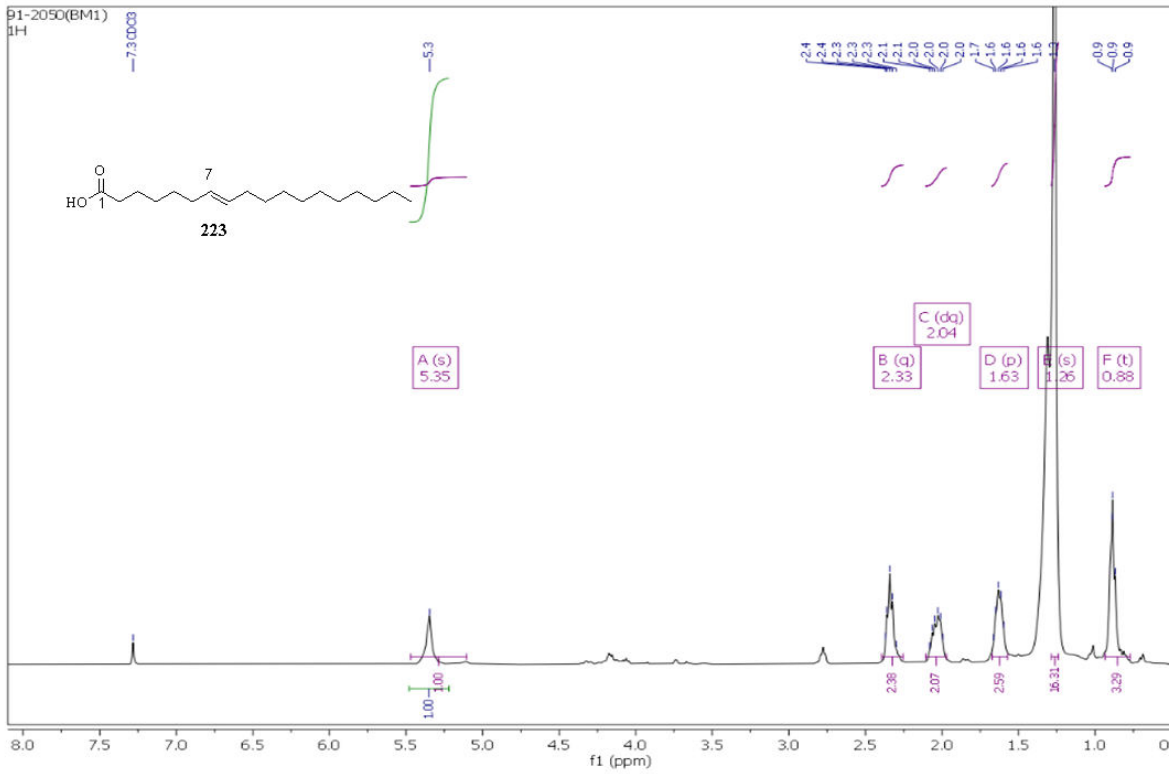

Appendix 1B: ^{13}C NMR (101 MHz, $CDCl_3$) spectrum of (*E*)-octadec-7-enoic acid (**223**)

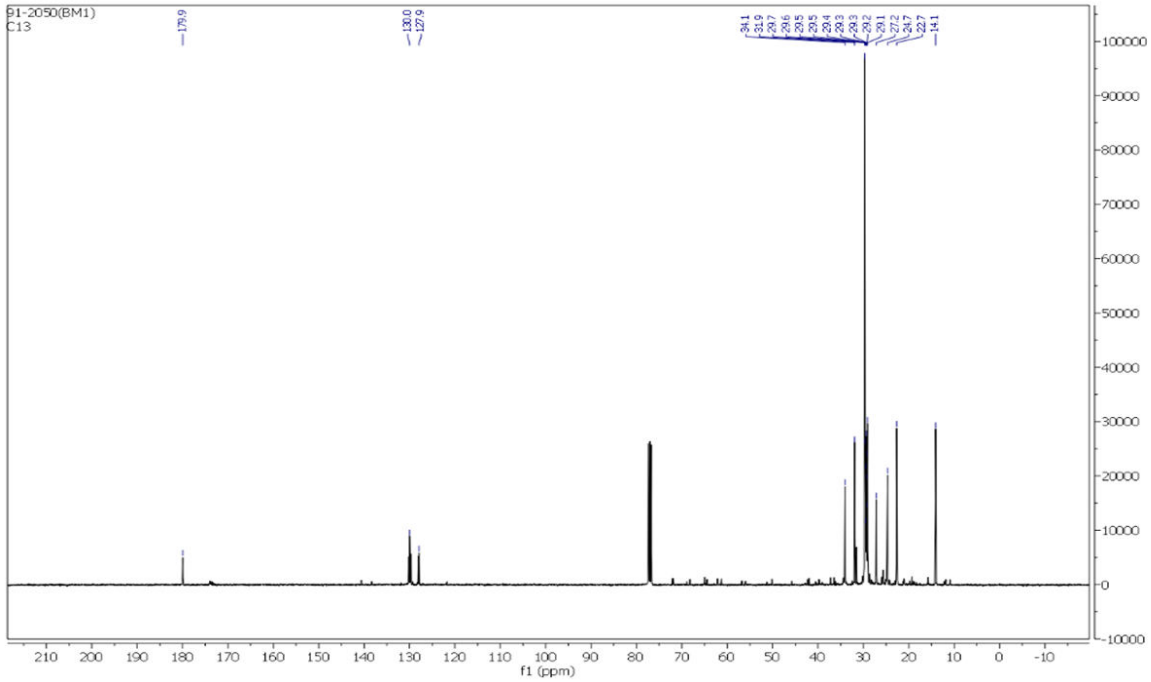

Appendix 1C: DEPT-135 NMR (101 MHz, $CDCl_3$) spectrum of (*E*)-octadec-7-enoic acid (**223**)

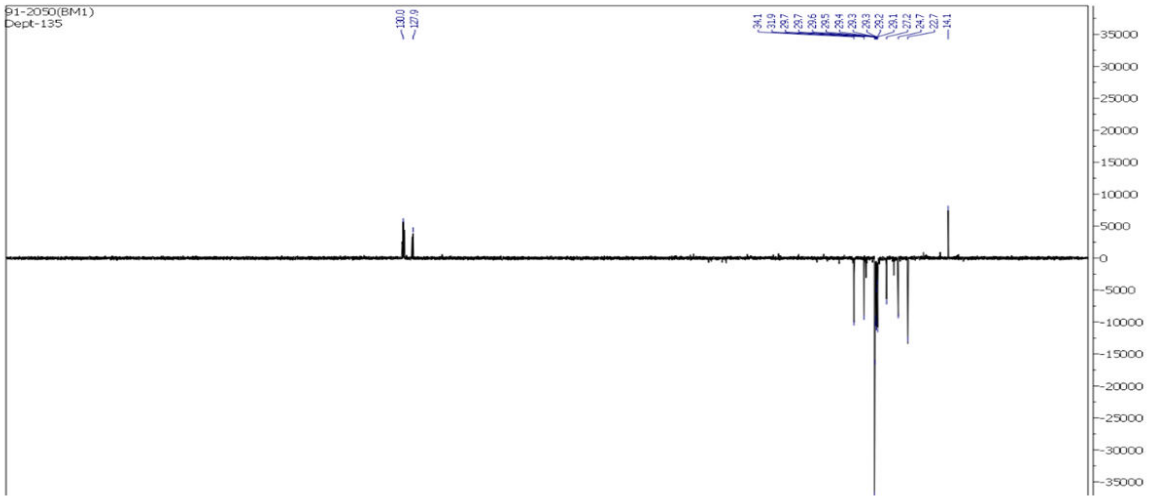

Appendix 2A: ^1H NMR (400 MHz, $CDCl_3$) spectrum of stigmast-4-en-3-one (**224**).

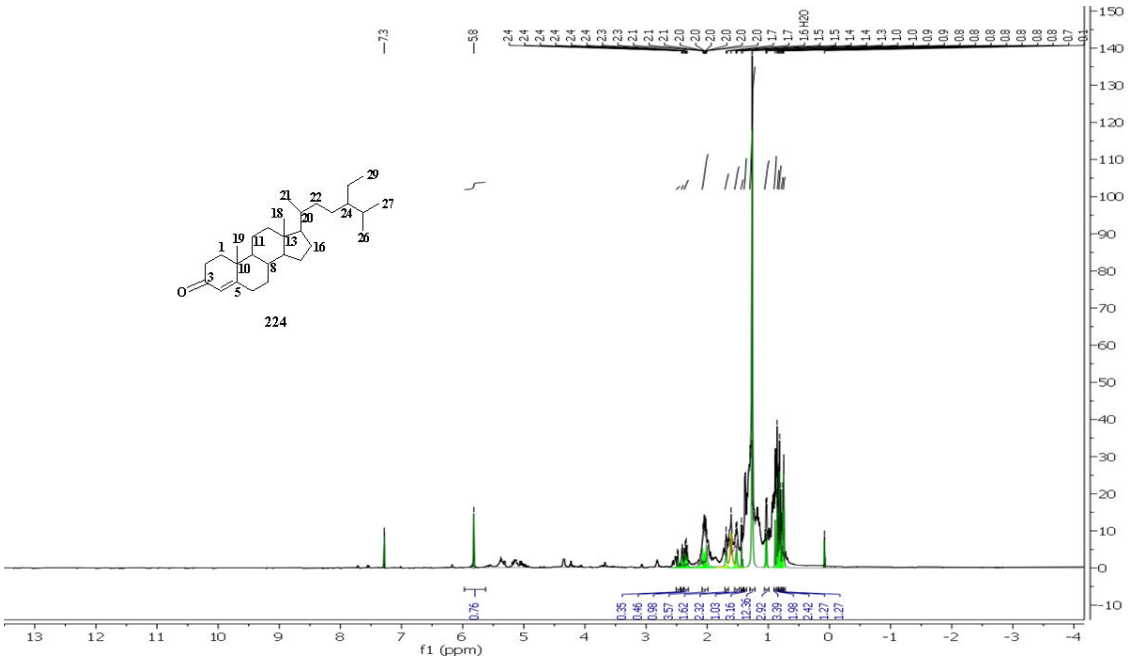

Appendix 2B: ^{13}C NMR (101 MHz, $CDCl_3$) spectrum of stigmast-4-en-3-one (**224**)

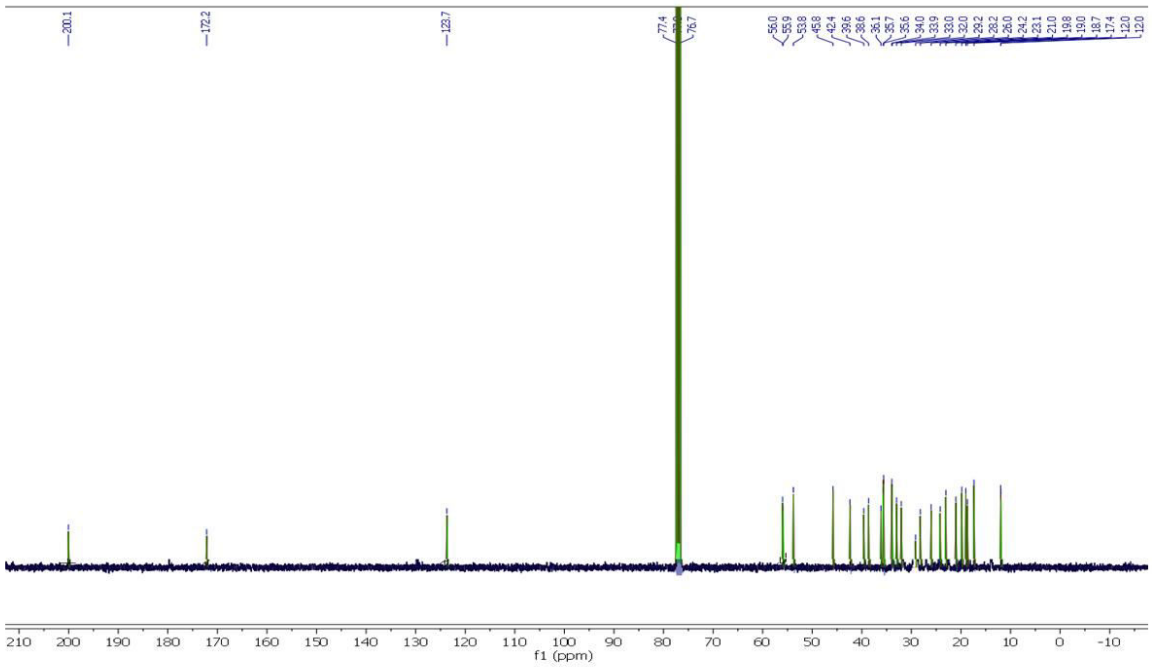

Appendix 2C: DEPT-135 NMR (101 MHz, $CDCl_3$) spectrum of stigmast-4-en-3-one (**224**)

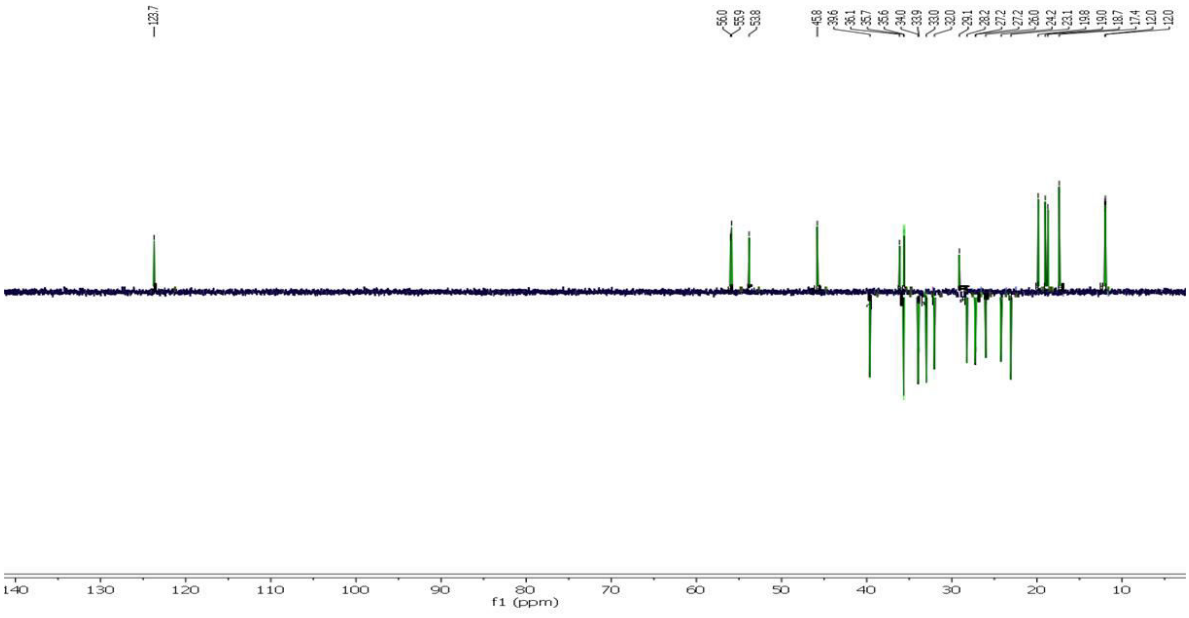

Appendix 3A: ^{1}H NMR (400 MHz, $CDCl_3$) spectrum of 1,3-dilinoleoyl-2-oleine (**225**)

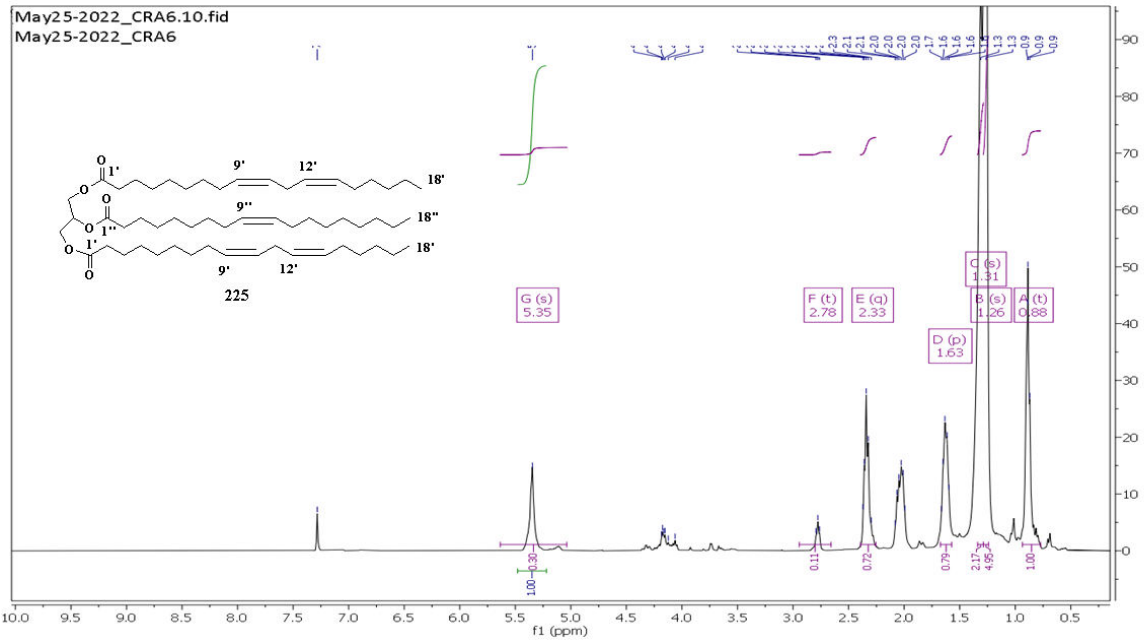

Appendix 3B: ^{13}C NMR (101 MHz, $CDCl_3$) spectrum of 1,3-dilinoleoyl-2-oleine (**225**)

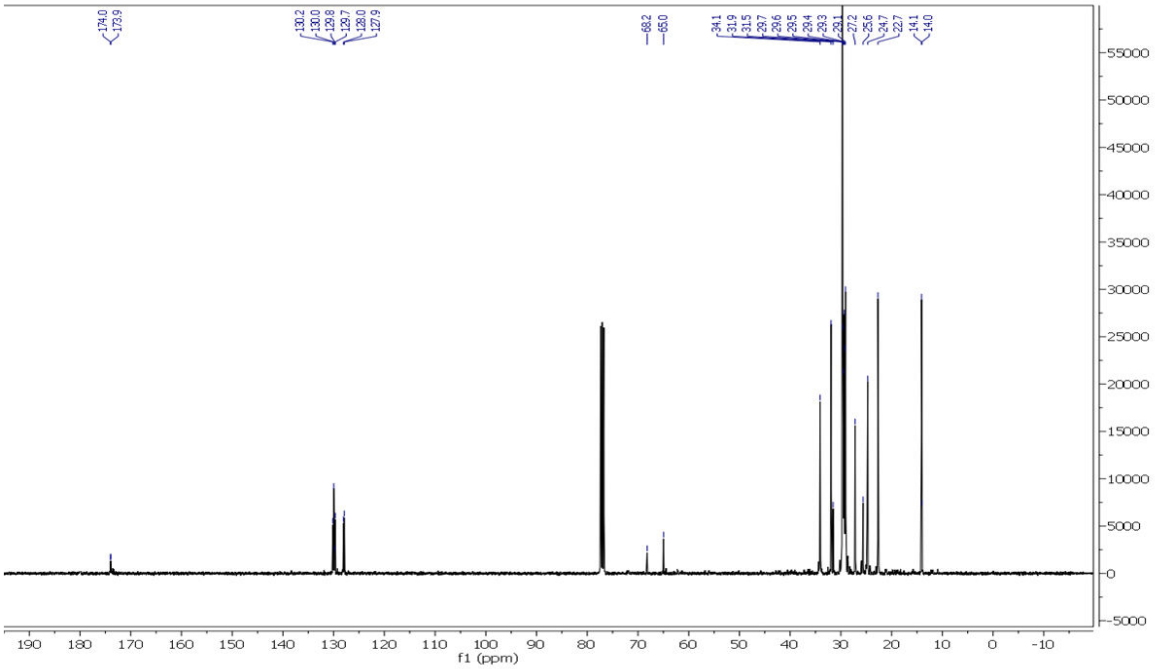

Appendix 3C: DEPT-135 NMR (101 MHz, $CDCl_3$) spectrum of 1,3-dilinoleoyl-2-oleine (**225**)

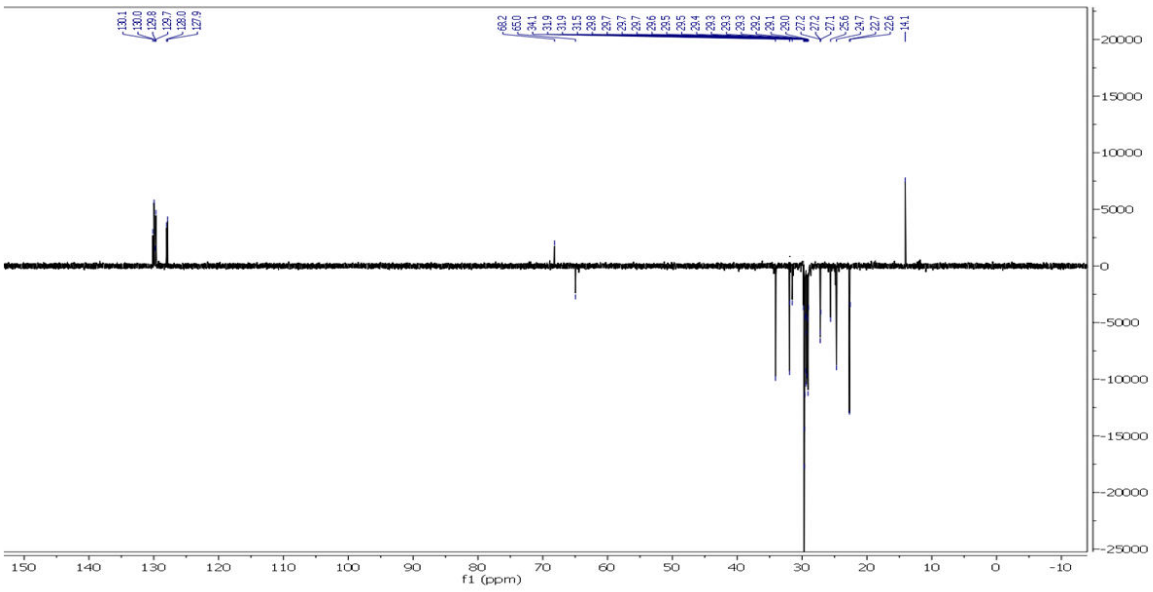

Appendix 4A: ^1H NMR (400 MHz, $CDCl_3$) spectrum of 6-hydroxy-3,5,7,4′-tetramethoxyflavone (226).

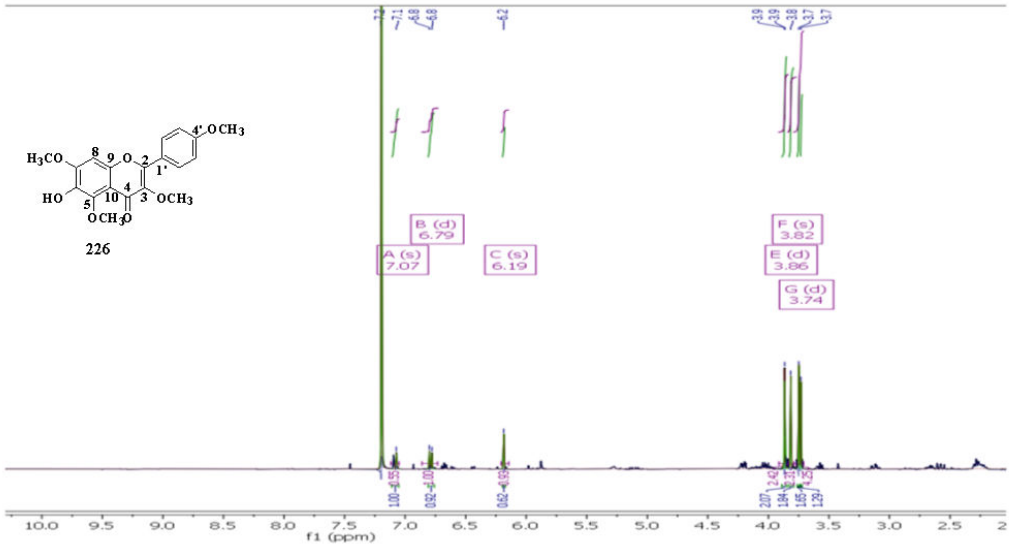

Appendix 4B: ^{13}C NMR (101 MHz, $CDCl_3$) spectrum of 6-hydroxy-3,5,7,4′-tetramethoxyflavone (**226**).

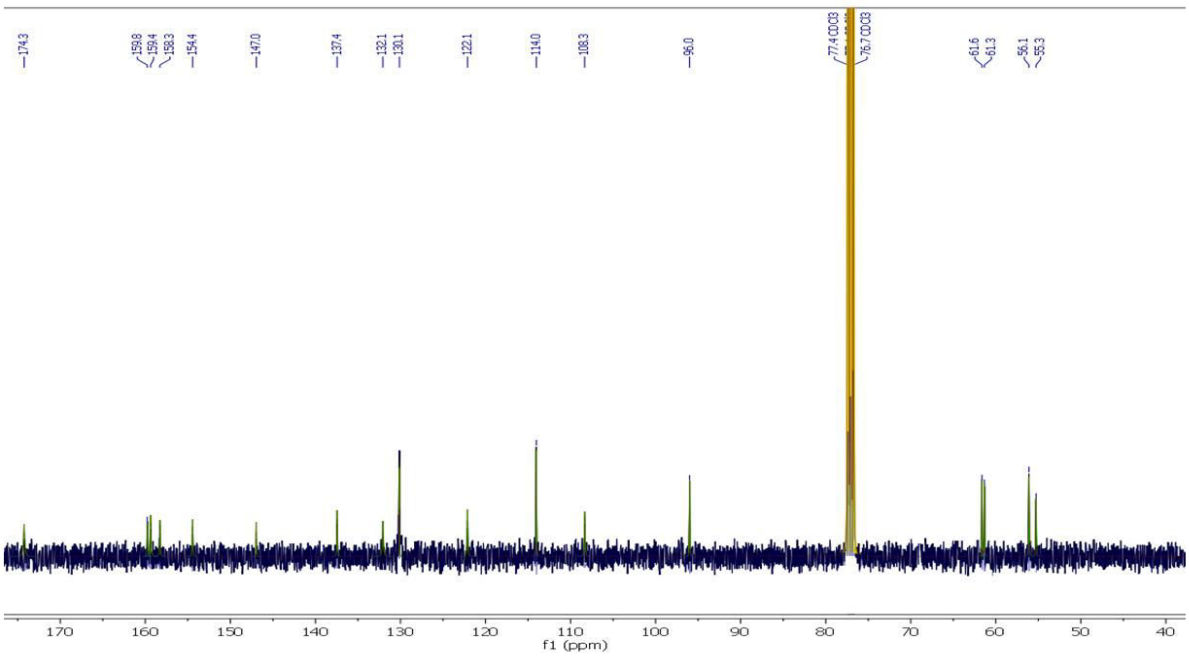

Appendix 4C: DEPT-135 NMR (101 MHz, $CDCl_3$) spectrum of 6-hydroxy-3,5,7,4′-tetramethoxyflavone **(226)**.

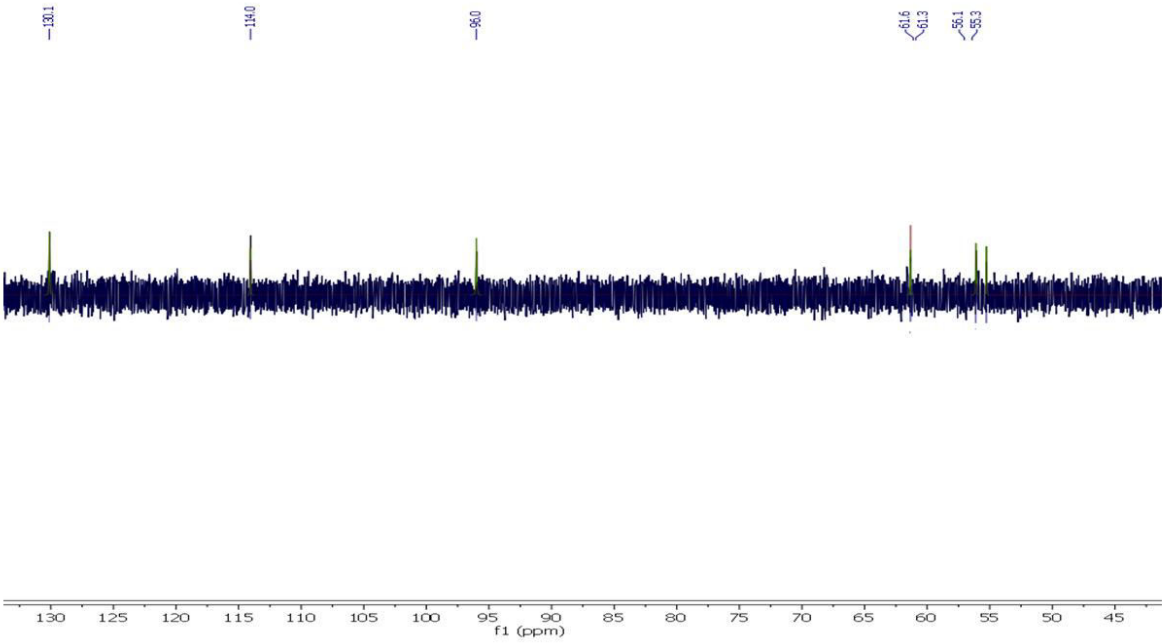

Appendix 4D: ^{1}H-^{1}H COSY spectrum of 6-hydroxy-3,5,7,4′-tetramethoxyflavone (**226**).

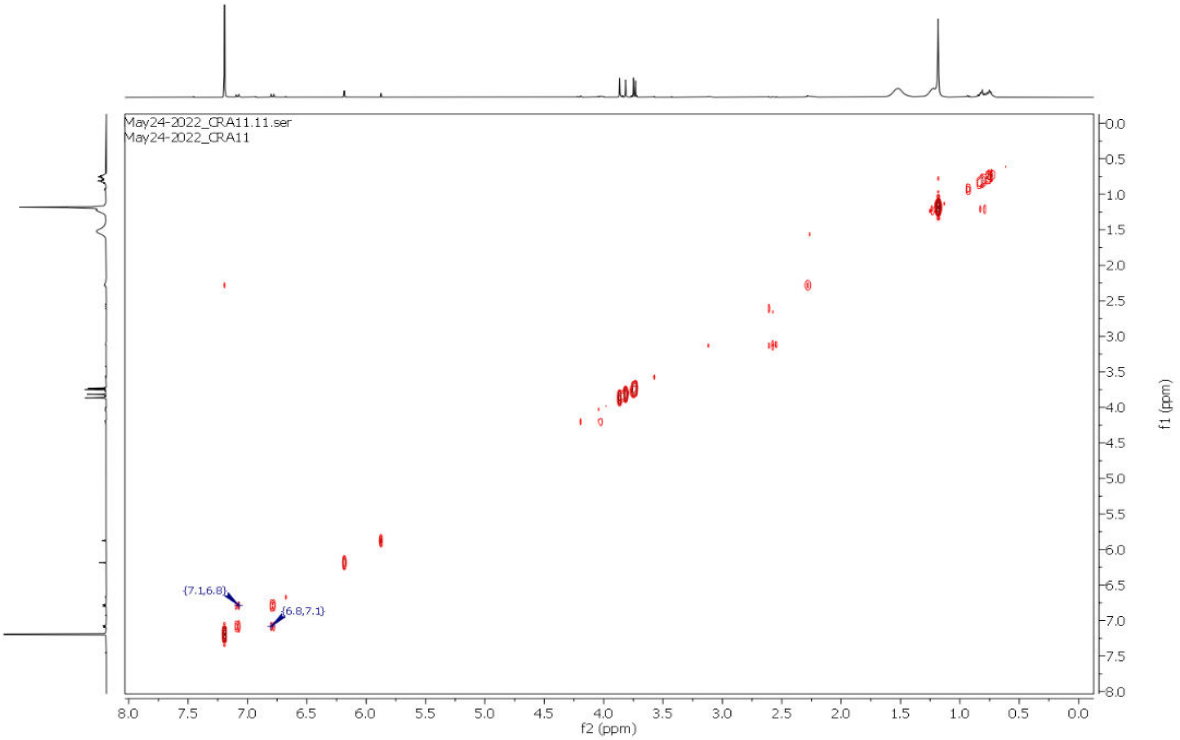

Appendix 4E: HSQC correlation of 6-hydroxy-3,5,7,4′-tetramethoxyflavone (**226**).

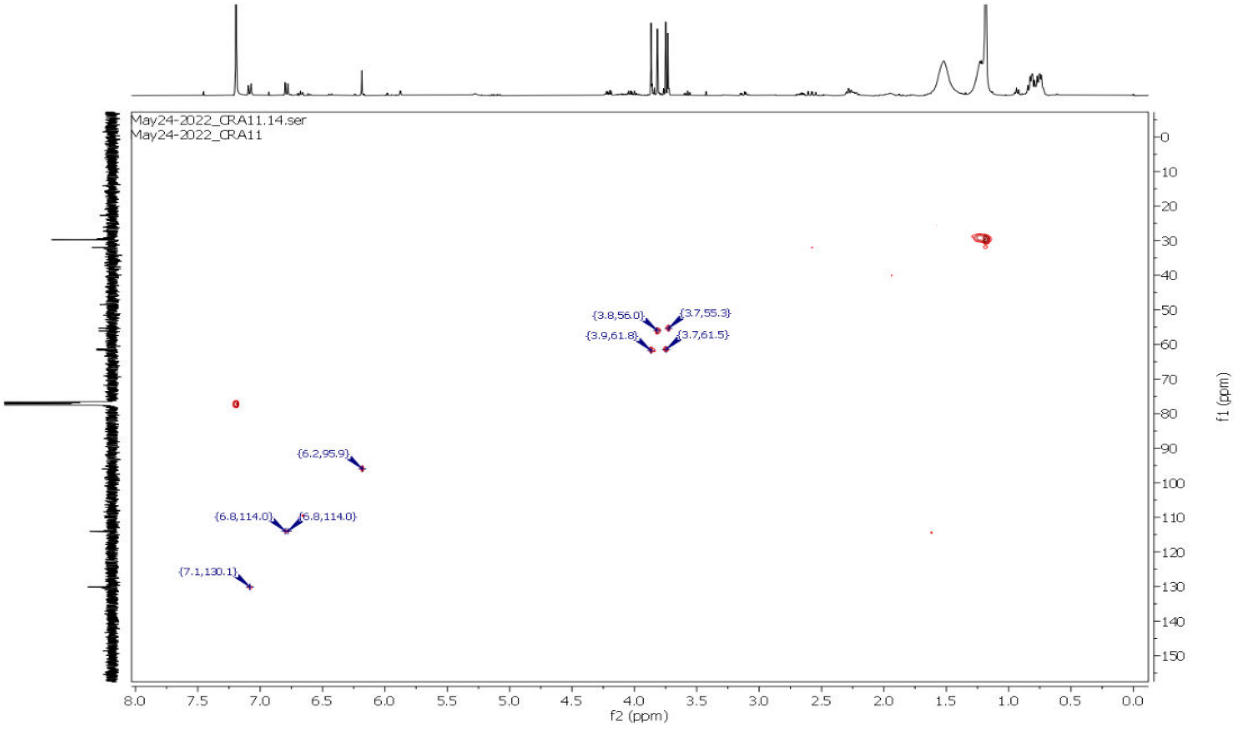

Appendix 4F: HMBC correlation of 6-hydroxy-3,5,7,4′-tetramethoxyflavone (**226**).

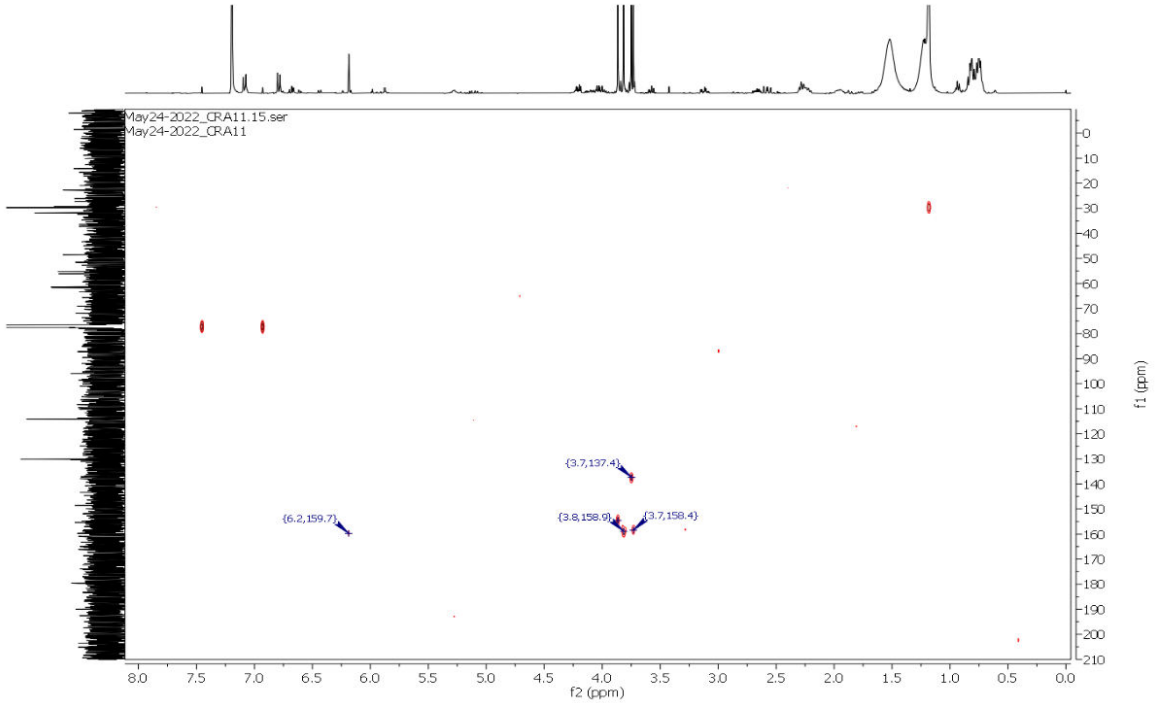

Appendix 5A: ^{1}H NMR (400 MHz, $CDCl_3$) spectrum of penicilloitins B (**227**).

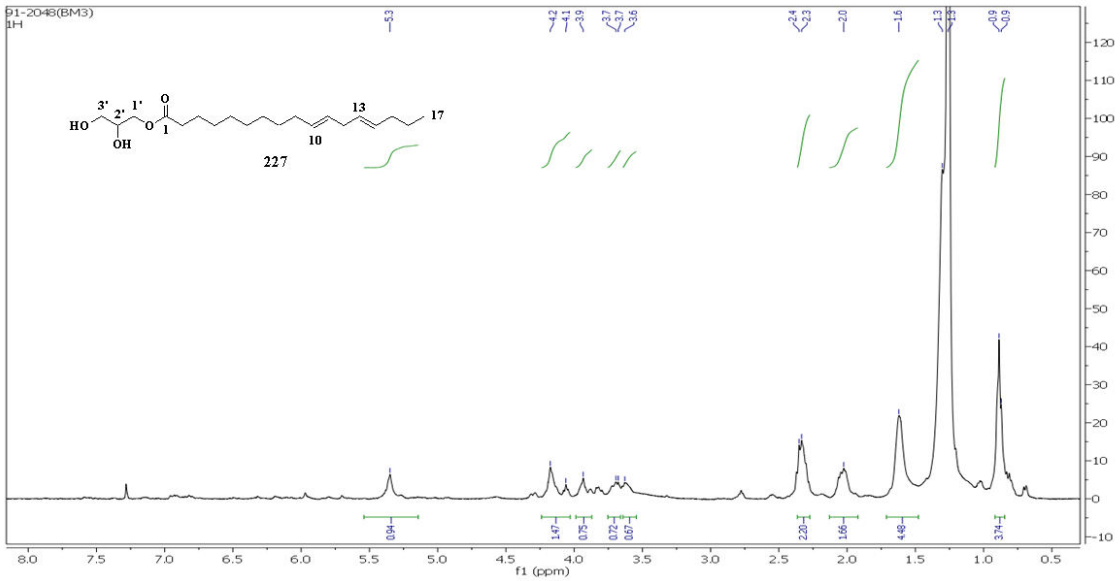

Appendix 5B: ^{13}C NMR (101 MHz, $CDCl_3$) spectrum of penicilloitins B (**227**).

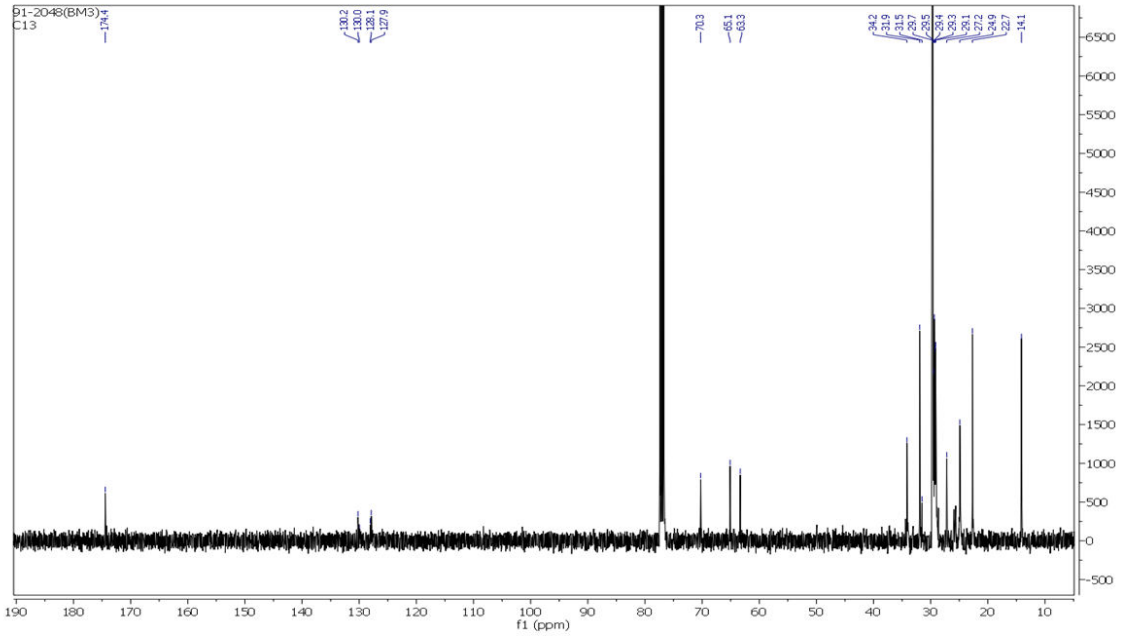

Appendix 5C: DEPT-135 NMR (101 MHz, $CDCl_3$) spectrum of penicilloitins B (**227**).

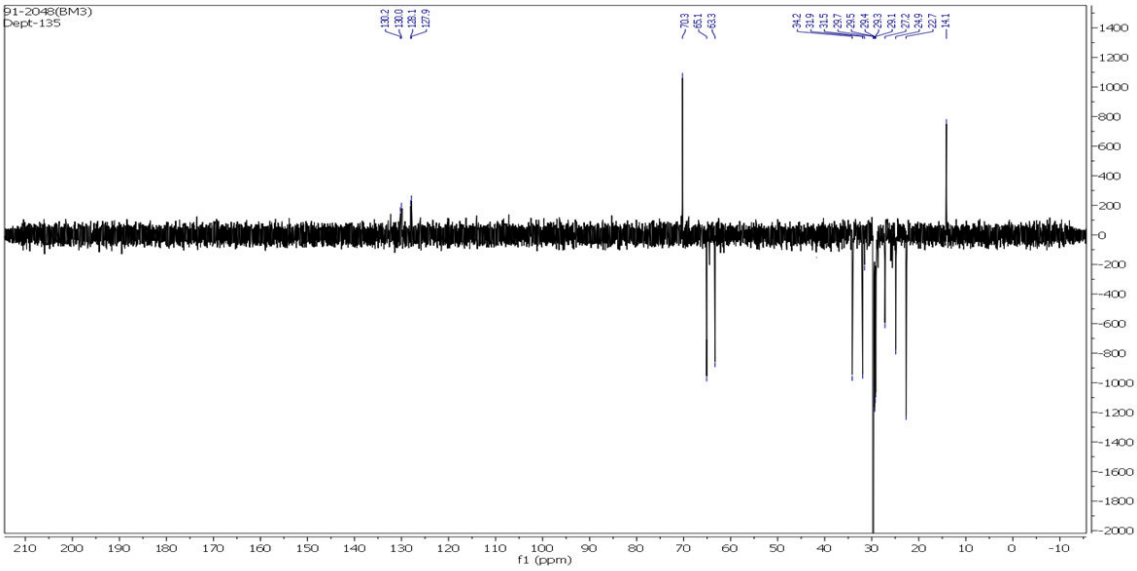

Appendix 6A: ^{1}H NMR (400 MHz, $CDCl_3$) spectrum of *para*-methoxy benzoyl-sitosterol-3-O-*β*-D-glucopyranoside (**228**).

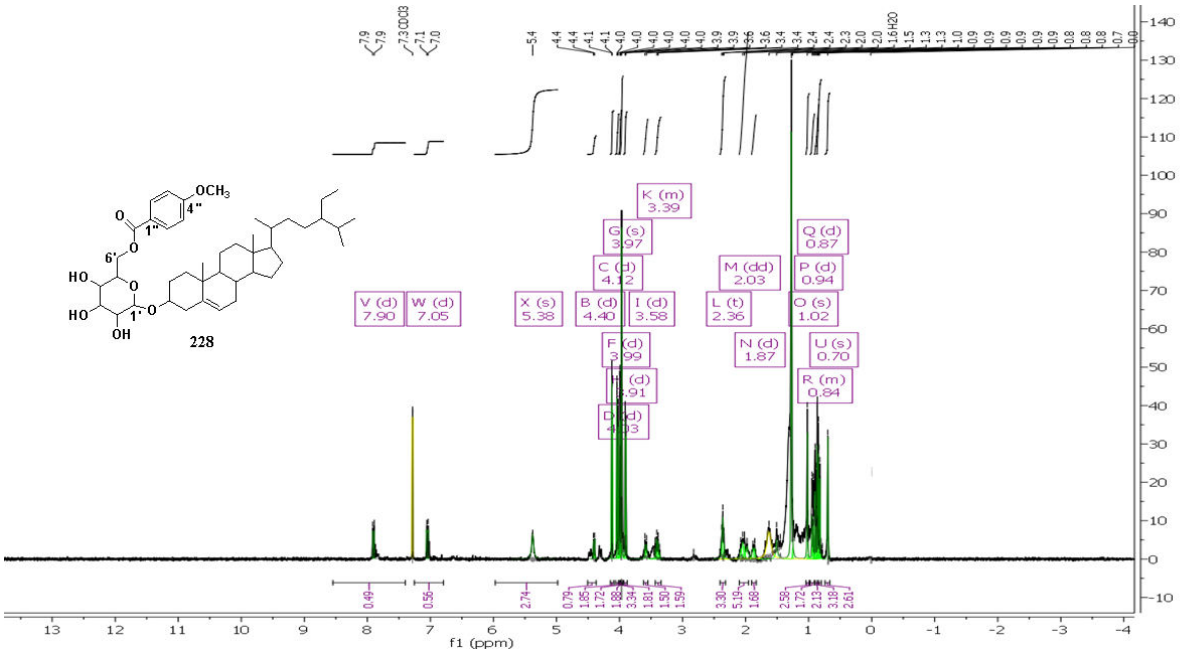

Appendix 6B: ^{13}C NMR (101 MHz, $CDCl_3$) spectrum of *para*-methoxy benzoyl-sitosterol-3-O-*β*-D-glucopyranoside (**228**).

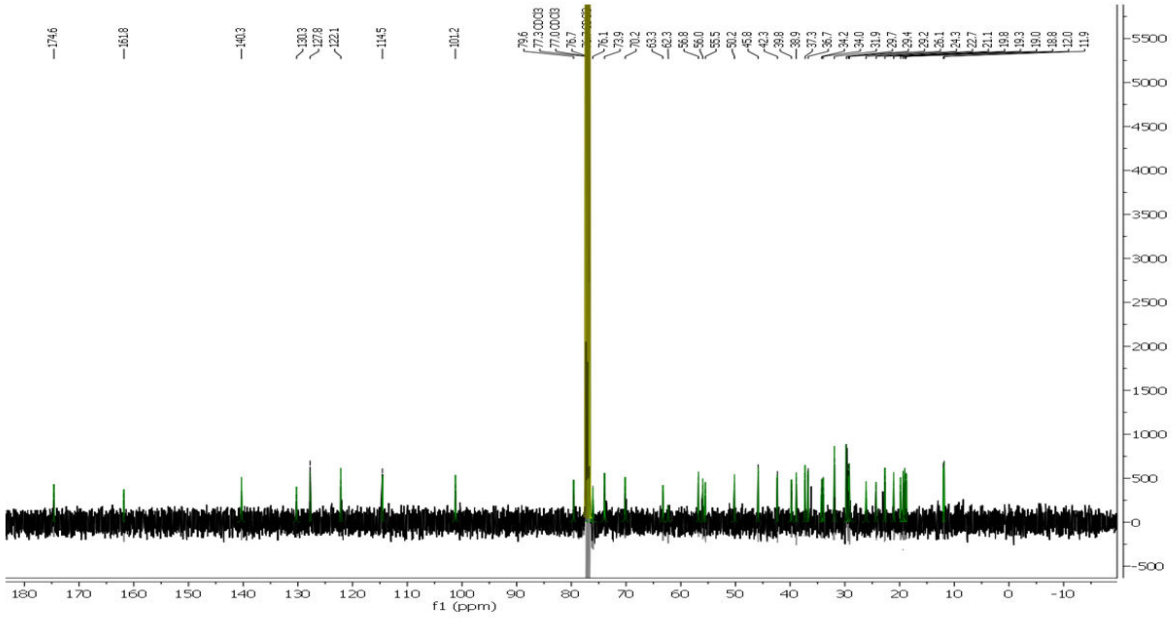

Appendix 6C: DEPT-135 NMR (101 MHz, $CDCl_3$) spectrum of *para*-methoxy benzoyl-sitosterol-3-O-β-D-glucopyranoside (**228**).

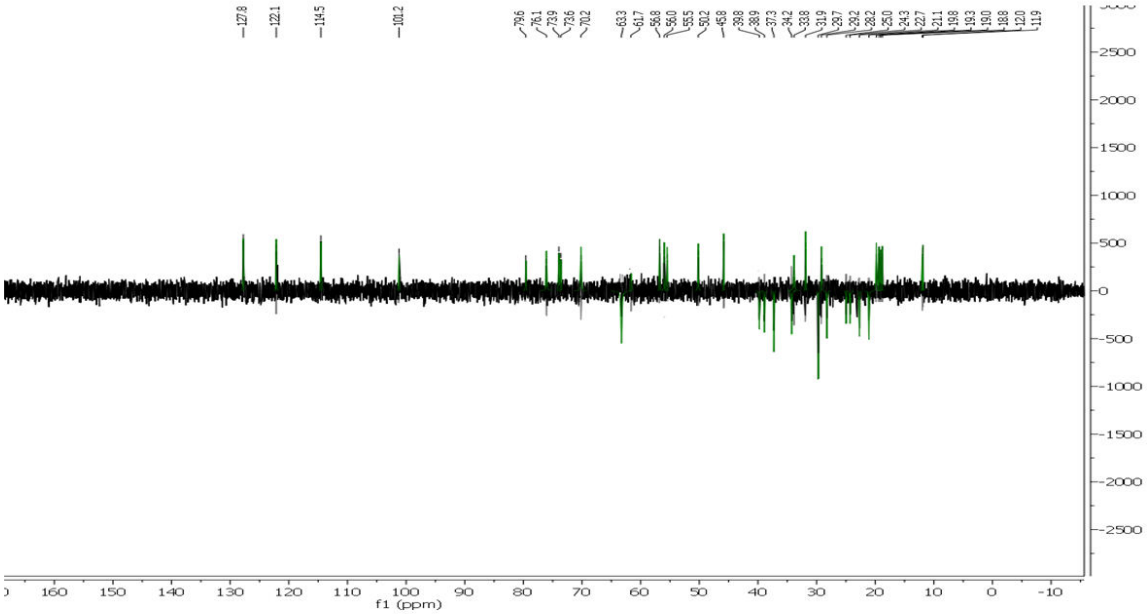

Appendix 7A: ^1H NMR (400 MHz, $CDCl_3$) spectrum of ethyl (E)-octadec-9-enoate (**229**).

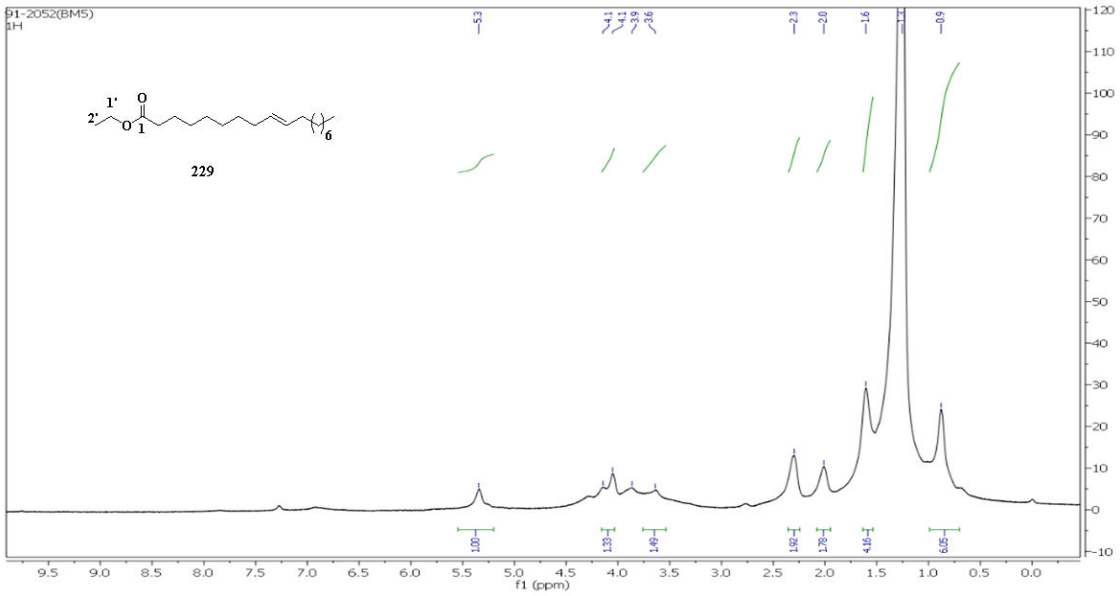

Appendix 7B: ^{13}C NMR (101 MHz, $CDCl_3$) spectrum of ethyl (E)-octadec-9-enoate (**229**).

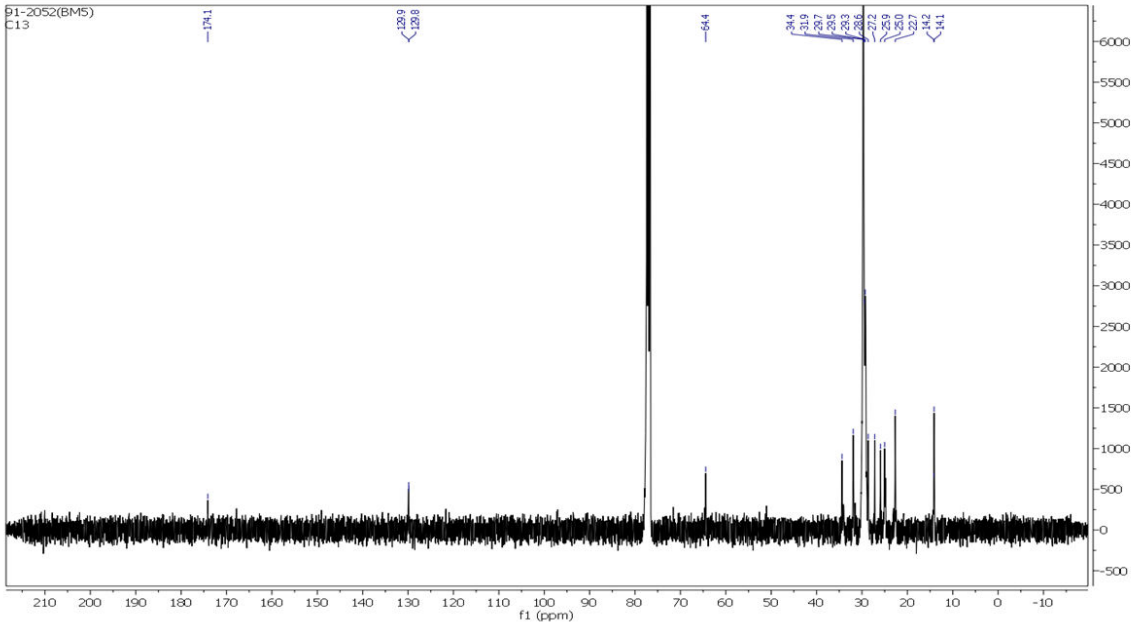

Appendix 7C: DEPT-135 NMR (101 MHz, $CDCl_3$) spectrum of ethyl (E)-octadec-9-enoate (**229**).

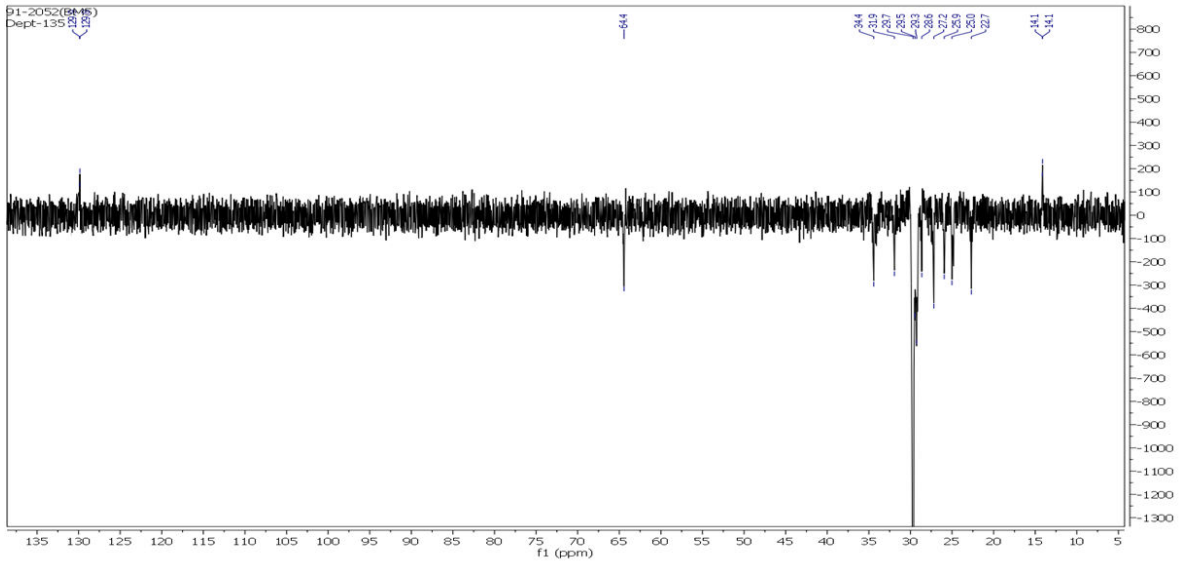

Appendix 8A: ^{1}H NMR (400 MHz, MeOD) spectrum of sucrose (**230**).

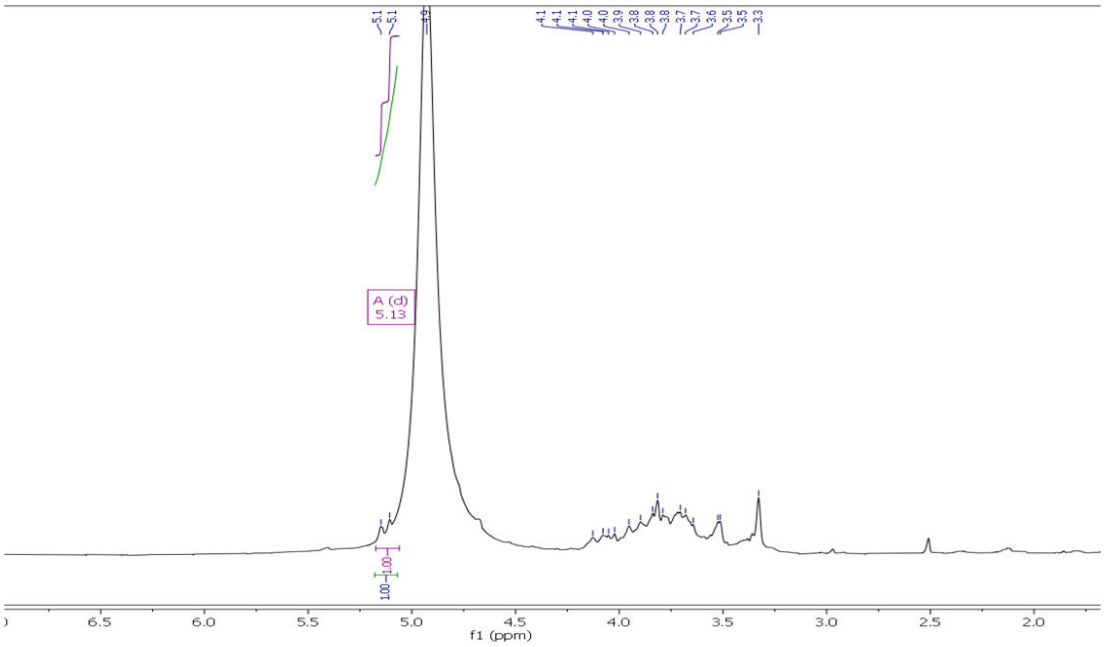

Appendix 8B: ^{13}C NMR (101 MHz, MeOD) spectrum of sucrose (**230**).

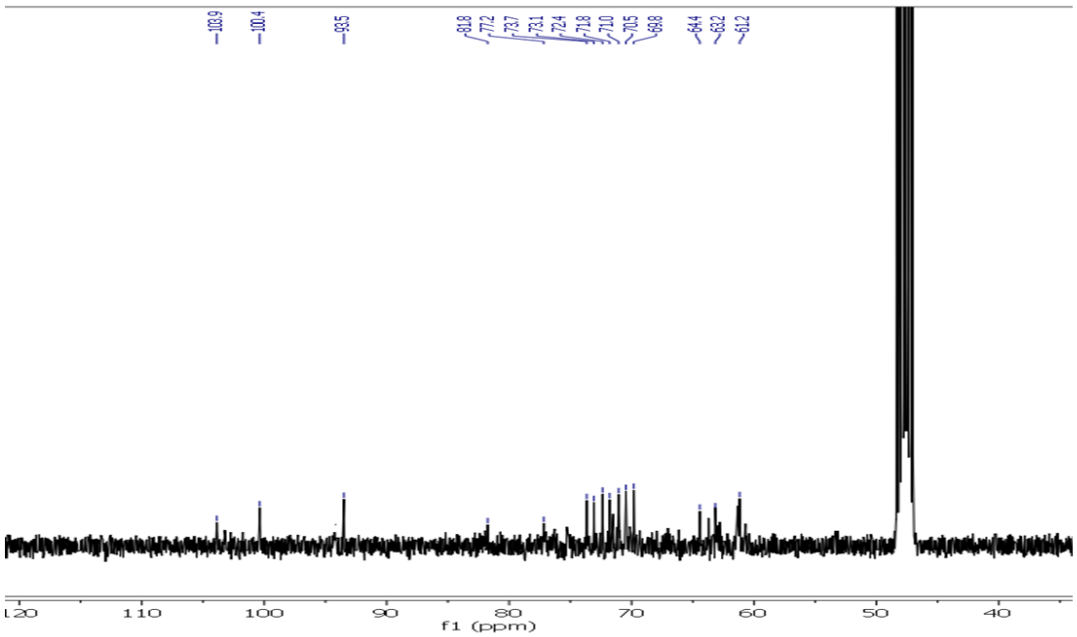

Appendix 8C: DEPT-135 NMR (101 MHz, MeOD) spectrum of sucrose (**230**).

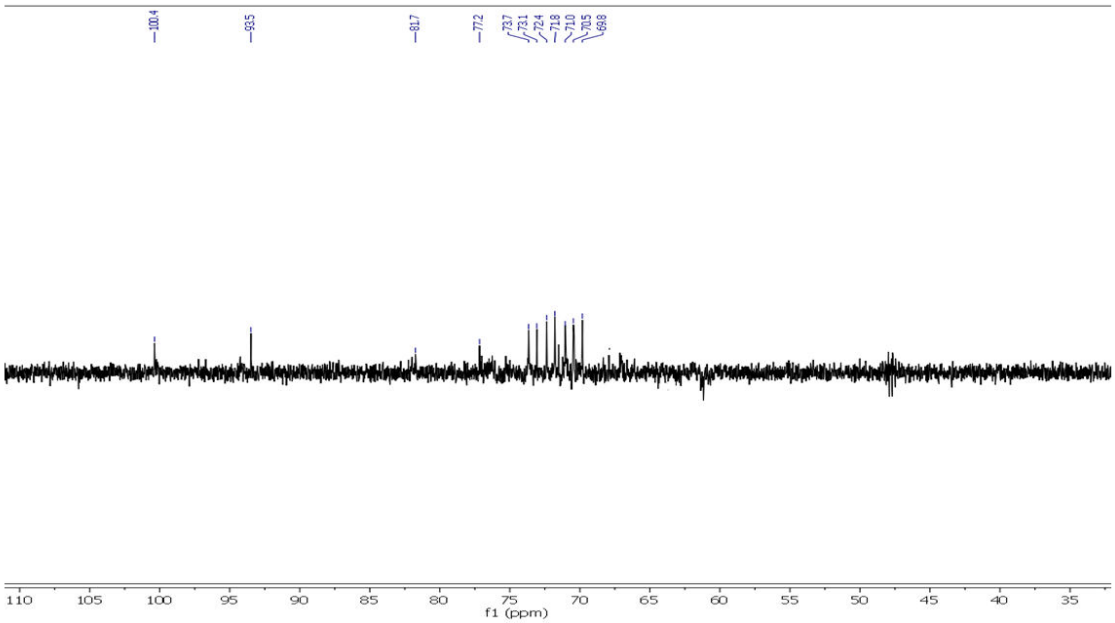

Appendix 9A: ^{1}H NMR (400 MHz, $CDCl_3$) spectrum of calotroproceryl acetate A (96).

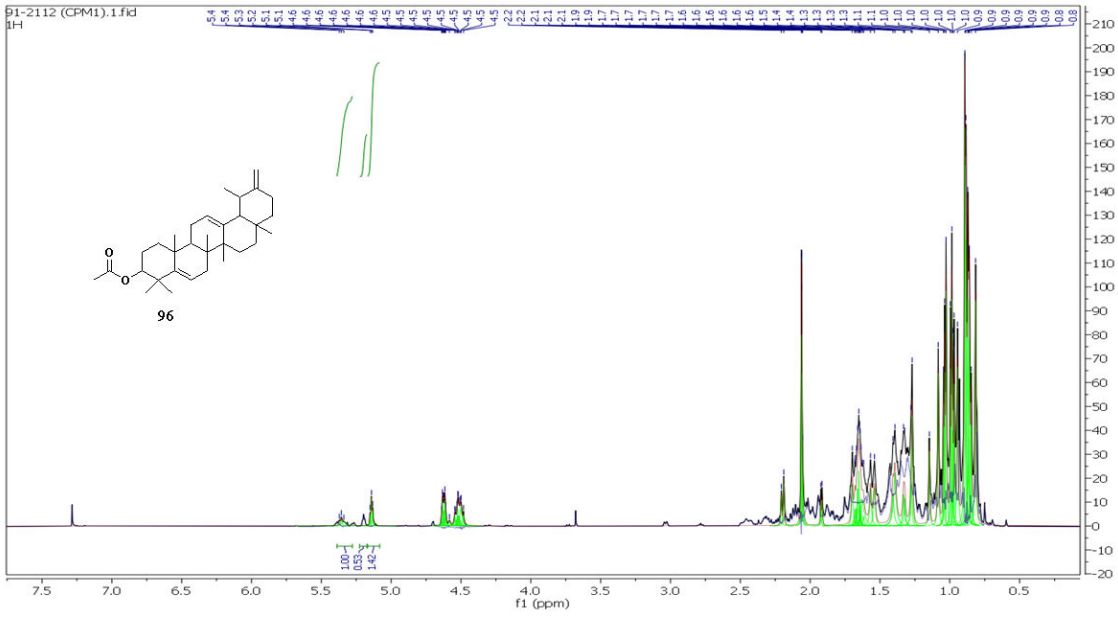

Appendix 9B: ^{13}C NMR (101 MHz, $CDCl_3$) spectrum of calotroproceryl acetate A (**96**).

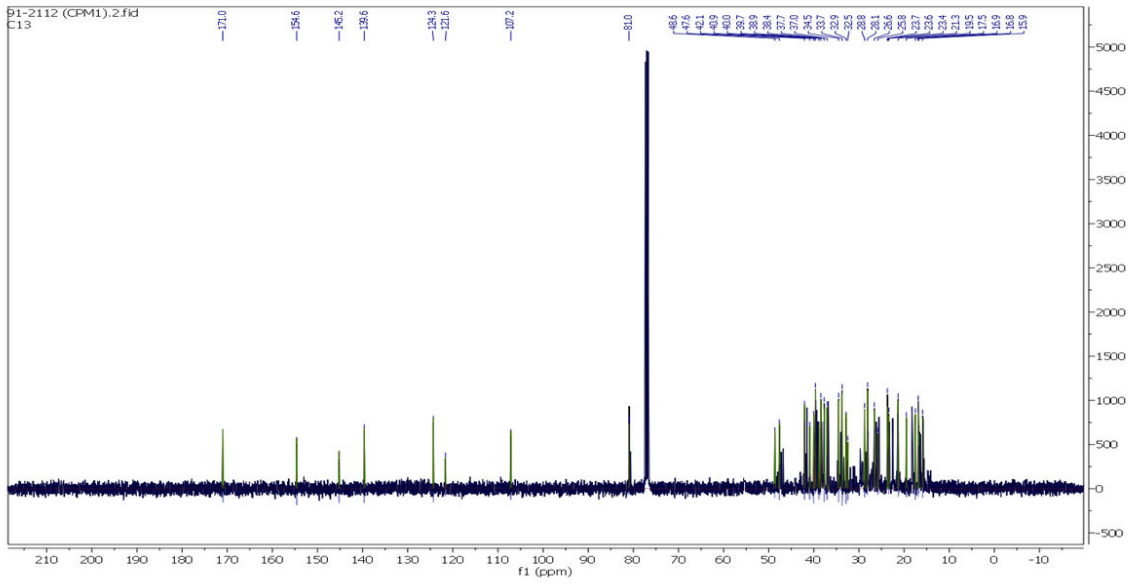

Appendix 9C: DEPT-135 NMR (101 MHz, $CDCl_3$) spectrum of calotroproceryl acetate A (96).

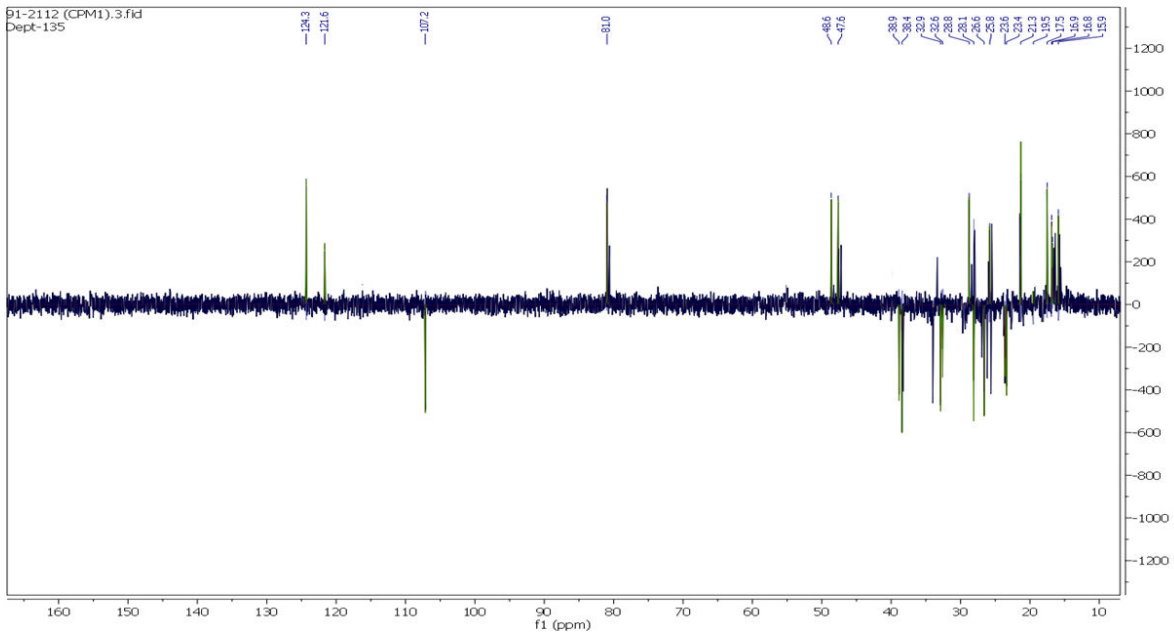

Appendix 10A: ^{1}H NMR (400 MHz, $CDCl_3$) spectrum of *β*-sitosteryl linoleate (**82**).

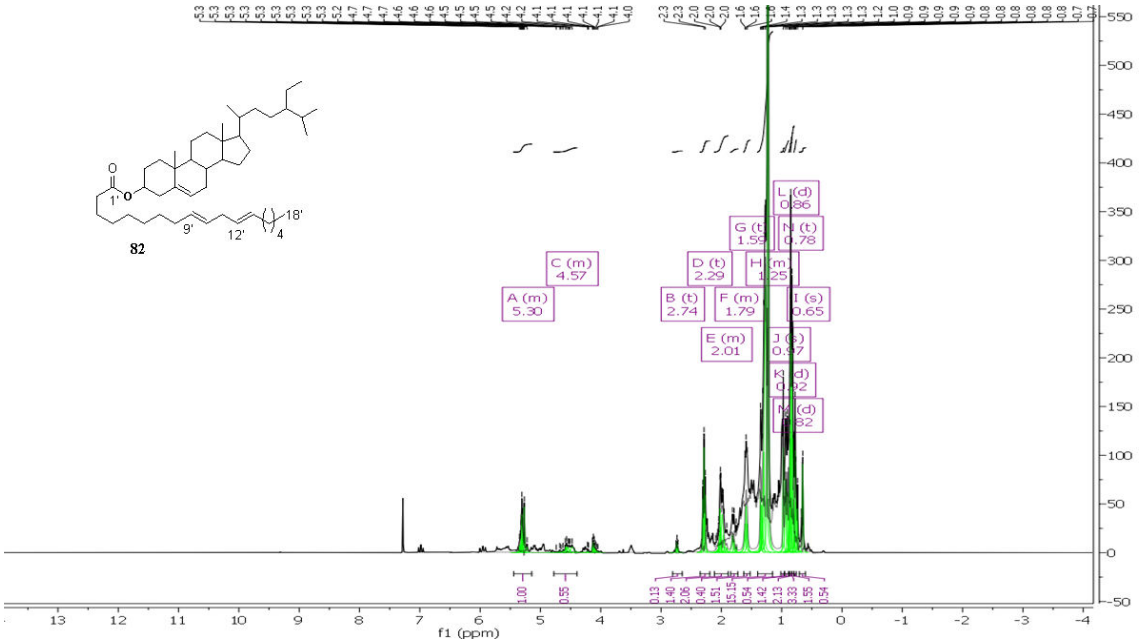

Appendix 10B: ^{13}C NMR (101 MHz, $CDCl_3$) spectrum of *β*-sitosteryl linoleate (**82**).

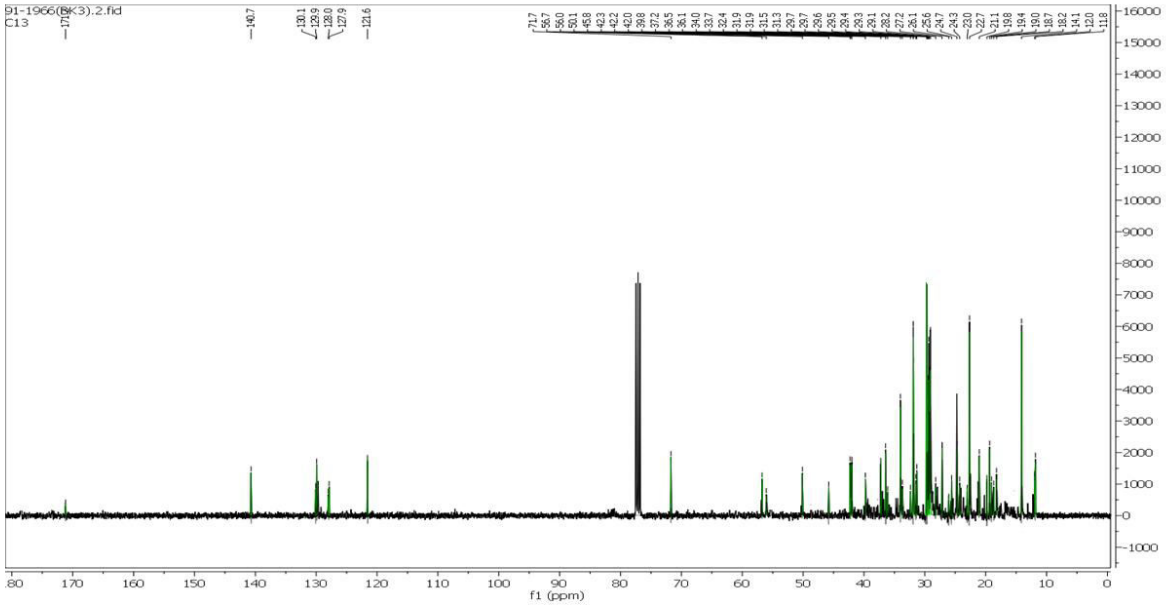

Appendix 10C: DEPT-135 NMR (101 MHz, $CDCl_3$) spectrum of β-sitosteryl linoleate (**82**).

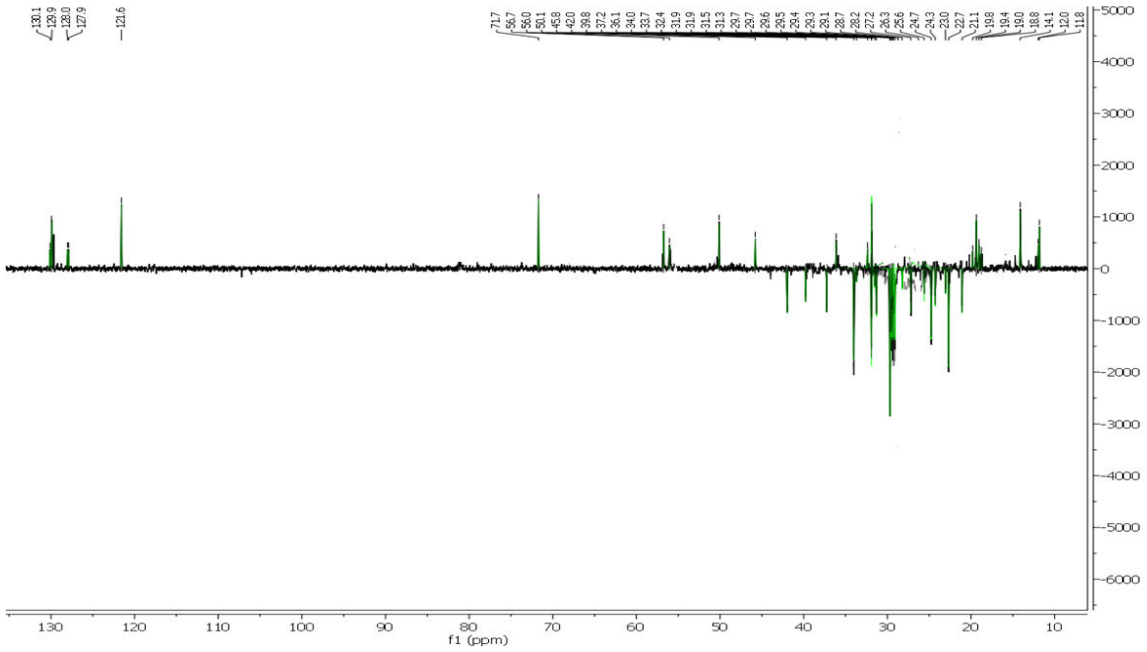

Appendix 11A: ^{1}H NMR (400 MHz, $CDCl_3$) spectrum of α-amyrin (**87**).

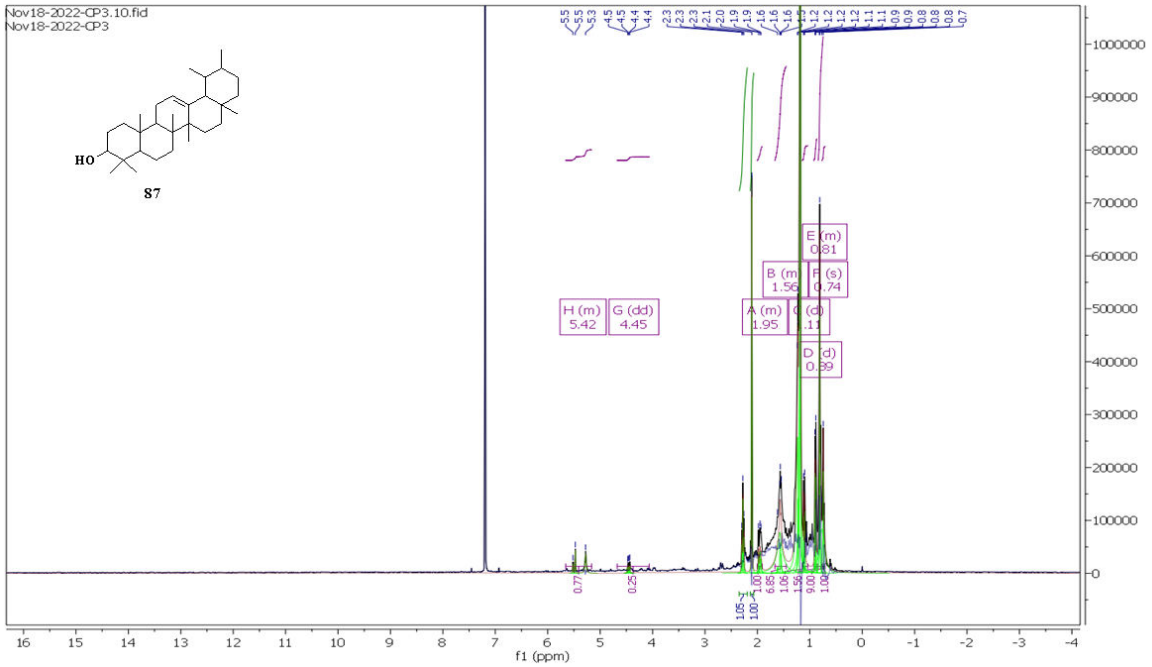

Appendix 11B: ^{13}C NMR (101 MHz, $CDCl_3$) spectrum of α-amyrin (**87**).

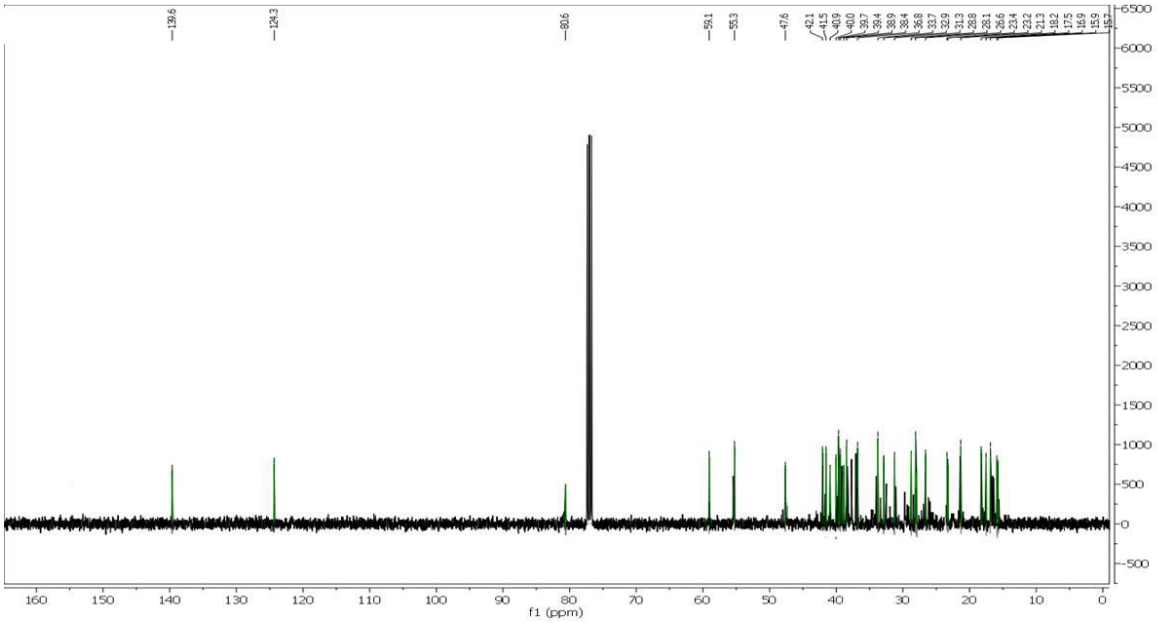

Appendix 11C: DEPT-135 NMR (101 MHz, $CDCl_3$) spectrum of α-amyrin (**87**).

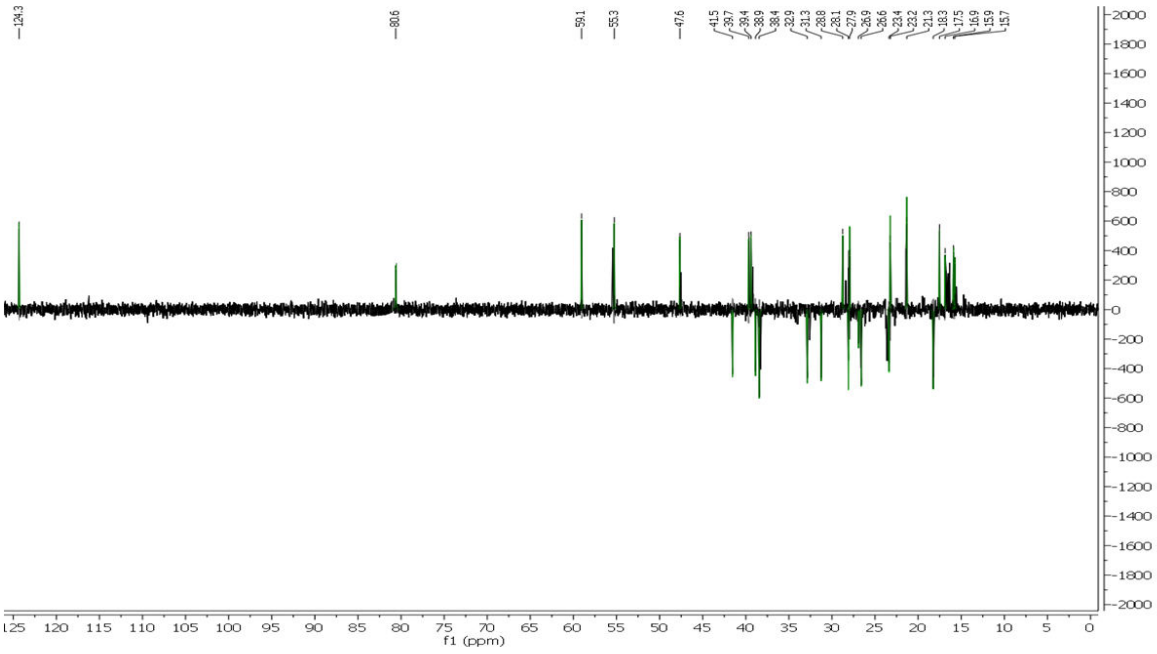

Appendix 12A: ^{1}H NMR (400 MHz, $CDCl_3$) spectrum of compound (**231**).

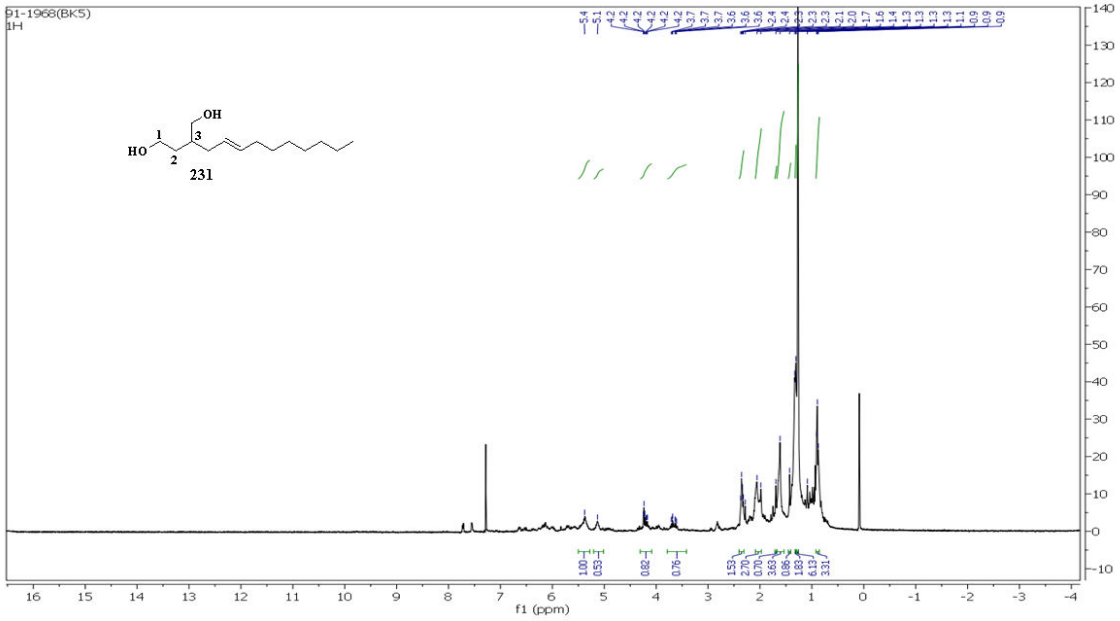

Appendix 12B: ^{13}C NMR (101 MHz, $CDCl_3$) spectrum of compound (**231**).

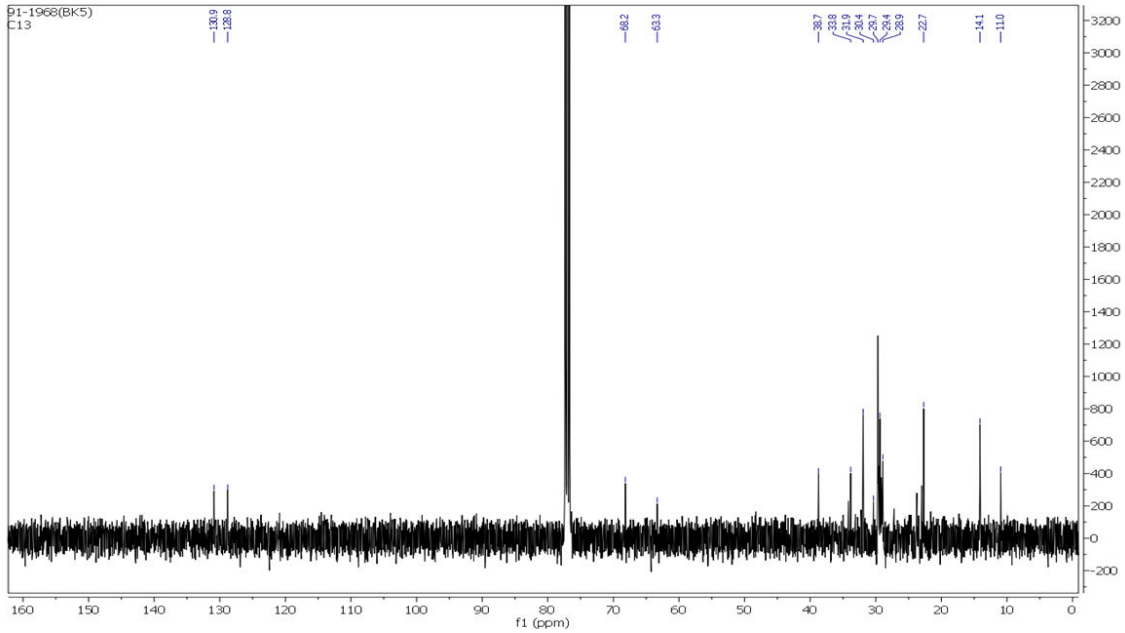

Appendix 12C: DEPT-135 NMR (101 MHz, $CDCl_3$) spectrum of compound (**231**).

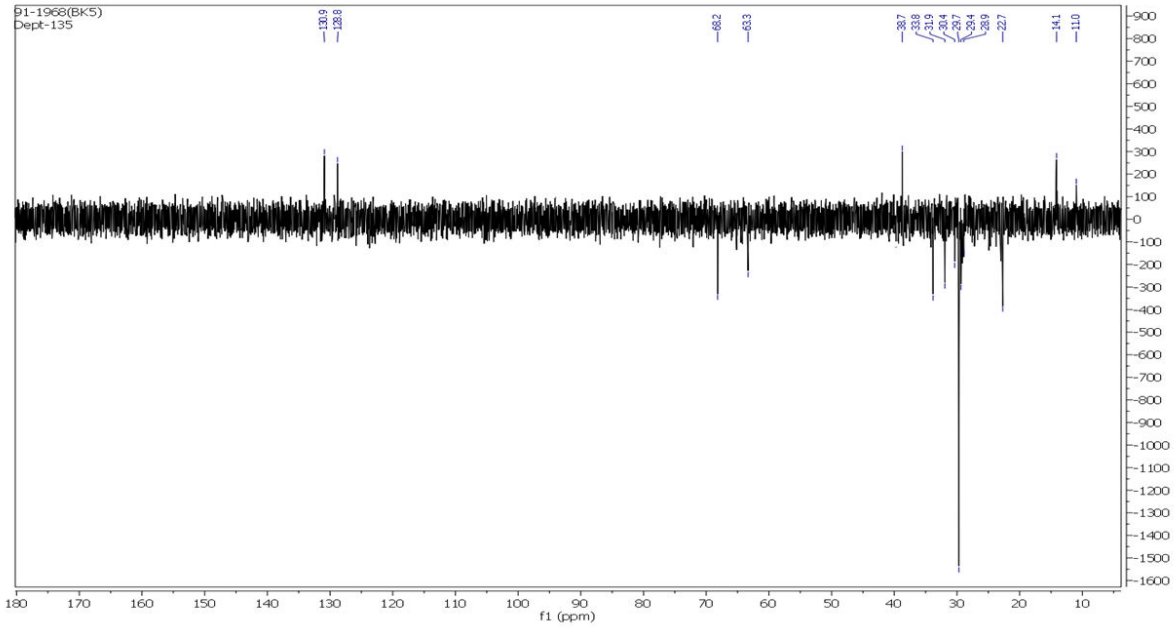

Appendix 13A: ^1H NMR (400 MHz, $CDCl_3$) spectrum of spinasterol acetate (**232**).

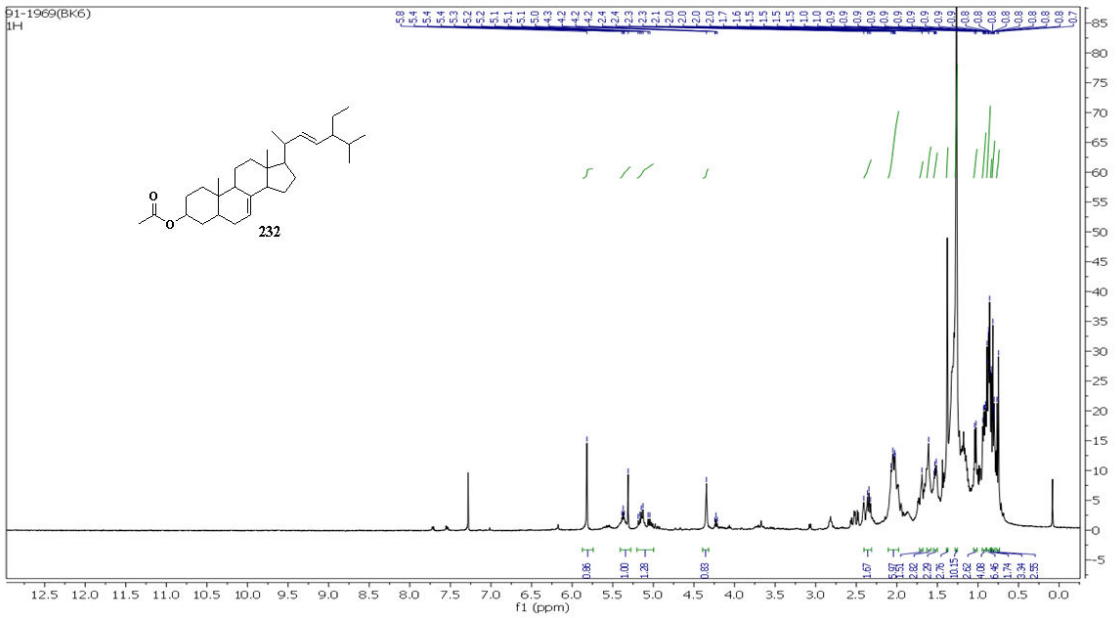

Appendix 13B: ^{13}C NMR (101 MHz, $CDCl_3$) spectrum of spinasterol acetate (**232**).

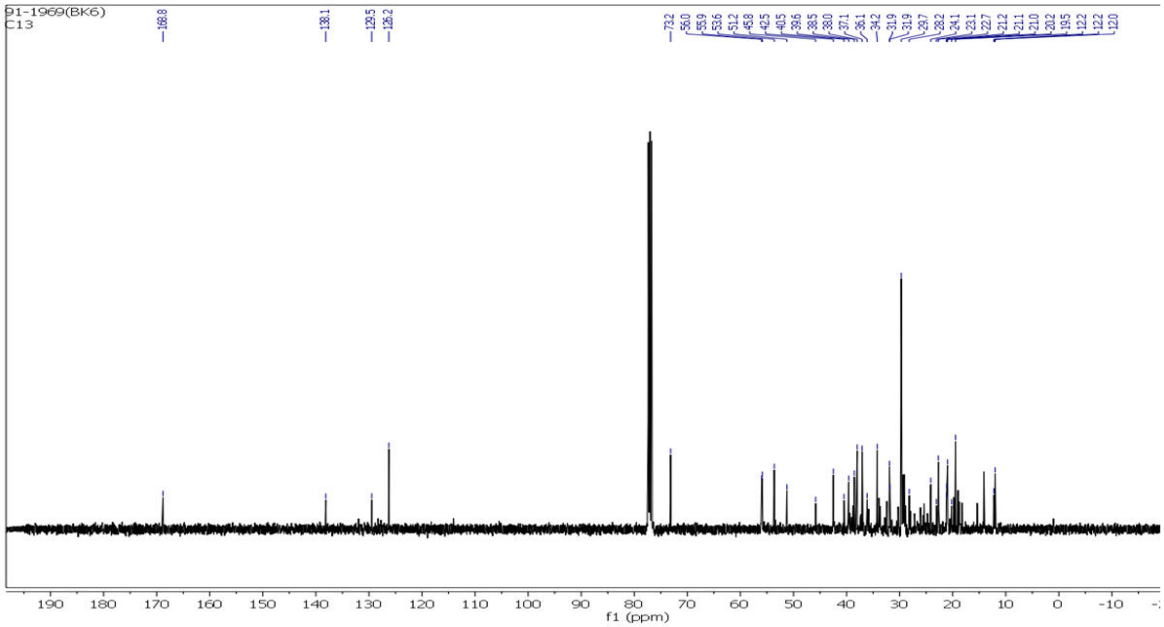

Appendix 13C: DEPT-135 NMR (101 MHz, $CDCl_3$) spectrum of spinasterol acetate (**232**).

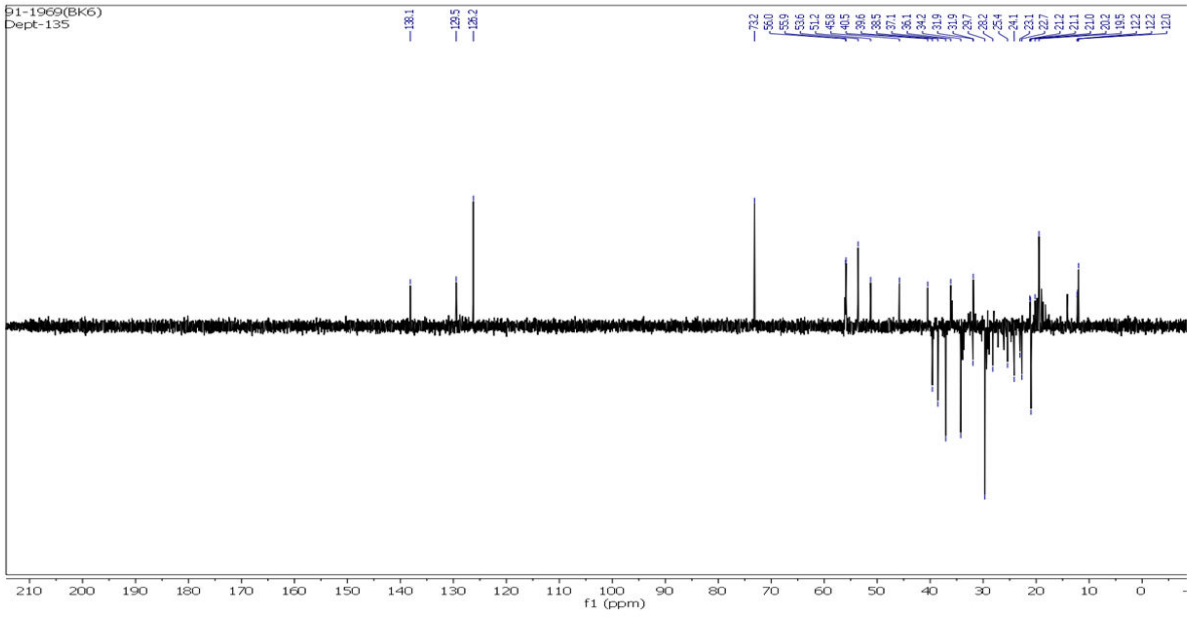

Appendix 14A: ^{1}H NMR (400 MHz, MeOD) spectrum of calotropursenol B (**233**).

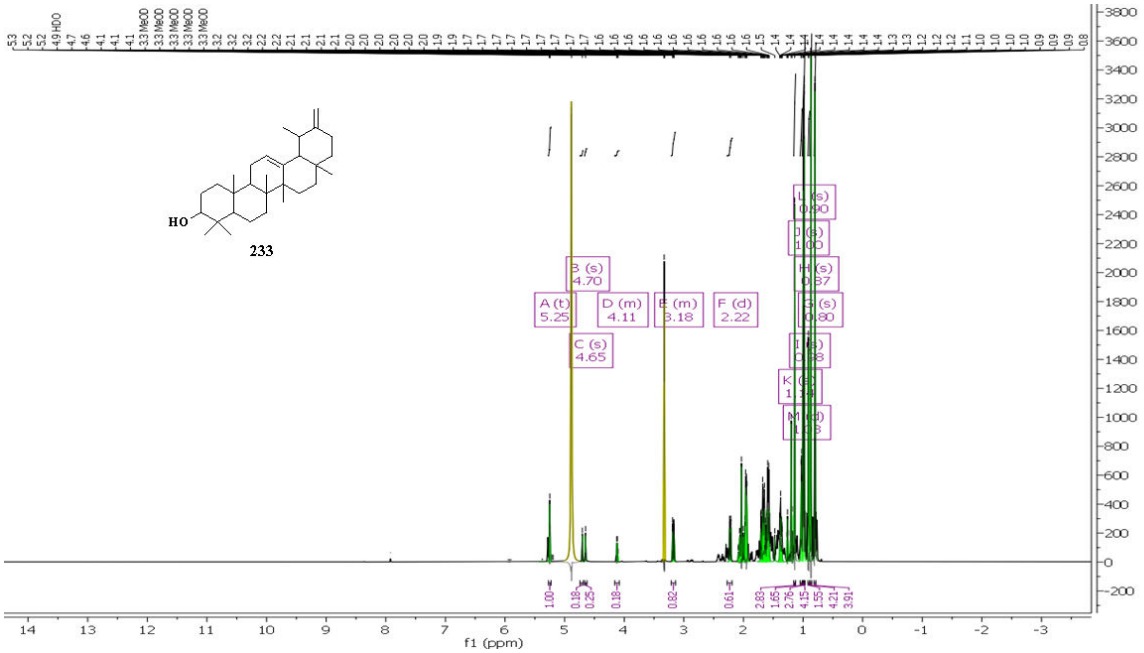

Appendix 14B: ^{13}C NMR (101 MHz, MeOD) spectrum of calotropursenol B (**233**).

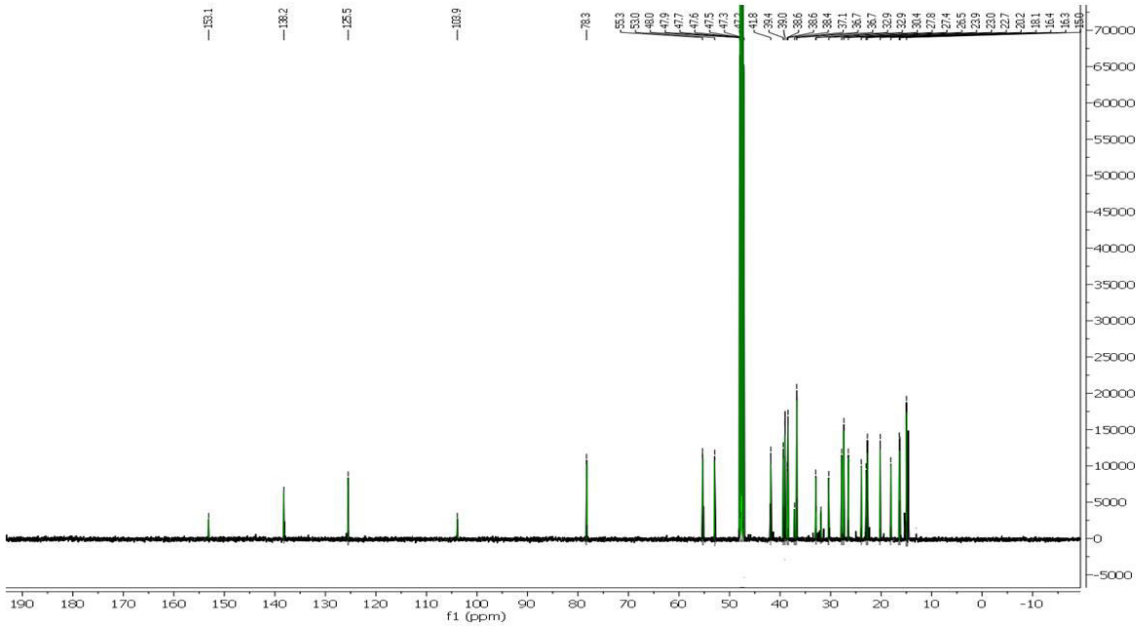

Appendix 14C: DEPT-135 NMR (101 MHz, MeOD) spectrum of calotropursenol B (**233**).

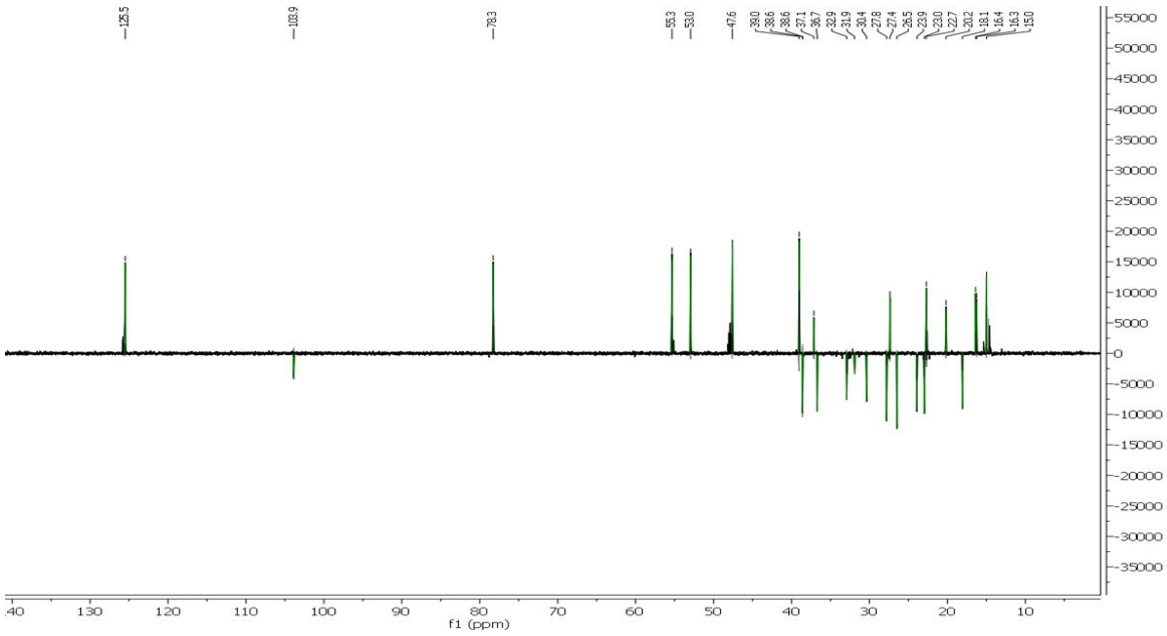

Appendix 15A: ^{1}H NMR (400 MHz, $CDCl_3$) spectrum of calotroprocerol A (**97**).

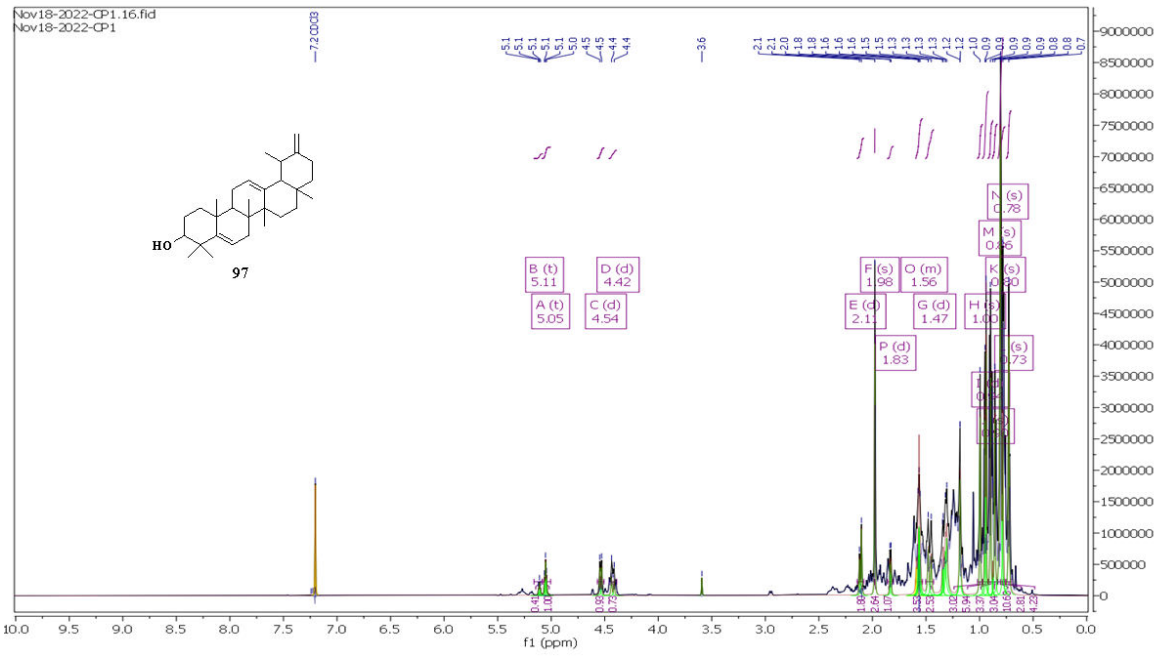

Appendix 15B: ^{13}C NMR (101 MHz, $CDCl_3$) spectrum of calotroprocerol A (**97**).

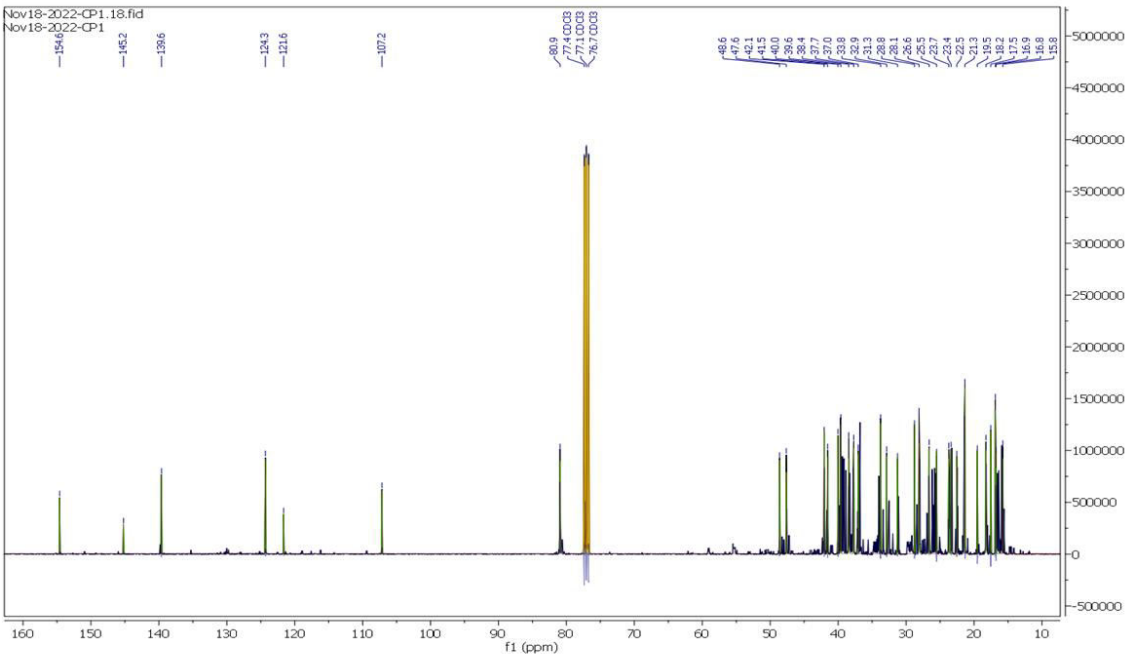

Appendix 15C: DEPT-135 NMR (101 MHz, $CDCl_3$) spectrum of calotroprocerol A (**97**).

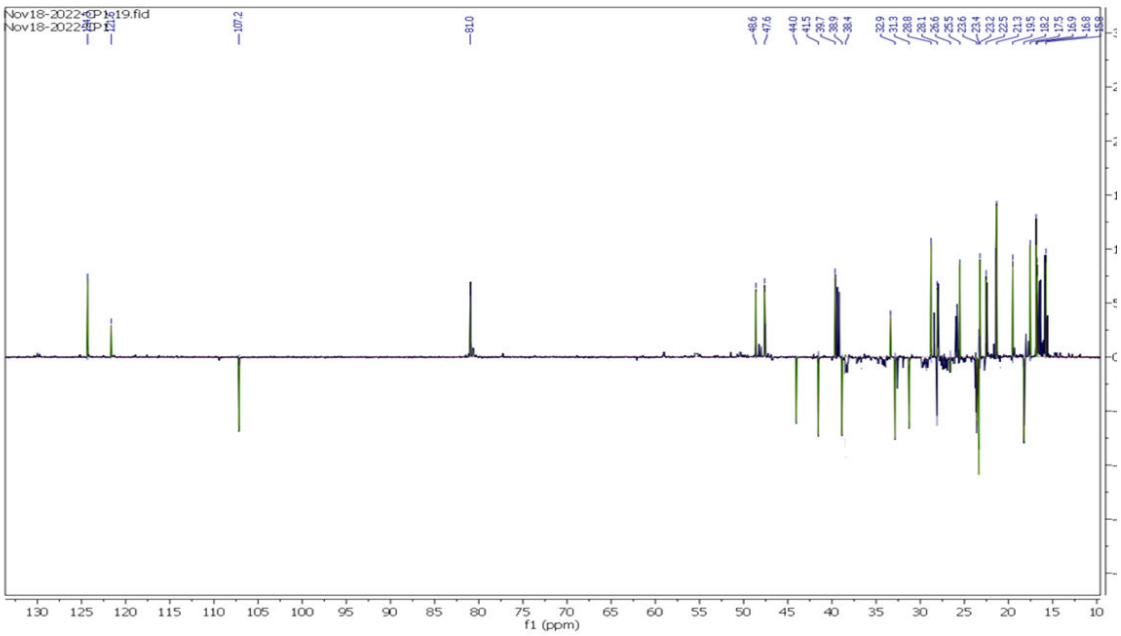

Appendix 15D: ^{1}H-^{1}H COSY spectrum of calotroproceroⅼ A (**97**).

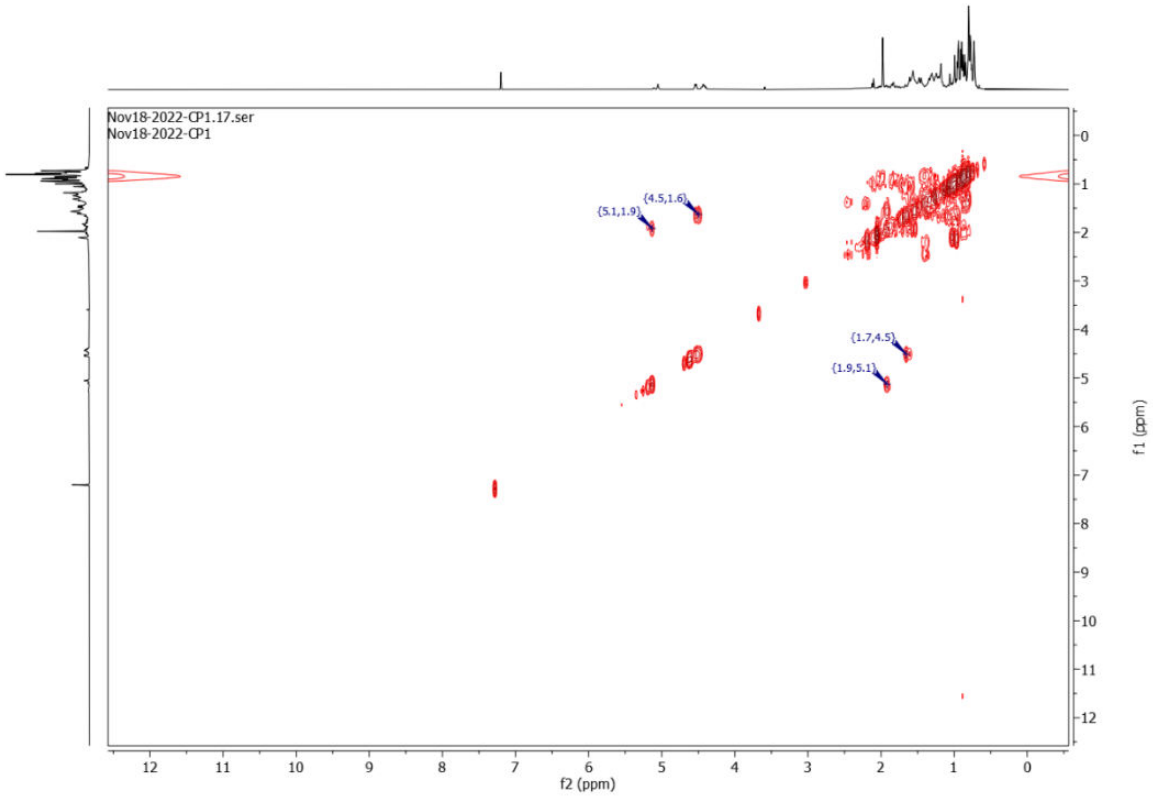

Appendix 15E: HSQC correlation of calotroproceroⅼ A (**97**).

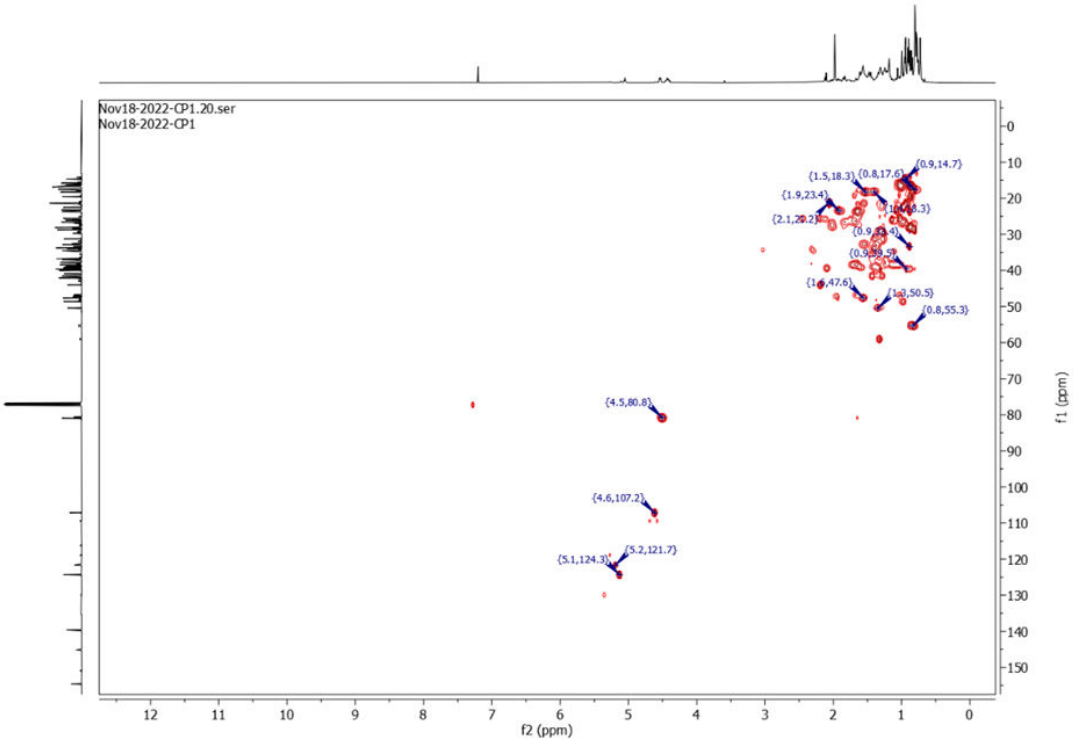

Appendix 15F: HMBC correlation of calotroproceroⅼ A (**97**).

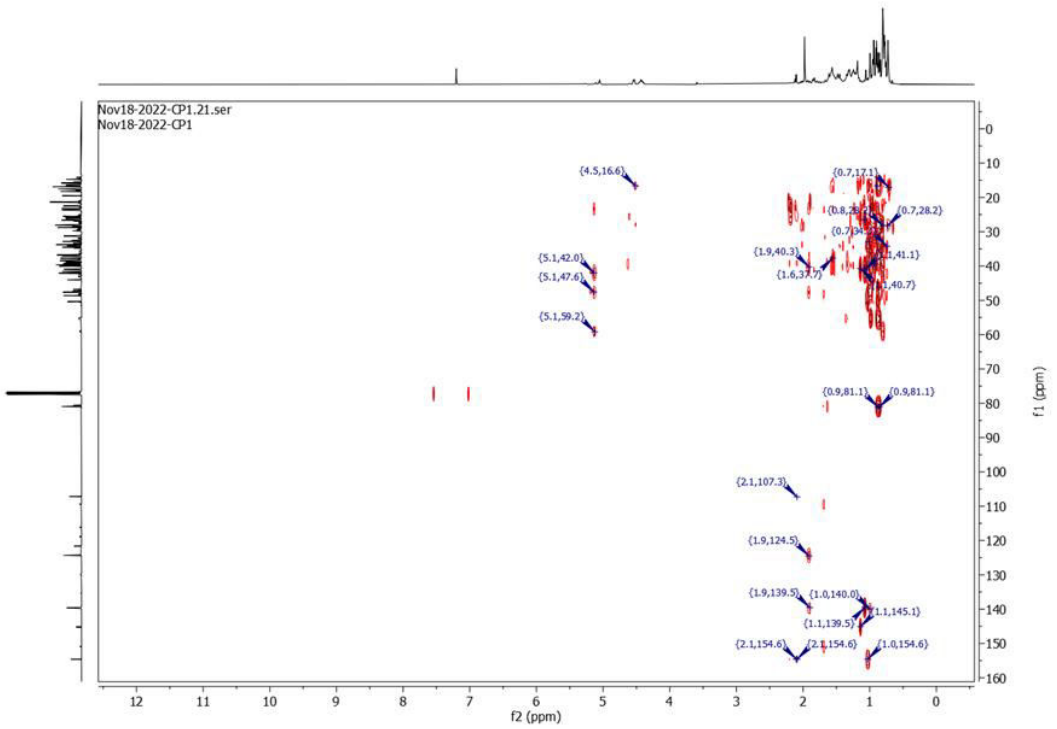

Appendix 16A: ^{1}H NMR (400 MHz, $CDCl_3$) spectrum of 11-oxo-α-amyrin ethylated (**234**).

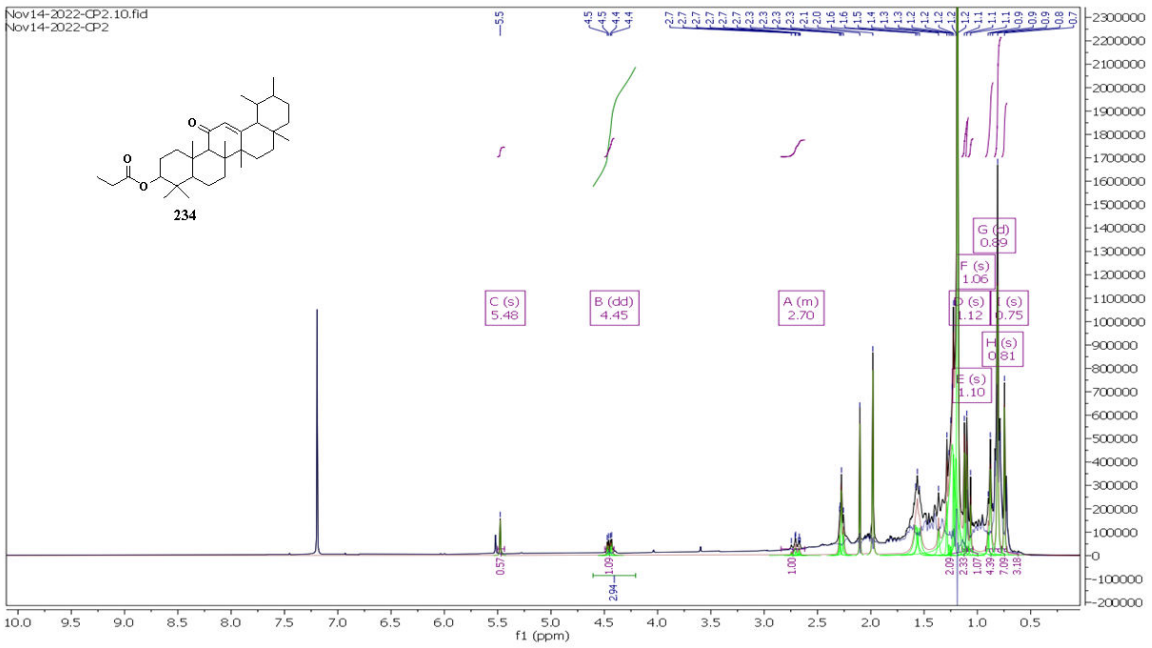

Appendix 16B: ^{13}C NMR (101 MHz, $CDCl_3$) spectrum of 11-oxo-α-amyrin ethylated (**234**).

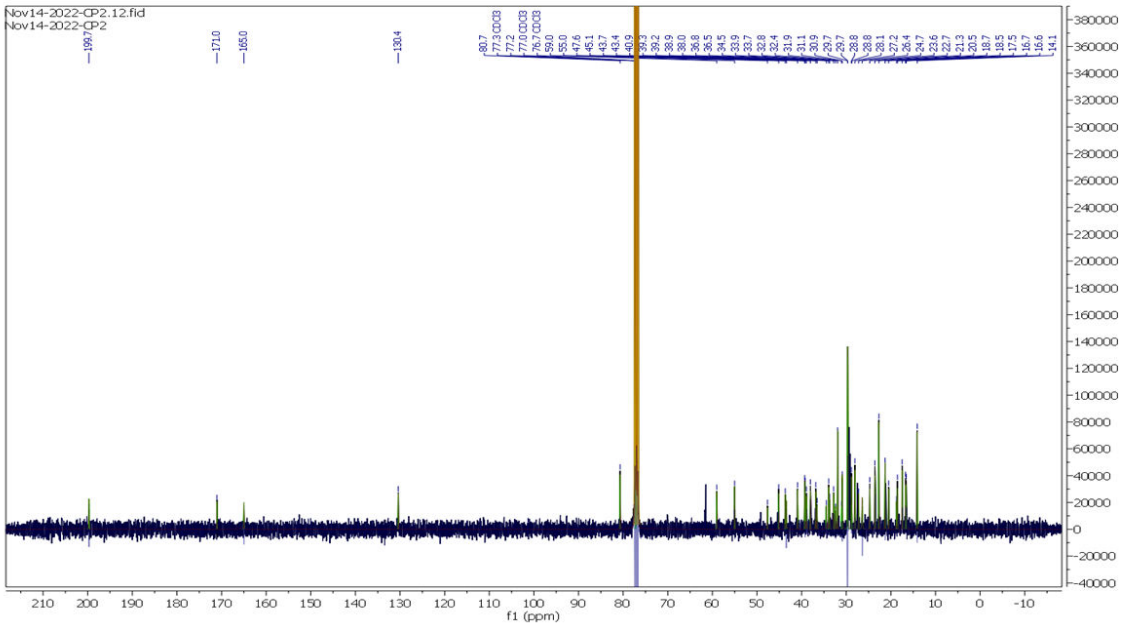

Appendix 16C: DEPT-135 NMR (101 MHz, $CDCl_3$) spectrum of 11-oxo-α-amyrin ethylated (**234**).

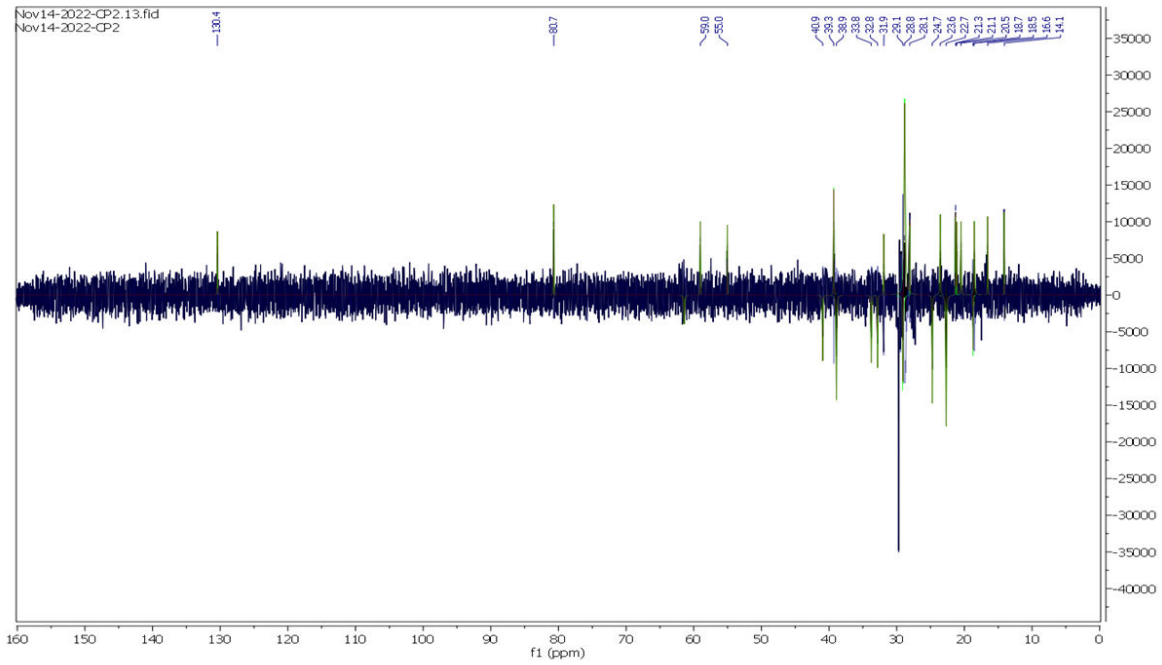

Appendix 16D: ^{1}H-^{1}H COSY spectrum of 11-oxo-α-amyrin ethylated (**234**).

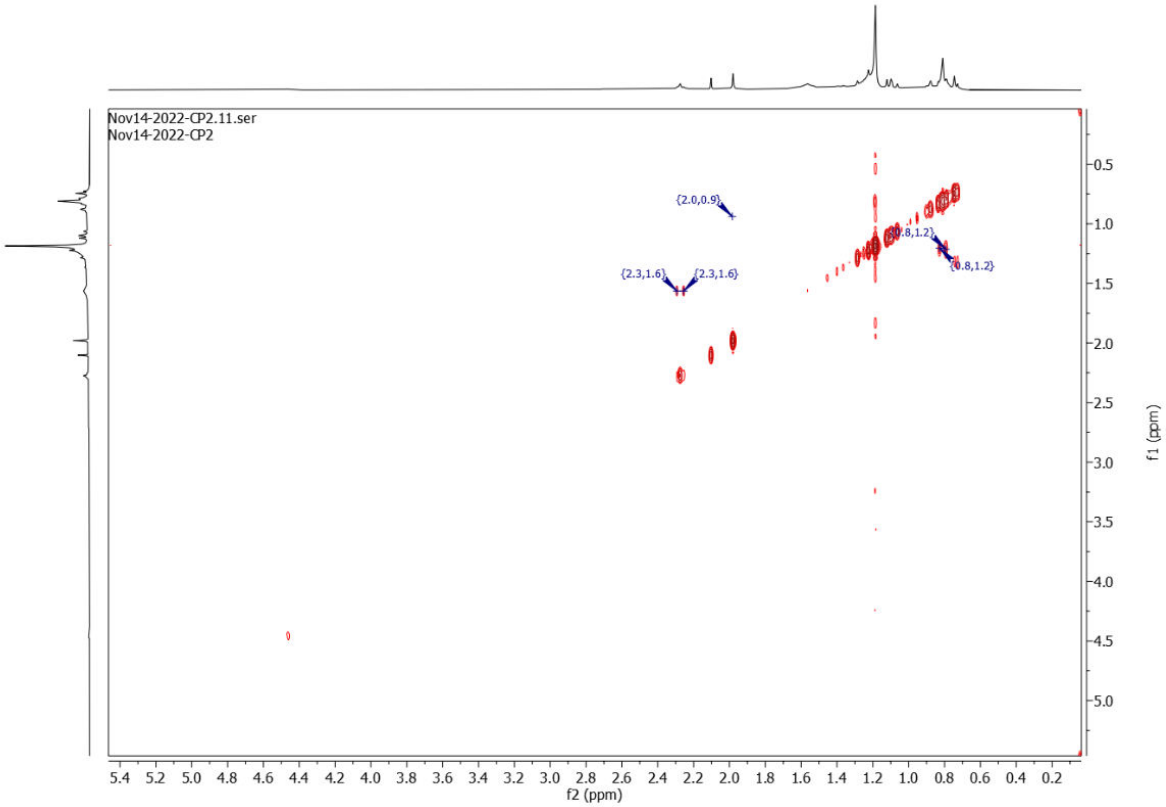

Appendix 16E: HSQC correlation of 11-oxo-α-amyrin ethylated (**234**).

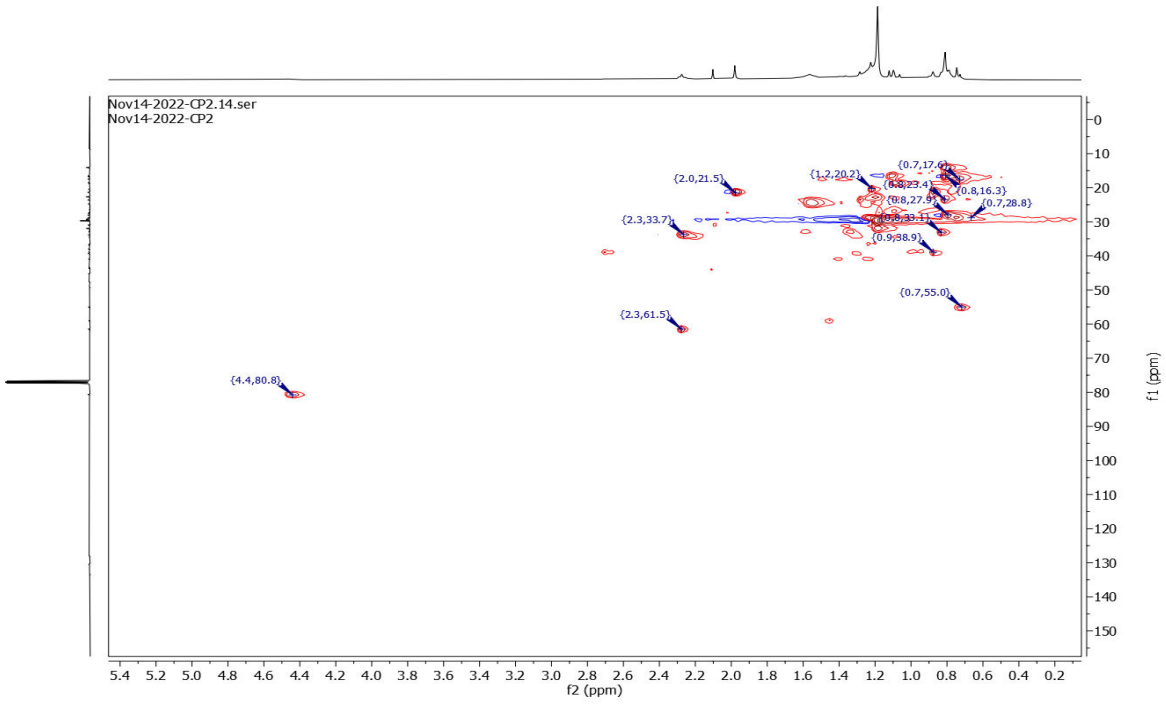

Appendix 16F: HMBC correlation of 11-oxo-α-amyrin ethylated (**234**).

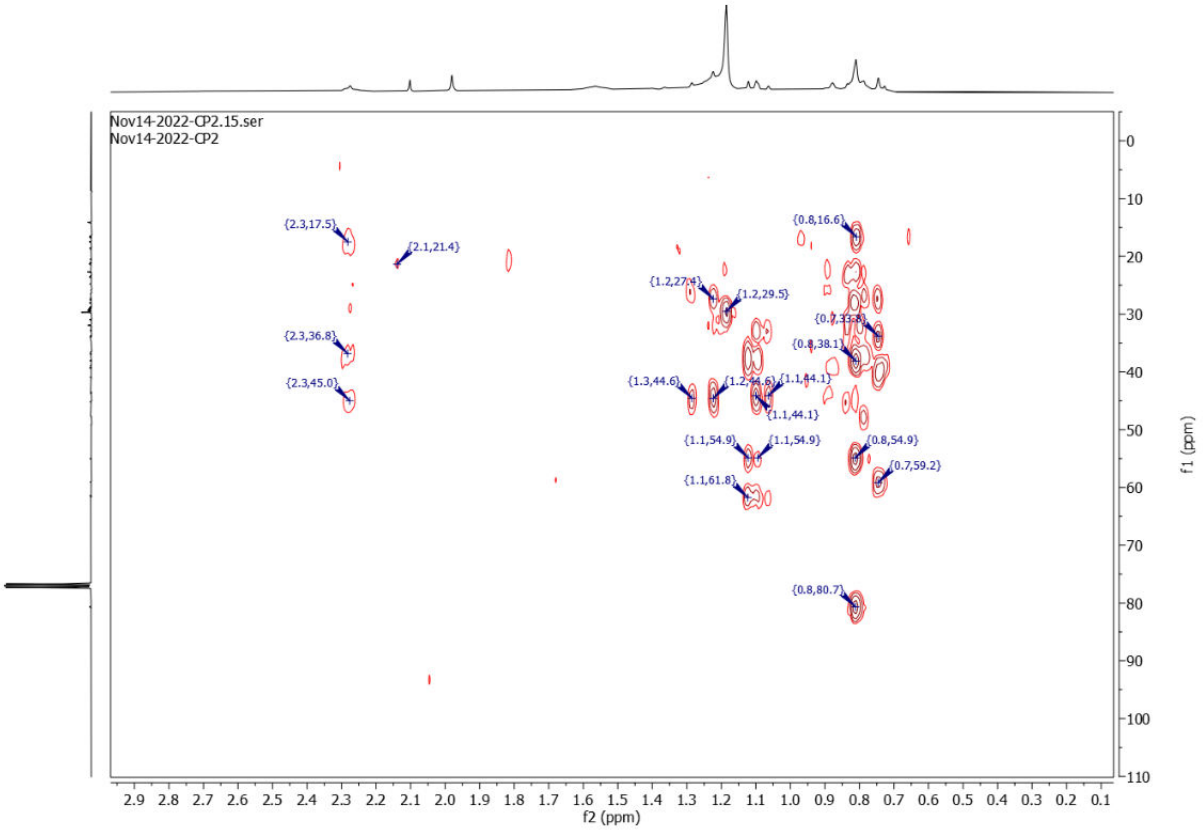

Appendix 17A: ^{1}H NMR (400 MHz, $CDCl_3$) spectrum of calotroprocerol B (**98**).

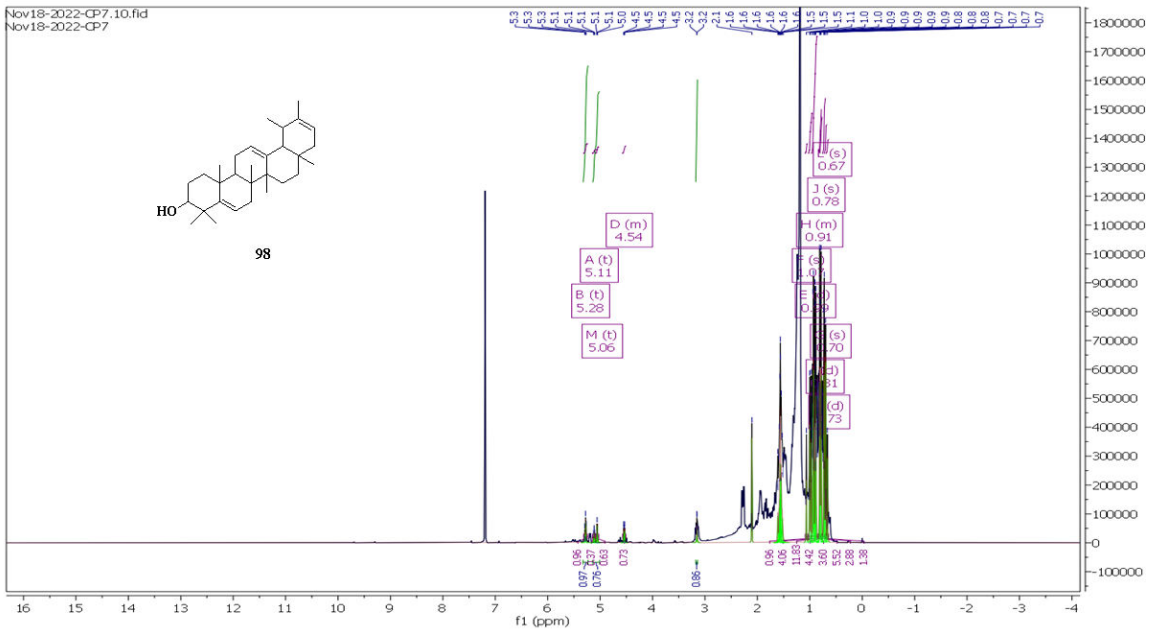

Appendix 17B: ^{13}C NMR (101 MHz, $CDCl_3$) spectrum of calotroprocerol B (**98**).

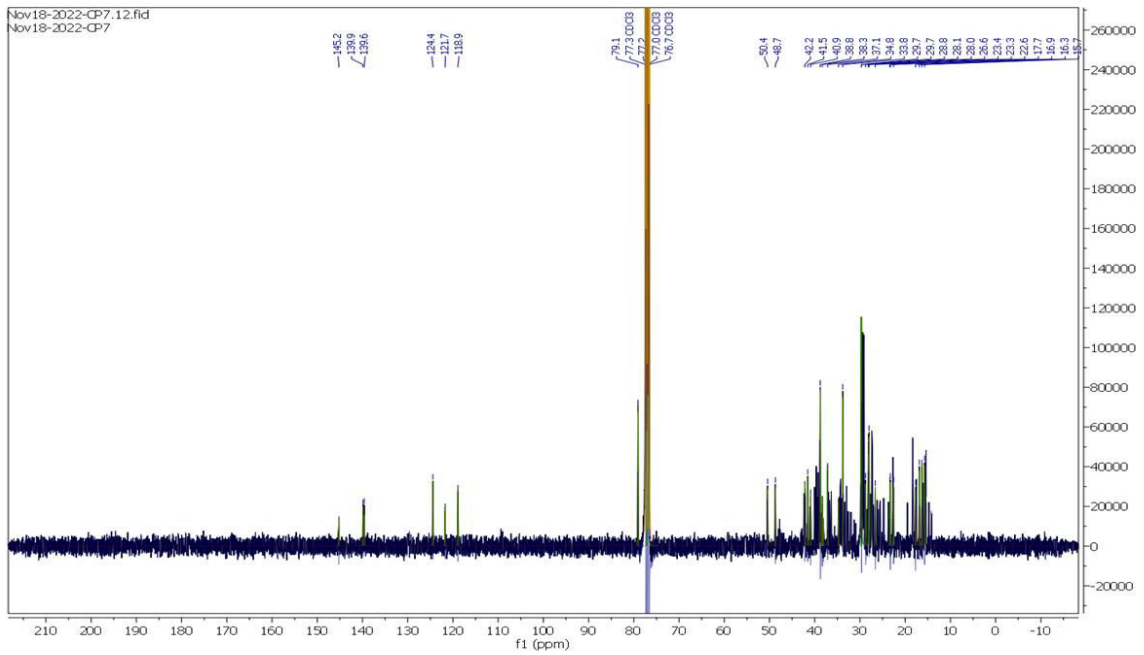

Appendix 17C: DEPT-135 NMR (101 MHz, $CDCl_3$) spectrum of calotroprocerol B (**98**).

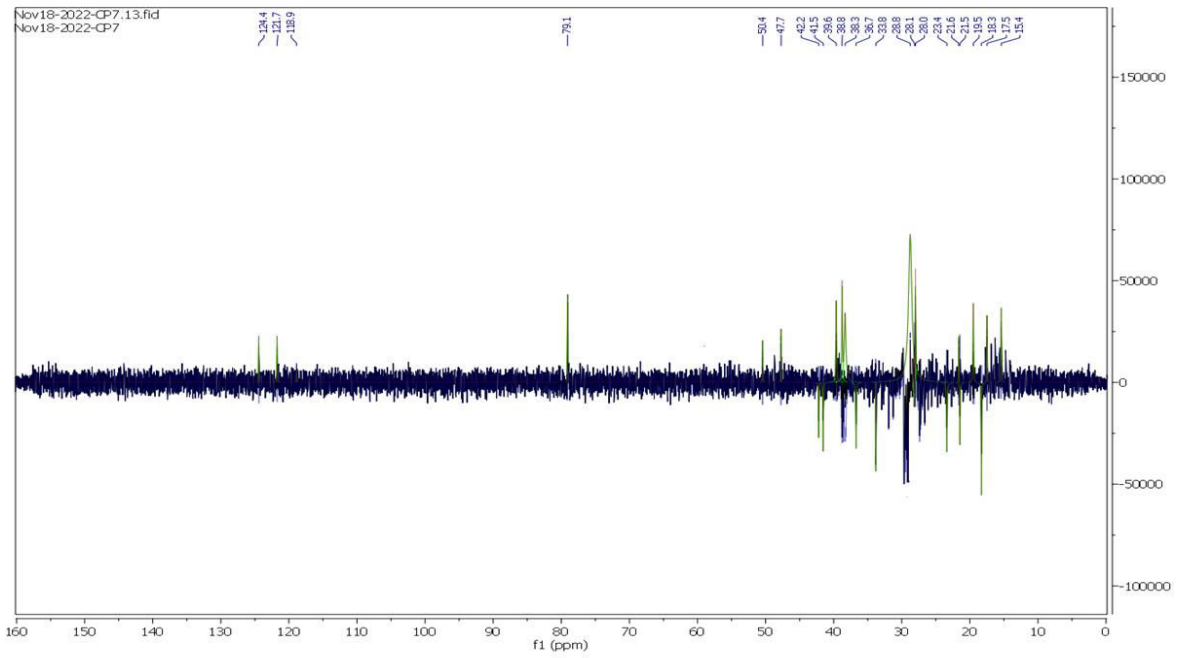

Appendix 18A: ^{1}H NMR (400 MHz, $CDCl_3$) spectrum of lauric acid (**238**).

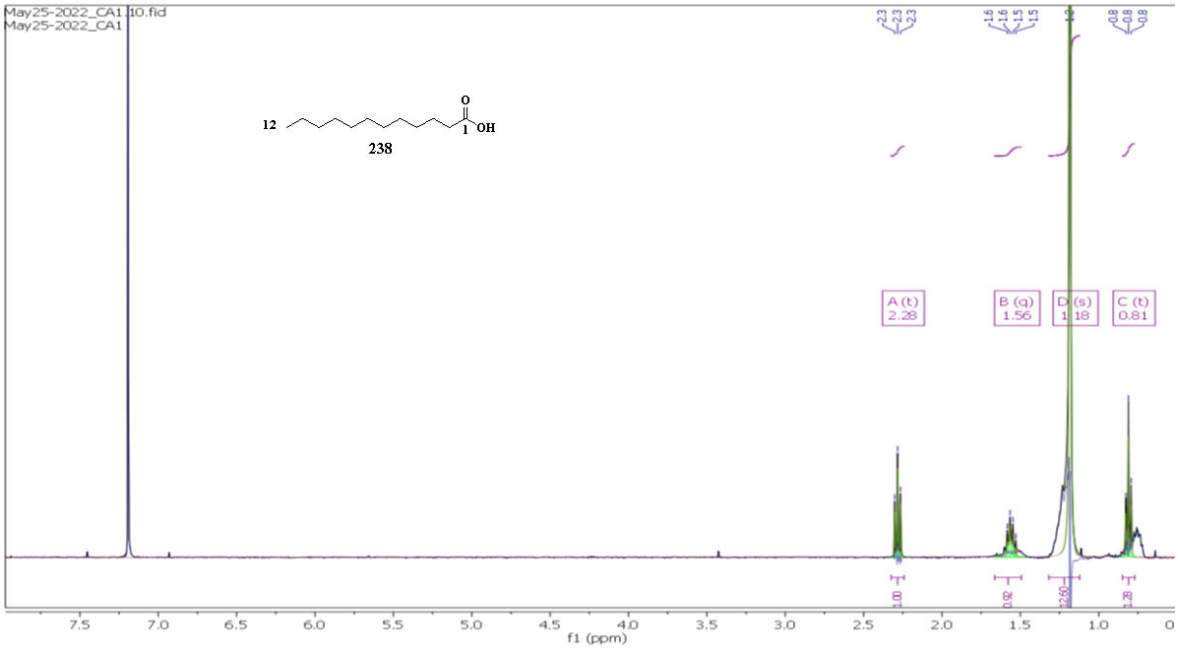

Appendix 18B: ^{13}C NMR (101 MHz, $CDCl_3$) spectrum of lauric acid (238).

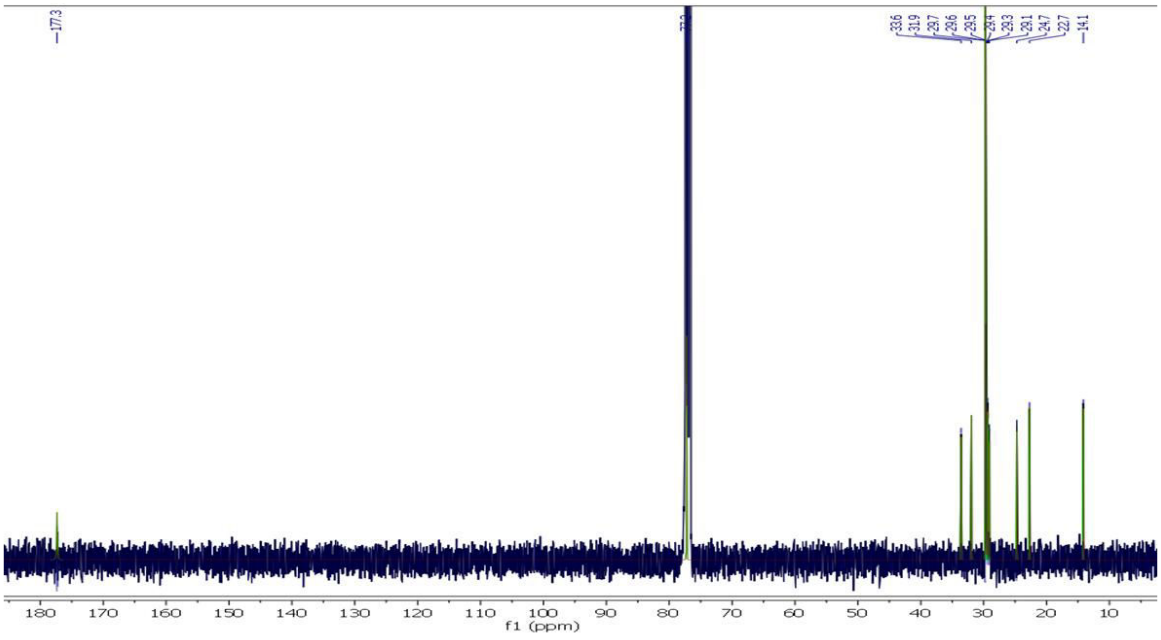

Appendix 18C: DEPT-135 NMR (101 MHz, $CDCl_3$) spectrum of lauric acid (**238**).

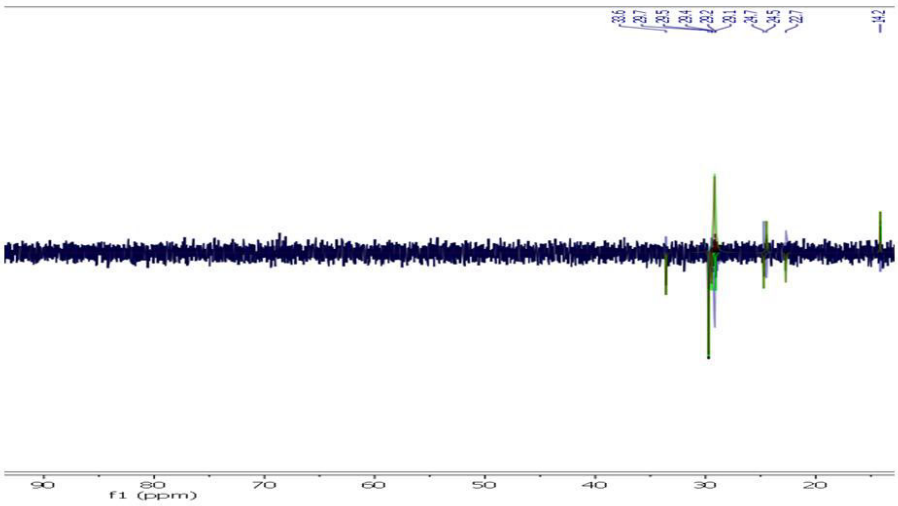

Appendix 18D: ^{1}H-^{1}H COSY spectrum of lauric acid (238).

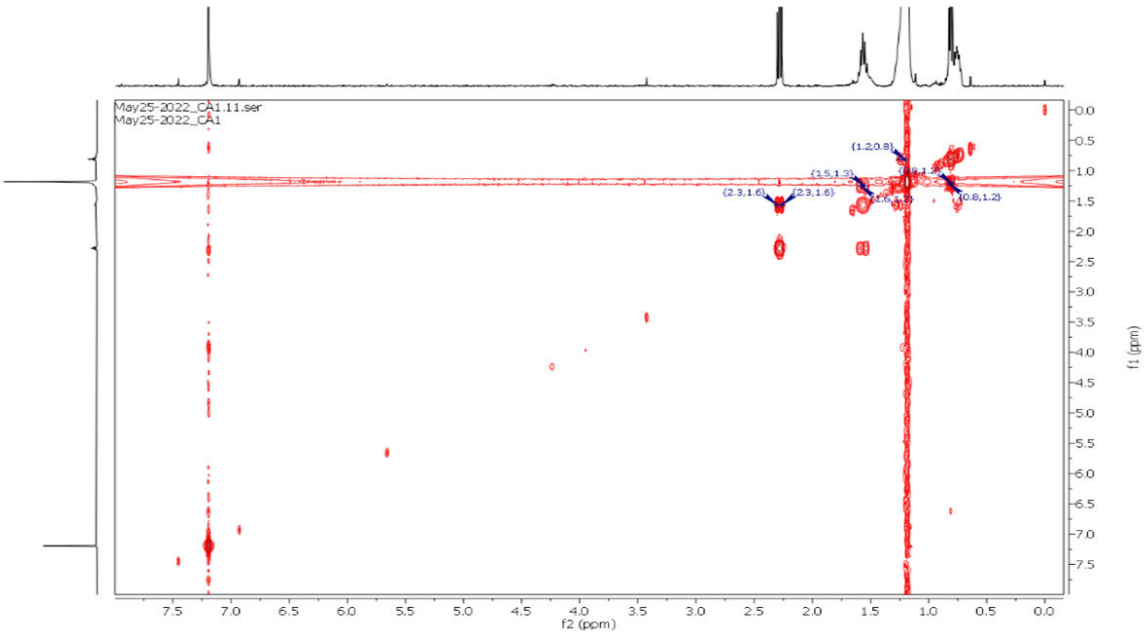

Appendix 18E: HSQC correlation of lauric acid (**238**).

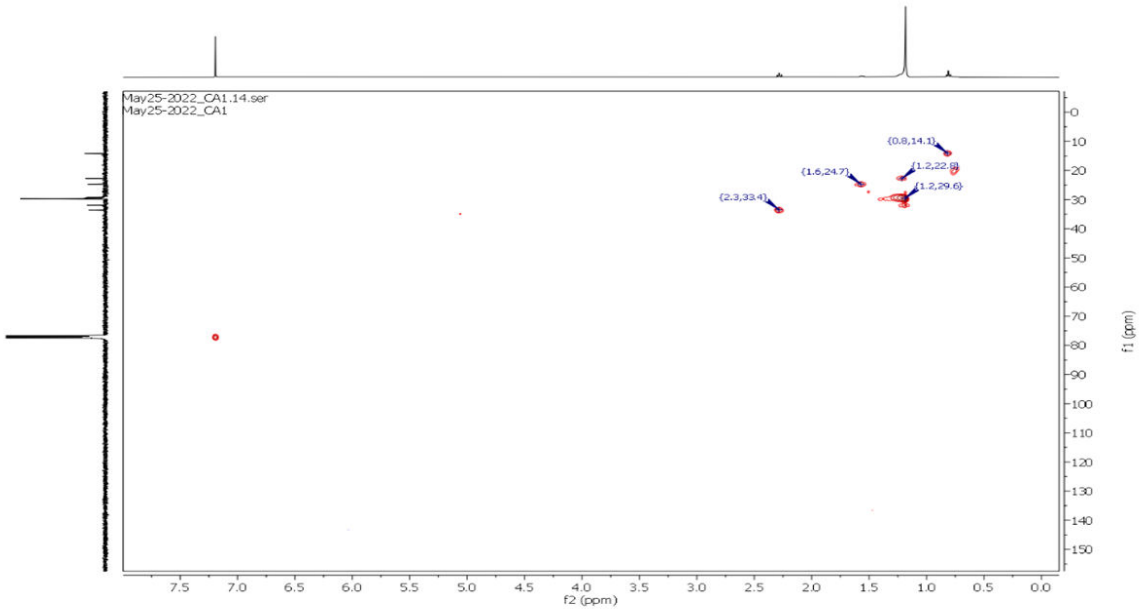

Appendix 18F: HMBC correlation of lauric acid (**238**).

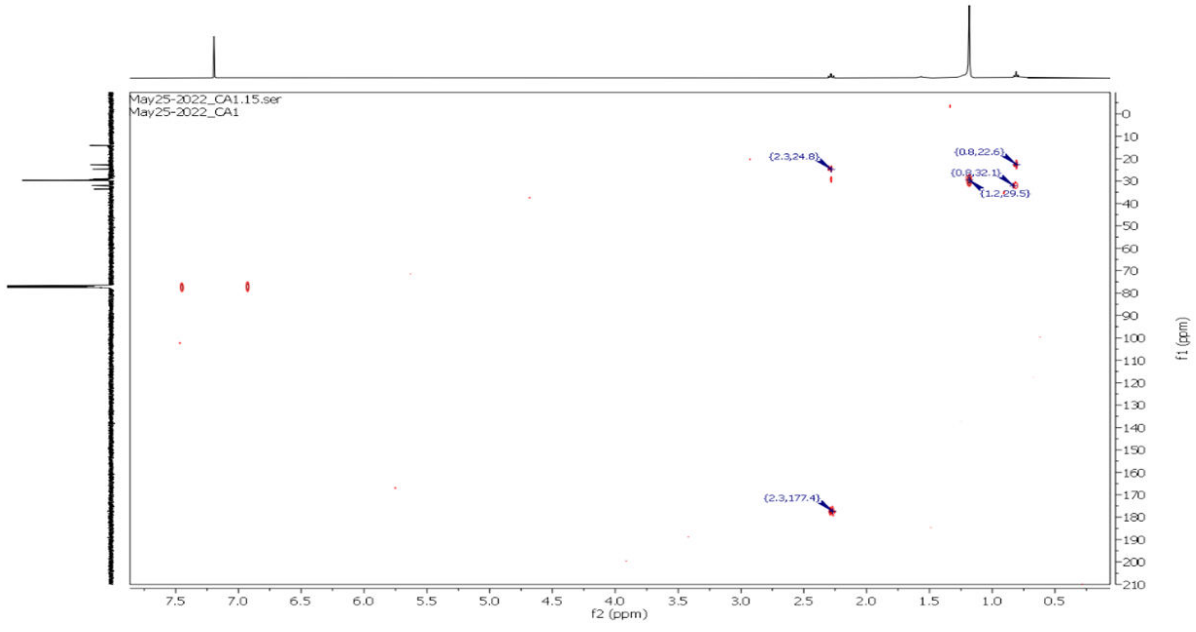

Appendix 19A: ^{1}H NMR (400 MHz, $CDCl_3$) spectrum of bis(2-ethylheptyl) phthalate (**239**).

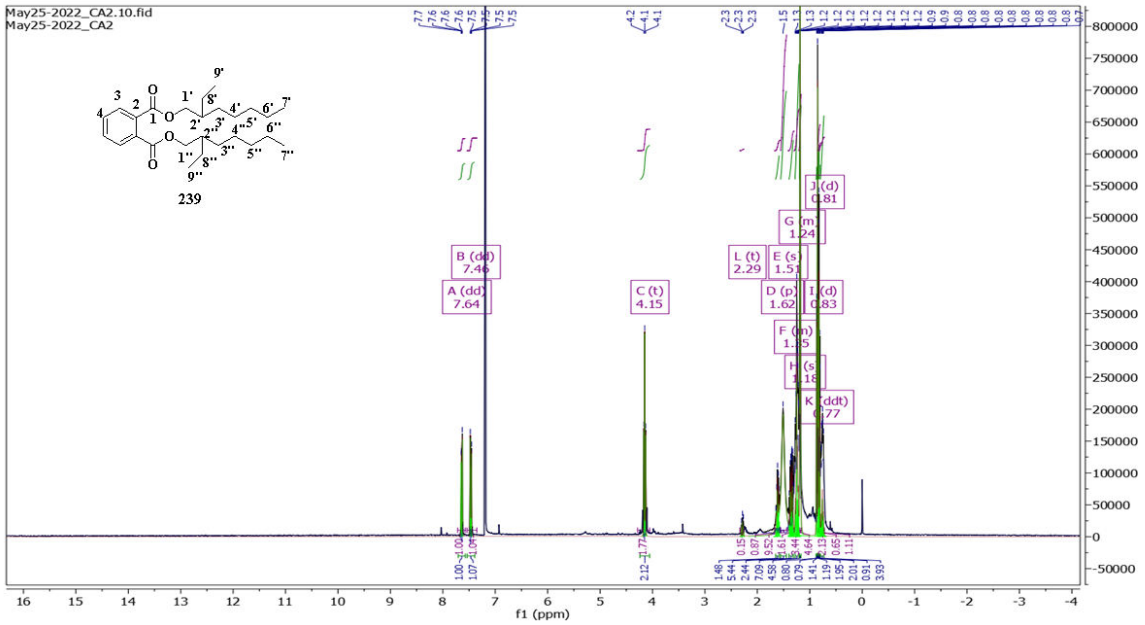

Appendix 19B: ^{13}C NMR (101 MHz, $CDCl_3$) spectrum of bis(2-ethylheptyl) phthalate (**239**).

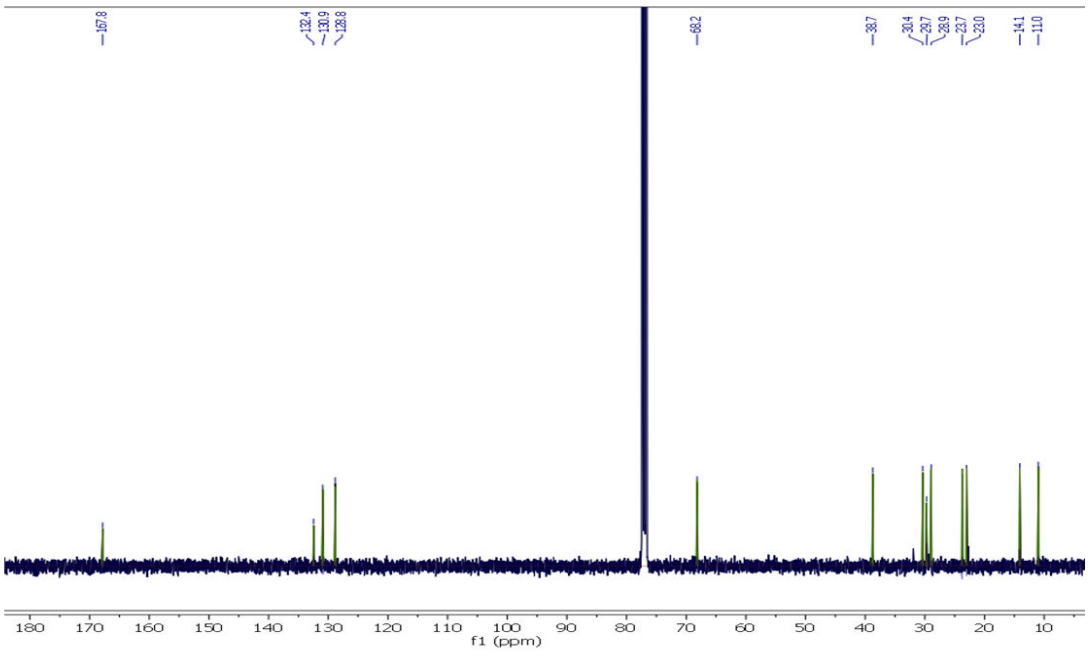

Appendix 19C: DEPT-135 NMR (101 MHz, $CDCl_3$) spectrum of bis(2-ethylheptyl) phthalate (**239**).

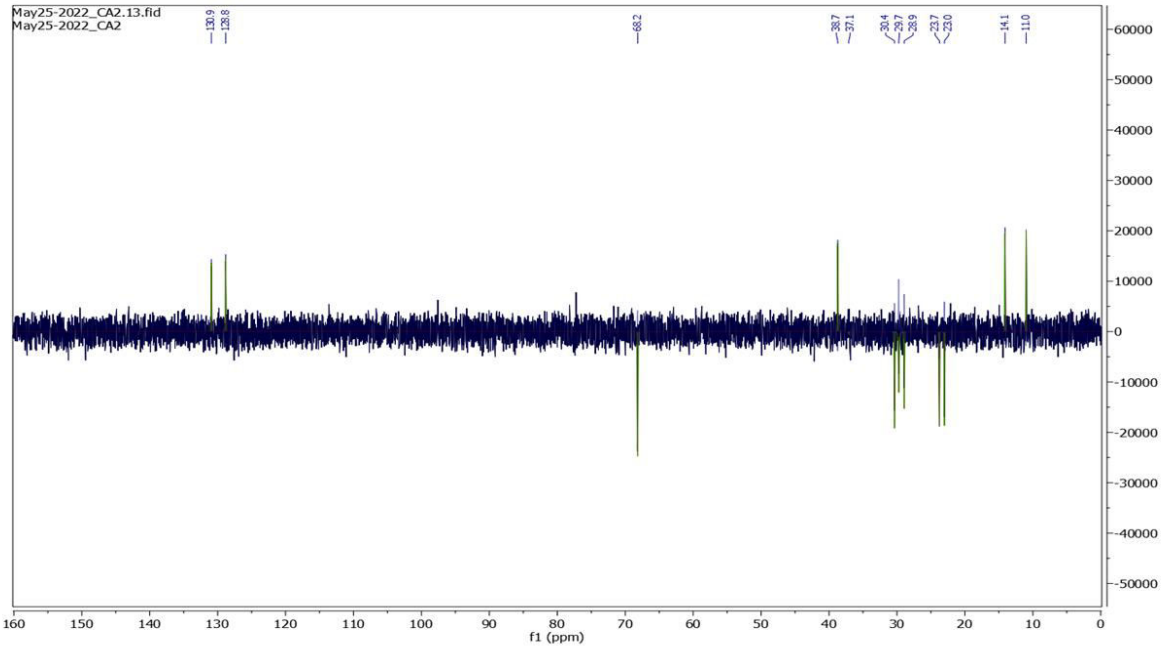

Appendix 19D: ^{1}H-^{1}H COSY spectrum of bis(2-ethylheptyl) phthalate (**239**).

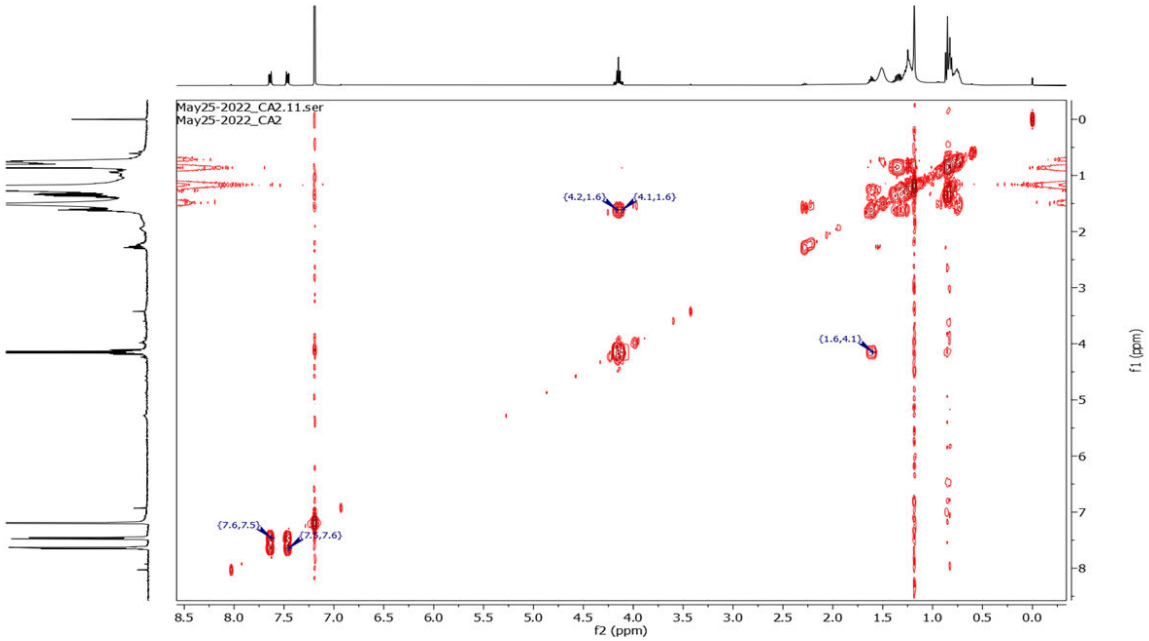

Appendix 19E: HSQC correlation of bis(2-ethylheptyl) phthalate (**239**).

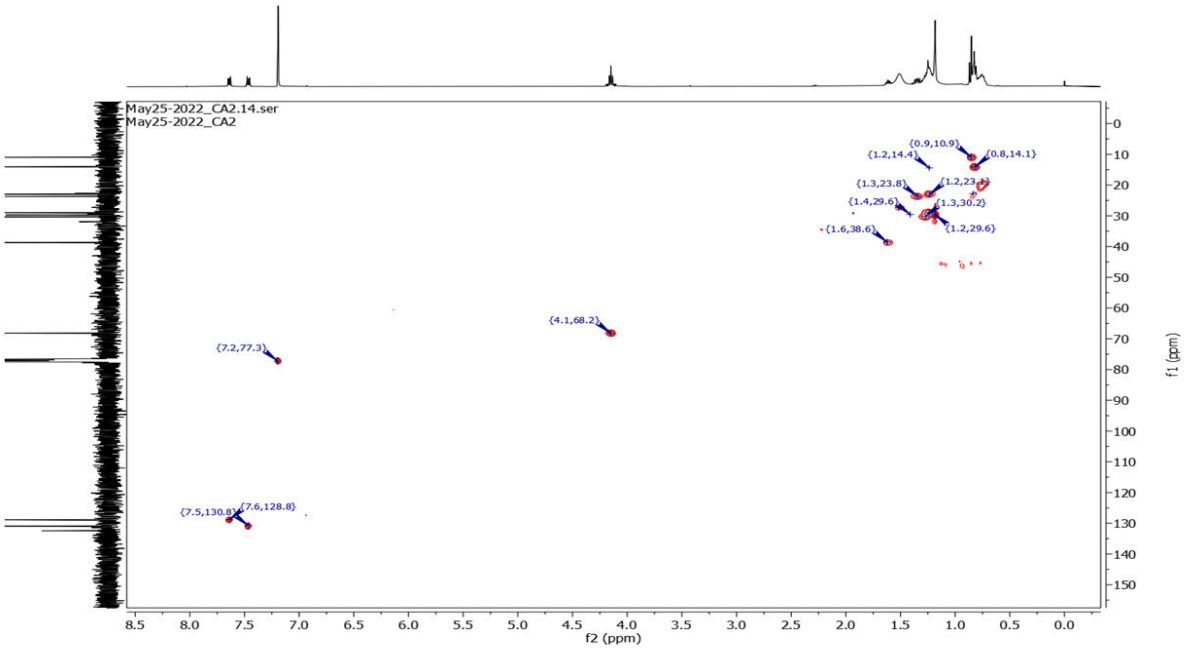

Appendix 19F: HMBC correlation of bis(2-ethylheptyl) phthalate (**239**).

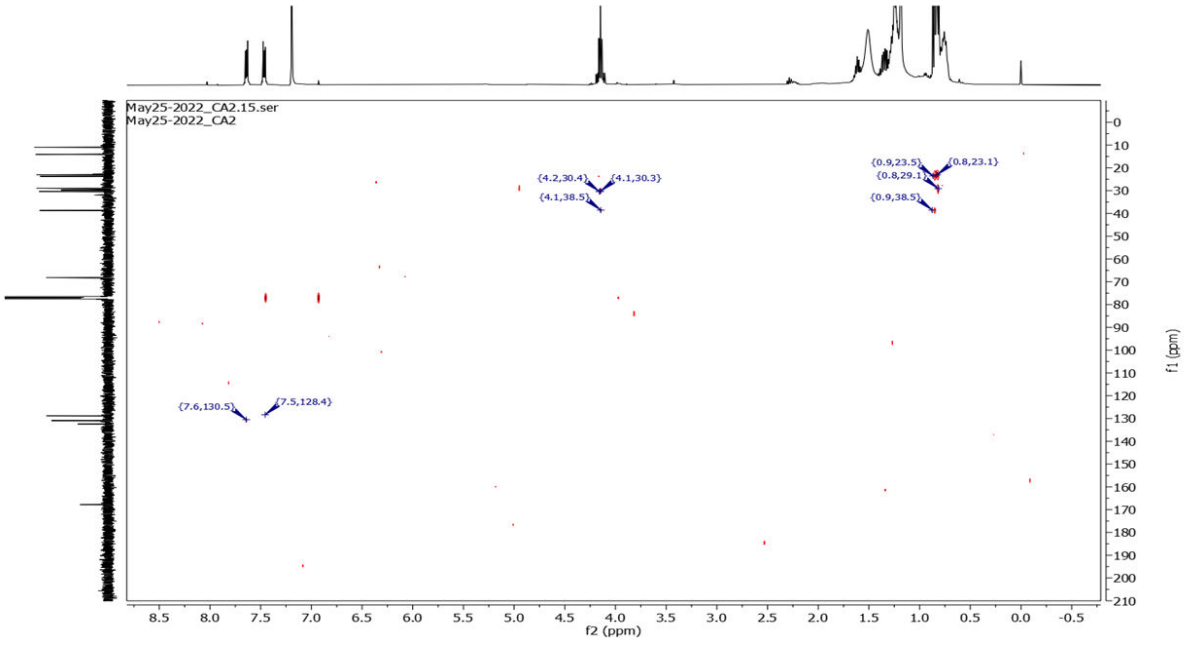

Appendix 20A: ^{1}H NMR (400 MHz, $CDCl_3$) spectrum of oleic acid (**240**).

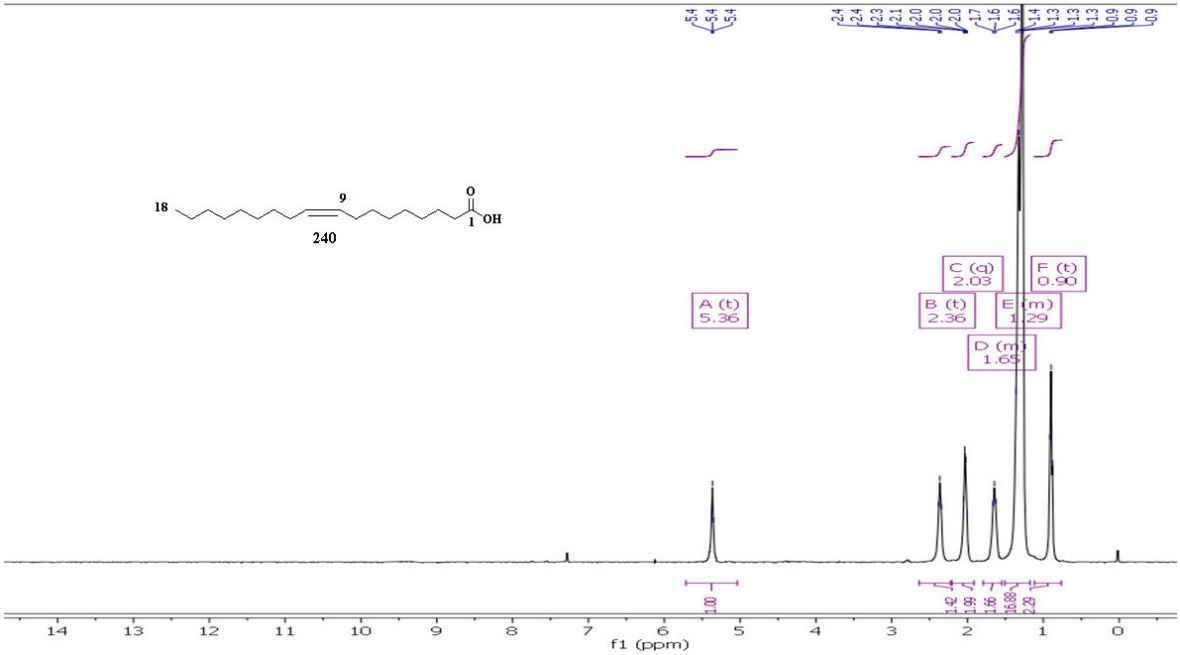

Appendix 20B: ^{13}C NMR (101 MHz, $CDCl_3$) spectrum of oleic acid (**240**).

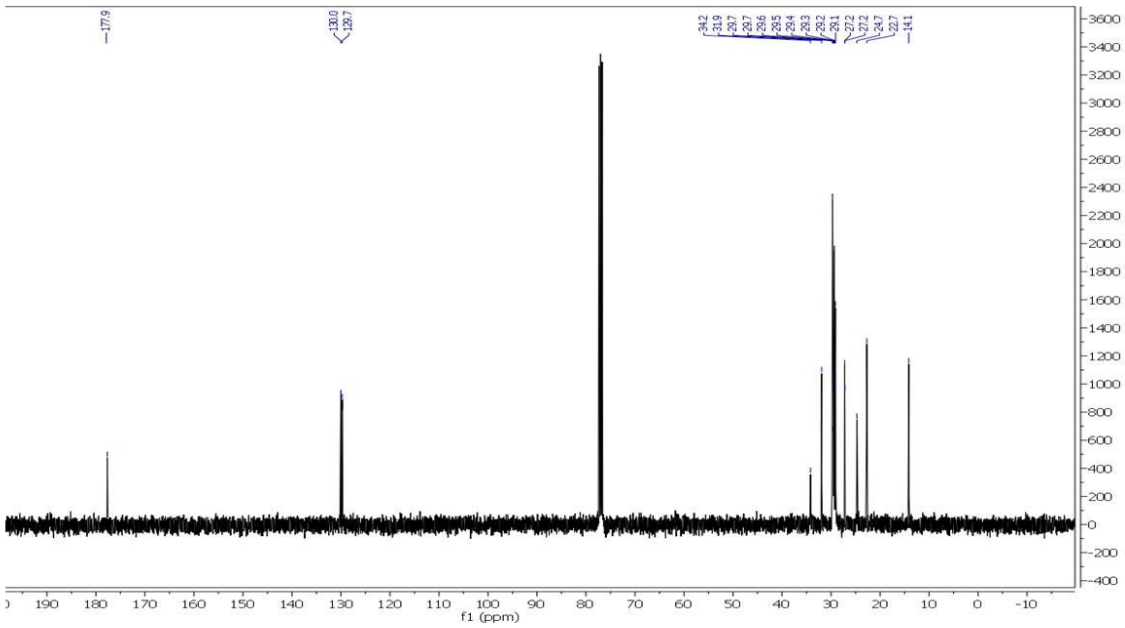

Appendix 20C: DEPT-135 NMR (101 MHz, $CDCl_3$) spectrum of compound oleic acid (**240**).

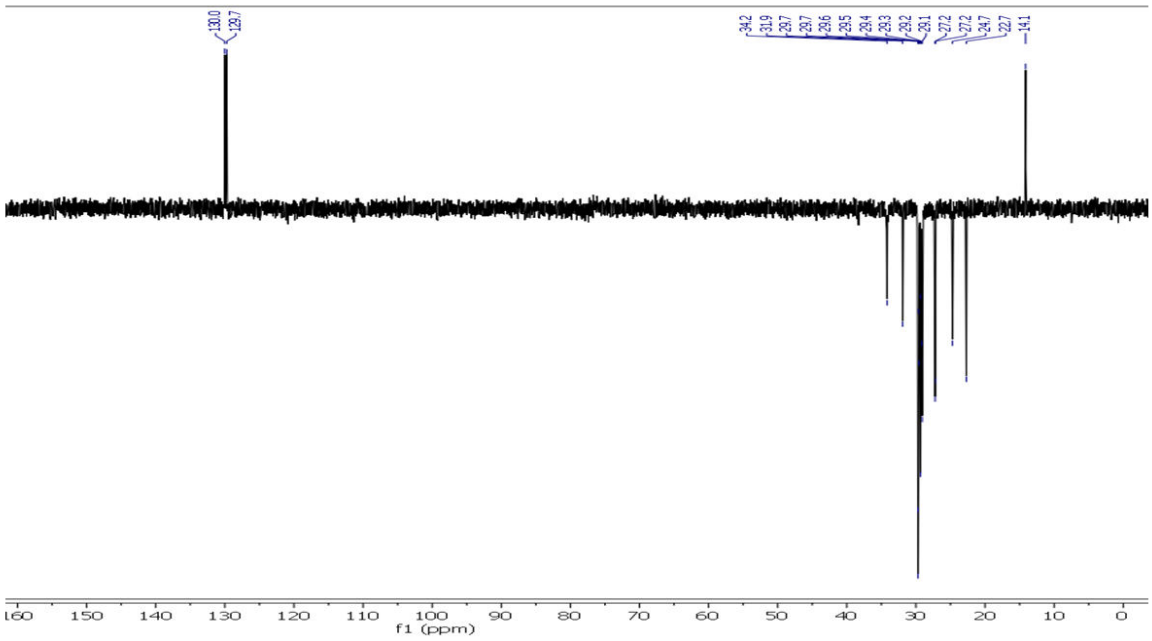

Appendix 21A: ^1H NMR (400 MHz, $CDCl_3$) spectrum of myristic acid (**241**).

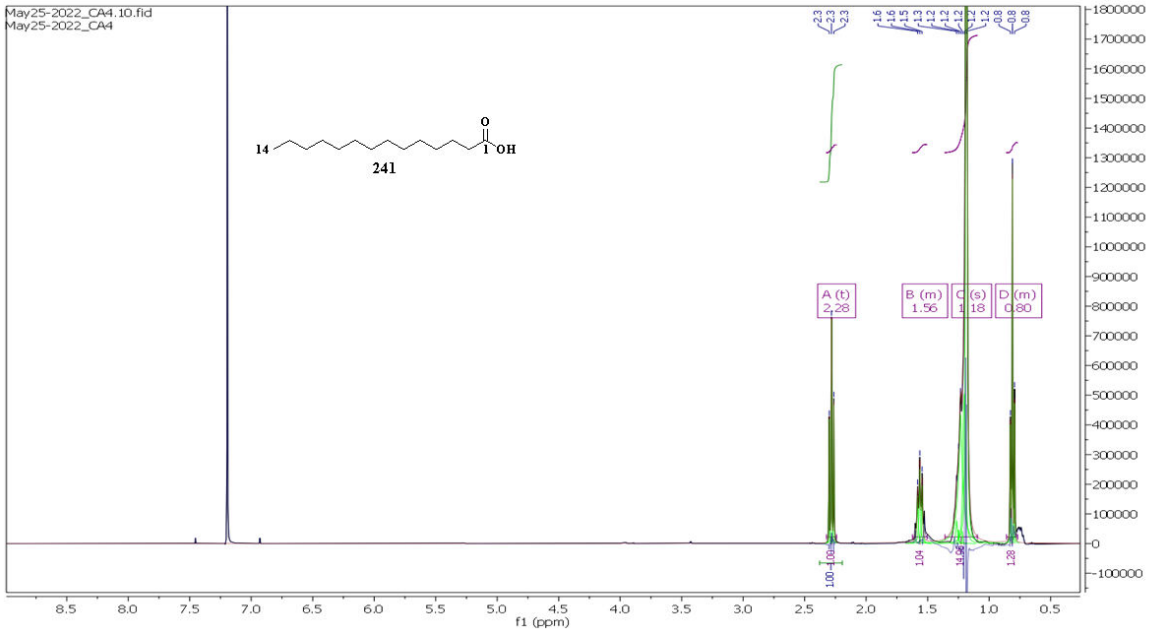

Appendix 21B: ^{13}C NMR (101 MHz, $CDCl_3$) spectrum of myristic acid (**241**).

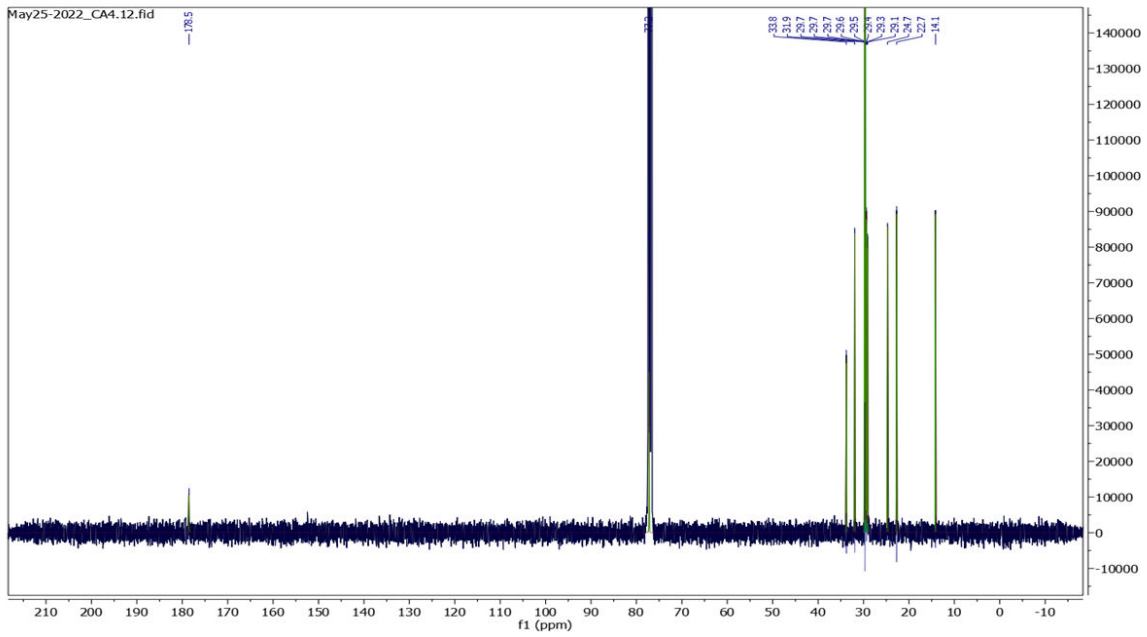

Appendix 21C: DEPT-135 NMR (101 MHz, $CDCl_3$) spectrum of myristic acid (**241**).

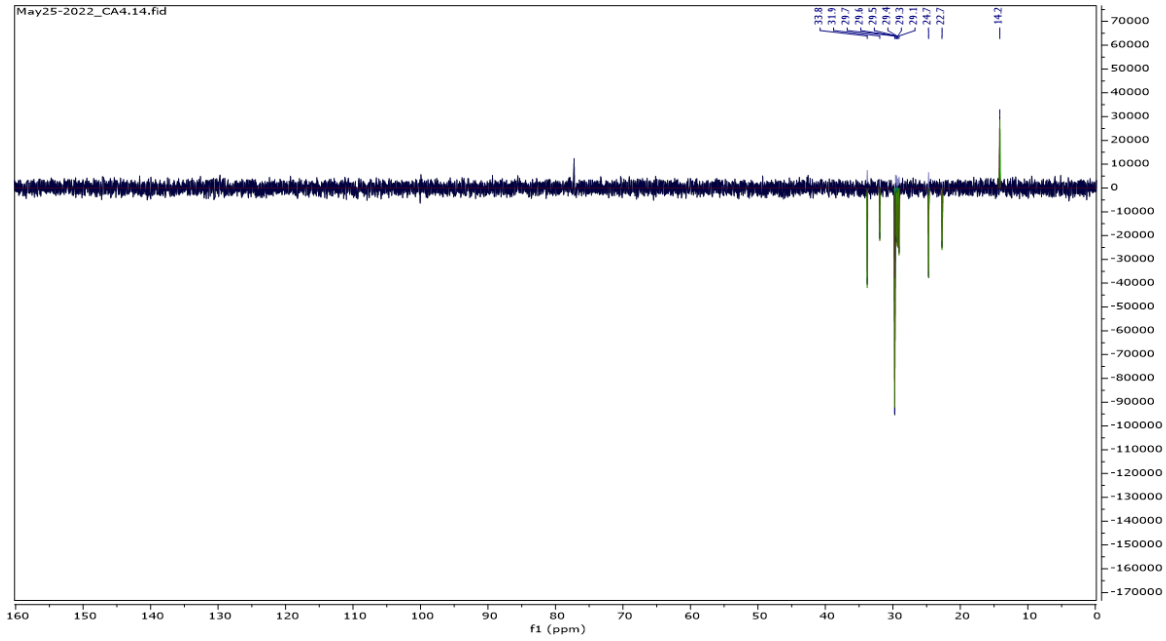

Appendix 21D: ^{1}H-^{1}H COSY spectrum of myristic acid (**241**).

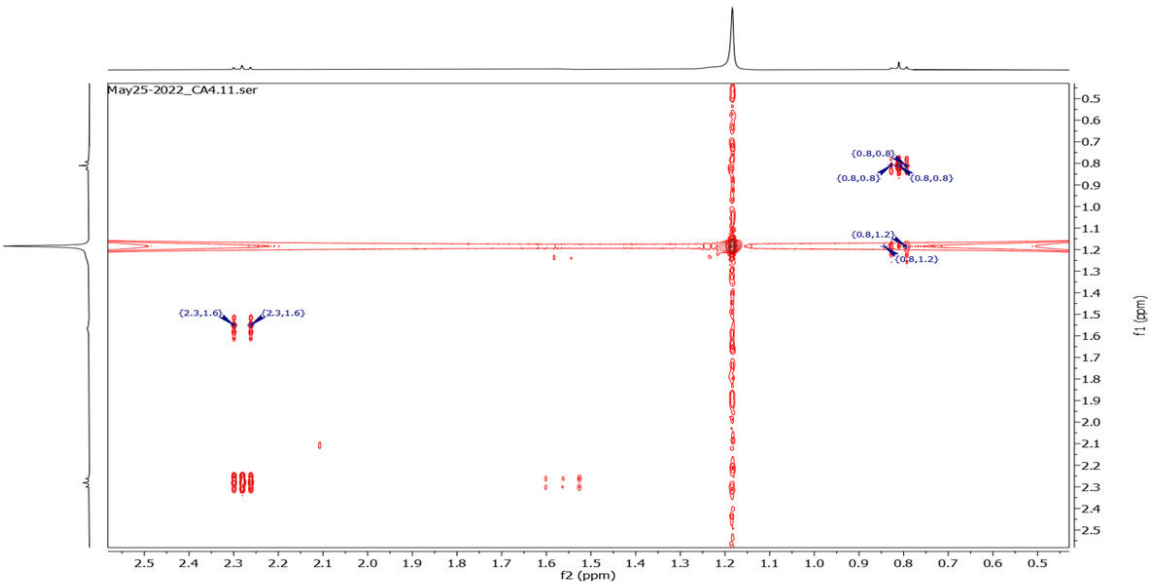

Appendix 21E: HSQC correlation of myristic acid (**241**).

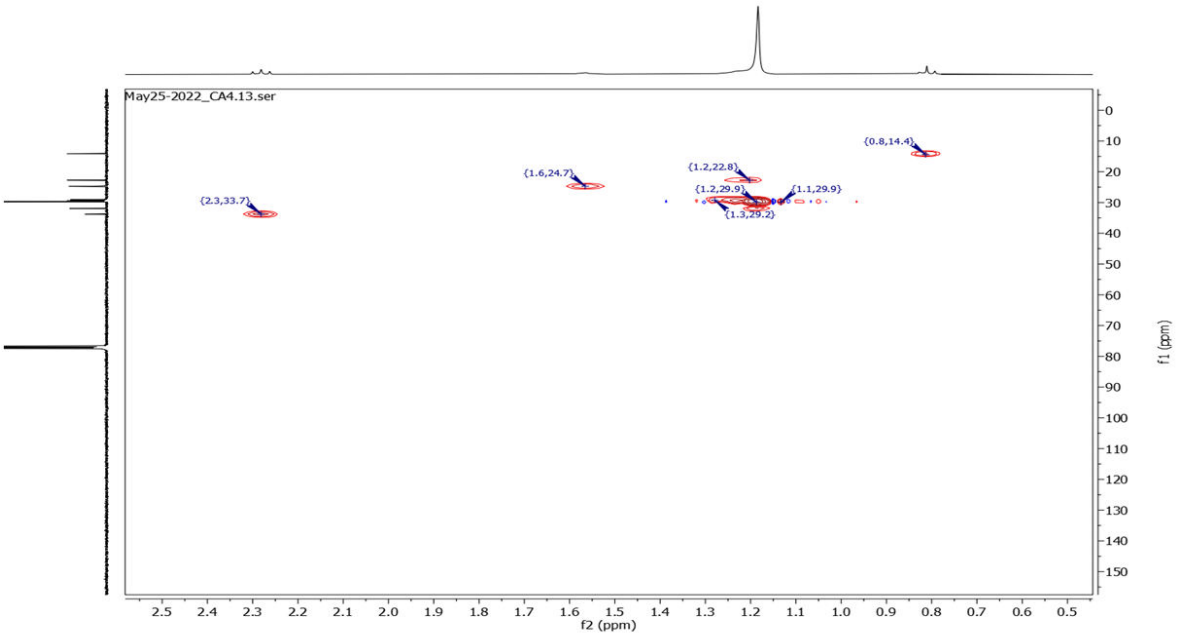

Appendix 21F: HMBC correlation of myristic acid (**241**).

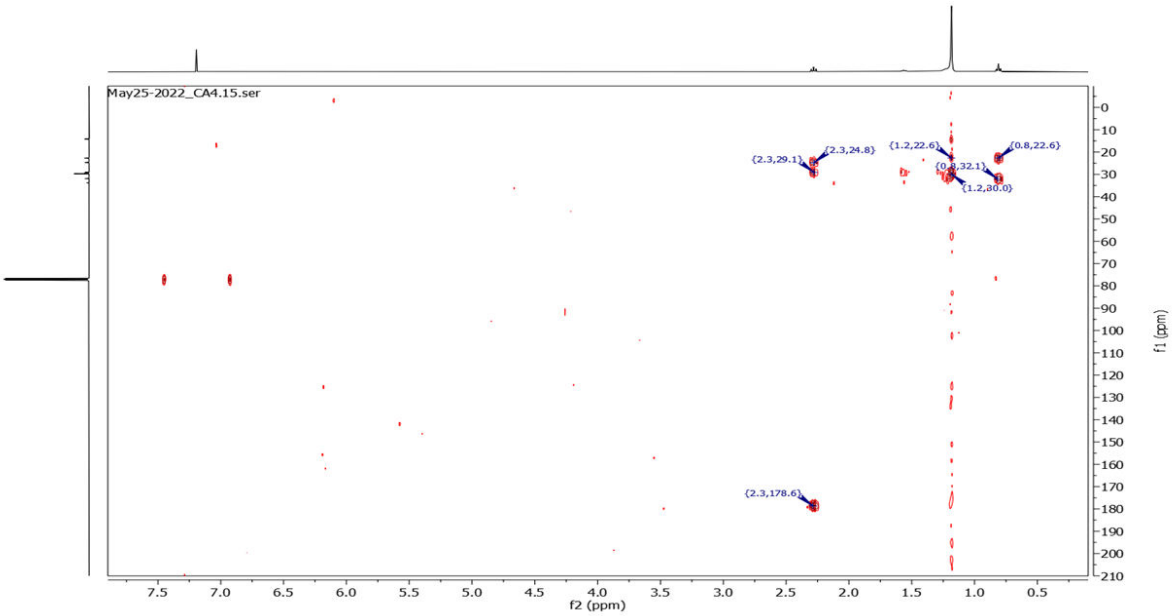

Appendix 22A: ^{1}H NMR (400 MHz, $CDCl_3$) spectrum of stigmasterol (**79**).

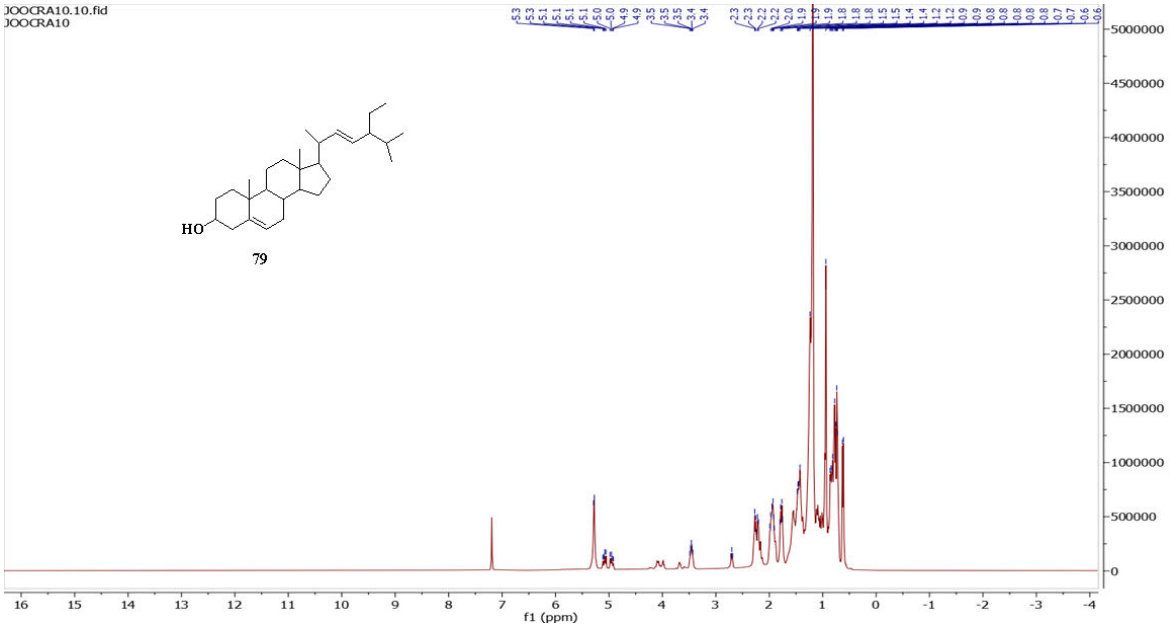

Appendix 22B: ^{13}C NMR (101 MHz, $CDCl_3$) spectrum of stigmasterol (**79**).

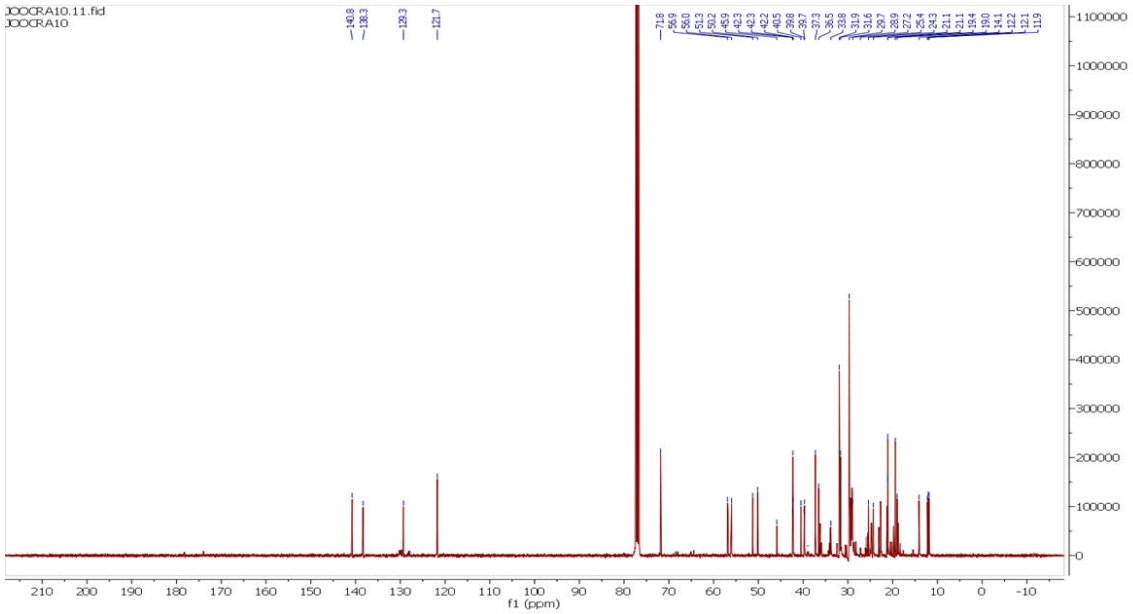

Appendix 22C: DEPT-135 NMR (101 MHz, $CDCl_3$) spectrum of stigmasterol (**79**).

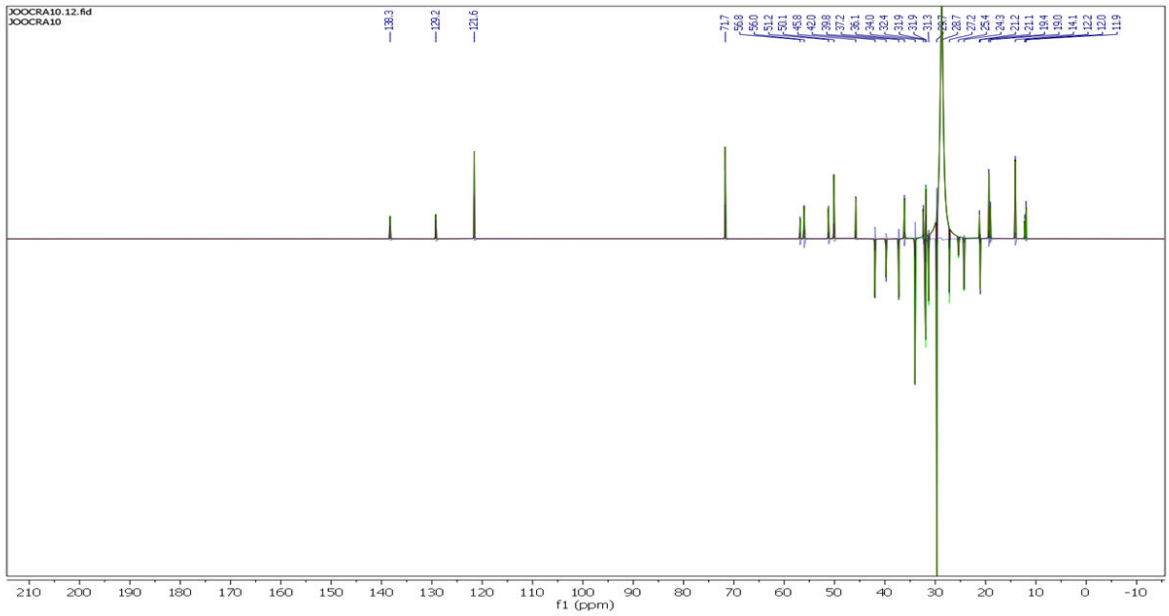

Appendix 23A: ^{1}H NMR (400 MHz, $CDCl_3$) spectrum of *β*-sitosterol (**78**).

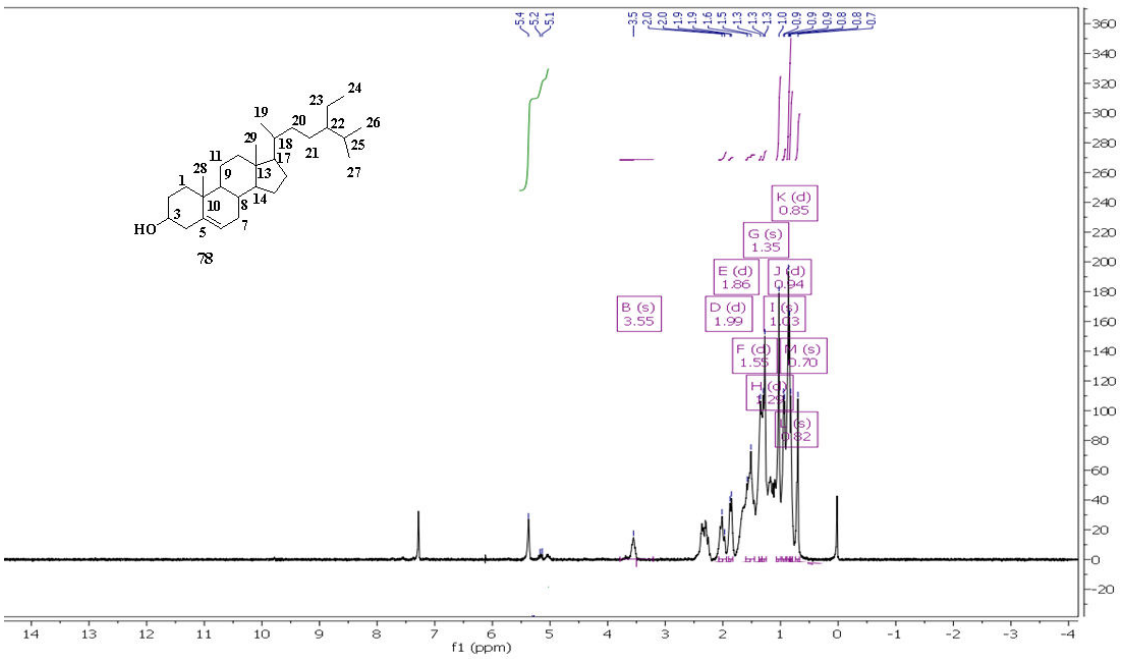

Appendix 23B: ^{13}C NMR (101 MHz, $CDCl_3$) spectrum of *β*-sitosterol (**78**).

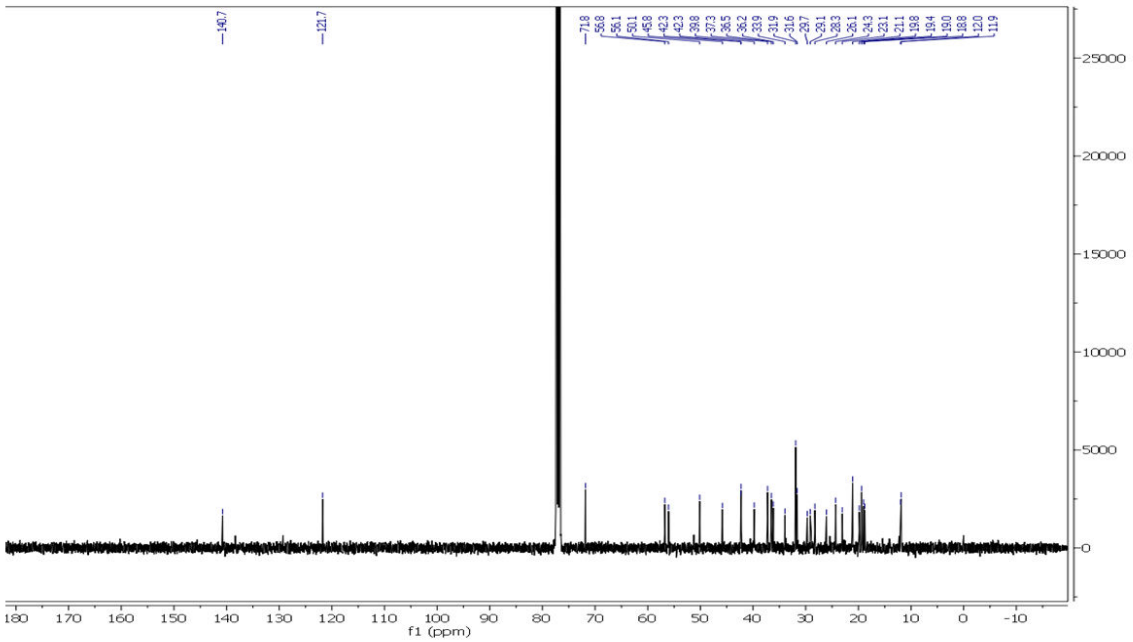

Appendix 23C: DEPT-135 NMR (101 MHz, $CDCl_3$) spectrum of *β*-sitosterol (**78**).

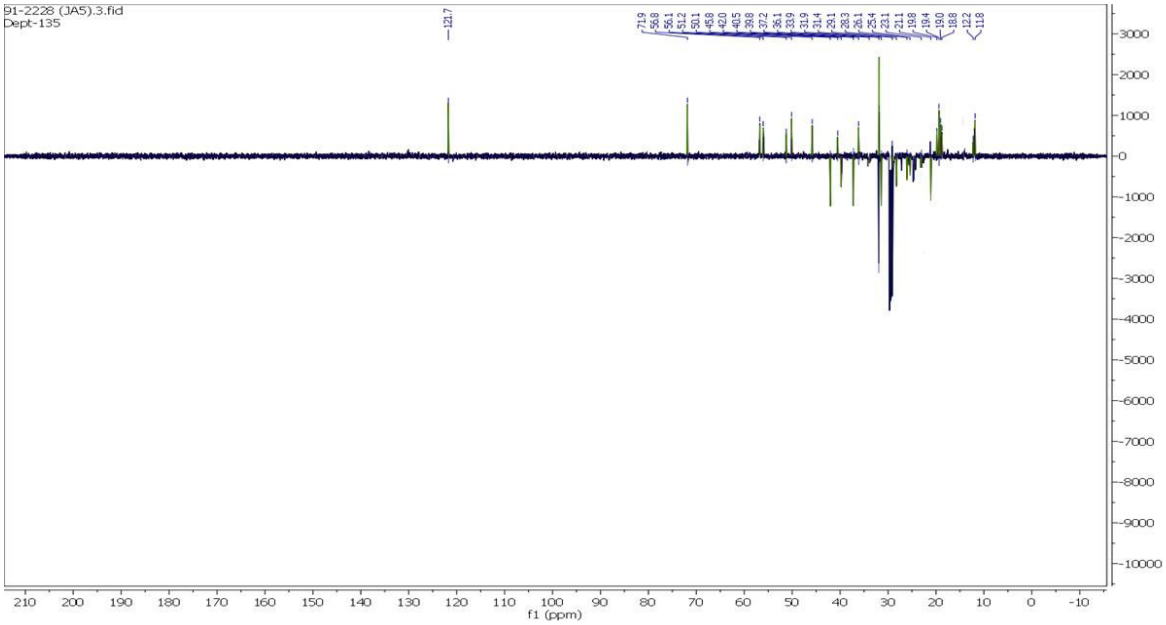

Appendix 24A: ^{1}H NMR (400 MHz, $CDCl_3$) spectrum of 5-methoxy durmillone (**242**).

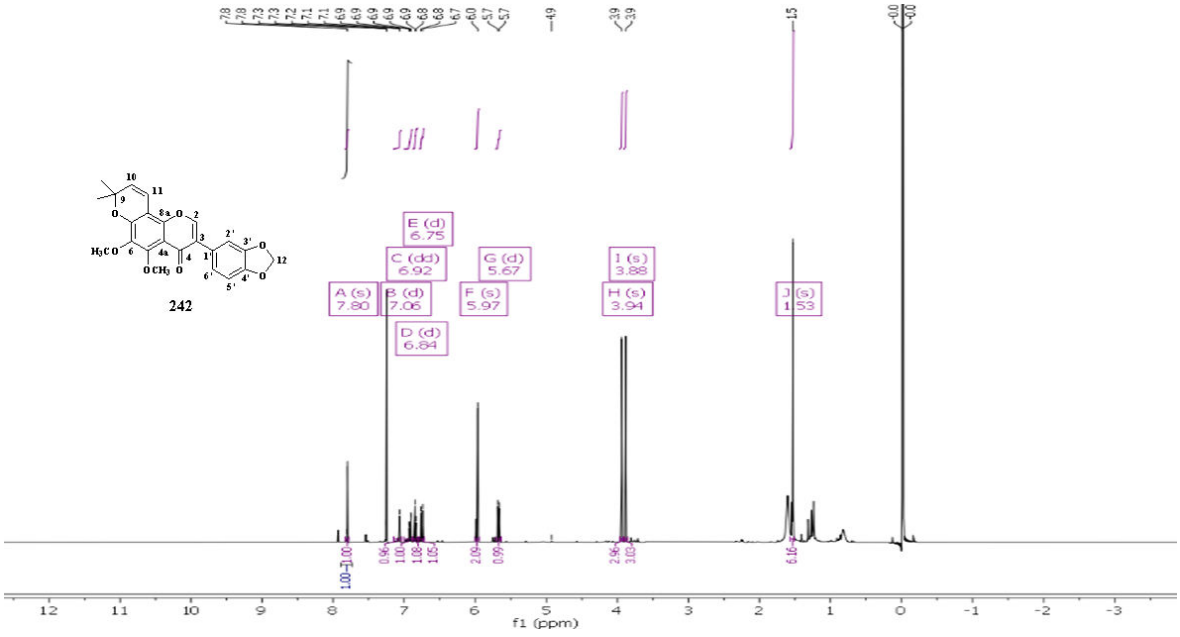

Appendix 24B: ^{13}C NMR (101 MHz, $CDCl_3$) spectrum of 5-methoxy durmillone (**242**).

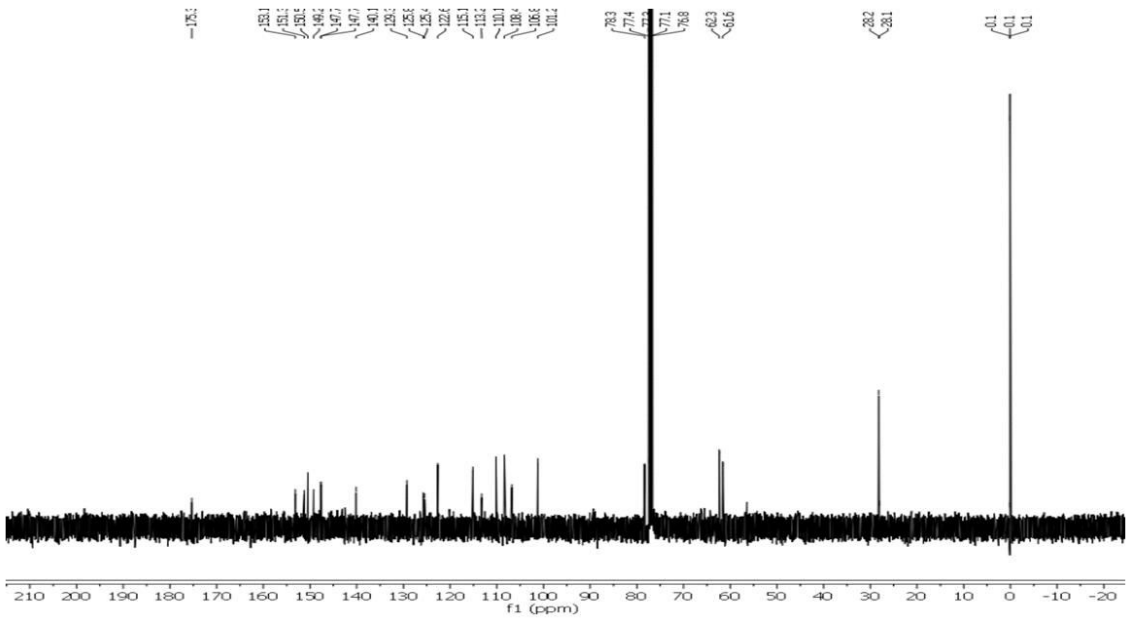

Appendix 24C: DEPT-135 NMR (101 MHz, $CDCl_3$) spectrum of 5-methoxy durmillone (**242**).

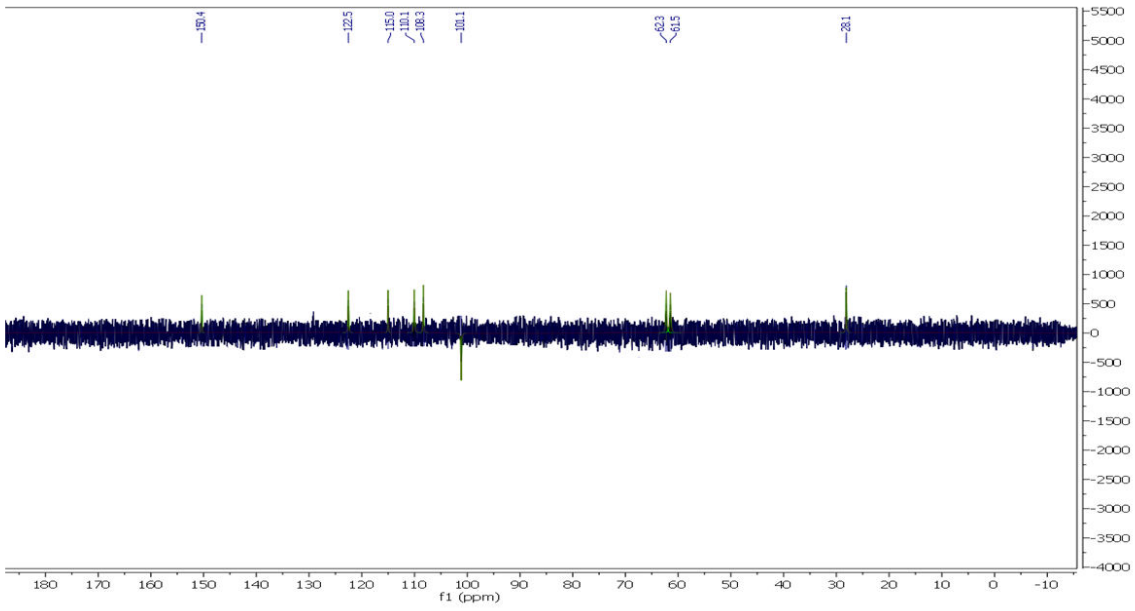

Appendix 24D: ^{1}H-^{1}H COSY spectrum of 5-methoxy durmillone (**242**).

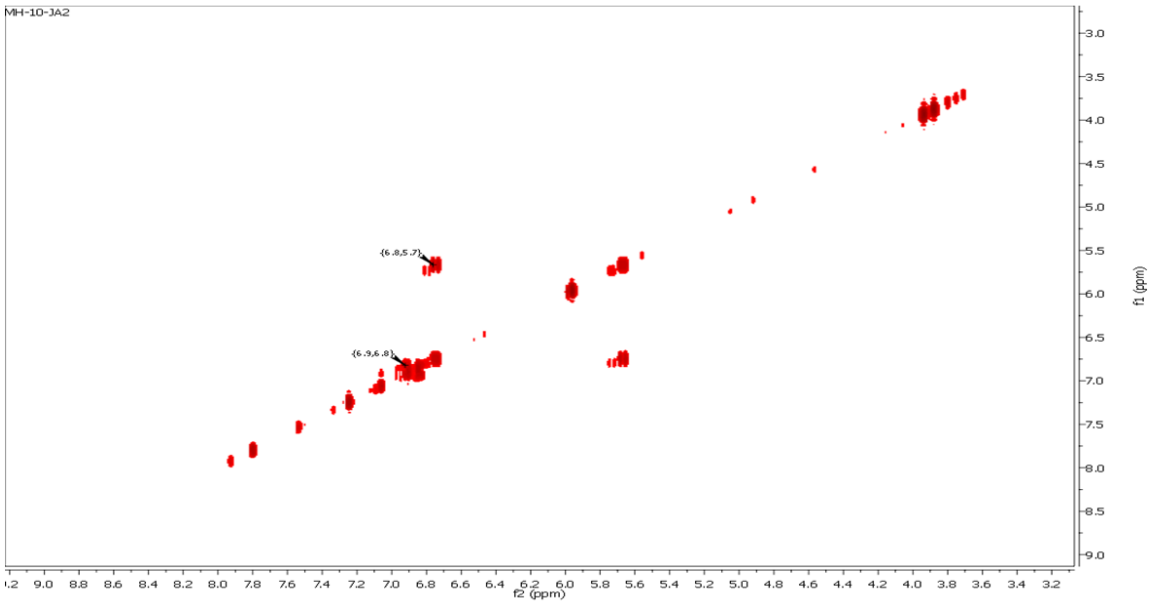

Appendix 24E: HSQC correlation of 5-methoxy durmillone (**242**).

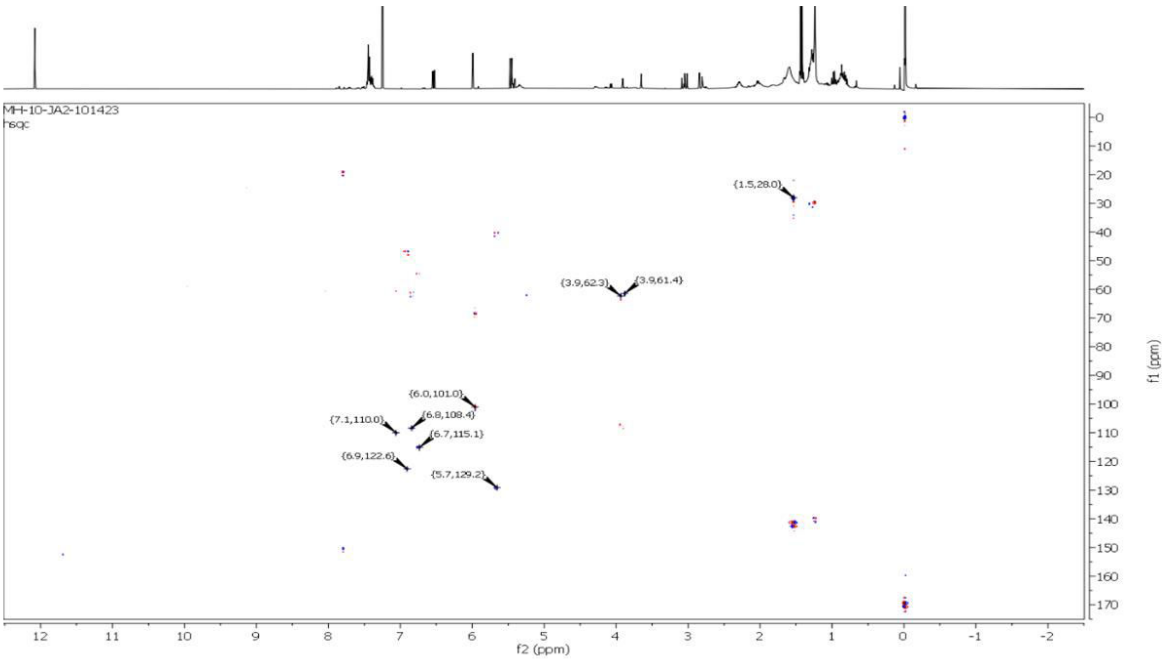

Appendix 24F: HMBC correlation of 5-methoxy durmillone (**242**).

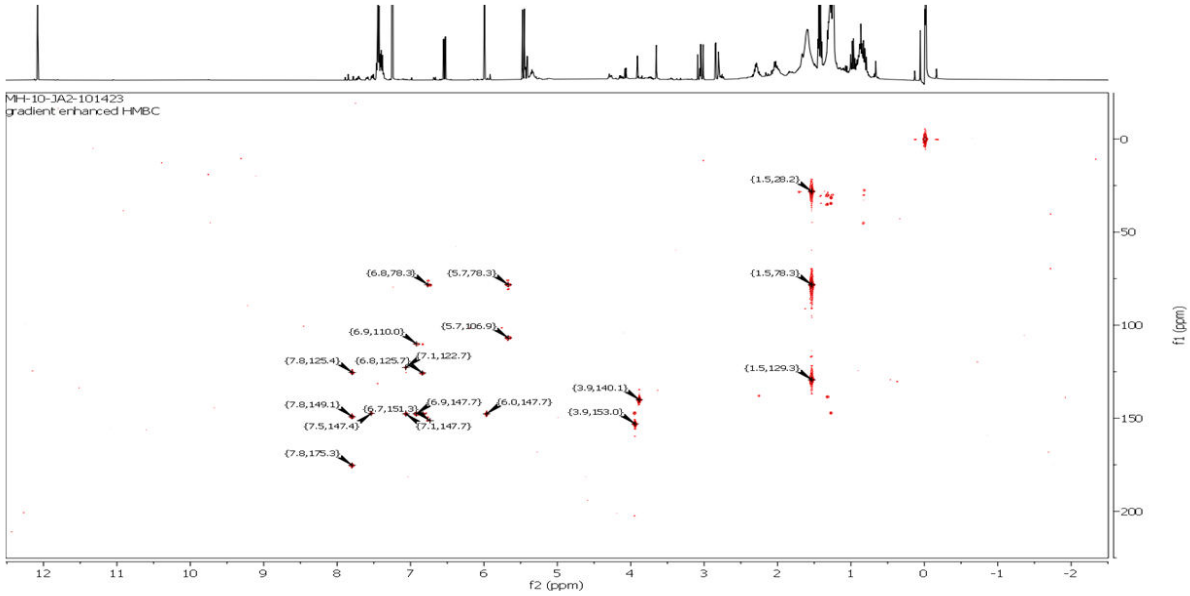

Appendix 25A: ^{1}H NMR (400 MHz, DMSO) spectrum of *trans-resveratr*ol (**243**).

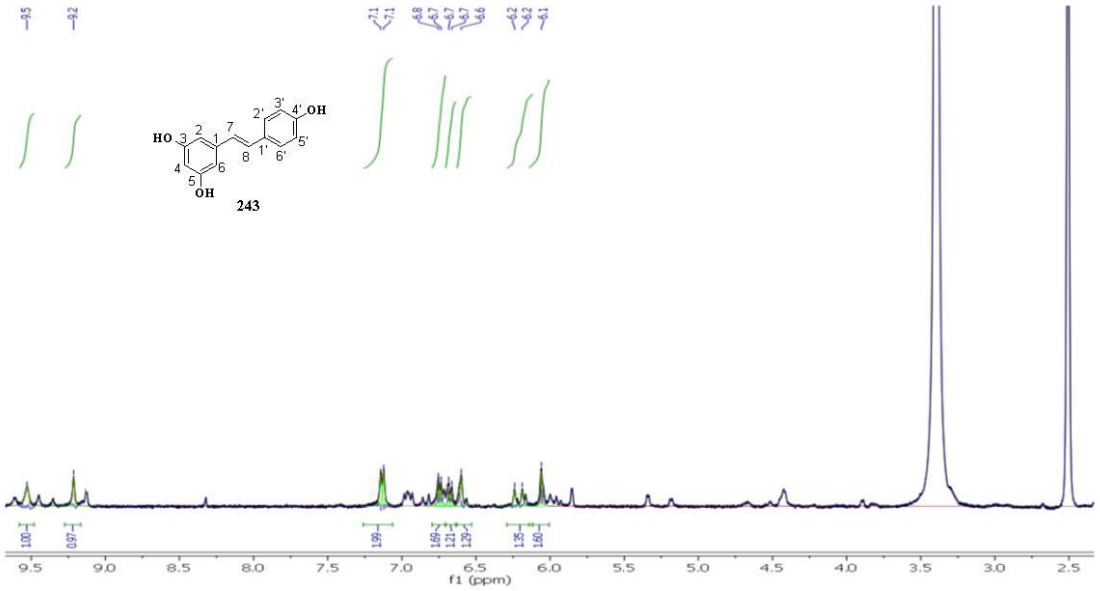

Appendix 25B: ^{13}C NMR (101 MHz, DMSO) spectrum of *trans-resveratr*ol (**243**).

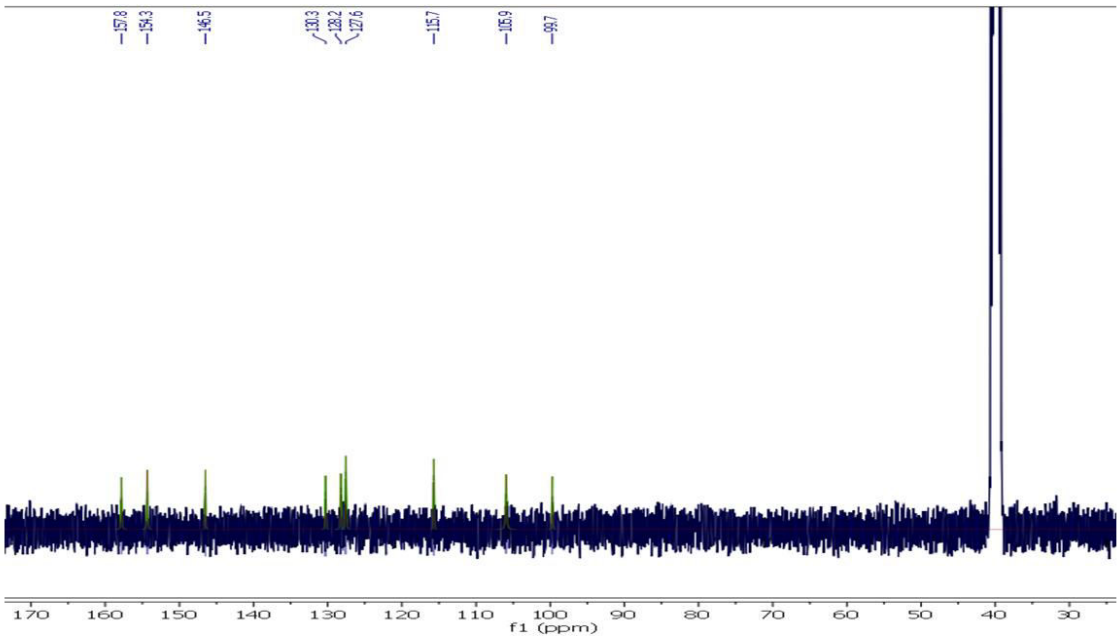

Appendix 25C: DEPT-135 NMR (101 MHz, DMSO) spectrum of *trans-resveratr*ol (**243**).

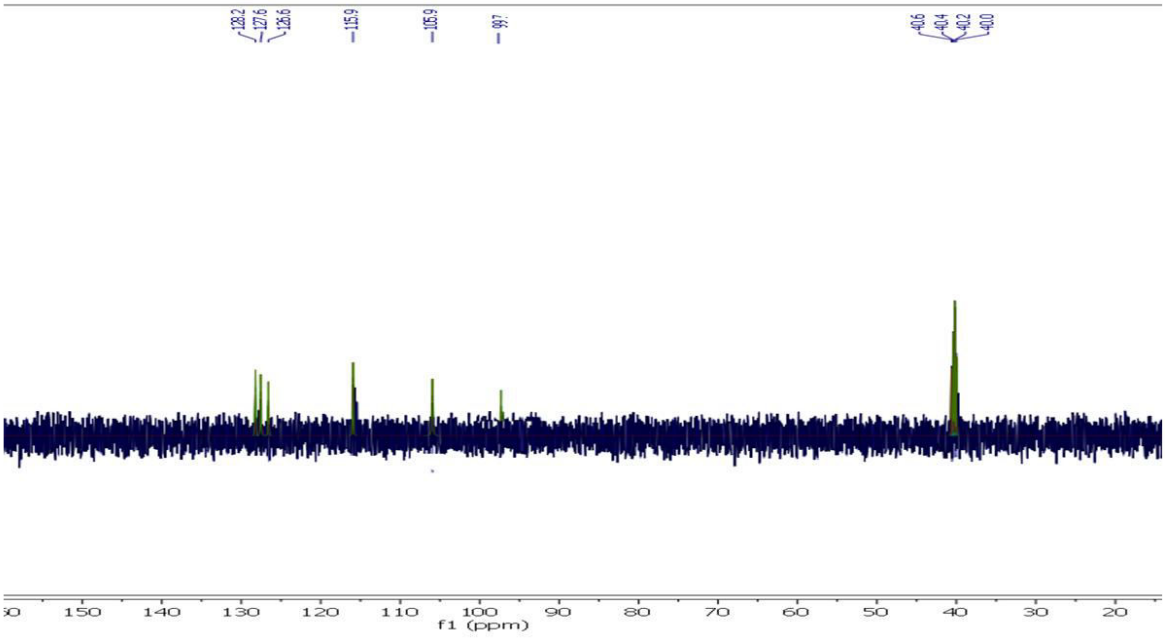

Appendix 26A: ^{1}H NMR (400 MHz, DMSO) spectrum of tricuspidatol A (**244**).

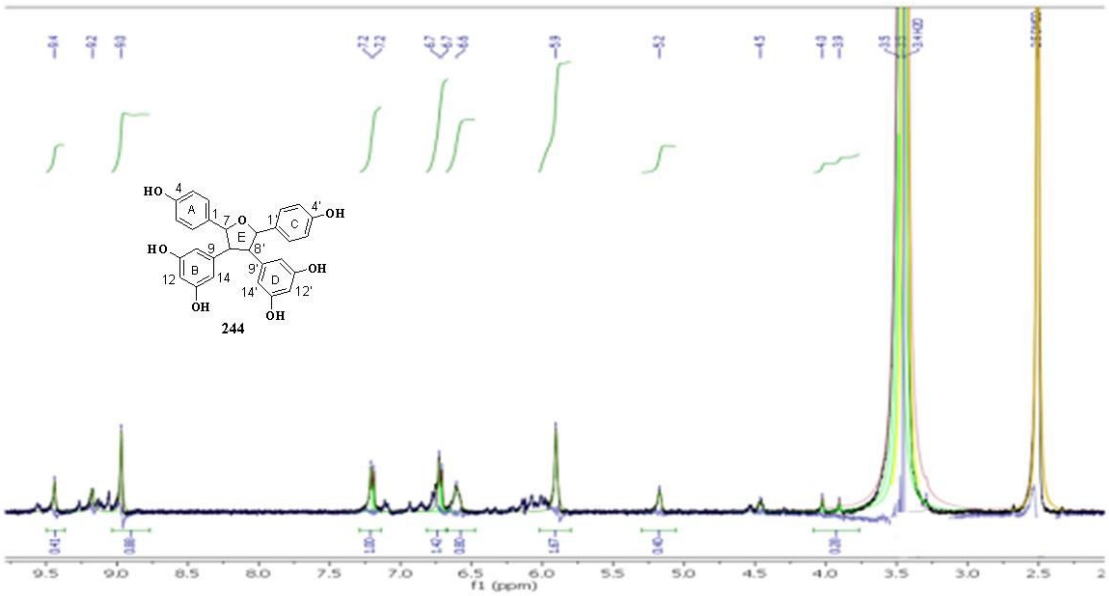

Appendix 26B: ^{13}C NMR (101 MHz, DMSO) spectrum of tricuspidatol A (**244**).

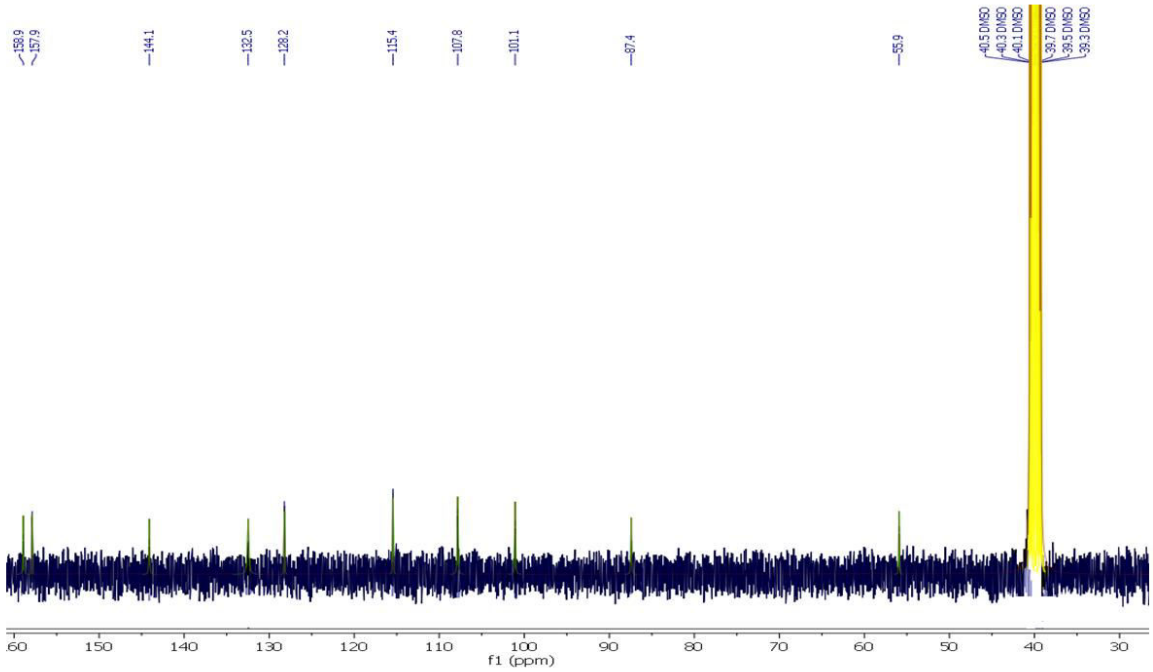

Appendix 26C: DEPT-135 NMR (101 MHz, DMSO) spectrum of tricuspidatol A (**244**).

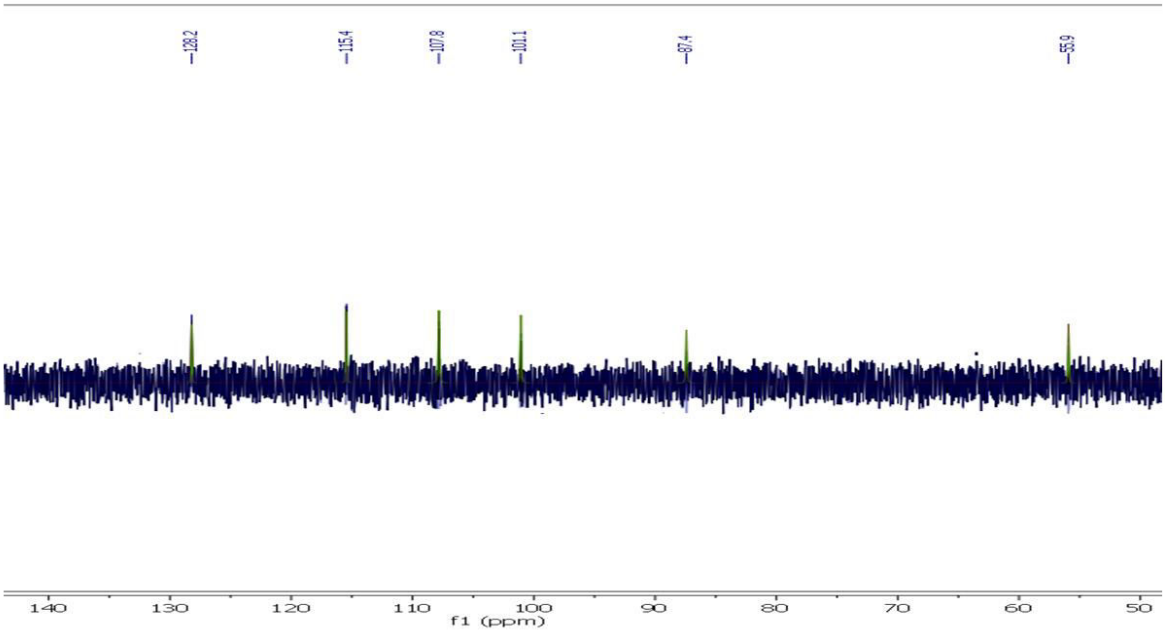

Appendix 27A: ^{1}H NMR (400 MHz, Acetone-d_6) spectrum of kaempferol-3-O-α rhamnopyranoside (**245**).

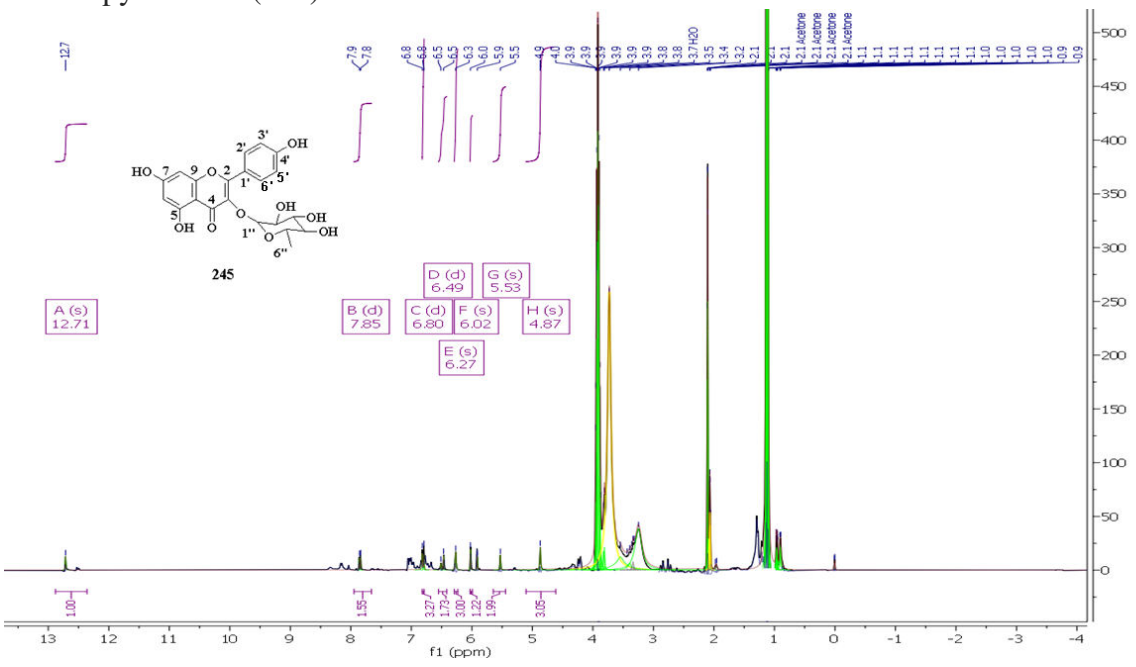

Appendix 27B: ^{13}C NMR (101 MHz, Acetone-d6) spectrum of kaempferol-3-O-α rhamnopyranoside (**245**).

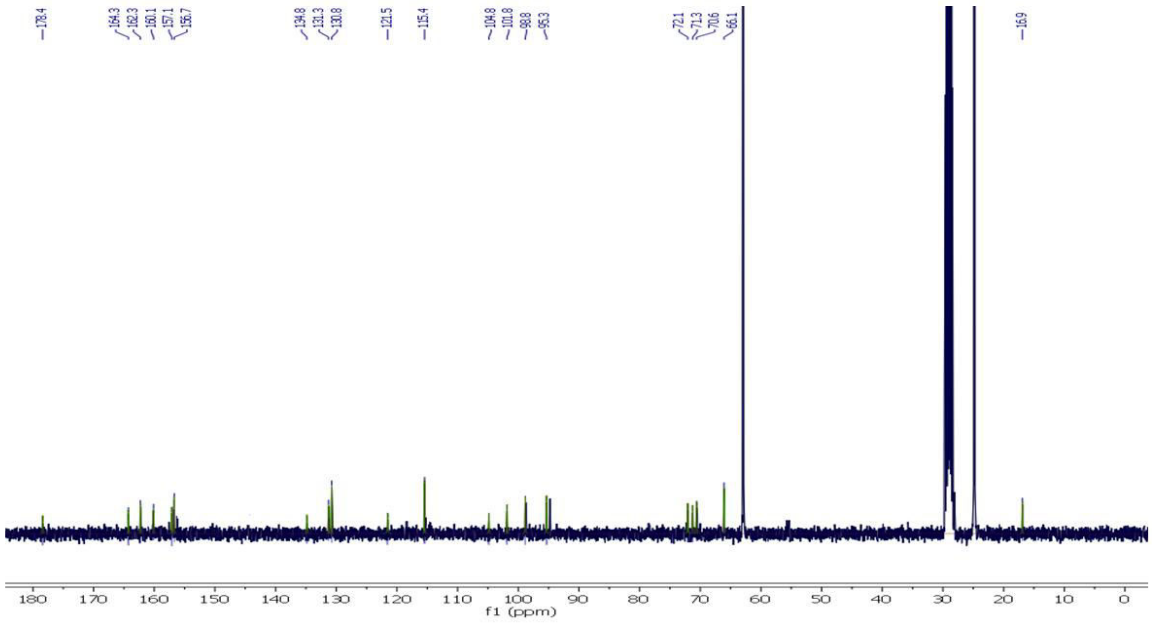

Appendix 27C: DEPT-135 NMR (101 MHz, Acetone-d6) spectrum of kaempferol-3-O-α rhamnopyranoside (**245**).

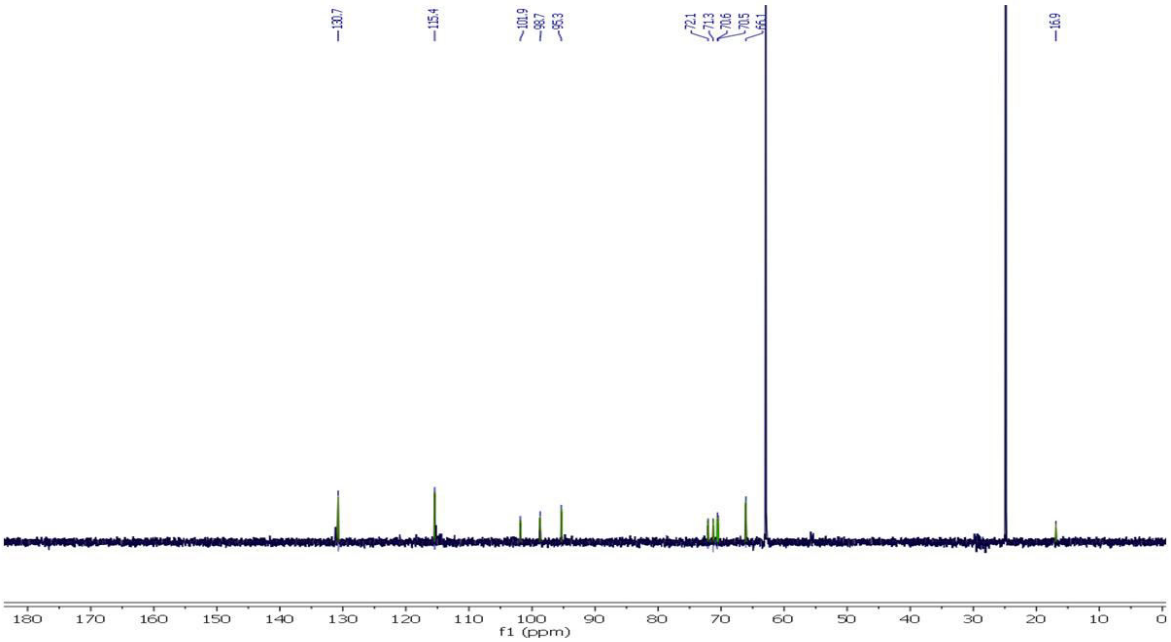

Appendix 28A: ^{1}H NMR (400 MHz, DMSO) spectrum of kaempferol-3-O-rutinoside (**246**).

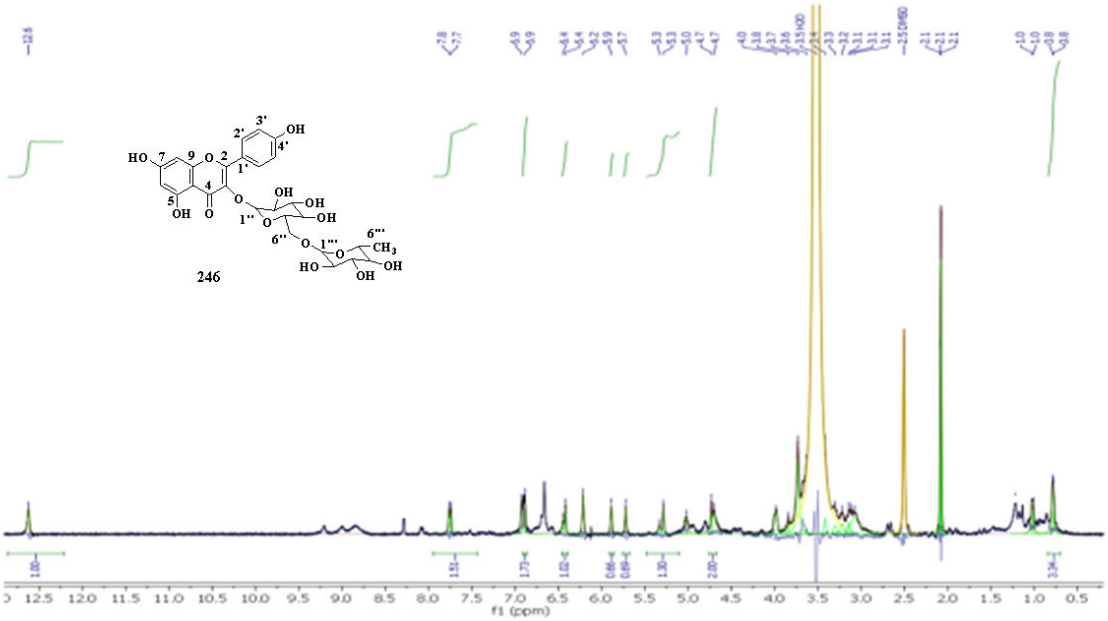

Appendix 28B: ^{13}C NMR (101 MHz, DMSO) spectrum of kaempferol-3-O-rutinoside (**246**).

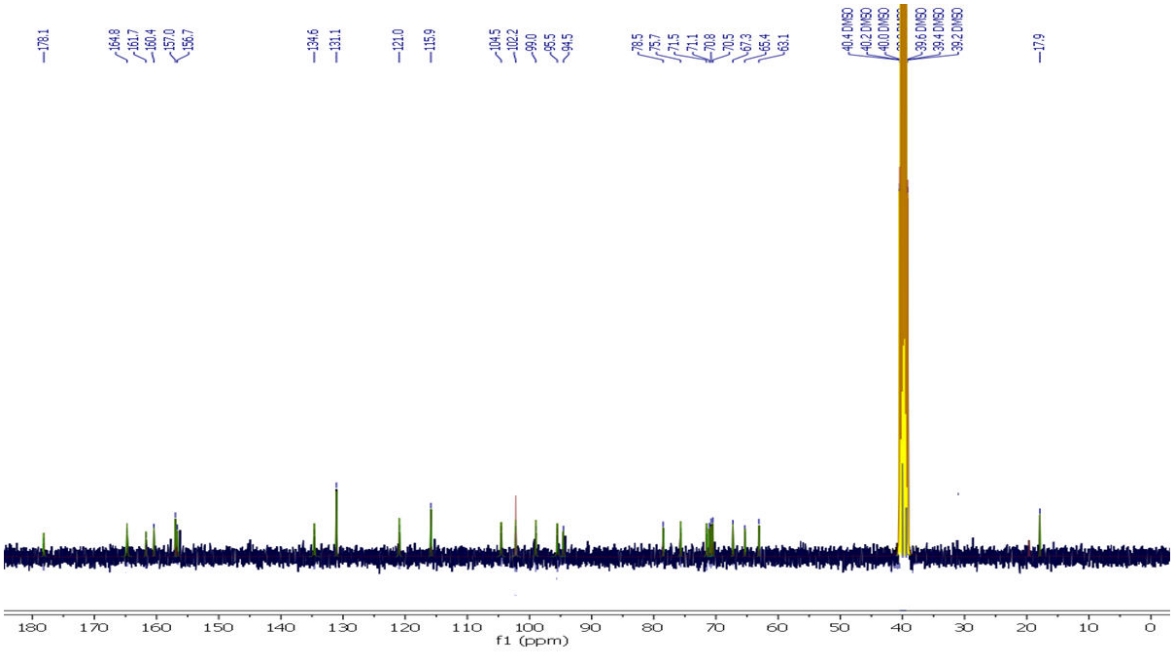

Appendix 28C: DEPT-135 NMR (101 MHz, DMSO) spectrum of kaempferol-3-O-rutinoside (**246**).

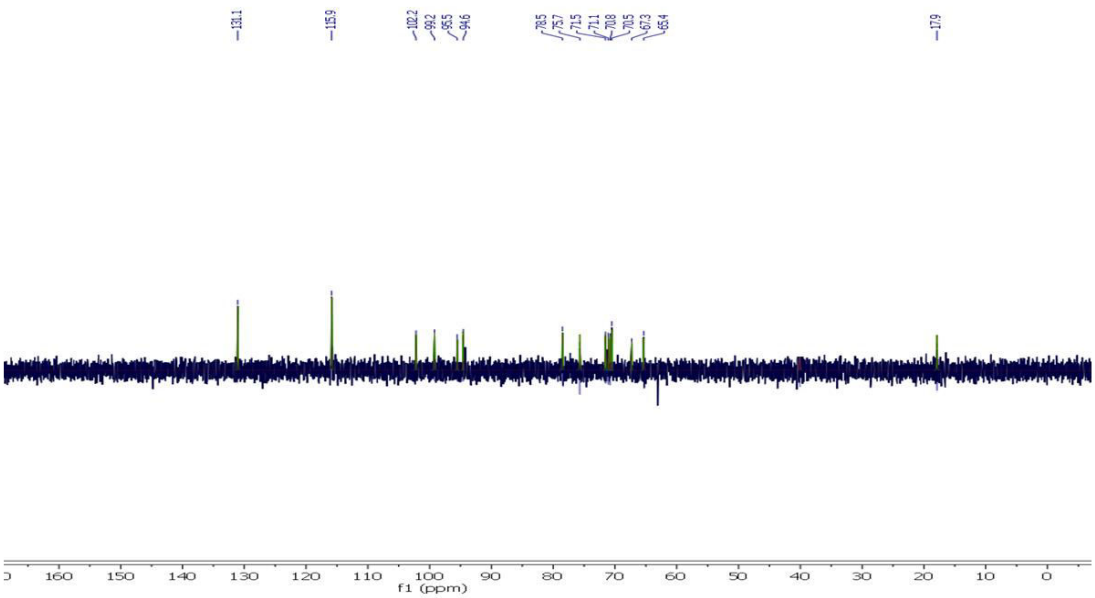

Appendix 29A: ^{1}H NMR (400 MHz, $CDCl_3$) spectrum of 3′-(4′′-methoxy phenyl)-3′-oxo-propionyl hexadecanoate (**247**).

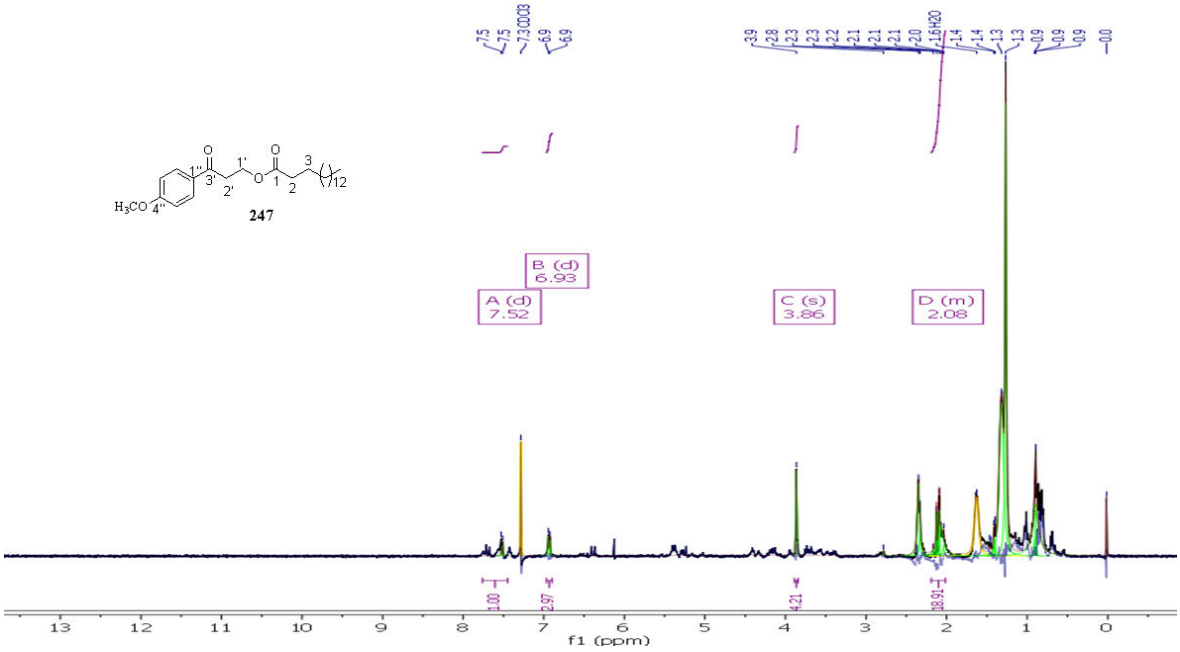

Appendix 29B: ^{13}C NMR (101 MHz, $CDCl_3$) spectrum of 3′-(4′′-methoxy phenyl)-3′-oxo-propionyl hexadecanoate (**247**).

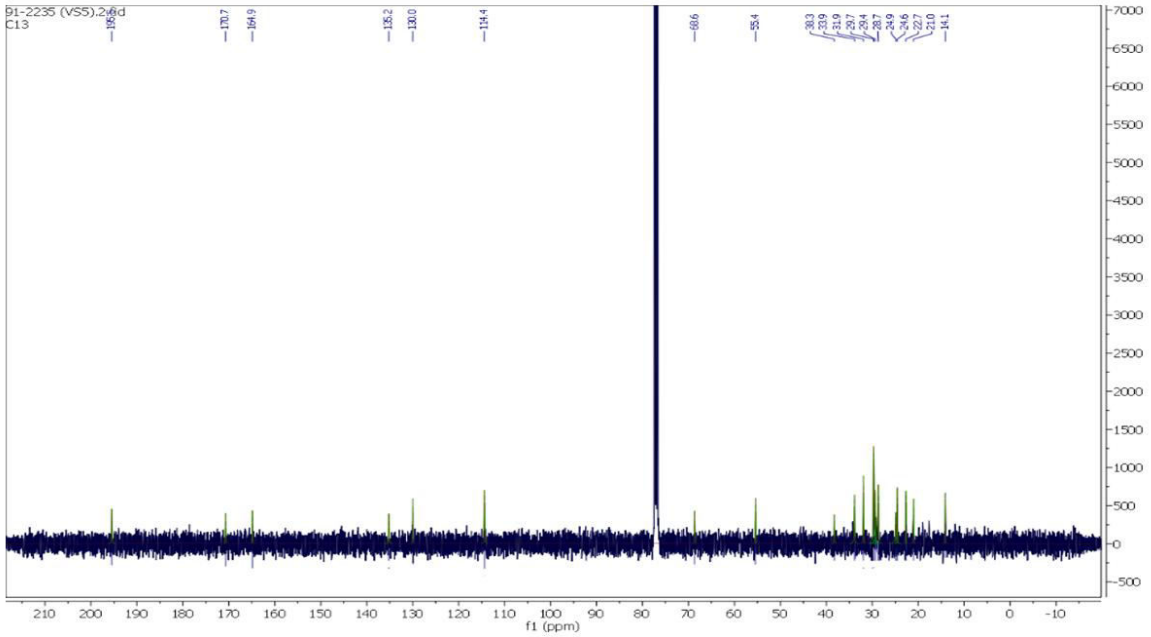

Appendix 29C: DEPT-135 NMR (101 MHz, $CDCl_3$) spectrum of 3′-(4′′-methoxy phenyl)-3′-oxo-propionyl hexadecanoate (**247**).

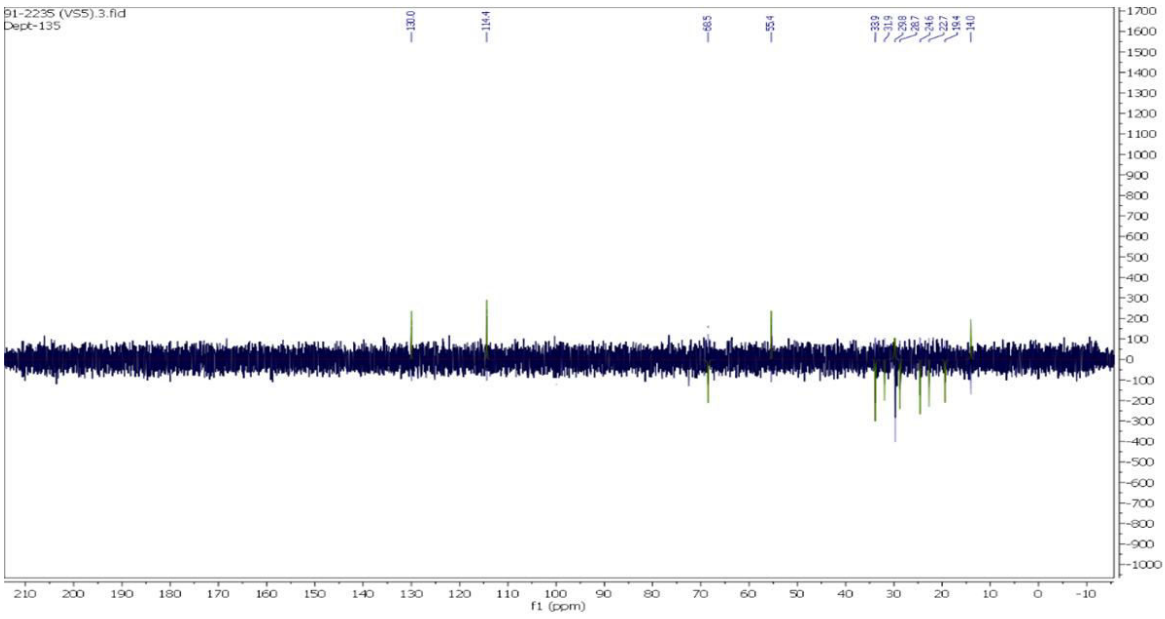

Appendix 30A: IR spectrum of compound **248**

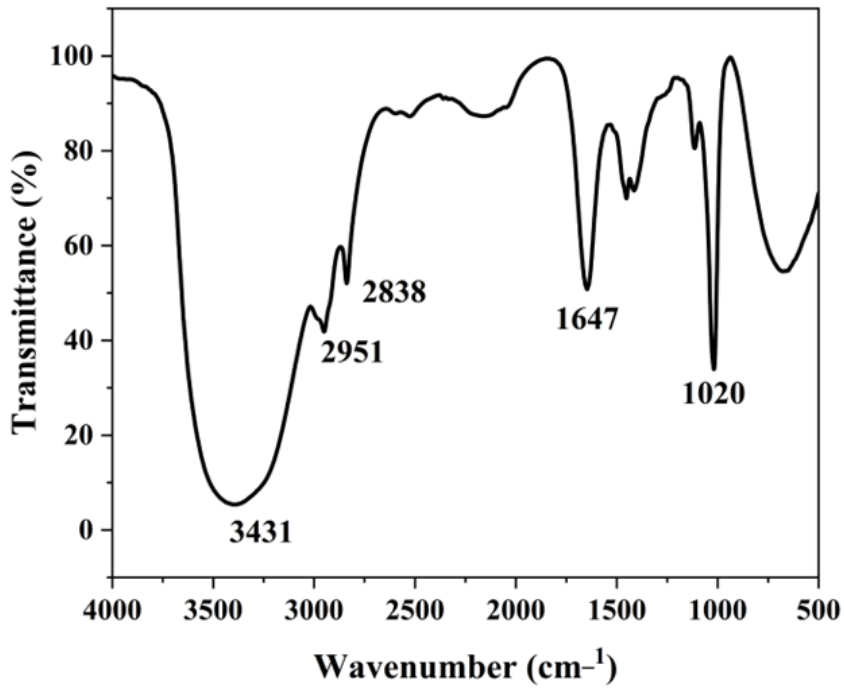

Appendix 30B: ^{1}H NMR (400 MHz, DMSO) spectrum of harpagoside (**248**).

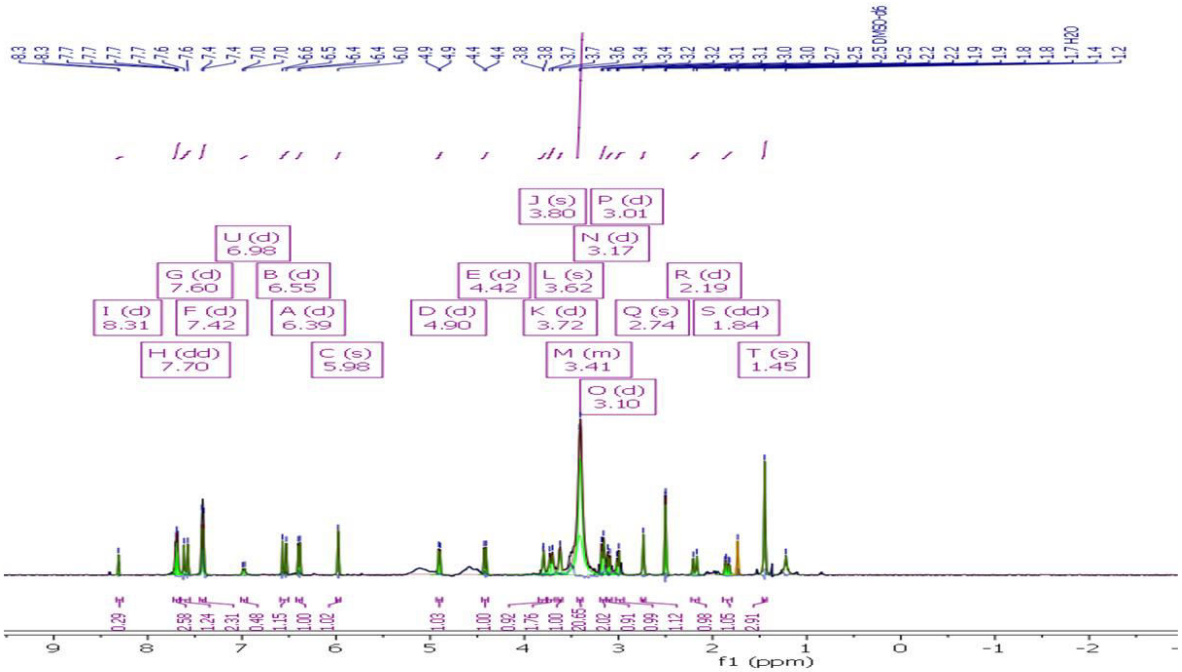

Appendix 30C: ^{13}C NMR (101 MHz, DMSO) spectrum of harpagoside (**248**).

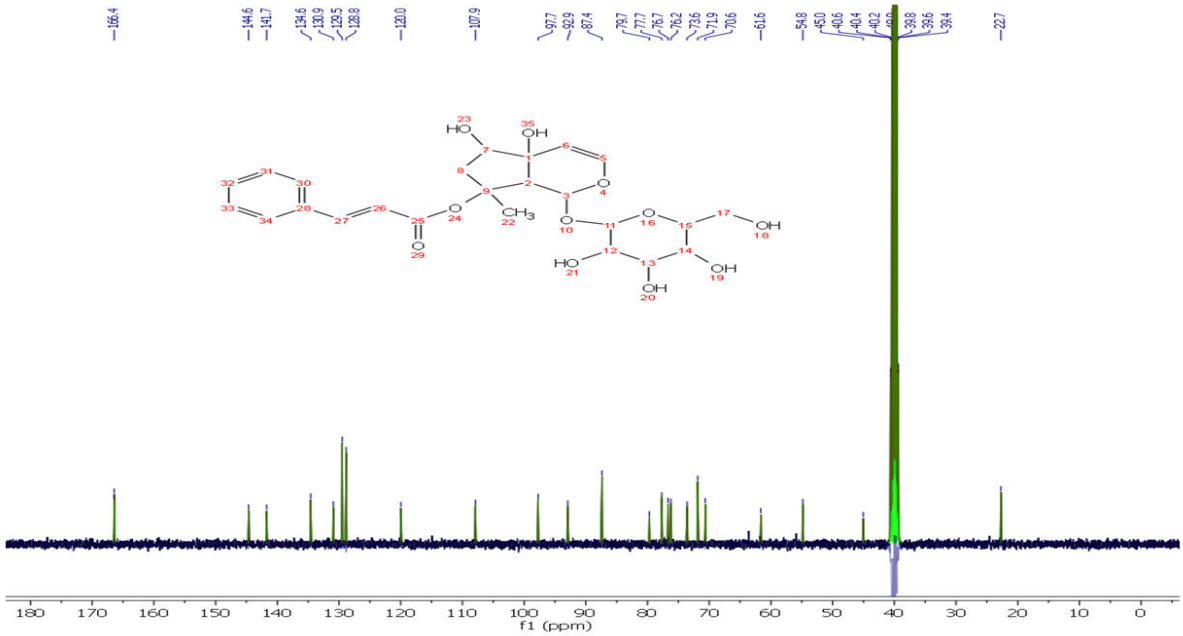

Appendix 30D: DEPT-135 NMR (101 MHz, DMSO) spectrum of harpagoside (**248**).

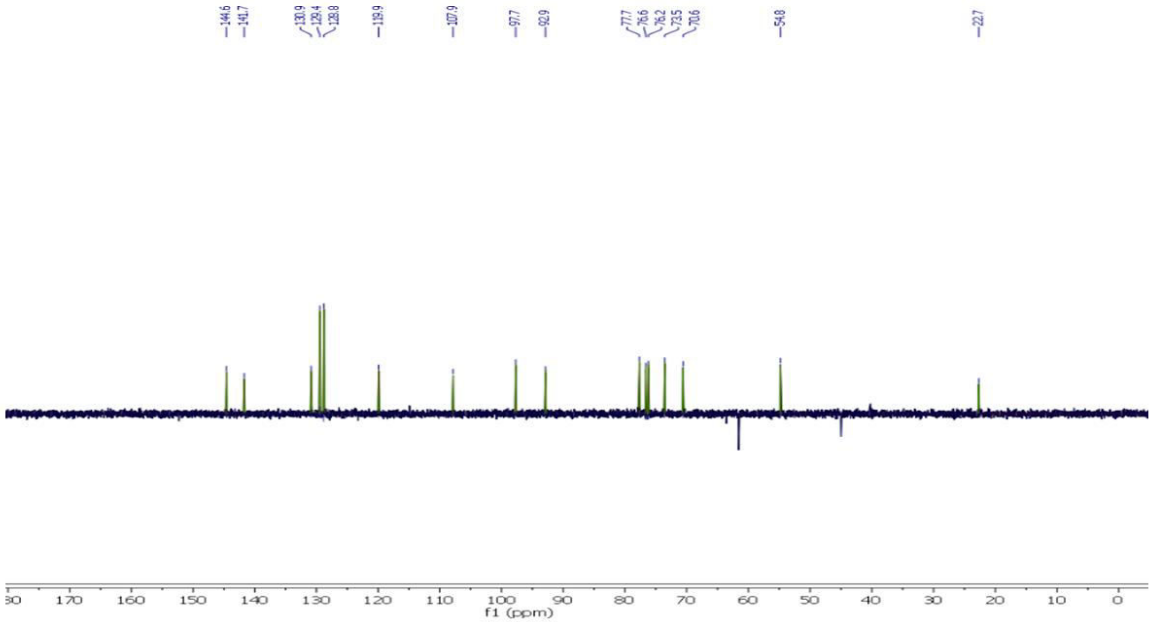

Appendix 31A: IR spectrum of compound **249.**

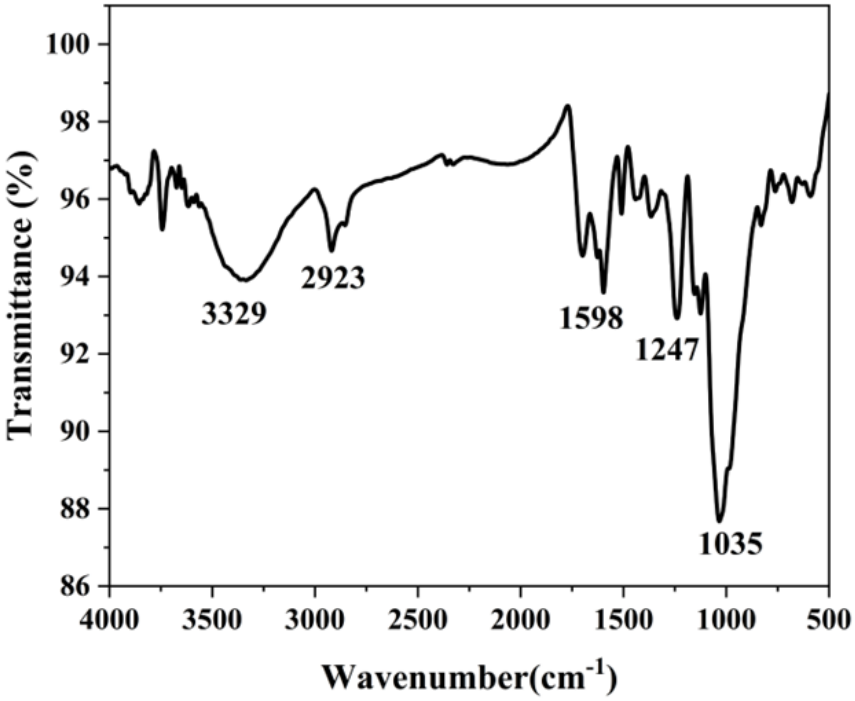

Appendix 31B: ^{1}H NMR (400 MHz, Acetone-d6)spectrum of pulverulentoside I (**249**).

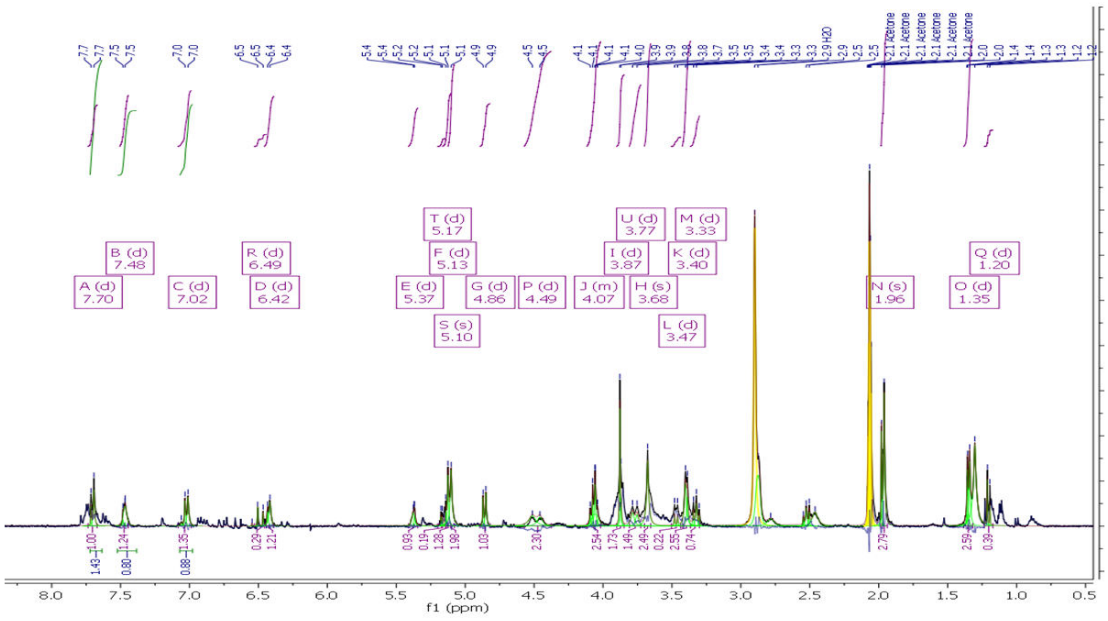

Appendix 31C: ^{13}C NMR (101 MHz, Acetone-d6)spectrum of pulverulentoside I (**249**).

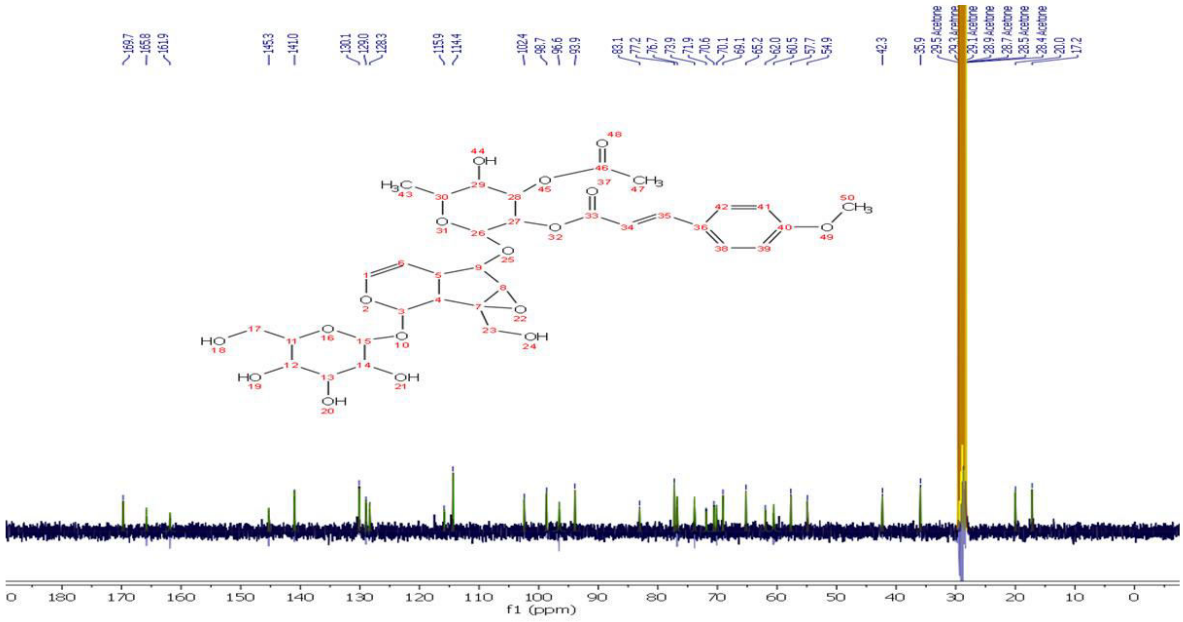

Appendix 31D: DEPT-135 NMR (101 MHz, Acetone-d6) spectrum of pulverulentoside I (**249**).

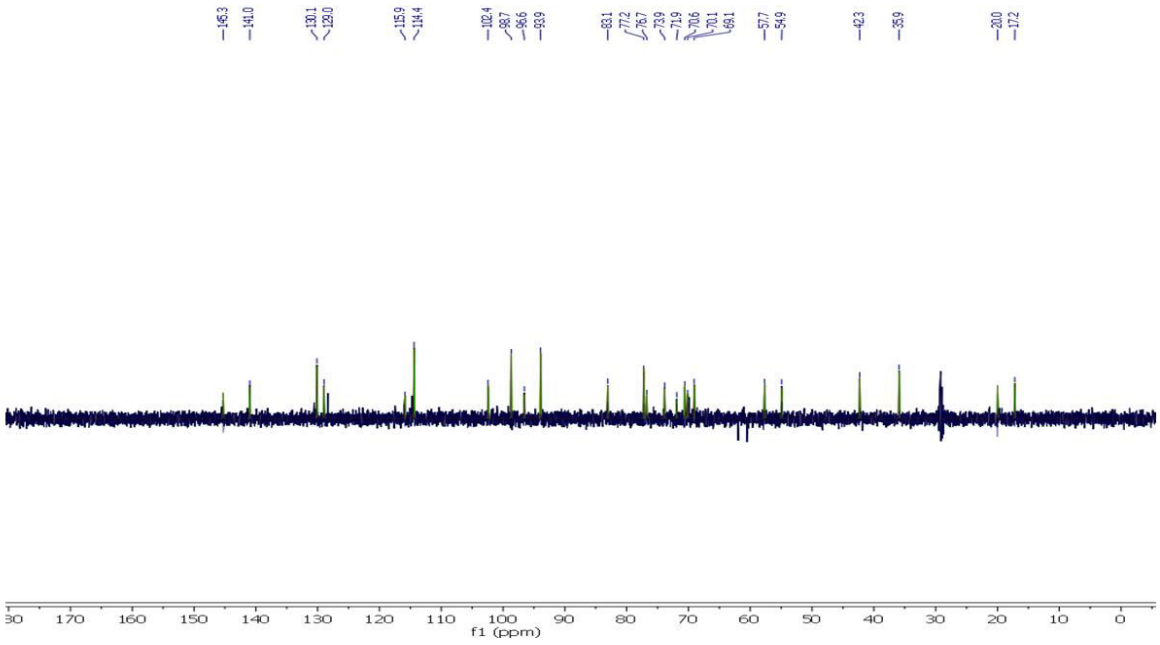

Appendix 32A: ^{1}H NMR (400 MHz, MeOD)spectrum of scrophuloside B4 (**250**).

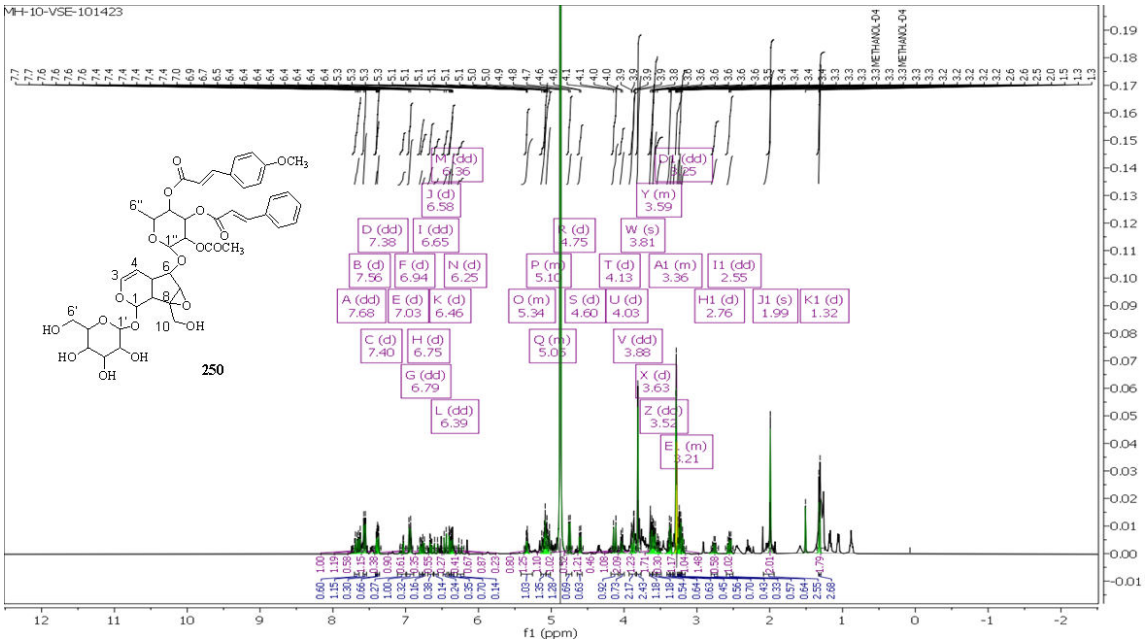

Appendix 32B: ^{13}C NMR (101 MHz, MeOD)spectrum of scrophuloside B4 (**250**).

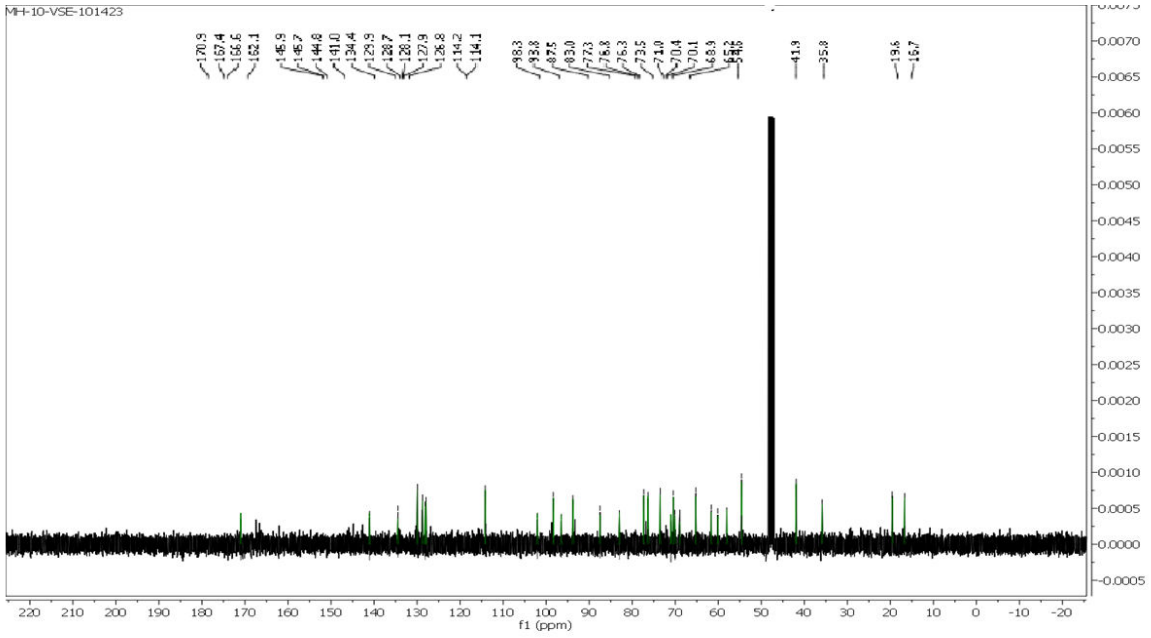

Appendix 32C: DEPT-135 NMR (101 MHz, MeOD) spectrum of scrophuloside B4 (**250**).

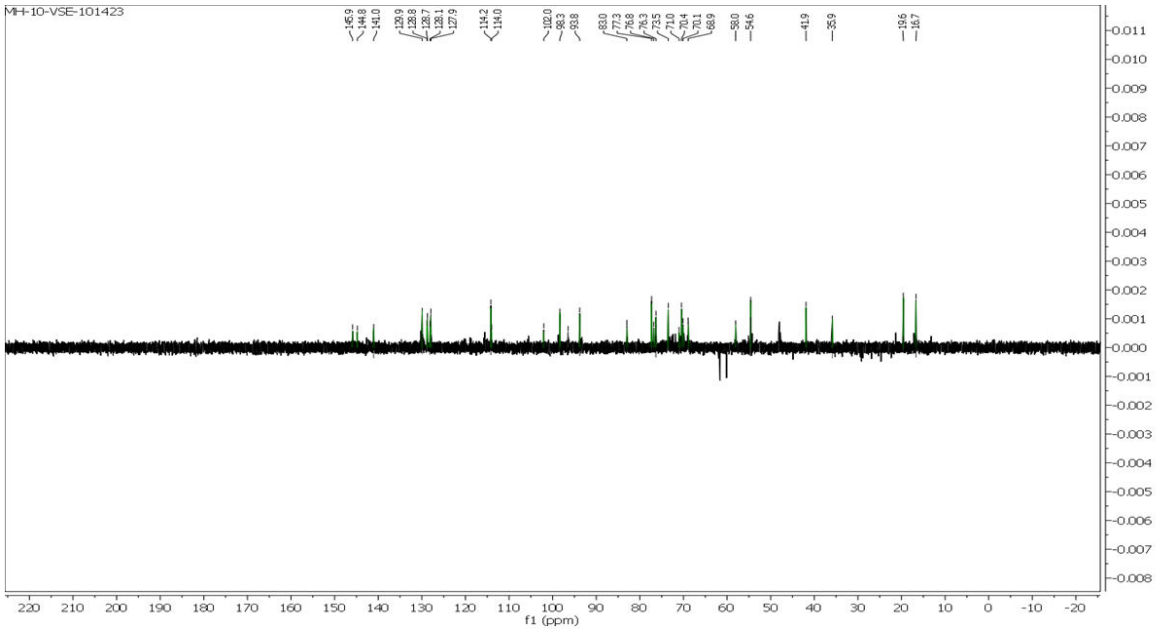

Appendix 33A: ^{1}H NMR (400 MHz, MeOD)spectrum of scropolioside A (**251**).

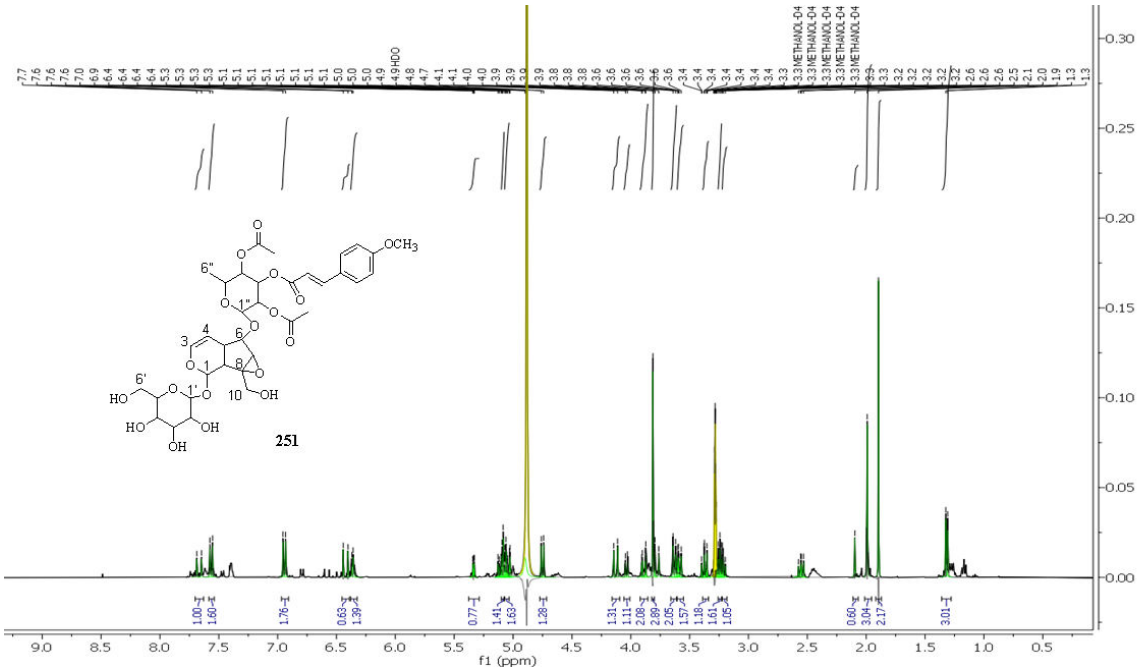

Appendix 33B: ^{13}C NMR (101 MHz, MeOD) spectrum of scropolioside A (**251**).

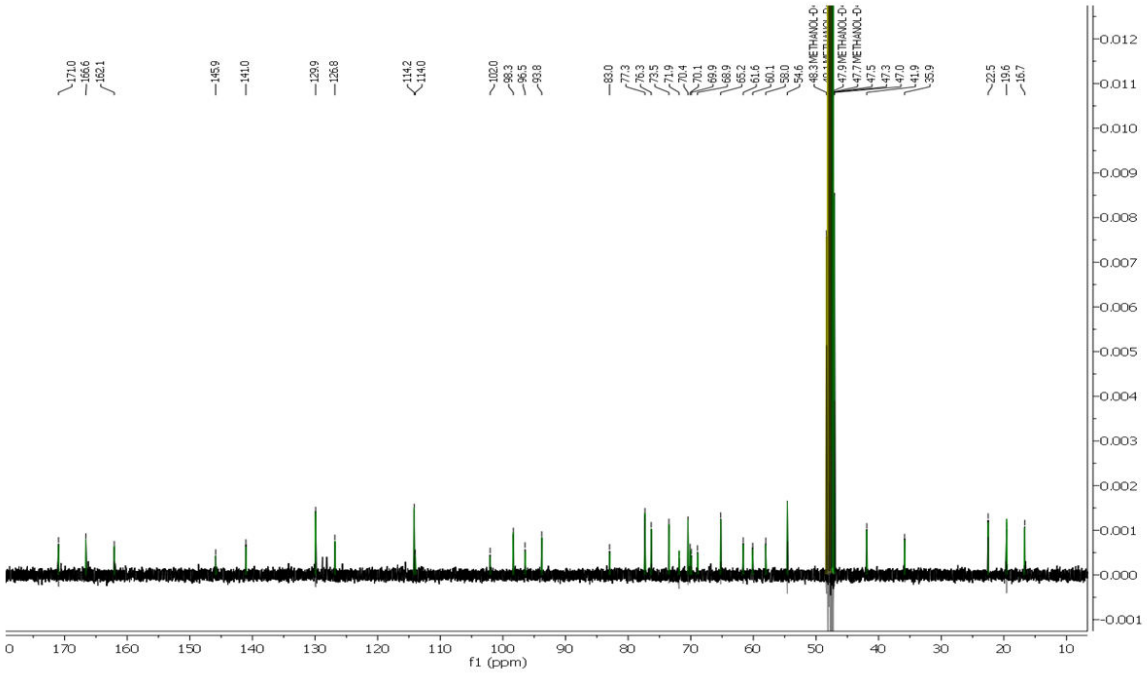

Appendix 33C: DEPT-135 NMR (101 MHz, MeOD) spectrum of scropolioside A (**251**).

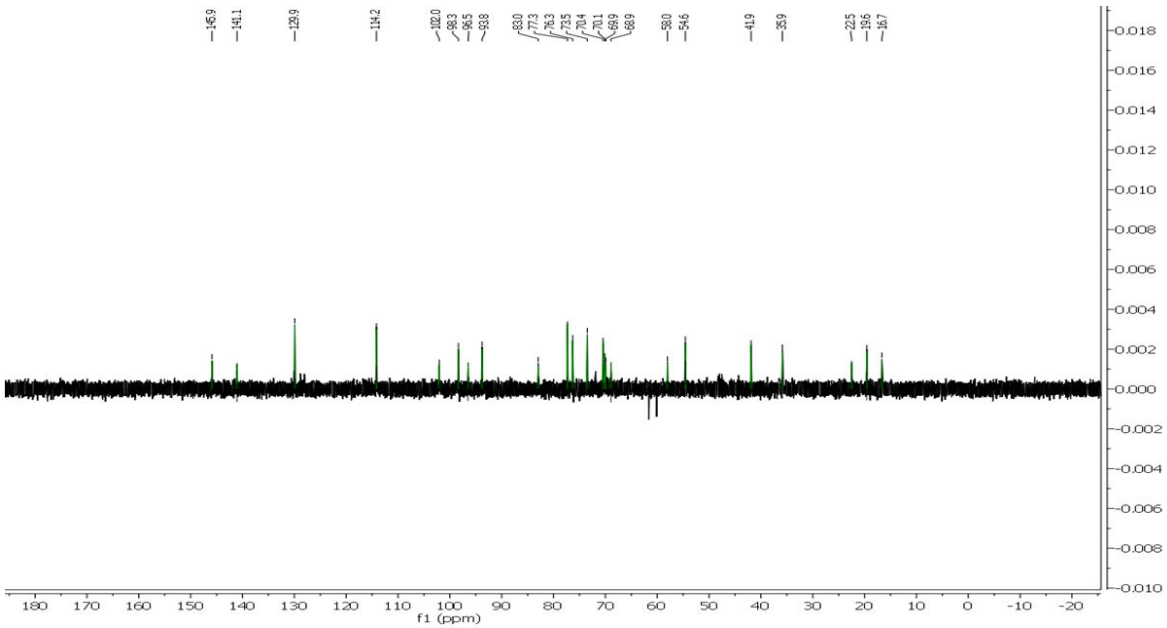

Appendix 34A: ^{1}H NMR (400 MHz, MeOD) spectrum of scropolioside-D2 (**252**).

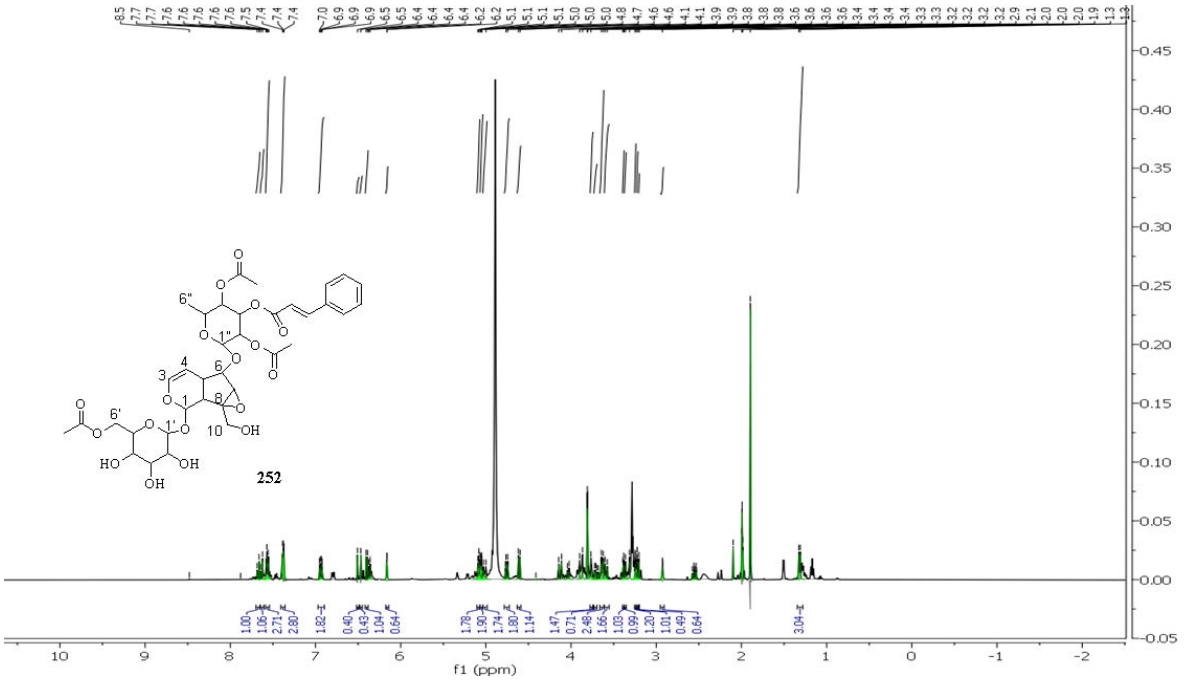

Appendix 34B: ^{13}C NMR (101 MHz, MeOD) spectrum of scropolioside-D2 (**252**).

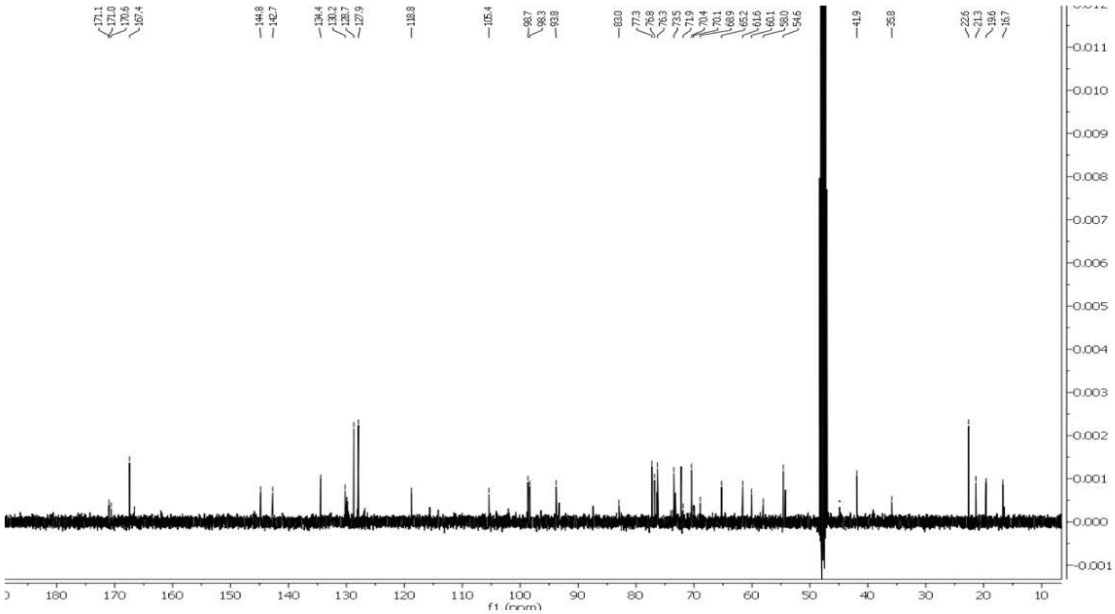

Appendix 34C: DEPT-135 NMR (101 MHz, MeOD) spectrum of scropolioside-D2 (**252**).

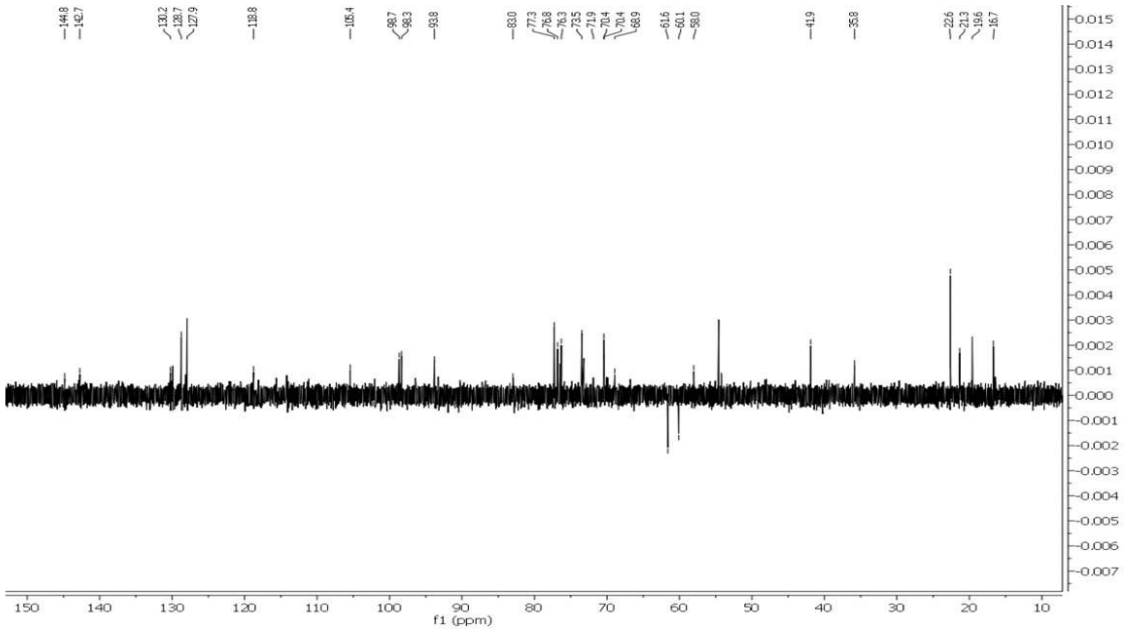

Appendix 35A: IR spectrum of compound **253.**

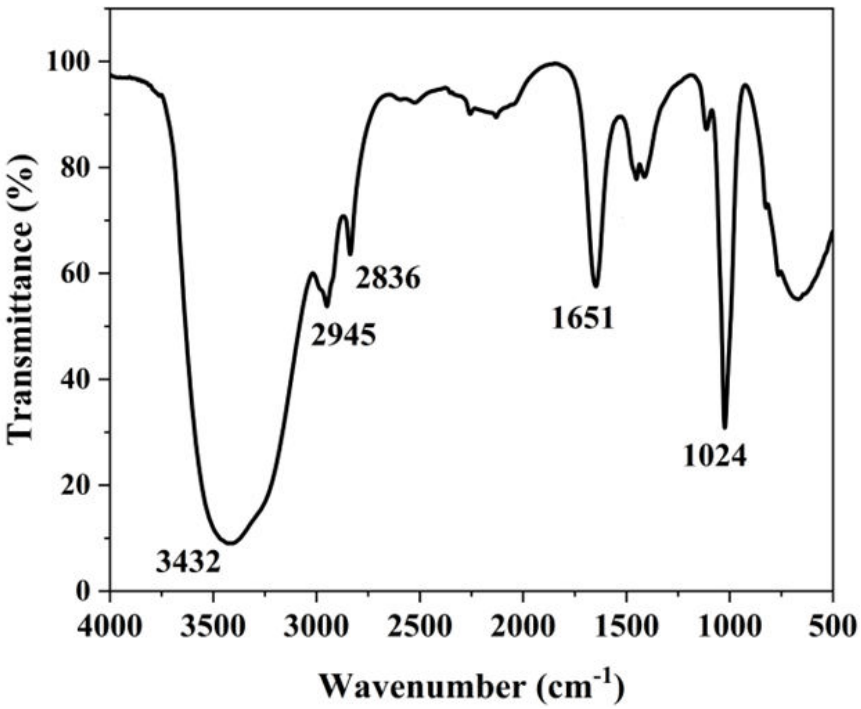

Appendix 35B: ^{1}H NMR (400 MHz, DMSO) spectrum of harpagide 6-*O*-β-glucoside (**253**).

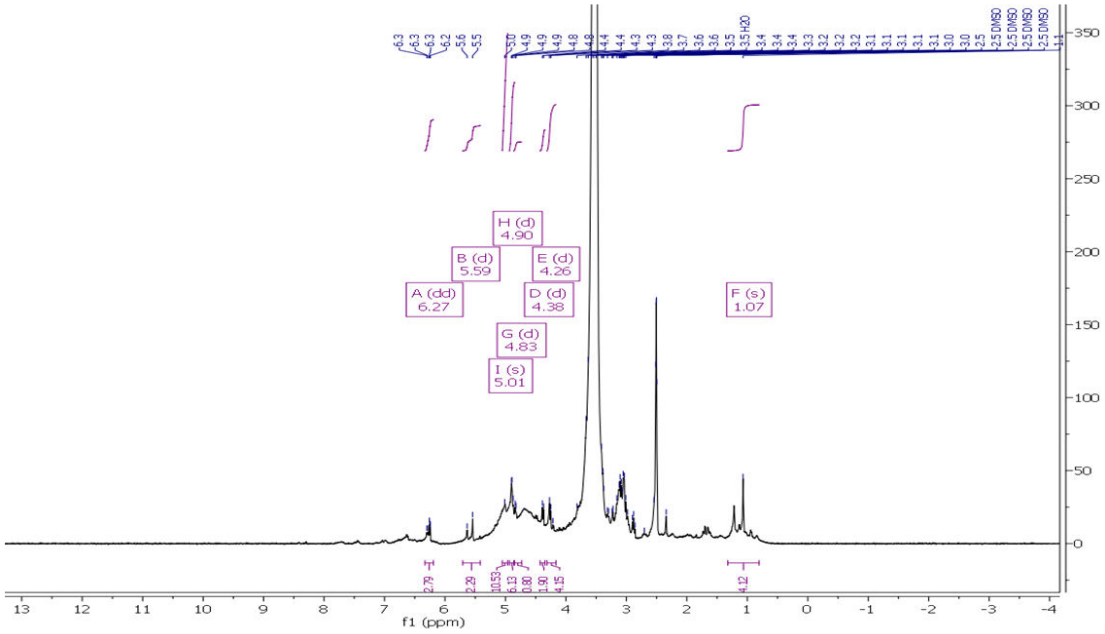

Appendix 35C: ^{13}C NMR (101 MHz, DMSO) spectrum of harpagide 6-*O*-β-glucoside (**253**).

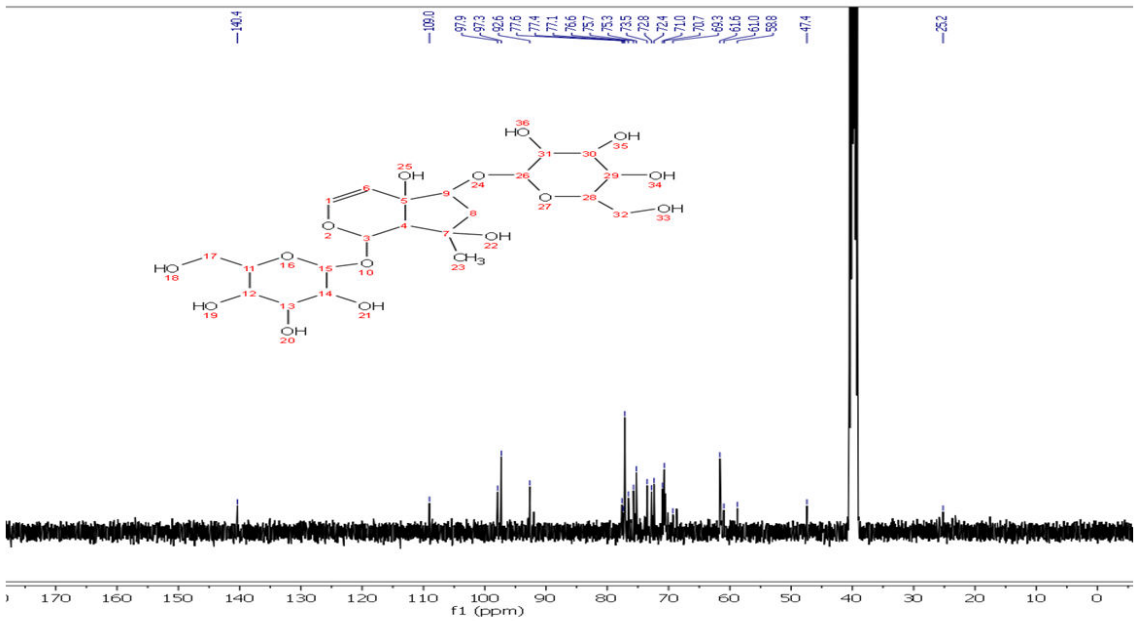

Appendix 35D: DEPT-135 NMR (101 MHz, DMSO) spectrum of harpagide 6-*O*-β-glucoside (**253**).

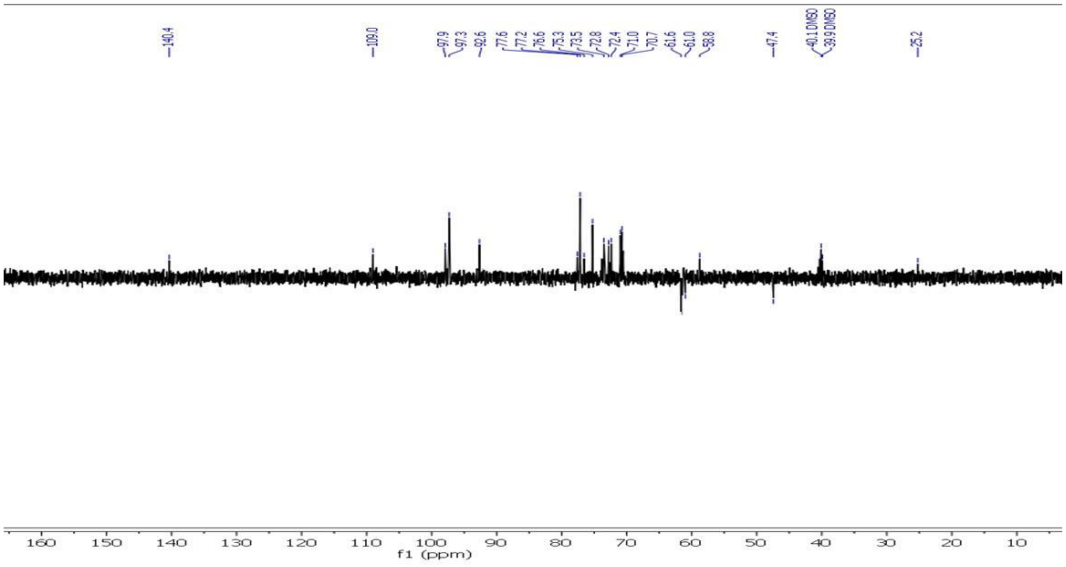

Appendix 36A: IR spectrum of compound **230.**

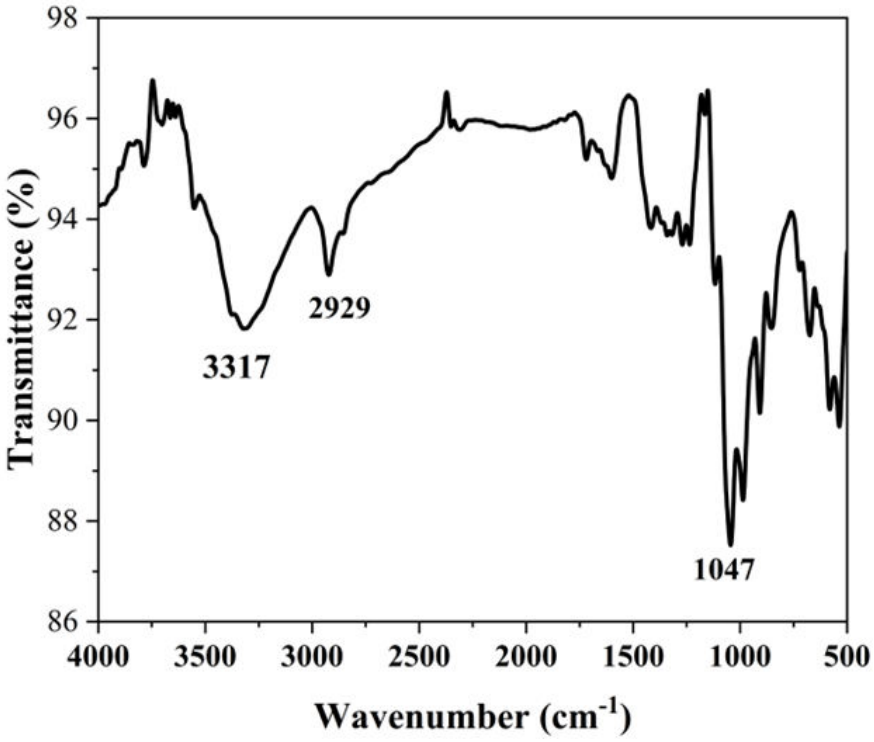

Appendix 36B: ^{1}H NMR (400 MHz, DMSO) spectrum of sucrose (**230**).

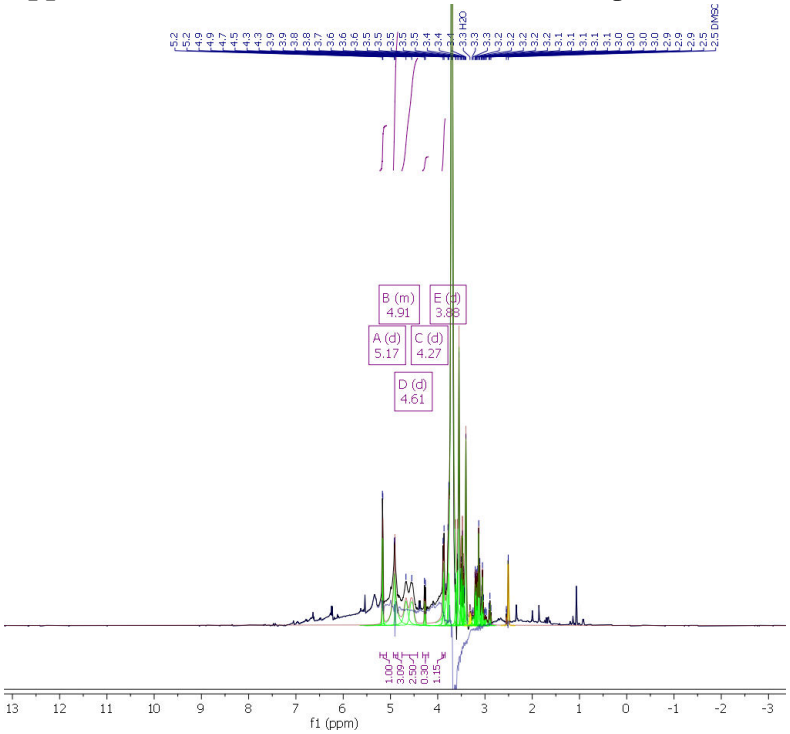

Appendix 36C: ^{13}C NMR (101 MHz, DMSO) spectrum of sucrose (**230**).

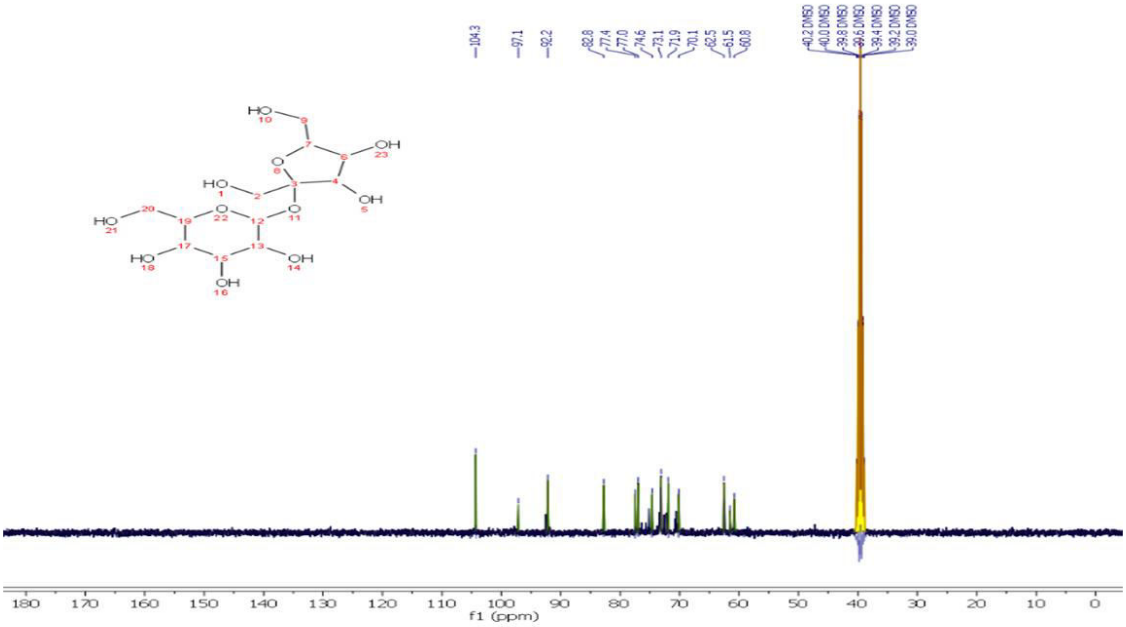

Appendix 36D: DEPT-135 NMR (101 MHz, DMSO) spectrum of sucrose (**230**).

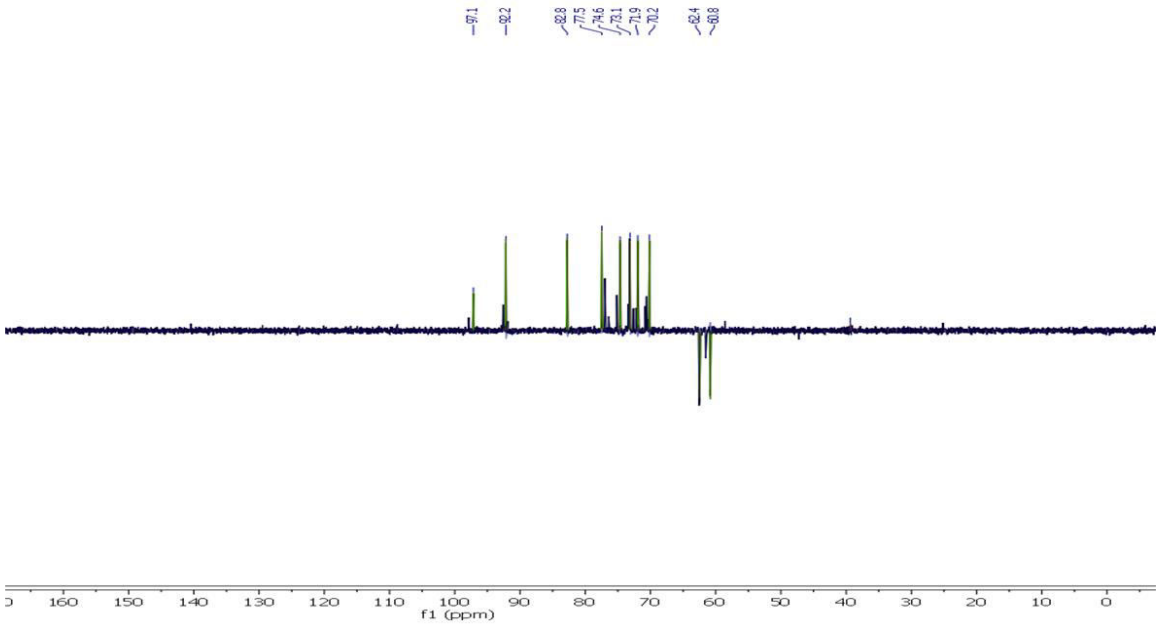

Appendix 37A: ^{1}H NMR (400 MHz, $CDCl_3$) spectrum of 22, 23-dihydrospinasterol acetate (**254**).

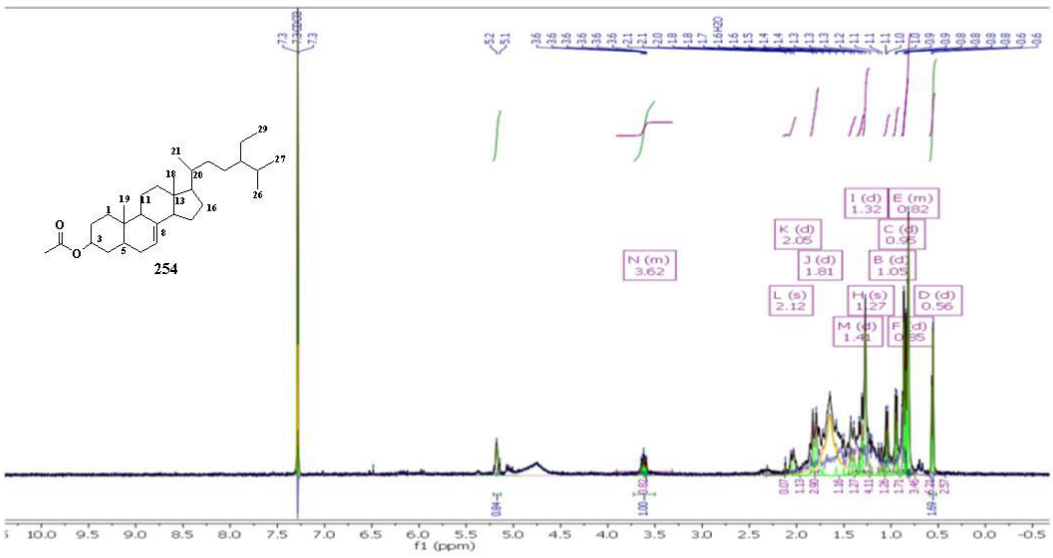

Appendix 37B: ^{13}C NMR (101 MHz, $CDCl_3$) spectrum of 22, 23-dihydrospinasterol acetate (**254**).

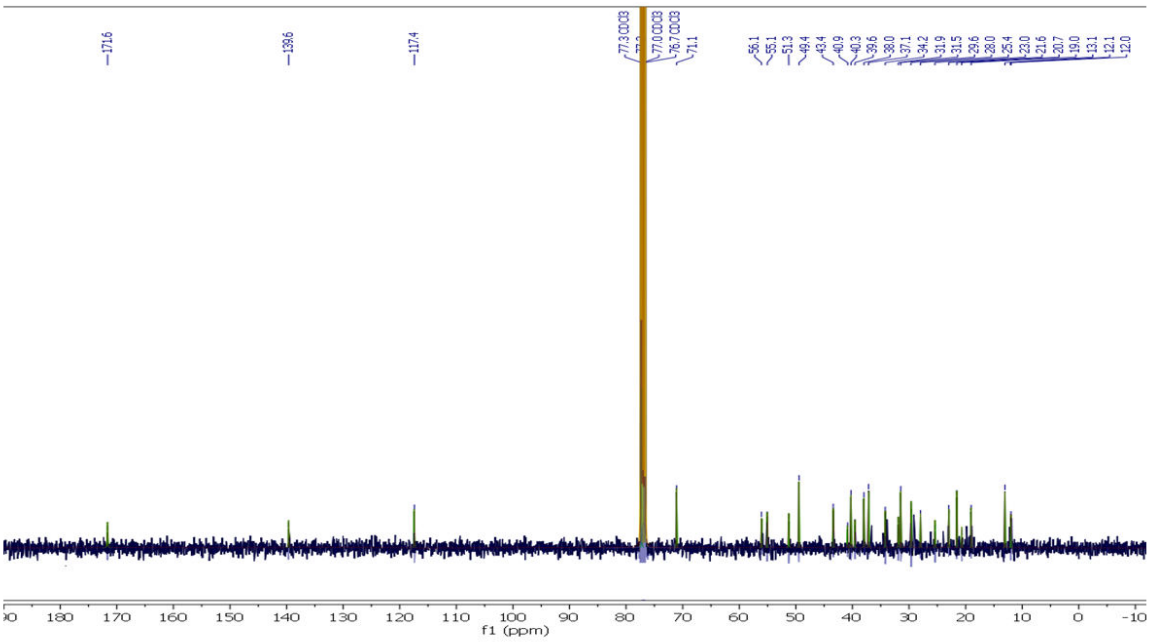

Appendix 37C: DEPT-135 NMR (101 MHz, $CDCl_3$) spectrum of 22, 23-dihydrospinasterol acetate (**254**).

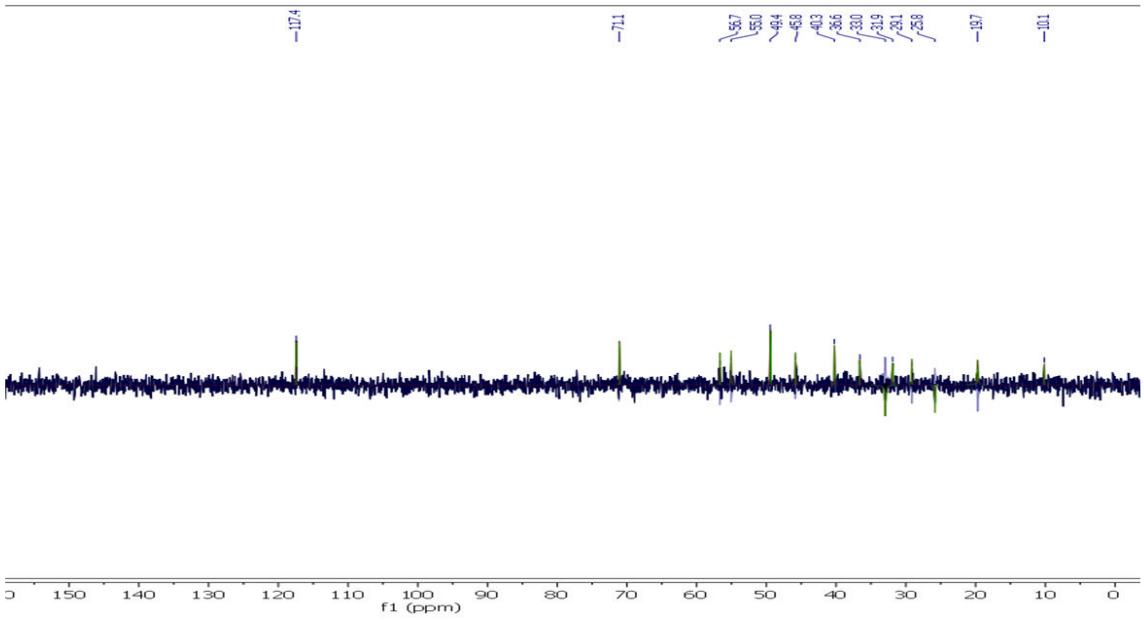

Appendix 38A: ^{1}H NMR (400 MHz, $CDCl_3$) spectrum of stigmasterol-3-O-β-D-glucoside (**255**).

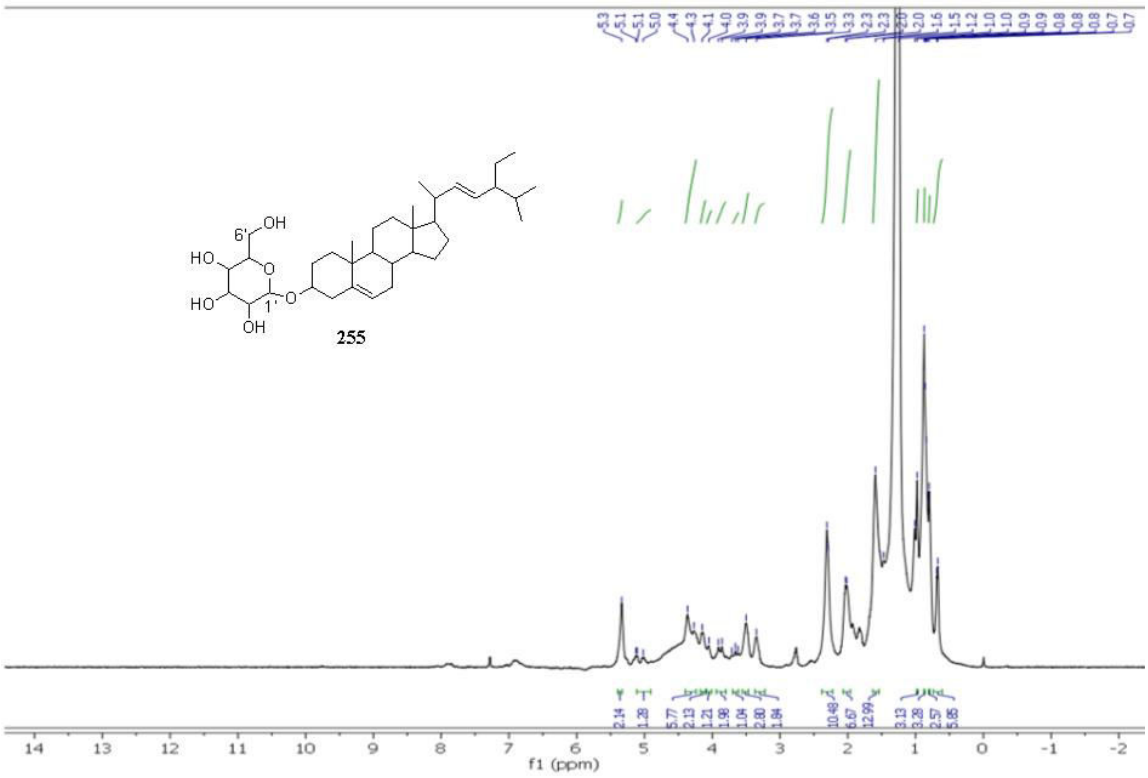

Appendix 38B: ^{13}C NMR (101 MHz, $CDCl_3$) spectrum of stigmasterol-3-O-β-D-glucoside (**255**).

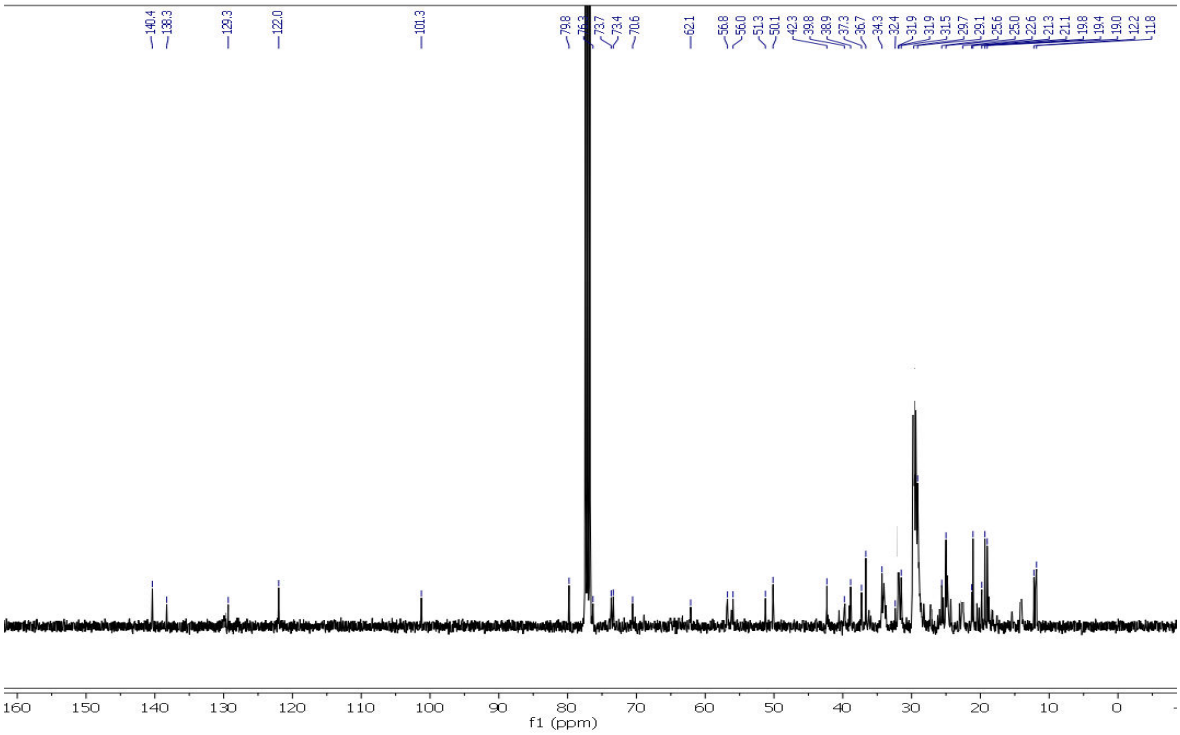

Appendix 38C: DEPT-135 NMR (101 MHz, $CDCl_3$) spectrum of stigmasterol-3-O-*β*-D-glucoside (**255**).

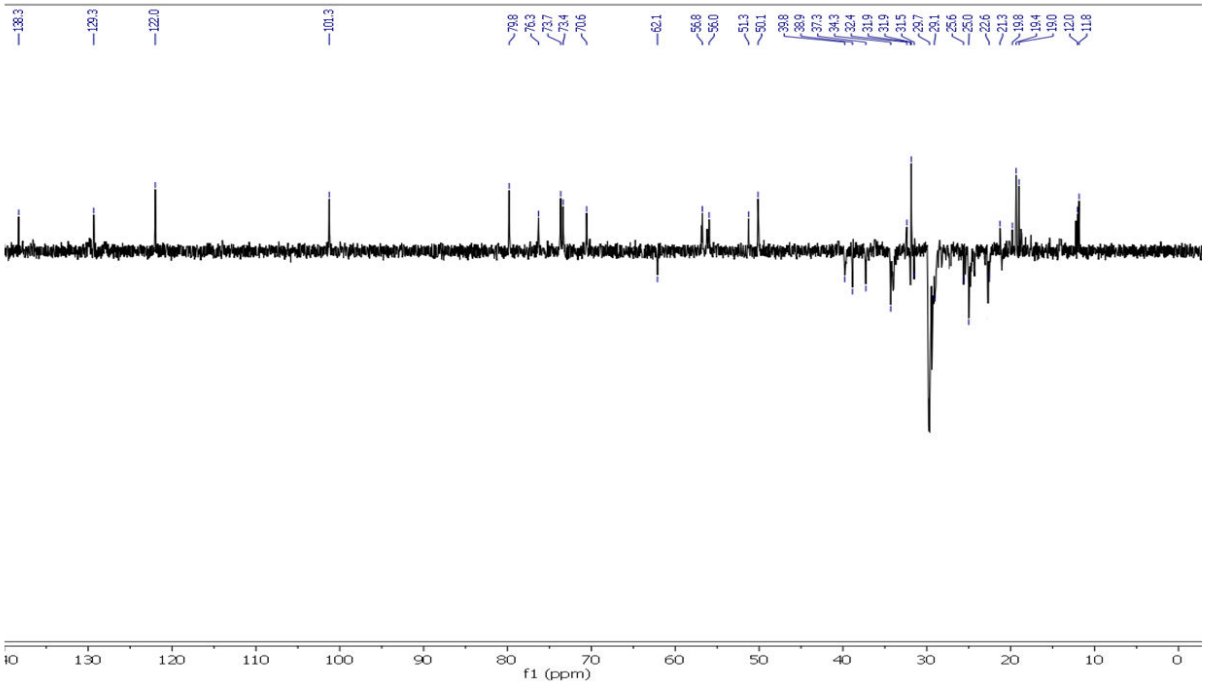

Appendix 39A: Chemical composition of the essential oils from bulbs of *C. abyssinicum* (BCA), and aerial parts of *C. abyssinica* (ACA).

Compound name	**RT**	**% Area**	
		BCA	ACA
γ-Caprolactone	9.09	0.54	-
(E)-Oct-2-enal	9.58	0.15	-
Phenylethanol	10.9	0.15	0.6
Camphor	11.9	0.36	0.21
Borneol	12.6	0.24	-
dl-Isopulegol	12.7	-	0.17
Octanoic acid	12.81	0.31	-
1-Dodecene	13.38	2.14	-
Dodecane	13.64	0.37	-
S-Verbenone	14.06	0.17	-
Benzofuran, 2,3-dihydro-	14.3	-	0.27
Phenethyl isocyanate	14.4	-	0.27
Benzenepropanenitrile	15.2	-	21.15
Capric acid	16.27	1.24	-
Isobornyl acetate	16.53	0.25	-
Indole	16.7	-	0.52
2-Methoxy-4-vinyl-phenol	17.4	-	0.25
Piperonal	18.01	0.59	-

Cyclotetradecane	18.32	0.29	-
Isoeugenol	18.79	0.14	-
γ-n-Amylbutyrolactone	18.96	0.25	-
Cysteamine S-sulfate	19.17	0.30	-
4a-Methyldecahydro-2H-benzo[a]cyclohepten-2-one	19.28	0.15	-
1-Adamantanecarboxylic acid, 5-tetradecyl ester	19.99	0.15	-
Tetradecane	20.11	1.38	-
Isocaryophyllene	20.81	0.23	-
***cis*-Geranylacetone**	21.9	-	0.35
Tenocyclidine	21.94	0.20	-
Isoshyobunone	22.22	0.26	-
1-Dodecanol	22.4	1.61	-
Benzene, (2-isothiocyanatoethyl)-	22.4	-	33.24
Carotol	22.59	0.17	-
3-Furanacetic acid, 4-hexyl-2,5-dihydro-2,5-dioxo-	22.76	0.77	-
***trans*-.β.-Ionone**	22.8	-	1.12
Methyl phenethylcarbamate	22.9	-	0.61
β-Himachalene	23.28	0.25	-
Phenol, 2,4-bis(1,1-dimethylethyl)-	23.6	-	4.26
Cyclohexanebutanal, 2-methyl-3-oxo-, cis-	23.8	-	0.54
1,3-Benzenediol, 5-pentyl-	24.02	0.59	0.26
2(4H)-Benzofuranone, 5,6,7,7a-tetrahydro-4,4,7a-trimethyl-, (R)-	24.2	-	0.91
Ethylene thiourea	25.09	0.23	0.19
Megastigmatrienone	25.1	-	0.45
Hexadecane	26.10	0.90	-
1-Isobutyl-7,7-dimethyl-1,3,4,5,6,7a-hexahydroisobenzofuran-3a-ol	29.50	0.17	-
Myristic acid	30.72	1.84	0.25
(*E*)-Atlantone	30.93	0.18	-
Octadecane	31.54	0.80	-
Stearyl alcohol	31.72	0.28	-
Phthalic acid, cylclohexylmethyl pentyl ester	32.3	-	0.55
Aspidospermidin-17-ol, 1-acetyl-16-methoxy-	32.70	0.15	-
2-Pentadecanone, 6,10,14-trimethyl-	32.7	-	0.89
Ethyl (9Z,12Z)-9,12-octadecadienoate	33.07	0.36	-
i-Propyl 12-methyltetradecanoate	33.16	0.24	-
1,2-Benzenedicarboxylic acid, bis(2-methylpropyl) ester	33.36	9.08	-
2,5-Octadecadiynoic acid, methyl ester	33.78	0.16	-
9-Hexadecenoic acid, methyl ester, (Z)-	34.2	-	0.2
rans-Geranylgeraniol	34.5	-	0.42
7,9-Di-tert-butyl-1-oxaspiro(4,5)deca-6,9-diene-2,8-dione	34.61	0.41	-
Palmitic acid ME	34.71	0.42	0.44
Linoleic acid	35.15	0.88	-

Palmitic acid	36.00	27.16	-
Mono(2-ethylhexyl) phthalate	36.5	-	0.21
Probucol	36.60	1.44	-
Diisooctylphthalate	36.69	2.04	11.14
1,2-Ethanediylbis(carbamodithioato)(2-)-manganese	37.06	1.32	-
β-Citronellol, triethylsilyl ether	37.76	0.43	-
Butyl-2-methylpropylphthalate	37.88	1.22	-
***E*-11-Tetradecenol, trimethylsilyl ether**	37.97	1.17	-
L-Serine, O-(phenylmethyl)-	38.26	0.77	-
9,12-Octadecadienoic acid (Z,Z)-, methyl ester	38.69	2.21	0.34
13-Methyltetradec-9-enoic acid methyl ester	38.8	3.05	-
9-Octadecenoic acid (Z)-, methyl ester	38.8	-	0.56
i-Propyl 11,12-methylene-octadecanoate	38.98	1.29	-
Phytol	39.1	-	3.57
Methyl 16-hydroxy-hexadecanoate	39.40	0.66	-
Linoleic acid	39.7	-	0.58
9,12-Octadecadienoic acid, ethyl ester	40.2	-	0.39
Ethyl Oleate	40.3	-	0.68
Stearic acid	40.34	4.52	-
Oleic Acid	40.4	-	-
***tert*-Hexadecanethiol**	41.02	2.15	-
Octadecane	41.1	-	0.30
Cyclotetradecane	41.2	-	0.25
Tricosane	43.13	3.91	-
2,2'-Biphenol, 3,3',5,5'-tetrakis(1,1-dimethylethyl)-	44.58	2.36	0.32
Cyclohexadecane	45.10	12.74	9.44
Phthalic acid, 2-cyclohexylethyl isobutyl ester	45.19	1.43	-
Phthalic acid, nonyl 2-pentyl ester	45.54	0.42	-
Phthalic acid, butyl undecyl ester	45.2	-	0.23
2-([(2-Ethylhexyl)oxy]carbonyl)benzoic acid	45.5	-	0.25
Phthalic acid, butyl tetradecyl ester	45.66	0.31	-
Hentriacontane	45.9	-	2.85
1,2-Benzenedicarboxylic acid, dinonyl ester	46.5	-	0.23

Appendix 39B: Chemical components (%) of the essential oils from leaves, flowers, and seeds of *C. procera.*

Compound name	**% Area**			**RT**	**RI**
	Leaves	Flowers	Seeds		
p-Cresol	1.32	0.48	-	8.5	699
Perhydropyridazine	-	-	0.32	15	400

Phenol, 2-methoxy-	0.36	-	-	10.1	700
3-Mercaptohexanol	0.34	-	-	10.8	601
Phenylethanol	0.92	0.29	-	10.9	799
Phenol, 4-ethyl-	-	0.37	-	12.5	800
1-Nonanol	-	0.23	-	12.7	899
Nonadecane	-	-	0.77	31.5	1900
3,6-Nonadien-1-ol, (E, Z)-	0.92	-	-	12.3	899
1-Dodecene	0.74	-	-	12.7	1199
Tetradecane	-	-	0.71	20.1	1400
Benzofuran, 2,3-dihydro-	0.75	2.12	-	14.2	800
Capric acid	-	0.29	-	15.9	1000
Guaiacol, 4-ethyl-	-	0.24	-	16.3	900
Promecarb-M	-	0.49	-	17.6	1001
1-Undecanol	-	-	0.13	20.3	1099
1-Dodecanol	-	-	1.29	22.4	1199
Cyclodecanone	-	0.43	-	18.3	999
1,5,5-Trimethyl-6-methylene-cyclohexene	0.29	-	-	15	999
Carane, 4,5-epoxy-, trans	0.38	-	-	15.4	999
Cyclotetradecane	0.28	-	-	16	1400
3,6-Dimethyl-2,3,3a,4,5,7a-hexahydrobenzofuran	0.71	-	-	16.3	1000
Phenol, 5-methyl-2-(1-methylethyl)-	1.23	0.59	-	16.7	1000
Mono(2-ethylhexyl) phthalate	-	-	0.49	44.4	
Prop-2-en-1-one, 1-(6,6-dimethylbicyclo [3.1.1]hept-2-en-2-yl)-	0.34	-	-	16.9	1201
2-methoxy-4-vinyl-phenol	3.38	4.69	-	17.4	901
2(3H)-Furanone, dihydro-5-pentyl-	-	0.49	0.49	18.9	900
4-Hydroxy-3-methoxybenzaldehyde	-	0.58	-	20.0	800
Phenol, 2-cyclohexyl-	1.37	-	-	17.6	1201
(2E)-3,7-Dimethyl-2,6-octadienal	0.56	-	-	17.9	1002
4,4,6-Trimethyl-cyclohex-2-en-1-ol	1.14	-	0.27	18.3	899
2-Cyclopenten-1-one, 3-methyl-2-(2-pentenyl)-, (Z)-	0.57	-	-	19.1	1100
Ylangenal	-	1.06	-	28.3	1501
Vanillin lactoside	0.32	-	-	20.1	2000
Phenol, 2,4-bis(1,1-dimethylethyl)-	-	-	23.39	23.6	1400
Naphthalene, 2-methoxy-	0.36	-	-	21.6	1100
Acorenone B	0.41	-	-	21.8	1500
Cyclotetradecane	0.55	0.71	0.56	16	1400
trans-.beta.-Ionone	2.27	-	-	22.8	1299
Octadecane	0.48	0.44	-	23.1	1799
2,4-Di-tert-butylphenol	0.57	0.33	-	23.5	1400
1,8(2H,5H)-Naphthalenedione, hexahydro-8a-methyl-, cis-	-	0.29	-	23.9	1100

Lauric acid	-	0.95	-	25.1	1199
Isoshyobunone	-	0.24	-	26.6	1501
beta.-Eudesmol	-	0.31	-	27.6	1500
10,10-Dimethyl-3-oxatricyclo [7.1.1.0]undecan-4-one	0.51	-	-	24	1200
2(4H)-Benzofuranone, 5,6,7,7a-tetrahydro-4,4,7a-trimethyl-, (R)-	0.27	-	-	24.1	1100
2H-1-Benzopyran-2-one, 3,4-dihydro-4,4-dimethyl-	0.32	-	-	24.3	1101
Benzaldehyde, 4-(dimethylamino)-	0.52	-	-	24.4	901
1H-Benzocycloheptene, 2,4a,5,6,7,8-hexahydro-3,5,5,9-tetramethyl-, (R)-	-	-	0.27	23.3	1500
1,1,4,7-Tetramethyldecahydro-1H-cyclopropa[e]azulen-4-ol	1.24	0.41	-	25.1	1499
9,12-Octadecadienoic acid (Z, Z)-	-	2.86	2.43	39.6	1799
9,12-Octadecadienoic acid, ethyl ester	-	-	2.57	40.3	1900
1-Oxaspiro [2.5]octane, 5,5-dimethyl-4-(3-methyl-1,3-butadienyl)-	0.36	-	-	25.7	1400
Linoleic acid	0.67	0.25	0.22	26.4	1801
Stearic acid ME	-	-	0.76	39.4	1900
1,4-Methanoazulen-7(1H)-one, octahydro-4,8,8,9-tetramethyl-, (+)-	0.28	-	-	26.6	1501
τ-Cadinol	0.27	-	-	27.3	1500
Turmerone	1.08	2.71	-	28	1500
2H-Benzocyclohepten-2-one, decahydro-9a-methyl-, trans-	-	0.32	-	29.3	1200
4,6,6-Trimethyl-2-(3-methylbuta-1,3-dienyl)-3-oxatricyclo [5.1.0.0(2,4)] octane	0.53	-	-	28.3	1501
Tridecanal	4.44	-	-	29.3	1300
(E)-Atlantone	-	-	0.16	30.9	1499
Heptane, 1,1'-thiobis-	2.28	-	-	29.4	1400
5,7-Dodecadiyn-1,12-diol	-	-	0.29	33.8	1201
Myristic acid	3.12	2.53	-	30.6	1399
Anthracene	-	0.27	-	30.9	1399
3-Cyclopentylpropionic acid, benzyl ester	-	0.44	-	31.7	1500
Cyclohexadecane	3.27	0.68	14.46	31.4	1600
Octadecahydro-benzo[cd]pyrene	-	0.36	-	32.1	1901
Phthalic acid, 5-ethyl-1,3-dioxan-5-yl pentyl ester	0.39	-	-	32.1	2001
Aspidospermidin-17-ol, 1-acetyl-16-methoxy-	-	0.38	0.12	33.4	2200
2-Pentadecanone, 6,10,14-trimethyl-	1.12	-	-	32.7	1799
Phthalic acid, 2-cyclohexylethyl butyl ester	-	0.35	0.99	34.5	2000
Pentadecanoic acid	1.11	-	-	33.1	1500
Stearyl alcohol	-	-	0.29	31.7	1800
Butyl-2-methylpropylphthalate	0.49	3.30	1.45	33.3	1600
Ethyl (9Z,12Z)-9,12-octadecadienoate	1.24	-	--	33.9	1999
9-Hexadecenoic acid, methyl ester, (Z)-	0.34	-	1.01	34.2	1699

1,2-Benzenedicarboxylic acid, bis(2-methylpropyl) ester	-	8.58	0.65	33.3	1600
Farnesol (E), methyl ether	0.74	-	-	34.5	1600
Hexadecanoic acid, methyl ester	2.98	-	-	34.7	1700
.beta.-Citronellol, triethylsilyl ether	-	-	0.29	34	1599
Palmitic acid ME	-	0.863	1.43	34.7	1700
Palmitic acid	-	-	20.87	35.1	1600
7,9-Di-tert-butyl-1-oxaspiro (4,5)deca-6,9-diene-2,8-dione	-	-	0.49	34.6	1699
Palmitoleic acid	2.52	2.292	-	35.1	1600
Hexadecanoic acid	2.39	44.08	-	36.4	1600
Diisooctylphthalate	27.42	-	3.53	36.9	2399
Kaur-16-ene	1.084	0.65	-	37.4	1999
Estra-1,3,5(10)-trien-17.beta.-ol	-	-	0.62	37.2	1799
E-11-Tetradecenol, trimethylsilyl ether	-	-	0.53	37.6	1700
11,14-Octadecadienoic acid, methyl ester	-	0.81	-	38.7	1899
L-Serine, O-(phenylmethyl)-	-	-	0.88	38.2	1000
9-Octadecenoic acid (Z)-	-	0.28	-	40.3	1800
Ethyl Oleate	-	-	5.68	40.3	2000
Methyl 9-cis,11-trans-octadecadienoate	2.26	-	-	38.7	1899
13-Octadecenoic acid, methyl ester	3.63	-	-	38.8	1899
Phytol	7.54	-	-	39.1	2000
6-Octadecenoic acid, methyl ester	-	-	3.02	38.8	1899
Heptadecanoic acid, 16-methyl-, methyl ester	0.50	-	-	39.4	1900
Methyl dihydromalvalate	-	1.27	-	38.8	1899

RT = Retention time, RI = Retention indices, alkane standards (C7-C31).

Appendix 39C: Chemical compositions of essential oils from *J. schimperiana* roots, and leaves essential oils.

Compound name	**RI**	**% Area**	
		Root	Leaves
2-Oxaadamantane	1036	0.17	-
Heptanoic Acid	1078	0.84	-
Phenylethanol	1114	0.24	-
2,6-Nonadienal, (E, E)-	1146	0.56	-
Ethyltetramethylcyclopentadiene	1165	-	0.21
Phenol, 2-cyclohexyl-	1177	0.39	0.35
Octanoic acid	1183	2.06	-
α-Terpineol	1188	0.35	-
Benzothiazole	1195	0.17	-
1-Benzoxepin-2(3H)-one, octahydro-	1204	0.91	-
Cyclodecanone	1208	-	0.43
Phenethyl isocyanate	1225	-	0.19
Aspidospermidin-17-ol, 1-acetyl-16-methoxy-	1250	-	0.18
3,7-Dimethylocta-2,6-dien-1-ol	1255	1.09	-

2,5-Octadecadiynoic acid, methyl ester	1263	-	0.18
(2E)-3,7-Dimethyl-2,6-octadienal	1269	-	0.18
Vanillin lactoside	1273	-	0.26
Thymol	1288	9.32	-
Cinnamyl alcohol	1309	0.25	-
Naphthalene, 2-methoxy-	1341	0.74	-
3-Pyridinemethanol, 4,5-dihydroxy-6-methyl-	1359	-	0.25
2(3H)-Furanone, dihydro-5-pentyl-	1362	0.76	0.69
Eugenol	1366	0.24	0.22
Capric acid	1380	2.25	0.25
***trans*-β-Damascenone**	1381	-	0.19
4,6,10,10-Tetramethyl-5-oxatricyclo [4.4.0.0(1,4)]dec-2-en-7-ol	1390	-	0.15
***trans*-β-Ionone**	1395	-	2.45
Methyl 4,6-tetradecadiynoate	1400	-	0.3
α-Cedrene	1408	0.19	-
3(2H)-Furanone, 2-hexyl-5-methyl-	1446	0.35	-
Humulenol-II	1457	0.29	-
Methyl 3-methoxysalicylate	1459	1.02	-
Benzene, (2-isothiocyanatoethyl)-	1465	-	1
Megastigmatrienone	1473	-	0.59
Benzoic acid, 2,3-dimethoxy-, methyl ester	1483	0.55	-
1-Isopropyl-2,3,4,5-tetramethylbenzene	1485	-	0.15
2,4-Di-tert-butylphenol	1513	0.26	0.45
α-Cedrane	1530	0.36	-
1-Naphthalenemethanol, 1,4,4a,5,6,7,8,8a-octahydro-2,5,5,8a-tetramethyl-	1535	-	0.65
Lauric acid	1570	1.62	-
Isoshyobunone	1585	0.36	-
Diethyl Phthalate	1591	0.41	-
1,9-dimethyl-4-propan-2-yl-8-spiro [4.5]dec-9-enone	1632	-	0.16
.tau.-Cadinol	1639	0.47	-
Cyclotetradecane	1673	0.3	1.3
Ylangenal	1674	0.89	-
Tumerone	1680	0.21	-
α-Bisabolol	1685	-	0.87
Limonen-6-ol, pivalate	1691	-	0.17
Widdrenal	1724	-	0.16
Oxiraneoctanoic acid, 3-octyl-, methyl ester	1745	-	0.15
1,3-Benzenediol, 5-pentyl-	1770	-	0.63
Myristic acid	1774	2.01	2.58
Anthracene	1793	0.31	0.29
Octadecane	1800	-	0.17
Thiosulfuric acid (H2S2O3), S-(2-aminoethyl) ester	1829	0.16	0.87
2-Pentadecanone, 6,10,14-trimethyl-	1847	-	6.63
Farnesol (E), methyl ether	1849	-	1.56
Pentadecanoic acid	1869	0.83	1.1
Benzofuran, 4,5,6,7-tetrahydro-2,7-dimethyl-4-(1-methylethyl)-	1870	0.18	-

Diisobutyl phthalate	1873	1.34	12.9
Cyclohexadecane	1883	-	6.3
Butyl-2-methylpropylphthalate	1892	3.96	2.3
Cholestan-3-ol, 2-methylene-, (3. beta.,5.alpha.)-	1912	0.2	-
Palmitic acid ME	1926	0.31	-
1-Ethynyl-3, trans(1,1-dimethylethyl)-4,cis-methoxycyclohexan-1-ol	1927	-	0.2
Hexadecanoic acid, methyl ester	1927	-	1.9
14-Pentadecenoic acid	1930	0.38	-
cis-1,2-Cyclododecanediol	1936	-	0.46
Palmitoleic acid	1953	0.86	0.29
L-Serine, O-(phenylmethyl)-	1965	-	0.2
n-Hexadecanoic acid	1991	32.4	30.3
Phthalic acid, butyl cycloheptyl ester	2027	-	0.56
Stearyl alcohol	2081	3.17	-
9-Octadecenoic acid (Z)-	2102	0.43	-
Phytol	2109	-	3.9
Linoleic acid	2140	6.21	0.19
(-)-Isolongifolol, methyl ether	2150	0.37	-
9,12-Octadecadienoic acid (Z, Z)-	2156	5.76	1.3
10-Methoxy-nb-alpha-methylcorynantheol	2157	0.455	-
Ethyl (9Z,12Z)-9,12-octadecadienoate	2159	0.19	2.45
Palmitamide	2182	-	1.3
Diisooctylphthalate	2186	11.11	-
11,14-Octadecadienoic acid, methyl ester	2314	0.34	0.31
Phthalic acid, nonyl oct-3-yl ester	2493	0.32	-
Didecyl phthalate	3096	0.31	-
Diisononylphthalate	3122	0.42	11.3

Appendix 39D: Chemical compositions of essential oils from leaves, and roots of *V. siniaticum*.

RI	**Compound name**	**% Area**	
		Leaves	Roots
981	Hexanoic acid	-	1.4
1004	Dodecane	0.23	-
1033	Benzyl alcohol	1.01	-
1078	Heptanoic acid	-	0.35
1103	Tetrahydrofuran-2-ol, 3,4-di[1-butenyl]-	0.25	-
1111	5,7-Undecadienol	0.25	-
1121	Phenylethanol	2.72	0.37
1178	Phenol, 2-cyclohexyl-	0.19	0.2
1180	Octanoic acid	0.26	0.87
1190	4-Cyano-3,5-dimethylphenol	0.48	1.67
1192	1-Dodecene	1.51	-
1199	4,4,6-Trimethyl-cyclohex-2-en-1-ol	-	0.57

1219	Benzofuran, 2,3-dihydro-	0.42	-
1244	Benzenepropanenitrile	0.27	-
1251	Anisaldehyde	0.33	-
1273	Tetradecane	1.20	-
1277	Benzaldehyde, 4-methoxy-	-	0.46
1280	Nonanoic acid	0.96	-
1280	1,13-Tetradecadien-3-one	0.38	-
1286	Aspidospermidin-17-ol, 1-acetyl-16-methoxy-	0.45	-
1305	Mesityl isocyanate	-	0.23
1312	2-methoxy-4-vinyl-phenol	0.56	-
1318	Benzofuran-5-carbaldehyde	0.59	1.56
1359	Eugenol	0.41	-
1367	2(3H)-Furanone, dihydro-5-pentyl-	-	0.37
1373	Capric acid	0.22	0.83
1379	2-Buten-1-one, 1-(2,6,6-trimethyl-1,3-cyclohexadien-1-yl)-, (E)-	0.48	-
1389	4,6,10,10-Tetramethyl-5-oxatricyclo [4.4.0.0(1,4)]dec-2-en-7-ol	0.16	-
1442	Cyclohexanebutanal, 2-methyl-3-oxo-, cis-	0.51	-
1450	5,5,8a-Trimethyl-3,5,6,7,8,8a-hexahydro-2H-chromene	0.36	-
1464	1-Dodecanol	1.49	-
1465	Benzene, (2-isothiocyanatoethyl)-	7.65	-
1467	trans-β-Ionone	0.52	-
1472	Megastigmatrienone	0.48	-
1478	γ-Cadinene	-	0.28
1499	α-Selinene	-	0.2
1503	Thiosulfuric acid (H2S2O3), S-(2-aminoethyl) ester	0.25	-
1513	Tridecanal	-	0.35
1517	Hexadecane	1.45	-
1525	2,4-Di-tert-butylphenol	30.6	0.21
1527	β-Himachalene	0.33	-
1533	Cyclopropane, 1-methyl-1-(1-methylethyl)-2-nonyl-	0.35	-
1538	2(4H)-Benzofuranone	0.68	-
1550	Octadecane	-	0.3
1581	Caryophyllene oxide	-	0.45
1594	Diethyl Phthalate	0.89	0.94
1644	.tau.-Cadinol	-	1.4
1666	Patchouli alcohol	0.54	-
1673	Cyclotetradecane	0.95	-
1674	Ylangenal	-	1.88
1680	α-Bisabolol	0.20	-
1691	2-Naphthaleneacetaldehyde	0.18	-
1724	5,7-Dodecadiyn-1,12-diol	0.21	-
1779	(*E*)-Atlantone	0.16	-

1813	Nonadecane	0.85	-
1860	9-t-Butyltricyclo[4.2.1.1(2,5)]decane-9,10-diol	-	0.35
1883	Cyclohexadecane	15.5	34.5
1892	Butyl-2-methylpropylphthalate	3.56	-
1912	1,2-Benzenedicarboxylic acid, dinonyl ester	-	0.22
1920	Palmitic acid	4.42	-
2040	3-Epi-cedrenol, methyl ether	-	0.3
2063	Stearyl alcohol	0.29	-
2099	10-Methoxy-nb-alpha-methylcorynantheol	-	1.9
2124	β-Citronellol, triethylsilyl ether	0.72	-
2147	Linoleic acid	0.79	-
2152	Mono(2-ethylhexyl) phthalate	0.20	-
2169	Diisooctylphthalate	1.86	36.7
2177	Stearic acid	0.24	-
2300	*cis, cis*-7,10,-Hexadecadienal	-	0.3
2405	Cyclopropanenonanoic acid, 2-[(2-butylcyclopropyl)methyl]-, methyl ester	2.19	-
2406	Phthalic acid, oct-3-yl pentyl ester	0.31	-
2545	L-Serine, O-(phenylmethyl)-	0.20	-
2577	*tert*-Hexadecanethiol	1.55	-
2933	2,2'-Biphenol, 3,3',5,5'-tetrakis(1,1-dimethylethyl)-	2.27	-
2943	5-Hexadecenoic acid, 2-methoxy-, methyl ester	-	0.8
2968	Phthalic acid, butyl tetradecyl ester	0.38	-
2993	1,2-Benzenedicarboxylic acid, monononyl ester	1.22	-
3100	Didecyl phthalate	-	1.5
3105	Phthalic acid, butyl undecyl ester	0.23	-
3107	Di-isononyl phthlate	-	8.2
3112	Phthalic acid, nonyl 2-pentyl ester	0.46	-
3167	Phthalic acid, 2-cyclohexylethyl isobutyl ester	1.21	0.4

RI = Retention indices, based on HP-5MS capillary column (non-polar column) and alkane standards (C7-C31).

Appendix 39E: Chemical compositions of essential oils from seeds, and roots of *L. abyssinica*

Compound name	**RT**	**% Area**	
		Seed	Roots
Bis(4-hydroxyphenyl) methnl 2-naphthylmethane	6.9	1.01	0.22
Benzaldehyde, 4-hydroxy-	7.7	-	0.2
(Cyclopropyl) trivinylsilane	7.7	0.64	-
2,5-Norbornanediol	8.7	0.20	-
Cyclohexanol, 3,3,5-trimethyl-, cis-	9.3	0.19	-
p-Cresol	9.6	1.1	-
Phenol, 2-methoxy-	10.1	6.08	0.4
Trans-1-methyl-2-nonyl-cyclohexane	10.4	0.29	-

Benzaldehyde, 4-hydroxy-	10.9	-	0.2
Phenol, 3,4-dimethyl-	11.9	0.26	-
Phenol, 3-ethyl-	12.5	0.89	-
1-Undecen-10-al	12.7	-	0.18
2-Methoxy-5-methylphenol	13.4	2.46	-
Benzofuran, 2,3-dihydro-	14.2	0.38	-
2-(2-Isopropenyl-5-methylcyclopentylmethoxy) tetrahydropyran	14.5	0.18	-
Guaiacol, 4-ethyl-	16.2	2.9	-
DOM	16.3	-	0.21
Indole	16.7	0.96	-
(+)-3-Carene, 4-isopropenyl-	16.9	-	0.18
2-methoxy-4-vinyl-phenol	17.4	1.48	0.26
Phenol, 2-cyclohexyl-	17.6	-	0.8
4,4,6-Trimethyl-cyclohex-2-en-1-ol	18.3	-	0.35
Phenol, 2,6-dimethoxy-	18.6	0.91	-
Eugenol	18.8	0.47	-
Ethanol, 2-(3,3-dimethylbicyclo [2.2.1]hept-2-ylidene)-	18.9	0.17	-
2(3H)-Furanone, 5-heptyldihydro-	19.0	-	0.23
Capric acid	19.1	-	0.32
Phenol, 2-methoxy-4-propyl-	19.1	0.81	-
1H-Indole, 3-methyl-	19.7	0.37	-
Phenol, 2-methoxy-4-(1-propenyl)-, (Z)-	20.4	0.27	-
***trans*-Isoeugenol**	21.7	1.86	-
2,6-Di-tert-butyl-4-methyl-phenol	22.3	-	0.18
7-Octadecyne, 2-methyl-	22.7	0.16	-
2-Tridecanone	23.1	-	0.23
2,4-Di-tert-butylphenol	23.5	-	0.43
Cyclohexanebutanal, 2-methyl-3-oxo-, cis-	23.8	-	0.33
MOPPP-M 2ET	24	-	0.24
Ethanone, 1-(2,6-dihydroxy-4-methoxyphenyl)-	24	0.24	-
Hydroxy citronellal	25	-	0.28
Lauric acid	25	-	0.63
(*Z*)-2-nonadecene	28.4	0.21	-
Myristic acid	30.6	-	2.2
Phthalic acid, cylclohexylmethyl pentyl ester	31.9	-	0.28
Phthalic acid, 5-ethyl-1,3-dioxan-5-yl pentyl ester	32	-	0.39
Cyclotetradecane	32.7	0.22	-
Pentadecanoic acid	33.1	-	0.73
Phthalic acid, isobutyl 2-propylpentyl ester	33.3	0.37	-
1,2-Benzenedicarboxylic acid, bis(2-methylpropyl) ester	33.3	-	7.2
Phthalic acid, isobutyl octadecyl ester	34.4	-	0.25
Palmitic acid ME	34.7	1.10	-

Pyrrolo[1,2-a]pyrazine-1,4-dione, hexahydro-3-(2-methylpropyl)-	34.9	0.72	-
Palmitoleic acid	35.1	-	1.67
***n*-Hexadecanoic acid**	35.7	2.87	14.5
2-([(2-Ethylhexyl)oxy]carbonyl)benzoic acid	36.4	-	0.63
Diisooctylphthalate	36.7	19.98	-
Diisooctylphthalate	36.8	-	34.3
1,2-Benzenedicarboxylic acid, dinonyl ester	38.0	1.24	0.52
Methyl 9-cis,11-trans-octadecadienoate	38.7	0.79	-
Phthalic acid, nonyl oct-3-yl ester	38.8	0.34	-
Heptadecanoic acid, 10-methyl-, methyl ester	39.4	0.37	-
9,12-Octadecadienoic acid (Z, Z)-	39.5	4.73	-
Thiosulfuric acid ($H_2S_2O_3$), S-(2-aminoethyl) ester	40.2	0.88	0.5
Cyclotetradecane	40.4	-	0.3
Linoleic acid	40.7	0.26	0.3
Stearyl alcohol	42.2	-	8.6
Cyclohexadecane	42.3	32.22	21.7
Didecyl phthalate	45.1	1.191	-
Di-isononyl phthalate	45.4	7.979	-

Appendix 40A: The GC-MS chromatogram of *C. abyssinicum* bulbs (a), and *C. abyssinica* aerial parts (b) essential oils.

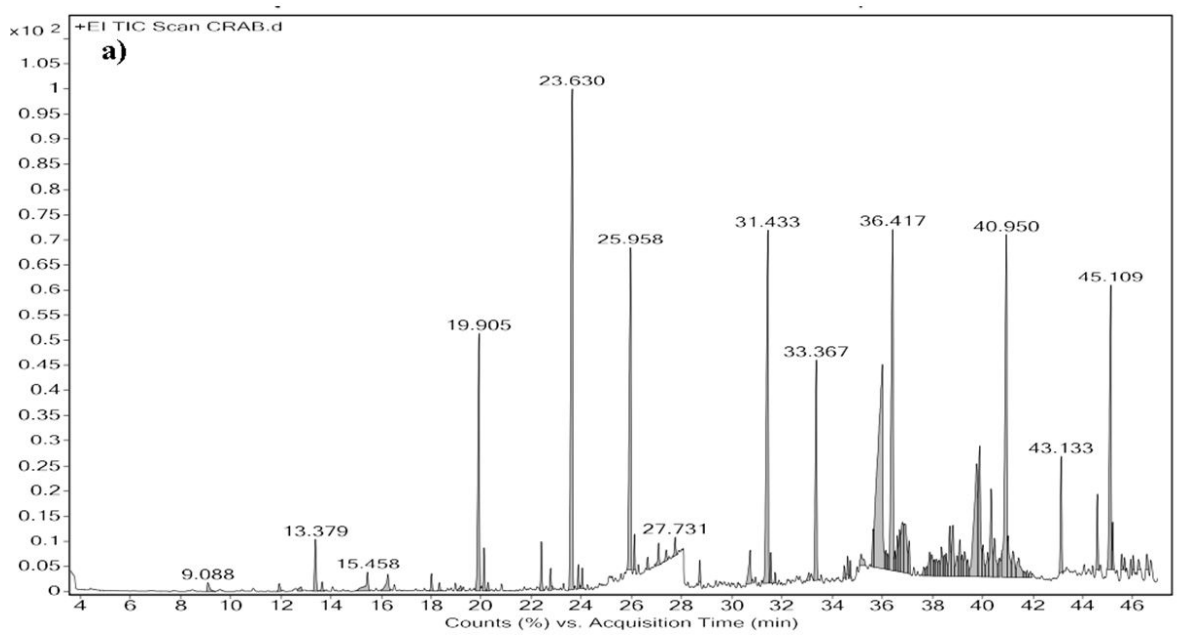

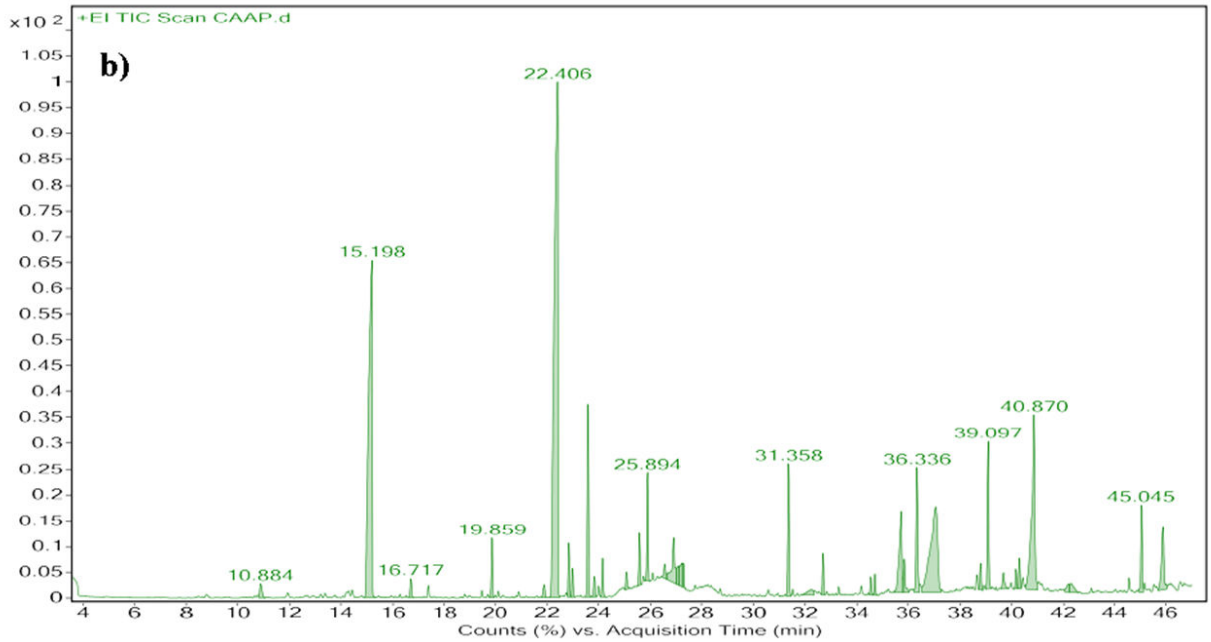

Appendix 40B: The GC-MS chromatogram of *C. procera* leaves (a), flowers (b), and seeds (c) essential oils.

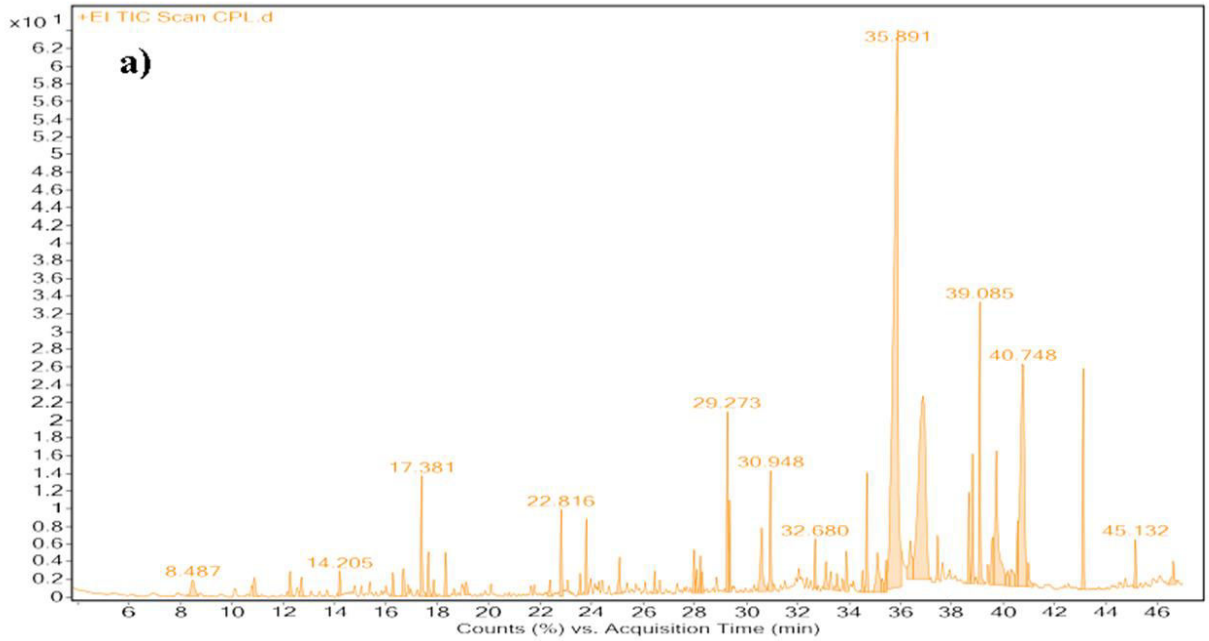

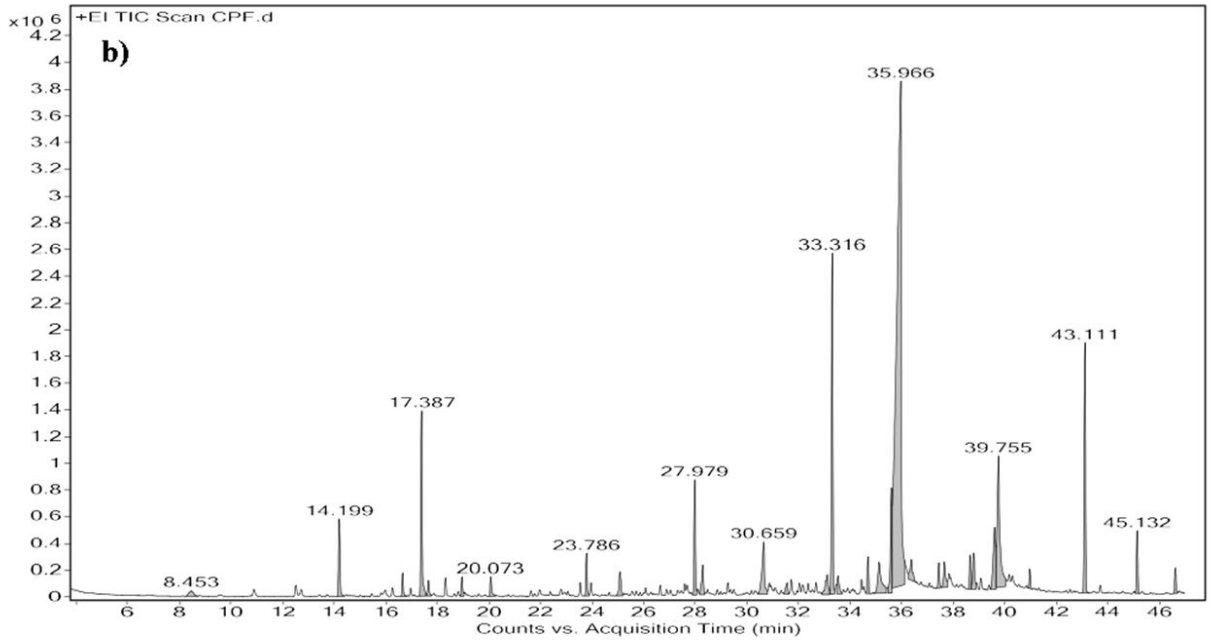
+EI TIC Scan CPF.d
b)
x10 6
35.966
33.316
43.111
17.387
39.755
27.979
14.199
45.132
30.659
23.786
20.073
8.453
Counts vs. Acquisition Time (min)

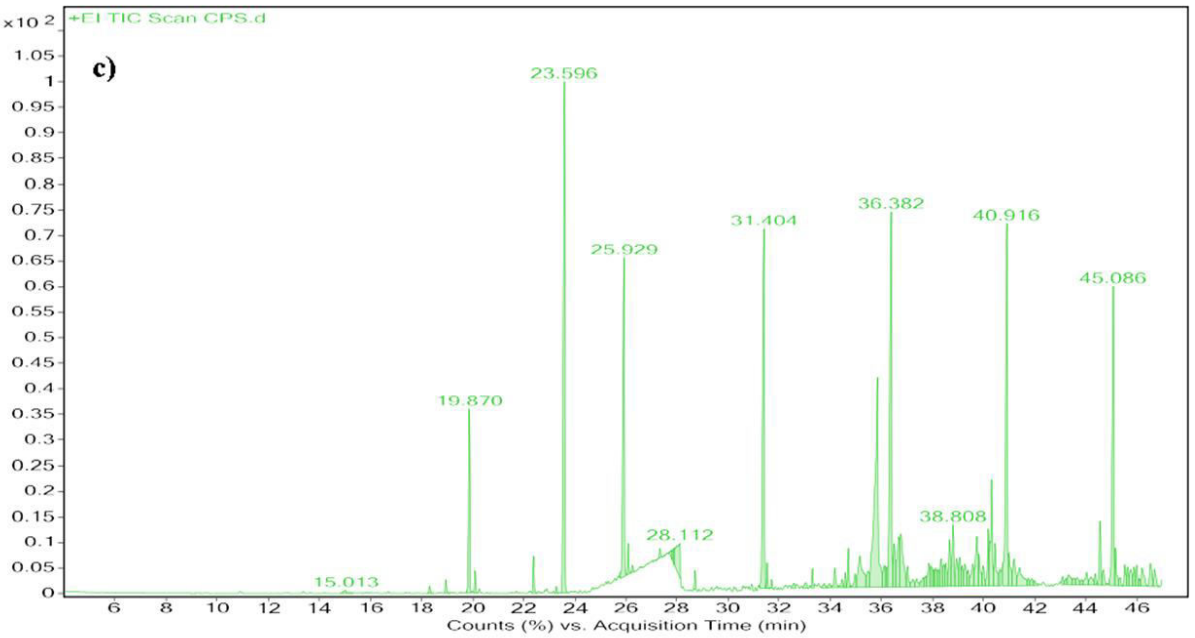
+EI TIC Scan CPS.d
c)
x10 2
23.596
36.382
31.404
40.916
25.929
45.086
19.870
38.808
28.112
15.013
Counts (%) vs. Acquisition Time (min)

Appendix 40C: The GC-MS chromatogram of *J. schimperiana* roots (a), and leaves (b) essential oils.

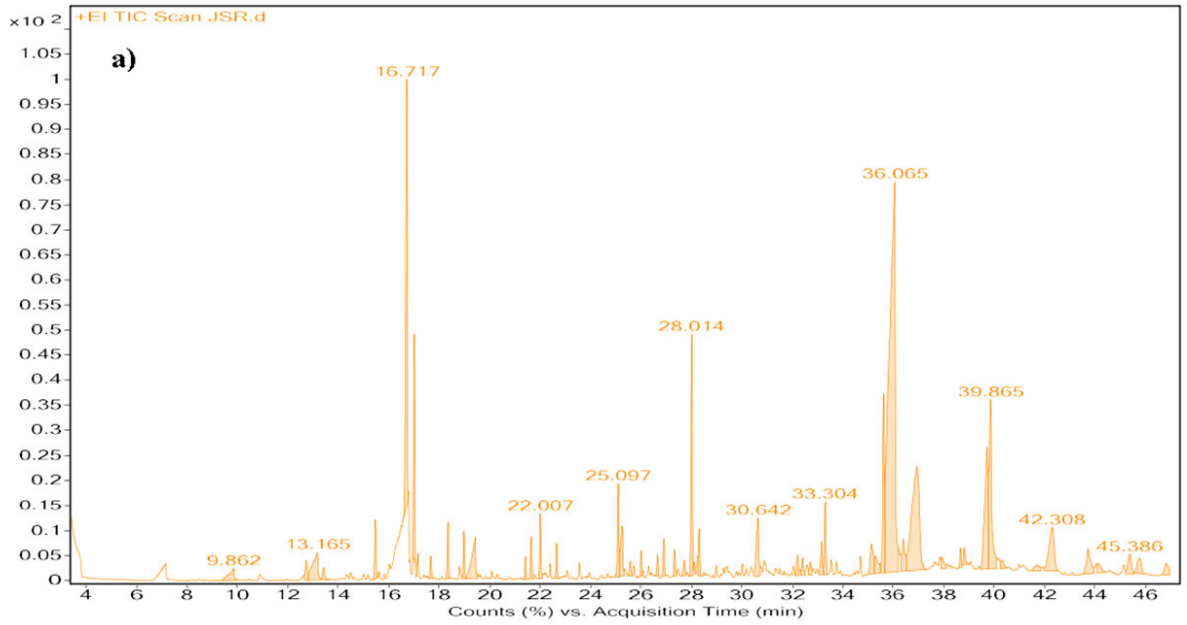

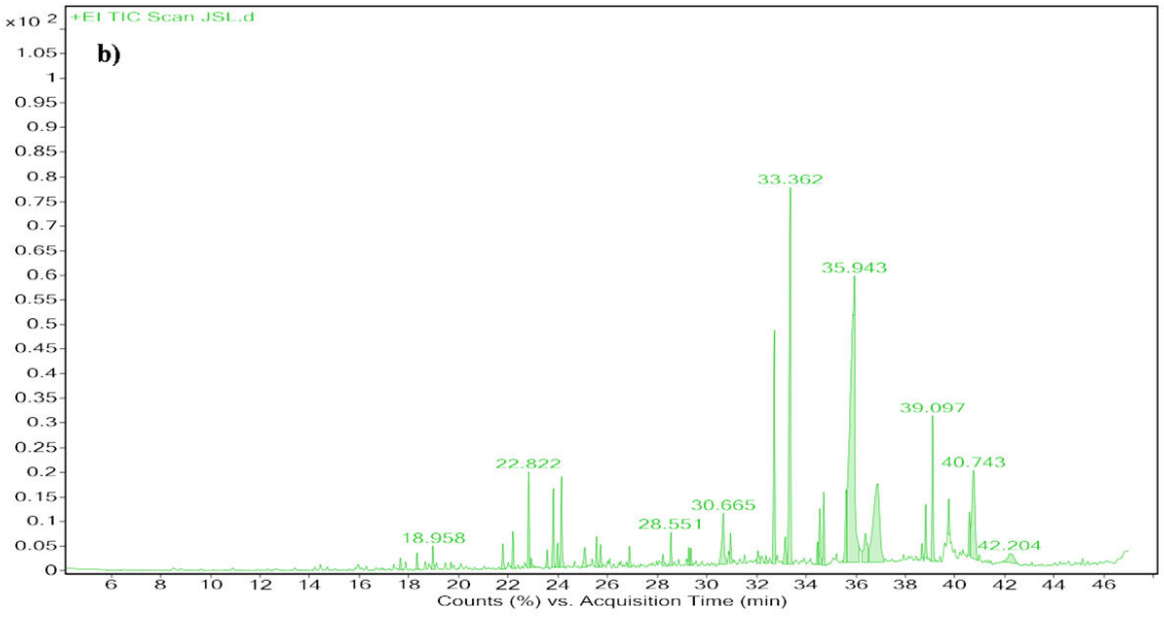

Appendix 40D: The GC-MS chromatogram of *V. siniaticum* leaves (a), and roots (b) essential oils.

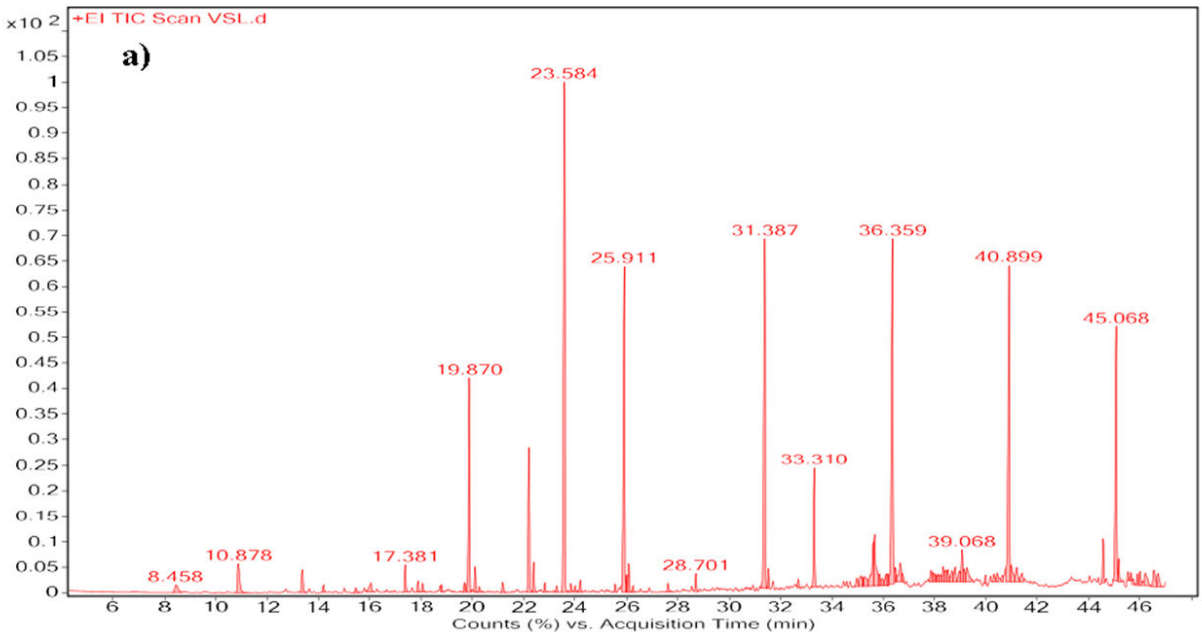

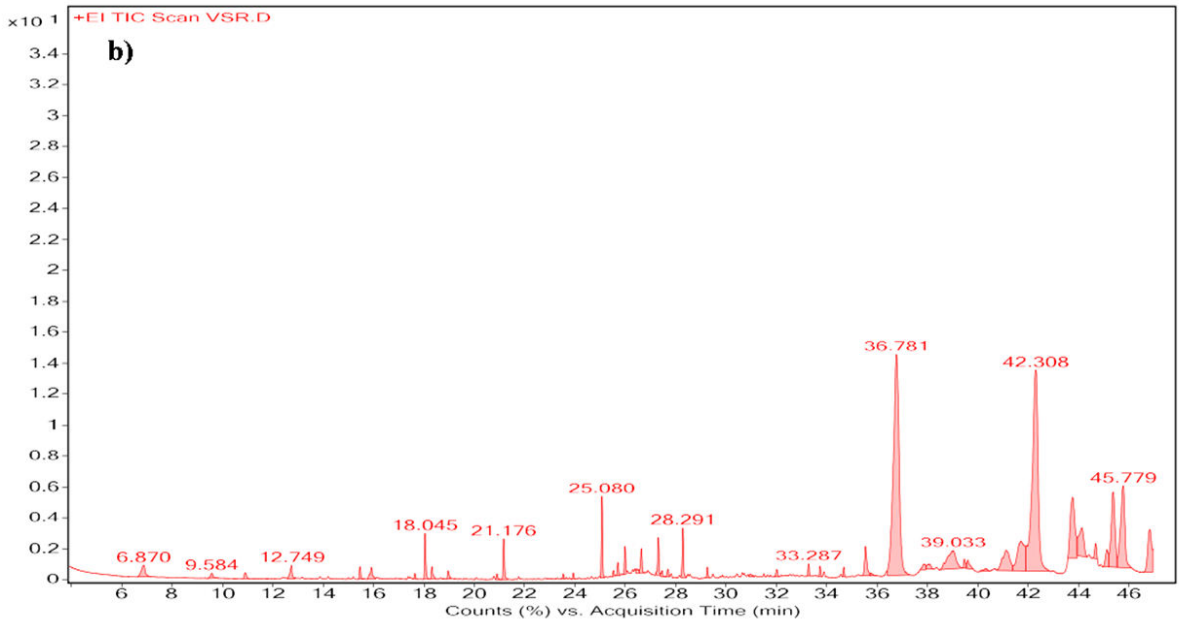

Appendix 40E: The GC-MS chromatogram of *L. abyssinica* seeds (a), and roots (b) essential oils.

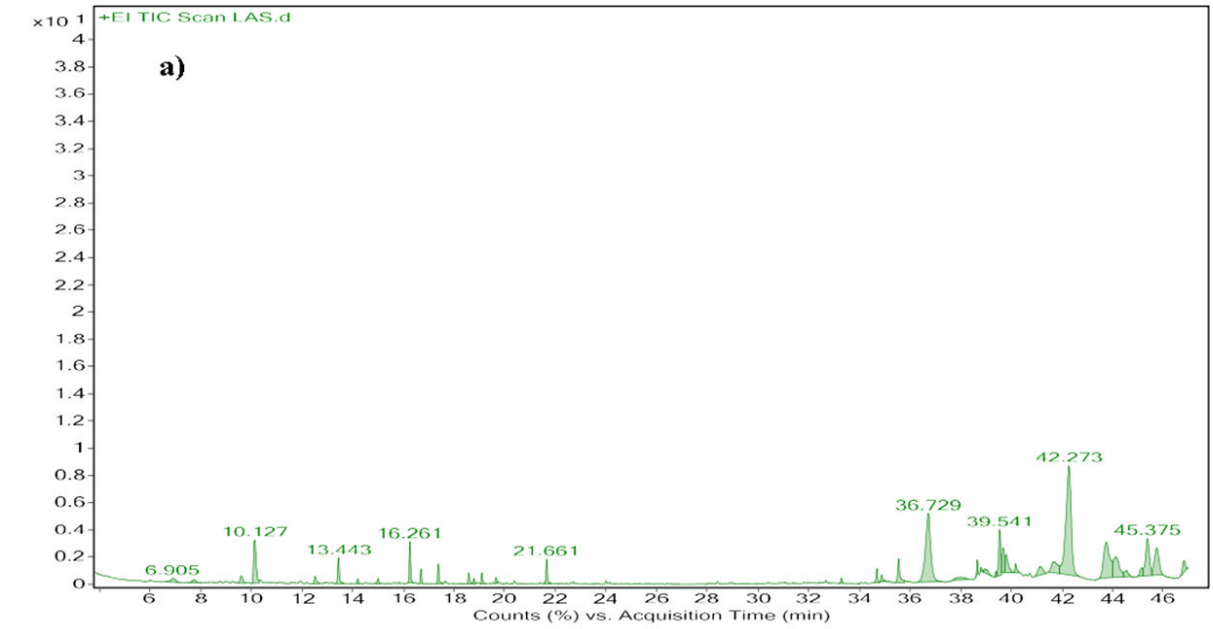

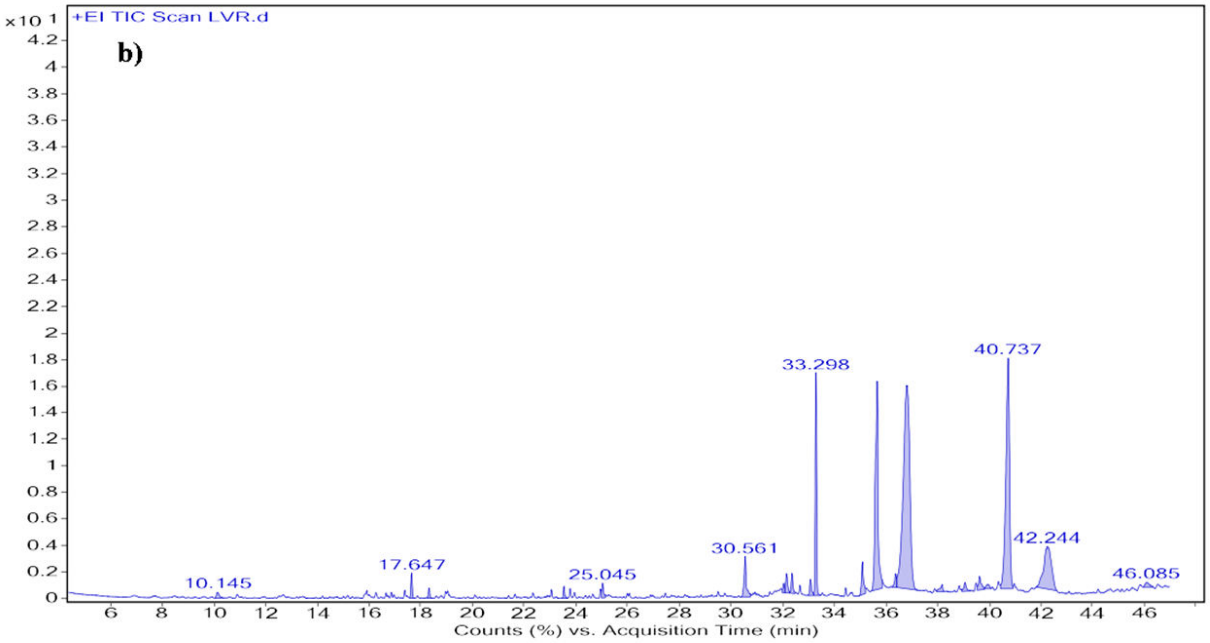

Appendix 41A: Molecular docking results of isolated compounds against *E. coli* Gyrase B (PDB ID 7P2W).

			Residual interactions	
Ligands	**Binding**	**H-bond**	Hydrophobic,	Van der Waals

	Affinity (kcal/mol)		Electrostatic, and Others	
224	– 8.9	Gly-77	Val-118	Gly-117, Asp-49, Asn-46, Glu-50, Gly-101, Asp-73, Thr-165, Ile-78, Pro-79, Arg-76, Ile-94
226	– 7.8	Thr-165, Gly-77, Val-43	Ile-78, Asn 46, Ala 47, Val-120, Val-167, Ile-78 Ile-94, Ile-78, Val-118, Val-118, Val-118	Ala-100, Met-95, Ala-47, Asp-73, Glu-50, Arg-76, Pro-79
227	-6.0	Val-120, Asn-40	Val-43, Val-71, Val-167	Gly-77, Asp-73, Glu-50, Pro-79, Gly-119, Ser-121, Leu-98, Val-97, Thr-165
228	-5.4	Arg-76	Pro-79	Asn-46, Glu-50, Gly-77, Asp-49, Gly-117, Val-120, Arg-136
229	-5.0	--	Ala-47, Val-71, Ile-78, Pro-79, Ile-94,	Asn-46, Asp-73, Glu-50, Gly-77, Thr-165
239	– 7.1	Arg-76	Glu-50, Val-120, Val-167, Ile-94, Ile-78, Ile-78, Val-118, Val-118, Ile-78	Gly-117, Gly-101, Asp-49, Asn-46, Ala-47, Asp-73, Val-43, Thr-165, Pro-79
240	– 6.5	Val-167, Asp-73, Thr-165	Val-120, Ile-78, Ile-78, Val-118, Val-118, Val-118	Asp-49, Pro-79, Arg-76, Asn-46, Ala-47, Val-43, Val-71, Gln-72, Met-166, Glu-50
241	– 6.1	Asp-73, Val-167	Val-120, Ile-94, Arg-76, Pro-79, Ile-78, Ile-78, Ile-78, Val-118, Val-118	Arg-136, Gly-77, Glu-50, Asn-46, Val-43, Thr-165, Ala-47, Gln-72, Val-71, Met-166, Ile-59
78	– 8.7	Asp-73	Ala-90, Val-118, Ile-78, Val-93, Ile-94, Ile-94, His-83	Pro-79, Ala-100, Gly-101, Arg-76, Asp-49, Asn-46, Glu-50, Ala-47, Thr-165
79	– 7.5	Asp-73, Glu-50	Ile-78, Ile-94, Ala-100, Val-118	Gly-101, Asp-49, Asn-46, Ala-47, Thr-165, Pro-79, Ala-90, His-83, Val-93
96	-6.7	Asn-46	Ile-94, Pro-79, Ile-78	Glu-50, Asp-73, Thr-165, Arg-136
97	– 8.0	—	Ile-78, Ile-94, Val-118	Pro-79, Gly-117, His-116, Asn-46, Arg-76, Asp-49, Glu-50, Ala-53
98	– 8.6	Thr-165	—	Asp-49, Arg-76, Glu-50, Ala-47, Asn-46, Asp-73, Gly-77, Ile-78, Pro-79, Ile-94, Val-118, Gly-101, Gly-102, Gly-117, His-116
231	- 5.5	Asn-46	--	Val-43, glu-50, Pro-79, Gly-77, Ile-78, Thr-165, Val-120, Val-167, Val-71, Gn-72
234	– 7.6	Arg-76, Arg-76	Pro-79	Ala-90, Ile-94, Val-118, Gly-117, Asp-49, Glu-50, Ala-53, Leu-52
87	– 8.2	His-83	Val-118	Arg-76, Glu-50, Ile-78, Ile-94, Pro-79, Ala-90, Pro-84
243	-6.3	Gly77, Asp73, Thr165	Arg76, Glu50, Ile78	Ala47, Gly164, Gly75, Pro79, Arg136
244	-7.3	Arg136, Asp49,	Arg76, Asn46;	Ile94, Ala53, Asp73, Ala47,

		Asp49, Glu50	Ala47, Arg76, Pro79, Ile78	Thr165, Gly77
245	-6.7	Asn46, Arg76, Thr165, Asp73	Asn46, Ala47, Ile78, Ile94	Gly75, Gly77, Glu50, Ala47, Val43
246	-8.1	Asn46, Arg76, Glu50, Asp49	Glu50, Pro79, Ile78, Ile78	Gly77, Gly75, Gly164, Thr165, Asp73, Ala47, Ala53, Val120, Gly119
247	-6.4	Val71, Thr165, Glu50	Pro79, Ala90, Val93, Ala100, Val118, Val43, Val71, Ile94, Val93, His83, His83, Ile78, Val120	Met-166, Gly-77, Ala-47, Asp-73, Asn-46, Arg-76
248	-6.9	His116, Asp49	Ile78, Val118, Val120	Leu-52, Val-43, Val-167, Gly-117, Thr-165, Asn-46, Glu-50, Arg-76, Ala-53
249	-7.9	Arg76, Arg76, Gly117, Asp49, Asp73, Asp49	Ile78, Val43, Val167, Val118, Val120	Pro-79, Leu-52, Ala-53, His-116, Glu-50, Asn-46, Ile-94, Thr-165, Ala-47, Val-71
253	-7.3	Asp73, Ala100	-	Ile-94, Pro-79, Val-118, Ile-78, Val-120, Val-167, Val-43, Thr-165, Val-71, Ala-71, Ala-47, Asn-46, Glu-50, Asp-49, Arg-76, Gly-102, Gly-101
254	– 8.6	Gly-77, Gly-77	Ile-78	Ala-53, Val-118, Ile-94, Arg-76, Pro-79, Glu-50, Arg-136, Thr-165, Asn-46, Asp-49, Gly-117, His-116
Amoxicillin	– 7.6	Arg-76, Arg-76, Glu-50, Glu-50, Asn-46	Ile-78, Asn 46, Ala 47, Val-118, Val-120	His-116, Gly-117, Asp-73, Asp-49, Thr-165, Val-43, Val-167, Leu-52, Ala-53, His-55, Pro-79
Ciprofloxacin	-6.7	Asn46, Arg76, Gly77, Asp73, Glu50	Glu50, Arg76, Pro79, Ile94, Ile78	Gly-75, Gly-164, Thr-165

Appendix 41B: Molecular docking results of isolated compounds against human myeloperoxidase (PDB ID 1DNU).

Ligands	**Binding Affinity (kcal/mol)**	**H-bond**	**Residual interactions**	
			Hydrophobic	Van der Waals
239	– 6.5	Arg-333, Arg-333, Arg-424, Arg-424	Arg-333, Arg-333, His-95, His-336, His-336	Phe-146, Phe-147, Leu-415, Phe-407, Leu-420, Glu-102, Glu-242, Asp-94, Phe-99, Gln-91, Leu-417, Arg-239, Asn-421, Thr-100
240	– 5.3	Arg-239, Arg-333, Arg-333, Asp-98, Asp-98	Arg-239, Arg-239, His-95, Phe-99, Phe-407	Leu-417, Gln-91, Glu-102, Glu-242, Thr-100, Asp-94, Phe-366, Thr-329
241	– 4.3	Arg-323 (Dist. 2.0332 Å), Arg-323 (Dist. 2.4029 Å), Ala-35, Arg-31	Ala-152, Ala-28, Ala-28	Asn-162, Thr-159, Ile-160, Pro-34, Leu-33
79	– 8.2	Asp-218	Pro-220, Leu-420, Phe-407	Arg-239, Phe-366, Glu-242, Phe-99, Leu-216, Asp-219, Glu-116, Met-411, Leu-415, Phe-147, Arg-424, Phe-146

97	– 10.3	Asp-94	Phe-407	Phe-366, Met-411, Phe-147, Leu-406, Leu-415, Leu-420, Arg-424, Leu-417, His-336, Arg-333, His-95, Asp-98, Arg-239, Phe-99, Glu-102
234	– 10.1	Arg-239, Arg-333, Arg-333	Pro-220, Phe-366	His-336, Asn-421, Phe-99, Leu-417, Thr-100, His-95, Leu-406, Glu-242, Phe-407, Thr-238, Leu-216
87	– 10.8	Glu-102	Leu-216	Phe-407, Pro-220, Phe-366, Arg-239, Thr-238, Phe-99, Arg-424
245	-8.8	Thr100, Asp94	-	Gln91, His336, Glu242, Arg239, Thr329, Asp98, Arg333, Phe99, Pro101, Glu102, Phe407, Leu417
246	-10.1	Ala35, Asn162, Arg323, Arg31	Arg323, Arg31, Ala35, Ile160	Ala28, Ala152, Thr159, Cys153, Arg161, Ile160, Ala35, Pro34, Val30, Trp32, Pro34, Leu22
248	-10.3	Gln91, Arg239, Arg424, Asp94, Asp98, Thr329, Glu102	Gly90, Gln91	-
249	-9.2	Asn162, Arg323, Phe29, Arg31, Ile160	Arg31, Ile160	Ala-152, Ile-158, Ala A-28, Thr D-159, Ala B-28, Asn-162, Leu-33, Trp-32, Pro A-34, Asp-321, Val A-30, Val B-30, Arg-31, Ala-35, Pro B-34, Phe-29, Thr C-159
250	-9.4	Arg31, Arg323, Ser319	Ala152, Cys153, Ala28, Ala152	Val-320, Phe-439, Trp-32, Leu-33, Arg-31, Ala-35, Pro-34, Leu-33, Trp-32, Ile-160, Asn-162, Asp-321, Pro-34, Leu-33, Trp-32, Arg-323, Val-30, Cys-158, Thr-159, Phe-29, Val-30,
251	-9.6	Gln91, Gln91, Arg239, Arg333, Glu116	Gly90; Gln91, Leu338	Asp-94, Glu-102, Pro-220, Thr-100, Met-411, Ile-339, Ala-104, His-336, Phe-332, Gly-335, Met-87, Phe-99, Phe-407, Leu-406, Leu-417, His-95, Glu-242
252	-9.5	Gln91, Arg239, Glu102	Met87, His336	Thr-238, Phe-99, Phe-366, Glu-242, His-95, Ile-339, Gly-335, Asp-94, Arg-333, Thr-329, Asp-98, Thr-100, Phe-407, Phe-147, Glu-116, Ala-104, Pro-103
253	-9.2	Gln91, Glu102, Asp94, Phe332, Met87, Gly335	-	Leu-338, Ile-339, His-336, Asn-421, Phe-99, Arg-239, Arg-424, Glu-242, Leu-417, Arg-333, His-95, Gly-90
Amoxicillin ($C_{16}H_{19}N_3O_5S$)	– 9.2	Gln-91, Arg-333, Arg-424, His-336, Phe-332, Phe-332	His-336 Gly 90, Gln 91	Asp-98, Thr-329, Ile-339, His-95, Arg-239, Thr-100, Phe-99, Glu-102, Leu-417, Asp-94, Tyr-334, Gly-335
Ascorbic Acid ($C_6H_8O_6$)	– 8.1	Gln-91, Thr-100, Arg-239, Arg-239, Arg-333, Arg-333,	Asp-94, Arg-333	His-336, Phe-332, Phe-99, Thr-329, His-95, Asp-98

		Arg-333		

Appendix 41C: Molecular docking value of isolated compounds against human topoisomerase IIα (PDB ID: 4fm9).

Ligands	Affinity (kcal/mol)	H-bond	Residual interactions	
			Hydrophobic	Van dar Waals
224	– 8.5	Gln-542	Leu-592, Pro-593	Arg-672, Glu-682, Leu-705, Glu-596, Gln-544, Tyr-590, Ile-577, Ser-591, Asp-543, Ser-547, Glu-702, Lys-550, Tyr-686
226	– 7.4	Gln-544, Asp-831, Gln-544, His-759, Lys-728, Lys-728	Pro-724, His-759, Pro-724	His-758, Glu-837, Val-836, Leu-829, Ser-717, Arg-727, Glu-712, Ser-709
228	-6.8	Leu-685, Glu-702	Glu-682, Pro-593, Leu-705	Gln-544, Asp-543, Arg-672, Ser-547, Lys-550, Tyr-686, Ser-591, Tyr-684, Leu-592, Lys-599, Ser-709, Asp-831, Asp-832,
229	-5.5	--	Pro-593, Leu-685, Tyr-686, Leu-705	Asp-543, Gln-542, Lys-550, Ile-577, Ser-591, Ser-709
232	-6.5	Arg-124, Asn-76	Pro-40, Pro-45, Ile-119, Phe-120, Leu-116	Ile-361, Thr-353, Ser-354, Asn-465, Thr-464
78	– 7.7	Lys-728	Pro-724, Lys-676, Phe-1003	Gly-1007, Arg-727, Arg-673, Glu-712, Arg-672, Ser-717, Glu-839, Leu-829, Asp-831, Glu-837
239	-6.1		Val-928, Arg-929, Leu-995	Lys-863, Lys-990, DTD-13,DCD-14, DCD-11
240	-5.1	ARG-727, ILE-715, SER-717, PRO-724	Arg-713, Pro-724, Pro-724, Pro-724 Pro-724 Leu-829, Tyr-757, His-759	
241	-4.5	ASP-543	Pro-593, Pro-593, Leu-705, Leu-685, Leu-705, Leu-705, Phe-668, Tyr-686	
79	-8.2			Val-928, Thr-993, Arg-929,Thr-930,Thr-934,Lys-863,DC-9,DC-11,Glu-854,DG-7,DT-6,DA-12
97	-9.9	LYS-863, GLU-854	LYS990	DT-13, DA-12, THR-993,ARG-929,DC-9,DA-8,THR-934,TYR-935,THR-930,GLN-938,VAL-939,
234	-9.1			DA-8, DC-5, LYS-798,DG-10,DC-9,DT-12,DC-8,DT-7,
87	-8.2	HIS-758	-	GLY-1007, GLU-839,GLU-837,ARG-727,PRO-724,LYS-728,HIS-759,ASP-831,GLU-712,LEU-829,ARG-672,ARG-673
98	– 9.1	Arg-727	—	Arg-673, Gly-1007, Lys-676, Glu-712, Phe-1003, Pro-724, Ser-717, Glu-839, Leu-829, Arg-672
248	-8.8	Glu839, Met669, Val1006	Phe1003, Pro724	Ser-717, Arg-727, Glu-712, Arg-713, Lys-676, Arg-672, Arg-673, Cys-1008, Asn-708, His-1005, Trp-840
249	-9.4	Arg672, Arg673, Ser717, Lys728,	Leu829, Pro724, Phe1003	Pro-716, Lys-723, Arg-727, Glu-837, Gly-1007, Lys-676, Lys-827, Glu-839, Arg-713, Gly-725, Tyr-757

		His758, His759, Glu712, Ile715, Leu722		
250	-9.2	Arg31, Arg323, Ser319	La152, Cys153, Ala28, Ala152	Asp-321, Pro-34, Leu-33, Trp-32, Ile-160, Arg-323, Val-30, Cys-158, Thr-159, Asn-162, Val-90, Phe-29, Thr-159, Ile-160, Pro-34, Ala-35, Arg-31, Leu-33, Trp-32, Phe-439, Val-320
251	-8.6	Arg31, Arg323, Ser319	Ala152, Cys153, Ala28, Ala152	Asp-321, Pro-34, Leu-33, Trp-32, Ile-160, Arg-323, Val-30, Cys-158, Thr-159, Asn-162, Val-90, Phe-29, Thr-159, Ile-160, Pro-34, Ala-35, Arg-31, Leu-33, Trp-32, Phe-439, Val-320
252	-8.8	Arg672, Arg673, Arg672, Gly1007	Phe1003	Arg-727, Pro-724, Leu-829, Glu-839, Val-1006, Asp-831, Arg-675, Tyr-684, Leu-680, Pro-681, Glu-682, Pro-593, Glu-597, Ser-600, Gly-679, Lys-676, Ser-717
253	-8.3	Ser717, Glu839, His1005, Glu839, Glu712, Glu839	-	Ser-709, Arg-713, His-759, Lys-728, Tyr-757, Pro-724, Arg-672, Lys-676, Arg-673, Val-1006, Gly-1007, Phe-1003, Trp-840, Asp-1004, Pro-838, Leu-829, Asp-831, Arg-727, Glu-837
254	– 7.8	Asn-708, Leu-705	Leu-705	Gln-544, Ser-709, Leu-592, Asp-831, Lys-614, Asp-832, Tyr-612, Pro-593, Lys-599, Phe-595, Glu-682, Arg-672, Asn-833, Phe-668
Vosaroxin	-7.2	Ser-591, Leu-685, Leu-592	Leu-705, Ile-577, Pro-593	Glu-682, Tyr-684, Arg-672, Gln-542
Revlimid	– 7.4	Gln-542, Gln-544, Glu-702, Pro-593, Lys-550, Lys-550	Pro-593, Leu-705	Ser-591, Glu-682, Tyr-686, Ser-547, Asp-543, Ile-577, Ser-709, Asn-708, Arg-672

Appendix 41D: Molecular docking results of isolated compounds against *S. aureus* Gyrase (PDB ID 2XCT).

			Residual interactions	
Ligands	**Binding Affinity (kcal/mol)**	**H-bond**	Hydrophobic	Van der Waals
224	– 7.5	Ser-1084, Ser-1084	Ala-1120	Ala-1118, Ala-1119, Ser-438, Asp-437, DG-9, DA-11, DT-10, Tyr-1087, Ser-1084, Glu-1088, Met-1121, Asp-1083, Arg-1122
226	– 9.6	Arg-1122, Arg-1122, Arg-1122, Asp-1083	Ala-1120, Ala-1120	DT-10, Arg-1122, Asp-1083, Phe-1123, Ala-1119, Ser-438, Asp-437
239	– 5.8	Met-1121, Arg-1122, Arg-1122, Arg-1122, Arg-1122, Arg-1122	Asp-1083, Ala-1120, Met-1121, Tyr-1087	Asp-1083, Ser-1084, Ala-1119, Ala-1118, Glu-1088, DT-10, Phe-1123, Asp-437, DG-9, Ser-438
240	– 6.0	Asp-437, Ser-438, Ser-438, Ser-438	Arg-458, Arg-458	Gly-459, DT-10, Ala-439, Phe-1123, Gly-436, Gly-584, Arg-1122
241	– 5.6	DG-9, Asp-437	Phe-1123, Phe-1123	Arg-458, Gly-1082, Arg-1122, DT-10, Gly-459, DA-13, His-1081, Mn-2492

78	– 7.0	Glu-1088, Ser-1084	Ala-1120, Met-1121, Arg-1122	Arg-1122, Asp-1083, Ser-1084, DT-10, DA-11, Met-1121, Asp-1083, DG-9, Tyr-1087
79	– 7.9	Ser-1084	Ala-1120	Ser-438, Glu-1088, Tyr-1087, Ser-1084, Ala-1119, DT-10, Asp-437, Met-1121, Arg-1122, Asp-1083
97	– 10.1	Asp-1083	Ala-1120	Tyr-1087, Ala-1119, Glu-1088, Met-1121, Ser-1084, Asp-1083, Arg-1122, Ala-1120, DG-9, DT-10, Ser-438, Asp-437
98	– 9.8	Glu-1088	Ala-1120, Met-1121	Arg-1122, Ser-1084, Asp-1083, DA-11, DT-10, Ala-1120, Met-1121, Ala-1119, Tyr-1087, DG-9
234	– 9.4	DA-11, DC-12 (Dist. 2.59726 Å), DC-12 (Dist. 2.5525 Å)	—	DT-10, Arg-1122, Asp-1083, Met-1121, Ala-1120, DG-9, Ala-1119, Glu-1088, Tyr-1087, Ser-1084
87	– 9.8	Glu-1088	Met-1121	Ser-1084, DT-10, Asp-1083, Ala-1119, Met-1121, Ala-1120, Tyr-1087, DG-9, Arg-1122
254	– 7.9	DT-10	Met-1121, Ala-1120, Ala-1120	DT-10, Asp-1083, Ser-1084, Tyr-1087, Met-1121, Glu-1088, Ala-1119, Arg-1122, DG-9
Amoxicillin	– 10.0	Asp-437, Asp-437, Asp-437, Ser-438, Ser-438, Ala-439, Leu-457,	Asp-508, Phe-1123	Gly-584, Gly-582, Gly-436, Pro-1080, Mn-2492, Gly-459, Glu-435, Arg-458, DA-13

A = adenine; G = guanine; C = cytosine; U = uracil

Appendix 41E: Molecular docking results of isolated compounds against N-Terminal Domain of PqsA in a Complex with 6-Fluoroanthraniloyl-AMP (PDB ID 5OE3).

			Residual interactions	
Ligands	**Binding Affinity (kcal/mol)**	**H-bond**	Hydrophobic, Electrostatic, and Others	Van der Waals
224	– 8.0	Arg-386, Tyr-392	Leu-358	Glu-331, Glu-343, Cys-332, Gly-376, Gly-355, Arg-354, Asn-180, Ser-177, Pro-356, Ala-156, Arg-179, Pro-360
226	– 8.5	Ala-21, Ala-21, Ser-31, Asp-19, Asp-19, Ala-245	Arg-200, Thr-29, Thr-29, Ala-21, Ala-21, Ala-21	Phe-246, His-24, Thr-29, Thr-20, Arg-200, Gln-34, Leu-30, Arg-247
239	– 6.4	Ala-21, His-24, His-24, Arg-200, Thr-20	Ala-21, Ala-21	Thr-29, Gly-198, Ser-226, His-24, Asp-19, Thr-20, Arg-200
240	– 5.4	Gly-210, Tyr-163, Phe-209, Phe-209	Lys-206, Ile-257, Pro-205, Pro-205, Pro-234, Pro-234, Val-254, Val-254, Phe-209, Phe-209, Phe-209, Phe-209	Ile-204, Thr-164, Ile-208, Thr-304, Trp-233
241	– 5.1	Ile-342, Arg-386, Arg-386, Arg-386	Arg-186, Ala-187, Pro-356, Pro-326, Pro-328, Pro-328	Glu-343, Glu-191, Gly-329, Cys-332, Glu-331, Arg-333, Thr-341, Leu-334
78	– 7.9	Arg-333, Arg-333	Pro-326	Leu-325, Gly-390, Gly-329, Arg-386, Tyr-330, Gly-355, Glu-331, Pro-356, Tyr-392, Cys-332, Glu-343

79	– 8.5	Gln-34, Ala-245	Ala-21	Ser-226, Thr-20, Thr-29, Arg-200, His-24, Phe-246, Arg-247, Ser-31, Ala-21, Asp-19, Gly-198
97	– 10.2	Thr-29	Ala-21	Arg-200, His-24, Thr-29, Ala-21, Phe-246, Thr-20, Gly-198, Ser-226, Asp-19, Ser-31
98	– 10.4	Ala-245	Ala-21	Thr-29, Arg-200, His-24, Phe-246, Thr-20, Gly-198, Ala-21, Asp-19, Ser-31
234	– 11.0	His-24, Arg-200, Arg-200	His-24	Ala-245, Phe-246, Thr-29, Arg-200, Thr-20, Ala-21, Ser-226, Gly-198, Gln-28, Gly-27
87	– 9.9	Arg-200	His-24, Phe-246	Arg-200, Asp-19, Thr-20, Ala-21, Gly-198, His-24, Thr-29, Gly-27, Ala-245
243	-7.0	Gly-27, Asp-19 Gln-28, Asn-242 Ser-31	Leu-228, Phe-246 Ala-245	Arg26, Tyr25, His24, Thr29, Arg200
244	-8.6	Arg-333, Leu-358, Ser-359, Gly-329, Cys-332	Glu-331, Leu-358	Thr341, Pro360, Glu-343, Arg179, Gly390, Arg386, Gly355, Pro356, Tyr330, Tyr392, Pro326, Gly376
245	-9.2	Arg-333, Arg-386, Glu-343, Tyr-330, Arg186	Glu331, Pro328, Pro328, Pro356, Pro326, Arg333	Ala345, Thr341, Cys332, Gly329, Glu191, Ala187, Gly390
246	-10.4	Arg-186, Arg-354, Arg-333, Arg-386, Cys-332, Gly-390, Glu-388, Asp-387	Glu-343, Arg-186, Arg-356, Pro-356	Leu325, Pro326, Leu182, Gly183, Gly355, Glu-331, Trp-377, Thr341, Ala345
254	– 8.2	Ala-345, Glu-343	Ala-345, Val-10, Pro-155, Ala-5, Ala-5	Thr-3, Leu-178, Arg-179, Arg-386, Glu-344, Glu-388, Leu-182, Arg-13
Amoxicillin	– 8.1	Arg-333, Arg-333, Arg-333, Tyr-392, Arg-186, Arg-186, Arg-186, Cys-332, Arg-179	Glu-343, Arg-333	Glu-388, Ala-345, Thr-341, Leu-182, Leu-178, Pro-356, Gly-390, Arg-386, Glu-331

List of published articles from this work

1. Tegegn, G., Melaku, Y., Eswaramoorthy, R., & Endale, M. (2022). Pharmacokinetics, drug-likeness, antibacterial and antioxidant activity of secondary metabolites from the root's extracts of *Crinum abyssinicum* and *Calotropis procera* and *in silico* molecular docking study. *International Journal of Secondary Metabolites*, 9(4), 467-492.

2. Tegegn G, Melaku Y, Aliye M, Abebe A, Abdissa N, Meresa A, Degu S, Hunsen M, Hussein AA, Endale M. (2024). In vitro antimicrobial and antioxidant activities, essential oil composition, and in silico molecular modeling analysis of secondary metabolites from roots of *Verbascum sinaiticum*. *Zeitschrift für Naturforschung C*, Doi: 10.1515/znc-2023-0157.

3. Tegegn, G., Melaku, Y., Eswaramoorthy, R., Aliye, M., Abebe, A., Degu, S., Hunsen M, & Endale, M. (2023). Essential Oil Composition, In Vitro Antidiabetic, Cytotoxicity, Antimicrobial, Antioxidant activity, and In Silico Molecular Modeling Analysis of Secondary Metabolites from *Justicia schimperiana*. Submitted to *Zeitschrift für Naturforschung C*, Accepted.
4. Tegegn, G., Melaku, Y., Eswaramoorthy, R., Garg, A., Abebe, A., Degu, S., & Endale, M. (2023). *In Vitro* Antidiabetic, Cytotoxicity, Antimicrobial and Antioxidant Activity of Secondary Metabolites from *Calotropis procera*: A Combined Experimental and Computational Study. Submitted to ABC (Springer Open Publishers), under review.
5. Tegegn, G., Melaku, Y., Eswaramoorthy, R., Aliye, M., Abebe, A., Degu, S., & Endale, M. (2023). Integrated Experimental and Computational Study of Secondary Metabolites from *Caylusea abyssinica* and *Lagenaria abyssinica*: *In Vitro* Antidiabetic, Cytotoxic, Antimicrobial, and Antioxidant Activities. Submitted to ABC (Springer Open Publishers), under review.